

Membrane protein glycan markers of epithelial ovarian cancer: Discrimination of serous tumours of ovary, peritoneum and tube

Merrina Anugraham

Master of Biotechnology (2010), Macquarie University, Australia

A thesis submitted for the Degree of
Doctor of Philosophy



Department of Chemistry and Biomolecular Sciences,
Faculty of Science and Engineering,
Macquarie University, Sydney, Australia

May 2015

In loving memory of my beloved aunt who endured her battle
with cancer through courage, strength, love and grace



Table of Contents

Statement of Declaration	vi
Abstract.....	vii
Acknowledgements	ix
Publications.....	xi
Presentations/Awards.....	xiii
Abbreviations.....	xv
CHAPTER I: INTRODUCTION.....	1
1.0 Cancers of the Ovary, Fallopian Tube and Peritoneum	2
1.0.1 Epithelial Ovarian Cancer (EOC)	3
1.0.1.1 Epidemiology and Etiology of Epithelial Ovarian Cancer	3
1.0.2 Serous Cancers of Non-ovarian Origin.....	5
1.0.2.1 Primary Fallopian Tube Serous Carcinoma (PFTSC)	5
1.0.2.2 Primary Peritoneal Serous Carcinoma (PPSC)	5
1.1 Origin of Ovarian Cancer	6
1.1.1 Dualistic Model for Ovarian Cancer Carcinogenesis	8
1.1.2 Identifying the Site of Origin of Serous Cancers	9
1.1.2.1 Role of OSE in Ovarian Cancer	9
1.1.2.2 Emergence of Distal Fallopian Tube as a Site of Serous Carcinogenesis	10
1.1.3 Current Model of Serous Carcinogenesis	12
1.1.4. Molecular Distinction between Serous Pelvic Carcinomas	14
1.2 Diagnosis, Treatment and Management of Serous Cancers.....	16
1.2.1 Diagnosis and Screening of EOC.....	16
1.2.2 Treatment Types.....	16
1.2.3. Molecular Targeted Therapies in EOC	18
1.3 Experimental Models of High Grade Serous Carcinomas	20
1.4 Overview of Section I: Highlights and Challenges in EOC	23
1.5 Glycosylation in Cancer	24
1.5.1 Glycosylation in EOC.....	26
1.5.1.1 Detection of Anti-glycan Auto-antibodies in Serum of EOC Patients	28
1.6 Historical Overview of Glycobiology.....	29
1.6.1 <i>N</i> - and <i>O</i> - Glycosylation.....	29
1.6.1.1 Synthesis of <i>N</i> -glycans in Eukaryotes.....	32

1.6.1.2 Synthesis of <i>O</i> -glycans in Eukaryotes	35
1.6.2 Synthesis of Glycolipids in Eukaryotes	37
1.7 Glyco-epigenetic Regulation in Ovarian Cancer	39
1.8 Overview of Section II: Highlights and Challenges in EOC Glycosylation	41
1.8.1 Publication 1: Cell Surface Protein Glycosylation in Cancer	42
1.9 Mass Spectrometric and Non-Mass Spectrometric Methods of Glycan Characterisation	64
1.9.1 Mass Spectrometric Analysis of Glycans	64
1.9.2 Basic Principles of Mass Spectrometry	64
1.9.3 Ionisation Methods in Mass Spectrometry	65
1.9.4 Mass Analysers in Mass Spectrometry	66
1.9.4.1 Tandem Mass Spectrometry (MS ⁿ)	68
1.9.4.2 Collision Induced Dissociation (CID)	68
1.9.5 Nomenclature for the Fragmentation of Glycoconjugates	70
1.9.5.1 Fragmentation of Glycans in Positive Ion Mode	71
1.9.5.2 Fragmentation of Glycans in Negative Ion Mode	72
1.9.6 Chromatographic Interface for LC-MS of Glycans	74
1.9.6.1 Specific Chromatographic Features of Porous Graphitised Carbon Chromatography	74
1.9.7 Bioinformatics Tools for Glycan Structure Determination	78
1.9.8 Non-Mass Spectrometric Methods of Glycan Detection	79
1.10 Overview of Section IV: Highlights and Challenges in Glycan Structural Identification	82
1.11 Aims of Research Project	83
CHAPTER II	84
2.0 Publication II: Specific glycosylation of membrane proteins in epithelial ovarian cancer cell lines: glycan structures reflect gene expression and DNA methylation status	85
2.1 Supplementary Data	105
2.2 Overview of Chapter II	113
CHAPTER III	114
3.0 Introduction	115
3.1 Materials and Methods	119
3.2 Results	125
3.3 Discussion	163
3.4 Supplementary Data	170
3.5 Overview of Chapter III	171

CHAPTER IV	172
4.0 Publication III: A platform for the structural characterization of glycans enzymatically released from glycosphingolipids extracted from tissue and cells	173
4.1 Supplementary Data.....	190
4.2 Overview of Chapter IV: Publication III	192
4.3 Publication IV: The glycosphingolipid P ₁ is an ovarian cancer-associated carbohydrate antigen involved in migration.....	193
4.4 Supplementary Information.....	205
4.5 Supplementary Data.....	210
4.6 Overview of Chapter IV: Publication IV	215
CHAPTER V: CONCLUSIONS AND FUTURE DIRECTIONS	216
5.0 Thesis Overview.....	217
5.1 Methodology and Analytical Considerations	218
5.2 Biological Insights Derived From Membrane Glycosylation of Serous Cancers	220
5.3 Translational ('bench-to bedside') Implications for Ovarian Cancer Research	225
5.4 Future Directions/ Suggestions.....	226
CHAPTER VI: REFERENCES.....	227
6.0 References	228
APPENDICES	258
Appendix A: FIGO staging	259
Appendix B: Biosafety Approval -MEA020712BHA	261
Appendix C: Ethics Approval-(5201100778)	266
Appendix D: Northern Translational Cancer Research Grant.....	267

Statement of Declaration

I hereby certify that the work presented in this thesis entitled, 'Membrane protein glycan markers of epithelial ovarian cancer: Discrimination of serous tumours of ovary, peritoneum and tube' has not previously been submitted for a degree nor has it been submitted as part of the requirements for a degree to any other university or institution other than Macquarie University. This thesis is an original piece of research and is the result of my own work except where appropriately acknowledged. I consent to a copy of this thesis being available in the University library for relevant consultation, loan and photocopying forthwith.

Merrina Anugraham

May 2015

Abstract

Epithelial ovarian cancer is characterised by a low 5-year survival rate of 43% of those diagnosed. The overall prognosis is poor due to many factors such as the lack of reliable and sensitive markers for early stage detection, the heterogeneity of the tumours, rapid metastasis of the disease which extends beyond the ovaries and the different cancer tissue origins (ovary, peritoneum and tube). As these cancers are derived from the epithelial surface, the comprehensive glycosylation of the cell membrane proteins and lipids from cell lines and serous cancer tissues was investigated to unravel cancer-specific biomarkers for improved diagnosis and personalised tumour-specific treatments.

In the first phase of this study, *N*- and *O*-glycans were enzymatically released by PNGase F and reductive β -elimination, respectively, from extracted membrane glycoproteins derived from '*in vitro*'-based cell line models of cancerous and non-cancerous ovarian cells. Released glycan alditols were separated using porous graphitised carbon (PGC) chromatography, analysed using electrospray ionisation mass spectrometry (LC-ESI-MS/MS) and characterised based on negative ion tandem MS fragmentation patterns and LC retention times. Glycan structural features such as bisecting *N*-acetylglucosamine (GlcNAc) and sialylated *N*-*N*-diacetyllactosamine (LacdiNAc)-type structures, together with increased levels of α 2-6 sialylation were detected on membrane glycoproteins derived from ovarian cancer cells. The corresponding gene expression and epigenetic regulation of specific glycosyltransferases responsible for the biosynthesis of relevant *N*-glycan structures were also investigated using qRT-PCR and de-methylation by 5-Aza treatment. Their presence correlated with the corresponding glycosyltransferase gene expression of *ST6GAL1*, *B4GALNT3*, and *MGAT3*, in which *MGAT3* was found to be also epigenetically regulated by DNA hypomethylation.

The presence of specific glycan structures implicated in the preliminary cell-line models were further verified in membrane proteins of serous cancer tissues from different origins (14 ovarian, 14 peritoneal and 4 tubal). Several statistical analyses such as analysis of variance (ANOVA), principal component analysis (PCA), partial-least-square discrimination analysis (PLSDA) and receiver-operating curve (ROC) were employed to evaluate differences in the expression of glycan structures and to discriminate between all three serous cancers. Bi-antennary sialylated *N*-glycans with prominent α 2-6 sialylation appeared to be the most common feature in all serous cancer tissues, whilst the unique expression of

sialylated LacdiNAc *N*-glycans was detected specifically in serous ovarian-derived cancer tissues and these structures were statistically classified as 'highly accurate' biomarkers of serous ovarian cancer by ROC. The expression of 11 *N*-glycans, including the LacdiNAc-type glycans contributed significantly ($p=0.00186$) to the classification accuracy (78.6 %) of serous ovarian and peritoneal cancers.

In addition to the structural identification of serous cancer membrane *N*- and *O*-glycans, a second analytical platform employing PGC-LC-ESI-MS/MS was also developed to characterise glycans released enzymatically (Endoglycoceramidase II) from PVDF-immobilised glycosphingolipids (GSLs) derived from cancer tissue samples and cell line. The analysis of the glycosylation of ovarian cancer membrane lipids revealed the presence of several isomeric and isobaric structures which were differentiated using specific diagnostic and structural feature ions produced by negative ion mode MS/MS fragmentation. This approach led to the identification of P blood group-related as well as fucosylated/non-fucosylated Type 1 and Type 2 antigens which were not expressed on *N*- and *O*-glycans of membrane proteins of serous cancers analysed in this study. These antigens were also implicated in the immune recognition by auto-antibodies found in the plasma and ascites fluid of ovarian cancer patients.

The identification and understanding of the regulation of membrane protein and lipid glycan epitopes unique to ovarian cancer could be utilised to distinguish serous ovarian from peritoneum and tubal cancers. More importantly, such structures may facilitate the diagnosis and development of different drug targets to improve survival rates of this malignancy.

Acknowledgements

First and foremost, I would like to express my sincere appreciation and heartfelt gratitude to my supervisor, Prof. Nicolle H. Packer for giving me the opportunity to carry out this PhD research project and most of all, for her invaluable guidance and excellent supervision in terms of her advice and insightful comments given throughout the duration of my research. She has been very involved in every aspect of this research project and her constructive reviews and feedback has provided me with the confidence to write and explore ways of analyzing and presenting my research work. I have been very fortunate to have met and worked with a very dedicated and passionate supervisor of high caliber who has been a good role model and a key source of inspiration for me, not just in the field of glycomics, but also as a competent woman pursuing an academic career in science.

I am also very grateful to my dedicated principal collaborator in Switzerland, Dr. Viola Heinzelmann-Schwarz, who initiated this research project with my supervisor and provided not just precious tissues and cell lines, but also dedicated her time and effort to ensure the research project was aligned with potential clinical outcomes in ovarian cancer. Her team of researchers in Hospital University Basel, Switzerland have also assisted me in every way and made my short stay in Switzerland so memorable and fun. A special acknowledgement is also expressed to her post-doc, Dr Francis Jacob, who supported this research in every way possible. He critically reviewed countless number of manuscript drafts, provided constructive comments and helpful suggestions and also drove me to the Swiss Alps to experience my first snowfall. I would also like to acknowledge Dr. Sheri Nixdorf (Lowy Cancer Research Centre, UNSW, Sydney) for her kind assistance in providing me with cell lines and for also guiding me during my visits to the lab.

My PhD experience would not have been complete without the help and support of post-docs and students from the 'Glyco' group headed by my supervisor. Specifically, I would like to say a big 'thank you' to Dr. Arun Vijay Everest-Dass for his invaluable guidance and technical advice regarding the use of mass spectrometry and data analysis. He has also been instrumental in helping me understand the complicated world of sugar fragmentation as well as patiently reviewed and edited most of my manuscripts (even during coffee breaks!) A very special appreciation is also attributed to Dr. Liisa Kautto throughout the 3.5 years for efficiently guiding and briefing me on equipment usage and for always ensuring that students had a safe and clean working environment in the laboratory. I also want to thank my officemate, Vignesh Venkatakrishnan for kindly offering his assistance as well as various

snacks and participating in amusing and informative conversations in the office which ranged from cricket, politics, music and history. I would also like to acknowledge past and present group members, Morten Anderson, Matthew Campbell, Chi-Hung Lin, Robyn Peterson, Jenny Chik, Jodie Abrahams, Katherine Wongtrakul-kish, Zeynap Sumer-Bayraktar, Lee Ling Yen and Maja Christiansen for their friendship and support. I am also grateful to Dr. John Merrick for his kind words of advise and encouragement and to my ex-lab mate, Cheah Wai Yuen, a dear friend throughout these 3.5 years, who always offered me assistance in the lab and with my research project as well as cheerfully organised numerous dinner gatherings in her house.

I would also like to take this opportunity to thank Macquarie University for the provision of the International Macquarie University Research Scholarship (iMQRES) for 3.5 years and the staff at the Australian Proteome Analysis Facility for enabling me to carry out a majority of my analytical work using the mass spectrometric facilities in their laboratory. Specifically, I like to thank Dr. Dana Pascovici for her guidance in the choice of statistical tools employed in this thesis. She has always been willing to assist in the data analyses and to provide valuable feedback for all my questions. I am also grateful to Prof Helena Nevalainen for allowing me to use her laboratory and to her efficient administrative staff of CBMS, Catherine Wong and Michelle Kang for reminding me of various deadlines and processing times for travel claims and HDR budgets.

I am so thankful and blessed to have wonderful and supportive parents, family members and friends in Malaysia (Marilyn, Denny, David and Suba) and Australia (Uncle Mat, Athai, Shahmani, Terence, Lata, Raj, Monica and Franco) who have continually been my source of strength, motivation and love. This thesis is lovingly dedicated to my parents, Michael Anugraham and Marie Thomas, who have always supported my decision to pursue my studies and taught me the value of patience, gratitude and humility. These values will forever be cherished and have helped shape my attitude and perspectives in life. I would also like to thank my loving fiancé, Paul Townsend, for being very supportive and accommodating throughout my PhD candidature and a heartfelt gratitude is also extended to his amazing parents for their care, concern and love. Above all, I thank the good Lord for blessing me with physical and mental strength, good health and tremendous opportunities to advance my knowledge. This thesis would not have been accomplished without the guidance, expertise, love and support of all the people mentioned here whom he has strategically placed in my life to cherish always.

Publications

1. Christiansen MN*, Chik J*, Lee LY*, **Anugraham M***, Abrahams JL*, Packer NH*. Cell surface protein glycosylation in cancer. *Proteomics*. **14** (4-5): 525-46. (2014)
2. **Anugraham M***, Jacob F*, Nixdorf S, Everest-Dass AV, Heinzelmann-Schwarz V, Packer NH. Specific glycosylation of membrane proteins in epithelial ovarian cancer cell lines: glycan structures reflect gene expression and DNA methylation status. *Molecular and Cellular Proteomics*. **13**(9): 2213-32 (2014)
3. Jacob F, **Anugraham M**, Pochechueva T, Tse BW, Alam S, Guertler R, Bovin NV, Fedier A, Hacker NF, Huflejt ME, Packer NH, Heinzelmann-Schwarz VA. The glycosphingolipid P1 is an ovarian cancer-associated carbohydrate antigen involved in migration. *British Journal of Cancer*. **111**: 1634–1645 (2014)
4. **Anugraham M**, Everest-Dass AV, Jacob F, Packer NH. A platform for the structural characterization of glycans enzymatically released from glycosphingolipids extracted from tissues and cells. *Rapid Communications in Mass Spectrometry*. **29** (7): 541-5 (2015)

* equal authorship

I, Merrina Anugraham, was the co-author for **Publication 1** and **2**, second author for **Publication 3** and first author for **submitted Publication 4**, presented in this thesis in Chapter 1 (as a review), Chapter 2 and Chapter 4 respectively.

In **Publication 1**, the ovarian cancer review section, together with the associated glycosyltransferases and sialylation section were prepared by myself, while the Figures were prepared by myself and Ling Lee Y. The overall design, structure and content for the conclusion section were contributed equally by all co-authors.

In **Publication 2**, all glycan-based experiments pertaining to sample processing, data analysis and manuscript preparation was performed by myself. The qRT-PCR experiments were performed equally by myself (in Switzerland) and Dr. Francis Jacob (in Sydney and Switzerland). Dr Francis also performed DNA de-methylation experiments and provided assistance in manuscript design and preparation. Dr. Sheri Nixdorf (Sydney) kindly provided cultured cell lines and assisted in manuscript revision. Dr. Arun-Vijay Everest Dass gave

technical support and assisted in glycan structural interpretation as well as critically reviewed the manuscript.

In **Publication 3**, all glycan-based experiments pertaining to tissue sample processing, culturing of cell line, MS-structural glycan interpretation and manuscript preparation (glycan section) was performed by myself.

In **Publication 4**, all glycan-based experiments pertaining to tissue sample processing, culturing of cell line, MS analysis and manuscript preparation was performed by myself. Dr. Arun-Vijay Everest Dass gave technical support and assisted in MS-glycan structural interpretation as well as critically reviewed the manuscript. Dr Francis provided the cell line and critically reviewed the manuscript.

My supervisor, Prof. Nicolle H. Packer supervised, critically reviewed and edited all four manuscripts and my principal collaborator from Switzerland, Dr. Viola Heinzelmann-Schwarz, supervised, critically reviewed and edited two manuscripts.

Presentations/Awards

* Poster/oral presenter

Poster Presentation 1

*Merrina Anugraham, Sheri Nixdorf, Viola Heinzelmann-Schwarz, Nicolle H. Packer (2012)
Ovarian cancer biomarkers: Differential expression of sugars on their cell membranes.
Poster presentation at **Sydney Cancer Conference 2012 (SCC2012): Cancer research network**, held on the 27- 28th of September 2012, University of Sydney, NSW, Australia.

Poster Presentation 2

*Merrina Anugraham, Sheri Nixdorf, Viola Heinzelmann-Schwarz, Nicolle H. Packer (2012)
Ovarian cancer biomarkers: Differential expression of sugars on their cell membranes.
Poster presentation at **Proteomics and Beyond Symposium 2012**, held on the 7th of November, 2012, Macquarie University, NSW, Australia.

Poster Presentation 3

*Merrina Anugraham, Sheri Nixdorf, Viola Heinzelmann-Schwarz, Nicolle H. Packer (2012)
Discovering glycan biomarkers of ovarian cancer by LC-MS/MS: Comparing *N*-glycans released from proteins in cancer cell lines and tissues. Poster presentation at **Mass Spectrometry: Applications to the Clinical Lab (MSACL), 2013**, held on the 9-13th of February, 2013, San Diego, California

Poster Presentation 4

*Francis Jacob, Merrina Anugraham, Shahidul Alam, Tatiana Pochechueva, Nicolai Bovin
Glycosphingolipid P1 is expressed on ovarian cancer cells and can be detected by anti-P1 antibodies from ovarian cancer ascites. Poster presentation at **International Symposium on Chemical Glycobiology, 2013**, held on June 21-July 1st, 2013, Shanghai, China.

Poster Presentation 5

*Merrina Anugraham, Arun Everest-Dass, Francis Jacob, Sheri Nixdorf, Viola Heinzelmann-Schwarz, and Nicolle H. Packer
N-glycosylation reveals differences between cancer subtypes of the ovary, tube and peritoneum. Poster presentation at the **27th International Carbohydrate Symposium, 2014 (ICS27)**, held on 12-17th of January, 2014, Bangalore, India.

Poster Presentation 6

Merrina Anugraham, Francis Jacob, Reto Kohler, Sheri Nixdorf, Arun Everest-Dass, Andre, Fedier,*Viola Heinzelmann-Schwarz, Nicolle H. Packer (2014). Presence of bisecting GlcNAc-modified proteins on ovarian cancer cells associates with elevated expression of the epigenetically regulated MGAT3 gene. Poster presentation at the **15th Biennial Meeting of the International Gynecologic Cancer Society, 2014** (IGCSMEL-2014) held on 8-11th of November, 2014, Melbourne, Australia

Oral Presentation 1

*Merrina Anugraham, Francis Jacob, Sheri Nixdorf, Viola Heinzelmann-Schwarz, Nicolle H. Packer (2013). Characterization of cell surface glycosylation in ovarian cancer leads to identification of dysregulation in MGAT3 and ST6GAL-1 gene expression. Oral presentation at the **22nd International Symposium on Glycoconjugates 2013** (GLYCO22) held on 23-28th of June, 2013, Dalian, China. In proceeding of: GLYCO 22 XXII International Symposium on Glycoconjugates. *Glycoconj J.* 30:281–461. doi 10.1007/s10719-013-9474-x.

Oral Presentation 2

*Nicolle H. Packer (2013). Glycosylation of proteins in cancer. Oral presentation held on 2nd of September, 2013 at Perth Cancer Club, Perth, Australia.

Travel Awards/Grants

The following travel awards and grants have been attained during the candidature of my thesis and are kindly acknowledged:

- Young Investigator Travel Award (USD 800) - Mass Spectrometry:Applications to the Clinical Lab (MSACL2013), San Diego, California
- Travel Grant (USD 800) - 22nd International Symposium on Glycoconjugates 2013 (GLYCO22), Dalian, China
- 2012 Northern Translational Cancer Research Unit Research Scholar Award - Anugraham (AUD 5000) from Cancer Institute, NSW, Australia (Aris Project No: 9201200676).
- Postgraduate Research Fund (PGRF) Award with DVC-Research Commendation (AUD 5500) for travel to 27th International Carbohydrate Symposium, 2014 (ICS27), Bangalore, India and lab visit to Switzerland

Abbreviations

APC	Adenomatous polyposis coli
ANOVA	Analysis of Variance
AUC	Area under the curve
BRAF	B-Raf proto-oncogene, serine/threonine kinase
BRCA1	Breast cancer type 1 susceptibility protein
BRCA2	Breast cancer type 2 susceptibility protein
BSO	Bilateral salphingo-oophorectomy
CA125	Cancer antigen 125
CCNE1	Cycline E1
Cer	Ceramide
CICs	Cortical inclusion cysts
CID	Collision induced dissociation
DAPK	Death-associated protein kinase 1
ECM	Extracellular matrix
EGFR	Epidermal growth factor receptor
EIC	Extracted ion chromatography
ELISA	Enzyme-linked immunosorbent assay
EOC	Epithelial ovarian cancer
EpCAM	Epithelial cell adhesion molecule
ERRB2	Human epidermal growth factor receptor-2 gene
ESI	Electrospray ionisation
FAB	Fast atom bombardment
FIGO	International Federation of Gynaecologists and Obstetricians
FSH	Follicle stimulating hormone
Gal	Galactose
GalNAc	<i>N</i> -acetylgalactosamine
GBP	Glycan binding protein
GlcNAc	<i>N</i> -acetylglucosamine
GSL	Glycosphingolipid
HE4	Human epididymis protein 4
HER2/neu	Human epidermal growth factor receptor 2
HGSC	High grade serous carcinomas
HIF-1 α	Hypoxia-inducible factor 1-alpha
HPLC	High performance liquid chromatography
hTERT	Human telomerase reverse transcriptase
KRAS	Kirsten rat sarcoma viral oncogene homolog
LacdiNAc	<i>N,N'</i> -diacetyllactosamine
LC	Liquid chromatography
LGSC	Low grade serous carcinomas
LH	Luteinizing hormone
MALDI	Matrix- assisted laser desorption ionization
Man	Mannose

MAPK/ERK	MAPK; mitogen-activated protein kinases, ERK; extracellular signal-regulated kinases
MCSF	Macrophage colony-stimulating factor
MS	Mass spectrometry
mTOR	Mammalian target of rapamycin
Neu5Ac	Neuraminic acid/ Sialic acid
OEI	Ovarian epithelium inclusions
OSE	Ovarian surface epithelium
PCA	Principal component analysis
PFTSC	Primary fallopian tube serous carcinomas
PGA	Printed glycan array
PGC	Porous graphitised carbon
PLSDA	Partial least squares discriminant analysis
PPSC	Primary peritoneal serous cancer
PTEN/P13kAKT	Phosphatase and tensin homolog (PTEN)/Phosphatidylinositol-4,5-bisphosphate 3-kinase
PVDF	Polyvinylidene difluoride
ROC	Receiver operating characteristics
SEOC	Serous epithelial ovarian cancer
STIC	Serous tubal intraepithelial carcinomas
TIC	Tubal intraepithelial carcinomas
TLIT	Tubal lesions in transition
TP53	Tumour suppressor gene
VEGF	Vascular endothelial growth factor
WNT5A	Wingless-type MMTV integration site family, member 5A

CHAPTER I: INTRODUCTION

Literature Review

1.0 Cancers of the Ovary, Fallopian Tube and Peritoneum

The development of cancer is a complex, multistep process, harbouring a series of cumulative events (eg. activation of proto-oncogenes, loss of tumour suppressor genes and promoter hypermethylation) which eventually leads to the transformation of microscopically normal cells to malignant, cancerous cells. These defective, abnormal cells eventually form lumps or tumours which invade the surrounding tissues of the body. These cells are also able to spread to other parts of the human body, through the lymph vessels and blood, in a process called metastasis. If the spread of these tumours persist throughout the entire body, they can cause further damage and result in death (Bray, Ren *et. al.*, 2013). In females, gynaecological cancers typically arise from organs of the reproductive system which are located deep within the lateral wall of the pelvis such as the ovaries, uterus and fallopian tubes. In some cases, cancer is also thought to develop within non-ovarian tissue origins such as the peritoneum as shown in **Figure 1**.

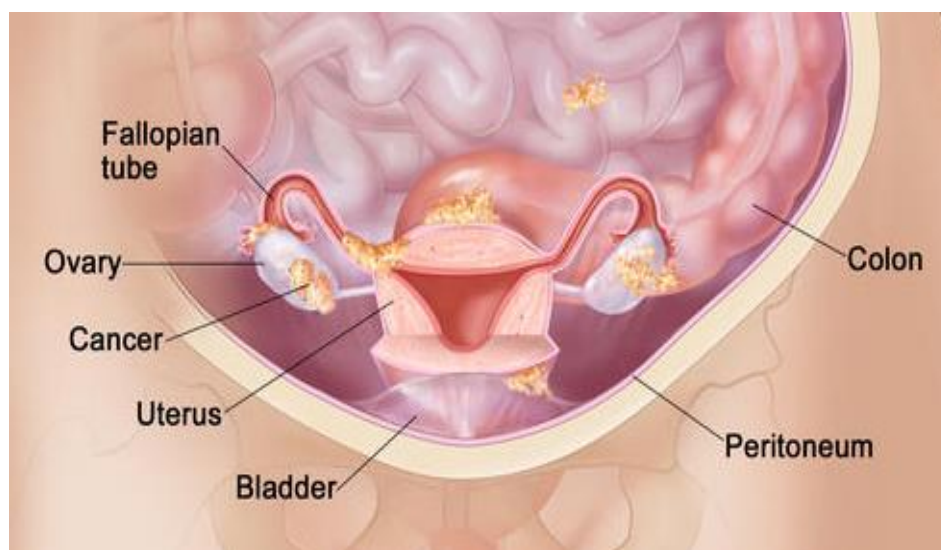


Figure 1: Anatomic location of cancers of the ovary, fallopian tube and peritoneum.
Sourced from Terese Winslow (2010).

1.0.1 Epithelial Ovarian Cancer (EOC)

As the name suggests, epithelial ovarian cancers (EOC) are thought to arise from the simple cuboidal surface epithelium of the ovary, accounting for approximately 90 % of ovarian cancer cases worldwide (Colombo, Peiretti *et. al.*, 2010). This group of ovarian tumours occurs primarily in middle-aged or older women and represents the highest mortality rate among all gynaecological cancers. These tumours are classified into five histological subtypes designated as follows: *serous (low and high grade)*, *mucinous*, *endometrioid (low and high grade)*, *clear cell* and *transitional cell (Brenner type)*. An overview of each cancer subtype within this category of ovarian tumours, with respect to their specific characteristic features is detailed in **Table 1**.

1.0.1.1 Epidemiology and Etiology of Epithelial Ovarian Cancer

Epithelial ovarian cancer is the seventh most commonly diagnosed cancer in the world among women, accounting for almost 4 % of all gynaecological cancers (Ferlay, Soerjomataram *et. al.*, 2013). It is referred to as the ‘silent killer’ due to its asymptomatic nature and is known to have the highest mortality rates per year than any other cancer of the female reproductive system (Sankaranarayanan and Ferlay, 2006). On a worldwide basis, it is estimated that 239 000 new cases will be diagnosed and 151 000 women will die from this disease annually (Ferlay, Soerjomataram *et. al.*, 2013). The median age of diagnosis for ovarian cancer is 60 years and the lifetime risk for women in developed countries is approximately 1 in 70 (Cannistra, 2004). Several risk factors for ovarian cancer have been established and these include age, family history of the disease and lifestyle factors such as smoking and alcohol consumption, while the protective factors include the use of oral contraceptive and oophorectomy (removal of ovaries) (Permuth-Wey and Sellers, 2009). In Australia, ovarian cancer was the second most commonly diagnosed gynaecological cancer in 2010, with 1305 cancer cases reported in women (AIHW, 2014). According to the recent statistics from the 2012 Australian Institute of Health and Welfare (AIHW), in the year 2014, about 1470 Australian women are expected to be diagnosed with ovarian cancer and this figure is expected to rise to 1640 in 2020 (AIHW, 2012). The overall five-year survival rate for women diagnosed with this disease is only 43 % as compared to 89 % for breast cancer (AIHW, 2012).

Table 1: Classification of Epithelial Ovarian Cancer (EOC)			
Subtype	Age at diagnosis (incidence rates)	Characteristic Features	References
Serous	59.4 (60-80 %)	<ul style="list-style-type: none"> – Most common subtype – Low-grade serous carcinomas (LGSC) have low-grade nuclei with infrequent mitotic figures and evolve from adenofibromas or borderline tumors; high grade serous carcinomas (HGSC) exhibit high-grade nuclei and numerous mitotic figures. – Presented as a large mass in the ovary (bilateral involvement in 2/3 cases) – Abundant papillary or micro-papillary projections within the cyst cavity and surface of tumour – Often accompanied by metastasis within the omentum (peritoneum layer surrounding abdominal organs) 	(Chen, Ruiz <i>et. al.</i> , 2003; Levanon, Crum <i>et. al.</i> , 2008; Vang, Shih Ie <i>et. al.</i> , 2009)
Endometrioid	60 (10-25 %)	<ul style="list-style-type: none"> – Derived from cells identical to internal lining of uterine endometrium – Low-grade adenocarcinomas and seem to arise from endometriotic cysts associated with endometriosis; high-grade carcinomas are morphologically indistinguishable from HGSCs and often express WT1. – Usually confined to the ovaries (unilateral) and diagnosed at early FIGO stages (I and II) – Predominantly cystic or solid in appearance 	(Scully, Young <i>et. al.</i> , 1998; Chen, Ruiz <i>et. al.</i> , 2003; Prat, 2012)
Mucinous	54.7 (5-10 %)	<ul style="list-style-type: none"> – Derived from cells identical to intestinal epithelium or endocervical epithelium – Presented as a large unilateral tumours – Abundant papillary or micro-papillary projections within the cyst cavity, large areas of necrosis and solid areas – Presence of tenacious mucus 	(Scully, Young <i>et. al.</i> , 1998; Chen, Ruiz <i>et. al.</i> , 2003)
Clear-cell	50 (4-5 %)	<ul style="list-style-type: none"> – 50-70 % have endometriosis – Presented as a large unilateral tumours – Predominantly cystic or solid with polypoid masses protruding into lumen – Abundant clear cytoplasm; prominent cell membrane – Poor prognosis for Stage 1 cancers with 5-year survival rates of 69 % 	(Scully, Young <i>et. al.</i> , 1998; Chen, Ruiz <i>et. al.</i> , 2003)
Transitional cell (Brenner type)	50 (2 %)	<ul style="list-style-type: none"> – Derived from cells identical to the internal lining of the urinary bladder or urothelium – Presented as unilateral tumours – Predominantly cystic or solid with papillary or polypoid projections – Morphologically and phenotypically similar to serous tumours – 70-100 % present at advanced stages; better response to chemotherapy 	(Nucci and Oliva, 2009)

1.0.2 Serous Cancers of Non-ovarian Origin

1.0.2.1 Primary Fallopian Tube Serous Carcinoma (PFTSC)

Primary fallopian tube serous carcinoma (PFTSC) is a rare malignancy, predominantly of the serous histotype (Nordin, 1994; Alvarado-Cabrero, Young *et. al.*, 1999; Piura and Rabinovich, 2000), that clinically and histologically resembles serous epithelial ovarian cancer (SEOC) (Jeung, Lee *et. al.*, 2009). It accounts for approximately 0.1-1.8 % of all female gynaecological cancers (Riska, Leminen *et. al.*, 2003), with a 5-year survival rate of about 30 to 50 % (Rosen, 1993; Rauthe, 1998). The peak incidence for patients with PFTSC is between the ages of 60 and 64 years of age, with the mean age of onset being 55 years (Cohen, Thoas *et. al.*, 2000). It is thought that the true incidence of PFTSC may have been underestimated and these tumours may have been misclassified as SEOC due to their similar histological appearance (Henderson, Harper *et. al.*, 1977). Nevertheless, as compared to SEOC, PFTSC is often present at early FIGO stages (Appendix A: **Table 1**), with a much worse prognostic outcome. Despite this, the management and treatment of PFTSC are similar to EOC, in terms of surgical management and adjuvant chemotherapy (Kosary and Trimble, 2002).

1.0.2.2 Primary Peritoneal Serous Carcinoma (PPSC)

Primary peritoneal serous carcinoma (PPSC) is a rare primary malignancy of the peritoneum (Eltabbakh and Piver, 1998; Hou, Liang *et. al.*, 2012). The peritoneum is a serous membrane, composed of a layer of mesothelium which forms the lining of the abdominal cavity. The primary function of the peritoneum is to support the abdominal organs and to serve as a conduit for the nerves, blood and lymph vessels. The origin of PPSC has not been well characterized and early studies have shown that it is thought to arise from the mesothelium layer of the peritoneum (Raju, Fine *et. al.*, 1989), or from the coelomic epithelium lining the abdominal cavity due to oncogenic stimulus (Truong, Maccato *et. al.*, 1990). This rare clinical entity was first identified by Swerdlow in 1959 (Swerdlow, 1959), in which it exhibited characteristics such as diffuse peritoneal tumor implants, usually involving the omentum and upper abdomen. The prognosis of PPSC is relatively poor with 5-year survival rates ranging between 0-26.5 % (Fromm, Gershenson *et. al.*, 1990). The diagnosis of PPSC is rarely considered preoperatively (Eddy, 1984; Liu, Lin *et. al.*, 2011) and is based on the FIGO staging established for EOC (Appendix A: **Table 2**).

1.1 Origin of Ovarian Cancer

The origin and molecular pathogenesis of epithelial ovarian cancer have perplexed investigators for many years, in which several time-honoured concepts have been recently reviewed (Kurman and Shih Ie, 2010) and summarised as follows: a) high-grade serous carcinomas remain the vast majority of ovarian cancers and are therefore regarded as a single disease, b) ovarian cancer is thought to originate from the ovarian surface epithelium (OSE), which eventually undergoes malignant transformation and c) ovarian cancer spreads from the ovary to other distant sites such as the pelvis and the abdomen. These views have also formed the basis for the proposal of several early hypotheses linked to factors such as ovulation, inflammation, and hormonal changes relating to the origin and development of ovarian cancer. The two main traditional and long-held theories that have been extensively described in numerous studies which are associated with decreased risks due to the decreased number of ovulatory cycles are described below:

a) Incessant ovulation hypothesis

The incessant ovulation hypothesis was initially proposed by Fathalla and co-workers in 1971 (Fathalla, 1971) and the notion was later supported by several other researchers in the following years (Casagrande, Louie *et. al.*, 1979; Moorman, Schildkraut *et. al.*, 2002; Purdie, Bain *et. al.*, 2003; Tung, Wilkens *et. al.*, 2005). This hypothesis is based on the repeated cycles of ovarian follicular rupture and subsequent repair during the ovulation process which leads to the increased likelihood of genetic abnormalities to the ovarian surface epithelium. This hypothesis seems to be in agreement with increased risk factors associated with early menarche, late menopause and nulliparity, all of which contribute to increased ovulation episodes (Choi, Wong *et. al.*, 2007). In agreement, other conditions in which ovulation is suppressed such as prolonged breastfeeding or lactation, oral contraceptive use and multiple pregnancies, have been reported to lower the risk of developing ovarian cancer (Ford, Easton *et. al.*, 1994; Greenlee, Murray *et. al.*, 2000). While much of the incessant ovulation theory reconciles with epidemiological and experimental results from previous studies and points to the protective effects of anovulatory effects against ovarian cancer, the suppression of ovulation alone is insufficient to understand the underlying mechanism in the development of ovarian cancer. Moreover, this hypothesis also fails to provide an explanation for the increased risks associated with twin pregnancies (Lambe, Wu *et. al.*, 1999), obesity among women (Mink, Folsom *et. al.*, 1996; Frost and Coleman, 1997; Purdie, Bain *et. al.*, 2001) and polycystic ovarian syndrome (PCOS) (Schildkraut, Schwingl *et. al.*, 1996). This led to the disagreement by several researchers in recent years (Levanon, Crum

et. al., 2008; Gross, Kurman *et. al.*, 2010; Li, Fadare *et. al.*, 2012; Sherman-Baust, Kuhn *et. al.*, 2014), in which several other alternative theories have been proposed to understand the causative mechanisms behind the development of ovarian cancer.

b) Gonadotropin theory

The second prevailing hypothesis, known as the ‘gonadotropin theory’ was proposed by Cramer and Welch in 1983 (Cramer, Hutchison *et. al.*, 1983; Cramer and Welch, 1983), in which it was thought that the excessive levels of gonadotropin (FSH and LH) stimulation of the ovarian surface epithelium (OSE) contributed to ovarian cancer carcinogenesis (Cramer and Welch, 1983). While FSH and LH receptors are found on all normal ovaries, their presence has only been implicated in about 60 % of malignancies (Zheng, Lu *et. al.*, 2000). To date, there has been no direct evidence or studies demonstrating that the exposure to gonadotropins is capable of transforming OSE to malignant phenotype (Landen, Birrer *et. al.*, 2008). Nevertheless, there have been several animal model studies which indicate that gonadotropins promote tumour proliferation (Parrott, Doraiswamy *et. al.*, 2001), angiogenesis (Schiffenbauer, Abramovitch *et. al.*, 1997) and vascular endothelial growth factor (VEGF) expression (Wang, Luo *et. al.*, 2002) as well as *in vitro* studies which demonstrate that the overexpression of FSH and LH is associated with the activation of potential oncogenes (Tashiro, Katabuchi *et. al.*, 2003; Ji, Liu *et. al.*, 2004). These studies suggest the role of gonadotropins in promoting the progression, rather than the cause, of ovarian cancer. This theory, however, does not shed any light as to why invasive carcinomas such as endometrioid and mucinous types are frequently associated with borderline tumours derived from the ovary, while the serous subtype is rarely confined to the ovary and may potentially originate from extra-ovarian sites (Karst and Drapkin, 2010).

1.1.1 Dualistic Model for Ovarian Cancer Carcinogenesis

Based on the above views, a majority of efforts have focused on the ovary for the early detection of ovarian cancer and for the development of new chemotherapeutic drugs and delivery routes, irrespective of their histological subtypes (Kurman and Shih Ie, 2008; Suh, Park *et. al.*, 2010). Unfortunately, these efforts have not been successful in improving the overall survival rates of ovarian cancer over the past 50 years, and thereby the general views regarding the histogenesis, as outlined above, have been regarded as deeply flawed (Levanon, Crum *et. al.*, 2008; Kurman and Shih Ie, 2010). In 2004, a dualistic model of ovarian cancer was proposed by Shih *et. al.*, categorizing the development of ovarian cancer into two groups, designated as Type I and Type II (Shih Ie and Kurman, 2004). This model is largely based on the fact that high grade serous carcinomas differ from all other ovarian tumours in terms of their molecular pathogenesis, genetic alterations, prognosis and morphological characteristics outlined in **Table 2**.

Type	Characteristic Features	Genetic Mutations	References
Type I	<ul style="list-style-type: none"> – Slow growing, clinically indolent tumours – Present a low stage; low proliferation potential – Exhibit shared lineage between benign neoplasms and low-grade carcinomas – Low grade serous, mucinous, endometrioid and clear cell carcinomas – 5-year survival rates of 55 % 	<ul style="list-style-type: none"> – Genetically more stable – Distinctive patterns of high frequency mutations in different histologic cell types – KRAS, BRAF and ERBB2 mutations in majority of low grade ovarian cancers – TP53 mutations are rare 	(Singer, Oldt <i>et. al.</i> , 2003; Shih Ie and Kurman, 2004; Cho and Shih Ie, 2009; Kuo, Guan <i>et. al.</i> , 2009; Shih Ie, Chen <i>et. al.</i> , 2010)
Type II	<ul style="list-style-type: none"> – Highly aggressive tumours with rapid spread throughout pelvic region – Often associated with non-ovarian serous carcinomas arising from the fallopian tube and peritoneum – Bilateral involvement of both ovaries and peritoneal membranes – Exhibit glandular, papillary and solid patterns – Present at advanced FIGO stages III and IV; appear without definitive precursor lesion – High grade serous, endometrioid, malignant mixed mesodermal, undifferentiated carcinomas 	<ul style="list-style-type: none"> – Genetically unstable – High frequency TP53 mutations (> 80 % cases) – Amplification of CCNE1 – Majority of cases are associated with BRCA1 mutations – Predominantly cystic or solid in appearance 	(Shaw, McLaughlin <i>et. al.</i> , 2002; Cho and Shih Ie, 2009; Lynch, Casey <i>et. al.</i> , 2009)

1.1.2 Identifying the Site of Origin of Serous Cancers

1.1.2.1 Role of OSE in Ovarian Cancer

Studies have shown that human OSE cells are composed of uncommitted mesothelial cells that express epithelial and mesenchymal markers such as vimentin and N-cadherin (Blaustein, 1984; Auersperg, Wong *et. al.*, 2001; Drapkin and Hecht, 2002), and do not typically express certain ovarian cancer markers such as E-cadherin, CA125 and HE4 (Maines-Bandiera and Auersperg, 1997; Piek, Dorsman *et. al.*, 2004). The single epithelial layer of the OSE constitutes less than 1 % of the total ovarian mass, and yet, it is thought to be the source of more than 90 % of ovarian cancers which are epithelial in origin. Interestingly, numerous studies on the ovaries have found no precursor lesions in the ovary (Cheng, Liu *et. al.*, 2005; Naora, 2005; Levanon, Crum *et. al.*, 2008; Kurman and Shih Ie, 2010; Li, Fadare *et. al.*, 2012) and there is increasing evidence that a majority of the borderline tumours and low-grade serous ovarian carcinomas arise from cortical inclusion cysts (CICs) embedded within the ovarian parenchyma, under the OSE layer (Levanon, Crum *et. al.*, 2008).

Several studies have examined the epithelium of ovaries obtained as part of risk-reducing bilateral salphingo-oophorectomy (BSO) procedures in high-risk women, but their findings did not establish a consistent relationship between these CICs and high grade serous ovarian carcinomas (Resta, Russo *et. al.*, 1993; Salazar, Godwin *et. al.*, 1996; Werness, Afify *et. al.*, 1999; Casey, Bewtra *et. al.*, 2000; Okamura and Katabuchi, 2001; Piek, Verheijen *et. al.*, 2003; Folkins, Jarboe *et. al.*, 2008). These observations, together with the earlier proposed Type I and II classification of ovarian tumours have led to the suggestion that high grade serous carcinoma is fundamentally different from other ovarian carcinomas. It also became apparent that there is likely to be no single location for all these epithelial ovarian cancers and hence, the search for a precursor lesion for high grade serous cancers has intensified in recent years (Levanon, Crum *et. al.*, 2008; Erickson, Conner *et. al.*, 2013).

1.1.2.2 Emergence of Distal Fallopian Tube as a Site of Serous Carcinogenesis

The fallopian tube has traditionally been viewed as a minor anatomical feature of the female reproductive system and thus, only a limited amount is known regarding its normal cellular biology (Li, Fadare *et. al.*, 2012). The role of the fallopian tube was first implicated in a study investigating serous neoplasia associated with early adenocarcinoma of the fallopian tube, in which tubal intraepithelial carcinomas (TIC) were found in approximately 5 to 10 % of serous ovarian cancer cases. The authors commented on the importance of rigorous sectioning of the fallopian tube to detect for precursor lesions (Bannatyne and Russell, 1981). This observation, together with various published studies looking at TIC incidence, as summarised in **Table 3**, culminated in the proposal that serous TICs (STIC) are almost exclusively detected in the fimbrial region of the fallopian tube, rather than the ovaries and may potentially be the source of serous carcinogenesis in both women with BRCA mutations and those with unknown genetic predisposition for ovarian cancer (Levanon, Crum *et. al.*, 2008; Li, Fadare *et. al.*, 2012).

The delayed appreciation of the role of the distal fallopian tube as the precursor lesion in pelvic serous carcinomas of the ovary, fallopian tube and peritoneum (Levanon, Crum *et. al.*, 2008) was due to a number of reasons. Firstly, a significant proportion of high grade serous carcinomas are present as large ovarian masses, with ovarian cases outnumbering other pelvic serous carcinomas, such as those of the fallopian tube and peritoneum by a 50:1 ratio (Levanon, Crum *et. al.*, 2008). Therefore, it appears reasonable to understand why traditional models of ovarian cancer carcinogenesis were focused mainly on the OSE of the ovaries. Furthermore, it is also widely accepted that customary practices, involving the examination of the entire fallopian tube (including the fimbrial end) in most high grade serous carcinomas by pathologists are not required and are rather limited to the central fallopian tube (Hu, Taymor *et. al.*, 1950). Nevertheless, the identification of putative and possible precursor fallopian tube lesions, together with p53 mutations described in the fallopian tube (Lee, Miron *et. al.*, 2007) provides additional evidence for the concept that serous carcinogenesis could begin in the fallopian tube and not the ovary. It has also been hypothesised that hereditary serous carcinomas could potentially originate from the fallopian tube cells, which in turn, sheds cells onto the surface of the ovary, therefore creating the appearance of an ovarian source of cancer cell origin (Piek, Verheijen *et. al.*, 2003).

Table 3: Clinico-pathological findings of tubal intraepithelial carcinomas (TICs) in BRCA and non-BRCA mutation carriers

Mutation Carriers	Clinico-pathological Findings	Source of Experimental Samples	References
BRCA 1 and/or BRCA 2	Dysplastic changes, also known as tubal lesions in transition (TLIT) which resemble high grade serous carcinomas (HGSC) were identified in fallopian tubes of women who were either a) genetically predisposed to developing ovarian cancer or had BRCA mutations	Prophylactically removed fallopian tubes (n=12)	(Piek, van Diest <i>et. al.</i> , 2001)
	1) Early 'serous' cancerous lesions associated with serous tubal intra-epithelial carcinoma (STIC) of the fimbria end of the distal fallopian tube 2) No precursor lesion observed on ovarian surface epithelium (OSE)	BRCA1/2 mutation carriers with ovarian/fallopian tube cancer (n=7)	(Finch, Shaw <i>et. al.</i> , 2006)
	Increased risk (120-fold) in developing fallopian tube cancers	BRCA1 mutation carriers (n=483)	(Brose, Rebbeck <i>et. al.</i> , 2002)
	1-5 % diagnosed with early tubal cancer were associated with TICs in the distal end of the fallopian tube; patients had a higher risk of developing serous fallopian tube carcinoma, not serous ovarian	Fallopian tubes (n=28)	(Cass, Holschneider <i>et. al.</i> , 2005)
	1) STICs in fallopian tubes and high grade serous cancers are comprised of only secretory cell-type epithelium 2) Secretory cell proliferations are associated with nuclear p53 alterations	Prophylactically removed fallopian tubes (n=41)	(Lee, Miron <i>et. al.</i> , 2007)
	24 % had p53 signatures; 53 % identified in fallopian tubes containing STICs	BSO samples; BRCA mutations (n=41)	(Lee, Miron <i>et. al.</i> , 2007)
	93 % had TP53 mutations in the TICs and corresponding metastasized tumours; hypothesized monoclonal origin for these cancers	Pelvic high-grade serous cancers (HGSCs)(n=29)	(Kuhn, Kurman <i>et. al.</i> , 2012)
	38 % harboured at least one p53 signature in the fallopian tube; One OSE specimen exhibited p53 signatures in ovary	Prophylactically removed fallopian tubes and ovaries (n=75)	(Folkins, Jarboe <i>et. al.</i> , 2008)
Non-BRCA	1) 100 % , 66.7 % and 66.7 % of fallopian tubes derived from tubal, ovarian and peritoneal cancers, respectively, contained areas with STICs 2) 93 % of all TICs located at distal end of tubal fimbriae	Fallopian tube specimens from patients with ovarian (n=30); peritoneal (n=6) and tubal (n=5) cancer	(Kindelberger, Lee <i>et. al.</i> , 2007)
	TICs associated with the development of serous-type histology and not in mucinous or endometrioid histologies	Ovarian (n=37), peritoneal (n=8) and fallopian tube (n=7)	(Przybycin, Kurman <i>et. al.</i> , 2010)
	33 % of patients had p53 signatures; 53 % identified in fallopian tubes containing STICs	BSO samples; non-BRCA mutations (n=58)	(Lee, Miron <i>et. al.</i> , 2007)

n= number of samples examined

1.1.3 Current Model of Serous Carcinogenesis

Based on the above mentioned findings and clinico-pathological observations, a high-grade serous carcinogenesis development model has been recently proposed as shown in **Figure 2** (Li, Fadare *et. al.*, 2012). This model supports the notion that the development of both low and high-grade serous carcinomas is likely to arise from the secretory cell proliferations of the fallopian tube, which acquire DNA damage leading to chromosomal instability and further genetic alterations. In high-grade serous cancers, TP53 mutations occur in the early process of carcinogenesis, and may result in the accumulation of p53 signatures. It is presumed that a subset of p53 signatures undergo specific molecular events which cannot be reversed due to the loss of BRCA functions, eventually transforming to the malignant precursor lesion, serous TIC (STIC). BRCA1 and BRCA2 genes encode nuclear proteins that participate in the DNA repair process via non-homologous recombination (Venkitaraman, 2002). These lesions form papillary tufts on the fimbrial end, which consists of loosely cohesive cells and are easily shed or implanted on the surface of the ovary or peritoneum. Given this scenario, it is possible that, in the absence of serous invasive fallopian tube carcinoma, serous carcinomas of ‘ovarian’ or ‘peritoneal’ origin may develop from the detachment and implantation of these tubal-derived cells. Similarly, serous carcinomas can also be present as fallopian tube cancers or primary peritoneal cancers, if there is no significant involvement of the ovaries. This theory also gives precedence as to why Type II serous tumours often involve the pelvic cavity and spread early on in the carcinogenesis process.

On the other hand, low-grade serous cancers typically develop in a step-wise fashion as well, starting from the tubal epithelial cells which attach to the OSE and invaginate into the ovarian stroma to form ovarian epithelial inclusions (OEI). The acquisition of KRAS, BRAF or ERBB2 gene mutations in the tubal-derived OEIs and possibly other mutations lead to the development of serous borderline tumours and eventually to low-grade serous tumours. In some cases, it is possible for these tubal-derived OEIs to acquire TP53 gene mutations and develop into high-grade serous tumours. This may partially explain why in a significant subset of high grade serous carcinomas, there is no association with STICs in the fallopian tubes, even after extensive examination.

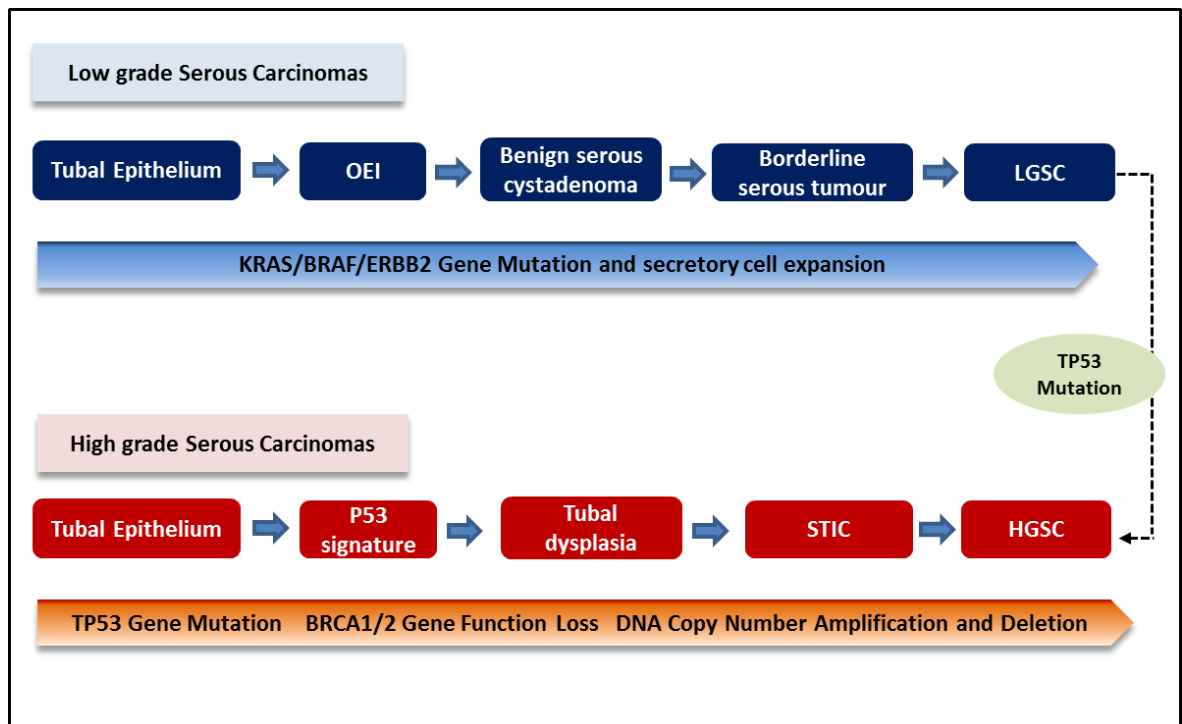


Figure 2: Molecular changes and pathways associated with the development of low and high grade serous carcinogenesis. Low grade serous cancers are characterised by molecular changes including KRAS, BRAF, or ERBB2 mutations and develop from the tubal epithelia to form ovarian epithelial inclusions (OEI). Further growth of OEI results in the step-wise fashion development of serous cystadenoma, serous borderline tumor, and LGSC. In contrast, high-grade serous cancers (HGSC) develop in a different pathway, and are characterised by p53 gene mutation that starts from the tubal epithelia and develop into the latent pre-cancer (p53 signature), tubal dysplasia), early cancer (serous intraepithelial carcinoma, STIC) and HGSC. Reproduced from Li. J. *et al.* (2012)

1.1.4. Molecular Distinction between Serous Pelvic Carcinomas

The histologic distinction between serous carcinomas of the ovary, fallopian tube and peritoneum is quite difficult to achieve especially in cases of advanced disease which often involves more than one site of origin. To date, most studies have used immunohistochemistry profiling to distinguish serous cancers from other subtypes such as endometrioid and mucinous tumours, while very few comparative studies have been performed to distinguish serous cancers of the ovary, peritoneum and fallopian tube (**Table 4**). In addition, apart from serous ovarian cancer, large scale studies of serous peritoneal and tubal cancer groups have been difficult to accomplish due to their rarity of diagnosis. Nevertheless, it has been previously noted that the similarities between serous peritoneal and ovarian cancers do not enable a preoperative distinction between these neoplasms, given their close histological and clinical similarities. In fact several studies have shown that primary peritoneal serous cancers and primary ovarian carcinomas are immunohistochemically indistinguishable (Bloss, Liao *et. al.*, 1993; McCluggage and Wilkinson, 2005), where both cancer serous entities were found to express estrogen receptor (ER), cytokeratin 7 (CK7), Wilm's tumour suppressor gene (WT1), and cancer antigen 125 (CA 125) (von Riedenauer, Janjua *et. al.*, 2007). Studies of clonality have provided further evidence suggesting that primary peritoneal cancers are multifocal in origin, unlike serous ovarian cancers which are clonal in origin (Schorge, Muto *et. al.*, 1998). Taken together, uncovering the potential molecular differences between serous ovarian and peritoneal cancers may be appropriate and could possibly have further implications for their specific diagnosis and treatment options (Jordan, Green *et. al.*, 2008).

Table 4: Comparison of Profiling between SEOC, PPSC and PFTSC					
Category	Immunohistochemistry Marker	High Grade Serous Carcinomas			References
		Serous Epithelial Ovarian Carcinomas (SEOC)	Primary Peritoneal Serous Carcinoma (PPSC)	Primary Fallopian Tube Serous Carcinoma (PFTSC)	
Gene Mutation	P53	+(n=10/22), (n=76/178)	+(n=8/26), (n=6/6)	+(n=26/43), (n=51/63)	(Lacy, Hartmann <i>et. al.</i> , 1995; Rosen, Ausch <i>et. al.</i> , 2000; Halperin, Zehavi <i>et. al.</i> , 2001; Madore, Ren <i>et. al.</i> , 2010; Hou, Liang <i>et. al.</i> , 2012)
Hormone Receptors	Oestrogen	+(n=16/22)	+(n=8/26)		(Halperin, Zehavi <i>et. al.</i> , 2001)
	Progesterone	+(n=20/22)	+(n=12/26)		(Halperin, Zehavi <i>et. al.</i> , 2001)
Growth Factor Receptors	EGFR	+ membrane (n=44/121) + cytoplasm (n=81/121)	+(n=4/6)		(Noske, Schwabe <i>et. al.</i> , 2011; Hou, Liang <i>et. al.</i> , 2012)
	VEGF		+(n=6/6)		(Hou, Liang <i>et. al.</i> , 2012)
Molecular Markers	Ki-67 (cell proliferation marker)	+(n=6/22)	+(n=10/26)		(Halperin, Zehavi <i>et. al.</i> , 2001)
	HER 2/neu	+(n=2/22), (n=4/18)	+(n=10/26), (n=11/32)	+(n=11/43)	(Lacy, Hartmann <i>et. al.</i> , 1995; Chen, Yamada <i>et. al.</i> , 2003)
	Wilm's tumour suppressor protein (WTI)	+(n=124/180)			(Madore, Ren <i>et. al.</i> , 2010)
	Vimentin		+(n=6/6)		(Hou, Liang <i>et. al.</i> , 2012)
Components of wnt signalling pathway	β- catenin	+(n=5/173)	+(n=6/6)		(Madore, Ren <i>et. al.</i> , 2010)
	E-cadherin		+(n=6/6)		(Hou, Liang <i>et. al.</i> , 2012)
	Wnt5a	+(n=30/38)	-(n=0/6)		(Badiglian Filho, Oshima <i>et. al.</i> , 2009)

n= number of samples examined; + positive staining; - negative staining

1.2 Diagnosis, Treatment and Management of Serous Cancers

1.2.1 Diagnosis and Screening of EOC

Epithelial ovarian cancer (EOC) is regarded as a ‘silent killer’, with over 75 % of women being diagnosed at stages III and IV, when the disease has spread beyond the ovary and throughout the abdomen (Ahmed, Wiltshaw *et. al.*, 1996; Jemal, Murray *et. al.*, 2005). This dismaying fact is largely attributed to the lack of early-stage symptoms of ovarian cancer which are often thought to be subtle or absent. In 2000, Goff, *et. al.* developed a ‘symptom index’ which constituted more than 12 episodes of at least one of the following: a) pelvic or abdominal pain, b) urgent need to urinate and increased frequency, c) difficulty while eating or early satiety for less than a year (Goff, Mandel *et. al.*, 2000). Although these symptoms were not formulated as a screening tool, it was envisaged that it would increase awareness both in women and their medical practitioners, thereby resulting in a quicker diagnosis of EOC. To date, there has been no single effective screening test for asymptomatic women, although large population-based screening trials based on CA-125 and transvaginal ultrasound have been carried out recently in USA (Buys, Partridge *et. al.*, 2011) and is currently in progress in UK (Raja, Chopra *et. al.*, 2012). The three general approaches towards the screening and diagnosis of EOC are summarised in **Table 5**.

1.2.2 Treatment Types

For most women with early stage (stage I) ovarian cancers, the standard treatment is usually an operation, known as laparotomy, which allows the surgeon to remove as much of the tumour as possible and to also confirm the diagnosis that has been made. During this surgery, a bilateral salpingo-oophorectomy (removal of ovaries and fallopian tubes), total abdominal hysterectomy (removal of uterus and cervix) and removal of omentum (fat pad surrounding abdominal organs) will be carried out. For a majority of patients (~ 75 %) who are diagnosed with advanced stages of EOC, including serous cancer of the fallopian tube and peritoneum, the standard treatment includes primary cytoreductive surgery, followed by extensive chemotherapeutic regimens (Raja, Chopra *et. al.*, 2012).

Table 5: Screening and Diagnosis of EOC

Detection Methods	Description	Method	Randomised Screening Trials/ Experiment(s)	Clinical Evaluation	References
Transvaginal or Pelvic Sonography ⁺ (TVS)	Imaging technique performed for women with a high risk of developing EOC or after pelvic examination reveal abnormalities	Ultrasound instrument is placed in the vagina, providing detailed images of pelvic structures (eg. size and shape of ovaries)	1) Screening resulted in 326 laparotomies and 5 detected cases of primary ovarian cancers (Total n=5000) 2) Screening and surgery performed on 44 women; 3 cases of ovarian cancer (Total n=3000)	Both methods are not sensitive or specific to be recommended as a general screening procedure	(Campbell, Bhan <i>et. al.</i> , 1989; van Nagell, Higgins <i>et. al.</i> , 1990)
CA125 ⁺	1) Monoclonal antibody recognising soluble form of CA125 in serum 2) Used clinically in ovarian cancer screening, from age 35 onwards or 5-10 yrs earlier than earliest age of EOC diagnosis	Commercially available diagnostic kits that measure serum level of the CA125 antigen	1) Elevated in 85 % of serum of clinically advanced EOC patients 2) Pre-operative serum levels of CA125 < 35U/ml (cut-off point) in 50 % of clinical stage 1 ovarian cancer cases 3) Elevated CA125 levels in benign conditions; endometriosis; ovulation and pregnancy	1) Utilised clinically for detection, diagnosis, monitoring and prognosis. 2) Remains the standard component of routine management of women with advanced ovarian cancer	(Bast, Feeney <i>et. al.</i> , 1981; Ismail, Rotmensch <i>et. al.</i> , 1994; Miller, Deaton <i>et. al.</i> , 1996; Bon, Kenemans <i>et. al.</i> , 1999; van Haaften-Day, Shen <i>et. al.</i> , 2001; Cheng, Wang <i>et. al.</i> , 2002; Blagden and Gabra, 2008)
CA125 and tumour markers	Potential serum/tissue tumour markers: a) HE4 (human epididymis proteins) b) mesothelin c) kallikreins 6,10 and 11 d) M-CSF e) osteopontin f) soluble EGF receptor	CA125 serum marker is used in conjunction with additional tumour markers	1) Tissue microarray on ovarian cancers: a) weak or absent CA125 (n=65) b) kallikrein 6 and 10, osteopontin and claudin-3 (n=296) c) mucin-like glycoprotein (n= 281) d) VEGF (n=239) e) mesothelin (n=100) f) HE4 (n=94) Total: n=296 - <i>Mesothelin and HE4: good specificity when compared with normal tissue</i>	Not currently being used in clinic –currently being investigated in clinical trials	(Rosen, Wang <i>et. al.</i> , 2005)

+ = Detection methods used simultaneously; n= number of prospective patients

1.2.3. Molecular Targeted Therapies in EOC

As a result of the improved understanding of the various molecular pathways in carcinogenesis and tumour growth, many potential therapeutic targets have been identified to be used either in combination with chemotherapy or alone (Salani, Backes *et. al.*, 2009). Some of the drugs that have been trialed and are currently being investigated are highlighted in **Table 6**. These drugs have been developed to block membrane-bound growth receptors, ligands and pathways associated with ovarian cancer. While many of these are aimed specifically to patients with recurrent disease, they are still in the early stages of development with preclinical and clinical trials exploring the use of these molecular agents as first-line therapy for EOC. At present, Bevacizumab, a monoclonal antibody directed towards the VEGF receptor, has shown some promise in ovarian cancer treatment and is thoroughly being investigated. The exploration of therapeutic approaches for the treatment of malignant ascites has also been a clinical priority, with several novel angiogenic and non-angiogenic drug targets identified in recent years (Salani, Backes *et. al.*, 2009). Additional research is also being carried out, focusing on immune-based therapy such as vaccines (Chianese-Bullock, Irvin *et. al.*, 2008) and new monoclonal antibodies (Bookman, Darcy *et. al.*, 2003; Makhija, Amler *et. al.*, 2010) to treat patients with primary or re-current ovarian, peritoneal and fallopian tube cancers.

Table 6: Molecular Targets in Ovarian Cancer Treatment			
Drug	Mechanism of Action	Effect	References
Bevacizumab (Avastin)	mAb against VEGF; inhibits endothelial cell migration, proliferation, differentiation and vascular permeability	Response rate as a single agent: 10-22 %; in combination with cytotoxic agents: 24-78 %	(Monk, Han <i>et al.</i> , 2006; Burger, Sill <i>et al.</i> , 2007; Richardson, Backes <i>et al.</i> , 2008; Wright, Secord <i>et al.</i> , 2008)
Temsirolimus	PK13-mTOR and HIF-1 α inhibition; modulates cell growth and metabolism	Phase II studies show safety and effectiveness in ovarian cancer	(Mabuchi, Altomare <i>et al.</i> , 2007; Campone, Levy <i>et al.</i> , 2009)
Cetuximab (ErbB receptor family)	Chimeric human-murine mAb that binds the EGFR; inhibition of cell proliferation, enhanced apoptosis, reduced angiogenesis, invasiveness and metastasis	Phase II studies of cetuximab combined with carboplatin or carboplatin with paclitaxel did not result in improved PFS	(Konner, Schilder <i>et al.</i> , 2008; Secord, Blessing <i>et al.</i> , 2008)
Gefitinib (ErbB receptor family)	Inhibitor of EGFR signaling	No significant response	(Schilder, Sill <i>et al.</i> , 2005; Posadas, Liel <i>et al.</i> , 2007)
Erlotinib (ErbB receptor family)	Inhibitor of EGFR tyrosine kinase receptor	Phase II study: 6% response rate, no improvement when combined with bevacizumab	(Gordon, Finkler <i>et al.</i> , 2005; Nimeiri, Oza <i>et al.</i> , 2008)
Sorafenib (VEGF receptor family)	Oral multikinase inhibitor; targeting MAPK/ERK signalling pathway; suppression of angiogenesis-inhibition of VEGF 1, 2 and 3.	Partial response 43 % (6 of 13 patients) in combination with bevacizumab	(Azad, Posadas <i>et al.</i> , 2008)
Catumaxomab (Intraperitoneal)	Rat/murine hybrid antibody anti-epithelial cell-adhesion molecule and anti-CD3	Phase I/II dose-escalating (advanced ovarian cancer with recurrent malignant ascites; reduction in ascites; significant elimination of EpCAM tumour cells with acceptable toxicity	(Burges, Wimberger <i>et al.</i> , 2007)
⁹⁰ Y-muHMFG1 (ip.)	MUC1 antibody	Phase III trial comparing standard treatment plus ⁹⁰ Y-muHMFG1; improved survival in patients with highest anti-MUC1 IgG response	(Verheijen, Massuger <i>et al.</i> , 2006; Oei, Sweep <i>et al.</i> , 2008)
PTEN/P13kAKT pathway	Upregulation of the tumor suppressor gene PTEN; inactivation of the PTEN/P13kAKT pathway	Facilitate apoptosis and increase chemosensitivity	(Wu, Cao <i>et al.</i> , 2008)
Vascular disrupting agents	Target tumor vessels; cause tumour death	Phase II studies show no toxicity when combined with carboplatin and paclitaxel	(McKeage, Von Pawel <i>et al.</i> , 2008)

Sourced from Salani R. *et al.* (2009)

1.3 Experimental Models of High Grade Serous Carcinomas

Over the past 10 to 15 years, experimental model systems established to understand the biology of ovarian cancer have evolved significantly and a number of useful models have consistently been used in advanced translational research. A few of these models are described in **Table 7A** and **7B** to demonstrate their utility and feasibility as a research and analytical tool. Cell lines have long been considered important and useful ‘*in vitro*’ models in investigating the molecular events and pathological processes underlying the development of ovarian tumours. Besides that, cell lines have also been used to search for diagnostic and prognostic tumour markers as well as for therapeutic targets (Jacob, Nixdorf *et. al.*, 2014). Recently, the isolation and culturing of non-cancerous fallopian tube non-ciliated epithelium (FTNE) and ovarian epithelial (OCE) cells from the same healthy female has been described (Merritt, Bentink *et. al.*, 2013). This availability of ‘normal’ cells from different origins will enable researchers to clarify the apparent ambiguity in regards to the origin of ovarian cancer and to identify molecular and histological differences, not just between ‘non-cancerous’ and ‘cancerous’ epithelial cells, but also to distinguish ovarian, tubal and peritoneal cancers. Apart from ‘*in vitro*’ models, several other models such as three-dimensional, ‘*ex vivo*’ and ‘*in vivo*’ models of ovarian cancer have also been continually developed to replicate the molecular events that underlie the dissemination of tumour cells from the primary tumour as well as to highlight the contributions of the extracellular matrix (ECM), stromal and inflammatory cells in ovarian cancer (Lengyel, Burdette *et. al.*, 2014).

Table 7A: Development of cellular models in EOC

Models	Source	Significance	Example(s)	References
Ovarian Surface Epithelium (OSE)	Rodent: a) Rat OSE (ROSE) b) Mouse OSE (MOSE)	1) Isolation and transformation of rat OSE (ROSE) using Kirsten murine sarcoma virus (Ki-MSV) 2) Simulation of incessant ovulation for repeated ' <i>in vitro</i> ' passaging of cells; exhibited increased proliferation and tumorigenic properties 3) Transformed cells displayed similar genomic and proliferative patterns observed in ovarian tumours	a) OV3121 b) OV3121-ras4 c) OV3121-ras7 d)p53-def-MOSE	(Adams and Auersperg, 1981; Godwin, Testa <i>et. al.</i> , 1992; Testa, Getts <i>et. al.</i> , 1994; Roby, Taylor <i>et. al.</i> , 2000)
	Human OSE (HOSE)	1) Immortalisation of human-derived HOSE cells achieved via retroviral transduction of either the simian virus 40 T antigen (SV40-Tag) or the human papilloma virus E6/E7 oncogenes 2) Proliferative lifespan increased without tumorigenic properties; stable after many passages	a) HOSE 6.3 b) HOSE 17.1 c) HOSE 105 d) HOSE 129 e) HOSE 130	(Maines-Bandiera, Kruk <i>et. al.</i> , 1992; Tsao, Mok <i>et. al.</i> , 1995; Kusakari, Kariya <i>et. al.</i> , 2003; Jacob, Nixdorf <i>et. al.</i> , 2014)
Fallopian Tube Epithelial Cells (FTEC)	Fresh primary fallopian tube specimen	1) Developed to study neoplastic transformation of normal fallopian tube epithelium; ' <i>ex vivo</i> ' culture system with air-surface liquid interface 2) Preserve natural architecture, orientation, polarity and biological functions displayed by ' <i>in vivo</i> ' FTECs. 3) Long term propagations of cells using hTERT transduction and SV40-Tag sufficient to overcome senescence without inducing tumour formation	a) NT/T-S	(Ando, Kobayashi <i>et. al.</i> , 2000; Levanon, Ng <i>et. al.</i> , 2010; Karst, Levanon <i>et. al.</i> , 2011)
Ovarian Cancer Cell Lines	Tumours: a) Primary tumour b) Metastasised tumours c) Resistant tumours	1) Grown continuously in culture; allow repeated experiments to be performed without the necessary requirements or limitations observed for ' <i>in vivo</i> ' models. 2) Developed for the study of neoplastic transformation and chemotherapy resistance development in tumours	Primary tumour: A2780, IGROV1, ES-2 Metastasised tumours: CAOV-4, EFO27, TO14 Resistant tumours: A2780cis	(Jacob, Nixdorf <i>et. al.</i> , 2014) [ATCC; http://www.Igcstandards-atcc.org]
	Fluid: a) Ascites fluid b) Pleural Fluid	1) Developed for the study of neoplastic transformation and chemotherapy resistance development in tumours	Ascites fluid: SKOV3, OVCAR3, EFO-21, OV-56 Pleural fluid: COV504, PEA1, PEO4	(Jacob, Nixdorf <i>et. al.</i> , 2014) [ATCC; http://www.Igcstandards-atcc.org]

Table 7B: Development of ‘ <i>ex vivo</i> ’ and ‘ <i>in vivo</i> ’ models in EOC				
Models	Source	Significance	Example(s)	References
3D cultures	OvCa cells/primary cells with 3D matrix	1) Cell lines and primary cell lines are grown with different forms of ECM (eg. purified proteins such as collagen, Matrigel) 2) Early events following the cell-matrix contact allow for evaluation of gene expression changes that accompany metastatic anchoring 3) Screening of new drugs that are able to penetrate deep into the hypoxic and acidic region of the 3D culture	Growth factor-reduced Matrigel OvCa model	(Adams and Auersperg, 1981; Mullen, Ritchie <i>et. al.</i> , 1996; Barbolina, Adley <i>et. al.</i> , 2007)
	OvCa spheroids/multicellular aggregates	1)OvCa spheroids (30 to 200um) isolated from patients ascites or produced by growing OVCa cells on non-adherent plate, spinner flasks or hanging-drop culture method 2) Multicellular aggregate formation facilitate metastasis and can adhere to both omentum and exposed ECM 3) Useful for monitoring unique mRNA profiles that resemble <i>in vivo</i> tumours	Cell lines for multicellular aggregate (MCA) formation: DOV13 and OVCA433 cells	(Allen, Porter <i>et. al.</i> , 1987; Gilead and Neeman, 1999; Lin and Chang, 2008)
	Peritoneal and organ explants	1) Dissected peritoneal explants are pinned to optically clear silastic resin and incubated with OvCa cells or multicellular aggregates 2) Explants can be histologically sectioned and used to quantify tumour cell penetration 3)Ability to monitor the extent and kinetics of adhesion, observe early events in peritoneal anchoring and test potential anti-adhesive therapeutics	3D alginate scaffolds of ovarian surface cells, mouse oviducts and baboon fimbria	(Kenny, Kaur <i>et. al.</i> , 2008; Jackson, Inoue <i>et. al.</i> , 2009; King, Quartuccio <i>et. al.</i> , 2011)
Cell Line Xenografts (murine)	Cell lines Ovarian and fallopian tubes from primary ovarian tumors	1) Developed to recapitulate tumor heterogeneity with recruitment of host stromal cells and maintenance of both tumor stroma and tumor/non-tumor vasculature interactions 2) Most OvCa cell lines can be transfected or transduced to express fluorescent or bioluminescent vectors to enable longitudinal optical imaging of tumor growth	Serous-type cancers: OvCa (OVCAR3, SKOV3, PEO23 etc.) Clear cell –type cancers (ES-2, TOV-21G) Primary and fallopian tube cells	(Hua, Christianson <i>et. al.</i> , 1995; Miyajima, Nakano <i>et. al.</i> , 1995; Provencher, Lounis <i>et. al.</i> , 2000; Hu, Hofmann <i>et. al.</i> , 2005)
Genetically engineered mouse models (GEMM)	a) Ovarian surface epithelium, fallopian tube	1) Genes (p53, RB, Myc, Akt, Pten) are expressed or deleted specifically in the ovary and fallopian tube to evaluate the physiological relevance of defined genetic changes 2) These preclinical models are useful to study drug resistance and for discovery of serum biomarkers	Transgenic mice infected with a) OSE cells (p53-depleted with presence of oncogenes) and b) targeted deletion of BRCA1/2	(Orsulic, Li <i>et. al.</i> , 2002; Chodankar, Kwang <i>et. al.</i> , 2005)

1.4 Overview of Section I: Highlights and Challenges in EOC

- Serous cancers comprise a group of pelvic cancers of the ovary, primary peritoneal and fallopian tube cancers.
- For all three serous epithelial cancers, their specific diagnosis can only be ascertained based on surgical staging and examination by pathologists based on the recommended FIGO guidelines.
- Misclassification of serous tumours based on their origin (ovarian, peritoneal or tubal) often occurs when the primary site of cancer is unknown.
- Serous cancers of the ovary, peritoneum and tube are treated identically, namely with maximal cytoreductive surgery and platinum-based chemotherapy.
- The identification of the secretory epithelium cells of the fallopian tube has emerged as a potential source for some of these serous cancers; leading to important implications for future differential detection, treatment and prevention.
- Early, non-invasive markers to detect tubal intraepithelial carcinoma (TICs) of the fallopian tube are relatively unknown and are dependent on tubal tissue specimens obtained from bilateral-salpingo oophorectomy (BSO) procedures.
- Patients with molecular alterations in p53, BRCA 1 and BRCA 2 are susceptible to all three serous cancers.
- The expression of CA125, the most extensively studied serum marker for ovarian cancer, is not sensitive or specific enough to be used alone as an early detection marker.
- Most of the research so far has been carried out using BSO specimens and commercially available ovarian cancer cell lines with a major focus on ovarian carcinogenesis.

1.5 Glycosylation in Cancer

Aberrant glycosylation has been well documented in essentially all types of experimental and human cancer for over 35 years, in which many glycosylated epitopes constitute tumour-associated cancer antigens (TACAs) which play key roles in the development and progression of cancers (Hakomori, 1984). TACAs are differentially expressed by tumour and non-tumour cells and are involved in key pathophysiological processes during the various steps of tumour progression such as tumour growth, cell signalling, cell migration, invasion, metastasis, angiogenesis, and evasion of innate immunity (Hakomori, 1989; Hakomori, 1991; Fuster and Esko, 2005; Ghazarian, Itoni *et. al.*, 2011). These glycosylated structures have also been studied extensively for the use as specific tumour biomarkers and potential therapeutic targets (Hakomori, 1989; Pochechueva, Jacob *et. al.*, 2012). Despite the long-standing argument of whether aberrant glycosylation is a cause or consequence of carcinogenesis, many studies have indicated that in most cases this phenomenon is the result of initial oncogenic transformation and is a key event in the induction of tumour invasion and metastasis.

The mechanisms in which glycosylation promotes or inhibits tumour invasion and metastasis represent a crucial aspect in cancer research and to date, this area of study is less understood and has indeed, received very little attention from most cell biologists involved in cancer research (Hakomori, 2002; Pochechueva, Jacob *et. al.*, 2012). This is largely due to complexities in the structural and functional concepts of glycosylation in cancer as opposed to the more well-defined functional roles of certain genes and proteins that govern the majority of the cancer cell phenotypes and the molecular events associated with apoptosis (Hiraishi, Suzuki *et. al.*, 1993; Kakugawa, Wada *et. al.*, 2002), motility (Zeng, Gao *et. al.*, 2000), cell signalling (Zheng, Fang *et. al.*, 1994; Isaji, Sato *et. al.*, 2006), angiogenesis (Saito, Miyoshi *et. al.*, 2002) and many more. The major roles of glycosylation in regards to the aberrant expression of glycan structures and their implication in the promotion or inhibition of tumour progression is highlighted in **Figure 3**.

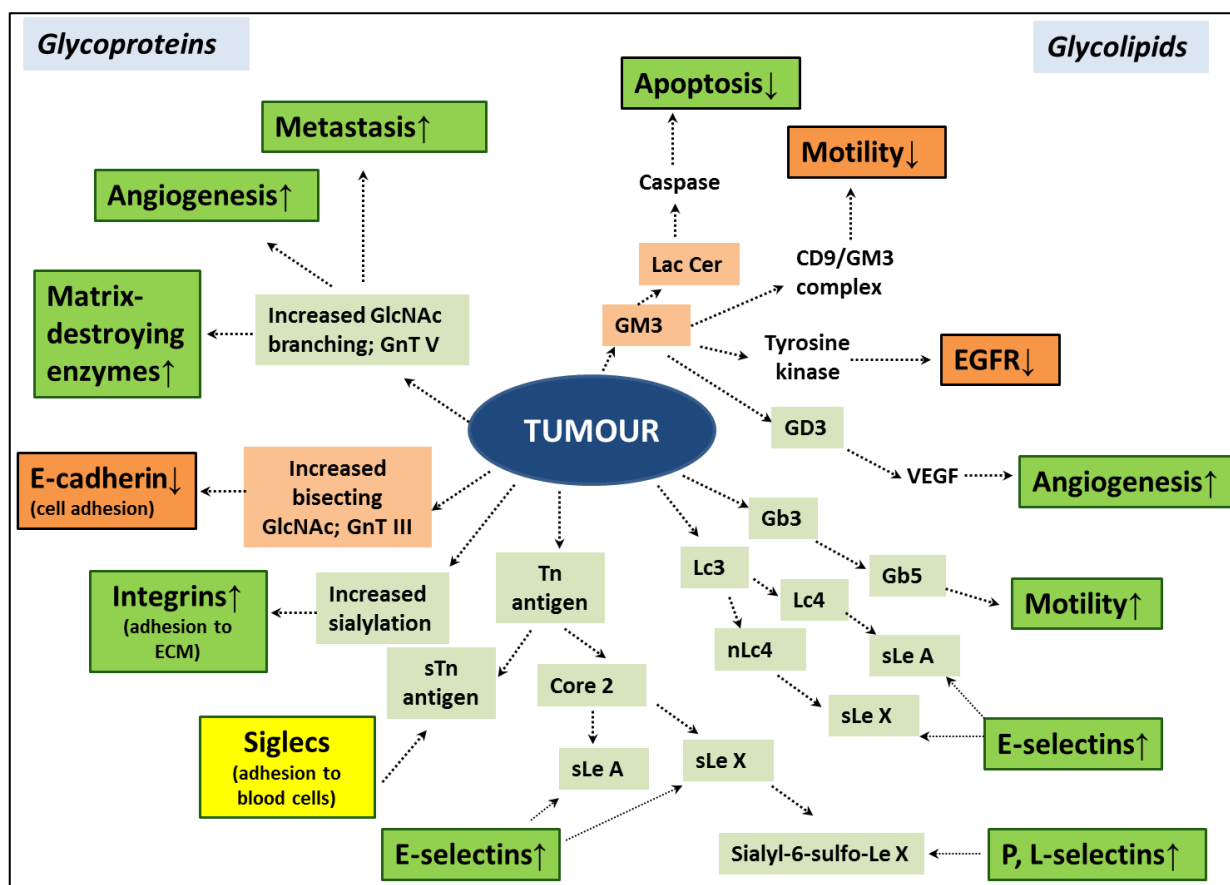


Figure 3: The known involvement of glycoprotein *N*-glycans (GlcNAc branching, bisecting GlcNAc, sialylation), *O*-glycans (Tn, sTn, Core 2, sLeA, sLeX, Sialyl-6-sulfo-LeX) and glycolipids (LacCer, Lc3, Lc4, nLc4, GD3, GM3, Gb5) in various processes in cancer. Cancer is defined by several key phenotypes: apoptosis, motility, angiogenesis, EGF receptor tyrosine kinase, matriptase (matrix-destroying enzyme) activity, self-adhesion (through cadherin), adhesion to ECs and platelets (through E-, L-or P-selectin), adhesion to ECM (through integrin), adhesion to blood cells (through siglecs). The consequence of the expression of different glycosylation features (light orange and light green boxes) in cancer and their corresponding regulation of each phenotype (↑, ↓) as are indicated. Phenotypes displaying ↑ or ↓ in orange boxes inhibit tumour invasiveness, while green boxes promote invasiveness. Yellow coloured box appear to have variable or unclear effect on tumour invasiveness. Figure revised and reproduced from Hakomori, S. (2002).

1.5.1 Glycosylation in EOC

Cellular glycosylation changes, which give rise to the expression of tumour-associated glycans in ovarian cancer have also been investigated using several approaches such as immunohistochemistry and lectins, in which the differential expression of carbohydrate antigens between normal tissue and ovarian cancer tissue (Dietel, 1983; Ryuko, Iwanari *et. al.*, 1993; Tashiro, Yonezawa *et. al.*, 1994) as well as between tumour histotypes (Federici, Kudryashov *et. al.*, 1999; Abbott, Nairn *et. al.*, 2008; Abbott, Lim *et. al.*, 2010) have been observed. In addition, significant technological advancements in mass spectrometry-based glycomics over the past few years have also led to the discovery and identification of specific glycan profiles on serum and secreted glycoproteins, particularly implicating increased branching, core fucosylation and sialylation (Kui Wong, Easton *et. al.*, 2003; Saldova, Royle *et. al.*, 2007; Biskup, Braicu *et. al.*, 2013; Kim, Ruhaak *et. al.*, 2014).

The majority of studies investigating glycosylation changes at a cellular level have been carried out using established ovarian cancer cell lines. Although cell lines do not provide an ideal representation of tumour micro- and macro-heterogeneity, substantial changes pertaining to malignant characteristics can be investigated in order to identify relevant glycan expression patterns. For instance, glycoproteins with terminal α 2-6-linked sialic acids have been detected using *Sambucus nigra* (SNA-1) lectin in a number of ovarian cancer cell lines (Escreveente, Machado *et. al.*, 2006) while another lectin-based study indicated that α 2-6 sialylation of β 1 integrin, a membrane-associated glycoprotein, confers a more metastatic phenotype through its increased adhesion to, and migration on, collagen I (Christie, Shaikh *et. al.*, 2008). Apart from sialylation, high-mannose type N-glycans derived from glycoproteins of SKOV 3 and OVCAR 3 ovarian cancer cell lines, including the well-known ovarian cancer biomarker, CA125 (Kui Wong, Easton *et. al.*, 2003; Machado, Kandzia *et. al.*, 2011) have been identified. Thomas *et. al.* and co-workers also recently developed a monoclonal antibody, TM10, which was shown to have specificity towards high mannose N-glycans on glycoproteins derived from a range of ovarian cancer cells (Newsom-Davis, Wang *et. al.*, 2009). This antibody however, was not tested on non-cancerous cells. Other less investigated N-glycan motifs such as core fucosylation and LacdiNAc-type were also reported on the glycoproteins of SKOV 3 cells, while bisecting-type N-glycans were found to be up-regulated on the CA125 glycoprotein (Kui Wong, Easton *et. al.*, 2003).

Tumour-specific glycan changes have also been observed on a number of cellular glycoproteins which have led to the identification of novel ovarian cancer biomarkers. In one particular targeted glycoproteomic study by Abbott *et. al.*, the differential binding of lectins specific for bisecting type and core fucosylated *N*-glycan structures were observed on epithelial endometrioid ovarian cancer tumours as compared to the normal ovarian tissue. The authors also validated this study by screening for glycoproteins bearing these specific glycan changes in the serum of ovarian cancer patients and confirmed the utility of these glycans in distinguishing patients' serum from normal serum (Abbott, Lim *et. al.*, 2010). In regards to alterations in *O*-glycosylation, a few studies have observed the increased expression of T_n and sialyl-T_n antigens in a range of malignant serous, endometrioid and mucinous ovarian tumours as compared to borderline tumours when examined immunohistochemically using newly developed antibodies (Inoue, Ton *et. al.*, 1991; Ogawa, Ghazizadeh *et. al.*, 1996). In all of the tissues examined, there was no expression of precursor T_n antigen without the presence of sialyl-T_n, thereby leading the authors to conclude that the accumulation of sialyl-T_n antigen is an early, pre-cancerous indicator of carcinogenesis of the ovary, providing additional prognostic information on patient outcomes. Likewise, the Lewis family antigens (Type 1 and Type 2 terminal structures, e.g., Lewis a/b and Lewis x/y antigens, respectively) was demonstrated in several studies of ovarian carcinomas (Tashiro, Yonezawa *et. al.*, 1994; Yin, Finstad *et. al.*, 1996). As part of this thesis, a publication that reviews the membrane glycosylation changes in epithelial ovarian cancer, in comparison to other cancers of the liver, breast, colon and melanoma has been recently published (**Section 1.8.1**).

1.5.1.1 Detection of Anti-glycan Auto-antibodies in Serum of EOC Patients

In ovarian cancer, the biological potential of altered glycosylation has been shown to be reflected by tumour-associated cancer carbohydrate antigens which are recognised by binding auto-antibodies in the serum. In a recent study by Jacob *et. al.* (2012), the authors characterised and evaluated the diagnostic potential of serum-based antibody recognition of carbohydrate antigens in ovarian cancer patients versus healthy controls using standardised printed glycan arrays (Jacob, Goldstein *et. al.*, 2012). Interestingly, serum antibodies directed at the P₁ antigen trisaccharide (Gal α 1-4Gal β 1-4GlcNAc β) were identified as a potential candidate biomarker for various ovarian cancer subtypes of ovarian origin, excluding the non-mucinous subtype, while a combinatory panel of six glycans comprising of biological and non-biological motifs such as Gal α 1-4Gal β 1-4GlcNAc β (P₁), Neu5Ac α 2-3Gal β 1-4-(6-Su)GlcNAc β , Neu5-Ac β 2-6GalNAc α , Neu5Ac β 2-6Gal β 1-4GlcNAc β , Neu5Ac α 2-3Gal β 1-3-(6-Su)GalNAc α and Gal β 1-4GlcNAc β 1-6Gal β 1-4GlcNAc β were found to generate a high discriminatory potential between the non-cancer and cancerous serum samples. It was hypothesised that the binding of the anti-glycan auto-antibodies may be directed towards the cell surface carbohydrate antigens which have become exposed to the antibodies during oncogenic transformation of cells and remodelling of extracellular matrices (Jacob, Goldstein *et. al.*, 2012). The structural glycan motifs identified in this serum-based study, however, have never, until now, been detected in cell lines or clinical tissue samples. Nevertheless, the realisation that specific glycan motifs could potentially be utilised for both diagnostic or therapeutic purposes, point to the critical need for structurally characterising membrane glycosylation changes in ovarian cancer, especially in the context of representative, clinically-derived samples.

1.6 Historical Overview of Glycobiology

As compared to other major classes of biomolecules such as DNA and proteins, carbohydrates have been primarily investigated as a source of energy and structural material that lacked any significant biological activities (Sharon, 1980). However, in the late 1980's, the development of new methodologies for the study of glycans paved the way for a new frontier of molecular biology, known as glycobiology, which combines traditional disciplines of carbohydrate chemistry with the modern understanding of cellular glycans (Rademacher, Parekh *et. al.*, 1988; Cabezas, 1994). The term 'glycobiology' encompasses the study of the structure, biology, biosynthesis and saccharides (glycans) that are present in nature and the proteins that recognize them. To date, it has become one of the most rapidly growing areas of research in the natural sciences, with a widespread significance in basic research, biomedicine, and biotechnology. More specifically, this field includes the study of chemistry of carbohydrates, enzymology, glycan recognition by proteins, glycan roles in complex biological systems and analytical techniques to unravel their structures (Sharon and Lis, 1993; Marino, Bones *et. al.*, 2010; Freire-de-Lima, 2014).

1.6.1 *N*- and *O*- Glycosylation

The term 'glycosylation' refers to the attachment of carbohydrate residues (glycans) to the aglycone (non-carbohydrate entity), forming a dense glycocalyx which covers all cell surfaces (Spiro, 2002; Lanctot, Gage *et. al.*, 2007) (**Figure 4**). Glycosylation is perhaps one of the most frequently observed and structurally diverse forms of post-translational protein modification, with over 50 % of proteins estimated as being substituted with glycans at several attachment sites (Apweiler, Hermjakob *et. al.*, 1999). Unlike the syntheses of other macromolecules such as proteins and nucleic acids which are well-defined and template-driven, the biosynthetic pathway of glycosylation is a complex event that is well coordinated by different repertoires of glycosyltransferases and glycosidases within the ER and Golgi apparatus of each cell (Spiro, 2002). Glycan structures are remarkably diverse as these cyclic residues can be linked through many different carbon positions to another monosaccharide ring structure, thus forming various branched or linear oligosaccharide structures (Varki, 2009). Glycans expressed on cell surfaces are the first to be encountered by neighbouring cells, thus mediating interactions between cells as well as the extracellular matrix (Crocker and Feizi, 1996; Solis, Jimenez-Barbero *et. al.*, 2001).

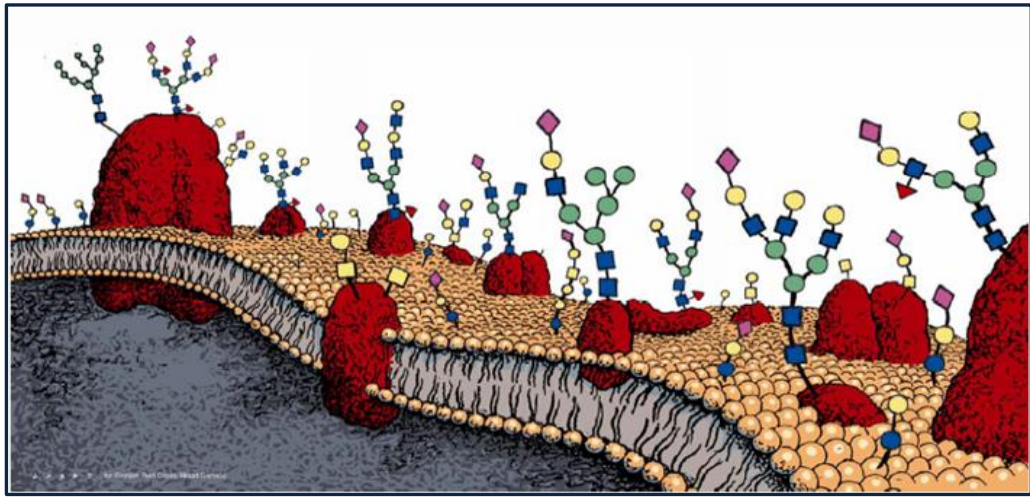


Figure 4: Glycosylation on the cell membrane. Sourced from Valmu, L. (2009)

Furthermore, these glycan chains can also significantly alter protein folding and conformation, which may in turn, modulate the function of a protein and their interactions with other proteins (Dwek, 1996). The final structure of the glycan is also dependent on the polypeptide backbone and a number of variable factors such as enzyme availability (glycosidases, glycosyltransferases) and substrate levels, which may change in a cell during growth, differentiation and development (Roth, 2002; Spiro, 2002). On eukaryotic cells, the common classes of glycans are defined according to the nature of the linkage to the respective aglycone. For instance, a glycoprotein is a glycoconjugate, in which the protein contains one or more glycan chains that are covalently attached via *N*- or *O*-linkages to the polypeptide backbone. *N*- and *O*-glycosylation represent the two major type of protein glycosylation as described below:

a) N-linked glycosylation (N-glycans)

N-linked glycosylation of proteins involves the covalent attachment of a glycan, linked via an *N*-glycosidic bond, to the amide group of the asparagine (Asn) residue within the amino acid sequence, Asn-X-Ser/Thr, where X can be any amino acid except proline (Pro). It is estimated that approximately 65% of the potential glycosylation sequons are occupied in proteins, in which 70% are of the Asn-X-Thr sequeon (Petrescu, Milac *et. al.*, 2004). Five different *N*-glycan linkages have been identified, of which the *N*-acetylglucosamine that is β -glycosidically to asparagine (GlcNAc β 1-Asn) is the most common (Stanley, Schachter *et. al.*, 2009). Other less common linkages to the Asn residue that have been described include glucose to Asn in laminin of mammals and Archaea, *N*-acetylgalactosamine (GalNAc) to asparagine in Archaea, glucose to Arg in sweet corn glycoprotein and rhamnose to Asn in bacteria. All GlcNAc reducing terminus *N*-glycans share a common pentasaccharide core

sequence, $\text{Man}\alpha 1-6(\text{Man}\alpha 1-3)\text{Man}\beta 1-4\text{GlcNAc}\beta 1-4\text{GlcNAc}\beta 1$, and are classified into three main classes: a) oligomannosidic glycans containing only mannose residues attached to the core, b) complex-type glycans, consisting of an “antennae” initiated by *N*-acetylglucosaminyltransferases (GlcNAcTs) attached to the core and c) hybrid glycans with mannose residues attached to the $\text{Man}\alpha 1-6$ arm of the core and GlcNAc initiated antennae on the $\text{Man}\alpha 1-3$ arm (Stanley, Schachter *et. al.*, 2009).

b) O-linked glycosylation (O-glycans)

O-linked glycosylation refers to the attachment of the glycan that is α -glycosidically linked via *N*-acetylgalactosamine (GalNAc) to the hydroxyl group of serine or threonine residues (Hanisch, 2001). Although these glycans do not share a common core structure such as *N*-glycans, they comprise of a number of different structural core classes. There are four main common *O*- glycan core structures, designated as Core 1 to Core 4 and the additional less commonly found types known as Core 5 to Core 8 (Brockhausen, Schachter *et. al.*, 2009). Mucin-type *O*-glycosylation represents the most common form in mammals, in which large mucinous glycoproteins are heavily *O*-glycosylated, ranging from single glycan chains to hundreds of large, branched glycans. Mucins, produced by the epithelial cells of salivary glands and mucous membranes are found primarily in mucous secretions and as transmembrane proteins of the cell surface (Tabak, 1995). There are also many other types of non-mucin *O*-glycans which include the α -linked *O*-mannose, α -linked *O*-fucose, β -linked *O*-xylose and β -linked *O*-GlcNAc (Hansen, Lund *et. al.*, 1996).

1.6.1.1 Synthesis of *N*-glycans in Eukaryotes

The *N*-linked glycosylation of proteins at the consensus sequence Asn-X-Ser/Thr is a co-translational event which occurs during protein synthesis. The biosynthesis of *N*-glycans is initiated on the cytoplasmic face of the endoplasmic reticulum (ER) membrane (**Figure 5**), in which the GlcNAc-P from UDP-GlcNAc is transferred to the membrane-bound lipid-like precursor dolichol phosphate (Dol-P), forming dolichol pyrophosphate *N*-acetylglucosamine (Dol-P-P-GlcNAc) (Kornfeld and Kornfeld, 1985; Schwarz and Aebi, 2011). This step is catalyzed by a specific enzyme, GlcNAc-1-phosphotransferase, that transfers the sugar linked to a phosphate (GlcNAc-1-P) from UDP-GlcNAc. Next, the other GlcNAc residue and five Man residues are subsequently transferred to form the Man₅GlcNAc₂-P-P-Dol precursor which translocates across the ER membrane, mediated by an enzyme known as ‘flippase’. The assembly of the mature *N*-glycan lipid-linked oligosaccharide precursor, Glc₃Man₉GlcNAc₂-P-P-Dol, is carried out in a sequential manner, through the addition of other glycan residues donated by Dol-P-Glc and Dol-P-Man. The entire synthesis of this 14-sugar *N*-glycan precursor is mediated by the action of glycosyltransferases in the asparagine-linked glycan (ALG) pathway. Once completed, the ‘*en bloc*’ transfer of this glycan precursor to a conserved Asn-X-Ser/Thr sequon of a folded protein is catalysed by the oligosaccharidetransferase complex (OST) (Schwarz and Aebi, 2011).

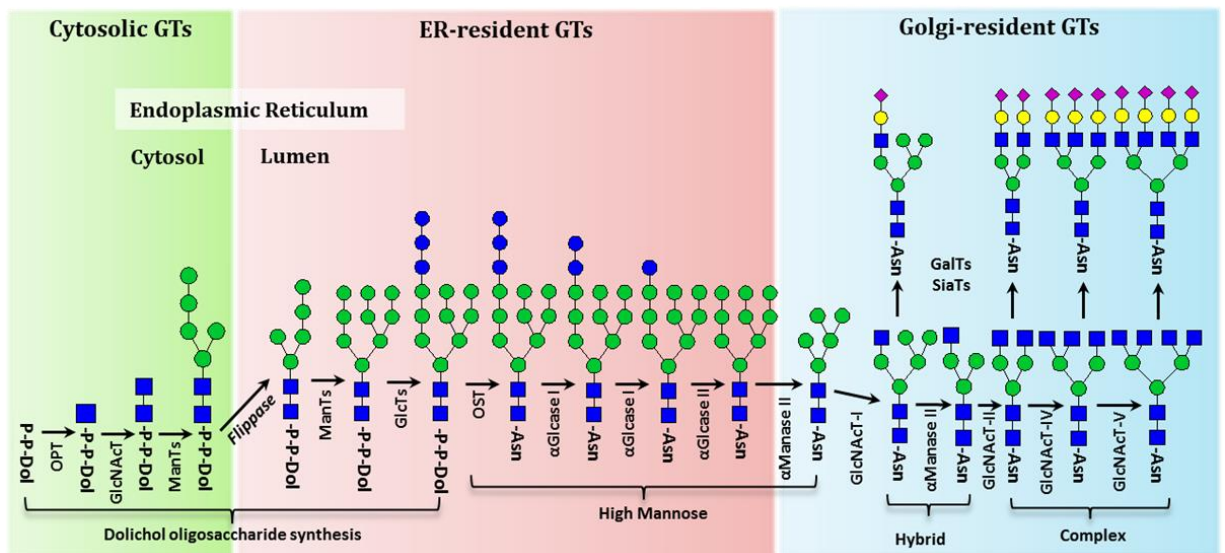


Figure 5: *N*-glycan biosynthesis pathway. Reproduced and revised from Ernst and Magnani (2009) and Schnaar R. L. *et. al.* (2008)

In the ER, the transferred, protein-bound *N*-glycan undergoes several processing steps which include the trimming of glucose and mannose residues at the non-reducing end by specific glycosidases (Taylor and Drickamer, 2006). Specifically, the α 1-2 linked glucose residue and the remaining two α 1-3 linked glucoses are trimmed by the enzyme, glucosidase I and II, respectively which reside in the lumen of the ER. In some cases, the removal of glucose residues may be inhibited by glucosidase I inhibitors, and the glycoproteins are partially trimmed by the ER α -mannosidase I, which removes terminal α 1-2Man residues, resulting in Glc₃Man₇₋₉GlcNAc₂ structures on mature glycoproteins. The majority of the glycoproteins, however, exit the ER with eight or nine Man residues and the trimming process of α 1-2Man residues resumes in the Golgi through the action of α 1-2 mannosidases, giving rise to the Man₅GlcNAc₂ intermediate. While this glycan intermediate is key to the formation of hybrid and complex-type glycans, not all glycoproteins are fully processed to Man₅GlcNAc₂ and these incompletely processed glycoproteins will carry *N*-glycans bearing Man₅₋₉ GlcNAc₂, also known as high mannose-type glycans (Stanley, Schachter *et. al.*, 2009).

Further processing takes place in the medial-Golgi after the de-mannosylation process, in which the *N*-acetylglucosaminyltransferase, GlcNAcT-I, adds an *N*-acetyl-glucosamine residue to the C2 of the α 1-3 mannose arm of the core Man₅GlcNAc₂ (Schachter, 2000). Once this transfer has been catalysed, subsequent processing by α -mannosidase II, another resident of the medial-Golgi is carried out to remove the remaining terminal Man residues, forming GlcNAcMan₃GlcNAc₂. The second *N*-acetylglucosamine is added to C-2 of the α 1-6-linked mannose arm by the action of GlcNAcT-II to yield the common precursor for biantennary, complex *N*-glycans. In the event that α -mannosidase II fails to trim GlcNAcMan₅GlcNAc₂, the peripheral α 1-3Man and α 1-6Man residues remain intact and hybrid glycan are formed. The complex *N*-glycans can be further extended, in which additional branches (antennae) can be initiated at the C-4 of the α 1-3 linked mannose arm by GlcNAcT-IV and C-6 of the α 1-6-linked mannose arm by GlcNAcT-V, yielding tri- and tetra-antennary *N*-glycans. Highly branched *N*-glycans can also be generated by the action of enzymes, GlcNAcT-VI, GlcNAcT-IX or GlcNAcT-Vb (Lau, Partridge *et. al.*, 2007). These branched structures are typically extended by galactose residues which are further capped by the transfer of sialic acids at the terminal non-reducing end (**Figure 6**). The core mannose can also be modified by another enzyme, GlcNAcT-III, which transfers *N*-acetylglucosamine to the β -linked mannose to generate the bisecting-type *N*-glycans. Similarly, the reducing-end GlcNAc can also be modified by a fucose residue to form core fucosylated *N*-glycans, a common modification observed in humans. Terminal fucosylation is

another common modification, in which fucose is linked to either the galactose (Gal) or *N*-acetyl-glucosamine (GlcNAc) residues of the antennae to form Lewis or blood group antigens (**Figure 6**). The addition of galactose, fucose and sialic acid residues are carried out sequentially by the action of respective galactosyltransferases, fucosyltransferases and sialyltransferases located in the Golgi. As a result of these extensions and modifications of the *N*-glycans, the final structure of the *N*-glycan can vary in different cells and tissues, leading to their structural diversity and complexity (Ohtsubo and Marth, 2006; Blixt and Razi, 2008).

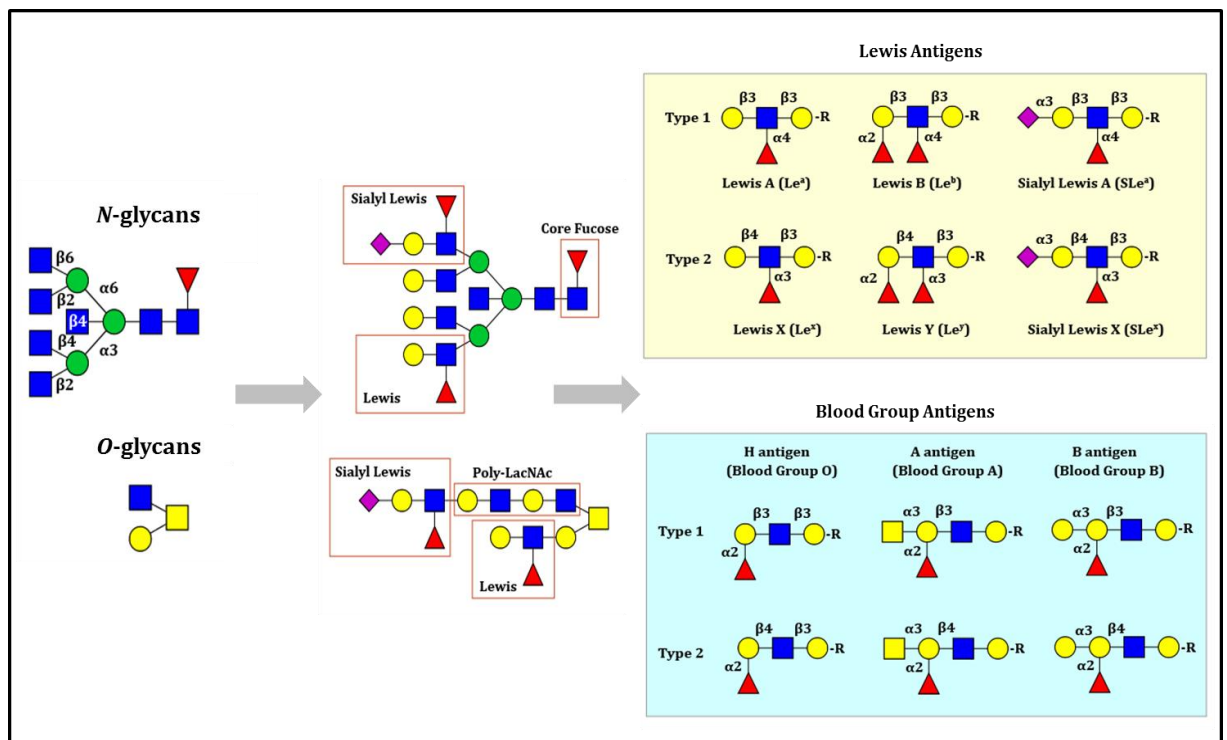


Figure 6: Common extensions/modifications in *N*- and *O*-glycans. Revised and reproduced from Varki, A. *et al.* (2009)

1.6.1.2 Synthesis of *O*-glycans in Eukaryotes

O-glycans typically contain between 1-20 monosaccharide residues, in which the simplest mucin *O*-glycan has a single *N*-acetylgalactosamine (GalNAc) residue linked to a serine or threonine, also known as the T_n antigen (Hanisch, 2001) (**Figure 7**). The most common *O*-glycan, however, is the Galβ1-3GalNAc disaccharide, found in many mucins and glycoproteins. It is also termed as Core 1 or T antigen and it forms the basic core structure for many longer and more complex *O*-glycans. Both T_n and T antigens, as their names suggest, are antigenic glycans and they may be modified by the addition of sialic acid, to form sialyl-T_n or sialyl-T antigens (Brockhausen, Schachter *et. al.*, 2009). The Core 1 *O*-glycan is further extended by the addition of the branching β1-6 *N*-acetylglucosamine (GlcNAc), to form another common core structure, Core 2, which is found in a variety of cells and tissues. Core 2 structures are also typically extended by repeating lactosamine units (Galβ1-4GlcNAc) which are further modified by fucose and sialic acid residues (Maemura and Fukuda, 1992; Tarp and Clausen, 2008). The linear Core 3 *O*-glycan is formed when a β1-3 *N*-acetylglucosamine is linked to the single GalNAc residue and this structure is converted to Core 4 *O*-glycan by the addition of β1-6 *N*-acetylglucosamine *via* the action of β1-6 *N*-acetylglucosaminyltransferase (Vavasseur, Yang *et. al.*, 1995; Iwai, Inaba *et. al.*, 2002). The expression of these structures is restricted to the salivary glands, intestinal and respiratory tracts and has been found only in secreted mucins. The least common core structures, Core 5 to Core 8 *O*-glycans are extremely restricted in their occurrence and the enzymes synthesising these structures have yet to be characterised (Brockhausen, Schachter *et. al.*, 2009). Nevertheless, they have been previously found in colonic and intestinal adenocarcinoma tissue, human intestinal and ovarian cyst, breast cancer tissues and human respiratory mucins (Hollingsworth and Swanson, 2004; Brockhausen, 2006). Many of the terminal structures of *O*-glycans are antigenic and have lectin binding sites, comprising of fucosylated, sialylated or sulphated motifs or polylactosamine repeating units.

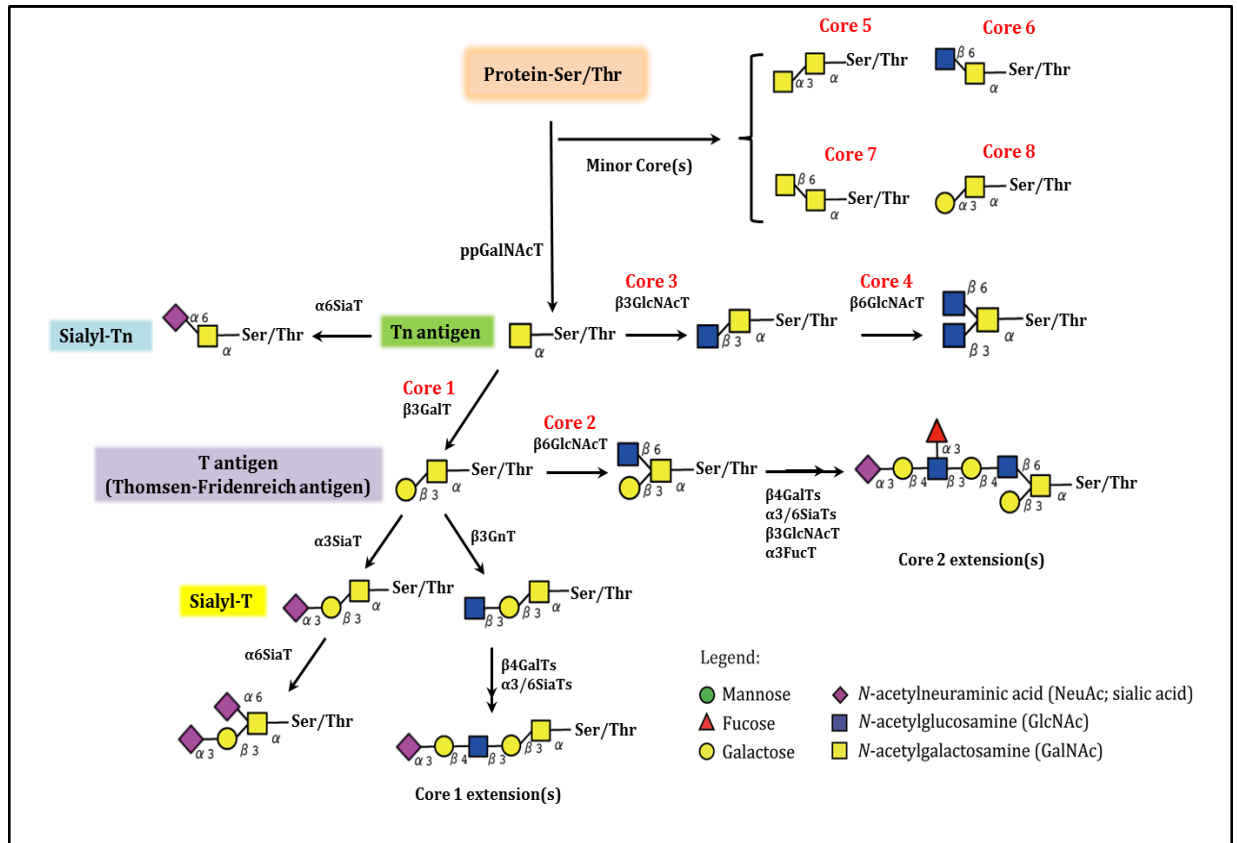


Figure 7: O-glycan biosynthesis pathway. Modified and adapted from Nakayama, Y. *et. al.* (2013)

1.6.2 Synthesis of Glycolipids in Eukaryotes

A majority of glycolipids in vertebrates are composed of glycosphingolipids (GSLs), a large and heterogeneous family of amphipathic lipids that are anchored to the cell membranes (Maccioni, Giraudo *et. al.*, 2002). The common lipid component of GSLs, ceramide, is composed of an amide-linked fatty acid and a long-chain amino alcohol (sphingosine) which vary in length, hydroxylation and saturation, thereby giving rise to a structural diversity of lipids (Farwanah and Kolter, 2012). Nevertheless, the major structural and functional classifications of GSLs have traditionally been based on the glycan portions of the glycolipid which contain more than ten monosaccharide units which differ in terms of their structure, linkage and composition. Despite the diverse glycoforms, most organisms express only a limited set of GSL core structures, also known as the GSL series, which share common carbohydrate sequences. The first monosaccharide residues linked to the 1-hydroxyl group of ceramides are typically β -linked galactose or glucose which forms GalCer and GlcCer, respectively (Chester, 1998). GalCer glycolipids and the sulfatide analogue (with sulfate residue on C-3 hydroxyl of galactose) represent the most abundant glycans in the brain, where they are implicated in the structural and functional roles of myelin. Interestingly, a sialylated form of GalCer (NeuAc α 2-3Gal β Cer), also known as GM4, has also shown to be associated with myelin. These GalCer glycolipids are rarely extended to form larger glycan chains as compared to members of the diverse and large GlcCer family of glycosphingolipids found in higher animals (Schnaar, Suzuki *et. al.*, 2009). In complex vertebrates, the C-4 hydroxyl of the glucose residue in GlcCer is substituted with the β -linked galactose, to form a lactosylceramide (Gal β 1-4Glc β Cer) (Hakomori, 2003). Additional glycans are then added to this moiety to generate a series of neutral 'core' structures that form the basis of glycosphingolipid nomenclature as shown in **Figure 8**.

The ganglio-series glycosphingolipids (gangliosides), are sialic acid-containing glycans which are formed by NeuAc:lactosylceramide α 2-3 sialyltransferase which catalyses the transfer of sialic acid to the lactosylceramide (Gal β 1-4Glc β Cer) to make the simple ganglioside, GM3. GM3 acts as the acceptor for UDP-GalNAc β 1-4 N-acetylgalactosaminyltransferase to subsequently generate larger gangliosides. The widely used nomenclature by Svennerholm has been used for gangliosides (Svennerholm, 1964). In this nomenclature, gangliosides are commonly known as GM1, GM2 or GM3, in which the first letter G refers to ganglioside series, the second letter refers to the number of sialic acid residues ('A'=0, 'M'=1, 'D'=2, etc), and the number (1, 2, 3, etc.) refers to the order of migration of the ganglioside based on thin-layer chromatography (e.g., GM3 > GM2 >

GM1). Apart from the ganglio-series, the globo and isoglobo-series have the lactosylceramide extended by galactose to form $\text{Gal}\alpha 1-4\text{Gal}\beta 1-4\text{Glc}\beta\text{Cer}$ and $\text{Gal}\alpha 1-3\text{Gal}\beta 1-4\text{Glc}\beta\text{Cer}$, respectively. On the other hand, the lacto- and neo-lacto series are comprised of the $\text{Gal}\beta 1-3\text{GlcNAc}\beta 1-3\text{Gal}\beta 1-4\text{Glc}\beta\text{Cer}$ and $\text{Gal}\beta 1-4\text{GlcNAc}\beta 1-3\text{Gal}\beta 1-4\text{Glc}\beta\text{Cer}$, respectively which extend the lactosylceramide with $\beta 1-3\text{GlcNAc}$ (Fujii, Numata *et. al.*, 2005). For these lacto- and neo-lacto series, sialic acid residues can also be attached to the galactose residues within the core structures. The function and diversity in glycosphingolipids greatly reflects the importance of these structures, not just in their interactions with carbohydrate binding lectins, but also in their interaction with proteins present in the same membrane (Brown and London, 2000). These glycosphingolipids are also expressed in a tissue specific pattern, with gangliosides, although broadly distributed, found predominantly in the brain, while neo-lacto series are commonly found on hematopoietic cells including leukocytes. In contrast, the globo-series structures are mostly found on erythrocytes, while the lacto-series have been identified in secretory organs (Schnaar, Suzuki *et. al.*, 2009).

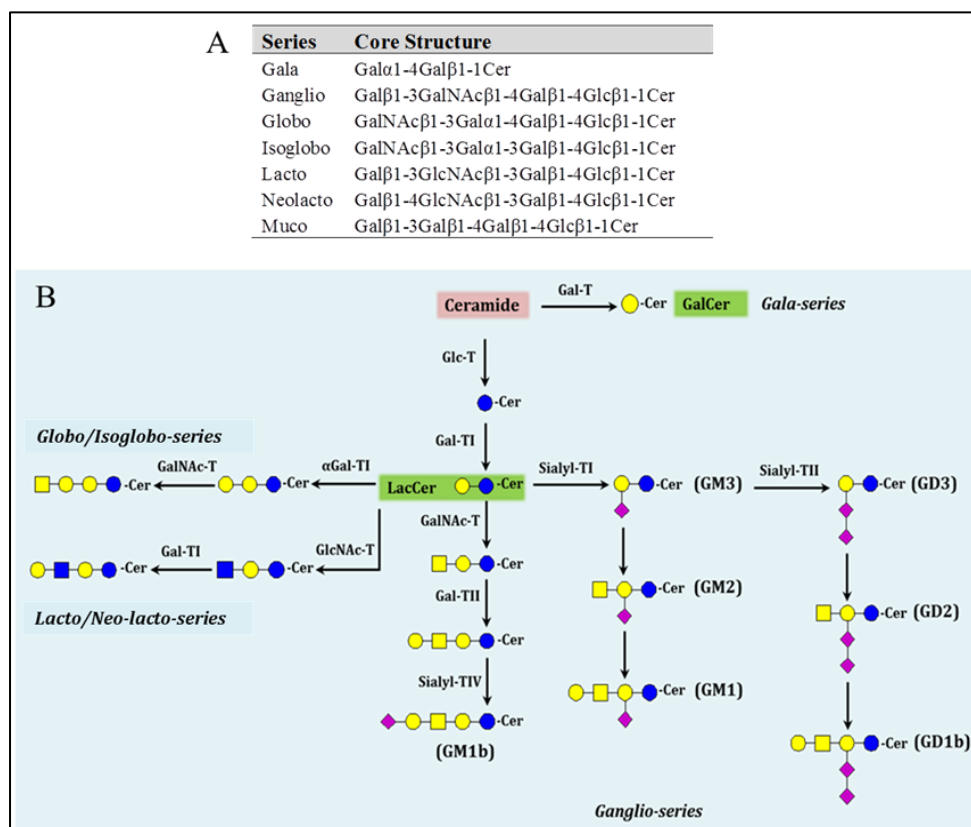


Figure 8: Glycosphingolipid (GSL) series of higher eukaryotes (A). In the synthetic pathway of glycosphingolipids, three alternate pathways (lacto/neolacto-series, globo/isoglobo-series, and ganglio-series) arise from LacCer while the Gala-series is formed from the GalCer (B). Modified and adapted from Tsukuda Y. *et. al.* (2012).

1.7 Glyco-epigenetic Regulation in Ovarian Cancer

Ovarian cancer is caused by progressive genetic alterations such as mutations in oncogenes, tumour suppressor genes, and other abnormalities as well as epigenetic alterations (Bast, Hennessy *et. al.*, 2009; Kwon and Shin, 2011). Epigenetics is defined as acquired heritable changes in gene expression that are not caused by alterations in DNA sequence (Esteller, 2008). These alterations result in abnormal gene transcriptional regulation which reflects in changes in their expression profiles, thus affecting apoptosis, cellular differentiation, proliferation and survival. In view of the fact that early diagnosis is critical for the successful treatment of EOC, specific methylated DNA markers can be detected in the blood plasma, serum and peritoneal fluid of ovarian cancer patients (Ibanez de Caceres, Battagli *et. al.*, 2004). In fact, it has been shown that a panel of tumour-specific methylation biomarkers of at least one of a panel of six tumour suppressor genes- BRCA1, RASSF1A, APC, p14, p16 and DAPK could be detected in serum of ovarian cancer patients with 100 % specificity and 82 % sensitivity (Ibanez de Caceres, Battagli *et. al.*, 2004).

Just like the expression of any gene in the human body, glycan biosynthesis can also be influenced by alteration of gene expression through epigenetic regulations such as DNA methylation or histone modification (Zoldos, Horvat *et. al.*, 2012; Zoldos, Horvat *et. al.*, 2013). The number of studies investigating the involvement of epigenetic factors in protein glycosylation, however, is rather limited (Horvat, Zoldos *et. al.*, 2011; Zoldos, Horvat *et. al.*, 2012). Nevertheless, to date, glycosylation events in cancer have been linked with epigenetic regulation, thereby emphasising the importance of identifying these epigenetic alterations to gain further insights into the link between these alterations at a genetic level with corresponding effects on glycosylation and glycan structures (Zoldos, Grgurevic *et. al.*, 2010). For the purpose of this thesis, DNA methylation changes associated with EOC, including glycosyltransferase genes involved in the glycosylation pathways, are described in **Table 8**.

Table 8: Epigenetic Regulation of Genes in EOC				
Epigenetic Regulation	Characteristics	Genes/Glycosyltransferase genes	Studies	References
DNA Hypermethylation	<p>1) Occurs at CpG-rich regions or CpG islands of genes, leading to inactivation of genes</p> <p>2) In normal cells, CpG islands of active vital genes are unmethylated to allow for gene activation</p>	<p>Tumour suppressor genes:</p> <p>1) BRCA1 2) BRCA2</p>	<p>1) 5-24 % of EOC 2) 14 % of sporadic EOC but not in hereditary EOC 3) No correlation of BRCA1 methylation with histological subtypes, grades or stages 4) BRCA2 promoter methylation is rarely observed in sporadic non-hereditary ovarian cancers</p>	<p>(Takai and Jones, 2002) (Esteller, Corn <i>et. al.</i>, 2001) (Baldwin, Nemeth <i>et. al.</i>, 2000; Strathdee, Appleton <i>et. al.</i>, 2001) (Bol, Suijkerbuijk <i>et. al.</i>, 2010) (Gras, Cortes <i>et. al.</i>, 2001).</p>
DNA Hypomethylation	<p>1) Contributes to structural chromosomal changes and chromosome instability through activation of proto-oncogenes, aberrant recombination and increased mutagenesis</p> <p>2) In normal cells, repeated genomic sequences are heavily methylated to prevent chromosomal re-arrangements</p>	<p>Non-glycosyltransferase genes:</p> <p>1) Methylation-controlled DNAJ (MCJ) 2) synuclein -γ (SNCG) 3) taxol-resistance associated gene (TRAG-3) 4) Insulin-like growth factor(IGF2) 5) Claudin-4 membrane protein</p> <p>Glycosyltransferase genes:</p> <p>1) ST3GAL4 2) MGAT5</p>	<p>1) Extensive hypomethylation in advanced-stage tumours 2) Serous and endometrioid tumours display higher DNA methylation as compared to mucinous subtype</p> <p>2) Global de-methylation correlates with increased expression of glycosyltransferase genes (increase in sialylation and tri-antennary branching and loss in core fucosylation)</p>	<p>(Ehrlich, 2002; Ehrlich, 2002; Eden, Gaudet <i>et. al.</i>, 2003; Strathdee, Vass <i>et. al.</i>, 2005; Czekierdowski, Czekierdowska <i>et. al.</i>, 2006) (Widschwendter, Jiang <i>et. al.</i>, 2004; Yao, Hu <i>et. al.</i>, 2004; Murphy, Huang <i>et. al.</i>, 2006; Litkouhi, Kwong <i>et. al.</i>, 2007)</p> <p>(Salдова, Dempsey <i>et. al.</i>, 2011)</p>

1.8 Overview of Section II: Highlights and Challenges in EOC Glycosylation

- Glycosylation is the most common post-translational modification of proteins and lipids and is highly reflective of changes in the cellular environment.
- Glycobiology is one of the most rapidly growing areas of research in today's post-genomic era and is likely to have a widespread significance in major research fields as development of new methodologies and technological advancements progress in the near future.
- The glycan structures of glycoproteins (*N*- and *O*-linked) and glycolipids are diverse, ranging from single monosaccharides to large, branched oligosaccharide structures.
- The mechanisms regulating the biosynthetic pathways of glycosylation such as availability of sugar nucleotide donors, transporters and glycosyltransferase enzymes are frequently disrupted in cancer, giving rise to aberrant glycosylation of tumour glycoproteins and glycolipids.
- In cancer, the presence of tumour-specific glycan antigens plays crucial roles in angiogenesis, cell adhesion, cell signalling and metastasis and many more processes.
- In ovarian cancer, aberrant glycosylation has been observed in a few studies investigating ovarian cancer cell lines and clinical tissues.
- Anti-glycan autoantibodies that appear to have discriminatory potential for ovarian cancer have been detected in sera of patients; reflecting the antigenic nature of glycans in ovarian cancer.
- There is a lack of studies on potentially different membrane glycosylation profiles of the non-ovarian derived serous cancer tissues (such as serous peritoneal and serous tubal cancers) which constitute high grade serous carcinomas of the pelvic cavity and are commonly grouped as EOC.
- Epigenetic alterations in EOC may potentially have a role in the regulation of cellular glycosylation and in the expression of key glycosyltransferases in EOC.

REVIEW

Cell surface protein glycosylation in cancer

Maja N. Christiansen*, Jenny Chik*, Ling Lee*, Merrina Anugraham*, Jodie L. Abrahams* and Nicolle H. Packer*

Department of Chemistry and Biomolecular Sciences, Faculty of Science, Biomolecular Frontiers Research Centre, Macquarie University, Sydney, Australia

Glycosylation of proteins is one of the most important PTMs, with more than half of all human proteins estimated to be glycosylated. It is widely known that aberrant glycosylation has been implicated in many different diseases due to changes associated with biological function and protein folding. In cancer, there is increasing evidence pertaining to the role of glycosylation in tumour formation and metastasis. Alterations in cell surface glycosylation, particularly terminal motifs, can promote invasive behaviour of tumour cells that ultimately lead to the progression of cancer. While a majority of studies have investigated protein glycosylation changes in cancer cell lines and tumour tissue for individual cancers, the review presented here represents a comprehensive, in-depth overview of literature on the structural changes of glycosylation and their associated synthetic enzymes in five different cancer types originating from the breast, colon, liver, skin and ovary. More importantly, this review focuses on key similarities and differences between these cancers that reflect the importance of structural changes of cell surface *N*- and *O*-glycans, such as sialylation, fucosylation, degree of branching and the expression of specific glycosyltransferases for each cancer. It is envisioned that the understanding of these biologically relevant glycan alterations on cellular proteins will facilitate the discovery of novel glycan-based biomarkers which could potentially serve as diagnostic and prognostic indicators of cancer.

Received: August 31, 2013
Revised: November 7, 2013
Accepted: November 11, 2013

Keywords:

Biomarkers / Cancer / Glycoproteomics / Glycosylation / Glycosyltransferases / Membrane proteins

1 Introduction

Cell surface glycans on membrane-bound proteins are involved in numerous essential biological functions including cell proliferation, differentiation and migration, cell–cell integrity and recognition, cell–matrix and host–pathogen interactions, immune modulation and signal transduction [1]. The glycans found in humans are predominantly attached to the protein in either of two ways: (i) a GlcNAc residue is added to the Asn residue within a consensus peptide se-

quence of Asn-X-Ser/Thr (where X can be any amino acid except proline) for *N*-glycans or (ii) a GalNAc residue is added to the hydroxyl group of Ser or Thr residue on the polypeptide for *O*-glycans. Proteins destined for the cell surface typically undergo glycosylation in the endoplasmic reticulum–Golgi pathway where a sequence of regulated events occur involving both catabolic and anabolic enzymes such as glycosidases and glycosyltransferases to create highly complex but specific glycan structures on the proteins [2].

It is now becoming increasingly evident that the expression of aberrant glycans is intimately associated with pathological conditions including cancer [3], possibly due to dysregulated transcription of enzymes of the glycosylation machinery. Many studies have shown that altered glycosylation patterns on the surface of cancer cells disrupt normal cellular

Correspondence: Professor Nicolle Packer, Department of Chemistry and Biomolecular Sciences, Faculty of Science, Biomolecular Frontiers Research Centre, Macquarie University, Bldg E8C Room 307, NSW 2109, Australia
E-mail: nicki.packer@mq.edu.au
Fax: +61-2-9850-8313

Abbreviations: AFP, alpha-fetoprotein; GnT-III, *N*-acetylglucosaminyltransferase III; GnT-V, *N*-acetylglucosaminyltransferase V; HCC, hepatocellular carcinoma; sTn, sialyl-Tn;

*These authors contributed equally to this work.

Colour Online: See the article online to view Fig. 1 in colour.

functions that eventually lead to their metastatic and invasive behaviours [4–8]. As the significance of glycosylation changes emerge, the search for glycan-based cancer biomarkers or drug targets has become an attractive and widely pursued field of research. Tumour-associated glycans located on the cell surface present themselves as probable cancer predictors and/or as viable options for drug targets as well as for monitoring drug responses. In this review, we focus mainly on cell surface glycosylation changes that have been investigated using cell culture-based models and/or the analysis of tumour tissue from patients across five different cancers, namely those of the breast, colon, liver, skin (melanoma) and ovary (summarised in Table 1). This review comprises three sections in which the first section highlights the use of cell lines and tissues and the various methodologies that have been applied in glycan-based studies. In the next section, we briefly describe the major glycan changes observed in each of the five cancers, followed by a comprehensive analysis of specific glycan epitopes/motifs displayed on the cell surface glycans across the different cancers. Ultimately, we aim to provide readers with an overview of similarities and differences associated with cell surface glycan alterations between these five cancers and how they may be implicated in carcinogenesis.

1.1 The use of cultured cells and tumour tissue for glycan-based studies

According to the most recent statistics, cancer accounted for an estimated 7.6 million deaths annually and remains a leading cause of mortality worldwide [9]. Although there is an improved understanding of cancer compared to decades ago, early diagnosis and treatment are still hampered by the highly complex nature of the disease. Nevertheless, much progress has been facilitated by the accessibility of both immortalised cultured cells and non-immortalised (primary) cells representing a myriad of cancer types collected at different stages which are made available for cancer studies. For example, over 200 melanoma cell lines have been thoroughly characterised for genetic abnormalities and global gene expression patterns that have helped in understanding the stepwise process of melanoma progression [10]. Cell lines that reflect various subtypes of cancers have also been analysed such as OVCAR3 and ES-2 for serous and clear cell subtypes in ovarian cancer and MCF-7 and MDA-MB-231 for luminal and basal subtypes in breast cancer. In addition, non-tumourigenic primary cell lines such as those derived from human mammary epithelial cells, hepatocytes or melanocytes can also be easily obtained for comparative studies. Traditionally, cell lines have been analysed extensively to investigate underlying pathology and potential disease biomarkers. However, with increased spotlight on the implications of altered glycosylation in cancers, these *in vitro* models are being increasingly used for detecting glycan changes that occur in cancer. It must be considered though that the process of glycosylation is enzymatically

driven and is highly dependent on the biochemical environment and cell type [11]. Consequently, the cell culturing process could potentially alter the biochemical environment of the cells and thus affect their cell surface glycosylation expression. It is therefore useful to compare the results of using cellular models of cancer with those obtained from diseased tissue analysis to investigate whether glycosylation is altered between these two approaches.

In breast cancer, several studies have demonstrated that the genetic diversity present in clinical tumours is largely mirrored in breast cancer cell lines [12–14] while another study showed that the glycoprotein profiles of various breast cancer cell lines corresponded to specific tumour subtypes [15]. Cell lines offer the potential to more easily study the different cancer cell subtypes; for example, a lectin-based microarray study that explored cell surface protein glycosylation signatures on various breast cancer cell lines did not identify consistent lectin-binding patterns between three breast cancer cell lines, namely the MCF-7, MDA-MB-231 and SK-BR-3 cell lines, which represent different breast cancer subtypes, that is, luminal, basal-like and ErbB2-overexpressing, respectively [16]. However, in a recent study of a panel of 60 cancer cell lines, markedly different gene expression profiles were obtained between the cultured cells, including those from breast and ovarian cancers, and their corresponding tumour tissues [17]. The genomic profiling of ovarian cancer cell lines has also failed to correlate with their relevant primary ovarian tumour subtypes [18] although numerous glycoproteomic and transcriptomic studies performed on ovarian tumour tissues have identified several glycan motifs which are associated with ovarian cancer subtypes [19–24].

Taken together, these studies suggest that although certain *in vitro* models do reflect changes occurring *in vivo*, other *in vitro* models do not necessarily mimic their corresponding primary tumours. Therefore, data obtained from *in vitro* models needs to be carefully interpreted and followed by subsequent validation studies using clinical tissue samples.

1.2 Methods used to study glycosylation in cancer

To date, numerous studies employing a variety of glycan detection methods have been carried out to compare glycosylation patterns between normal and malignant cancer samples (Table 1). A brief discussion of these methods, which include the use of orthogonal as well as more advanced mass spectrometric-based techniques to identify glycan changes in cancer is described below.

Investigation of glycan expression can be targeted (lectin based or antibody based) or non-targeted (MS based) (reviewed in [25]). Plant lectins which recognise specific glycan motifs are the most commonly exploited tool (reviewed in [26]) and have been used in several ways to detect differential cell surface glycan expression; such as lectin histochemical staining [27–31], lectin affinity chromatography [32–34], lectin blotting [33, 35–38], and lectin array [39]. The utility

Table 1. Cell surface glycan changes in different cancers

Glycan change	Regulation	Sample type (H/M)		Disease stage	Analytical method			Reference(s)	
		Tissue	Cell line		Cancer vs non-cancer	Early/late/metastatic	Mab		Lectin
Breast cancer									
Sialylation									
Sialyl Lewis A	↑, ↓	H	H	x	x	x			[69, 148, 149, 200]
Sialyl Lewis X	↑	H	H	x	x	x			[69, 75, 148, 149]
α2-3	↑	H	H	x	x		x		[29, 208]
α2-6	↑		H						[200]
α2-8	d		H		x				[155]
Fucosylation									
Core fucosylation	↑		H	x				x	[70]
Lewis A	↑	H	H	x	x				[148]
Lewis B	↑, ↓, d	H	H	x	x				[40, 41, 148]
Lewis X	↑, d	H	H	x	x				[41, 67, 75, 148, 170]
Lewis Y	↑, d	H	H	x	x				[40, 41, 148]
H epitope	d	H	H		x				[41]
Branching									
β1-6-branching	↑	H	H	x			x		[27, 28, 43, 71, 200]
Polylectosamine	↑	H	H	x				x	[43]
Truncation									
T, Tn	↑	H	H		x			x	[68, 188, 189]
Sialyl Tn	↑	H	H	x	x			x	[68], [188–190]
Colorectal cancer									
Sialylation									
Sialyl Lewis A	d	H	H		x				[150, 196, 209]
Sialyl Lewis X	↑, d	H	H	x	x		x	x	[48, 58, 84, 150, 196, 210]
Sialyl Lewis type	↑	H	H	x	x			x	[45]
α2-3	↑	H	H	x			x		[31]
Fucosylation									
Lewis A	d	H	H	x		x			[150]
Lewis X	↓, d	H	H	x	x			x	[48, 84, 150]
Branching									
Bisecting GlcNAc	↓	H	H	x				x	[45]
Truncation									
T	↑, ↓	H	H	x	x			x	[42, 84, 191]
Sialyl Tn	↑, d	H	H	x	x				[42, 84, 195–197, 199, 211]
Pauci-mannose type	↑	H	H	x				x	[45]
Liver cancer									
Sialylation									
Sialyl Lewis X	↑		H		x				[105]
α2-6	↑		H	x					[106]
Branching									
Tetra-antennary	↑	H	H	x				x	[107]
Melanoma									
Sialylation									
α2-3 and α2-6	↑		H		x		x		[37, 38]
Branching									
β1-6	↑	H	H	y	y		y	y	[37, 38]

Table 1. Continued

Glycan change	Regulation	Sample type (H/M)		Disease stage		Analytical method			Reference(s)
		Tissue	Cell line	Cancer vs non-cancer	Early/late/metastatic	Mab	Lectin	HPLC/MS	
Ovarian cancer									
Sialylation	↑	H			x	x			[126]
Sialyl Lewis A	↑	H			x	x			[24]
Sialyl Lewis X	↑				x	x			[132, 134]
α2–6	↑		H	x		x	x		[126, 134]
Fucosylation									
Lewis A	↑, nd	H	H	x	x	x			[126, 134]
Lewis B	↑, nd		H	x		x			[134]
Lewis X	↑, nd		H	x		x			[134]
Lewis Y	↑, d, nd	H	H	x	x	x			[126, 134, 174]
H epitope	↑	H			x	x			[126]
Branching									
Bisecting GlcNAc	↑		H	x				x	[131]
Truncation									
Sialyl Tn	↑, d	H		x	x	x			[19, 20, 23, 192, 193]
Other									
LactinAc	↑		H	x				x	[47, 133]
High mannose	↑		H	x		x		x	[47, 131, 206]

↑: increase; ↓: decrease; d: detected; nd: not detected; H: human; Mab: monoclonal antibody.

of lectins has been clearly demonstrated by their ability to identify the proteins that carry a tumour-specific glycan change. For example, high reactivity of the two lectins, PHA-E towards periostin and AAL towards thrombospondin, revealed increased bisecting *N*-acetylglucosamine glycosylation and core fucosylation, respectively, on both proteins, suggesting their use as glycomarkers for ovarian cancer [33]. Antibodies against glycan-associated antigens present on cancer cell surfaces have also been used on various platforms such as Western blots, flow cytometry and immunochemistry. These methods have been successfully applied to glycan studies in numerous cancers. In particular, the occurrence of highly expressed sialyl-Tn (sTn) and Lewis antigens in ovarian, breast and colon tumours were largely established by the use of antibodies against these epitopes. [20,40,41]. Specific glycan alterations identified by lectin- and antibody-based studies were also found to correlate with patient outcome. For example, the increased β1–6 branching of *N*-glycans in node-negative breast tumours [27] as well as the highly expressed Tn and sTn antigens in colorectal carcinoma tissues [42] were associated with poor prognosis of patients.

In recent years, detailed characterisation and extensive coverage profiling of glycan structures attached to proteins have been achieved using advanced instrumentation, in particular, MS. In most of these studies, glycans were enzymatically released from protein samples with or without subsequent chemical derivatisation prior to MS-based analysis via (i) permethylation [43,44]; (ii) 2-AB labelling [8,45] and (iii) as native or reduced forms [34,46–50]. It is evident that MS-based glycomics is becoming indispensable for structural analysis of glycans and glycoconjugates. Due to its non-targeted nature, structures associated with cancer which were not previously identified using conventional techniques may potentially be discovered [8,48]. One current disadvantage is the relatively low throughput nature of glycan analysis by MS since the data analysis requires manual interpretation and detailed assignment of structures. This task is challenging and time-consuming due to the structural complexity, heterogeneity and non-template driven nature of glycans, although computational tools are currently undergoing development to overcome this bottleneck [51, 52].

A large number of studies have also been carried out to identify specific glycosyltransferases involved in the glycosylation pathway in cancers. Most studies measure the mRNA expression of specific glycosyltransferases [38, 53–57] or perform whole transcriptome analysis [2] while others assay directly for the enzyme expression [58–61]. One interesting outcome of these studies is that the correlation between specific glycan expression and their regulation in the enzymatic synthetic pathway is not always consistent. For instance, increased levels of Tn, sTn, T and Lewis X (Le^x) antigens in colon cancer tissue homogenates were not necessarily matched by the activity levels of glycosyltransferases responsible for their synthesis [59]. Notably, elevated expression of cell surface sialyl Lewis X (sLe^x) antigens correlated with those of fucosyltransferase mRNA transcripts in cultured colon cancer cells

but this trend was not observed in tissue samples [55]. Studies have also manipulated glycosyltransferase expression levels in cell lines [62, 63] or introduced specific glycosylation alterations in murine models, for example, by injecting high mucin-producing colon cells [64], to evaluate the effects of the glycan changes on tumour development and metastasis.

The methods used to characterise the glycosylation of proteins in cancer are thus diverse and the strengths and limitations of each of these approaches complicates the comparison of the analytical results and the deductions made from many of these studies.

2 Glycosylation in cancer

Here we will describe the current knowledge of the changes in protein *N*- and *O*-glycosylation that have been observed in five different cancers, viz. breast, colon, liver, skin (melanoma) and ovarian. Details of the various studies reporting these changes are summarised in Table 1.

2.1 Breast cancer

Breast cancer remains the leading cause of death for women worldwide [9]. Detailed cDNA microarray studies on breast cancer tumours unveiled characteristic molecular expression patterns that clustered the disease into five subtypes, namely, luminal A or B, basal-like, ErbB2-amplified and normal-like [65]. Some key differentiators are the status of cell surface receptors, that is, presence of estrogen receptor (ER) and progesterone receptor for luminal A/B subtypes; presence of human epidermal growth factor receptor 2 for ErbB2-amplified subtype and the absence of all three receptors for basal/normal-like subtypes. The clinical implications are huge as this differentiation has allowed for more effective targeted therapies and improved prediction of treatment responses for breast cancer patients.

Early evidence that suggested the involvement of glycans in breast cancer came largely from studies using breast cancer cultured cells and breast tumour tissues [41, 66]. Common cultured cells include cell lines BT20, MCF-7, SKBR3 and MDA-MB-231. The use of antibodies and lectins that recognised specific carbohydrate structures have identified the presence or over-expression of Lewis-type epitopes such as Le^x, sLe^x and Lewis Y (Le^y) and β 1–6 branching of the *N*-glycans as well as short *O*-glycan residues such as T and sTn antigens on cell and tissue membranes [41, 66–71]. Overall increases in branching of *N*-linked glycans, truncation of *O*-linked glycans, sialylation and fucosylation of *N*- and/or *O*-linked glycans are common features observed in breast malignancy. Concomitantly, these changes have been correlated with altered expression of the relevant enzymes responsible for their occurrence such as sialyltransferases, fucosyltransferases, *N*-acetylglucosaminyltransferases and galactosyltransferases [2, 72–74]. Several studies also demonstrated

a positive correlation of cancer-associated glycan structures with metastasis and prognosis of patients [27, 40, 75].

Major efforts have also been directed towards detecting glycan changes in patient serum with the hope of discovering clinically useful biomarkers, particularly for early-stage breast cancer. Current serum biomarkers for breast cancer – CA 15–3 (or CA27.29) and carcinoembryonic antigens both lack sensitivity and specificity and are not suitable for the screening of breast cancer. Comparative profiling of glycans from serum proteins of breast cancer and healthy patients have revealed similar trends of altered glycosylation to those found on the cancer cell surface, which include a general increase in *N*-glycan branching, sialylation and fucosylation [70, 76–78]. Interestingly, one study observed a higher mannose content in serum from breast cancer patients but this alteration has not been reported on cancer cell surface glycans [79].

In addition to overall global glycomic changes to the proteome, numerous breast cancer-associated proteins that bear altered glycan epitopes have also been identified such as EGFR, CD44, TGF β R, 4F2 antigen, Basigin and the notch receptors [80]. Given that more than 50% of proteins are estimated to be glycosylated [81], much more remains to be discovered. Although glycosylation sites in some of these proteins are able to be predicted, detailed site-specific characterisation of glycan changes on each glycosylation site may be essential to understand the roles of these glycan alterations in breast cancer.

2.2 Colorectal cancer

Colorectal cancer is a major and prevalent type of malignancy worldwide, being the third most common in males and second most common in females [9]. It has a relatively high incidence and mortality with an estimate of over 1 million new cases and half a million deaths each year [9]. For this cancer type, alterations of glycans and glycoproteins have been known since the late 1980s [42] and investigations have continued until recent times [45, 49, 82]. The methods, sample types and techniques used have been varied depending on approach and encompass cell lines, animal models as well as clinical samples.

For clinical colon cancer samples, alterations in glycan expression have been observed in patient serum as well as in tissue. In serum, carbohydrate antigens such as CA-19–9 and CA242 are increased in patients with colon carcinomas [83]. In tissue, the main glycan changes observed on the cell surface are Tn and Lewis antigens, as well as their sialylated forms [42, 58, 84]. For the majority of these studies, investigations have used the targeted approach of immunohistochemistry, where only a limited suite of glycans were assayed. Use of non-targeted glycomic approaches such as LC MS has lagged behind, most likely due to the low-throughput nature. Some understanding of the biosynthetic regulation of glycosylation in colon cancer has been obtained through assaying the expression of glycosyltransferase genes, usually at the

transcriptomic level [57,85]. Less is known about the protein expression associated with the glycan alterations, probably due to their relatively low abundance in the proteome due to heterogeneity, as well as the ion suppression of glycopeptides in classic proteomic studies.

Investigations into the biosynthetic regulation of cancer-associated glycan changes and their subsequent functional impact on cancer progression have been performed in *in vitro* cell models of colorectal cancer using cell lines such as HT29 [86], WiDR [87] and LS174T [88]. Increased expression of mucins was associated with increased metastasis [89] and increased fucosylation with increased cellular adhesion [87]. Perhaps the most interesting observation was that cell surface glycan expression and the correlation with relevant glycosyltransferase transcripts [55] or enzymatic activities [59] were not always well defined in tissue. In contrast, surface glycan expression appears to be more easily associated with the synthetic glycosylation pathway in cell culture [55,90]. These findings in particular suggest differences between tissue and cell models, particularly in the complexity of glycan biosynthetic regulation.

2.3 Liver cancer

Primary liver cancer includes different subtypes of cancer originating from the liver and includes hepatocellular carcinoma (HCC), cholangiocarcinoma, angiosarcoma and hepatoblastoma. The most common of the primary liver cancers is HCC representing over 90% of cases [91]. HCC is currently the fifth most prevalent cancer, is the third leading cause of cancer-related death worldwide [92] and is the focus of liver cancer research. It usually arises as a result of long-term underlying liver disease and is the main cause of death in patients with liver cirrhosis [93]. Patients with HCC have a dismal prognosis, with 5-year survival rates as low as 18%, partly due to tumours being commonly diagnosed at advanced stages [94].

The majority of studies involving glycosylation changes associated with liver cancer have been conducted using patient serum samples. Since most of the proteins in serum are of hepatic origin, the close relationship between liver and serum suggests that aberrant glycosylation of liver proteins may be reflected in the serum [95]. Even though this review focuses on changes in cell surface protein glycosylation in cancer, one well-documented example of glycosylation alterations to a serum protein in liver cancer should be mentioned first, namely alpha-fetoprotein (AFP), which is currently one of the few successful/approved glyco biomarkers [96–98]. The AFP abundance is generally raised as a result of liver disease and the change in glycoforms of AFP has been shown to be a good indicator of disease progression, distinguishing HCC from chronic liver disease [99]. Various AFP glycoforms are present in benign liver disease, chronic hepatitis, liver cirrhosis as well as HCC. However, there is one particular glycoform known as AFP-L3 (lectin fraction 3) that correlates well with liver cancer. AFP-L3 is the major glycoform

found in serum of HCC patients and carries an additional α 1–6-linked fucose residue (core fucose) and represents a good marker for malignancy. At present, the cut-off index for fucosylation is set to 10% (positive when AFP-L3 >10% of total AFP) [100], in which HCC patients tested positive for AFP-L3 over this threshold have the potential for faster tumour growth and early metastasis [101, 102]. For chronic hepatitis or liver cirrhosis patients who are considered high-risk groups for HCC, AFP-L3 can detect liver tumours with a diameter of less than 2 cm [103] with a lead time of 9–12 months compared to imaging techniques [104] with sensitivity of the test increasing with tumour size and aggressiveness of HCC. Clearly, these results indicate that the different glycosylation of AFP-L3, although unknown as to its function, is useful for early diagnosis of HCC due to its high specificity.

There are some studies where liver tissue from HCC patients and hepatocellular cell lines has been investigated as well. An up-regulation of sLe^x [105] and α 2–6-linked sialylation [106] as well as tetra- antennary glycans [107] has been described in some of these cases. However, most studies measure either the regulation or activity of specific glycosyltransferases, with reporting of an increase in enzymes responsible for core fucosylation [108,109] and branching [4, 56, 109, 110]. The glycosyltransferase regulation is not directly linked to structural changes in the glycans in most cases, making it difficult to ascertain how cell surface protein glycan expression is regulated.

2.4 Melanoma

Melanoma is the least common but most life-threatening form of skin cancer, with about 200 000 new cases diagnosed worldwide each year (<http://www.aimatmelanoma.org>). If detected at an early stage before metastasis has occurred, surgical removal of the primary lesion results in a survival rate of over 90%. This survival rate drastically decreases to 13% for patients diagnosed after metastasis to distant organs has occurred.

Alterations in cell surface glycosylation have been found to contribute to the invasive and metastatic potential of the melanoma tumour cells and poor prognosis of patients with studies of the glycosylation of human melanoma cell lines and the popular murine B16 melanoma tumour model providing valuable information on the cell surface protein glycosylation changes associated with the development and progression of melanoma [111–113]. Over 5000 independent cell line strains are available for the study of melanoma, covering the different stages of disease progression from primary melanomas to metastases in distant organs such as lymph nodes and the brain [10].

The studies carried out include interaction of glycosylated cell adhesion proteins with extracellular matrix proteins [34,38], glycosyltransferase expression profiling [38] and the use of lectins to identify characteristic glycan changes

[37,38,114]. Other methods include the use of sialic acid determination using HPLC and sialidase treatment [111], MALDI MS/MS and HPLC analysis of *N*-glycans released from isolated glycoproteins from melanoma cell lines [8,34,114,115]. These studies have reported changes in sialic acid linkage and fucosylation of individual proteins, as well as an increase in both the total cell surface abundance and number of proteins bearing β 1–6-branched tri- and tetra-antennary *N*-glycans in the progression from primary to metastatic melanoma.

Although extensive studies have been carried out on melanoma cell lines and mouse model systems, there is limited evidence on whether the observed changes in these systems are consistent with the glycosylation profiles of tumour tissue from patients, probably due to the small sample size of melanoma tissue.

2.5 Ovarian cancer

Ovarian cancer, derived from the ovary, fallopian tube or peritoneum, is the sixth most common cause of cancer worldwide with the highest mortality rate among all gynaecological cancers [116]. The histological subtypes for ovarian cancer such as serous, mucinous, endometrioid and clear cell are all associated with different genetic risk factors and distinct molecular events during oncogenesis [117,118]. The serous subtype, however, represents over 75% of ovarian cancers and is characterised by a 5-year survival rate of only 10–20% [119,120]. This poor prognosis is due to an array of factors which include the anatomical location of the ovaries within the abdominal cavity, lack of early symptoms and diagnostic biomarkers as well as inadequate screening methods. At present, CA125 is the only clinical marker used for the detection of ovarian cancer, despite limitation in terms of its sensitivity and specificity [121]. Due to their morphological heterogeneity and location, most ovarian cancers are diagnosed at advanced stages when metastasised to distant sites and are usually treated in the same manner; namely with maximal cytoreductive surgery [122,123] followed by platinum-based chemotherapy [124,125].

Several approaches have been explored to identify glycosylation changes that give rise to the expression of tumour-associated glycans such as Tn and sTn antigens which have been found in ovarian cancer tissue. Conventional methods such as the use of immunohistochemical staining using monoclonal antibodies have shown differential expression of carbohydrate antigens between normal tissue and ovarian cancer tissue [19–21] and facilitated the characterisation of ovarian cancer tumour subtypes [126]. Multi-lectin affinity chromatography has also been employed for the enrichment of glycoproteins to aid in the detection of specific glycosylation changes between healthy and diseased cancer tissue [33,53].

While a majority of proteomics-based experiments have focused mainly on body fluids such as serum [127–129] and secreted glycoproteins [130,131], there is a lack of informa-

tion regarding the cell surface protein glycosylation of ovarian cancer tissues and cell lines. However, over the past few years, MS-based glycomics has led to the discovery and identification of glycans associated with ovarian cancer progression. For instance, studies associated with cellular glycan changes have been reported for the SKOV3, PA-1, OV4, OVM, m130, GG and RMG-1 cell lines in which several glycans with Lewis antigens or LacdiNAc motifs were detected as possible markers of ovarian carcinoma [47,132–134]. Besides that, mass spectrometric profiling of ovarian cancer tissue also revealed the overexpression of cancer-associated terminal β -*N*-acetyl-D-glucosamine (GlcNAc) in protein and lipid-linked glycoconjugates [135].

Although the ovary has traditionally been thought to be the origin of ovarian cancer development, the clinical focus has shifted from the ovaries to other potential sites of origin such as the fallopian tube and peritoneum [136–138]. Hence, the recent identification of serum anti-glycan antibodies which differentiated ovarian cancers according to their origin serves as a good indicator that glycosylation changes on a cellular level may evoke specific antibody responses that can be monitored for diagnostic and prognostic purposes [139]. Owing to the fact that 90% of ovarian cancers are epithelial cancers [140], novel glycan alterations on the cell surface represent a vital source of drug targets and biomarkers which could be utilised as alternative treatment strategies to improve survival rates of this disease.

3 Glycan changes associated with cancer

Glycosylation changes to the cell membrane proteins have thus been associated with all of the described cancers and have been investigated in detail for some cases. Specifically, sialylation, fucosylation, branching and truncation of both *N*- and *O*-glycans appear to be a common theme amongst the cancer-associated changes in glycan structures and are described in the following sections. A detailed overview of these glycan alterations (Table 1) and the key glycosyltransferase changes (Table 2) observed in cancer is provided. An illustrative diagram depicting the reported cancer-associated glycosylation changes, with their known corresponding glycosyltransferases, is also shown in Fig. 1.

3.1 Sialylation

Sialic acids, which include the nine-carbon monosaccharide, *N*-acetylneuraminic acid, are widely distributed in nature as terminal sugars on various glycoconjugates [141]. The addition of sialic acid residues, also termed sialylation, is an important modification in cellular glycosylation as sialylated glycans mediate various roles in cellular recognition, cell adhesion and cell-to-cell signalling [142]. The four major families of sialyltransferases are classified according to the carbohydrate linkage in which they transfer the sialic acid residues,

Table 2. Glycosyltransferase regulation of cell surface glycans in various cancers

Glycosyltransferase change	Regulation	Sample type (H/M)		Disease stage		Analytical method		Reference(s)
		Tissue	Cell line	Cancer vs non-cancer	Early/late/metastatic	RT-PCR	Enzyme assay ^{a)}	
Breast cancer								
Sialylation								
ST3GAL 1	↑	H	H	x		x		[72]
ST3GAL 3	↑, ↓	H		x	x ^{b)}	x		[2, 74, 153, 200]
ST3GAL 4	↑	H			x	x		[200]
ST3GAL 6	↑, ↓	H		x	x ^{c)}	x		[2, 5]
ST6GAL 1	↑	H			x ^{b)}	x		[74]
ST6GALNAC 2	↑		H		x	x		[200]
ST8SIA 1	↑		H		x	x		[200]
ST3GAL 1	↑		H	x	x	x	x	[60]
Fucosylation								
FUT 8	↑	H		x		x		[2]
FUT 2, 3, 4, 5, 11	↑	H	H	x	x ^{c)}	x		[2, 5, 200]
FUT 4, 9, 10	↓	H		x		x		[2]
Branching								
MGAT5	↑	H, M		x			x	[71]
MGAT 4, 5B ^{d)}	↓	H		x		x		[2]
MGAT3	↓	H		x		x		[2]
Truncation								
GALNT 2, 3, 5, 6, 7, 10	↑	H	H	x		x		[2, 200]
Other								
B4GALT 1, 2, 3, 5	↑	H	H	x		x		[2, 200]
GCNT 1	↑	H	H	x		x		[2, 200]
GALNT 14	↑	H		x			x	[73]
Colorectal cancer								
Sialylation								
ST3GAL 1	↑	H		x		x		[212]
ST3GAL 3	↑	H			x	x		[213]
ST3GAL 4	↑, ↓	H		x	x	x, NB		[57, 212]
ST6GAL 1	↑	H		x		x		[213]
ST3GAL 2	↑	H		x		x		[57]
ST3GAL transferase	↑	H		x			x	[59]
ST6GALNAC transferase	↓	H	H	x			x	[59, 90]
Fucosylation								
FUT 8	↑	H		x			WB	[87]
FUT 3	↑, ↓, d	H	H	x		x		[55, 57, 213]
FUT 1, 4, 6	↑	H		x		x		[57, 58, 212, 213]
Branching								
MGAT3	↑	H		x		x		[213]
Truncation								
GALNAC transferase	↓	H		x			x	[59]
Other								

Table 2. Continued

Glycosyltransferase change	Regulation	Sample type (H/M)		Disease stage		Analytical method		Reference(s)
		Tissue	Cell line	Cancer vs non-cancer	Early/late/metastatic	RT-PCR	Enzyme assay ^{a)}	
B4GALNT 2	↑	H		x			x	[85]
B3GNT 6, B6GN transferase	↑		H	x			x	[90]
C1GALT 1	↑	H		x			x	[59]
Liver cancer								
Sialylation								
ST6GAL 1	↑↓	H		x	x		x	[106]
Fucosylation								
FUT 8	↑	H		x			x	[108, 109]
α2/α3 fucosyltransferase	↓	H		x			x	[109]
Branching								
MGAT5	↑	H	H	x	x		x, WB	[4, 56, 110, 176]
MGAT3	↑	H		x			x	[108]
Other								
Mannosyltransferase	↑	H		x			x	[109]
Galactosyltransferase	↑	H		x			x	[109]
Melanoma								
Sialylation								
ST3GAL 3, 4	↑		H			x		[38]
Fucosylation								
FUT 1	nd		H			x		[38]
FUT 4	nd		H			x		[38]
Branching								
MGAT5	↑		H			x		[38]
Ovarian cancer								
Sialylation								
ST3GAL 1	↑	H		x		x		[54]
ST3GAL 3, 5, 6	↓	H		x		x		[54]
ST6GAL 1	↑	H		x		x		[54]
Fucosylation								
FUT 1, 2	↑		H	x		x		[7]
FUT 3, 4, 5, 6	↑	H	H	x	x		x	[134]
FUT 8	↑	H, M		x		x		[53]
FUT 9, 10	↑	H	H	x	x	x	x	[134]
Bisecting								
MGAT3	↑	H, M		x		x		[53]

↑: increase; ↓: decrease; d: detected; nd: not detected; H: human; M: mouse; WB: Western blot; NB: Northern blot.

a) Assay for glycosyltransferase activity unless otherwise indicated.

b) High grade vs low grade.

c) ER+ vs ER– tumour.

d) MGAT5B has been reported to catalyse mainly the formation of β1,6GlcNAc-branch on O-mannosyl glycans in brain [214].

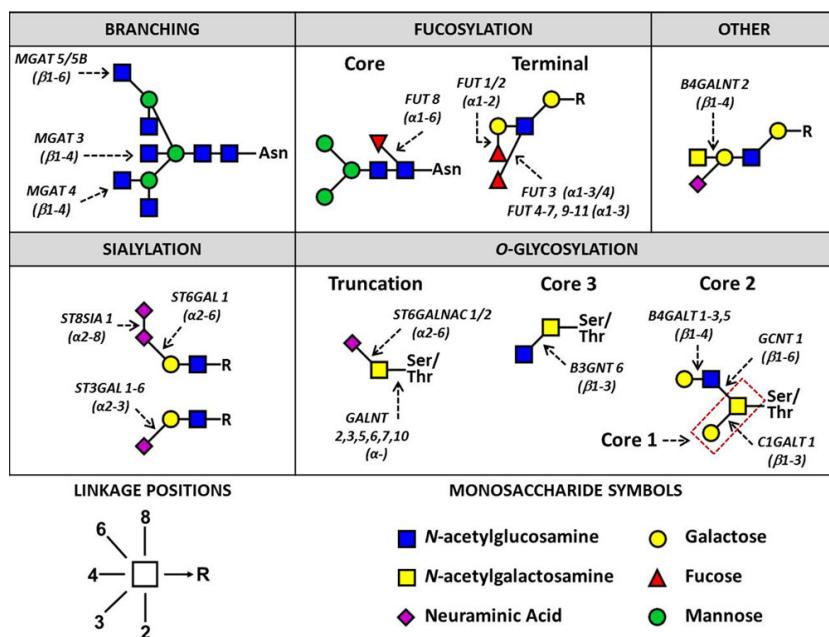


Figure 1. Representative diagram illustrating the glycosyltransferase genes involved in various *N*- and *O*-glycan changes in breast, colorectal, ovarian, liver and melanoma cancers. R indicates *N*- and *O*-glycans.

namely the ST6Gal (α 2–6 linkage), ST3Gal (α 2–3 linkage), ST6GalNAc (α 2–6 linkage) and ST8Sia (α 2–8 linkage) [143] as shown in Fig. 1.

Sialylated Lewis epitopes such as sLe^x (NeuAc α 2–3Gal β 1–3(Fuc α 1–4)GlcNAc β) and sLe^a (NeuAc α 2–3Gal β 1–4(Fuc α 1–3)GlcNAc β) are structurally related and have been frequently investigated in a majority of cancer studies [144–146]. It has also been shown that the aberrant expression of these epitopes is implicated in cancer metastasis through the adhesion of tumour cells to the endothelium [144, 147]. For instance, in breast cancer, the occurrence of both sLe^x and sLe^a, was found to be highly expressed in breast carcinoma with lymph node metastases [69, 75, 148]. Their occurrence also had an inverse relationship to the expression of the epithelial marker, E-cadherin, a membrane glycoprotein commonly associated with epithelial–mesenchymal transition [149]. Apart from the presence of sLe^x in ovarian cancer, sLe^a also appears to be a key antigenic determinant for mucinous ovarian tumours, indicating that its expression is more discriminatory for this subtype as compared to other ovarian cancer subtypes such as serous and endometrioid [126].

The preferential up-regulation of sLe^x, a notable feature observed in metastatic tissue (e.g. lymph node) as compared to primary cancer tissue, has also been shown to be indicative of malignancy and disease progression [5, 84, 145]. This trend has been observed in colon cancer, in which the expression of sLe^x correlated with metastasis and a higher incidence of recurrence and poor prognosis. Likewise, in ovarian cancer, this epitope is associated with metastasis although there was no correlation with patient prognosis [23, 24, 145, 150]. Sim-

ilarly, sLe^x was also present in the hepatocytes surrounding the metastatic carcinoma site in liver cancer but not detected in normal livers [151]. In contrast, for melanoma cancer, a separate study showed that the excessive expression of sLe^x on short chain polylactosamine *N*-glycans in α 1–3 fucosyltransferase III-transfected B16-F1 melanoma cells led to subsequent tumour rejection by natural killer cells [152].

The prevalence of either α 2–3 or α 2–6 sialylation has also been extensively studied for each cancer type in terms of the expression of sialyltransferases and glycan structures bearing these epitopes. For instance, α 2–3 or α 2–6-sialylated glycans were found to be involved in conferring a metastatic phenotype in melanoma cell lines [37] while another recent study revealed higher mRNA expression levels of α 2–3 sialyltransferases, ST3GAL3 and ST3GAL4, which were specific for *N*-glycan lactosamine chains bearing Gal β 1–3 and Gal β 1–4, respectively. Similarly, the impact of sialylation type was also observed in colorectal cancer, in which α 2–3-sialylated structures detected using *Maackia amurensis* lectin also showed positive correlation with lymph node metastases and lymphatic invasion [31]. In breast cancer, the associated sialyltransferases, ST3Gal3 for *N*-glycans and ST3Gal1 for *O*-glycans, were also found to be up-regulated in most breast cancer studies [74, 153]. Glycoproteins with terminal α 2–6-linked sialic acids, however, have been up-regulated in several ovarian cancer cell lines while another study indicated that α 2–6 sialylation of β 1 integrin, a membrane-associated glycoprotein, conferred metastatic and adhesive properties to ovarian cancer cells [132, 134]. The expression of α 2–6-sialylated glycoproteins was also observed in liver

cancer and the corresponding mRNA expression of ST6GAL1 was a consequence of the neoplastic transformation of hepatocytes [106, 154]. It should also be noted that changes on the cell surface glycosylation upon malignant transformation have also revealed the novel occurrence of α 2–8-linked polysialic *O*-glycans that correlated with enhanced metastatic properties of MCF-7 breast cancer cells [155].

Overall, the accumulating evidence in the cancers described clearly highlights the important role of sialylation of glycoproteins in tumour metastasis, a critical event in cancer development and progression. In particular, the up-regulation of sLe^x is commonly observed across different cancer types such as breast, ovarian, liver and colorectal cancer, whilst the differential expression of α 2–3 and α 2–6 sialylation in cancer was found to correlate with metastasis in all five cancers as opposed to the novel α 2–8-linked polysialic *O*-glycans observed only in breast cancer so far.

3.2 Fucosylation

L-fucose is a common component of many *N*- and *O*-linked glycans produced by mammalian cells. Two key features that distinguish this monosaccharide from other hexoses include the lack of a hydroxyl group at the six-carbon position of the sugar ring and the L-configuration. Fucose, also classified as a deoxyhexose, frequently exists as a non-extendable modification of glycans and plays a functional role in regulating ontogeny and cellular differentiation [156]. Hence it is no surprise that fucosylation is differentially regulated in cancerous compared to non-malignant conditions. Fucosylated glycans are synthesised by a range of fucosyltransferases (encoded by FUT1–11) and can be generally divided into two subcategories, core fucosylated and terminally fucosylated glycans.

3.2.1 Core fucosylation

Core fucosylation is the addition of α 1–6-linked fucose to the innermost GlcNAc residue of *N*-glycans which is synthesised by a single α 1–6 fucosyltransferase (encoded by FUT8, Fig. 1). Up-regulation of core fucosylation and the associated FUT8 gene seems to be an important factor in most cancers (refer to Tables 1 and 2). Core fucosylation has been found to be elevated in liver, colon and ovarian cancerous tissue [53, 157, 158] and the increase is reflected in the serum levels of HCC and ovarian cancer patients [157, 159]. Increased core fucosylation has also been observed on the cell surface of colon and breast cancer cell lines [2, 55, 87]. In addition to the increase in core fucosylation, the transcription of FUT8 is enhanced in HCC liver tissue and breast tumour tissue [2, 108] with a significant increase of the substrate GDP-fucose levels reported in HCC [160]. It should also be noted that a recent study found similar levels of fucosylation in HCC tissue as compared to the surrounding healthy tissue, after measuring

high expression levels of FUT8 enzyme in tumour tissue as compared to the surrounding non-tumour tissue [161], suggesting that there may be an abnormal secretion of fucosylated proteins into the serum of HCC patients [107]. Various studies on colorectal cancer cell lines [162–165] have also identified the role of core fucosylation in E-cadherin-dependent adhesion [55, 87], since both have shown to be up-regulated in cancerous tissue. FUT8 knockout colorectal cancer cells mediate loose cell–cell contacts whereas FUT8-transfected cells increase adhesion and aggregation, thereby supporting the role of core fucosylation in cell adhesion and cancer metastasis. Core fucosylation has also been linked to antibody-dependent cellular cytotoxicity [166] and a positive correlation was observed between increased dimerization and phosphorylation of EGFR [158] in breast cancer cells, further demonstrating the impact of core fucosylation in breast malignancy through enhanced EGFR-mediated cellular activities.

3.2.2 Terminal fucosylation

Cell surface glycans also frequently carry fucose residues in a α 2–3 and/or 4 linkage at the terminus of the *N*- and *O*-linked glycan structures, giving rise to the formation of specific Lewis blood group antigens, such as (Le^x/^y) and (Le^a/^b). Several fucosyltransferases are involved in the formation of Lewis antigens including those coded by FUT1–7 and FUT9 [167] with FUT3–7 and 9 gene products known to produce the Le^x structure [167–169] (Fig. 1). FUT1–2 genes, on the other hand, are involved in creating the precursor of the H antigen. Although fucosylation is essential for normal biological functions, a change in fucosylation has been strongly implicated in cancer and increasing metastatic potential. Le^x antigens, for instance, have been found to be differentially expressed in colon [150] and breast [80, 169] cancer tissues. More specifically, a comparison between adjacent and carcinoma tissue in colon cancer showed an increase of Le^x and sLe^x in the tumour tissues, in which patients having both epitopes had shorter life spans than those without them [150]. A similar association was seen in breast cancer where overexpression of the sLe^x correlated with lymph node metastases, poor prognosis and lower survival rates in breast cancer [170]. This indicated that varying levels of fucosylation of glycans on tumour tissue proteins corresponded to higher malignancy and poorer prognosis in both colon and breast cancer.

Le^x antigens have also been found in colorectal, breast and ovarian cancer cell lines. sLe^x was found to promote adhesion of some breast cancer cell types to activated endothelial cells [41, 171], a trend that was also observed in colorectal cancer cell lines as a result of overexpression of sLe^x [172]. It was also shown that increased expression of the Le^x antigen correlated with higher mRNA levels of FUT3 in colorectal cell lines although this association could not be verified in tissue [55]. Other studies have identified FUT6 as the predominant gene involved in the synthesis of sLe^x expression

by the use of non-transfected and FUT6-transfected colon cancer cells [58]. Moreover, transfection of the FUT6 gene not only induced synthesis of sLe^x, but also enhanced the adhesion of breast cancer cells to the endothelial cells. In another study, FUT6 expression was found to be directly related to the elevated amount of sLe^x found in breast tumour tissue [169]. Similarly, the effect of FUT7 transfection on cell adhesion has also been investigated in colorectal cells [172] and resulted in the overexpression of sLe^x as well as increased adhesive capabilities of the cells.

In addition to Le^x and sLe^x, Le^y antigens have been found in breast [80] and ovarian cancer cell lines [134] as well as on the ovarian cancer antigens CA125 and MUC-1 and the membrane-associated family of EGF receptors [173, 174]. Serous and endometrioid ovarian tumours were also characterized by a high expression of Le^y and H (type 2) antigens as compared to an increase in Le^a antigens in mucinous tumours [126]. Furthermore, α 1-2 fucosyltransferase, which is involved in the expression of Le^y, has been correlated with increasing proliferation, cell adhesion, invasion, metastasis and drug resistance [7, 175] in ovarian cancer. Conversely, other fucosyltransferases seem to be down-regulated in some cancers, for instance α 2/ α 3 fucosyltransferases in HCC were significantly lower in tumour compared to non-tumourous tissue [109] while the FUT1 gene product was not detectable in 25% of tested melanoma cell lines [38].

The overall evidence from the investigated cancers highlights the importance of fucosylation in cancer and cancer progression. More specifically, core fucosylation is preferentially up-regulated in breast and liver cancer while the corresponding increase of the FUT8 enzyme has also been reported in all of the cancers except melanoma. The regulation of terminally fucosylated glycan structures and their related fucosyltransferases, however, appears to be varied across the five cancers, despite the Le^x epitope being consistently up-regulated in most cases.

3.3 Branching and bisecting GlcNAc

3.3.1 Branching of *N*-glycans

Tetra-antennary *N*-linked glycans are formed by the action of *N*-acetylglucosaminyltransferase V (GnT-V), which catalyses the addition of β 1-6-GlcNAc to the six arm of the *N*-glycan core. Increases in these branched structures have been associated with cancer and there is evidence for their involvement in the progression of all five of the cancers examined in this review.

Elevated presence of β 1-6 branching on cell surface *N*-glycans has been consistently observed in several comparative studies of tumour with normal tissues in both breast cancer and HCC [27, 28, 43, 66, 107]. Some of these studies had evidence not only at the cell surface *N*-glycan structural level but showed correlation with increased activity of GnT-V and its corresponding MGAT5 (Fig. 1) gene expression [71, 107]. An

increase in branching structures has been shown to not only be associated with the initial stages of cancer but also with the progression to advanced stages and metastasis. Studies using GnT-V knockout and antisense cell lines have demonstrated the involvement of β 1-6 branching in the migratory behaviour and metastatic phenotype, particularly in breast, colon and HCC cells [176–179]. Higher levels of GnT-V expression were positively correlated with the histological grade and tumour node metastasis (TNM) classification in tissue from patients with cirrhosis, well-differentiated and poorly differentiated liver tumours, consistent with earlier findings that elevated GnT-V correlates with HCC and its progression [4, 56, 110].

Comparison of the PHA-L lectin (specific for β 1-6-branched complex-type *N*-glycans) binding patterns between primary and metastatic melanoma cell lines showed an increase in not only the intensity of lectin staining in cells from metastatic sites but also an increase in the number of proteins containing β 1-6-branched glycans [37], indicating an increased activity of the GnT-V enzyme and availability of its substrates in metastatic melanoma. The reactivity of breast tumour tissue with PHA-L from different stages of disease also correlated with tumour progression while highly branched *N*-glycans have been suggested as a predictive tumour marker for the identification of node-negative breast cancer patients [27, 28]. Overall, the use of PHA-L to isolate proteins from colon cancer and melanoma cell lines and breast tumour tissue, and their identification by MS, has identified tumour-associated cell surface glycoproteins including TIMP-1, EGFR, TGFR, integrin subunits, *N*-cadherin, periostin, LAMP 1, matriptase L1-CAM, Mac-2-binding protein and melanoma cell adhesion molecule [32, 114, 180–184].

Thus, this specific structural change of increased *N*-glycan branching on proteins in these cancers, together with the supporting correlation with the synthetic enzyme responsible for this structure appears to be an important hallmark of the cancer cell, particularly of the metastatic process.

3.3.2 Bisecting GlcNAc

Bisecting GlcNAc *N*-glycan structures are a result of the expression of *N*-acetylglucosaminyltransferase III (GnT-III), the enzyme responsible for adding a β 1-4-linked GlcNAc residue to the core of *N*-glycans by the MGAT3 gene, and are known to regulate cell adhesion [185]. GnT-III has also been shown to be expressed at a significantly higher level in hepatic nodules compared to surrounding control liver tissue [108], suggesting a possible correlation between GnT-III and the early pre-cancerous stage of liver cancer. Additionally, GnT-III serum activity is raised in HCC patients compared to patients with chronic hepatitis and healthy controls, although there is some evidence that the GnT-III activity in serum and tissue is elevated in cirrhosis as well as in the malignant transformation of the liver [108, 186].

Differential binding of the PHA-E lectin specific for bisecting *N*-glycan structures and a substantial increase of the gene (MGAT3, Fig. 1) transcripts responsible for GnT-III expression in ovarian cancer tumours were observed compared to normal ovarian tissue. [53]. Other studies have indicated the role of bisecting *N*-glycans in promoting metastasis and tumourigenesis [187]. The clinical marker for ovarian cancer, CA125, isolated from OVCAR3 cell line has also been shown to carry bisecting GlcNAc *N*-linked glycans using a combination of mass spectrometric approaches, FAB-MS, MALDI-TOF, and CAD-MS/MS [131].

In contrast to their metastatic correlation in ovarian cancer and HCC, bisecting GlcNAc structures have been shown to prevent metastasis in a melanoma mouse model. The introduction of the MGAT3 gene into mouse cells led to the suppression of lung metastasis due to the competition between the enzymes GnT-V and GnT-III, resulting in a subsequent decrease of β 1–6 structures and increase in bisecting GlcNAc, with concomitant alterations in biological function of cell surface glycoproteins including E-cadherin [115].

Overall, the disruption in regulation of the MGAT3 and MGAT5 genes and the abundance of bisecting and β 1–6 branched *N*-glycans, respectively, displayed on cell adhesion proteins have been associated with the migratory and invasive behaviour of cancer cells in both rodent and cell culture models of liver, colon, ovarian, breast cancer and melanoma.

3.4 Truncated *O*-glycans

Shortened or truncated glycans appear to be another long-reported feature that is commonly increased during cancer, whereas they are either absent or only weakly expressed in normal tissues. Examples of these truncated antigens include antigens T (or core 1), Tn and their sialylated forms (sT/Tn) on the *O*-glycans attached to mucins. These truncated glycans have been shown to be generally increased in tumours across different carcinomas, including breast [68, 188–190], colorectal [42, 191] and ovarian cancer [19–21, 192–194].

Of these, sTn is notably increased in breast, ovarian and colorectal cancers. In colorectal cancer, multiple immunohistochemical studies have been reported and the majority of these patients (83.4% of 407 patients across six studies) [42, 195–199] were reported as sTn positive while the antigen was not generally observed in normal tissues. A similar finding was observed for breast [62, 200] and ovarian cancer tissues [19–21, 192–194]. The increased expression of this sTn antigen is also frequently associated with poorer prognosis, lower survival rates and metastatic progression [22–24, 197, 201] across these different cancers. This suggests that these structures may play an important role through mechanisms such as alteration of cellular adhesion, which is implicated in the metastatic cascade [202].

Interestingly, conflicting results have been obtained using the colorectal cancer cell line, LS174T. In this study [203], subclones of LS174T were selected for secretion of mucins

with truncated glycans (LS-C) as well as more fully glycosylated mucins (LS-B) [204]. Since liver is a commonly observed metastatic site [205], the colonisation of liver by these subclones was investigated in athymic mice. Unexpectedly, the subclone of the LS147T cell line with the more fully glycosylated mucin colonised the liver of athymic mice to a greater extent. In addition, adhesion to hepatic endothelial cells, a likely contributor towards liver metastasis, was also greater by the subclone with the more fully glycosylated mucin than by the subclone with truncated glycans on the mucins [203]. However, adhesion to basement membrane matrix (Matrigel) was greater for truncated LS-C cells than for LS-B cells. Therefore, the effect of the truncated and extended glycans on the mucins and their impact on cellular adhesion during colorectal cancer progression is more complex than we understand at present. It is also unknown how or whether the truncated *O*-glycans may mediate metastatic progression in the other cancers detailed in this review.

Taken together, up-regulation of sTn in tumours is frequently observed on the mucins of epithelial cancers such as breast, ovarian and colon, and its overexpression is commonly associated with poorer prognosis and metastatic progression.

3.5 High-mannose *N*-glycans

High-mannose *N*-glycan-related glycan changes have also been observed as a notable feature in some cancer cell types such as ovarian and liver cancer. In ovarian cancer, high-mannose type *N*-glycans have been observed on the total glycoproteins derived from cancer cell lines, SKOV-3 [47] as well as on the glycoprotein CA125 derived from OVCAR3 cells [131]. Besides that, a monoclonal antibody, TM10, was recently developed that demonstrated specificity towards high-mannose *N*-glycans on glycoproteins derived from a range of ovarian cancer cells, PEA-1, PEO-1 and SKOV-3 [206]. In liver cancer, slight up-regulation of mannosyltransferase activity was observed in tumours compared to non-tumour tissues [109]. This implied an increased expression of high-mannose glycans, although this was not directly determined. Interestingly, elevation of high-mannose glycans has also been previously reported in serum of humans and mouse models of breast cancer [207]. Whilst there is some evidence to suggest increased expression of high-mannose glycans in some cancer types, it is unknown at present what role high-mannose glycans play in cancer.

4 Conclusions and future perspectives

The extensive literature findings summarised in this review provide compelling evidence which signifies the biologically important role of cell surface protein glycosylation in cancer, particularly with regard to the specific *N*- and *O*-glycan structures involved in disease state and progression. Despite the fact that every cancer develops and behaves differently,

several conclusions can be drawn regarding the similarities and differences arising from the glycosylation patterns of the proteins in the five different cancers investigated in this review. These conclusions have the caveat that the different studies have involved various methodologies including structural glycan analysis, determination of enzyme activities and levels of gene expression, and were carried out on a range of diverse cell lines and/or tissue samples. In addition, the lack of observation of a particular structure may simply reflect the inability of the method used in a particular study to identify it.

Firstly, the increase in sialylation observed in all the cancers has been shown to promote cancer metastasis and to a certain extent, is indicative of poor patient prognosis, although there is no single specific sialylation change associated with all the cancers. *N*-glycans bearing α 2–3-linked sialylation is up-regulated in breast, colon and melanoma whereas the α 2–6-linked sialylation is typically associated with liver, melanoma and ovarian cancers. The general trend for sialylated Lewis antigens x/y/a/b expression varies, although sLe^x has been found to be up-regulated in all cancers except for melanoma.

Secondly, core fucosylation also appears to correlate strongly with malignancy as evidenced by its observed high expression in breast, colon, ovarian and liver cancer and its association with increased cell adhesion and aggregation. Importantly, the presence of core fucosylated glycans on the cell surface is also largely mirrored by their presence in the sera for those cancers investigated, thereby substantiating the potential for further use of specific protein glycoforms for early cancer detection. As for the terminal fucosylated Lewis structures, no general trend was observed due to their differential expression in all five cancers, except for breast and colon cancer, in which Le^x and sLe^x corresponded to increased cell adhesion and reduced patient survival rates.

Additionally, although β 1–6 *N*-glycan branching is clearly implicated in all cancers reviewed, the role of bisecting-type *N*-glycans appears not to be universally associated with different cancers. In particular, their occurrence in ovarian and liver cancer correlated with metastasis and tumour progression but was found to suppress melanoma. Therefore, there appears to be some evidence to suggest that the functional role of bisecting glycans is cancer specific. However, more studies are needed to ascertain and elucidate the different mechanisms underlying this difference in expression of this *N*-glycan structure between cancer types.

Moreover, alterations in the expression of the truncated *O*-glycan, sTn, as well as high-mannose *N*-glycans, have been associated with the cancers reviewed. sTn was observed to be generally increased in breast, ovarian and colon cancers, and was associated with poorer prognosis, lower survival rates and metastatic progression. Whilst this suggests that they are implicated in cancer, the role of truncated *O*-glycans on aspects of cancer progression, such as cellular adhesion, is complex. On the other hand, for high-mannose *N*-glycans, there is evidence to suggest they are increased on the cell

surface of ovarian and liver cancers. Therefore, they may also be involved in cancer although their role is unknown at present.

Overall, alterations in the expression of sialylation, core fucosylation, truncation, bisecting and high-mannose glycans, and their implicated role in cancer progression strongly suggest differential regulation of their corresponding glycosyltransferases in cancer. In this regard, perhaps the most intriguing observations are the common increase of FUT8, ST3GAL1 and ST6GAL1 which accounts for the core fucosylated and sialylated glycans observed in most of these cancers. Although the expression of cell surface tumour-associated glycans is largely a result of the complex interplay between multiple glycosyltransferases in the glycosylation pathway, FUT8, ST3GAL1 and ST6GAL1 may produce key enzymatic alterations that can be targeted by inhibitors in future therapeutic applications, since the increased expression of glycan structures created by these enzymes has been observed in most of the cancers studied.

Although it is clear there are both similarities and differences in cell surface glycan expression between different cancers, it is also worth noting that this review encompasses the observations made on samples from both in vitro cultured cells as well as ex vivo tissues. This has yielded some discrepancies between data collected from both sample types such as notable differences in gene expression profiles from breast, colon and ovarian tumours compared to their cultured counterparts [17, 55]. This raises the question as to whether cell lines are a reliable source for investigating surface glycosylation changes in cancer that are clinically relevant and highlights the importance of validating in vitro discoveries in appropriate clinical samples, although sample availability is frequently limited. Nevertheless, while cell cultures may not capture the full complexity of glycan heterogeneity, use of these in vitro models has given some insight into the regulation of cell surface glycan expression and allows genomic manipulation to determine the biological impact of changes in the glycosylation pathway in the development and progression of cancer.

The majority of glycan expression studies reviewed here, including those with clinical samples, was carried out using targeted approaches, commonly immunohistochemistry with monoclonal antibodies or lectins against specific glycan epitopes. This approach has relatively high throughput, in which large patient cohorts can be studied and observations made with high statistical confidence. The non-targeted use of LC-MS/MS has been applied to a much lesser extent despite its potential for uncovering novel cancer-associated glycans. Current developments in glycan-specific chromatography, mass spectrometric workflows and bioinformatics tools will facilitate and increase the speed and accuracy of this type of data acquisition and analysis. Therefore, it is envisioned that the future expanded employment of LC-MS/MS combined with judicious use of cells lines and tissue samples, is likely to continue to discover cancer-specific glycan alterations, which together with associated cancer-specific glycoproteins, will

become strong candidate biomarkers and therapeutic targets for future cancer diagnosis and treatment.

The authors have declared no conflict of interest.

5 References

- [1] Varki, A., Biological roles of oligosaccharides: all of the theories are correct. *Glycobiology* 1993, **3**, 97–130.
- [2] Potapenko, I. O., Haakensen, V. D., Luders, T., Helland, A. et al., Glycan gene expression signatures in normal and malignant breast tissue; possible role in diagnosis and progression. *Mol. Oncol.* 2010, **4**, 98–118.
- [3] Dube, D. H., Bertozzi, C. R., Glycans in cancer and inflammation [mdash] potential for therapeutics and diagnostics. *Nat. Rev. Drug Discov.* 2005, **4**, 477–488.
- [4] Wei, T., Liu, Q., He, F., Zhu, W. et al., The role of N-acetylglucosaminyltransferases V in the malignancy of human hepatocellular carcinoma. *Exp. Mol. Pathol.* 2012, **93**, 8–17.
- [5] Julien, S., Ivetic, A., Grigoriadis, A., QiZe, D. et al., Selectin ligand Sialyl-Lewis x antigen drives metastasis of hormone-dependent breast cancers. *Cancer Res.* 2011, **71**, 7683–7693.
- [6] Kim, Y.-S., Ahn, Y. H., Song, K. J., Kang, J. G. et al., Overexpression and β -1,6-N-acetylglucosaminylation-initiated aberrant glycosylation of TIMP-1: a “double whammy” strategy in colon cancer progression. *J. Biol. Chem.* 2012, **287**, 32467–32478.
- [7] Liu, J. J., Lin, B., Hao, Y. Y., Li, F. F. et al., Lewis(y) antigen stimulates the growth of ovarian cancer cells via regulation of the epidermal growth factor receptor pathway. *Oncol. Rep.* 2010, **23**, 833–841.
- [8] Hoja-Lukowicz, D., Link-Lenczowski, P., Carpentieri, A., Amoresano, A. et al., L1CAM from human melanoma carries a novel type of N-glycan with Galbeta1-4Galbeta1-motif. Involvement of N-linked glycans in migratory and invasive behaviour of melanoma cells. *Glycoconj. J.* 2013, **30**, 205–225.
- [9] Jemal, A., Bray, F., Center, M. M., Ferlay, J. et al., Global cancer statistics. *CA: Cancer J. Clin.* 2011, **61**, 69–90.
- [10] Herlyn, M., Fukunaga-Kalabis, M., What is a good model for melanoma? *J. Invest. Dermatol.* 2010, **130**, 911–912.
- [11] Butler, M., Optimisation of the cellular metabolism of glycosylation for recombinant proteins produced by mammalian cell systems. *Cytotechnology* 2006, **50**, 57–76.
- [12] Kao, J., Salari, K., Bocanegra, M., Choi, Y.-L. et al., Molecular profiling of breast cancer cell lines defines relevant tumor models and provides a resource for cancer gene discovery. *PLoS One* 2009, **4**, e6146.
- [13] Neve, R. M., Chin, K., Fridlyand, J., Yeh, J. et al., A collection of breast cancer cell lines for the study of functionally distinct cancer subtypes. *Cancer Cell* 2006, **10**, 515–527.
- [14] Lacroix, M., Leclercq, G., Relevance of breast cancer cell lines as models for breast tumours: an update. *Breast Cancer Res. Treat* 2004, **83**, 249–289.
- [15] Yen, T.-Y., Macher, B. A., McDonald, C. A., Alleyne-Chin, C., Timpe, L. C., Glycoprotein profiles of human breast cells demonstrate a clear clustering of normal/benign versus malignant cell lines and basal versus luminal cell lines. *J. Proteome Res.* 2011, **11**, 656–667.
- [16] Tao, S.-C., Li, Y., Zhou, J., Qian, J. et al., Lectin microarrays identify cell-specific and functionally significant cell surface glycan markers. *Glycobiology* 2008, **18**, 761–769.
- [17] Gillet, J.-P., Varma, S., Gottesman, M. M., The clinical relevance of cancer cell lines. *J. Natl. Cancer Inst.* 2013, **105**, 452–458.
- [18] Houshdaran, S., Hawley, S., Palmer, C., Campan, M. et al., DNA methylation profiles of ovarian epithelial carcinoma tumors and cell lines. *PLoS One* 2010, **5**, e9359.
- [19] Tashiro, Y., Yonezawa, S., Kim, Y. S., Sato, E., Immunohistochemical study of mucin carbohydrates and core proteins in human ovarian tumors. *Hum. Pathol.* 1994, **25**, 364–372.
- [20] Ryuko, K., Iwanari, O., Kitao, M., Moriaki, S., Immunohistochemical evaluation of sialosyl-Tn antigens in various ovarian carcinomas. *Gynecol. Oncol.* 1993, **49**, 215–224.
- [21] Dietel, M., Discrimination between benign, borderline, and malignant epithelial ovarian tumors using tumor markers: an immunohistochemical study. *Cancer Detect. Prev.* 1983, **6**, 255–262.
- [22] Kobayashi, H., Terao, T., Kawashima, Y., Sialyl Tn as a prognostic marker in epithelial ovarian cancer. *Br. J. Cancer* 1992, **66**, 984–985.
- [23] Davidson, B., Berner, A., Nesland, J. M., Risberg, B. et al., Carbohydrate antigen expression in primary tumors, metastatic lesions, and serous effusions from patients diagnosed with epithelial ovarian carcinoma: evidence of up-regulated Tn and Sialyl Tn antigen expression in effusions. *Hum. Pathol.* 2000, **31**, 1081–1087.
- [24] Davidson, B., Gotlieb, W. H., Ben-Baruch, G., Kopolovic, J. et al., Expression of carbohydrate antigens in advanced-stage ovarian carcinomas and their metastases-A clinicopathologic study. *Gynecol. Oncol.* 2000, **77**, 35–43.
- [25] Zaia, J., Mass spectrometry and glycomics. *OMICS* 2010, **14**, 401–418.
- [26] Wu, A. M., Lisowska, E., Duk, M., Yang, Z., Lectins as tools in glycoconjugate research. *Glycoconj. J.* 2009, **26**, 899–913.
- [27] Handerson, T., Camp, R., Harigopal, M., Rimm, D., Pawelek, J., β 1,6-Branched oligosaccharides are increased in lymph node metastases and predict poor outcome in breast carcinoma. *Clin. Cancer Res.* 2005, **11**, 2969–2973.
- [28] Fernandes, B., Sagman, U., Auger, M., Demetrio, M., Dennis, J. W., β 1–6 Branched oligosaccharides as a marker of tumor progression in human breast and colon neoplasia. *Cancer Res.* 1991, **51**, 718–723.
- [29] Cui, H., Lin, Y., Yue, L., Zhao, X., Liu, J., Differential expression of the alpha2,3-sialic acid residues in breast cancer is associated with metastatic potential. *Oncol. Rep.* 2011, **25**, 1365–1371.
- [30] Taeda, Y., Nose, M., Hiraizumi, S., Ohuchi, N., Expression of L-PHA-binding proteins in breast cancer: reconstitution and molecular characterization of beta 1–6 branched

- oligosaccharides in three-dimensional cell culture. *Breast Cancer Res. Treat.* 1996, **38**, 313–324.
- [31] Fukasawa, T., Asao, T., Yamauchi, H., Ide, M. et al., Associated expression of alpha2,3sialylated type 2 chain structures with lymph node metastasis in distal colorectal cancer. *Surg. Today* 2013, **43**, 155–162.
- [32] Drake, P. M., Schilling, B., Niles, R. K., Prakobphol, A. et al., Lectin chromatography/mass spectrometry discovery workflow identifies putative biomarkers of aggressive breast cancers. *J. Proteome Res.* 2012, **11**, 2508–2520.
- [33] Abbott, K. L., Lim, J. M., Wells, L., Benigno, B. B. et al., Identification of candidate biomarkers with cancer-specific glycosylation in the tissue and serum of endometrioid ovarian cancer patients by glycoproteomic analysis. *Proteomics* 2010, **10**, 470–481.
- [34] Kremser, M. E., Przybylo, M., Hoja-Lukowicz, D., Pohec, E. et al., Characterisation of alpha3beta1 and alpha(v)beta3 integrin N-oligosaccharides in metastatic melanoma WM9 and WM239 cell lines. *Biochim. Biophys. Acta* 2008, **1780**, 1421–1431.
- [35] Brooks, S. A., Hall, D. M. S., Buley, I., GalNAc glycoprotein expression by breast cell lines, primary breast cancer and normal breast epithelial membrane. *Br. J. Cancer* 2001, **85**, 1014–1022.
- [36] Rambaruth, N. D. S., Greenwell, P., Dwek, M. V., The lectin Helix pomatia agglutinin recognises O-GlcNAc containing glycoproteins in human breast cancer. *Glycobiology* 2012, **22**, 839–848.
- [37] Litynska, A., Przybylo, M., Pohec, E., Hoja-Lukowicz, D. et al., Comparison of the lectin-binding pattern in different human melanoma cell lines. *Melanoma Res.* 2001, **11**, 205–212.
- [38] Laidler, P., Litynska, A., Hoja-Lukowicz, D., Labedz, M. et al., Characterization of glycosylation and adherent properties of melanoma cell lines. *Cancer Immunol. Immunother.* 2006, **55**, 112–118.
- [39] Chen, S., Zheng, T., Shortreed, M. R., Alexander, C., Smith, L. M., Analysis of cell surface carbohydrate expression patterns in normal and tumorigenic human breast cell lines using lectin arrays. *Anal. Chem.* 2007, **79**, 5698–5702.
- [40] Madjd, Z., Parsons, T., Watson, N., Spendlove, I. et al., High expression of Lewisy/b antigens is associated with decreased survival in lymph node negative breast carcinomas. *Breast Cancer Res.* 2005, **7**, R780–R787.
- [41] Sakamoto, J., Furukawa, K., Cordon-Cardo, C., Yin, B. W. T. et al., Expression of Lewis, Lewisb, X, and Y blood group antigens in human colonic tumors and normal tissue and in human tumor-derived cell lines. *Cancer Res.* 1986, **46**, 1553–1561.
- [42] Itzkowitz, S. H., Yuan, M., Montgomery, C. K., Kjeldsen, T. et al., Expression of Tn, sialosyl-Tn, and T antigens in human colon cancer. *Cancer Res.* 1989, **49**, 197–204.
- [43] Abbott, K. L., Aoki, K., Lim, J.-M., Porterfield, M. et al., Targeted glycoproteomic identification of biomarkers for human breast carcinoma. *J. Proteome Res.* 2008, **7**, 1470–1480.
- [44] North, S. J., Huang, H.-H., Sundaram, S., Jang-Lee, J. et al., Glycomics profiling of Chinese hamster ovary cell glycosylation mutants reveals N-glycans of a novel size and complexity. *J. Biol. Chem.* 2010, **285**, 5759–5775.
- [45] Balog, C. I. A., Stavenhagen, K., Fung, W. L. J., Koeleman, C. A. et al., N-glycosylation of colorectal cancer tissues. *Mol. Cell. Proteomics* 2012, **11**, 571–585.
- [46] Kirmiz, C., Li, B., An, H. J., Clowers, B. H. et al., A serum glycomics approach to breast cancer biomarkers. *Mol. Cell. Proteomics* 2007, **6**, 43–55.
- [47] Machado, E., Kandzia, S., Carilho, R., Altevogt, P. et al., N-Glycosylation of total cellular glycoproteins from the human ovarian carcinoma SKOV3 cell line and of recombinantly expressed human erythropoietin. *Glycobiology* 2011, **21**, 376–386.
- [48] Robbe-Masselot, C., Herrmann, A., Maes, E., Carlstedt, I. et al., Expression of a core 3 disialyl-Le(x) hexasaccharide in human colorectal cancers: a potential marker of malignant transformation in colon. *J. Proteome Res.* 2009, **8**, 702–711.
- [49] Larsson, J. M., Karlsson, H., Crespo, J. G., Johansson, M. E. et al., Altered O-glycosylation profile of MUC2 mucin occurs in active ulcerative colitis and is associated with increased inflammation. *Inflamm. Bowel Dis.* 2011, **17**, 2299–2307.
- [50] Holmén Larsson, J. M., Karlsson, H., Sjövall, H., Hansson, G. C., A complex, but uniform O-glycosylation of the human MUC2 mucin from colonic biopsies analyzed by nanoLC/MSn. *Glycobiology* 2009, **19**, 756–766.
- [51] Deshpande, N., Jensen, P. H., Packer, N. H., Kolarich, D., GlycoSpectrumScan: fishing glycopeptides from MS spectra of protease digests of human colostrum sIgA. *J. Proteome Res.* 2009, **9**, 1063–1075.
- [52] Apte, A., Meitei, N., in: Li, J. (Ed.), *Functional Glycomics*, Humana Press 2010, pp. 269–281.
- [53] Abbott, K. L., Nairn, A. V., Hall, E. M., Horton, M. B. et al., Focused glycomic analysis of the N-linked glycan biosynthetic pathway in ovarian cancer. *Proteomics* 2008, **8**, 3210–3220.
- [54] Wang, P. H., Lee, W. L., Juang, C. M., Yang, Y. H. et al., Altered mRNA expressions of sialyltransferases in ovarian cancers. *Gynecol. Oncol.* 2005, **99**, 631–639.
- [55] Hanski, C., Klusmann, E., Wang, J., Böhm, C. et al., Fucosyltransferase III and sialyl-Le(x) expression correlate in cultured colon carcinoma cells but not in colon carcinoma tissue. *Glycoconj. J.* 1996, **13**, 727–733.
- [56] Ito, Y., Miyoshi, E., Sakon, M., Takeda, T. et al., Elevated expression of UDP-N-acetylglucosamine: α -mannoside β 1,6 N-acetylglucosaminyltransferase is an early event in hepatocarcinogenesis. *Int. J. Cancer* 2001, **91**, 631–637.
- [57] Kudo, T., Ikehara, Y., Togayachi, A., Morozumi, K. et al., Up-regulation of a set of glycosyltransferase genes in human colorectal cancer. *Lab. Invest.* 1998, **78**, 797–811.
- [58] Trinchera, M., Malagolini, N., Chiricolo, M., Santini, D. et al., The biosynthesis of the selectin-ligand sialyl Lewis x in colorectal cancer tissues is regulated by fucosyltransferase VI and can be inhibited by an RNA interference-based approach. *Int. J. Biochem. Cell Biol.* 2011, **43**, 130–139.

- [59] Yang, J. M., Byrd, J. C., Siddiki, B. B., Chung, Y. S. et al., Alterations of O-glycan biosynthesis in human colon cancer tissues. *Glycobiology* 1994, 4, 873–884.
- [60] Brockhausen, I., Yang, J. M., Burchell, J., Whitehouse, C., Taylor-Papadimitriou, J., Mechanisms underlying aberrant glycosylation of MUC1 mucin in breast cancer cells. *Eur. J. Biochem.* 1995, 233, 607–617.
- [61] Raval, G. N., Parekh, L. J., Patel, D. D., Jha, F. P. et al., Clinical usefulness of alterations in sialic acid, sialyl transferase and sialoproteins in breast cancer. *Indian J. Clin. Biochem.* 2004, 19, 60–71.
- [62] Julien, S., Krzewinski-Recchi, M. A., Harduin-Lepers, A., Gouyer, V. et al., Expression of sialyl-Tn antigen in breast cancer cells transfected with the human CMP-Neu5Ac:GalNAc α 2,6-sialyltransferase (ST6GalNAc I) cDNA. *Glycoconj. J.* 2001, 18, 883–893.
- [63] Lin, S., Kemmner, W., Grigull, S., Schlag, P. M., Cell Surface [alpha]2,6-sialylation affects adhesion of breast carcinoma cells. *Exp. Cell Res.* 2002, 276, 101–110.
- [64] Kuan, S. F., Byrd, J. C., Basbaum, C. B., Kim, Y. S., Characterization of quantitative mucin variants from a human colon cancer cell line. *Cancer Res.* 1987, 47, 5715–5724.
- [65] Perou, C., Sorlie, T., Eisen, M., Rijn, M. et al., Molecular portraits of human breast tumours. *Nature* 2000, 406, 747–752.
- [66] Dennis, J., Laferte, S., Waghorne, C., Breitman, M., Kerbel, R., Beta 1–6 branching of Asn-linked oligosaccharides is directly associated with metastasis. *Science* 1987, 236, 582–585.
- [67] Vredenburg, J. J., Simpson, W., Memoli, V. A., Ball, E. D., Reactivity of anti-CD15 monoclonal antibody PM-81 with breast cancer and elimination of breast cancer cells from human bone marrow by PM-81 and immunomagnetic beads. *Cancer Res.* 1991, 51, 2451–2455.
- [68] Imai, J., Ghazizadeh, M., Naito, Z., Asano, G., Immunohistochemical expression of T, Tn and sialyl-Tn antigens and clinical outcome in human breast carcinoma. *Anticancer Res.* 2001, 21, 1327–1334.
- [69] Renkonen, J., Paavonen, T., Renkonen, R., Endothelial and epithelial expression of sialyl Lewis x and sialyl Lewis a in lesions of breast carcinoma. *Int. J. Cancer* 1997, 74, 296–300.
- [70] Kyselova, Z., Mechref, Y., Kang, P., Goetz, J. A. et al., Breast cancer diagnosis and prognosis through quantitative measurements of serum glycan profiles. *Clin. Chem.* 2008, 54, 1166–1175.
- [71] Dennis, J. W., Laferte, S., Onco developmental expression of -GlcNAc β 1–6Man α 1–6Man β 1- branched asparagine-linked oligosaccharides in murine tissues and human breast carcinomas. *Cancer Res.* 1989, 49, 945–950.
- [72] Burchell, J., Poulsom, R., Hanby, A., Whitehouse, C. et al., An α 2,3 sialyltransferase (ST3Gal I) is elevated in primary breast carcinomas. *Glycobiology* 1999, 9, 1307–1311.
- [73] Wu, C., Guo, X., Wang, W., Wang, Y. et al., N-Acetylgalactosaminyltransferase-14 as a potential biomarker for breast cancer by immunohistochemistry. *BMC Cancer* 2010, 10, 123.
- [74] Recchi, M. A., Hebbbar, M., Hornez, L., Harduin-Lepers, A. et al., Multiplex reverse transcription polymerase chain reaction assessment of sialyltransferase expression in human breast cancer. *Cancer Res.* 1998, 58, 4066–4070.
- [75] Nakagoe, T., Fukushima, K., Itoyanagi, N., Ikuta, Y. et al., Expression of ABH/Lewis-related antigens as prognostic factors in patients with breast cancer. *J. Cancer Res. Clin. Oncol.* 2002, 128, 257–264.
- [76] Abd Hamid, U. M., Royle, L., Saldova, R., Radcliffe, C. M. et al., A strategy to reveal potential glycan markers from serum glycoproteins associated with breast cancer progression. *Glycobiology* 2008, 18, 1105–1118.
- [77] Saldova, R., Reuben, J. M., Abd Hamid, U. M., Rudd, P. M., Cristofanilli, M., Levels of specific serum N-glycans identify breast cancer patients with higher circulating tumor cell counts. *Ann. Oncol.* 2011, 22, 1113–1119.
- [78] Alley, W. R., Madera, M., Mechref, Y., Novotny, M. V., Chip-based reversed-phase liquid chromatography–mass spectrometry of permethylated N-linked glycans: a potential methodology for cancer-biomarker discovery. *Anal. Chem.* 2010, 82, 5095–5106.
- [79] de Leoz, M. L. A., Young, L. J. T., An, H. J., Kronewitter, S. R. et al., High-mannose glycans are elevated during breast cancer progression. *Mol. Cell. Proteomics* 2011, 10, M110.002717.
- [80] Listinsky, J. J., Siegal, G. P., Listinsky, C. M., The emerging importance of α -L-fucose in human breast cancer: a review. *Am. J. Transl. Res.* 2011, 3, 292–322.
- [81] Apweiler, R., Hermjakob, H., Sharon, N., On the frequency of protein glycosylation, as deduced from analysis of the SWISS-PROT database. *Biochim. Biophys. Acta* 1999, 1473, 4–8.
- [82] Misonou, Y., Shida, K., Korekane, H., Seki, Y. et al., Comprehensive clinico-glycomics study of 16 colorectal cancer specimens: elucidation of aberrant glycosylation and its mechanistic causes in colorectal cancer cells. *J. Proteome Res.* 2009, 8, 2990–3005.
- [83] Hundt, S., Haug, U., Brenner, H., Blood markers for early detection of colorectal cancer: a systematic review. *Cancer Epidemiol. Biomarkers Prev.* 2007, 16, 1935–1953.
- [84] Bresalier, R. S., Ho, S. B., Schoepfner, H. L., Kim, Y. S. et al., Enhanced sialylation of mucin-associated carbohydrate structures in human colon cancer metastasis. *Gastroenterology* 1996, 110, 1354–1367.
- [85] Malagolini, N., Santini, D., Chiricolo, M., Dall'Olio, F., Biosynthesis and expression of the Sda and sialyl Lewis x antigens in normal and cancer colon. *Glycobiology* 2007, 17, 688–697.
- [86] Uemura, T., Shiozaki, K., Yamaguchi, K., Miyazaki, S. et al., Contribution of sialidase NEU1 to suppression of metastasis of human colon cancer cells through desialylation of integrin β 4. *Oncogene* 2009, 28, 1218–1229.
- [87] Osumi, D., Takahashi, M., Miyoshi, E., Yokoe, S. et al., Core fucosylation of E-cadherin enhances cell-cell adhesion in human colon carcinoma WiDr cells. *Cancer Sci.* 2009, 100, 888–895.

- [88] Bu, X. D., Li, N., Tian, X. Q., Huang, P. L., Caco-2 and LS174T cell lines provide different models for studying mucin expression in colon cancer. *Tissue Cell* 2011, 43, 201–206.
- [89] Bresalier, R. S., Niv, Y., Byrd, J. C., Duh, Q. Y. et al., Mucin production by human colonic carcinoma cells correlates with their metastatic potential in animal models of colon cancer metastasis. *J. Clin. Invest.* 1991, 87, 1037–1045.
- [90] Vavasseur, F., Dole, K., Yang, J., Matta, K. L. et al., O-Glycan biosynthesis in human colorectal adenoma cells during progression to cancer. *Eur. J. Biochem.* 1994, 222, 415–424.
- [91] Ma, Y. C., Yang, J. Y., Yan, L. N., Relevant markers of cancer stem cells indicate a poor prognosis in hepatocellular carcinoma patients: a meta-analysis. *Eur. J. Gastroenterol. Hepatol.* 2013, 25, 1007–1016.
- [92] El-Serag, H. B., Rudolph, K. L., Hepatocellular carcinoma: epidemiology and molecular carcinogenesis. *Gastroenterology* 2007, 132, 2557–2576.
- [93] Hernandez-Gea, V., Turon, F., Berzigotti, A., Villanueva, A., Management of small hepatocellular carcinoma in cirrhosis: focus on portal hypertension. *World J. Gastroenterol.* 2013, 19, 1193–1199.
- [94] Padhya, K. T., Marrero, J. A., Singal, A. G., Recent advances in the treatment of hepatocellular carcinoma. *Curr. Opin. Gastroenterol.* 2013, 29, 285–292.
- [95] Adamczyk, B., Tharmalingam, T., Rudd, P. M., Glycans as cancer biomarkers. *Biochim. Biophys. Acta* 2012, 1820, 1347–1353.
- [96] Oda, K., Ido, A., Tamai, T., Matsushita, M. et al., Highly sensitive lens culinaris agglutinin-reactive alpha-fetoprotein is useful for early detection of hepatocellular carcinoma in patients with chronic liver disease. *Oncol. Rep.* 2011, 26, 1227–1233.
- [97] Moriya, S., Morimoto, M., Numata, K., Nozaki, A. et al., Fucosylated fraction of alpha-fetoprotein as a serological marker of early hepatocellular carcinoma. *Anticancer Res.* 2013, 33, 997–1001.
- [98] Taniguchi, N., Toward cancer biomarker discovery using the glycomics approach. *Proteomics* 2008, 8, 3205–3208.
- [99] Dai, Z., Zhou, J., Qiu, S. J., Liu, Y. K., Fan, J., Lectin-based glycoproteomics to explore and analyze hepatocellular carcinoma-related glycoprotein markers. *Electrophoresis* 2009, 30, 2957–2966.
- [100] Debruyne, E. N., Delanghe, J. R., Diagnosing and monitoring hepatocellular carcinoma with alpha-fetoprotein: new aspects and applications. *Clin. Chim. Acta* 2008, 395, 19–26.
- [101] Yamashiki, N., Seki, T., Wakabayashi, M., Nakagawa, T. et al., Usefulness of *Lens culinaris* agglutinin A-reactive fraction of alpha-fetoprotein (AFP-L3) as a marker of distant metastasis from hepatocellular carcinoma. *Oncol. Rep.* 1999, 6, 1229–1232.
- [102] Kumada, T., Nakano, S., Takeda, I., Kiriya, S. et al., Clinical utility of *Lens culinaris* agglutinin-reactive alpha-fetoprotein in small hepatocellular carcinoma: special reference to imaging diagnosis. *J. Hepatol.* 1999, 30, 125–130.
- [103] Taketa, K., Endo, Y., Sekiya, C., Tanikawa, K. et al., A collaborative study for the evaluation of lectin-reactive alpha-fetoproteins in early detection of hepatocellular carcinoma. *Cancer Res.* 1993, 53, 5419–5423.
- [104] Li, D., Mallory, T., Satomura, S., AFP-L3: a new generation of tumor marker for hepatocellular carcinoma. *Clin. Chim. Acta* 2001, 313, 15–19.
- [105] Takada, A., Ohmori, K., Yoneda, T., Tsuyukawa, K. et al., Contribution of carbohydrate antigens sialyl Lewis A and sialyl Lewis X to adhesion of human cancer cells to vascular endothelium. *Cancer Res.* 1993, 53, 354–361.
- [106] Dall'Olio, F., Chiricolo, M., D'Errico, A., Gruppioni, E. et al., Expression of β -galactoside α 2,6 sialyltransferase and of α 2,6-sialylated glycoconjugates in normal human liver, hepatocarcinoma, and cirrhosis. *Glycobiology* 2004, 14, 39–49.
- [107] Mehta, A., Norton, P., Liang, H., Comunale, M. A. et al., Increased levels of tetra-antennary N-linked glycan but not core fucosylation are associated with hepatocellular carcinoma tissue. *Cancer Epidemiol. Biomarkers Prev.* 2012, 21, 925–933.
- [108] Blomme, B., Van Steenkiste, C., Callewaert, N., Van Vlierberghe, H., Alteration of protein glycosylation in liver diseases. *J. Hepatol.* 2009, 50, 592–603.
- [109] Hutchinson, W. L., Du, M.-Q., Johnson, P. J., Williams, R., Fucosyltransferases: differential plasma and tissue alterations in hepatocellular carcinoma and cirrhosis. *Hepatology* 1991, 13, 683–688.
- [110] Yao, M., Zhou, D.-P., Jiang, S.-M., Wang, Q.-H. et al., Elevated activity of N-acetylglucosaminyltransferase V in human hepatocellular carcinoma. *J. Cancer Res. Clin. Oncol.* 1998, 124, 27–30.
- [111] Passaniti, A., Hart, G. W., Cell surface sialylation and tumor metastasis. Metastatic potential of B16 melanoma variants correlates with their relative numbers of specific penultimate oligosaccharide structures. *J. Biol. Chem.* 1988, 263, 7591–7603.
- [112] Kawano, T., Takasaki, S., Tao, T. W., Kobata, A., N-linked sugar chains of mouse B16 melanoma cells and their low-metastasizing variant selected by wheat germ agglutinin. *Glycobiology* 1991, 1, 375–385.
- [113] Gorelik, E., Xu, F., Henion, T., Anaraki, F., Galili, U., Reduction of metastatic properties of BL6 melanoma cells expressing terminal fucose(α)1–2-galactose after α 1,2-fucosyltransferase cDNA transfection. *Cancer Res.* 1997, 57, 332–336.
- [114] Ochwat, D., Hoja-Lukowicz, D., Litynska, A., N-glycoproteins bearing beta1–6 branched oligosaccharides from the A375 human melanoma cell line analysed by tandem mass spectrometry. *Melanoma Res.* 2004, 14, 479–485.
- [115] Yoshimura, M., Ihara, Y., Matsuzawa, Y., Taniguchi, N., Aberrant glycosylation of E-cadherin enhances cell-cell binding to suppress metastasis. *J. Biol. Chem.* 1996, 271, 13811–13815.
- [116] Jemal, A., Siegel, R., Xu, J., Ward, E., Cancer statistics, 2010. *CA. Cancer J. Clin.* 2010, 60, 277–300.
- [117] Narod, S. A., Boyd, J., Current understanding of the epidemiology and clinical implications of BRCA1 and BRCA2

- mutations for ovarian cancer. *Curr. Opin. Obstet. Gynecol.* 2002, **14**, 19–26.
- [118] Alberts, D. S., Markman, M., Muggia, F., Ozols, R. F. et al., Proceedings of a GOG workshop on intraperitoneal therapy for ovarian cancer. *Gynecol. Oncol.* 2006, **103**, 783–792.
- [119] Fishman, D. A., Bozorgi, K., The scientific basis of early detection of epithelial ovarian cancer: the National Ovarian Cancer Early Detection Program (NOCEDP). *Cancer Treat. Res.* 2002, **107**, 3–28.
- [120] Ozols, R. F., Systemic therapy for ovarian cancer: current status and new treatments. *Semin. Oncol.* 2006, **33**, S3–S11.
- [121] Vician, M., Hrbaty, B., Vrtik, L., Simo, J. et al., (Surgical treatment of acute diverticulitis of the large intestine). *Rozhledy v. chirurgii : mesicnik Ceskoslovenske chirurgicke spolecnosti.* 2000, **79**, 275–278.
- [122] Crawford, S. C., Vasey, P. A., Paul, J., Hay, A. et al., Does aggressive surgery only benefit patients with less advanced ovarian cancer? Results from an international comparison within the SCOTROC-1 Trial. *J. Clin. Oncol.* 2005, **23**, 8802–8811.
- [123] Eltabbakh, G. H., Mount, S. L., Beatty, B., Simmons-Arnold, L. et al., Factors associated with cytoreducibility among women with ovarian carcinoma. *Gynecol. Oncol.* 2004, **95**, 377–383.
- [124] Bhoola, S., Hoskins, W. J., Diagnosis and management of epithelial ovarian cancer. *Obstet. Gynecol.* 2006, **107**, 1399–1410.
- [125] Friedlander, M., Buck, M., Wyld, D., Findlay, M. et al., Phase II study of carboplatin followed by sequential gemcitabine and paclitaxel as first-line treatment for advanced ovarian cancer. *Int. J. Gynecol. Cancer* 2007, **17**, 350–358.
- [126] Federici, M. F., Kudryashov, V., Saigo, P. E., Finstad, C. L., Lloyd, K. O., Selection of carbohydrate antigens in human epithelial ovarian cancers as targets for immunotherapy: serous and mucinous tumors exhibit distinctive patterns of expression. *Int. J. Cancer* 1999, **81**, 193–198.
- [127] Jacob, F., Goldstein, D. R., Fink, D., Heinzlmann-Schwarz, V., Proteogenomic studies in epithelial ovarian cancer: established knowledge and future needs. *Biomark. Med.* 2009, **3**, 743–756.
- [128] Annunziata, C. M., Azad, N., Dharmoon, A. S., Whiteley, G., Kohn, E. C., Ovarian cancer in the proteomics era. *Int. J. Gynecol. Cancer* 2008, **18**(Suppl 1), 1–6.
- [129] Nossov, V., Amneus, M., Su, F., Lang, J. et al., The early detection of ovarian cancer: from traditional methods to proteomics. Can we really do better than serum CA-125? *Am. J. Obstet. Gynecol.* 2008, **199**, 215–223.
- [130] Saldova, R., Dempsey, E., Perez-Garay, M., Marino, K. et al., 5-AZA-2'-deoxycytidine induced demethylation influences N-glycosylation of secreted glycoproteins in ovarian cancer. *Epigenetics* 2011, **6**, 1362–1372.
- [131] Kui Wong, N., Easton, R. L., Panico, M., Sutton-Smith, M. et al., Characterization of the oligosaccharides associated with the human ovarian tumor marker CA125. *J. Biol. Chem.* 2003, **278**, 28619–28634.
- [132] Christie, D. R., Shaikh, F. M., Lucas, J. A. t., Lucas, J. A., 3rd, Bellis, S. L., ST6Gal-I expression in ovarian cancer cells promotes an invasive phenotype by altering integrin glycosylation and function. *J. Ovarian. Res.* 2008, **1**, 3. doi: 10.1186/1757-2215-1-3.
- [133] Yu, S. Y., Chang, L. Y., Cheng, C. W., Chou, C. C. et al., Priming mass spectrometry-based sulfoglycomic mapping for identification of terminal sulfated lacdiNAc glycotope. *Glycoconj. J.* 2013, **30**, 183–194.
- [134] Escrevente, C., Machado, E., Brito, C., Reis, C. A. et al., Different expression levels of alpha3/4 fucosyltransferases and Lewis determinants in ovarian carcinoma tissues and cell lines. *Int. J. Oncol.* 2006, **29**, 557–566.
- [135] Satomaa, T., Heiskanen, A., Leonardsson, I., Angstrom, J. et al., Analysis of the human cancer glycome identifies a novel group of tumor-associated N-acetylglucosamine glycan antigens. *Cancer Res.* 2009, **69**, 5811–5819.
- [136] Kindelberger, D. W., Lee, Y., Miron, A., Hirsch, M. S. et al., Intraepithelial carcinoma of the fimbria and pelvic serous carcinoma: evidence for a causal relationship. *Am. J. Surg. Pathol.* 2007, **31**, 161–169.
- [137] Lee, Y., Miron, A., Drapkin, R., Nucci, M. R. et al., A candidate precursor to serous carcinoma that originates in the distal fallopian tube. *J. Pathol.* 2007, **211**, 26–35.
- [138] Jarboe, E., Folkins, A., Nucci, M. R., Kindelberger, D. et al., Serous carcinogenesis in the fallopian tube: a descriptive classification. *Int. J. Gynecol. Pathol.* 2008, **27**, 1–9.
- [139] Jacob, F., Goldstein, D. R., Bovin, N. V., Pochechueva, T. et al., Serum antiglycan antibody detection of nonmucinous ovarian cancers by using a printed glycan array. *Int. J. Cancer.* 2012, **130**, 138–146.
- [140] Colombo, N., Peiretti, M., Parma, G., Lapresa, M. et al., Newly diagnosed and relapsed epithelial ovarian carcinoma: ESMO Clinical Practice Guidelines for diagnosis, treatment and follow-up. *Ann. Oncol.* 2010, **21** (Suppl 5), v23–v30.
- [141] Wang, P. H., Altered glycosylation in cancer: sialic acids and sialyltransferases. *J. Cancer Mol.* 2005, **1**, 73–81.
- [142] Varki, A., Schauer, R., *Essentials of Glycobiology*, Cold Spring Harbor Laboratory Press, Cold Spring Harbor (NY) 2009.
- [143] Tsuji, S., Molecular cloning and functional analysis of sialyltransferases. *J. Biochem.* 1996, **120**, 1–13.
- [144] Ugorski, M., Laskowska, A., Sialyl Lewis(a): a tumor-associated carbohydrate antigen involved in adhesion and metastatic potential of cancer cells. *Acta Biochim. Pol.* 2002, **49**, 303–311.
- [145] Nakamori, S., Kameyama, M., Imaoka, S., Furukawa, H. et al., Increased expression of Sialyl Lewisx antigen correlates with poor survival in patients with colorectal carcinoma: Clinicopathological and Immunohistochemical Study. *Cancer Res.* 1993, **53**, 3632–3637.
- [146] Ravindranath, M. H., Amiri, A. A., Bauer, P. M., Kelley, M. C. et al., Endothelial-selectin ligands sialyl Lewis(x) and sialyl Lewis(a) are differentiation antigens immunogenic in human melanoma. *Cancer* 1997, **79**, 1686–1697.

- [147] Renkonen, J., Paavonen, T., Renkonen, R., Endothelial and epithelial expression of sialyl Lewis(x) and sialyl Lewis(a) in lesions of breast carcinoma. *Int. J. Cancer* 1997, **74**, 296–300.
- [148] Narita, T., Funahashi, H., Satoh, Y., Watanabe, T. et al., Association of expression of blood group-related carbohydrate antigens with prognosis in breast cancer. *Cancer* 1993, **71**, 3044–3053.
- [149] Jeschke, U., Mylonas, I., Shabani, N., Kunert-Keil, C. et al., Expression of sialyl lewis X, sialyl Lewis A, E-cadherin and cathepsin-D in human breast cancer: immunohistochemical analysis in mammary carcinoma in situ, invasive carcinomas and their lymph node metastasis. *Anticancer Res.* 2005, **25**, 1615–1622.
- [150] Nakagoe, T., Fukushima, K., Nanashima, A., Sawai, T. et al., Expression of Lewis(a), sialyl Lewis(a), Lewis(x) and sialyl Lewis(x) antigens as prognostic factors in patients with colorectal cancer. *Can. J. Gastroenterol.* 2000, **14**, 753–760.
- [151] Jagirdar, J., Thung, S. N., Shah, K. D., Nudelman, E. et al., Expression of sialylated Lewis(x) antigen in chronic and neoplastic liver diseases. *Arch. Pathol. Lab. Med.* 1992, **116**, 643–648.
- [152] Ohyama, C., Tsuboi, S., Fukuda, M., Dual roles of sialyl Lewis X oligosaccharides in tumor metastasis and rejection by natural killer cells. *EMBO J.* 1999, **18**, 1516–1525.
- [153] Hebbar, M., Krzewinski-Recchi, M. A., Hornez, L., Verdier, A. et al., Prognostic value of tumoral sialyltransferase expression and circulating E-selectin concentrations in node-negative breast cancer patients. *Int. J. Biol. Markers* 2003, **18**, 116–122.
- [154] Dall'Olio, F., The sialyl- α 2,6-lactosaminy-structure: Biosynthesis and functional role. *Glycoconj. J.* 2000, **17**, 669–676.
- [155] Martersteck, C. M., Kedersha, N. L., Drapp, D. A., Tsui, T. G., Colley, K. J., Unique alpha 2, 8-polysialylated glycoproteins in breast cancer and leukemia cells. *Glycobiology* 1996, **6**, 289–301.
- [156] Becker, D. J., Lowe, J. B., Fucose: biosynthesis and biological function in mammals. *Glycobiology* 2003, **13**, 41R–53R.
- [157] Zhao, Y.-Y., Takahashi, M., Gu, J.-G., Miyoshi, E. et al., Functional roles of N-glycans in cell signaling and cell adhesion in cancer. *Cancer Sci.* 2008, **99**, 1304–1310.
- [158] Liu, Y.-C., Yen, H.-Y., Chen, C.-Y., Chen, C.-H. et al., Sialylation and fucosylation of epidermal growth factor receptor suppress its dimerization and activation in lung cancer cells. *Proc. Natl. Acad. Sci.* 2011, **108**, 11332–11337.
- [159] Alley, W. R., Jr., Vasseur, J. A., Goetz, J. A., Svoboda, M. et al., N-linked glycan structures and their expressions change in the blood sera of ovarian cancer patients. *J. Proteome Res.* 2012, **11**, 2282–2300.
- [160] Miyoshi, E., Moriwaki, K., Nakagawa, T., Biological function of fucosylation in cancer biology. *J. Biochem.* 2008, **143**, 725–729.
- [161] Ji, J., Gu, X., Fang, M., Zhao, Y. et al., Expression of alpha 1,6-fucosyltransferase 8 in hepatitis B virus-related hepatocellular carcinoma influences tumour progression. *Digest. Liver Dis.* 2013, **45**, 414–421.
- [162] Niv, Y., Byrd, J. C., Ho, S. B., Dahiya, R., Kim, Y. S., Mucin synthesis and secretion in relation to spontaneous differentiation of colon cancer cells in vitro. *Int. J. Cancer* 1992, **50**, 147–152.
- [163] Chen, T. R., Drabkowski, D., Hay, R. J., Macy, M., Peterson, W., Jr., WiDr is a derivative of another colon adenocarcinoma cell line, HT-29. *Cancer Genet. Cytogenet.* 1987, **27**, 125–134.
- [164] Noguchi, P., Wallace, R., Johnson, J., Earley, E. M. et al., Characterization of WiDr: a human colon carcinoma cell line. *In Vitro* 1979, **15**, 401–408.
- [165] Kawasaki, N., Lin, C. W., Inoue, R., Khoo, K. H. et al., Highly fucosylated N-glycan ligands for mannan-binding protein expressed specifically on CD26 (DPPVI) isolated from a human colorectal carcinoma cell line, SW1116. *Glycobiology* 2009, **19**, 437–450.
- [166] Ferrara, C., Grau, S., Jäger, C., Sondermann, P. et al., Unique carbohydrate-carbohydrate interactions are required for high affinity binding between Fc γ RIII and antibodies lacking core fucose. *Proc. Natl. Acad. Sci.* 2011, **108**, 12669–12674.
- [167] Miyoshi, E., Moriwaki, K., Nakagawa, T., Biological function of fucosylation in cancer biology. *J. Biochem.* 2008, **143**, 725–729.
- [168] Kannagi, R., in: Taniguchi, N., Honke, K., Fukuda, M., Clausen, H., et al. (Eds.), *Handbook of Glycosyltransferases and Related Genes*, Springer, Japan 2002, pp. 237–245.
- [169] Matsuura, N., Narita, T., Hiraiwa, N., Hiraiwa, M. et al., Gene expression of fucosyl- and sialyl-transferases which synthesize sialyl Lewis(x), the carbohydrate ligands for E-selectin, in human breast cancer. *Int. J. Oncol.* 1998, **12**, 1157–1164.
- [170] Ura, Y., Dion, A. S., Williams, C. J., Olsen, B. D. et al., Quantitative dot blot analyses of blood-group-related antigens in paired normal and malignant human breast tissues. *Int. J. Cancer* 1992, **50**, 57–63.
- [171] Elola, M. T., Capurro, M. I., Barrio, M. M., Coombs, P. J. et al., Lewis x antigen mediates adhesion of human breast carcinoma cells to activated endothelium. *Possible involvement of the endothelial scavenger receptor C-type lectin.* *Breast Cancer Res. Treat.* 2007, **101**, 161–174.
- [172] Yue, L., Yu, H., Zhang, C., Liu, J., The effect of overexpression of α 1,3-fucosyltransferase VII on adhesive capability of human colon carcinoma HT-29 cells to HUVECs. *Adv. Mat. Res.* 2012, **345**, 250–256.
- [173] Basu, A., Murthy, U., Rodeck, U., Herlyn, M. et al., Presence of tumor-associated antigens in epidermal growth factor receptors from different human carcinomas. *Cancer Res.* 1987, **47**, 2531–2536.
- [174] Yin, B. W., Finstad, C. L., Kitamura, K., Federici, M. G. et al., Serological and immunochemical analysis of Lewis y (Ley) blood group antigen expression in epithelial ovarian cancer. *Int. J. Cancer* 1996, **65**, 406–412.
- [175] Iwamori, M., Tanaka, K., Kubushiro, K., Lin, B. et al., Alterations in the glycolipid composition and cellular properties of ovarian carcinoma-derived RMG-1 cells on transfection of the alpha1,2-fucosyltransferase gene. *Cancer Sci.* 2005, **96**, 26–30.

- [176] Guo, H.-B., Zhang, Y., Chen, H.-L., Relationship between metastasis-associated phenotypes and N-glycan structure of surface glycoproteins in human hepatocarcinoma cells. *J. Cancer Res. Clin. Oncol.* 2001, **127**, 231–236.
- [177] Seiberger, P. J., Chaney, W. G., Control of metastasis by Asn-linked, β 1–6 branched oligosaccharides in mouse mammary cancer cells. *Glycobiology* 1999, **9**, 235–241.
- [178] Guo, H. B., Randolph, M., Pierce, M., Inhibition of a specific N-glycosylation activity results in attenuation of breast carcinoma cell invasiveness-related phenotypes: inhibition of epidermal growth factor-induced dephosphorylation of focal adhesion kinase. *J. Biol. Chem.* 2007, **282**, 22150–22162.
- [179] Guo, H.-B., Johnson, H., Randolph, M., Nagy, T. et al., Specific posttranslational modification regulates early events in mammary carcinoma formation. *Proc. Natl. Acad. Sci.* 2010, **107**, 21116–21121.
- [180] Kim, Y. S., Hwang, S. Y., Kang, H. Y., Sohn, H. et al., Functional proteomics study reveals that N-Acetylglucosaminyltransferase V reinforces the invasive/metastatic potential of colon cancer through aberrant glycosylation on tissue inhibitor of metalloproteinase-1. *Mol. Cell. Proteomics* 2008, **7**, 1–14.
- [181] Przybylo, M., Martuszczyńska, D., Pochec, E., Hoja-Lukowicz, D., Lityńska, A., Identification of proteins bearing β 1–6 branched N-glycans in human melanoma cell lines from different progression stages by tandem mass spectrometry analysis. *Biochim. Biophys. Acta* 2007, **1770**, 1427–1435.
- [182] Ihara, S., Miyoshi, E., Nakahara, S., Sakiyama, H. et al., Addition of β 1–6 GlcNAc branching to the oligosaccharide attached to Asn 772 in the serine protease domain of matriptase plays a pivotal role in its stability and resistance against trypsin. *Glycobiology* 2004, **14**, 139–146.
- [183] Guo, H.-B., Lee, I., Kamar, M., Akiyama, S. K., Pierce, M., Aberrant N-glycosylation of β 1 integrin causes reduced α 5 β 1 integrin clustering and stimulates cell migration. *Cancer Res.* 2002, **62**, 6837–6845.
- [184] Siddiqui, S. F., Pawelek, J., Handerson, T., Lin, C. Y. et al., Coexpression of β 1,6-N-acetylglucosaminyltransferase V glycoprotein substrates defines aggressive breast cancers with poor outcome. *Cancer Epidemiol. Biomarkers Prev.* 2005, **14**, 2517–2523.
- [185] Akama, R., Sato, Y., Kariya, Y., Isaji, T. et al., N-acetylglucosaminyltransferase III expression is regulated by cell-cell adhesion via the E-cadherin-catenin-actin complex. *Proteomics* 2008, **8**, 3221–3228.
- [186] Ishibashi, K., Nishikawa, A., Hayashi, N., Kasahara, A. et al., N-Acetylglucosaminyltransferase III in human serum, and liver and hepatoma tissues: Increased activity in liver cirrhosis and hepatoma patients. *Clin. Chim. Acta* 1989, **185**, 325–332.
- [187] De Santis, G., Miotti, S., Mazzi, M., Canevari, S., Tomassetti, A., E-cadherin directly contributes to PI3K/AKT activation by engaging the PI3K-p85 regulatory subunit to adherens junctions of ovarian carcinoma cells. *Oncogene* 2009, **28**, 1206–1217.
- [188] Lloyd, K. O., Burchell, J., Kudryashov, V., Yin, B. W., Taylor-Papadimitriou, J., Comparison of O-linked carbohydrate chains in MUC-1 mucin from normal breast epithelial cell lines and breast carcinoma cell lines. Demonstration of simpler and fewer glycan chains in tumor cells. *J. Biol. Chem.* 1996, **271**, 33325–33334.
- [189] Lavrsen, K., Madsen, C. B., Rasch, M. G., Woetmann, A. et al., Aberrantly glycosylated MUC1 is expressed on the surface of breast cancer cells and a target for antibody-dependent cell-mediated cytotoxicity. *Glycoconj. J.* 2013, **30**, 227–236.
- [190] Soares, R., Marinho, A., Schmitt, F., Expression of sialyl-Tn in breast cancer. Correlation with prognostic parameters. *Pathol. Res. Pract.* 1996, **192**, 1181–1186.
- [191] Campbell, B. J., Finnie, I. A., Hounsell, E. F., Rhodes, J. M., Direct demonstration of increased expression of Thomsen-Friedenreich (TF) antigen in colonic adenocarcinoma and ulcerative colitis mucin and its concealment in normal mucin. *J. Clin. Invest.* 1995, **95**, 571–576.
- [192] Ogawa, H., Ghazizadeh, M., Araki, T., Tn and sialyl-Tn antigens as potential prognostic markers in human ovarian carcinoma. *Gynecol. Obstet. Invest.* 1996, **41**, 278–283.
- [193] Inoue, M., Ton, S. M., Ogawa, H., Tanizawa, O., Expression of Tn and sialyl-Tn antigens in tumor tissues of the ovary. *Am. J. Clin. Pathol.* 1991, **96**, 711–716.
- [194] Ohno, S., Ohno, Y., Nakada, H., Suzuki, N. et al., Expression of Tn and sialyl-Tn antigens in endometrial cancer: its relationship with tumor-produced cyclooxygenase-2, tumor-infiltrated lymphocytes and patient prognosis. *Anticancer Res.* 2006, **26**, 4047–4053.
- [195] Imada, T., Rino, Y., Hatori, S., Takahashi, M. et al., Sialyl Tn antigen expression is associated with the prognosis of patients with advanced colorectal cancer. *Hepato-gastroenterology* 1999, **46**, 208–214.
- [196] Akamine, S., Nakagoe, T., Sawai, T., Tsuji, T. et al., Differences in prognosis of colorectal cancer patients based on the expression of sialyl Lewis^x, sialyl Lewis^x and sialyl Tn antigens in serum and tumor tissue. *Anticancer Res.* 2004, **24**, 2541–2546.
- [197] Itzkowitz, S. H., Bloom, E. J., Kokal, W. A., Modin, G. et al., Sialosyl-Tn. A novel mucin antigen associated with prognosis in colorectal cancer patients. *Cancer* 1990, **66**, 1960–1966.
- [198] Ohshio, G., Yoshioka, H., Manabe, T., Sakahara, H. et al., Expression of sialosyl-Tn antigen (monoclonal antibody MLS102 reactive) in normal tissues and malignant tumors of the digestive tract. *J. Cancer Res. Clin. Oncol.* 1994, **120**, 325–330.
- [199] Thor, A., Ohuchi, N., Szpak, C. A., Johnston, W. W., Schlom, J., Distribution of Oncofetal Antigen Tumor-associated Glycoprotein-72 Defined by Monoclonal Antibody B72.3. *Cancer Res.* 1986, **46**, 3118–3124.
- [200] Carcel-Trullols, J., Stanley, J. S., Saha, R., Shaaf, S. et al., Characterization of the glycosylation profile of the human breast cancer cell line, MDA-231, and a bone colonizing variant. *Int. J. Oncol.* 2006, **28**, 1173–1183.

- [201] Miles, D. W., Happerfield, L. C., Smith, P., Gillibrand, R. et al., Expression of sialyl-Tn predicts the effect of adjuvant chemotherapy in node-positive breast cancer. *Br. J. Cancer* 1994, 70, 1272–1275.
- [202] Paschos, K. A., Canovas, D., Bird, N. C., The role of cell adhesion molecules in the progression of colorectal cancer and the development of liver metastasis. *Cell. Signal.* 2009, 21, 665–674.
- [203] Bresalier, R. S., Byrd, J. C., Brodt, P., Ogata, S. et al., Liver metastasis and adhesion to the sinusoidal endothelium by human colon cancer cells is related to mucin carbohydrate chain length. *Int. J. Cancer* 1998, 76, 556–562.
- [204] Ogata, S., Chen, A., Itzkowitz, S. H., Use of model cell lines to study the biosynthesis and biological role of cancer-associated sialosyl-Tn antigen. *Cancer Res.* 1994, 54, 4036–4044.
- [205] Cunningham, D., Atkin, W., Lenz, H.-J., Lynch, H. T. et al., Colorectal cancer. *Lancet* 2010, 375, 1030–1047.
- [206] Newsom-Davis, T. E., Wang, D., Steinman, L., Chen, P. F. et al., Enhanced immune recognition of cryptic glycan markers in human tumors. *Cancer Res.* 2009, 69, 2018–2025.
- [207] de Leoz, M. L., Young, L. J., An, H. J., Kronewitter, S. R. et al., High-mannose glycans are elevated during breast cancer progression. *Mol. Cell. Proteomics* 2011, 10, M110 002717.
- [208] Ulloa, F., Real, F. X., Differential distribution of sialic acid in α 2,3 and α 2,6 linkages in the apical membrane of cultured epithelial cells and tissues. *J. Histochem. Cytochem.* 2001, 49, 501–509.
- [209] Nakamori, S., Kameyama, M., Imaoka, S., Furukawa, H. et al., Involvement of carbohydrate antigen sialyl Lewis X in colorectal cancer metastasis. *Dis. Colon Rectum* 1997, 40, 420–431.
- [210] Nakamori, S., Kameyama, M., Imaoka, S., Furukawa, H. et al., Increased expression of sialyl Lewisx antigen correlates with poor survival in patients with colorectal carcinoma: Clinicopathological and Immunohistochemical Study. *Cancer Res.* 1993, 53, 3632–3637.
- [211] Ogata, S., Koganty, R., Reddish, M., Michael Longenecker, B. et al., Different modes of sialyl-Tn expression during malignant transformation of human colonic mucosa. *Glycoconj. J.* 1998, 15, 29–35.
- [212] Ito, H., Hiraiwa, N., Sawada-Kasugai, M., Akamatsu, S. et al., Altered mRNA expression of specific molecular species of fucosyl- and sialyl-transferases in human colorectal cancer tissues. *Int. J. Cancer* 1997, 71, 556–564.
- [213] Petretti, T., Kemmner, W., Schulze, B., Schlag, P. M., Altered mRNA expression of glycosyltransferases in human colorectal carcinomas and liver metastases. *Gut* 2000, 46, 359–366.
- [214] Lee, J. K., Matthews, R. T., Lim, J. M., Swanier, K. et al., Developmental expression of the neuron-specific N-acetylglucosaminyltransferase Vb (GnT-Vb/IX) and identification of its in vivo glycan products in comparison with those of its paralog, GnT-V. *J. Biol. Chem.* 2012, 287, 28526–28536.

1.9 Mass Spectrometric and Non-Mass Spectrometric Methods of Glycan Characterisation

1.9.1 Mass Spectrometric Analysis of Glycans

Mass spectrometry has emerged as an enabling and indispensable technology which caters for the quantitative and qualitative applications in both discovery and targeted analysis of glycans and glycoconjugates from biological samples (Zaia, 2008). In the recent years, the combinatory power of mass spectrometry with other advanced separation techniques such as high-pressure liquid chromatography (HPLC) has been widely demonstrated in the field of glycomics, allowing for the sensitive detection and structural characterisation of specific glycan structural determinants. This analytical approach has been used in this thesis to identify specific membrane glycosylation changes implicated in serous cancers of the ovary, peritoneum and fallopian tube.

1.9.2 Basic Principles of Mass Spectrometry

Mass spectrometry is an analytical technique that is routinely used to provide both quantitative (molecular mass/concentration) and qualitative information on any molecule upon their conversion to ions (Ho, Lam *et. al.*, 2003). Basically, mass spectrometers consist of three essential elements, namely the a) ionisation source, b) mass analyser and c) detector (**Figure 9**). In brief, the molecules or analyte of interest are introduced to the ionisation source within the mass spectrometer, where they are first ionised to become either positive- or negatively charged ions. These charged ions then travel through the mass analyser where they can be isolated electrically (or magnetically) according to their respective mass-to-charge ratio (m/z). These ions eventually reach the detector and are transformed into electrical signals which are then integrated by a computer system. The signals are displayed graphically as a mass spectrum representing relative abundance of each signal (y-axis) according to their mass-to-charge ratios (x-axis).

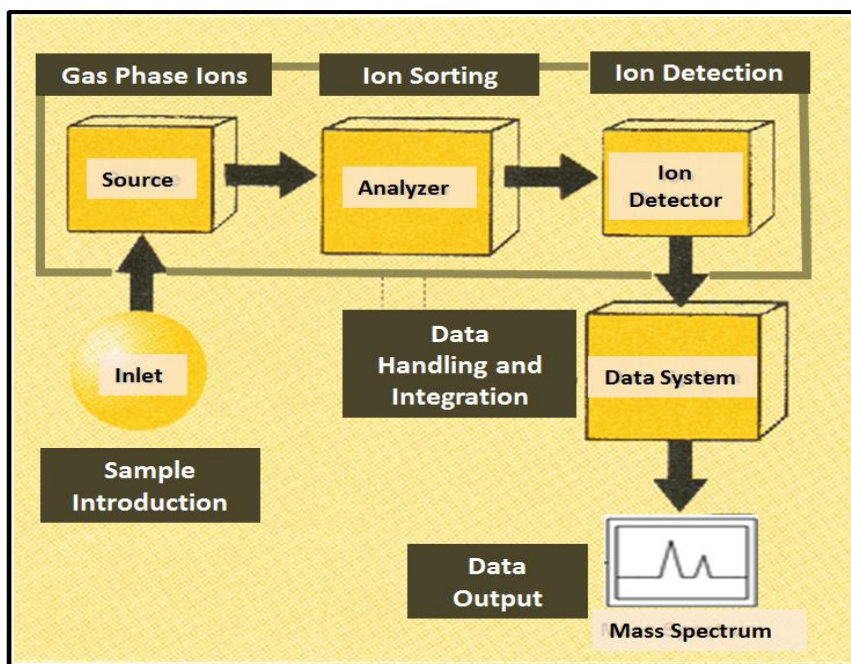


Figure 9: Components of a mass spectrometer. Sourced and modified from Barofsky, D.F (1999)

1.9.3 Ionisation Methods in Mass Spectrometry

In mass spectrometry, the ion source is of primary importance and is often considered as the ‘heart’ of the mass spectrometer (Chait, 1972). Very often, the success of any mass spectrometric analysis largely depends on the choice of ion source. The mode of ion production (negative or positive) is also a crucial factor which is determined by the sample that is investigated. These mass ions are subsequently interpreted by the chemist to yield vital information pertaining to molecular structure, composition etc. The conventional ionisation method, also known as electron impact (EI), is achieved by electron capture or electron ejection of vaporised samples which results in the formation of radical anions or cations, respectively (Munson and Field, 1966). These conditions are not ideal for large molecules or for most biological samples as specific sample characteristics such as thermal stability and volatility are required for efficient ionisation. Due to the limitations observed for EI ionisation, other ionisation methods such as chemical ionisation (CI) and plasma desorption (PD) were subsequently developed, resulting in the formation of protonated (or deprotonated) ions which were more stable than the formation of radical ions in EI-MS (El-Anead, Cohen *et. al.*, 2009). PD ionisation, in particular, is also regarded as one of the early ‘soft’ ionisation methods capable of analysing biological molecules up to a molecular weight

(MW) of 100,000 Daltons (Da). The term ‘soft’, in this context, refers to the minimum internal energy that is transmitted to the analytes during the ionisation process. In the following years, additional soft ionisation methods such as matrix assisted laser desorption ionisation (MALDI) and electrospray ionisation (ESI) have revolutionised the way in which mass spectrometers are utilised and have enabled analytical chemists to study biological molecules such as glycoconjugates (glycans, glycolipids, glycoproteins), proteins, peptides and DNA. A brief description of each of the three methods mentioned earlier and its application in the field of glycomics are described in **Table 9**.

1.9.4 Mass Analysers in Mass Spectrometry

A mass analyser is a component of the mass spectrometer in which the newly generated gas phase ions, upon ionization, are separated based on their mass-to-charge ratio (m/z) (El-Aneed, Cohen *et. al.*, 2009). The five main relevant features for measuring the performance of a typical mass analyser are mass range limit, sensitivity, mass accuracy, resolution analysis speed and transmission (Hoffmann and Stroobant, 2013). Several types of mass analysers have been developed based on their different separation principles highlighted in **Table 10**. The mass analyser used in this study consist of the quadrupole ion trap mass analyser which offers advantages due to its small and compact size, low costs, sensitivity and capacity to perform tandem MS experiments. During the detection process, the electrode potential is altered to produce ion instabilities, thus ejecting these ions in order of increasing m/z ratio.

Table 10: Mass Analysers		
Type of Analysers	Symbol	Principle of separation
Electric sector	ESA	Kinetic energy
Magnetic sector	B	Momentum
Quadrupole	Q	m/z (trajectory stability)
Ion trap	IT	m/z (resonance frequency)
Time-of-flight	TOF	Velocity (flight time)
Fourier transform ion cyclotron resonance	FTICR	m/z (resonance frequency)
Fourier transform orbitrap	FT-OT	m/z (resonance frequency)

Table 9: Ionisation Methods in Mass Spectrometry

Ionization Source	Process	Significance	Advantages/Disadvantages	References
Fast atom bombardment (FAB)	Bombardment of analyte with high-energy atomic beam (argon) resulting in molecular spluttering and subsequent desorption of secondary ions from liquid to gaseous phase	1) Formation of protonated (M+H) or deprotonated (M-H) molecular ions 2) Establishment of systematic nomenclature for glycan fragmentation	Advantages: 1) Small percentage of parent ions acquire sufficient energy to undergo fragmentation of labile bonds 2) Can obtain compositional and sequence information Disadvantages: 1) Analytes must be dissolved in special liquid matrix (glycerol, thioglycerol)	(Barber, 1981; Barber, Bordoli <i>et al.</i> , 1982) (Roberts, Santikarn <i>et al.</i> , 1988; Haslam, Morris <i>et al.</i> , 2001) (Roboz, 2002) (Dell and Ballou, 1983; Egge, Dell <i>et al.</i> , 1983; Kamerling, Heerma <i>et al.</i> , 1983; Ciucanu and Costello, 2003). (Domon and Costello, 1988)
Matrix-assisted laser desorption/ionisation (MALDI)	Analyte molecules are mixed with small, laser-absorbing organic molecules (eg. 2,5-dihydroxybenzoic acid) and the sample mixture is evaporated on a metal target placed in a vacuum source. Matrix co-crystallizes with analyte to form gas phase ions through a laser beam (nitrogen)	1) Leading ionisation source for protein/peptide sequencing 2) Extensively used for glycan analysis	Advantages: 1) 10 to 100 times more sensitive than FAB without any prior derivatisation 2) Tolerant to salts and other contamination Disadvantages: 1) Ionisation efficiency of neutral glycans are low 2) Matrix used is not ideal for acidic glycans 3) Glycans need to be permethylated as ionised as sodium cations	(Mock, Davey <i>et al.</i> , 1991; Strupat, Karas <i>et al.</i> , 1991; Harvey, 1993; Zaia, 2010)
Electrospray Ionisation (ESI)	Sample is dissolved in a suitable polar solvent and introduced to the ion source via a spray needle. High electrical potential at the tip of the needle generates charged droplets that result in desorption and ejection of ions into the gaseous phase.	1) Extensively used for glycan analysis 2) Generates multiple charged ions for large biomolecules	Advantages: 1) Useful for analysis of glycans with fragile constituents (sialic acids and sulphates) 2) Coupling with HPLC chromatography Disadvantages: 1) Presence of contaminants such as salts and/or detergents in the sample solution which can affect the sensitivity	(Iribarne and Thomson, 1976; Kobarle, 2000) (Vanderschaeghe, Festjens <i>et al.</i> , 2010) (Zaia, 2010)

1.9.4.1 Tandem Mass Spectrometry (MSⁿ)

Although single stage MS experiments have proven to be valuable for glycan structural determination based on molecular weight information in a MS spectra (Costello, Contado-Miller *et. al.*, 2007; El-Aneed, Cohen *et. al.*, 2009), many aspects of their structural features such as sequence, linkage positions and branching patterns are not able to be determined by MS alone due to the complexity and heterogeneity of the isobaric glycan structures. The use of tandem MS in the field of glycomics, has therefore, become an indispensable tool, driven by the need to elucidate the specific structural features which are relevant in biomarker discovery, pathogen recognition and the understanding of various disease processes. Tandem MS relies on the isolation of a specific m/z ion (eg. parent ion, precursor ion) which is then subjected to high energy fragmentation, thereby yielding subsequent fragments or product ions which correspond to various sub-structures (Lapadula, Hatcher *et. al.*, 2005; Zaia, 2010; Everest-Dass, Kolarich *et. al.*, 2013). Multiple fragmentation experiments performed in stages are represented as MSⁿ, where n refers to the number of stages. For instance, the first stage of a tandem MS is known as MS² and the subsequent dissociation of product ions from MS² are termed as MS³, MS⁴ and so on (Zhang, Singh *et. al.*, 2005).

1.9.4.2 Collision Induced Dissociation (CID)

In a tandem MS experimental set up, multiple mass analysers are connected in a series, in which ion isolation is performed by the first analyser, followed by fragmentation of that ion in a collision cell and finally separation of the fragment ions based on their m/z values by another analyser (**Figure 10**). The ion selected for MS/MS analysis undergoes collision with a stream of inert gas atoms in the collision cell, resulting in the transfer of kinetic energy internally, causing these ions to dissociate by the rupturing of bonds. This process is known as collisionally-activated dissociation (CAD) or more commonly referred to as collision-induced dissociation (CID). Typically, the most abundant product ion corresponds to the dissociation of the weakest bond. It must be emphasized that the interpretation of glycoconjugate product ions from MS/MS or multistage MS data is considerably more laborious than interpreting MS/MS spectra of peptides. For branched structures such as glycans, fragmentation can occur from the non-reducing end of the antennae and from the reducing end, giving rise to a higher level of complexity. Several studies have shown that CID-derived mass spectra have been successful in providing information on the linkage position (Chai, Piskarev *et. al.*, 2001; Everest-Dass, Kolarich *et. al.*, 2013), stereochemistry of

individual monosaccharide residues (Mueller, Domon *et. al.*, 1988) and well as branching patterns (Chai, Piskarev *et. al.*, 2002; Harvey, 2005c). For instance, oligosaccharides containing the same monosaccharide residues could have different branching patterns and very often show distinct fragment ion spectra due to the differences in steric environments between such isomers, thereby resulting in different bond energies and resultant product ion spectra.

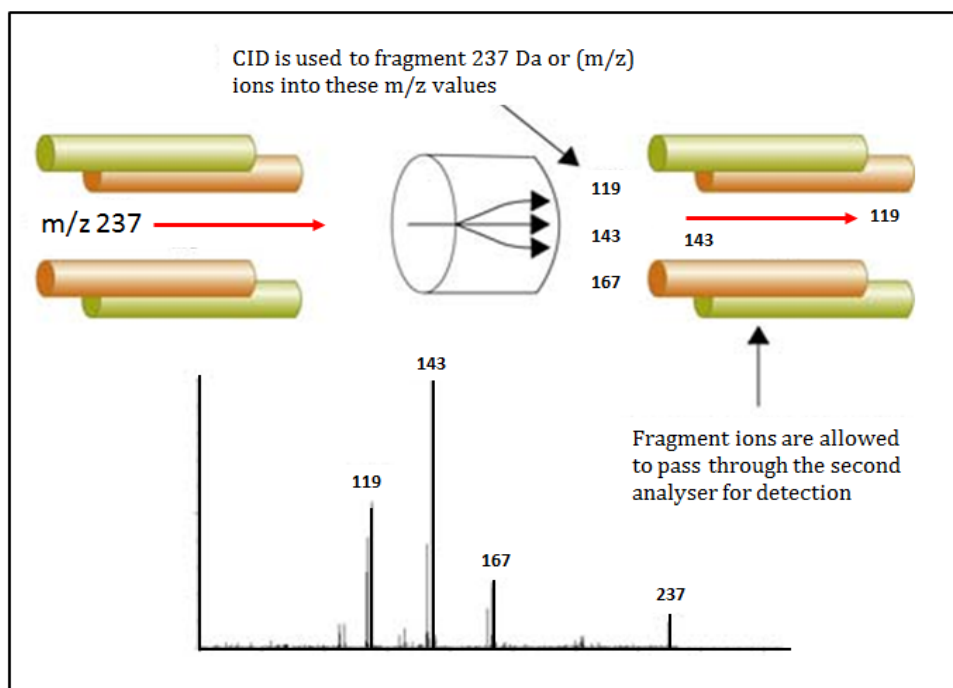


Figure 10: Collision-induced dissociation (CID) of a precursor ion m/z 237¹⁻ being fragmented in the MS/MS collision cell. Sourced from http://www.waters.com/waters/en_US

1.9.5 Nomenclature for the Fragmentation of Glycoconjugates

To facilitate the understanding of glycan fragmentation using tandem MS, the carbohydrate fragmentation nomenclature established by Domon and Costello (Domon and Costello, 1988) has been widely used throughout the mass spectrometry field. In principle, the two major types of fragmentation commonly observed for glycans are cleavages arising from the rupturing of glycosidic bonds between sugar residues and within the sugar ring (internal cross ring). As shown in **Figure 11**, fragment ions containing the non-reducing end of the oligosaccharide are labelled as A, B and C, while fragment ions containing the reducing end (aglycone) oligosaccharide are labelled as X, Y, and Z. The subscripts indicate the number of individual sugar residues from the non-reducing end. Cleavage ions which arise from the rupturing of glycosidic bonds are represented as B, C, Y and Z, in which the B, Y and C ions consist of an oxonium, protonated species ion and protonated molecular ion respectively while the Z ion is a result of a glycosidic cleavage (O-C bond). The cross ring fragment ions, namely the A and X ions are labelled by assigning a subscript number to the cleaved bond in a clockwise fashion as illustrated in **Figure 11**. The mechanisms detailing two-bond ring cleavages have been previously described (Spengler, Dolce *et. al.*, 1990; Hofmiester, Zhou *et. al.*, 1991) and are particularly useful for determining residue linkages and branching structures (Ashline, Singh *et. al.*, 2005; Zaia, 2010).

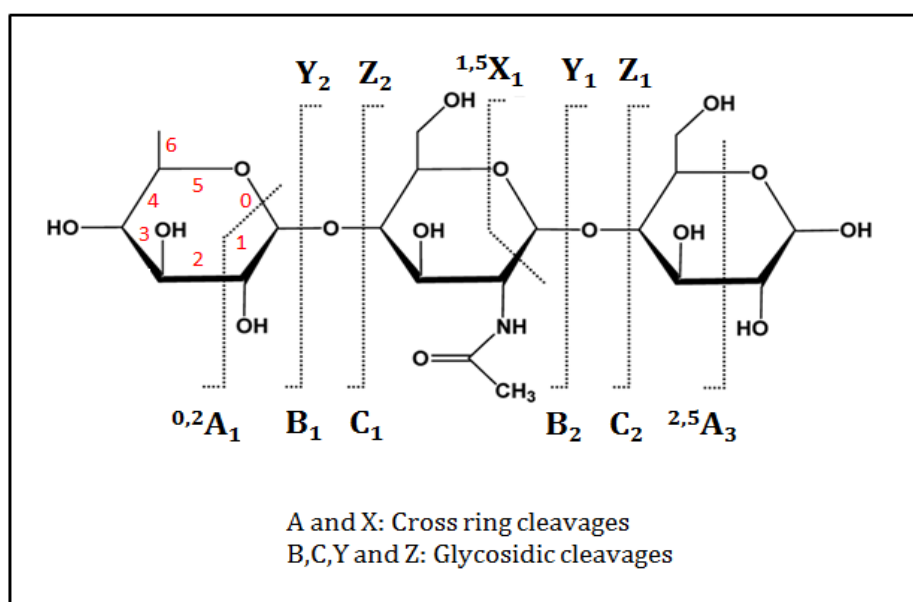


Figure 11: Nomenclature for fragmentation of oligosaccharides established by Domon and Costello (1998).

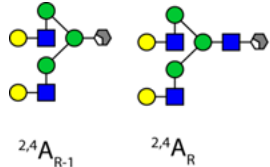
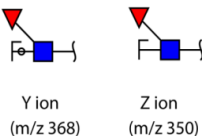
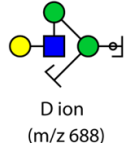

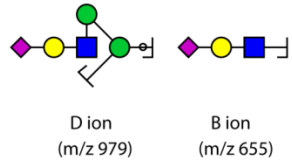
Sourced and modified from Broadbelt, J.S. (2014)

1.9.5.1 Fragmentation of Glycans in Positive Ion Mode

The CID fragmentation pattern of $[M+H]^+$ ions of native oligosaccharides, although not particularly informative, gives rise to mainly B and Y ions which are useful in assigning oligosaccharide sequences and determining glycan classes (Domon and Costello, 1988; Dell, 1990). These cleavages occur towards the HexNAc residues at the reducing-end of complex-type *N*-glycans, therefore allowing the definitive assignment of lactosamine (Gal-GlcNAc) disaccharide antennae at the non-reducing end. Similarly, high-mannose type oligosaccharides produce a series of glycosidic cleavages from successive losses of hexose residues, resulting in a generally more uniform product ion pattern as compared to complex type *N*-glycans. Cross ring cleavages, on the other hand, are typically low in abundance as compared to the glycosidic cleavages, and are observed primarily from protonated ions generated from fragmentation of small oligosaccharides. These observations have led to subsequent efforts to increase the structural information obtained from the fragment ion mass spectra (Zaia, 2004) (Orlando, Allen Bush *et. al.*, 1990). To date, permethylation of glycans ionised as $[M+Na]^+$ ions has become the preferred choice for analysis of glycans in positive ion mode as it enhances ionisation and improves MS sensitivity, leading to accurate structural assignments when tandem MS is performed (Dell, Reason *et. al.*, 1994; Viseux, de Hoffmann *et. al.*, 1997; Sheeley and Reinhold, 1998). Besides that, permethylation also stabilises glycans containing labile groups such as sialic acids by converting their carboxyl groups to methyl esters (Ariga, Kohriyama *et. al.*, 1987; Zaia, 2008), thereby permitting the simultaneous analysis of neutral and acidic glycans. This procedure also allows for reversed phase chromatography to be used in front of the MS for removal of salts and separation of glycans. Permethylation, however, involves some complicated sample preparation and subsequent clean-up steps that could possibly lead to sample losses, especially for small amounts. Nevertheless, permethylated oligosaccharides have been extensively studied using MALDI-MS and ESI-MS and their fragmentation properties are well established (Costello, Contado-Miller *et. al.*, 2007).

1.9.5.2 Fragmentation of Glycans in Negative Ion Mode

The negative ion tandem MS spectra of glycans which typically gives rise to $[M-H]^{-1}$ or $[M+X]^{-1}$, where X is an anion product (eg. Cl^{-} , NO_3^{-}), although less frequently investigated, has been observed to differ considerably from that of positive ion mode fragmentation (Wheeler and Harvey, 2000; Chai, Piskarev *et. al.*, 2001; Chai, Piskarev *et. al.*, 2002; Sagi, Peter-Katalinic *et. al.*, 2002; Quemener, Desire *et. al.*, 2003). Several studies on free neutral glycans derived from sources such as human milk (Pfenninger, Karas *et. al.*, 2002) and urine (Chai, Piskarev *et. al.*, 2001) as well as acidic glycans from oranges (Quemener, Desire *et. al.*, 2003) have shown that the fragment ion spectra comprises of prominent C-type ions and A-type cross ring fragment ions, unlike the B- and Y-type glycosidic cleavages in positive ion mode spectra. These observations can be rationalized by the mechanism known as ‘proton abstraction’, in which hydrogen is removed from various hydroxyl groups, thus leaving an electron-dense centre that continuously feeds electrons into the sugar rings and results in subsequent cleavages (Harvey, 2005a; Harvey, 2005b). The specific fragmentation mechanisms accounting for some of these diagnostic ions are crucial to understanding how these glycans fragment in negative ion mode and are shown in **Table 11**. Specific features that were reported to be characteristic of N-glycans in negative ion mode fragmentation included the composition of glycan constituents on both the 3- and 6-antennae, presence of bisecting GlcNAc on the branching mannose and location of fucose residues on the reducing-end chitobiose core GlcNAc, as well as terminal fucose on the antennae. Likewise, unique fragmentation ions have also been observed in negative ion mode of O-glycans, particularly the determination of various isomeric and isobaric structures pertaining to various blood group antigens (Everest-Dass, Abrahams *et. al.*, 2013; Everest-Dass, Kolarich *et. al.*, 2013).

Table 11: Structural feature ions in negative ionisation mode			
Compositional Features	Cleavage ions	Fragmentation Location	References
Chitobiose Core	^{2,4} A type cleavage of GlcNAc residues as a result of proton abstraction from the 3-position of the reducing-terminal GlcNAc Example: ^{2,4} A _R , ^{2,4} A _{R-1}	 ^{2,4} A _{R-1} ^{2,4} A _R	(Harvey, 2005c; Harvey, Royle <i>et. al.</i> , 2008)
Core Fucosylation	Z and Y ions which correspond to the composition of reduced GlcNAc and fucose residue	 Y ion (m/z 368) Z ion (m/z 350)	(Harvey, 2005c; Harvey, Royle <i>et. al.</i> , 2008)
6-Antennae	C/Z cleavage ion (also known as D ion) formed as a result of the loss of chitobiose core GlcNAc residues (C ion) and 3-antennae substituents (Z ion) Example: D and D-18 (H ₂ O) ions	 D ion (m/z 688)	(Harvey, Royle <i>et. al.</i> , 2008; Everest-Dass, Kolarich <i>et. al.</i> , 2013)
3- or 6-Antennae	A-type cross ring cleavage ion formed by the cleavage of Man residues at the 3- and 6-antennae Example: ^{1,3} A ion	 ^{1,3} A ion (m/z 424)	(Harvey, 2005c)
Sialylated Antennae	D ion which correspond to the composition of the sialylated 6-antennae B ion which corresponds to the 3- or 6-antennae containing sialic acid	 D ion (m/z 979) B ion (m/z 655)	(Nakano, Saldanha <i>et. al.</i> , 2011; Everest-Dass, Abrahams <i>et. al.</i> , 2013)

1.9.6 Chromatographic Interface for LC-MS of Glycans

In view of the complex heterogeneity of *N*- and *O*-glycans, refined systems for the separation of oligosaccharide mixtures are deemed vital and necessary for the further elucidation of their structural features (Davies and Hounsell, 1996; Davies and Hounsell, 1998). The importance of chromatographic separation of glycans prior to MS has thus been increasingly acknowledged as desirable in the field of analytical chemistry and has, over the last few years, resulted in the use of high performance liquid chromatography (HPLC) and capillary electrophoresis (CE) in glycan analysis. HPLC, in particular, has been noted to have a high resolving capability and can be coupled easily to various detectors such as MS or interface with other chromatographic methods. The chromatographic matrices currently used for the separation of glycans are shown in **Table 12**, highlighting their features with regard to chromatographic behaviour and suitability for coupling to MS.

1.9.6.1 Specific Chromatographic Features of Porous Graphitised Carbon Chromatography

The porous graphitised carbon (PGC) chromatographic matrix was first introduced in 1979 (Knox and Gilbert, 1981; Gilbert, Knox *et. al.*, 1982), in the form of porous glassy carbon, which was further improved to produce porous graphitised carbon (Knox and Kaur, 1986), displaying good stability and chromatographic performance. During the manufacturing process, silica-based material is impregnated with a homogenous mixture of phenol and hexamine and polymerised at 160 °C. Upon polymerisation, this polymer complex is pyrolysed under nitrogen at 1000 °C to produce highly porous amorphous carbon. Graphitisation is achieved through additional heat treatment at temperatures above 2000 °C using argon gas, resulting in a structurally rearranged crystalline surface without the presence of micropores (**Figure 12**). From a molecular perspective, the PGC surface architecture is two-dimensional, composed of flat sheets of hexagonally arranged carbon atoms connected through covalent linkages while the sheets are held together by Van der Waals interactions (Knox and Kaur, 1986). These unique features are thought to account for the increased rigidity and mechanical stability of PGC.

Today, PGC columns are commercially available from Thermo Fisher Scientific, under the trade name Hypercarb™ and have been used in a diverse range of applications, mainly for the separation of closely related substances (Emery, 1989; Tanaka, Tanigawa *et. al.*, 1991; Wan, Shaw *et. al.*, 1995) and polar analytes (Tanaka, Tanigawa *et. al.*, 1991; Takeuchi, Kojima *et. al.*, 2000).

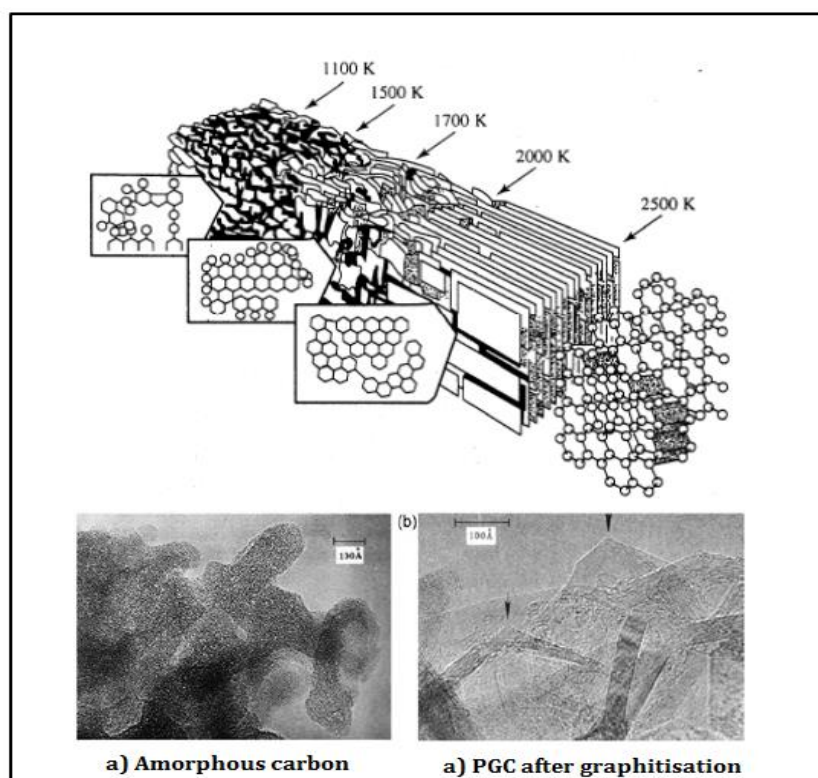


Figure 12: Heat graphitisation of amorphous carbon. Revised from Knox, J. *et. al.* (1986) and www.carbonandgraphite.org

In the past decade, PGC-LC-MS has demonstrated high sensitivity and superior resolution of native, underivatised *N*- and *O*-glycans as compared to conventional reversed-phased chromatography (Melmer, Stangler *et. al.*, 2011). This has led to the reliable separation of subtle differences in structures of the various glycoforms and it has, in fact, been regarded as a ‘glycomics’ method in particular (Backstrom, Thomsson *et. al.*, 2009; Pabst, Wu *et. al.*, 2010). More recently, PGC has also been developed into microfluidic chip-based formats with an integrated on-chip PNGase F reactor which is commercially available from Agilent Technologies Inc. for the high throughput analysis of IgG glycans (Ninonuevo, Perkins *et. al.*, 2008; Chu, Ninonuevo *et. al.*, 2009; Ni, Bones *et. al.*, 2013). One significant advantage of using underivatised glycans is that it avoids potential quantitative biases which could be due to incomplete chemical derivatisation, clean up or degradation (Palmisano, Larsen *et. al.*,

2013). Nevertheless, it must also be mentioned that carbon columns, in general strongly adsorb a variety of substances which may lead to the unstable retention times and increasing column back pressure. These problems, however, can be prevented by improving sample preparation steps through the use of desalting columns (Packer, Lawson *et. al.*, 1998) and occasional regeneration of the PGC column (Pabst and Altmann, 2008; Bereman, Williams *et. al.*, 2009).

Perhaps, one of the most remarkable features of PGC is the highly discriminative ability of PGC-LC towards isomeric and isobaric glycans structures with respect to the structure-retention time. These correlations have been well established using reference glycans in several studies (Karlsson, Schulz *et. al.*, 2004; Pabst, Bondili *et. al.*, 2007; Pabst, Wu *et. al.*, 2010; Jensen, Karlsson *et. al.*, 2012). For instance, PGC readily separates glycans with different sialic acid linkages ($\alpha 2-3/\alpha 2-6$), thus allowing the monitoring of relative quantitative as well as qualitative glycomic changes, as opposed to the used of stand-alone MS methods which require MS³ (Ito, Yamada *et. al.*, 2007), derivatisation (Wheeler, Domann *et. al.*, 2009; Alley and Novotny, 2010) or linkage-specific sialidases (Jensen, Karlsson *et. al.*, 2012) to determine such linkages. Larger sialoglycans with a high number of sialic acids residues have a greater retention on PGC as compared to smaller, less branched and less sialylated structures (Pabst, Bondili *et. al.*, 2007). Likewise, PGC has also been favoured for the analysis of glycans containing modifications such as sulfation of various *O*-linked glycans (Everest-Dass, Jin *et. al.*, 2012; Ozcan, An *et. al.*, 2013) and glycosaminoglycans (Zaia, 2013). Owing to the above mentioned properties and advantages of the PGC chromatography, the structural analysis of glycans released from both glycoproteins and glycolipids in this thesis has been carried out entirely using PGC-LC-ESI-MS/MS and specific features corresponding to their unique separation capabilities will be highlighted in the subsequent result chapters.

Table 12: Chromatographic Features of Liquid Chromatography Columns

Type	Properties	Advantages/Disadvantages	References
High-pH Anion-exchange Chromatography with Pulse Amperometric Detection (HPAEC-PAD)	<p>1) Strong basic eluents convert oligosaccharides into oxyanions which undergo interaction with the amino groups of the stationary phase column resin</p> <p>2) Separation of these bound oligosaccharides depends on factors such as charge, sugar composition, linkage and molecular size</p>	<p>Disadvantages:</p> <p>1) Requirement of high concentrations of the electrolyte</p> <p>2) Useful for monosaccharide analysis</p>	(Gohlke and Blanchard, 2008) (Bruggink, Wuhler <i>et al.</i> , 2005; Guignard, Jouve <i>et al.</i> , 2005) (Hardy and Townsend, 1988)
Reversed- phase Chromatography (RPC)	<p>1) Sugars are separated on the basis of hydrophobicity using a C18 column. As the size and polarity of the glycan increases, the degree to which it binds to the column decreases.</p> <p>2) Pairing of acidic glycans with amine groups in the mobile phase permits binding of glycans to the hydrophobic stationary phase, thus increasing their retention time</p>	<p>Disadvantages:</p> <p>1) Native glycans are too hydrophilic to adsorb to a reversed-phase matrix and are derivatised by reductive amination</p> <p>2) 3) Large acidic glycans typically elute earlier than neutral glycans and are poorly separated</p> <p>Advantages:</p> <p>1) Useful for detection of glycosaminoglycans</p> <p>2) Commonly used to separate fluorescently derivatised glycans</p>	(Hase, Ikenaka <i>et al.</i> , 1978; Hase, 1996; Lamari, Kuhn <i>et al.</i> , 2003) (Chen and Flynn, 2007) (Melmer, Stangler <i>et al.</i> , 2011). (Kuberan, Lech <i>et al.</i> , 2002; Thanawiroon, Rice <i>et al.</i> , 2004). (Kuberan, Lech <i>et al.</i> 2002, Thanawiroon, Rice <i>et al.</i> 2004).
Hydrophilic Interaction Chromatography (HILIC)	<p>1) Separates native glycans based on their hydrophilicity, depending on their properties such as polarity, size, charge and composition</p> <p>2) Retention mechanism is based on the hydrophilic partitioning of glycans to the aqueous organic layer surrounding the various stationary phases</p>	<p>Advantages:</p> <p>1) Neutral to acidic glycan classes can be separated without any recovery problems with high reproducibility of retention times</p> <p>2) Useful for detection of labeled <i>N</i>-glycans, glycopeptides, glycosaminoglycans</p>	(Alpert 1990, Hemstrom and Irgum 2006) (Palmisano, Larsen <i>et al.</i> , 2013) (Wuhler, Koeleman <i>et al.</i> , 2004; Zaia, 2010) (Hitchcock, Yates <i>et al.</i> , 2008)
Porous Graphitised Carbon Chromatography (PGCC)	<p>1) Retention mechanism is based on Polar Retention Effect on Graphite (PREG)</p> <p>2) Hydrophobic, polar and ionic interactions with the hexagonal graphite structures of PGC</p>	<p>Disadvantages:</p> <p>1) May have variable retention times due to fouling</p> <p>Advantages:</p> <p>1) Robustness against extreme temperature conditions, aggressive mobile phases, thermal stability and tolerance to extreme pH</p> <p>2) Separates neutral and acidic <i>N</i>-glycans, <i>O</i>-glycans and glycosaminoglycans</p>	(Packer, Lawson <i>et al.</i> , 1998; Kawasaki, Ohta <i>et al.</i> , 1999; Thomsson, Karlsson <i>et al.</i> , 1999). (Knox and Ross, 1997) (Pereira, 2008; West, Elfakir <i>et al.</i> , 2010) (Fan, Kondo <i>et al.</i> , 1994; Ruhaak, Deelder <i>et al.</i> , 2009)

1.9.7 Bioinformatics Tools for Glycan Structure Determination

Over the past few years, owing to the significant improvements in methods, a tremendous increase in analytical data on glycan structures has been generated and this has led to several funded initiatives which provide web-based bioinformatics resources (Apweiler, Hermjakob *et. al.*, 1999; Marchal, Golfier *et. al.*, 2003; Frank and Schloissnig, 2010). For instance, GlycoSuiteDB (<http://www.glycosuite.com>) is a relational database which contains most of the *N*- and *O*-glycan structures described in published scientific literature (Cooper, Joshi *et. al.*, 2003). Currently, GlycoSuiteDB has been incorporated into the recently established open-access platform for glycoinformatics, known as UniCarbKB (<http://unicarbkb.org>) (Campbell, Peterson *et. al.*, 2013). This new platform contains a growing, curated database of information on the glycan structures of glycoproteins that aims to increase further understanding of glycan structures, networks and pathways involved in glycosylation and glyco-mediated processes, through the integration of structural and experimental information. The GlycoMod online service, available at ExPASy website (<http://web.expasy.org/glycomod>), is also one of the most frequently used tools to deduce the potential glycan composition based on MS-derived mass and biosynthetic constraints (Cooper, Gasteiger *et. al.*, 2001). *De novo* sequencing tools based on MSⁿ fragmentation such as Glyco-Peakfinder (<http://www.glyco-peakfinder.org>) (Maass, Ranzinger *et. al.*, 2007) and the more recently developed GlycoWorkBench tool (<http://eurocarbdb.org/applications/ms-tools>) (Ceroni, Maass *et. al.*, 2008), which comprise of computer-assisted annotation of MS/MS fragments that was developed as part of the EUROCarbDB project (<http://eurocarbdb.org>). The above-mentioned tools have been used to assist in the identification of the structures of glycans derived from glycoproteins analysed in this thesis.

1.9.8 Non-Mass Spectrometric Methods of Glycan Detection

Various affinity-based detection methods using reagents such as glycan-binding lectins or glycan-binding antibodies have been developed to measure levels of specific glycans in a mixture (Cummings and Esko, 2009). These methods, although frequently used for the detection of glycans, do not provide a comprehensive structural elucidation of glycans, as compared to mass spectrometry or specific enzymatic methods. Nevertheless, these tools have been a valuable complement in providing information about terminal glycan epitopes observed as a result of biological variation and thus have facilitated the discrimination of several cancer-associated glycan antigens. While these methods have not been utilised in this thesis, they bear significant relevance to the identification of specific glycan motifs previously elucidated in ovarian cancer cell lines, serum and tissues and are briefly described as follows:

a) Lectin-based Identification of Glycans (for glycoproteins)

Lectins are composed of a group of non-enzymatic proteins which can recognise and bind to carbohydrates (mono- and oligosaccharides) (Boyd and Shapleigh, 1954; Goldstein, Hughes *et. al.*, 1980). Most of the lectins used as tools in glycobiology are derived from plants and have become commercially available as listed in **Table 13**. While most specificity studies have demonstrated that plant lectins exhibit a higher binding affinity for complex glycans/oligosaccharides than monosaccharides, the interactions between lectin-glycans are complex and not fully understood (Cummings and Etzler, 2009). Many lectins can recognise the non-reducing terminal monosaccharides on glycans, while others also recognise the internal sugars. Furthermore most lectins do not have absolute glycan specificities and can therefore bind to similar glycan structures with varying affinities (Narimatsu, Sawaki *et. al.*, 2010; Van Damme, 2011). Nevertheless, the use of lectin-based detection tools in glycosylation studies has been instrumental in the rapid glycosylation profiling of proteins, particularly in identifying the differential expression of *N*-glycan structures in various samples (Plavina, Wakshull *et. al.*, 2007; Van Damme, 2011). In addition, lectin affinity chromatographic enrichment is a routinely used methodology to concentrate or enrich for glycoproteins or peptides displaying specific glycan structures (Cummings and Kornfeld, 1982; Madera, Mechref *et. al.*, 2007). This technique, however, is more focused on *N*-linked protein glycosylation as existing limitations in the purification methods for *O*-linked glycoproteins do not enable sufficient lectin enrichment of the *O*-linked glycoproteins (Kim and Misek, 2011).

Table 13: Lectins commonly used for the enrichment of glycoproteins		
Lectin Name	Abbreviation	Oligosaccharide Specificity
<i>Concanavalin A</i>	Con A	N-linked high mannose or hybrid
<i>Phaseolus vulgarisleucoagglutinin</i>	PHA-L	N-linked tri and tetra-antennary
<i>Maackia amuerensis agglutinin</i>	MAA	Gal(β1-4)GlcNAc
<i>Vicia villosa agglutinin</i>	VAA	α- or β-linked GalNAc
<i>Sambucus nigra lectin</i>	SNA	Neu5Acα2-6Gal(β1-4)GlcNAc
<i>Maackia amuerensis lectin</i>	MAL	Neu5Acα2-3Gal(β1-4)GlcNAc
<i>Dolichos biflorusagglutinin</i>	DBA	β1-4GlcNAc oligomers
<i>Phaseolus vulgarislerythroagglutinin</i>	PHA-E	Bisecting GlcNAc
<i>Lotus tetragonolobuslectin</i>	LTL	Fuc(α1-3)GlcNAc
<i>Arachis hypogea-agglutinin (peanut)</i>	PNA	Gal(β1-3)GalNAc
<i>Wheat germ agglutinin</i>	WGA	Chitin oligomers, sialic acid
<i>Aleuria aurantia lectin</i>	AAL	Fuc(α1-6)GlcNAc (Core fucose), Fuc (α1-3)Gal(β1-4)GlcNAc (Lewis antigen)

b) Glycan-based Immunohistochemistry (for glycoproteins and glycolipids)

The fundamental basis of immunohistochemistry spans three main scientific disciplines; histology, immunology and chemistry, in which antigens within a tissue section can be detected by specific antibodies (Ramos-Vara, 2005). Immunogenic carbohydrate antigens are usually in the form of complex glycans bound to glycoconjugates such as glycoproteins and glycolipids expressed on the cell surface (Lloyd and Old, 1989). In several types of cancer including ovarian cancer, some of these carbohydrate antigens appear to be up-regulated and monoclonal antibodies have been raised against glycan motifs such as the T_n antigen (Kanitakis, al-Rifai *et. al.*, 1998), sialyl-T_n antigen (Kjeldsen, Clausen *et. al.*, 1988), Thomsen-Friedenreich antigen (T antigen) (Ghazizadeh, Oguro *et. al.*, 1990; Cao, Stosiek *et. al.*, 1996) and blood group antigens (Hanisch, Hanski *et. al.*, 1992) present on glycolipids and glycoproteins. These antigens have been shown to discriminate between malignant and non-malignant tissues as well between different histotypes (Yuan, Itzkowitz *et. al.*, 1986; Inoue, Ogawa *et. al.*, 1990; Remmers, Anderson *et. al.*, 2013). Similar to lectins, these antibodies recognise terminal glycan motifs, although additional sub-terminal motifs or sequences may be required for binding. Most of these monoclonal antibodies are murine-derived and comprise of primarily the IgM type, as compared to IgG type (Vollmers and Brandlein, 2006). While some antibodies can be obtained directly from individual laboratories, a variety of monoclonal antibodies is commercially available, but relatively more expensive than lectins.

c) Printed Glycan Array (PGA)

Glycan arrays are typically an extension of the ELISA assay and modern DNA protein microarray technologies (Culf, Cuperlovic-Culf *et. al.*, 2006). In recent years, a number of glycan-based array platforms have been developed based on the covalent or non-covalent immobilisation of glycans through natural or synthetic linkers to surfaces such as glass (Pochechueva, Jacob *et. al.*, 2011), silica (Chang, Han *et. al.*, 2010) or gold (Zhi, Laurent *et. al.*, 2008). In most cases, these synthetic glycans are modified to contain reactive primary amines at their reducing terminal end and printed arrays are overlaid with a buffer containing glycan binding proteins (GBP) to allow for simultaneous screening against multiple glycans. Glycan arrays, however, vary in terms of their specific glycan presentation, glycan source (natural or chemically synthesised), detection methods, assay conditions, microspheres (suspension arrays) and immobilisation methods (printed glycans on slides or ELISA); all of which contribute significantly to affinity and binding specificities (Lewallen, Siler *et. al.*, 2009; Oyelaran, Li *et. al.*, 2009). For instance, variability in binding results could lead to difficulties in data interpretation due to the potential identification of false-negative binding associated with altered glycan presentation which is largely associated with choice of linkers (Lewallen, Siler *et. al.*, 2009; Padler-Karavani, Song *et. al.*, 2012). Specifically, the degree to which linker chemistry affects the presentation of glycans has been shown to depend on both the length of the linker (short *vs.* long) and the orientation of the specific linker relative to the array surface (Grant, Smith *et. al.*, 2014). In addition, there are also inherent limitations regarding the structural diversity and size of carbohydrates presented on a glycan array which can also contribute significantly to the information acquired from a single experiment (Oyelaran and Gildersleeve, 2009).

1.10 Overview of Section IV: Highlights and Challenges in Glycan Structural Identification

- Mass spectrometry is an analytical technique that provides both relative quantitation and qualitative information on any molecule upon their conversion to ions.
- MALDI and ESI are the most popular ionisation sources commonly used in mass spectrometry of glycans.
- Two major types of fragmentation commonly observed for glycans are cleavages arising from the rupturing of glycosidic bonds between sugar residues and within the sugar ring (internal cross ring).
- Fragmentation patterns in positive and negative mode are different, giving rise to specific fragments which can be utilised to determine glycan structures.
- The utility of MSⁿ fragmentation in combination with the development of reference glycan structural databases is essential for the structural characterisation of glycans.
- Porous graphitised carbon is highly discriminative towards isomeric and isobaric glycans structures with respect to structure-retention time.
- Non-mass spectrometric glycan detection methods have been useful in determining terminal epitopes although they do not provide complete structural information of a particular glycan.

1.11 Aims of Research Project

The identification of key glycosylation changes in serous pelvic cancers of the ovary, fallopian tube and peritoneum offers a new approach to the understanding of this malignancy, in terms of its development and progression. With recent evidence implicating the fallopian tube as a potential source of high grade serous cancers, the research effort of this project parallels the present clinical perspectives and challenges aimed at distinguishing serous ovarian cancer from non-ovarian cancers derived from the fallopian tube and peritoneum. Specifically, the thorough investigation of the detailed structures of membrane glycosylation (both glycoproteins and glycolipids) using mass spectrometry is warranted, as a majority of serous cancers are thought to arise from epithelial cell neoplastic transformation.

In this research project, the comparison of cell line-derived glycosylation changes in commercially available cell lines was validated in clinically-derived serous cancer tissue samples and the degree to which these membrane protein glycans are statistically discriminative of the different epithelial serous cancer origins was investigated.

Specific Aims of the Research Project:

- 1) Compare the *N*- and *O*-glycosylation profiles and detailed structural glycan determinants of membrane proteins of non-cancerous and ovarian cancer cell lines. This investigation entails the identification of relevant glycosyltransferase genes and their epigenetic regulation in order to correlate the expression of observed membrane glycan structures with corresponding changes at the molecular DNA level (**Chapter 2**).
- 2) Compare the *N*- and *O*-glycosylation profiles and detailed structural glycan determinants of membrane proteins of serous cancer tissues derived from the ovary, fallopian tube and peritoneum and determine statistically significant specific glycosylation features distinguishing the three types, if possible (**Chapter 3**).
- 3) Optimise a detergent-free, enzymatic PVDF-based glycan release protocol for the elucidation of glycosphingolipid-derived glycan structures of selected serous cancer tissues and ovarian cancer cell lines and relate these changes to structures implicated by reported auto-antibody glycan recognition from array experiments (**Chapter 4**).

CHAPTER II

Rationale

To date, the membrane protein glycosylation profiles of epithelial ovarian cancer cells have never been simultaneously characterised, both in regard to their specific *N*- and *O*-glycan structures and in comparison with glycans derived from non-cancerous ovarian surface epithelial cells. The identification of these glycans, provides an insight into the aberrant glycosylation changes that are associated with ovarian cancer and potentially implicated in various processes in cancer such as metastasis, cell adhesion and cell proliferation. Therefore, a preliminary cell-line based glycosylation model comprising of non-cancerous (HOSE 6.3 and HOSE 17.1) and four cancerous epithelial ovarian cell lines (SKOV3, IGROV1, A2780 and OVCAR3) commonly used in ovarian cancer research were investigated using PGC-LC-ESI-MS/MS to identify specific membrane protein glycosylation changes in ovarian cancer. The corresponding glycosyltransferase gene expression, together with the associated epigenetic regulation at DNA level, which led to the synthesis of specific glycan features identified in the non-cancer and cancerous cell lines were also investigated.

2.0 Publication II: Specific glycosylation of membrane proteins in epithelial ovarian cancer cell lines: glycan structures reflect gene expression and DNA methylation status

tapraid4/zjw-macp/zjw-macp/zjw00814/zjw4806-14a xppws S=4 16/6/14 20:15 4/Color Figure(s) F1,3-5,T1 ARTNO: M113.037085

Research

© 2014 by The American Society for Biochemistry and Molecular Biology, Inc.
This paper is available on line at <http://www.mcponline.org>

2: A

Specific Glycosylation of Membrane Proteins in Epithelial Ovarian Cancer Cell Lines: Glycan Structures Reflect Gene Expression and DNA Methylation Status*

Merrina Anugraham^{‡**}, Francis Jacob^{§¶**}, Sheri Nixdorf[¶], Arun Vijay Everest-Dass[‡], Viola Heinzelmann-Schwarz^{§¶}, and Nicole H. Packer[‡]

Epithelial ovarian cancer is the fifth most common cause of cancer in women worldwide bearing the highest mortality rate among all gynecological cancers. Cell membrane glycans mediate various cellular processes such as cell signaling and become altered during carcinogenesis. The extent to which glycosylation changes are influenced by aberrant regulation of gene expression is nearly unknown for ovarian cancer and remains crucial in understanding the development and progression of this disease. To address this effect, we analyzed the membrane glycosylation of non-cancerous ovarian surface epithelial (HOSE 6.3 and HOSE 17.1) and serous ovarian cancer cell lines (SKOV 3, IGROV1, A2780, and OVCAR 3), the most common histotype among epithelial ovarian cancers. *N*-glycans were released from membrane glycoproteins by PNGase F and analyzed using nano-liquid chromatography on porous graphitized carbon and negative-ion electrospray ionization mass spectrometry (ESI-MS). Glycan structures were characterized based on their molecular masses and tandem MS fragmentation patterns. We identified characteristic glycan features that were unique to the ovarian cancer membrane proteins, namely the “bisecting *N*-acetyl-glucosamine” type *N*-glycans, increased levels of α 2-6 sialylated *N*-glycans and “*N,N*”-diacetyl-lactosamine” type *N*-glycans. These *N*-glycan changes were verified by examining gene transcript levels of the enzymes specific for their synthesis (*MGAT3*, *ST6GAL1*, and *B4GALNT3*) using qRT-PCR. We further evaluated

the potential epigenetic influence on *MGAT3* expression by treating the cell lines with 5-azacytidine, a DNA methylation inhibitor. For the first time, we provide evidence that *MGAT3* expression may be epigenetically regulated by DNA hypomethylation, leading to the synthesis of the unique “bisecting GlcNAc” type *N*-glycans on the membrane proteins of ovarian cancer cells. Linking the observation of specific *N*-glycan substructures and their complex association with epigenetic programming of their associated synthetic enzymes in ovarian cancer could potentially be used for the development of novel anti-glycan drug targets and clinical diagnostic tools. *Molecular & Cellular Proteomics* 13: 10.1074/mcp.M113.037085, 1–20, 2014.

Ovarian cancer is the fifth most common cause of cancer in women worldwide with the highest mortality rate among all gynecological cancers (1). Most patients are often diagnosed when the disease has already metastasized to distant sites, resulting in a poor 5-year survival rate of 15–30% when diagnosed at the advanced FIGO stages III–IV (2, 3). This poor prognosis is primarily attributed to difficulties in detecting the disease at an early stage, lack of noticeable early symptoms and inadequate screening methods. The most widely used clinical tumor marker for the diagnosis and management of this disease is CA125, a membrane-associated glycoprotein. However, its limited sensitivity and specificity impede the detection of early stage ovarian cancers (4–6).

Cellular glycosylation is a highly organized process in which the addition and modification of sugar or glycan residues on proteins and lipids are regulated by a large network of glycosyltransferases and glycosidases that are present in all tissues and cell types (7). The field of glycomics (study of glycans and glycan modifications) holds considerable promise as studies have begun to unravel the role of glycosylation in cancer (8–10). Upon malignant transformation, some of the enzymes in the glycosylation pathways are altered in their expression or activity and are thought to be associated with critical aspects of tumor development and metastasis. For example, β 1-6-*N*-acetyl-glucosaminyltransferase (GnT-V), which is responsi-

From the [‡]Department of Chemistry & Biomolecular Sciences, Biomolecular Frontiers Research Centre, Faculty of Science, Macquarie University, NSW 2109, Sydney, Australia; [§]Gynaecological Research Group, Department of Biomedicine, Women's University Hospital Basel, University of Basel, Basel 4003, Switzerland; [¶]Ovarian Cancer Group, Adult Cancer Program, Lowy Cancer Research Centre, Prince of Wales Clinical School, University of New South Wales, NSW 2052, Sydney, Australia

Received, December 12, 2013, and in revised form, May 4, 2014
Published, MCP Papers in Press, May 22, 2014, DOI 10.1074/mcp.M113.037085

Author contributions: M.A., F.J., V.H., and N.H.P. designed research; M.A. and F.J. performed research; S.N., A.V.E., and V.H. contributed new reagents or analytic tools; M.A., F.J., and A.V.E. analyzed data; M.A., F.J., and N.H.P. wrote the paper.

Alteration of Membrane Protein Glycosylation in Ovarian Cancer

ble for the expression of tri- or tetra-antennary β 1–6-GlcNAc-bearing *N*-glycans on the cell surface and secreted glycoproteins, is often overexpressed in various cancers and has been correlated with higher invasive potential (11), metastasis (12), vascular remodeling (13) and tumor growth (14).

Recent developments in mass spectrometric methodologies and ionization techniques have also significantly improved over the last decade, thereby facilitating the structural analysis of glycans (15, 16). Furthermore, the development of glyco-bioinformatics databases and tools such as UniCarb KB (17), GlycoMod (18), GlycoWorkBench (19), GlycReSoft (20), and Multiglycan (21) have accelerated the pace of glycan characterization. In ovarian cancer, the majority of studies investigating *N*-glycans have been performed using serum (22–25), in which significant cancer-associated changes such as increased levels of branching of the *N*-glycans attached to glycoproteins (24) and increased sialylation of *N*-glycopeptides (25) have been found. As 90% of ovarian cancers are of epithelial origin (26), an overview of the glycosylation landscape on cancer cell surface membrane glycoproteins is especially interesting as they have the potential to be used diagnostically, prognostically, and therapeutically (27).

In this study, we examined specific *N*-glycan changes on glycoproteins from non-cancerous ovarian surface epithelial and ovarian cancer cell lines based on their membrane *N*-glycomic profiles. In addition, we performed a gene expression analysis of relevant glycosyltransferases and evaluated the potential epigenetic influence on glycosyltransferase-encoding genes to better understand their complex association with cell surface glycosylation. The link between aberrant glycosylation and epigenetics in cancer is an emerging area of research that still remains poorly understood (28, 29). Unlike irreversible genetic changes that affect the activity of these enzymes, epigenetic modifications can potentially be reversed by therapies such as de-methylation, which may be able to target defective glycosylation pathways to prevent metastasis in cancer (30). Hence, the specific glycan structural and synthetic alterations reported here serve as a preface toward understanding the key steps involved in the development and progression of ovarian cancer via the regulation of specific glycosyltransferases and the expression of their corresponding glycan structural epitopes.

EXPERIMENTAL PROCEDURES

Materials—*N*-Glycosidase F (PNGase F, recombinant clone derived from *Flavobacterium meningosepticum* and expressed in *Escherichia coli*) and protease inhibitor mixture tablets were purchased from Roche Diagnostics (Basel, Switzerland). α 2–3 sialidase enzyme (Glyko® Sialidase S, recombinant derived from *Streptococcus pneumoniae* and expressed in *Escherichia coli*) was purchased from Prozyme (Hayward, CA). Immobilin-P polyvinylidene fluoride (PVDF, 0.2 μ m) was obtained from Millipore (Billerica, MA). Microtiter plates (Corning Costar® 96-well flat bottom) were purchased from Sigma Aldrich (St. Louis, MO). Cation exchange resin beads (AG50W-X8) was obtained from BioRad (Hercules, CA), and PerfectPure C18 Zip Tips were from Eppendorf (Hamburg, Germany). Mycoplasma detec-

tion kit VenorGeM® Mycoplasma Detection Kit was purchased from Minerva Biolabs GmbH (Berlin, Germany). RNA extraction NucleoSpin RNAII kit was obtained from Macherey & Nagel GmbH (Düren, Germany). Proteinase K was purchased from Finnzymes, ThermoFisher Scientific (Waltham, MA). EZ DNA Methylation-Gold™ Kit for bisulfite conversion was from Zymo Research (Irvine, CA). 5-aza-2'-deoxycytidine (5-Aza)² and primers were purchased from Sigma Aldrich (St. Louis, MO). Tris-hydrochloride (Tris-HCl), sodium chloride (NaCl), potassium hydroxide (KOH), ethylenediaminetetraacetic acid (EDTA), Triton X-114, polyvinyl pyrrolidone 40,000 (PVP40), and sodium borohydride (NaBH₄) were obtained from Sigma Aldrich (St. Louis, MO). Other reagents and solvents such as methanol, ethanol, and acetonitrile were of HPLC or LC/MS grade.

Cell Culture Preparation—Serous ovarian cancer cell lines (SKOV 3, IGROV 1, A2780, and OVCAR 3) were obtained from ATCC (Manassas) and were cultured in RPMI 1640 medium, supplemented with 10% fetal bovine serum. Normal, non-cancerous ovarian surface epithelial cell lines (HOSE 6.3 and HOSE 17.1) were obtained from the Garvan Research Institute (Sydney, Australia) and maintained in MCDB 105: Medium 199 (1:1, v/v) containing 10% fetal bovine serum (31). All cells were grown to 70% confluency at 37 °C in 5% CO₂. Detailed characteristics of the non-cancerous and cancerous cell lines used in this study are listed in [supplemental Table S1](#). For extraction of genomic DNA and total RNA, cells were lysed directly after washing without harvesting by trypsinization. All cultures were free of mycoplasma, as determined by qualitative PCR using VenorGeM® Mycoplasma Detection Kit.

Cell Membrane Preparation and Triton X-114 Phase Partitioning of Membrane Proteins—Approximately 4×10^7 cells were washed twice with PBS and pelleted through centrifugation at $2500 \times g$ for 20 mins to remove excess culture media. Cell pellets were re-suspended with 2 ml of lysis buffer (50 mM Tris-HCl, 100 mM NaCl, 1 mM EDTA, and protease inhibitor at pH 7.4) and stored on ice for 20 mins. The cells were lysed using a Polytron homogenizer (Omni TH, Omni International Inc, Kennesaw, GA) for 15 mins. Cellular debris and unlysed cells were removed by centrifugation at $2000 \times g$ for 20 mins at 4 °C. The supernatant was collected and diluted with 2 ml of Tris binding buffer (20 mM Tris-HCl, and 100 mM NaCl at pH 7.4) and sedimented by ultracentrifugation at $120,000 \times g$ for 80 mins at 4 °C. The supernatant was discarded and 140 μ l of Tris binding buffer was added into each sample to re-suspend the membrane pellet [modified from (32)]. A volume of 450 μ l of Tris binding buffer containing 1% (v/v) Triton X-114 was added to the suspended mixture, homogenized by pipetting and chilled on ice for 10 mins. Samples were heated at 37 °C for 20 mins and further subjected to phase partitioning by centrifugation at $200 \times g$ for 3 mins. The upper aqueous layer was carefully removed and stored at –20 °C until further analysis. The lower detergent layer containing the membrane proteins was mixed with 1 ml of ice-cold acetone and left overnight at –20 °C. Precipitated membrane proteins were pelleted by centrifugation at $1000 \times g$ for 3 mins and solubilized in 10 μ l of 8 M urea (32).

Enzymatic Release of *N*-glycans from Cell Membrane Proteins—*N*-glycans were prepared as previously described (33). Briefly, membrane proteins and glycoprotein standard (10 μ g of fetuin) were

¹ The abbreviations used are: 5-Aza, 5-aza-2'-deoxycytidine; Gal, galactosamine; Man, mannose; Glc, glucose; Fuc, fucose; GlcNAc, *N*-acetyl-glucosamine; LacdiNAc, *N,N'*-diacetyl-lactosamine; GalNAc, *N*-acetyl-galactosamine; Neu5Ac, *N*-acetyl-neuraminic acid; LC, liquid chromatography; ESI, electrospray ionization; BPC, base peak chromatogram; EIC, extracted ion chromatogram; PGC, porous graphitized carbon; FIGO, International Federation of Gynaecology and Obstetrics; MIQE, Minimum Information for Publication of Quantitative Real-Time PCR Experiments.

Alteration of Membrane Protein Glycosylation in Ovarian Cancer

spotted (2.5 $\mu\text{l} \times 4$ times) onto a polyvinylidene difluoride (PVDF) membrane (Sequi Blot 0.2 μm , Millipore). The PVDF membrane was dried overnight at room temperature prior to staining and de-staining of the bound membrane proteins. The stained protein spots were cut and placed in separate wells of a 96-well microtiter plate and 100 μl of blocking buffer was added to each well. Upon removing the blocking buffer, the wells were then washed with MilliQ water and PNGase F enzyme (2 μl of 1 U/ μl PNGase F and 8 μl of MilliQ water) was added to each well. A volume of 10 μl MilliQ water was added prior to an overnight incubation at 37 °C. The 96-well microtiter plate was sealed with parafilm to avoid sample evaporation. After sonication of the plate for 10 mins, ~20 μl of *N*-glycans were recovered from each well and combined with washings (50 μl of MilliQ water, twice) from the sample wells. To ensure a complete regeneration of the reducing terminus of the released *N*-glycans, 20 μl of 100 mM ammonium acetate (pH 5.0) was added to each sample (~120 μl) at room temperature for 1 h. After evaporation of the samples, the released *N*-glycans were reduced to alditols with 10 μl of 2 M NaBH₄ in 50 mM KOH and 10 μl of 50 mM KOH at 50 °C for 2 h and the reduction was quenched using 2 μl of glacial acetic acid.

Purification of *N*-glycan Alditols Derived from Cell Membrane Proteins—The *N*-glycan alditols were desalted using cation exchange columns prepared in-house. Approximately 45 μl of cation exchange resin beads (AG50W-X8) were deposited onto reversed phase $\mu\text{-C18}$ ZipTips (Perfect Pure, Millipore) placed in individual microfuge tubes. The tubes were then subjected to a brief spin followed by a series of individual prewashing steps as described previously (33). Approximately 20 μl of *N*-glycan alditols were applied to the column, eluted with MilliQ water (50 μl , twice) and dried. Residual borate was removed by drying the samples under vacuum after the addition of methanol (100 μl , thrice). The purified *N*-glycan alditols were resuspended in 15 μl of MilliQ water prior to mass spectrometry analysis.

LC-ESI-MS/MS of Released *N*-glycan Alditols—*N*-glycans were analyzed by nanoLC-MS/MS using an ion-trap mass spectrometer (LC/MSD Trap XCT Plus Series 1100, Santa Clara, CA), which was connected to an ESI source (Agilent 6330). Samples were injected onto a Hypercarb porous graphitized carbon capillary column (5 μm Hypercarb KAPPA, 180 $\mu\text{m} \times 100$ mm, Thermo Hypersil, Runcorn, UK) using an Agilent auto-sampler (Agilent 1100). The separation of *N*-glycans was carried out over a linear gradient of 0–45% (v/v) acetonitrile/10 mM ammonium bicarbonate for 85 mins followed by a 10 min wash-step using 90% (v/v) acetonitrile/10 mM ammonium bicarbonate at a flow rate of 2 $\mu\text{l}/\text{min}$. The sample injection volume was 7 μl and the MS spectra were obtained within the mass range of m/z 200– m/z 2200. The temperature of the transfer capillary was maintained at 300 °C and the capillary voltage was set at 3 kV. *N*-glycans were detected in the negative ionization mode as $[\text{M}-\text{H}]^-$ and $[\text{M}-2\text{H}]^{2-}$ ions. The MS data was analyzed and quantitated using Compass Data Analysis Version 4.0 software (Bruker Daltonics). Monosaccharide compositions of the measured monoisotopic masses were determined using the GlycoMod tool (18) available on the ExPASy server (<http://au.expasy.org/tools/glycomod>) with a mass tolerance of ± 0.5 Da. The proposed glycan structures were manually assigned and interpreted from the tandem MS fragmentation spectra and further characterized with the GlycoWorkBench software tool (19). In addition, the web-based LC-MS/MS database, UniCarb KB (17), was also utilized to confirm fragmentation and retention time of *N*-glycans based on previously reported glycan structures that were available in the online library (34–37). The assignment of sialic acid linkages on the *N*-glycan structures were carried out through specific exoglycosidase treatment described below. Furthermore, *N*-glycans from fetuin were also used to confirm these linkages as previously described (38). Other structural features such as the “bisecting

GlcNAc” structures were characterized from diagnostic fragment ions previously described in negative ion mode fragmentation of *N*-glycans (39–41).

Data Processing and Statistical Analysis of *N*-glycans—The MS ion intensity of each *N*-glycan composition was relatively quantified based on the peak areas of their extracted ion chromatogram (EIC) and expressed as a percentage of summed ion intensities for total *N*-glycans within each cell line. The glycan structures were classified into four major categories [high mannose/oligomannose, hybrid, complex (neutral and sialylated), and core fucosylated] based on the nomenclature proposed by Stanley *et al.* (2009) (42). Following normalization to 100%, the MS ion intensities were averaged for three replicates of each cell line and subjected to one-way analysis of variance (ANOVA) using SPSS Version 19.0 to assess their statistical significance at $p < 0.05$.

Specific α 2–3 Sialidase Digestion of *N*-glycan Samples—To verify the sialic acid linkages, 5 μl *N*-glycans (~30 μg of membrane proteins) were digested with 2 μl of α 2–3 sialidase S (2 mU) in 2 μl of 5X reaction buffer and made up to 10 μl with water. The reaction mixture was vortexed and incubated at 37 °C overnight prior to LC-ESI-MS analysis. A matched untreated glycan sample (3 μl) was made up to 10 μl with water and used as a control for comparison.

Compositional Monosaccharide Analysis—Compositional analysis of monosaccharides was performed to verify the presence of the monosaccharide residue, *N*-acetyl-galactosamine, on the released *N*-glycans of the non-cancerous and cancerous cell lines. For neutral amino monosaccharides, 20 μl of released *N*-glycan alditols were hydrolyzed by treatment with 4 M HCl (100 μl of 8 M HCl in 80 μl MilliQ water) at 100 °C for 6 h. Hydrolyzed samples were evaporated to dryness and reconstituted in 50 μl of internal standard (0.1 M 2-deoxy-D-glucose). Monosaccharide content was determined using a high-performance anion-exchange chromatography with pulsed amperometric detection (HPAEC-PAD) system that comprised of the Bio-LC (Dionex, Thermo Scientific, Sunnyvale, CA) equipped with gradient pumps (GS50, Dionex) and a pulsed amperometric detector (ED50A, Dionex). 20 μl of amino monosaccharides were injected for each sample in duplicate and separated isocratically on a Dionex CarboPac™ PA-10 column (2 \times 250 mm, Thermo Scientific) at a flow rate of 1.0 ml/min using 12 mM NaOH. Data was collected and analyzed using Chromeleon software (SP5 Build 1914, Dionex Version 6.70, Dionex Corporation).

Total RNA and Genomic DNA Extraction—In order to examine the potential gene expression of associated glycosyltransferases ($n = 17$) and reference genes ($n = 3$), non-cancerous ovarian surface epithelial and ovarian cancer cells were grown in 6-well plates (NUNC, Thermo Fisher Scientific, Roskilde, Denmark). Prior to cell lysis, cells were washed twice with PBS, and the cellular contents of two wells of a 6-well plate were combined. Total RNA extraction was performed using the NucleoSpin RNAII kit (Macherey-Nagel, Germany) according to the manufacturer's instructions. RNA was eluted in 50 μl of RNase free water. Total RNA was measured at $A_{260/230 \text{ nm}}$ and $A_{260/280 \text{ nm}}$ using the NanoDrop ND-1000 spectrophotometer (Thermo Fisher Scientific, Denmark). RNA integrity was confirmed via an electropherogram (Agilent Bioanalyzer RNA 6000 Nano).

For genomic DNA extraction, the cellular contents of two wells of a 6-well plate were combined. Cells were lysed using 250 μl of lysis buffer (20 mM Tris-HCl, 4 mM Na₂EDTA, and 100 mM NaCl) followed by the addition of 25 μl of 10% (w/v) SDS. The lysed cell suspensions were vortexed vigorously and subsequent Proteinase K digestion (2.5 μl) was performed for a minimum of 2 h at 55 °C. Residual undigested proteins were precipitated using 200 μl of 5.3 M NaCl followed by 13,000 $\times g$ centrifugation for 30 min at 4 °C. Supernatant was transferred to a new microfuge tube and an equal volume of ice-cold isopropanol was added. DNA was precipitated by inverting tubes

Q: C

AQ: D

Alteration of Membrane Protein Glycosylation in Ovarian Cancer

several times. Precipitated DNA was washed with 70% ethanol and dissolved in 10 mM of Tris-HCl at pH 8.5. DNA concentration was measured using spectrophotometry as described above for RNA.

Reverse Transcription (RT) and Quantitative PCR (qPCR)—Total RNA (1 µg) was reverse-transcribed using the iScript Reverse Transcription Superscript for RT-qPCR (Bio-Rad Laboratories, Australia) in a total volume of 20 µl according to the manufacturer's instructions. The complementary DNA (cDNA) was stored at −20 °C until further use. RT-qPCR was performed in concordance to MIQE guidelines (43). Reference genes were selected as previously described (44) and listed in Table II. Target gene primers were designed by QuantPrime (45). Primer sequences were cross-checked using the web-based tool *in-silico* PCR (<http://genome.ucsc.edu/cgi-bin/hgPcr>) on the human genome browser at UCSC (46) against gene and genomic targets. RT-qPCR was performed on the Applied Biosystems 7500 Fast Real Time PCR system (Applied Biosystems, Switzerland) in 96-well microtitre plates for all six cell lines (SKOV 3, IGROV 1, A2780, OVCAR 3, HOSE 6.3 and HOSE 17.1). Optimal reaction conditions were obtained using 1× SensiFast™ SYBR with low ROX as the reference dye (Biolabs, Switzerland), 400 nM specific sense, 400 nM specific antisense primer, RNase/DNase-free water, and cDNA template in a final reaction volume of 10 µl. Amplifications were performed starting with a 30 s enzyme activation at 95 °C, followed by 40 cycles of denaturation at 95 °C for 5 s, and then annealing/extension at 60 °C for 30 s. At the end of each run, a melting curve analysis was performed between 65–95 °C. All samples and negative controls were amplified in triplicates and the mean value obtained was then used for further analysis.

To compare the RNA transcript levels of six cell lines for 17 targeted genes, cycle of quantification (Cq) values were generated directly at a specific threshold. The fluorescence signals obtained at a defined RNA concentration were plotted and linear regression was performed to identify the best linear relationship representing the standard curve. The slope of the linear equation was applied to calculate the efficiency according to the equation, $E = (10^{[-1/\text{slope}]}) \times 100$. Raw data, including the melting and amplification curves, generated by the ABI 7500 software Version 2.0.6. (Applied Biosystems, Switzerland) were analyzed. Raw data were extracted and further data analysis was performed using the R statistical programming language Version 2.15.1 (<http://CRAN.R-project.org>).

5-aza-2'-deoxycytidine Treatment—To investigate the potential influence of DNA methylation on *MGAT3* and *ST6GAL1* expression, the DNA methyltransferase inhibitor 5-aza-2'-deoxycytidine (5-Aza) was applied to all cell lines as follows: 10⁶ cells were seeded in 6-well plates (NUNC, Thermo Fisher Scientific, Roskilde, Denmark) and incubated at 37 °C for 24 h. Culture medium was removed every 24 h and replaced by new medium containing 2.5 µM 5-Aza in 50% (v/v) acetic acid. Samples were harvested after 24 h, 48 h and 72 h of treatment. Total RNA was extracted as described above. Mock control cells were treated with 50% (v/v) acetic acid at a dilution identical to that of 5-Aza treated cells. The histone deacetylase inhibitor trichostatin A (TSA) was used as additional control (to exclude involvement of histone methylation) in which cells were treated with 5.0 µM TSA.

RESULTS

To identify specific membrane *N*-glycan changes in serous ovarian cancer cell lines (SKOV 3, IGROV 1, A2780, and OVCAR 3) and non-cancerous ovarian surface epithelial cell lines (HOSE 6.3 and HOSE 17.1), global glycosylation profiles of the glycans released from total membrane proteins by PNGase F were acquired using mass spectrometry. The glycan structures were assigned based on manual interpretation of the tandem MS fragment spectra.

Relative Quantitation of *N*-glycans of Membrane Proteins from Non-cancerous and Cancerous Cell Lines—The LC-ESI-MS/MS glycomic profiles were compared between the two non-cancerous and four cancerous cell lines to identify specific *N*-glycan alterations in terms of compositional and structural features. The major difference in structures between the *N*-glycans on membrane proteins from non-cancerous and cancerous cell lines are indicated in the representative glycomic profiles of one non-cancerous (HOSE 6.3) and one ovarian cancer (SKOV 3) cell line (Fig. 1).

In total, 53 individual *N*-glycan masses (including structural and compositional isomers) were detected across all six cell lines of which 33 *N*-glycan masses were present in all the non-cancerous and cancerous cell lines (Table I). In order to determine if there were quantitative differences between these glycans in the membrane proteins of the non-cancerous and cancerous cell lines, the common *N*-glycans present in both non-cancerous and cancerous cell lines were statistically analyzed based on their *N*-glycan classes [high mannose, hybrid, complex (neutral and sialylated) and core fucosylated]. As shown in Fig. 2, we observed significantly higher ($p < 0.05$) levels of high mannose *N*-glycans in the cancerous cell lines as compared with the non-cancerous cell lines with correspondingly lower levels of complex neutral ($p < 0.0001$) and complex sialylated *N*-glycans ($p < 0.05$) observed in ovarian cancer when compared with non-cancerous cell lines. Similarly, core fucosylated *N*-glycans were also found to be significantly lower ($p < 0.01$) in ovarian cancer cell lines as compared with the non-cancerous cell lines. No significant differences were observed in the overall expression of *N*-glycans in the total hybrid *N*-glycan subgroup. *O*-glycosylation was also investigated by reductive beta-elimination release from the membrane proteins of all the mentioned cell lines (non-cancer and cancerous) followed by PGC LC MS/MS. Less than five structures consisting of Core 1 and Core 2 *O*-glycans were found and there were no significant changes in the relative intensities of these structures between the non-cancer and cancer cell lines. Hence, the regulation of *O*-glycosylation was not further investigated.

α 2–6 Sialylation—Upon performing a one-way ANOVA analysis to determine quantitative differences between the non-cancerous and cancerous cell lines, each *N*-glycan subgroup was examined for qualitative differences arising because of the presence of specific structural isomers. Porous graphitized carbon (PGC) LC-ESI-MS enables the separation of isomers of differently linked sialylated *N*-glycans based on their corresponding retention times (Fig. 3). Both the complex and hybrid sialylated *N*-glycan subgroups were found to contain isomeric glycan structures pertaining to differences in α 2–6 or α 2–3 linked sialylation.

For example, the monosialylated biantennary complex *N*-glycan with m/z [1038.9]^{2−} detected in the cancer cell line, IGROV 1 [Fig. 3A(i)] consists of the monosaccharide composition (Neu5Ac)₁(Hex)₂(HexNAc)₂(dHex)₁ + (Man)₃(GlcNAc)₂

Alteration of Membrane Protein Glycosylation in Ovarian Cancer

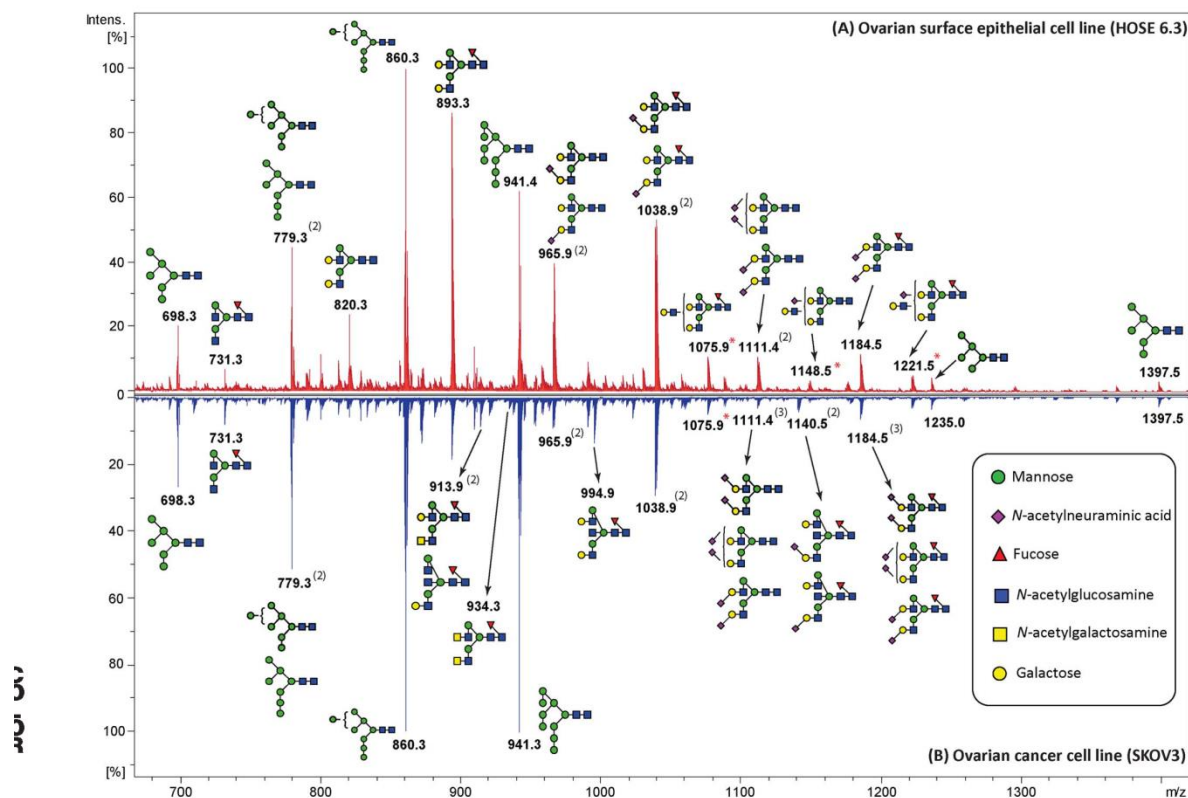


FIG. 1. Representative glycomic profiles of *N*-glycans released from membrane proteins of HOSE 6.3 and SKOV 3 cell lines. An overview of the representative average MS *N*-glycan profiles in the range of *m/z* 600–1400 of the non-cancerous human ovarian surface epithelial (HOSE 6.3) and ovarian cancer cell line (SKOV 3) membrane glycoproteins (LC elution time: 30 to 70 mins). The *N*-glycan structures were identified by tandem MS and are represented mainly by the doubly charged species ion, *m/z* [M-2H]²⁻. Singly charged [M-H]⁻ ions with *m/z* 1235.0 and *m/z* 1397.5 are also shown in the figure. Number of isomers corresponding to structurally resolved mass ions is indicated in parentheses (). *N*-glycan masses that were not structurally resolved and determined to consist of two or more isomer(s) are indicated with asterisks (*).

and comprises of two isomers; namely a sialylated, core fucosylated biantennary *N*-glycan with the Neu5Ac (sialic acid) linked either by a α 2–6 or α 2–3 linkage to the terminal Gal residue located on either arm. Sialylated isomers can be distinguished based on retention time differences as previously described (38, 40, 47) with the α 2–3 linked isomers having a stronger affinity to PGC and thereby eluting later as compared with the α 2–6 linked sialylated glycans. For the above *N*-glycan isomers, the α 2–6 linked sialic acid glycan isomers were shown to elute from the porous graphitized carbon column ~7–8 min earlier than the α 2–3 linked glycan isomers. The linkages were orthogonally verified using α 2–3 sialidase that resulted in the loss of the late eluting *N*-glycan peaks bearing the α 2–3-linked sialic acid [Fig. 3A(ii)]. This α 2–6 monosialylated fucosylated biantennary complex *N*-glycan (*m/z* [1038.9]²⁻) and the corresponding monosialylated, non-fucosylated structure of *m/z* [965.9]²⁻ [(Neu5Ac)₁(Hex)₂(HexNAc)₂ + (Man)₃(GlcNAc)₂] was observed only in the ovar-

ian cancer cells (supplemental Fig. S1A and S1B). The disialylated biantennary complex *N*-glycan with *m/z* [1184.5]²⁻ [(Neu5Ac)₂(Hex)₂(HexNAc)₂ (dHex)₁ + (Man)₃(GlcNAc)₂] (supplemental Fig. S1C) was also present with additional isomers in the ovarian cancer cells. As represented in Fig. 3B(i) and (ii), the extracted ion chromatograms (EIC) of *N*-glycans in the hybrid category also revealed the presence of additional isomers of the α 2–6 monosialylated *N*-glycan isomers with *m/z* [864.3]²⁻ [(Neu5Ac)₁(Hex)₂(HexNAc)₁ + (Man)₃(GlcNAc)₂], *m/z* [945.3]²⁻ [(Neu5Ac)₁(Hex)₃(HexNAc)₁ + (Man)₃(GlcNAc)₂] and *m/z* [937.3]²⁻ [(Neu5Ac)₁(Hex)₂(HexNAc)₁(dHex)₁ + (Man)₃(GlcNAc)₂] in all ovarian cancer cell lines but not in the non-cancerous cells.

Bisecting GlcNAc—Apart from the 33 *N*-glycans common to all analyzed cell lines, we identified six unique *N*-glycans (*m/z* [840.8]²⁻, *m/z* [913.9]²⁻, *m/z* [921.9]²⁻, *m/z* [994.9]²⁻, *m/z* [1177.5]²⁻, and *m/z* [1140.5]²⁻), which were present on the cell membrane proteins of all four cancerous cell lines, but not

Alteration of Membrane Protein Glycosylation in Ovarian Cancer

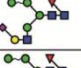
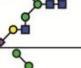
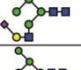
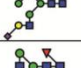
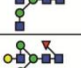
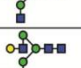
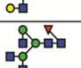
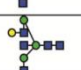
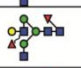

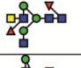
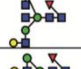
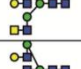
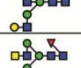
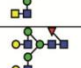
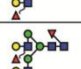
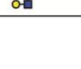
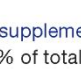
TABLE I

Proposed N-glycan structures detected on the membrane proteins of non-cancerous and ovarian cancer cells. N-glycan structures released from non-cancerous and ovarian cancer cell membrane proteins were separated by PGC-LC-ESI and their structures were assigned based on MS/MS fragmentation (where possible), retention time differences and biological pathway constraints. Structures were depicted according to the CFG (Consortium of Functional Glycomics) notation with linkage placement to indicate linkages for sialic acid and fucose residues. Specific linkages corresponding to Gal-GlcNAc (Type 1/Type 2) lactosamine linkages were not distinguished. N-glycan masses that were not structurally resolved and determined to consist of two or more isomer(s) are indicated with asterisks (*). Values represent mean ± S.D. of three separate experimental replicates

Type	No	Glycan Mass [M-H] ⁺	[M-2H] ²⁺	Glycan Structures	Average Relative Intensity (n=3)					
					Non-Cancerous Cells		Ovarian Cancer Cells			
					HOSE 6.3	HOSE 17.1	SKOV 3	IGROV 1	A2780	OVCAR 3
High Mannose	1	1235.4	617.2		0.60 ± 0.15	0.63 ± 0.15	0.66 ± 0.04	0.62 ± 0.06	1.61 ± 0.06	1.79 ± 0.15
	2	1397.6	698.3		3.85 ± 0.78	2.89 ± 0.82	5.03 ± 1.37	7.91 ± 0.15	4.84 ± 0.54	3.97 ± 0.36
	3a	1559.6	779.3		7.73 ± 0.51	4.40 ± 0.20	8.26 ± 0.15	11.30 ± 2.65	9.8 ± 2.20	6.72 ± 0.20
	3b	1559.6	779.3		1.90 ± 0.96	1.8 ± 0.75	1.86 ± 0.35	2.15 ± 0.20	2.53 ± 0.25	2.18 ± 0.13
	4	1721.6	860.3		15.40 ± 1.76	13.97 ± 3.84	22.86 ± 7.60	16.00 ± 3.73	17.29 ± 3.40	14.96 ± 0.81
	5	1883.8	941.4		14.11 ± 0.92	14.06 ± 0.93	25.21 ± 0.85	24.57 ± 6.02	20.84 ± 0.06	19.29 ± 0.23
Hybrid	6	2045.6	1022.3		0.68 ± 0.11	0.58 ± 0.10	1.16 ± 0.14	1.43 ± 0.61	1.16 ± 0.21	1.18 ± 0.17
	7	1260.5	-		0.15 ± 0.07	0.01 ± 0.00	0.04 ± 0.00	0.01 ± 0.00	0.01 ± 0.00	0.01 ± 0.00
	8	1422.6	710.8		0.00	0.00	0.00	0.21 ± 0.10	0.00	0.00
	9a	1567.6	783.3		0.00	0.00	0.04 ± 0.00	0.08 ± 0.03	0.22 ± 0.03	0.01 ± 0.00
	9b	1567.6	783.3		0.36 ± 0.12	0.31 ± 0.10	0.00	0.11 ± 0.05	0.17 ± 0.04	0.00
	10	1584.6	791.8		0.65 ± 0.14	0.56 ± 0.10	0.38 ± 0.13	0.34 ± 0.11	0.31 ± 0.05	0.55 ± 0.03
	11	1600.6	799.8		1.90 ± 0.36	1.44 ± 0.16	1.19 ± 0.54	1.04 ± 0.30	0.81 ± 0.11	2.21 ± 0.50
	12a	1713.6	856.3		0.00	0.12 ± 0.20	0.32 ± 0.35	0.7 ± 0.21	2.21 ± 0.10	0.43 ± 0.20
	12b	1713.6	856.3		1.72 ± 0.27	0.85 ± 0.15	0.35 ± 0.12	1.06 ± 0.42	2.36 ± 0.20	0.54 ± 0.18
	13a	1729.6	864.3		0.08 ± 0.25	0.02 ± 0.20	0.39 ± 0.25	0.38 ± 0.18	0.27 ± 0.05	0.99 ± 0.15
	13b	1729.6	864.3		0.84 ± 0.40	0.80 ± 0.10	0.14 ± 0.20	0.30 ± 0.29	0.67 ± 0.06	0.38 ± 0.10
	14	1746.6	872.8		0.18 ± 0.08	0.28 ± 0.10	0.50 ± 0.08	0.20 ± 0.00	0.45 ± 0.04	0.72 ± 0.31

Alteration of Membrane Protein Glycosylation in Ovarian Cancer

TABLE I—continued

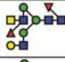
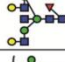
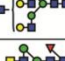
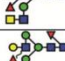
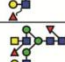
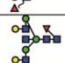
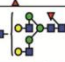
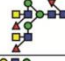
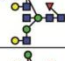
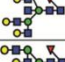
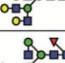


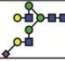
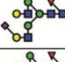
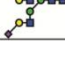

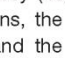
Type	No	Glycan Mass [M-H] ⁺	[M-2H] ²⁺	Glycan Structures	Average Relative Intensity (n=3)					
					Non-Cancerous Cells		Ovarian Cancer Cells			
					HOSE 6.3	HOSE 17.1	SKOV 3	IGROV 1	A2780	OVCA 3
Hybrid	15a	1875.6	937.3		0.00	0.00	0.41 ± 0.16	0.20 ± 0.25	0.69 ± 0.16	0.62 ± 0.18
	15b	1875.6	937.3		0.60 ± 0.06	0.36 ± 0.09	0.36 ± 0.12	0.41 ± 0.20	0.28 ± 0.14	0.60 ± 0.13
	16a	1891.6	945.3		0.06 ± 0.19	0.06 ± 0.12	0.68 ± 0.04	0.47 ± 0.22	0.63 ± 0.12	1.43 ± 0.38
	16b	1891.6	945.3		0.58 ± 0.10	0.42 ± 0.11	0.46 ± 0.03	0.43 ± 0.08	0.37 ± 0.03	0.7 ± 0.19
Complex Neutral	17	1463.6	731.2		0.59 ± 0.26	0.47 ± 0.06	0.90 ± 0.27	0.74 ± 0.03	0.76 ± 0.14	1.00 ± 0.17
	18	1625.6	812.3		1.63 ± 0.12	1.42 ± 0.19	0.76 ± 0.11	0.64 ± 0.14	1.40 ± 0.08	0.85 ± 0.35
	19	1641.6	820.3		4.65 ± 0.67	4.81 ± 0.76	0.87 ± 0.05	1.59 ± 0.62	0.91 ± 0.11	1.40 ± 0.24
	20	1666.4	832.8		0.28 ± 0.10	0.01 ± 0.00	1.31 ± 0.46	1.22 ± 0.40	0.77 ± 0.25	0.15 ± 0.05
	21	1682.6	840.8		0.00	0.00	0.30 ± 0.13	0.12 ± 0.05	0.70 ± 0.10	0.80 ± 0.16
	22	1771.8	885.4		0.47 ± 0.18	0.41 ± 0.04	0.00	0.00	0.00	0.00
	23	1787.6	893.3		14.43 ± 2.24	16.31 ± 2.81	3.14 ± 0.02	3.50 ± 0.22	3.81 ± 0.50	3.95 ± 0.91
	24	1812.8	905.9		0.00	0.00	0.00	0.24 ± 0.08	0.00	0.00
	25a	1828.8	913.9		0.00	0.00	0.12 ± 0.08	0.17 ± 0.13	1.70 ± 0.80	0.73 ± 0.18
	25b	1828.8	913.9		0.00	0.00	0.18 ± 0.04	0.49 ± 0.11	0.00	0.00
	26	1844.8	921.9		0.00	0.00	0.50 ± 0.09	1.37 ± 0.19	1.00 ± 0.13	1.60 ± 0.21
	27	1869.8	934.4		0.00	0.00	0.70 ± 0.30	0.51 ± 0.20	0.00	0.00
	28a	1933.6	966.3		1.90 ± 0.90	3.57 ± 0.59	0.00	0.00	0.00	0.00
	28b	1933.6	966.3		0.48 ± 0.11	0.83 ± 0.20	0.00	0.00	0.00	0.00

SI on the non-cancerous cell lines (Table I; supplemental Fig. 2). These *N*-glycans, representing ~5%-13% of total relative ion intensities of all four ovarian cancer cell lines (Fig. 2) consisted of bi- and tri-antennary *N*-glycans that was found to have a bisecting GlcNAc (*N*-acetyl glucosamine) residue attached in

a β 1–4 linkage to the innermost mannose of the *N*-glycan core. This linkage is catalyzed by the action of a specific enzyme, β 1–4-*N*-acetyl-glucosaminyltransferase III (GnT-III) encoded by the gene *MGAT3*. The structural assignment of the bisecting-type *N*-glycans was carried out based on the

Alteration of Membrane Protein Glycosylation in Ovarian Cancer

TABLE I—continued

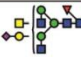

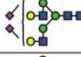
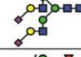

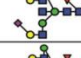
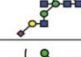

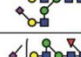
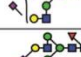
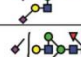
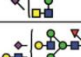
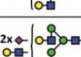
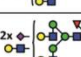
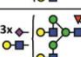
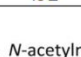





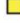

Type	No	Glycan Mass [M-H] [−]	[M-2H] ^{2−}	Glycan Structures	Average Relative Intensity (n=3)					
					Non-Cancerous Cells		Ovarian Cancer Cells			
					HOSE 6.3	HOSE 17.1	SKOV 3	IGROV 1	A2780	OVCA9
Complex Neutral	29	1974.8	986.9		0.00	0.00	0.00	0.79 ± 0.28	0.00	0.00
	30	1990.8	994.9		0.00	0.00	2.60 ± 0.10	2.62 ± 0.60	3.77 ± 0.80	5.93 ± 1.06
	31	2006.8*	1002.9		0.67 ± 0.25	1.14 ± 0.45	0.21 ± 0.07	0.31 ± 0.15	0.30 ± 0.12	0.27 ± 0.10
	32	2015.8	1007.4		0.00	0.00	0.00	0.14 ± 0.06	0.00	0.00
	33	2079.8	1039.4		0.32 ± 0.08	0.65 ± 0.15	0.00	0.00	0.00	0.00
	34	2120.8	1059.9		0.00	0.00	0.00	0.56 ± 0.19	0.00	0.00
	35	2136.6	1067.8		0.00	0.00	0.00	0.31 ± 0.15	0.00	0.00
	36	2152.8*	1075.9		2.44 ± 0.65	3.44 ± 0.62	0.92 ± 0.19	1.18 ± 0.16	1.10 ± 0.34	1.25 ± 0.31
	37	2162	1080.5		0.00	0.00	0.00	0.39 ± 0.09	0.00	0.00
	38a	2356	1177.5		0.00	0.00	0.00	0.00	0.18 ± 0.15	1.40 ± 0.44
	38b	2356	1177.5		0.00	0.00	0.40 ± 0.07	0.23 ± 0.02	0.22 ± 0.11	0.00
	39	2518	1258.5		0.01 ± 0.00	0.60 ± 0.18	0.40 ± 0.15	0.37 ± 0.10	0.16 ± 0.05	0.53 ± 0.18
Complex Sialylated	40a	1916.6	957.8		0.00	0.00	0.44 ± 0.00	0.07 ± 0.05	0.49 ± 0.03	0.58 ± 0.09
	40b	1916.6	957.8		0.74 ± 0.17	0.81 ± 0.06	0.11 ± 0.05	0.14 ± 0.06	0.39 ± 0.07	0.40 ± 0.14
	41a	1932.8	965.9		0.73 ± 1.20	0.79 ± 1.14	1.47 ± 0.36	1.38 ± 0.38	1.50 ± 0.26	2.09 ± 0.20
	41b	1932.8	965.9		3.57 ± 1.11	5.44 ± 1.35	1.03 ± 0.27	1.86 ± 0.49	1.12 ± 0.47	1.13 ± 0.11
	42a	2078.8	1038.9		0.81 ± 0.43	1.00 ± 0.20	5.15 ± 1.20	1.91 ± 0.23	3.80 ± 0.09	7.72 ± 1.34
	42b	2078.8	1038.9		9.36 ± 0.75	9.12 ± 0.25	3.49 ± 2.18	3.23 ± 0.14	2.85 ± 0.10	1.41 ± 1.55

MS/MS fragmentation described by Harvey (48). In negative mode fragmentation spectra of *N*-glycans, the D ion arises from the loss of the chitobiose core and the substituents forming the 3-antennae; thus the D ion mass corresponds to the composition of the 6-arm antenna as well as the two remaining branching core mannose residues. However, in bisecting type *N*-glycans, there is an additional loss of the β 1–4 linked GlcNAc, which results in the formation of the D-221 ion that is diagnostic for the presence of these structures. As observed in Fig. 4 (inset), the extracted ion chromatogram (EIC) of neutral bisecting GlcNAc *N*-glycan with m/z [994.9]^{2−} [(Hex)₂(HexNAc)₃(dHex)₁ + (Man)₃(GlcNAc)₂] is seen only in the ovarian cancer cell lines (Fig. 4C–4F). When this parent ion mass was fragmented, the D-221 fragment ion

F4

Alteration of Membrane Protein Glycosylation in Ovarian Cancer

TABLE I—continued

Type	No	Glycan Mass [M-H] ⁺	[M-2H] ²⁺	Glycan Structures	Average Relative Intensity (n=3)					
					Non-Cancerous Cells		Ovarian Cancer Cells			
					HOSE 6.3	HOSE 17.1	SKOV 3	IGROV 1	A2780	OVCAR 3
Complex Sialylated	43	2119.8 ^a	1059.4		0.00	0.00	0.17 ± 0.12	0.36 ± 0.15	0.00	0.00
	44a	2223.8	1111.4		0.00	0.00	0.05 ± 0.10	0.10 ± 0.03	0.20 ± 0.50	0.27 ± 0.13
	44b	2223.8	1111.4		0.23 ± 0.19	0.11 ± 0.14	0.18 ± 0.11	0.13 ± 0.08	0.60 ± 0.41	0.35 ± 0.26
	44c	2223.8	1111.4		0.66 ± 0.20	0.86 ± 0.10	0.15 ± 0.15	0.18 ± 0.10	0.33 ± 0.12	0.52 ± 0.14
	45	2265.8 ^a	1132.4		0.00	0.00	0.00	0.06 ± 0.02	0.00	0.00
	46a	2282.0	1140.5		0.00	0.00	0.54 ± 0.06	0.35 ± 0.14	1.10 ± 0.14	2.80 ± 0.50
	46b	2282.0	1140.5		0.00	0.00	0.36 ± 0.17	0.30 ± 0.17	0.00	0.00
	47	2297.8 ^a	1148.4		0.30 ± 0.00	0.53 ± 0.14	0.12 ± 0.02	0.23 ± 0.02	0.01 ± 0.00	0.01 ± 0.00
	48a	2370.0	1184.5		0.00	0.00	0.10 ± 0.19	0.42 ± 0.13	0.17 ± 0.19	0.12 ± 0.42
	48b	2370.0	1184.5		0.00	0.00	0.97 ± 0.30	0.38 ± 0.24	1.52 ± 0.20	0.35 ± 0.25
	48c	2370.0	1184.5		2.93 ± 0.76	2.32 ± 0.19	0.61 ± 0.21	0.53 ± 0.35	0.28 ± 0.31	1.60 ± 0.44
	49	2411.0	1205		0.00	0.00	0.03 ± 0.00	0.06 ± 0.02	0.00	0.00
	50	2444.0 ^a	1221.5		0.76 ± 0.40	1.31 ± 0.26	0.97 ± 0.30	0.65 ± 0.07	0.91 ± 0.15	1.12 ± 0.06
	51	2589.0 ^a	1294.0		0.16 ± 0.05	0.17 ± 0.09	0.03 ± 0.00	0.03 ± 0.00	0.01 ± 0.00	0.01 ± 0.00
	52	2735.0 ^a	1367.0		0.30 ± 0.14	0.23 ± 0.11	0.27 ± 0.09	0.03 ± 0.00	0.41 ± 0.13	0.37 ± 0.03
	53	3026.0 ^a	1512.5		0.19 ± 0.10	0.09 ± 0.02	0.15 ± 0.10	0.19 ± 0.08	0.01 ± 0.00	0.01 ± 0.00
Legend:  Mannose  Fucose  Galactose  N-acetylneuraminic acid  N-acetylglucosamine  N-acetylgalactosamine					Monosaccharide Linkage:  Unknown					

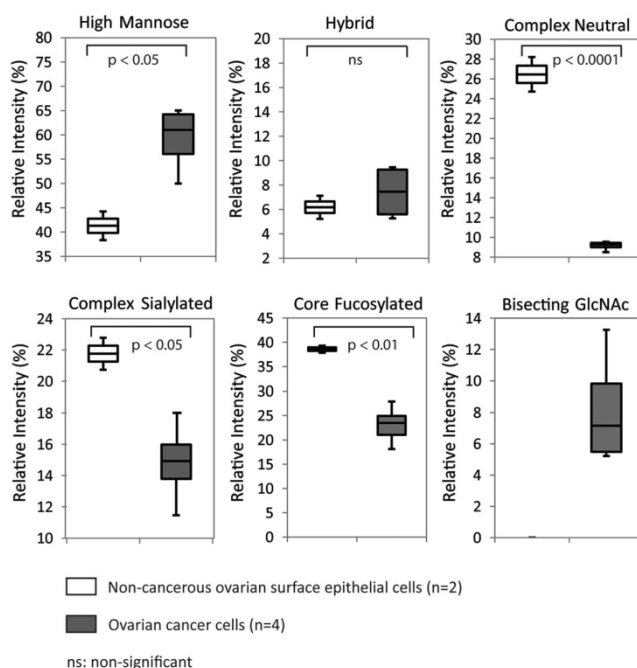
mass at m/z [670.3]¹⁻, which corresponds to the composition, Gal-GlcNAc-Man-Man - loss of H₂O was observed in the MS/MS spectra of all five bisecting type *N*-glycan structures as shown in Supplemental Fig. S3A–S3E. An example of another the diagnostic b-221 fragment ion at m/z [508.3]¹⁻ corresponding to GlcNAc-Man-Man - loss of H₂O, was also

observed in the MS/MS spectrum for the *N*-glycan with m/z [913.9]²⁻(supplemental Fig. S3F).

LacdiNAc-type N-glycans—Several *N*-glycans specific to only the cell membrane proteins of SKOV 3 and IGROV 1 cell lines were also detected at low intensities, in which their monosaccharide compositions were predicted to contain a

Alteration of Membrane Protein Glycosylation in Ovarian Cancer

Fig. 2. Quantitation of relative abundances based on structural *N*-glycan type (as shown in Table I). Box plots indicating changes in the relative ion intensities of 33 common *N*-glycans (high mannose, hybrid, complex neutral, complex sialylated, and core fucosylated) expressed in two non-cancerous human ovarian surface epithelial cells and four ovarian cancer cell lines. Levels of significant differences are indicated by respective *p* values for all categories except for bisecting GlcNAc. Data represents the mean of three technical replicates.



mixture of fucosylated, di-fucosylated and sialylated LacdiNAc motifs (Table I). We identified 4 *N*-glycans (m/z [913.9] $^{2-}$, m/z [934.4] $^{2-}$, m/z [1059.9] $^{2-}$, and m/z [1205.0] $^{2-}$) that were present in both the cell lines (supplemental Fig. S4) whereas the remaining six *N*-glycans (m/z [905.9] $^{2-}$, m/z [986.9] $^{2-}$, m/z [1007.4] $^{2-}$, m/z [1059.9] $^{2-}$, m/z [1080.5] $^{2-}$, and m/z [1132.4] $^{2-}$), consisted of mono and di-fucosylated LacdiNAc motifs that were present only in the IGROV 1 cell line (supplemental Fig. S5). The representative MS/MS fragmentation ion spectra of LacdiNAc-type *N*-glycan (m/z [934.4] $^{2-}$) as well as the fucosylated (m/z [1080.5] $^{2-}$) and sialylated (m/z [1205.0] $^{2-}$) LacdiNAc derivatives are shown in Fig. 5. The MS/MS fragmentation spectra, although at low intensities, contained adequate fragment ions corresponding to both glycosidic and cross ring cleavages to facilitate the identification of the LacdiNAc antennae on these *N*-glycans. As observed in Fig. 5A, the fragmentation spectra of the parent ion at m/z [934.4] $^{2-}$ [(HexNAc) $_4$ (dHex) $_1$ + (Man) $_3$ GlcNAc] $_2$ contained a prominent cross ring cleavage ion arising from the non-reducing terminal end of the *N*-glycan structure. This 1,3 A cross-ring cleavage ion at m/z [465.2] $^{1-}$, also termed as F ion, has a composition of GalNAc - GlcNAc-O-CH = CH-O- (GalNAc + GlcNAc + 59) that comprises the LacdiNAc disaccharide and two carbon atoms of the branching Man residue. Another pair of diagnostic ions that occurred as glycosidic cleavages at the non-reducing end was also observed as B/Y ions (m/z [405.2] $^{1-}$ and m/z [1463.6] $^{1-}$), clearly providing a definitive identification of the LacdiNAc antennae. Similarly, other de-

derivatives of the LacdiNAc motif such as the fucosylated LacdiNAc (GalNAc-(Fuc)GlcNAc) and sialylated LacdiNAc (Neu5Ac-GalNAc-GlcNAc) trisaccharides were also found to contain the B ion at m/z [551.2] $^{1-}$ and m/z [696.3] $^{1-}$ for the parent ion with m/z [1080.5] $^{2-}$ [(HexNAc) $_4$ (dHex) $_3$ + (Man) $_3$ GlcNAc] $_2$ and m/z [1205.0] $^{2-}$ [(Neu5Ac) $_2$ (Hex) $_1$ - (HexNAc) $_3$ (dHex) $_1$ + (Man) $_3$ GlcNAc] $_2$ respectively (Fig. 5B and 5C). The presence of the monosaccharide residue, *N*-acetyl-galactosamine (GalNAc) in the PNGase F released *N*-glycans was also verified through compositional monosaccharide analysis, which revealed trace amounts of GalNAc in the IGROV 1 cell line that was not detected in the other non-cancerous and cancerous cell lines (supplemental Table 2).

Gene Expression of Specific Glycosyltransferases in Ovarian Cancer Cell Lines—The detection of α 2–6 sialylation and bisecting GlcNAc in the *N*-glycans of all of the four ovarian cancer cell lines as compared with the non-cancerous cell lines may be attributed to the regulation of specific enzymes within the glycosylation pathway, specifically the α 2–6 sialyltransferase (*ST6GAL 1* gene) and the bisecting GlcNAc transferase (*MGAT 3* gene). Similarly, the identification of the LacdiNAc-type *N*-glycans, despite their low intensities, in two of the four ovarian cancer cell lines also warranted the investigation of specific gene expression of the various β 1–3/4 *N*-acetyl-galactosaminyltransferases (*B3GALNT* and *B4GALNT* genes). To determine this, the relative transcript abundance of these genes was investigated in the two

Alteration of Membrane Protein Glycosylation in Ovarian Cancer

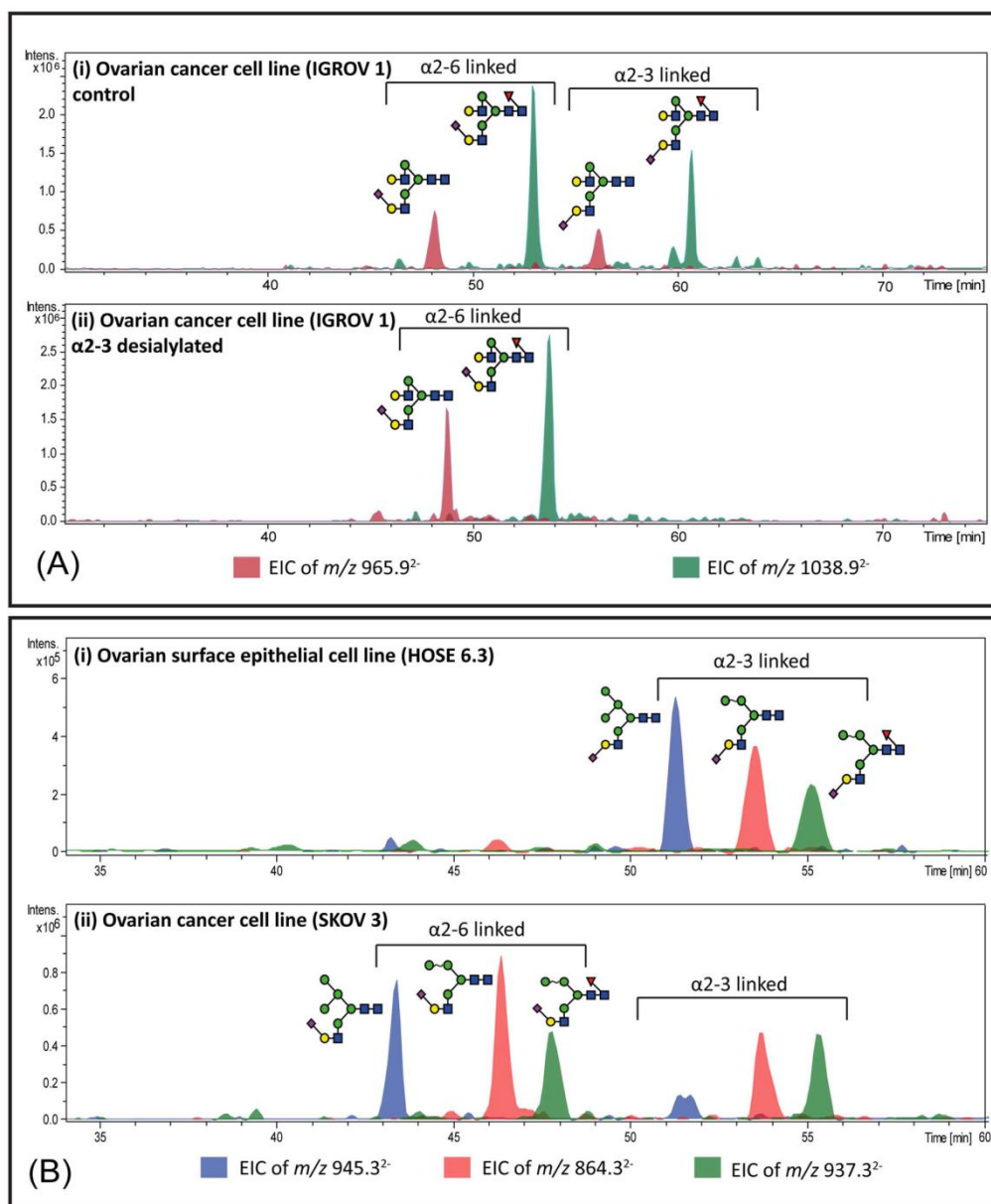


FIG. 3. Representative extracted ion chromatograms (EIC) of monosialylated *N*-glycans. A, PGC- LC allows for the separation of α 2–6 and α 2–3 sialylated *N*-glycans based on retention time. The EICs obtained from the ovarian cancer cell line, IGROV 1 depict two major monosialylated *N*-glycans (with and without fucose), m/z [965.9]²⁻ [(Neu5Ac)₁(Hex)₂(HexNAc)₂ + (Man)₃(GlcNAc)₂] and m/z [1038.9]²⁻ [(Neu5Ac)₁(Hex)₂(HexNAc)₂(dHex)₁ + (Man)₃(GlcNAc)₂], which display α 2–3 and α 2–6 sialylated isomers at separate retention times (i). To orthogonally confirm the identity of the isomers containing α 2–6 linked sialic acids, released *N*-glycans from the membrane proteins of IGROV1 cells were treated with α 2–3-linked sialidase. The lower panel depicts the loss of the α 2–3 sialylated isomers for both *N*-glycans (ii). B, The EICs of three monosialylated hybrid *N*-glycans with m/z [864.3]²⁻, m/z [945.3]²⁻ and m/z [937.3]²⁻ are represented and the separate retention times for isomers with α 2–6-linked and α 2–3-linked sialic acid are illustrated in (1) the non-cancerous epithelial cells (HOSE 6.3) and (2) ovarian cancer cell line (SKOV 3).

Alteration of Membrane Protein Glycosylation in Ovarian Cancer

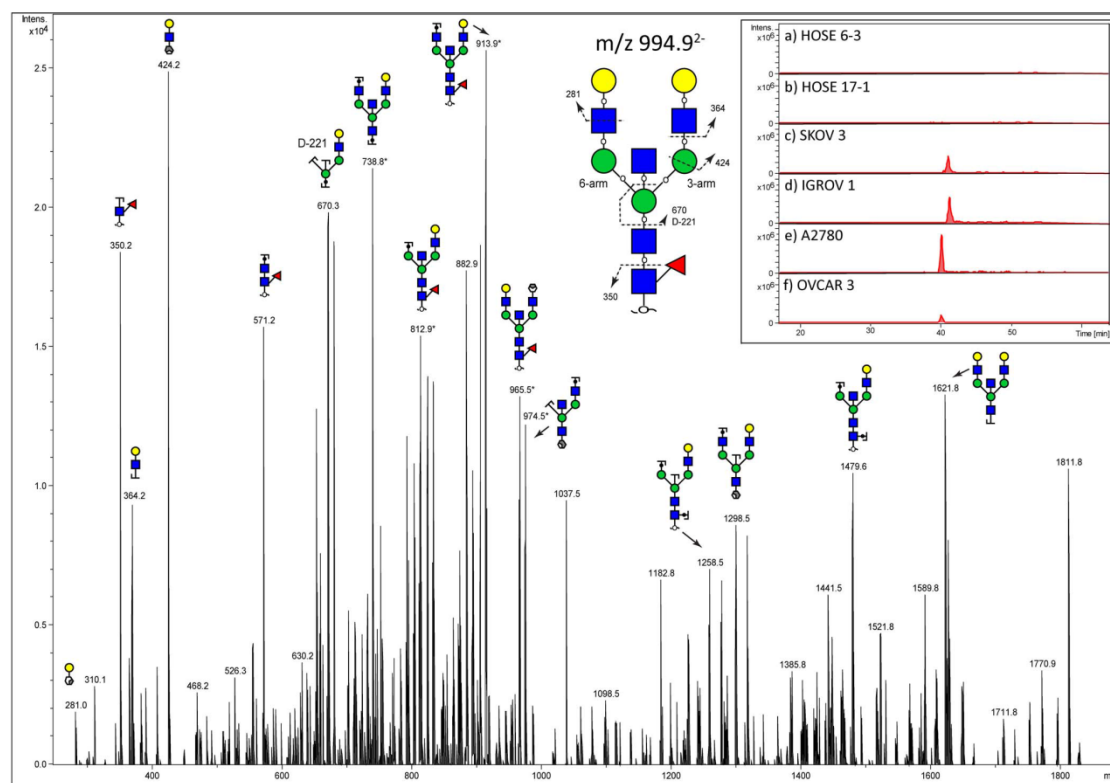


FIG. 4. Example of a MS² fragment ion spectra depicting the diagnostic ions of bisecting GlcNAc type *N*-glycans in ovarian cancer cells. In *N*-glycans, the D-221 ion is formed when the bisecting GlcNAc attached to the innermost Man residue is cleaved from the 6-antenna comprising of Gal-GlcNAc-bisecting GlcNAc-Man-Man. The fragment ion resulting from this specific cleavage of the bisecting bi-antennary *N*-glycan shown appears at *m/z* [670.3]⁺. The insert to the right represents the extracted ion chromatogram (EIC) of neutral bisecting GlcNAc *N*-glycan with *m/z* [994.9]²⁺ [(Hex)₂(HexNAc)₃ (dHex)₁ + (Man)₃(GlcNAc)₂] in noncancerous and ovarian cancer cell lines.

non-cancerous and four cancerous cell lines. In addition, we also profiled five *ST3Gal* sialyltransferases (*ST3GAL* 1–5) to determine the corresponding expression of enzymes responsible for the *N*-glycans bearing α 2–3 linked sialic acid residues, and six α 1–2/3/4/6 fucosyltransferases (*FUT* 2–5,8,9) that corresponded to *N*-glycans bearing either core and/or terminal fucosylation. According to MIQE guidelines, RNA integrity was based on the RNA integrity number (RIN) of which obtained values of $A_{260/280}$ (2.08–2.10), $A_{260/230}$ (1.95–2.21), and ratio 28S/18S (2.0–2.3) indicated purified and intact total RNA extracts. Each glycosyltransferase encoding gene ($n = 17$) and three reference genes (*HSPCB*, *SDHA*, and *YWHAZ*) were examined for qPCR assay performance on at least three 10-fold dilutions, ranging from a minimum of 50 pg to a maximum of 100 ng of initial total RNA. PCR efficiency was detected as being the lowest in *ST3GAL* 1 (83.3%) and the highest in *FUT* 5 (120.5%). The coefficient of determination (R^2) was always ≥ 0.910 (Table II). The remaining candidate genes for this study, namely

the α 1–3 fucosyltransferase 6 (*FUT* 6), α 1–3 fucosyltransferase 7 (*FUT* 7), and β 1–4 *N*-acetyl-galactosaminyltransferase 4 (*B4GALNT* 4) did not reveal reliable qPCR performance because of non-detectable expression of mRNA transcripts in all investigated cell lines ($n = 6$) and were therefore excluded from this study.

The ΔCq of each “glyco-gene” (normalized against the logarithmic mean of reference genes) was applied by visualizing and clustering “glyco-gene” expression among the tested cell lines (Fig. 6A). The expression of *ST6GAL* 1 ($p < 0.001$), *MGAT* 3 ($p < 0.001$), and *B4GALNT* 3 ($p = 0.015$) were significantly decreased in the non-cancerous cell lines as compared with the high expression observed in the ovarian cancer cell lines. In contrast, the non-cancerous cell lines showed significantly increased expression of *ST3GAL* 5 compared with all ovarian cancer cell lines ($p = 0.026$). *ST3GAL* 4 was abundantly expressed in both non-cancerous and ovarian cancer cell lines as compared with *ST3GAL* 3 that had varying transcript levels. The investigation of fucosyltransferase

F6

Alteration of Membrane Protein Glycosylation in Ovarian Cancer

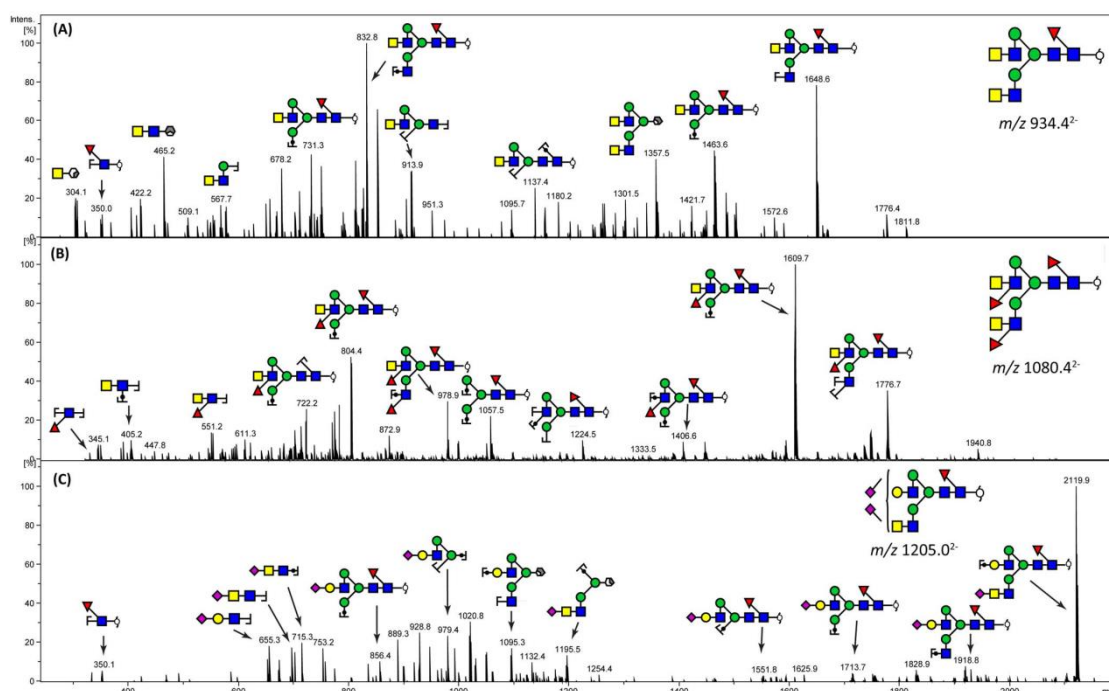


FIG. 5. Representative MS² fragment ion spectra depicting the diagnostic ions for LacdiNAc type *N*-glycans in ovarian cancer cells. A, Diagnostic ions characteristic for the identification of the HexNAc-HexNAc disaccharide, *m/z* [405.2][−] and *m/z* [465.2][−], are illustrated for the neutral bi-antennary core fucosylated *N*-glycan with *m/z* [934.4]^{2−} [(HexNAc)₄ (dHex)₁ + (Man)₃ (GlcNAc)₂]. Diagnostic ions, which are characteristic for terminal fucosylated LacdiNAc (*m/z* [551.2][−]) and sialylated LacdiNAc ([696.3][−]), are illustrated for *N*-glycans with *m/z* [1080.4]^{2−} [(HexNAc)₄ (dHex)₃ + (Man)₃ (GlcNAc)₂] B, and [1205.0]^{2−} [(Neu5Ac)₂ (Hex)₁ (HexNAc)₃ (dHex)₁ + (Man)₃ (GlcNAc)₂], respectively C.

encoding genes did not reveal any differential gene expression for core fucosylation (*FUT8*) and terminal fucosylation (*FUT2*, 4, and 5) between the non-cancerous and ovarian cancer cell lines, although a significant increase in gene expression for *FUT3* and *FUT9* was observed specifically in the OVCAR 3 cell line as compared with the other cell lines.

We used both the data on the *N*-glycan structures containing bisecting GlcNAc and α 2-6/α 2-3 sialylation as detected by LC-ESI-MS and the corresponding gene expression of the selected glycosyltransferases (*MGAT3*, *ST6GAL1*, and *ST3GAL5*) to investigate their potential correlation (Fig. 6B). This was achieved by calculating the total relative ion intensities for the bisecting GlcNAc *N*-glycans (*n* = 6 structures) and α 2-6/α 2-3 sialylated *N*-glycans (*n* = 11 structures) respectively, expressing them as a percentage of the total relative ion intensities of all *N*-glycans from each cell line and plotting these percentage values against the ΔCq of the corresponding glycosyltransferases. The linear dependence (*R*²) obtained revealed a strong correlation between bisecting GlcNAc and *MGAT3* expression (*r* = 0.79) and between α 2-6 sialylation and *ST6GAL1* expression (*r* = 0.76), whereas moderately linear association was observed between α 2-3 sialyla-

tion and *ST3GAL5* expression (*r* = 0.66). These correlations emphasize that the specific changes in *N*-glycan structures seen between non-cancerous and cancerous cells can be directly attributable to the expression of the genes responsible for their synthesis. In particular, the bisecting GlcNAcylation and α 2-6 sialylation of the glycan structures expressed on the membrane proteins of ovarian cancer cells are directly correlated with the increased expression of the genes, *MGAT3* and *ST6GAL1*.

DNA Hypermethylation and *MGAT3* Expression—The exclusive presence of bisecting GlcNAc on *N*-glycans from all tested ovarian cancer cell lines highly correlated with *MGAT3* expression, whereas the absence of bisecting GlcNAc in both non-cancerous cell lines was in full concordance with the reduced expression of *MGAT3*. In an attempt to understand the molecular mechanism underlying the decreased *MGAT3* transcription in the non-cancerous cells, we investigated whether epigenetic dysregulation by hypermethylation might be responsible for silencing the *MGAT3* gene in the non-cancerous cells. We treated the non-cancerous and ovarian cancer cell lines with 5-aza-2'-deoxycytidine (5-Aza), an inhibitor of DNA methyltransferase, and tested for *MGAT3* ex-

Alteration of Membrane Protein Glycosylation in Ovarian Cancer

TABLE II
Established target gene primers and reference genes. Comprehensive list of primers used for quantitative RT-qPCR and parameters providing efficiency (E) and correlation coefficient (R²) for each primer pair on target and reference genes were established by Jacob et al. (2013) (44)

Symbol	Gene name	Accession number	Chromosomal location	Forward primer 5'-3'	Reverse primer 5'-3'	E in %	R ²
MGAT3	mannosyl (β-1,4)-glycoprotein β-1,4-N-acetylglucosaminyl transferase	NM_002409.4	22q13.1	GGGATGAAGATGAGACGCTACAAAG	AGGACAGGGTCTTGAAAGAAATGTC	114.3	0.985
ST6GAL1	β-galactosamide α-2,6-sialyltransferase 1	NM_173217.2	3q27-q28b	CCATCCTCTGGGATGCTTGGTATC	ACGTCACTCTGGCGCTTGGATG	102.9	0.991
ST3GAL1	β-galactoside α-2,3-sialyltransferase 1	NM_173344.2	8q24.22	AGTACCGACTTTGTCTCAGGATG	TGGTCTTGGTCCCAACATCAGC	83.3	0.981
ST3GAL2	β-galactoside α-2,3-sialyltransferase 2	NM_006927.3	16q22.1	GCATGTGTGTGATGAGTGAACG	TTCTCCAGTAGTGTGCGCAGTTG	102.6	0.999
ST3GAL3	β-galactoside α-2,3-sialyltransferase 3	NM_174963	1p34.1	AGTGGCAGGACTTTAAGTGGTTG	AGAAGCCATCCGATGCACTCAC	91.4	0.983
ST3GAL4	β-galactoside α-2,3-sialyltransferase 4	NM_006278.2	11q24.2	CAGCCACGGAAGATTAAAGCAAG	GCAATGTGACCAAGTACACAG	111.3	0.999
ST3GAL5	β-galactoside α-2,3-sialyltransferase 5	NM_001042437.1	2p11.2	TGTGAGCCTGAGCCTGTAAGAG	TGCACAACTTGGGACGACATTCC	103.6	0.995
FUT2	α1-2 fucosyltransferase 2	NM_000511.5	19q13.3	TCACCGATGCTGGAGGGTTTC	AACGACAGCATGGCTTCTCTC	118.2	0.982
FUT3	α1-3/4 fucosyltransferase 3	NM_001097640.1	19p13.3	TCAGACAGTCCCAAGTTCAAGCC	TACAGTCGATCCCACTGTACCC	107.8	0.997
FUT4	α1-3 fucosyltransferase 4	NM_002033.3	11q21	TTTACCGAGGAGGAGCCAAAGG	GCTGGTTCTGCCACTGTCTATTG	100.0	0.999
FUT5	α1-3 fucosyltransferase 5	NM_002034.2	19p13.3	TGCATCACTATGGGTGACCTC	TGAGGATCGCAACACATCCAC	120.5	0.952
FUT8	α1-6 fucosyltransferase 8	NM_178155	14q24.3	GGCCTGTAAGTGAACATGCAC	TTTGTCTTCACTTCACTGACCC	89.4	0.998
FUT9	α1-3 fucosyltransferase 9	NM_006581.3	6q16	TGGCCTCAATTAGCCACCTTCAG	TGGACAAAGATGGCATCTTCAGG	93.1	0.987
B4GALNT1	beta-1,4-N-acetyl-galactosaminyl transferase 1	NM_001478.3	12q13.3	GAGCCTTCAGGCAGCTTCT	CCTAGGAGGCGAGTCAGGTT	98.1	0.910
B4GALNT3	beta-1,4-N-acetyl-galactosaminyl transferase 3	NM_173593.3	12p13.33	TGGCATAGACCTCGTGAAGGAC	ACAGTCTCCGAATGGCATC	100.4	0.998
B3GALNT1	beta-1,3-N-acetyl-galactosaminyltransferase 1	NM_003781.3	3q25	TGCTCTATCACGTGGTGCTCTC	ACGCGAGCCGAAGGTTCTTTAC	116.8	0.997
B3GALNT2	beta-1,3-N-acetyl-galactosaminyltransferase 2	NM_152490.2	1q42.3	TGCCCTTACTGAAGGAGGAAAGCAG	AGCTCGTGTGTTTCCACAGTCCATC	106.3	0.986
HSPCB	Heat shock protein 90 kDa alpha (cytosolic)	NM_007355	6p12	TCTGGGTATCGGAAAGCAAGCC	GTGCATCTCTCAGGCATCTTG	103.1	0.998
YWHAZ	Tyrosine 3-monooxygenase/tyroptophan 5-monooxygenase activation protein, zeta polypeptide	NM_003406	8q23.1	ACTTTTGGTACATTGTGGCTTCAA	CCGCCAGGACAAACCAAGTAT	101.2	0.998
SDHA	Succinate dehydrogenase complex, subunit A	NM_004168	5p15	TGGGAACAAGAGGCGCATCTG	CCACCAGTCATCAAAATTCATG	105.6	0.994

Alteration of Membrane Protein Glycosylation in Ovarian Cancer

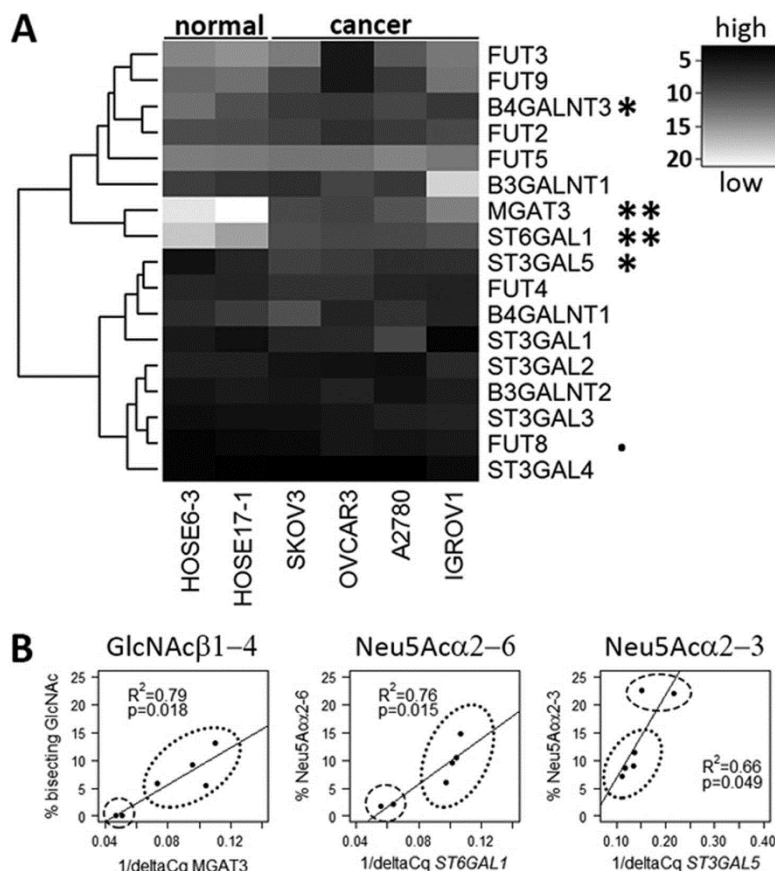


FIG. 6. Quantitative RT-PCR of mRNA transcripts of glycosyltransferase genes and scatterplot analysis of glyco-gene expression (*MGAT3* and *ST6GAL1*) with corresponding *N*-glycan structures. Gene expression levels of glycosyltransferase mRNA transcripts ($n = 17$) analyzed in two non-cancerous human ovarian surface epithelial cells (HOSE 6.3 and HOSE 17.1) and four ovarian cancer cell lines (SKOV 3, OVCAR 3, A2780, and IGROV 1). A, Normalized (ΔCq) and clustered "glyco gene" expression (row) among tested cell lines (column) visualized as heatmap. Dendrogram (row) shows clusters of correlating expression. Key at the right side indicates level of expression of transcripts from high (black) to low (white). Level of significant differences in transcript levels are indicated by asterisk (* $p < 0.1$; * $p < 0.05$; ** $p < 0.001$). Gene expression profiles of *MGAT3*, *ST6GAL1* and *ST3GAL5* show positive correlation with resulting glycan phenotype as illustrated by B, scatterplots of *MGAT3*, *ST6GAL1*, and *ST3GAL5* "glyco gene" expression (abscissa) and their corresponding relative MS ion intensities of bisecting GlcNAc, α 2-6 and α 2-3 sialylated *N*-glycan structures (ordinate). Scatterplot data points circled in dashes represent two non-cancerous human ovarian surface epithelial cells and data points circled in dots represent four ovarian cancer cell lines used in this study. Data represents the mean of three technical replicates.

pression. In addition, cells were treated with Trichostatin A (TSA), a selective inhibitor of class I and II histone deacetylases to exclude the potential alteration of *MGAT3* expression by histone epigenetic involvement. Within a 2 day-treatment period with 5-Aza, we observed a significant increase ($p < 0.05$) of *MGAT3* transcripts in non-cancerous cell lines as indicated by a relative *MGAT3* expression of up to 324-fold and 83-fold for HOSE 6.3 and HOSE 17.1, respectively (Fig. 7A). The reconstituted *MGAT3* gene PCR product for both non-cancerous cell lines was also visualized by agarose gel

electrophoresis (Fig. 7B). No or slightly increased *MGAT3* transcript levels were observed in the serous ovarian cancer cell lines with 5-Aza treatment except for IGROV1 cells that showed a 6.3-fold increase. TSA treatment revealed similar *MGAT3* expression in HOSE 17.1, OVCAR3, A2780, and IGROV1 cell lines with only minor variations in HOSE 6-3 and SKOV3. These data suggest that inhibition of DNA methyltransferases by 5-Aza subsequently lead to DNA hypomethylation, thereby increasing *MGAT3* expression in the two non-cancerous cell lines.

Alteration of Membrane Protein Glycosylation in Ovarian Cancer

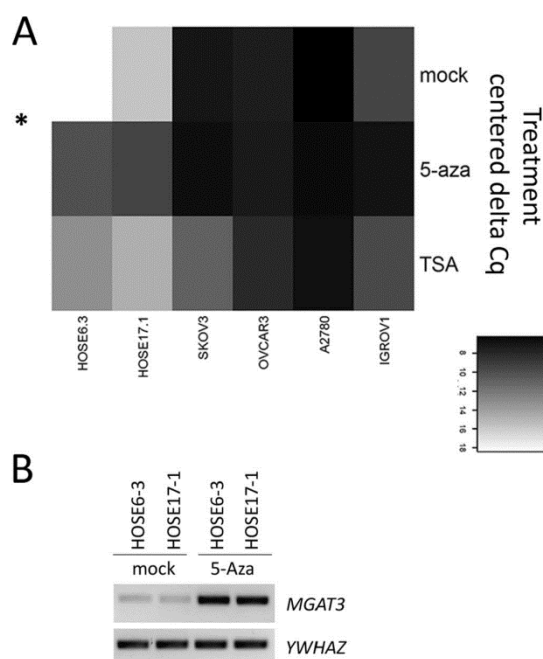


FIG. 7. Evidence of *MGAT3* gene silencing by DNA hypermethylation in non-cancerous human ovarian surface epithelial cells. To determine if *MGAT3* gene expression is regulated epigenetically by DNA methylation, all cell lines were treated with 5-Aza, a DNA methylation inhibitor, and tested for *MGAT3* expression. **A**, Heatmap illustration of *MGAT3* gene expression (ΔCq) normalized for all cell lines (abscissa) under different treatment conditions: no treatment (mock), Azacitidine (5-Aza), and Trichostatin A (TSA). In both non-cancerous cell lines, *MGAT3* gene expression was significantly increased after treatment with 5-Aza. Level of significant difference in transcript levels is indicated by asterisk (* $p < 0.05$). Transcription levels are based on 72 h treatment period. Key at the lower right side indicates level of *MGAT3* expression from high (black) to low (white). **B**, Reconstituted *MGAT3* (by 5-Aza and mock treatment) and reference gene (*YWHAZ*) expression in normal ovarian surface epithelial cell lines are visualized by agarose gel electrophoresis.

DISCUSSION

Post-translational modifications on proteins, such as glycosylation, offer researchers the possibility of exploring new potential biomarkers for early ovarian cancer detection and novel treatment options or therapies for this disease. The acquisition of structural information pertaining to membrane *N*-glycans is therefore important as it exposes new cell surface membrane glycan targets or modifications that represent key enzymatic changes that occur in cancer within the glycosylation machinery. It is becoming apparent that these glycan alterations are not necessarily the consequence of mutations and deletions at the DNA level of the respective glycosyltransferases, but may rather be caused by epigenetic modifications to the DNA such as hyper- or hypomethylation that

regulate variable gene expression (49). In this study, we identify specific *N*-glycan alterations on the cell surface membrane proteins of serous ovarian cancer cell lines that correlate with differential gene expression of the corresponding glycosyltransferase-encoded genes. We also show that the primary glycosyltransferase alteration is epigenetically regulated via DNA methylation.

A defining *N*-glycan structural feature unique to the ovarian cancer cell lines analyzed in this study was the presence of bisecting *N*-acetylglucosamine on several complex *N*-glycans, representing 5%–13% of the total *N*-glycans across four ovarian cancer cell lines. To our knowledge, no study has investigated bisecting GlcNAc structures on membrane proteins of serous ovarian cancer and normal human ovarian epithelial cells using *nano*ESI-LC-MS/MS to directly identify the presence of this determinant without the use of monoclonal antibodies or lectins. In a previous study by Wong *et al.* (2003), mono-fucosylated, bisecting GlcNAc *N*-glycans were identified on CA125, which was isolated by gel filtration from the conditioned media of the serous ovarian cancer cell line, OVCAR 3 (50). The authors confirmed the presence of bisecting GlcNAc using gas chromatography mass spectrometry (GC-MS) linkage analysis that identified a 3,4,6-linked Man residue of the *N*-glycan core, implying the presence of the 4-linked bisecting GlcNAc. For the first time, we have demonstrated that the expression of bisecting GlcNAc on *N*-linked glycoproteins is correlated with the expression of the *MGAT3* gene that expresses the enzyme that adds this monosaccharide in a β 1–4 linkage to the core of the *N*-glycans. This is consistent with a previous study using mouse models ($n = 9$) and human fresh frozen tissue samples ($n = 5$), in which there was elevated mRNA expression of *MGAT3* in endometrioid ovarian cancer in both species types as compared with normal ovaries (51). The authors used the lectin, *phytohemagglutinin E* (E-PHA), which has specificity toward binding to bisecting-type *N*-glycan determinants on glycoproteins. Positive staining for E-PHA was detected in normal controls and more than 2-fold increase of bisecting GlcNAc was detected in the ovarian cancer tissue samples (51). In our study, however, bisecting GlcNAc was completely absent in both non-cancerous cell lines and comprised up to 13% of the *N*-glycans in the cancer cells. The quantitative difference in observation could be caused by nonspecific cross reactive binding of the lectin or the variation in glycosylation of proteins between cell lines and tissues.

Importantly, this study provides strong evidence that the bisecting GlcNAc *N*-linked structures on the membrane proteins of serous ovarian cancer cells are a consequence of DNA hypomethylation. The suppression of *MGAT3* in non-cancerous cell lines was shown to be, at least partly, because of epigenetic silencing by DNA hypermethylation as evidenced by the reconstitution of the *MGAT3* gene expression after 5-Aza treatment. The enzyme, GnT-III, encoded by the *MGAT3* gene, is thus responsible for producing bisecting-

type *N*-glycans on the proteins of epithelial ovarian cancer cell lines. Bisecting GlcNAc addition has been thought to suppress metastasis by preventing the addition of branched-type complex *N*-glycans (52–54). This correlates strongly with our finding of an increased proportion of complex type *N*-glycans in the non-cancerous cells as compared with the serous ovarian cancer cells. A recent study demonstrated that *MGAT3* mediated E-cadherin *N*-glycosylation is involved in epithelial-mesenchymal transitions and their findings point to an involvement of DNA methylation as a regulatory mechanism of *MGAT3* (55). This supports our finding that the expression of bisecting GlcNAc on the entire *N*-glycoproteome is indeed a result of DNA hypomethylation of *MGAT3* transcriptional regulatory elements in serous ovarian cancer cells. However, the precise DNA region of the *MGAT3* gene that is affected by the hypomethylation is still under investigation as our preliminary method optimization has been hampered by the high amount of CpG islands surrounding the gene. It is possible that there are other factors besides DNA hypomethylation of *MGAT3* that can also stimulate the expression of *MGAT3* in all four serous ovarian cancer cells, although histone methylation does not appear to be significantly involved. Apart from DNA methylation, nucleosome occupancy is another regulatory element, in which nucleosome positioning could potentially influence the gene activation of *MGAT3* and thus regulate *MGAT3* expression. Studies have shown that both these epigenetic mechanisms form a combinatorial epigenetic profile of a genomic locus and are becoming increasingly associated with cancer (56, 57).

The other difference in the glycosylation of the *N*-linked glycans on the ovarian cancer cell glycoproteins was the exclusive expression of α 2–6 linked sialic acids. Sialylation of *N*-glycans is an important modification in cellular glycosylation and alterations in sialyltransferase expression have been implicated in tumor progression and metastasis (58). The sialylation of *N*-glycans is determined by the concerted action of sialyltransferases, which are classified into four families based on the specific linkage of the sialic acid residue transferred to the glycan substrate (59). The enzyme investigated in this study, *ST6GAL1*, terminally sialylates Gal β 1–4GlcNAc β motifs on *N*-glycans and the correlated overexpression of this gene in the serous ovarian cancer cells as compared with the non-cancerous cells is consistent with other findings reported for colorectal (60), breast (61), cervical (62), liver (63), and ovarian cancers (58). The presence of hybrid and complex *N*-glycans bearing α 2–6 sialylation in ovarian cancer cell lines is also in good agreement with another mass spectrometric-based analysis on the total serum glycome that revealed that α 2–6 sialylation of acute-phase glycoproteins in ovarian cancer patients' serum increased proportionally as compared with α 2–3 sialylation (64). The functional role of *ST6GAL1*-mediated sialylation of membrane proteins is yet to be fully understood although it has been shown that α 2–6 sialylation

of membrane-associated β_1 integrins in ovarian epithelial cells induces increased adhesion and invasive potential (65).

The contrasting prevalence of α 2–3 sialylation on membrane *N*-glycans in non-cancerous compared with ovarian cancer cells could be attributed to the overlapping enzyme specificities of the *ST3GAL* sialyltransferase family (66). Three of the five *ST3GAL* sialyltransferases (*ST3GAL3*, *ST3GAL4*, and *ST3GAL5*) profiled in this study are known to sialylate the Gal β 1–3/4GlcNAc β motif on glycoproteins and glycolipids (67–69). The preferential expression of *ST3GAL4* over *ST3GAL3* in all six tested cell lines in this study is consistent with results from the previously mentioned study using normal and serous ovarian cancer tissues (58). It is also interesting to note that the expression of *ST3GAL5*, was significantly reduced in all four ovarian cancer cell lines. The enzyme has also been reported to act exclusively on Gal β 1–4Glc-Cer motifs on glycolipids, giving rise to the synthesis of the α 2–3 sialylated ganglioside, GM $_3$ (70). Because our study was limited to the changes on the membrane *N*-glycoproteins, it will be worthwhile extending the scope of our analysis in the future to also investigate the differential expression of glycolipids in ovarian cancer.

Another exciting feature of this study is the presence of the “*N,N'*-diacetyl-lactosamine” (LacdiNAc) motif observed in some of the *N*-glycans of the ovarian cancer cell lines. This terminal modification, which also has been reported to occur as α 1–3-fucosylated (71, 72), 4-O-sulfated (73), or sialylated (74) derivatives, is less well understood as compared with the *N*-acetyl-lactosamine type antennae (LacNAc; Gal-GlcNAc). LacdiNAc-type *N*-glycans have been found on various mammalian glycoproteins such as the pituitary luteinizing hormone (75), glycodelin (76), and tenascin-R (77) as well as in other non-mammalian hosts such as the human parasite, *Schistosoma mansoni* (72). This disaccharide (GalNAc β 1–4GlcNAc) is synthesized by the action of specific β 4-GalNAc transferases, β 4GalNAcT3 and β 4GalNAcT4, which are differently expressed in various organs of the human body such as the stomach, colon, testes, and ovaries (78, 79). Studies have shown that this motif is also present in some *N*-glycans of tumor-associated glycoproteins such as secreted tissue plasminogen activator from Bowes melanoma cells (80) and secreted ribonuclease I from pancreatic tumor cells (81). Interestingly, this motif has been previously described in ovarian cancer in which LacdiNAc-type *N*-glycans were identified in SKOV 3- derived recombinant human EPO and endogenous glycoproteins of SKOV 3 cell lines using positive mode MALDI-TOF-TOF mass spectrometry (82). In addition to the identification of LacdiNAc, as well as sialylated LacdiNAc motifs, on membrane proteins using negative mode mass spectrometry in our study, the exclusive presence of fucosylated LacdiNAc-type *N*-glycans and the corresponding increase in gene expression of B4GALNT3 in the IGROV 1 cell line appear to be of significant interest. This is particularly because of the mixed histological classification of the tumor

Alteration of Membrane Protein Glycosylation in Ovarian Cancer

(endometrioid and serous) from which this IGROV 1 cell line is derived as compared with the rest of the ovarian cancer cell lines, which are mainly derived from serous type tumors. This observation, together with the recent findings of fucosylated as well as sulfated LacdiNAcs in a clear cell ovarian cancer cell line, RMG-1 (73), further substantiates the need to explore the significance of this motif, not only as a possible biomarker but also to aid in the differentiation between various histological subtypes of ovarian cancer.

The high mannose structures observed to comprise a greater proportion of the protein *N*-glycans in all four ovarian cancer cell lines were the most abundant structures as compared with the other *N*-glycan subgroups. A similar study involving cytosolic glycoproteins from breast cancer cell lines also showed that high mannose *N*-glycans were significantly elevated in invasive and noninvasive breast cancer cells as compared with the normal breast epithelial cells (83). Although it remains unclear whether high mannose glycans are a common feature of most cultured cell lines, the presence of high mannose structures reported here correlates with the study by Jacob *et al.* (2012) who showed that naturally occurring anti-glycan antibodies such as anti-Man, present in ovarian cancer patients' plasma exhibited specific binding of high mannose structures using a printed glycan-array technology (23). A recently developed monoclonal antibody, TM10, has also been shown to have specificity toward high mannose *N*-glycans on glycoproteins derived from human cancer cell lines, ranging from melanoma, prostate, breast, and ovarian cancer cell lines including SKOV 3 (84). One particular study indicated that cancer cells derived from A431 human squamous carcinoma cell line displayed high-mannose EGFR precursors on their cell surface because of their incomplete processing in the Golgi apparatus (85). Hence, it is possible that the synthetic processing of the *N*-glycans by the addition of other sugar residues to form complex structures on the cell surface membrane glycoproteins appears to be inhibited in cancer cells and this, together with the presence of bisecting GlcNAc, may explain the relatively low proportion of complex neutral and sialylated *N*-glycans observed in our study for the ovarian cancer cells.

At present, ovarian cancer treatment options are limited to only cytoreductive surgery and platinum-based chemotherapy of which more than 80% of patients undergo relapse caused by chemotherapy resistance (42). Attempts aimed at prolonging the remission of this disease and improving survival rates must be intensified through the development of novel biomarkers or molecular drug targets (86). The cell lines selected for this study, particularly the non-cancerous human ovarian surface epithelial cells, are representative of the cell line models currently used for studying ovarian cancer (31). Despite their potential utility, factors such as cell culture conditions and established choice of media may contribute to underlying cellular differences that must be taken into consideration in any *in vitro*-based studies. The determination of

specific structural and isomeric changes specific to ovarian cancer-associated membrane-derived *N*-glycans described in this study provides evidence for the potential of glycan candidates to detect and potentially treat ovarian cancer malignancy that must be further investigated *in vivo*. Furthermore, we highlight the importance of epigenetic modifications, such as DNA methylation, in ovarian cancer that is now shown to be pivotal in understanding the complex interplay between cellular glycosylation and glycosyltransferase expression.

* This work was supported by the Macquarie University Postgraduate Research Scholarship and Northern Translational Cancer Research Grant No: 1470100 by NSW Cancer Institute, Australia (M.A.), NSW Cancer Institute Grant No: 09CRF202 (V.H.S.), Krebsliga Beider Basel (V.H.S.), William Maxwell Trust (V.H.S.), Mary Elizabeth Courier Scholarship (V.H.S.), and Swiss National Foundation (F.J.).

§ This article contains supplemental Figs. S1 to S5 and Tables S1 and S2.

|| To whom correspondence should be addressed: Building E8C, Room 307, Department of Chemistry and Biomolecular Sciences, Macquarie University, New South Wales, 2109, Australia. Tel.: +61-2-9850 8176; Fax: +61-2-9850 8313; E-mail: nicki.packer@mq.edu.au.

** These authors contributed equally.

REFERENCES

- Jemal, A., Siegel, R., Xu, J., and Ward, E. (2010) Cancer statistics, 2010. *CA Cancer J. Clin.* **60**, 277–300
- Vathipadiekal, V., Saxena, D., Mok, S. C., Hauschka, P. V., Ozbun, L., and Birrer, M. J. (2012) Identification of a potential ovarian cancer stem cell gene expression profile from advanced stage papillary serous ovarian cancer. *PLoS One* **7**, e29079
- Berkenblit, A., and Cannistra, S. A. (2005) Advances in the management of epithelial ovarian cancer. *J. Reprod. Med.* **50**, 426–438
- Sasaroli, D., Coukos, G., and Scholler, N. (2009) Beyond CA125: the coming of age of ovarian cancer biomarkers. Are we there yet? *Biomark. Med.* **3**, 275–288
- Meyer, T., and Rustin, G. J. (2000) Role of tumour markers in monitoring epithelial ovarian cancer. *Br. J. Cancer* **82**, 1535–1538
- Jacob, F., Meier, M., Caduff, R., Goldstein, D., Pochechueva, T., Hacker, N., Fink, D., and Heinzelmann-Schwarz, V. (2011) No benefit from combining HE4 and CA125 as ovarian tumor markers in a clinical setting. *Gynecol. Oncol.* **121**, 487–491
- Paulson, J. C., and Colley, K. J. (1989) Glycosyltransferases. Structure, localization, and control of cell type-specific glycosylation. *J. Biol. Chem.* **264**, 17615–17618
- Taylor, A. D., Hancock, W. S., Hincapie, M., Taniguchi, N., and Hanash, S. M. (2009) Towards an integrated proteomic and glycomic approach to finding cancer biomarkers. *Genome Med.* **1**, 57
- Dube, D. H., and Bertozzi, C. R. (2005) Glycans in cancer and inflammation—potential for therapeutics and diagnostics. *Nat. Rev. Drug Discov.* **4**, 477–488
- Hakomori, S. (1996) Tumor malignancy defined by aberrant glycosylation and sphingo(glyco)lipid metabolism. *Cancer Res.* **56**, 5309–5318
- Yamamoto, H., Swoger, J., Greene, S., Saito, T., Hurh, J., Sweeley, C., Leestma, J., Mkrdchian, E., Cerullo, L., Nishikawa, A., Ihara, Y., Taniguchi, N., and Moskal, J. R. (2000) Beta1,6-N-acetylglucosamine-bearing *N*-glycans in human gliomas: implications for a role in regulating invasivity. *Cancer Res.* **60**, 134–142
- Couldrey, C., and Green, J. E. (2000) Metastases: the glycan connection. *Breast Cancer Res.* **2**, 321–323
- Taniguchi, N., Ihara, S., Saito, T., Miyoshi, E., Ikeda, Y., and Honke, K. (2001) Implication of GnT-V in cancer metastasis: a glycomic approach for identification of a target protein and its unique function as an angiogenic cofactor. *Glycoconj. J.* **18**, 859–865
- Demetriou, M., Nabi, I. R., Coppolino, M., Dedhar, S., and Dennis, J. W.

Alteration of Membrane Protein Glycosylation in Ovarian Cancer

- (1995) Reduced contact-inhibition and substratum adhesion in epithelial cells expressing GlcNAc-transferase V. *J. Cell Biol.* **130**, 383–392
15. Mechref, Y., Hu, Y., Garcia, A., Zhou, S., Desantos-Garcia, J. L., and Hussein, A. (2012) Defining putative glycan cancer biomarkers by MS. *Bioanalysis* **4**, 2457–2469
16. Harvey, D. J. (2000) Collision-induced fragmentation of underivatized N-linked carbohydrates ionized by electrospray. *J. Mass Spectrom.* **35**, 1178–1190
17. Hayes, C. A., Karlsson, N. G., Struwe, W. B., Lisacek, F., Rudd, P. M., Packer, N. H., and Campbell, M. P. (2011) UniCarb-DB: a database resource for glycomics discovery. *Bioinformatics* **27**, 1343–1344
18. Cooper, C. A., Gasteiger, E., and Packer, N. H. (2001) GlycoMod—a software tool for determining glycosylation compositions from mass spectrometric data. *Proteomics* **1**, 340–349
19. Ceroni, A., Maass, K., Geyer, H., Geyer, R., Dell, A., and Haslam, S. M. (2008) GlycoWorkbench: a tool for the computer-assisted annotation of mass spectra of glycans. *J. Proteome Res.* **7**, 1650–1659
20. Maxwell, E., Tan, Y., Tan, Y., Hu, H., Benson, G., Aizikov, K., Conley, S., Staples, G. O., Glysz, G. W., Smith, R. D., and Zaia, J. (2012) GlycoReSoft: a software package for automated recognition of glycans from LC/MS data. *PLoS One* **7**, e45474
21. Yu, C. Y., Mayampurath, A., Hu, Y., Zhou, S., Mechref, Y., and Tang, H. (2013) Automated annotation and quantification of glycans using liquid chromatography-mass spectrometry. *Bioinformatics* **29**, 1706–1707
22. Abbott, K. L., Lim, J. M., Wells, L., Benigno, B. B., McDonald, J. F., and Pierce, M. (2010) Identification of candidate biomarkers with cancer-specific glycosylation in the tissue and serum of endometrioid ovarian cancer patients by glycoproteomic analysis. *Proteomics* **10**, 470–481
23. Jacob, F., Goldstein, D. R., Bovin, N. V., Pochechueva, T., Spengler, M., Caduff, R., Fink, D., Vuskovic, M. I., Huflejt, M. E., and Heinzelmann-Schwarz, V. (2012) Serum antiglycan antibody detection of nonmucinous ovarian cancers by using a printed glycan array. *Int. J. Cancer* **130**, 138–146
24. Alley, W. R., Jr., Vasseur, J. A., Goelt, J. A., Svoboda, M., Mann, B. F., Matei, D. E., Menning, N., Hussein, A., Mechref, Y., and Novotny, M. V. (2012) N-linked glycan structures and their expressions change in the blood sera of ovarian cancer patients. *J. Proteome Res.* **11**, 2282–2300
25. Shetty, V., Hafner, J., Shah, P., Nickens, Z., and Philip, R. (2012) Investigation of ovarian cancer associated sialylation changes in N-linked glycopeptides by quantitative proteomics. *Clin. Proteomics* **9**, 10
26. Colombo, N., Peiretti, M., Parma, G., Lapresa, M., Mancari, R., Carinelli, S., Sessa, C., Castiglione, M., and Group, E. G. W. (2010) Newly diagnosed and relapsed epithelial ovarian carcinoma: ESMO Clinical Practice Guidelines for diagnosis, treatment and follow-up. *Ann. Oncol.* **5**, v23–30
27. Schiess, R., Wollscheid, B., and Aebersold, R. (2009) Targeted proteomic strategy for clinical biomarker discovery. *Mol. Oncol.* **3**, 33–44
28. Kim, Y. S., and Deng, G. (2008) Aberrant expression of carbohydrate antigens in cancer: the role of genetic and epigenetic regulation. *Gastroenterology* **135**, 305–309
29. Zoldos, V., Horvat, T., Novokmet, M., Cuenin, C., Muzinic, A., Pucic, M., Huffman, J. E., Gornik, O., Polasek, O., Campbell, H., Hayward, C., Wright, A. F., Rudan, I., Owen, K., McCarthy, M. I., Herceg, Z., and Lauc, G. (2012) Epigenetic silencing of HNF1A associates with changes in the composition of the human plasma N-glycome. *Epigenetics* **7**, 164–172
30. Saldova, R., Dempsey, E., Perez-Garay, M., Marino, K., Watson, J. A., Blanco-Fernandez, A., Struwe, W. B., Harvey, D. J., Madden, S. F., Peracaula, R., McCann, A., and Rudd, P. M. (2011) 5-AZA-2'-deoxycytidine induced demethylation influences N-glycosylation of secreted glycoproteins in ovarian cancer. *Epigenetics* **6**, 1362–1372
31. Tsao, S. W., Mok, S. C., Fey, E. G., Fletcher, J. A., Wan, T. S., Chew, E. C., Muto, M. G., Knapp, R. C., and Berkowitz, R. S. (1995) Characterization of human ovarian surface epithelial cells immortalized by human papilloma viral oncogenes (HPV-E6E7 ORFs). *Exp. Cell Res.* **218**, 499–507
32. Lee, A., Kolarich, D., Haynes, P. A., Jensen, P. H., Baker, M. S., and Packer, N. H. (2009) Rat liver membrane glycoproteome: enrichment by phase partitioning and glycoprotein capture. *J. Proteome Res.* **8**, 770–781
33. Jensen, P. H., Karlsson, N. G., Kolarich, D., and Packer, N. H. (2012) Structural analysis of N- and O-glycans released from glycoproteins. *Nat. Protoc.* **7**, 1299–1310
34. Estrella, R. P., Whitelock, J. M., Packer, N. H., and Karlsson, N. G. (2010) The glycosylation of human synovial lubricin: implications for its role in inflammation. *Biochem. J.* **429**, 359–367
35. Issa, S., Moran, A. P., Ustinov, S. N., Lin, J. H., Ligtenberg, A. J., and Karlsson, N. G. (2010) O-linked oligosaccharides from salivary agglutinin: *Helicobacter pylori* binding sialyl-Lewis x and Lewis b are terminating moieties on hyperfucosylated oligo-N-acetylactosamine. *Glycobiology* **20**, 1046–1057
36. Karlsson, N. G., and Thomsson, K. A. (2009) Salivary MUC7 is a major carrier of blood group I type O-linked oligosaccharides serving as the scaffold for sialyl Lewis x. *Glycobiology* **19**, 268–300
37. Everest-Dass, A. V., Jin, D., Thaysen-Andersen, M., Nevalainen, H., Kolarich, D., and Packer, N. H. (2012) Comparative structural analysis of the glycosylation of salivary and buccal cell proteins: innate protection against infection by *C. albicans*. *Glycobiology*
38. Nakano, M., Saldanha, R., Gobel, A., Kavallaris, M., and Packer, N. H. (2011) Identification of glycan structure alterations on cell membrane proteins in desoxyepithelone B resistant leukemia cells. *Mol. Cell. Proteomics* **10**, M111 009001
39. Everest-Dass, A. V., Kolarich, D., Campbell, M. P., and Packer, N. H. (2013) Tandem mass spectra of glycan substructures enable the multistage mass spectrometric identification of determinants on oligosaccharides. *Rapid Commun. Mass. Spectrom.* **27**, 931–939
40. Everest-Dass, A. V., Abrahams, J. L., Kolarich, D., Packer, N. H., and Campbell, M. P. (2013) Structural feature ions for distinguishing N- and O-linked glycan isomers by LC-ESI-IT MS/MS. *J. Am. Soc. Mass Spectrom.* **24**, 895–906
41. Harvey, D. J. (2005) Fragmentation of negative ions from carbohydrates: part 3. fragmentation of hybrid and complex N-linked glycans. *J. Am. Soc. Mass Spectrom.* **16**, 647–659
42. Stanley, P., Schachter, H., and Taniguchi, N. (2009) N-Glycans. In: Varki, A., Cummings, R. D., Esko, J. D., Freeze, H. H., Stanley, P., Bertozzi, C. R., Hart, G. W., and Etzler, M. E., eds. *Essentials of Glycobiology*, 2nd Ed., Cold Spring Harbor (NY)
43. Bustin, S. A., Benes, V., Garson, J. A., Hellemans, J., Huggett, J., Kubista, M., Mueller, R., Nolan, T., Pfaffl, M. W., Shipley, G. L., Vandesompele, J., and Wittwer, C. T. (2009) The MIQE guidelines: minimum information for publication of quantitative real-time PCR experiments. *Clin. Chem.* **55**, 611–622
44. Jacob, F., Guertler, R., Naim, S., Nixdorf, S., Fedier, A., Hacker, N. F., and Heinzelmann-Schwarz, V. (2013) Careful selection of reference genes is required for reliable performance of RT-qPCR in human normal and cancer cell lines. *PLoS One* **8**, e59180
45. Arvidsson, S., Kwasniewski, M., Riano-Pachon, D. M., and Mueller-Roeber, B. (2008) QuantPrime—a flexible tool for reliable high-throughput primer design for quantitative PCR. *BMC Bioinformatics* **9**, 465
46. Kent, W. J., Sugnet, C. W., Furey, T. S., Roskin, K. M., Pringle, T. H., Zahler, A. M., and Haussler, D. (2002) The human genome browser at UCSC. *Genome Res.* **12**, 996–1006
47. Pabst, M., Bondili, J. S., Stadlmann, J., Mach, L., and Altmann, F. (2007) Mass + retention time = structure: a strategy for the analysis of N-glycans by carbon LC-ESI-MS and its application to fibrin N-glycans. *Anal. Chem.* **79**, 5051–5057
48. Harvey, D. J., Crispin, M., Scanlan, C., Singer, B. B., Lucka, L., Chang, V. T., Radcliffe, C. M., Thobhani, S., Yuen, C. T., and Rudd, P. M. (2008) Differentiation between isomeric triantennary N-linked glycans by negative ion tandem mass spectrometry and confirmation of glycans containing galactose attached to the bisecting (beta1-4-GlcNAc) residue in N-glycans from IgG. *Rapid Commun. Mass. Spectrom.* **22**, 1047–1052
49. Rodriguez-Paredes, M., and Esteller, M. (2011) Cancer epigenetics reaches mainstream oncology. *Nat. Med.* **17**, 330–339
50. Kui Wong, N., Easton, R. L., Panico, M., Sutton-Smith, M., Morrison, J. C., Lattanzio, F. A., Morris, H. R., Clark, G. F., Dell, A., and Patankar, M. S. (2003) Characterization of the oligosaccharides associated with the human ovarian tumor marker CA125. *J. Biol. Chem.* **278**, 28619–28634
51. Abbott, K. L., Naim, A. V., Hall, E. M., Horton, M. B., McDonald, J. F., Moremen, K. W., Dinulescu, D. M., and Pierce, M. (2008) Focused glycomic analysis of the N-linked glycan biosynthetic pathway in ovarian cancer. *Proteomics* **8**, 3210–3220
52. Schachter, H. (1986) Biosynthetic controls that determine the branching and microheterogeneity of protein-bound oligosaccharides. *Adv. Exp. Med. Biol.* **205**, 53–85
53. Takahashi, M., Kuroki, Y., Ohtsubo, K., and Taniguchi, N. (2009) Core

Alteration of Membrane Protein Glycosylation in Ovarian Cancer

- ucose and bisecting GlcNAc, the direct modifiers of the N-glycan core: their functions and target proteins. *Carbohydr. Res.* **344**, 1387–1390
54. Lau, K. S., Partridge, E. A., Grigorian, A., Silvescu, C. I., Reinhold, V. N., Demetriou, M., and Dennis, J. W. (2007) Complex N-glycan number and degree of branching cooperate to regulate cell proliferation and differentiation. *Cell* **129**, 123–134
 55. Pinho, S. S., Oliveira, P., Cabral, J., Carvalho, S., Huntsman, D., Gartner, F., Seruca, R., Reis, C. A., and Oliveira, C. (2012) Loss and recovery of Mgat3 and Gnt-III Mediated E-cadherin N-glycosylation is a mechanism involved in epithelial-mesenchymal-epithelial transitions. *PLoS One* **7**, e33191
 56. Wilson, B. G., and Roberts, C. W. (2011) SWI/SNF nucleosome remodellers and cancer. *Nat. Rev. Cancer* **11**, 481–492
 57. Kelly, T. K., Liu, Y., Lay, F. D., Liang, G., Berman, B. P., and Jones, P. A. (2012) Genome-wide mapping of nucleosome positioning and DNA methylation within individual DNA molecules. *Genome Res.* **22**, 2497–2506
 58. Fwu, P. T., Wang, P. H., Tung, C. K., and Dong, C. Y. (2005) Effects of index-mismatch-induced spherical aberration in pump-probe microscopic image formation. *Appl. Opt.* **44**, 4220–4227
 59. Tsuji, S. (1996) Molecular cloning and functional analysis of sialyltransferases. *J. Biochem.* **120**, 1–13
 60. Dall'Olio, F., Chiricolo, M., and Lau, J. T. (1999) Differential expression of the hepatic transcript of beta-galactoside alpha2,6-sialyltransferase in human colon cancer cell lines. *Int. J. Cancer* **81**, 243–247
 61. Recchi, M. A., Hebbat, M., Hornez, L., Harduin-Lepers, A., Peyrat, J. P., and Delannoy, P. (1998) Multiplex reverse transcription polymerase chain reaction assessment of sialyltransferase expression in human breast cancer. *Cancer Res.* **58**, 4066–4070
 62. Wang, P. H., Lee, W. L., Lee, Y. R., Juang, C. M., Chen, Y. J., Chao, H. T., Tsai, Y. C., and Yuan, C. C. (2003) Enhanced expression of alpha 2,6-sialyltransferase ST6Gal I in cervical squamous cell carcinoma. *Gynecol. Oncol.* **89**, 395–401
 63. Pousset, D., Piller, V., Bureau, N., Monsigny, M., and Piller, F. (1997) Increased alpha2,6 sialylation of N-glycans in a transgenic mouse model of hepatocellular carcinoma. *Cancer Res.* **57**, 4249–4256
 64. Saldova, R., Royle, L., Radcliffe, C. M., Abd Hamid, U. M., Evans, R., Arnold, J. N., Banks, R. E., Hutson, R., Harvey, D. J., Antrobus, R., Petrescu, S. M., Dwek, R. A., and Rudd, P. M. (2007) Ovarian cancer is associated with changes in glycosylation in both acute-phase proteins and IgG. *Glycobiology* **17**, 1344–1356
 65. Christie, D. R., Shaikh, F. M., Lucas, J. A. t., Lucas, J. A., 3rd, and Bellis, S. L. (2006) ST6Gal-I expression in ovarian cancer cells promotes an invasive phenotype by altering integrin glycosylation and function. *J. Ovarian Res.* **1**, 3
 66. Harduin-Lepers, A., Recchi, M. A., and Delannoy, P. (1995) 1994, the year of sialyltransferases. *Glycobiology* **5**, 741–758
 67. Kitagawa, H., and Paulson, J. C. (1993) Cloning and expression of human Gal beta 1,3(4)GlcNAc alpha 2,3-sialyltransferase. *Biochem. Biophys. Res. Commun.* **194**, 375–382
 68. Kitagawa, H., and Paulson, J. C. (1994) Cloning of a novel alpha 2,3-sialyltransferase that sialylates glycoprotein and glycolipid carbohydrate groups. *J. Biol. Chem.* **269**, 1394–1401
 69. Ishii, A., Ohta, M., Watanabe, Y., Matsuda, K., Ishiyama, K., Sakoe, K., Nakamura, M., Inokuchi, J., Sanai, Y., and Saito, M. (1998) Expression cloning and functional characterization of human cDNA for ganglioside GM3 synthase. *J. Biol. Chem.* **273**, 31652–31655
 70. Harduin-Lepers, A., Mollicone, R., Delannoy, P., and Oriol, R. (2005) The animal sialyltransferases and sialyltransferase-related genes: a phylogenetic approach. *Glycobiology* **15**, 805–817
 71. Kavar, Z. S., Haslam, S. M., Morris, H. R., Dell, A., and Cummings, R. D. (2005) Novel poly-GalNAcbeta1-4GlcNAc (LacdiNAc) and fucosylated poly-LacdiNAc N-glycans from mammalian cells expressing beta1,4-N-acetylgalactosaminyltransferase and alpha1,3-fucosyltransferase. *J. Biol. Chem.* **280**, 12810–12819
 72. Wührer, M., Koelman, C. A., Deelder, A. M., and Hokke, C. H. (2006) Repeats of LacdiNAc and fucosylated LacdiNAc on N-glycans of the human parasite *Schistosoma mansoni*. *FEBS J.* **273**, 347–361
 73. Yu, S. Y., Chang, L. Y., Cheng, C. W., Chou, C. C., Fukuda, M. N., and Khoo, K. H. (2013) Priming mass spectrometry-based sulfoglycomics mapping for identification of terminal sulfated lacdiNAc glycotopes. *Glycoconj. J.* **30**, 183–194
 74. Saanen, J., Welgus, H. G., Flizer, C. A., Kalkkinen, N., and Helin, J. (1999) N-glycan structures of matrix metalloproteinase-1 derived from human fibroblasts and from HT-1080 fibrosarcoma cells. *Eur. J. Biochem.* **259**, 829–840
 75. Smith, P. L., and Baenziger, J. U. (1992) Molecular basis of recognition by the glycoprotein hormone-specific N-acetylgalactosamine-transferase. *Proc. Natl. Acad. Sci. U.S.A.* **89**, 329–333
 76. Dell, A., Morris, H. R., Easton, R. L., Panico, M., Patankar, M., Oehninger, S., Koistinen, R., Koistinen, H., Seppala, M., and Clark, G. F. (1995) Structural analysis of the oligosaccharides derived from glycodelin, a human glycoprotein with potent immunosuppressive and contraceptive activities. *J. Biol. Chem.* **270**, 24116–24126
 77. Woodworth, A., Fiete, D., and Baenziger, J. U. (2002) Spatial and temporal regulation of tenascin-R glycosylation in the cerebellum. *J. Biol. Chem.* **277**, 50941–50947
 78. Sato, T., Gotoh, M., Kiyohara, K., Kameyama, A., Kubota, T., Kikuchi, N., Ishizuka, Y., Iwasaki, H., Togayachi, A., Kudo, T., Ohkura, T., Nakanishi, H., and Narimatsu, H. (2003) Molecular cloning and characterization of a novel human beta 1,4-N-acetylgalactosaminyltransferase, beta 4GalNAc-T3, responsible for the synthesis of N,N'-diacetyllactosedi-amine, galNAc beta 1-4GlcNAc. *J. Biol. Chem.* **278**, 47534–47544
 79. Gotoh, M., Sato, T., Kiyohara, K., Kameyama, A., Kikuchi, N., Kwon, Y. D., Ishizuka, Y., Iwai, T., Nakanishi, H., and Narimatsu, H. (2004) Molecular cloning and characterization of beta1,4-N-acetylgalactosaminyltransferases IV synthesizing N,N'-diacetyllactosedi-amine. *FEBS Lett.* **562**, 134–140
 80. Chan, A. L., Morris, H. R., Panico, M., Etienne, A. T., Rogers, M. E., Gaffney, P., Creighton-Kempford, L., and Dell, A. (1991) A novel sialylated N-acetylgalactosamine-containing oligosaccharide is the major complex-type structure present in Bowes melanoma tissue plasminogen activator. *Glycobiology* **1**, 173–185
 81. Peracaula, R., Royle, L., Tabares, G., Mallorqui-Fernandez, G., Barrabes, S., Harvey, D. J., Dwek, R. A., Rudd, P. M., and de Llorens, R. (2003) Glycosylation of human pancreatic ribonuclease: differences between normal and tumor states. *Glycobiology* **13**, 227–244
 82. Machado, E., Kandzia, S., Carliho, R., Altevogt, P., Conradt, H. S., and Costa, J. (2011) N-Glycosylation of total cellular glycoproteins from the human ovarian carcinoma SKOV3 cell line and of recombinantly expressed human erythropoietin. *Glycobiology* **21**, 376–386
 83. Goetz, J. A., Mechref, Y., Kang, P., Jeng, M. H., and Novotny, M. V. (2009) Glycomic profiling of invasive and non-invasive breast cancer cells. *Glycoconj. J.* **26**, 117–131
 84. Newsom-Davis, T. E., Wang, D., Steinman, L., Chen, P. F., Wang, L. X., Simon, A. K., and Srean, G. R. (2009) Enhanced immune recognition of cryptic glycan markers in human tumors. *Cancer Res.* **69**, 2018–2025
 85. Johns, T. G., Mellman, I., Cartwright, G. A., Ritter, G., Old, L. J., Burgess, A. W., and Scott, A. M. (2005) The antitumor monoclonal antibody 806 recognizes a high-mannose form of the EGF receptor that reaches the cell surface when cells over-express the receptor. *FASEB J.* **19**, 780–782
 86. Yap, T. A., Carden, C. P., and Kaye, S. B. (2009) Beyond chemotherapy: targeted therapies in ovarian cancer. *Nat. Rev. Cancer* **9**, 167–181

2.1 Supplementary Data

Supplementary Table 1

Characteristics	HOSE 6.3	HOSE 17.1	SKOV 3	IGROV 1	A2780	OVCAR 3
Disease	ND	ND	Ovarian carcinoma	Ovarian carcinoma	Ovarian carcinoma	Ovarian carcinoma
Source	Human	Human	Human	Human	Human	Human
Tissue Origin	Normal ovary	Normal ovary	Ovary; ascites fluid	Right ovary	Ovary	Ovary; ascites fluid
Histology	-	-	Serous	Mixed; endometrioid and serous	Serous	Serous
Age of Patient (Yr.)	NA	NA	64	47	NA	60
Immortalization	Yes; HPV16 E6/E7 genes (retroviral vector)	Yes; HPV16 E6/E7 genes (retroviral vector)	No	No	No	No
Culture Media	MCDB 105:M199 (1:1, v/v); 10 % FBS	MCDB 105:M199 (1:1, v/v); 10 % FBS	RPMI 1640; 10 % FBS	RPMI 1640; 10 % FBS	RPMI 1640; 10 % FBS	RPMI 1640; 10 % FBS
Morphology	Epithelial; adherent monolayer	Epithelial; adherent monolayer	Epithelial; adherent monolayer	Epithelial; adherent monolayer	Epithelial; adherent monolayer	Epithelial; adherent monolayer
Tumorigenicity in nude mice	Non-tumorigenic	Non-tumorigenic	Tumorigenic	Highly tumorigenic	Tumorigenic	Tumorigenic
References	(1)	(1)	(2-5)	(2, 5, 6)	(2, 5, 7)	(2, 5)

Keywords:

ND: Non-diseased **NA:** Not available **HPV:** Human papillomavirus oncogenes

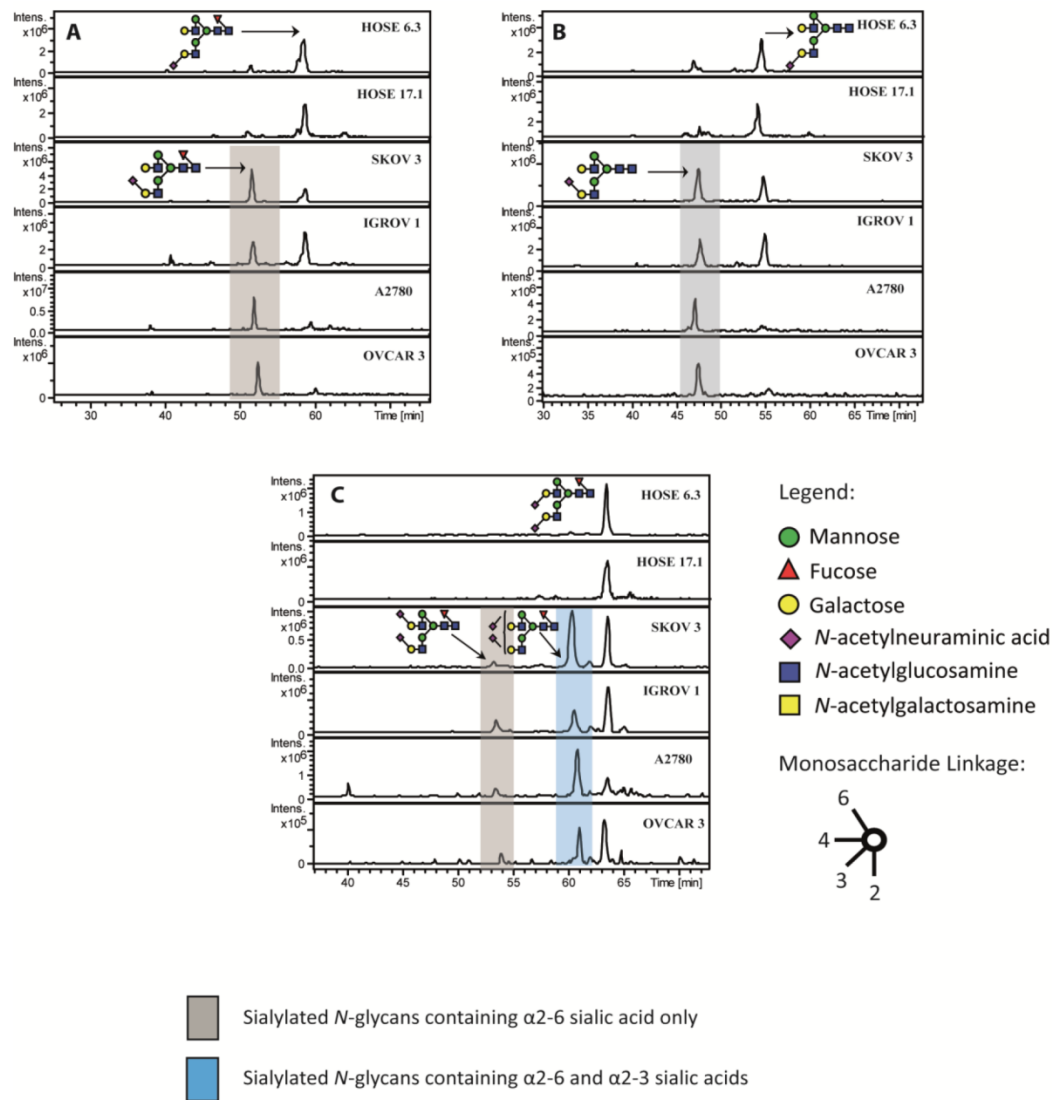
Source, clinical and pathological features of the two human immortalized ovarian surface epithelial cell lines and four epithelial ovarian cancer (EOC) cell lines used in this study. The ovarian cancer cell lines have been selected based on their serous histotype which represents the major subtype of ovarian cancer.

Supplementary Table 2

Amino Monosaccharides	Non-cancerous cell lines		Ovarian cancer cell lines			
	HOSE 6.3	HOSE 17.1	SKOV 3	IGROV 1	A2780	OVCAR 3
	(nM / μ l)		(nM / μ l)			
GlcNAc	132.5 \pm 3.0	215.8 \pm 0.75	77.0 \pm 1.5	203.0 \pm 1.5	113.5 \pm 13.4	126.5 \pm 12.7
(GalNAc)	<i>nd</i>	<i>nd</i>	<i>nd</i>	9.3 \pm 3.25	<i>nd</i>	<i>nd</i>

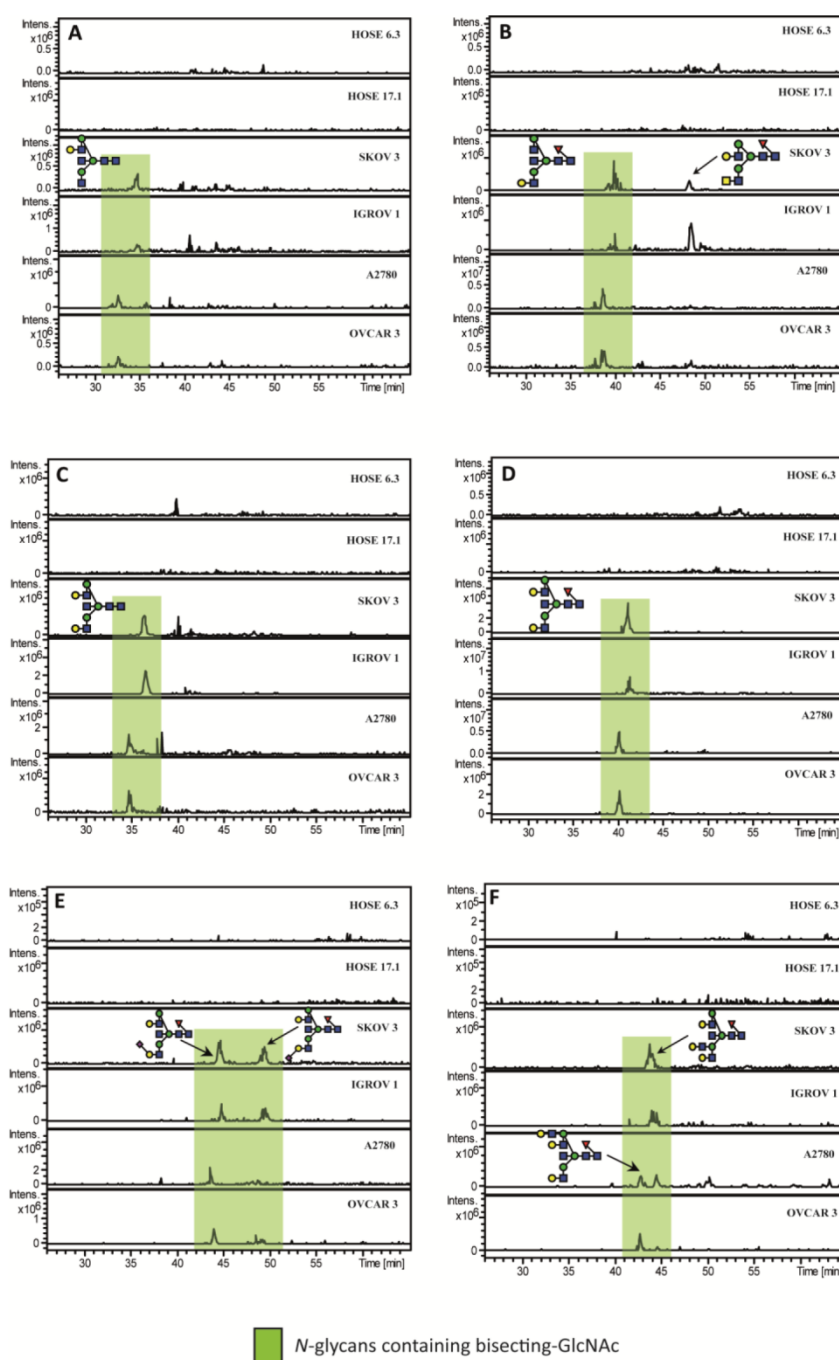
Monosaccharide amino analysis of hydrolysed *N*-glycans extracted from membrane glycoproteins of non-cancerous and ovarian cancer cell lines using high performance anion-exchange with pulsed amperometric detection (HPAEC-PAD). The values are represented as mean \pm SD values of duplicate measurements for each analysis. Abbreviations are indicated for the following: **GlcNAc**: *N*-acetyl-glucosamine; **GalNAc**: *N*-acetyl-galactosamine and *nd*: not-detected.

Supplementary Figure 1



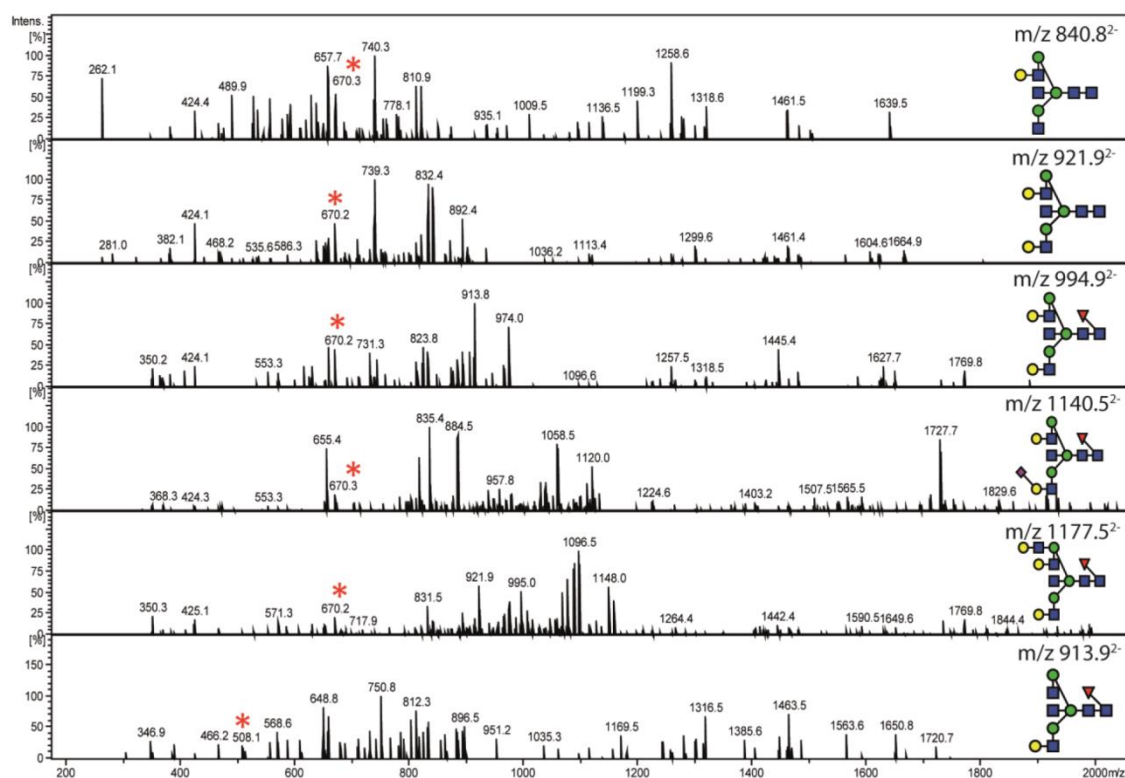
Extracted ion chromatograms (EIC) of monosialylated and di-sialylated biantennary complex *N*-glycans containing isomers with α 2-6-linked sialic acid are illustrated for m/z [1038.9]²⁻ (A), m/z [965.9]²⁻ (B) and m/z [1184.5]²⁻ (C) while the isomer containing both the α 2-6 and α 2-3-linked sialic acids is shown to be eluting at 61 mins for m/z [1184.5]²⁻ (C). These isomers were found to be present in cancer cells (SKOV 3, IGROV 1, A2780 and OVCAR 3) and are indicated by the shaded boxes.

Supplementary Figure 2



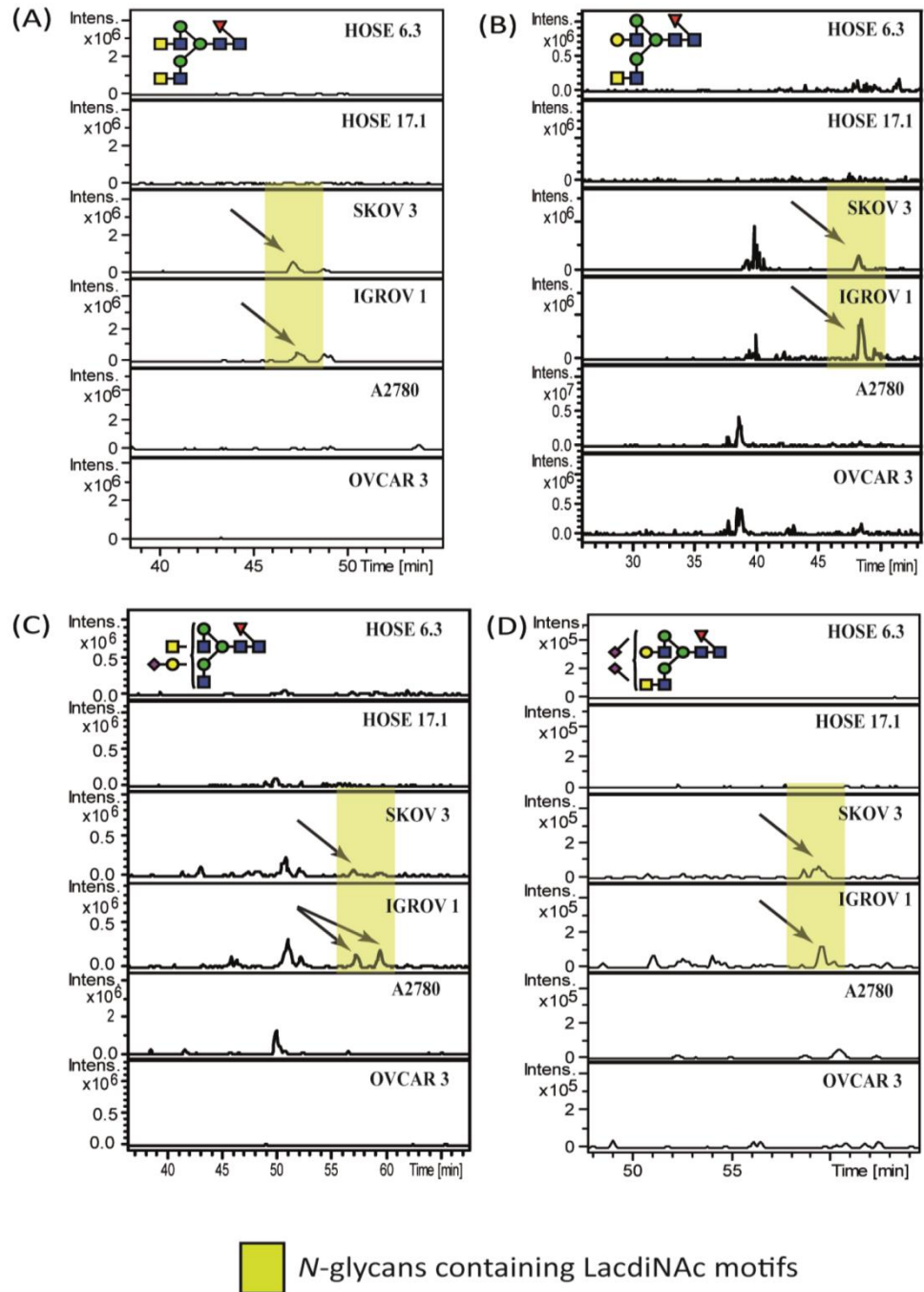
Extracted ion chromatograms (EIC) of bisecting-type complex *N*-glycans with *m/z* [840.8]²⁻ (A), *m/z* [913.9]²⁻ (B), *m/z* [921.9]²⁻ (C), *m/z* [994.9]²⁻ (D), *m/z* [1140.5]²⁻ (E) and *m/z* [1177.5]²⁻ (F) were found to be present in cancer cells (SKOV 3, IGROV 1, A2780 and OVCAR 3) and are indicated by the shaded boxes.

Supplementary Figure 3



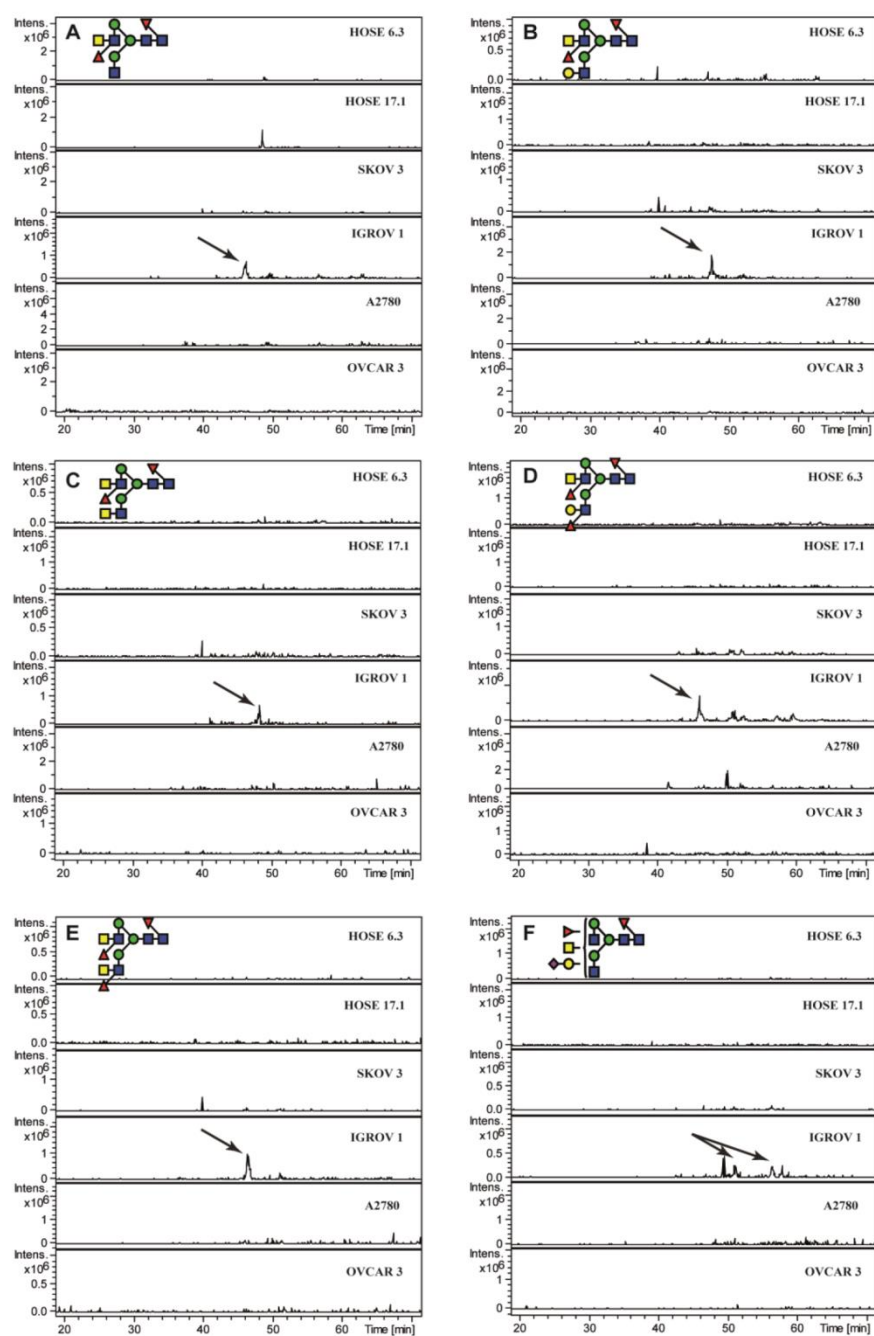
Negative ion MS/MS spectrum of bisecting-type *N*-glycans with m/z [840.8]²⁻ (A), m/z [921.9]²⁻ (B), m/z [994.9]²⁻ (C), m/z [1140.5]²⁻ (D), m/z [1177.5]²⁻ (E) and m/z [913.9]²⁻ (F). Diagnostic ion (D-221) at m/z [670.3]¹⁻ and m/z [508.1]¹⁻ are represented by the asterisks (*)

Supplementary Figure 4



Extracted ion chromatograms (EIC) of LacdiNAc-type complex *N*-glycans identified in ovarian cancer cells (SKOV3 and IGROV1) with m/z [934.4]²⁻ (A), m/z [913.9]²⁻ (B), m/z [1059.4]²⁻ (C) and m/z [1205.0]²⁻ (D) as indicated by the arrows.

Supplementary Figure 5



Extracted ion chromatograms (EIC) of LacdiNAc-type complex *N*-glycans identified in IGROV 1 ovarian cancer cells with m/z [905.9]²⁻(A), m/z [986.9]²⁻(B) and m/z [1007.4]²⁻(C), m/z [1059.9]²⁻(D), m/z [1080.5]²⁻(E) and m/z [1132.4]²⁻(F) as indicated by the arrows.

References

1. Tsao, S. W., Mok, S. C., Fey, E. G., Fletcher, J. A., Wan, T. S., Chew, E. C., Muto, M. G., Knapp, R. C., and Berkowitz, R. S. (1995) Characterization of human ovarian surface epithelial cells immortalized by human papilloma viral oncogenes (HPV-E6E7 ORFs). *Exp Cell Res* 218, 499-507
2. Buehler, M., Tse, B., Leboucq, A., Jacob, F., Caduff, R., Fink, D., Goldstein, D. R., and Heinzelmann-Schwarz, V. (2013) Meta-Analysis of Microarray Data Identifies GAS6 Expression as an Independent Predictor of Poor Survival in Ovarian Cancer. *Biomed Res Int* 2013, 238284
3. Shoemaker, R. H., Monks, A., Alley, M. C., Scudiero, D. A., Fine, D. L., McLemore, T. L., Abbott, B. J., Paull, K. D., Mayo, J. G., and Boyd, M. R. (1988) Development of human tumor cell line panels for use in disease-oriented drug screening. *Prog Clin Biol Res* 276, 265-286
4. Berger, S., Siegert, A., Denkert, C., Kobel, M., and Hauptmann, S. (2001) Interleukin-10 in serous ovarian carcinoma cell lines. *Cancer Immunol Immunother* 50, 328-333
5. Kurbacher, C. M., Korn, C., Dixel, S., Schween, U., Kurbacher, J. A., Reichelt, R., and Arenz, P. N. (2011) Isolation and culture of ovarian cancer cells and cell lines. *Methods Mol Biol* 731, 161-180
6. Benard, J., Da Silva, J., De Blois, M. C., Boyer, P., Duvillard, P., Chiric, E., and Riou, G. (1985) Characterization of a human ovarian adenocarcinoma line, IGROV1, in tissue culture and in nude mice. *Cancer Res* 45, 4970-4979
7. Hamilton, T. C., Young, R. C., and Ozols, R. F. (1984) Experimental model systems of ovarian cancer: applications to the design and evaluation of new treatment approaches. *Semin Oncol* 11, 285-298

2.2 Overview of Chapter II

- Non-cancerous ovarian epithelial cells (HOSE 6.3 and HOSE 17.1) and cancerous ovarian cells (SKOV3, IGROV1, OVCAR3, A2780) exhibit differences in their cellular membrane protein glycosylation profiles
- Cancerous ovarian cells display a significant increase in high mannose-type and a decrease in complex-type *N*-glycans as compared to non-cancerous cells
- In terms of their sialylation patterns, α 2-6 sialylated *N*-glycans are significantly increased for both hybrid and complex-type *N*-glycans in all four ovarian cancer cell lines
- Ovarian cancer cell lines also exhibit unique glycan motifs such as bisecting GlcNAc-type *N*-glycans and LacdiNAc-type *N*-glycans which are not observed in non-cancerous cells.
- Using MS/MS mass spectrometry and LC retention time, the structural features of these glycans can be elucidated using diagnostic fragment ions that represent specific cross ring and glycosidic cleavages and provide information on their specific linkage and branching patterns.
- The specific glycosylation features that are present on the cell surface of these cells are regulated by the expression of various glycosyltransferase genes. For instance, in ovarian cancer cells, the expression of α 2-6 sialylation, bisecting GlcNAc and LacdiNAc-type glycans correlate with their cellular expression of ST6GAL1, MGAT3 and B4GALNT3 genes, respectively.
- The presence of bisecting GlcNAc *N*-glycans on ovarian cancer cells is thought to be epigenetically regulated through DNA hypomethylation of MGAT3 gene.

CHAPTER III

Rationale

Serous cancers derived from the ovary, peritoneum and tube represent a group of cancers that are collectively treated and managed similarly, despite their distinct anatomical origins. In this study, the membrane protein *N*- and *O*-glycosylation of serous cancer tissues derived from ovarian, peritoneum and tubal origin were investigated to a) validate the presence of ovarian cancer-associated structural glycans previously identified in cancerous cell lines and b) identify common and discriminatory glycan structural features between the three serous cancer origins. Relative quantitative glycan profiling, together with the characterisation of isomeric and isobaric structural glycans were employed in this study. The differential expression of *N*- and *O*-glycans was evaluated by rigorous statistical methods to identify diagnostic and discriminatory serous cancer tissue-derived markers.

3.0 Introduction

Epithelial ovarian cancer (EOC) represents a heterogeneous disease which is classified into the serous, endometrioid, clear-cell, mucinous and undifferentiated subtypes based on their histopathologic features (Scully, 1998; Kurman and Shih Ie, 2010). EOC has the highest mortality rate within all gynaecological malignancies, where more than 75 % of tumours are presented at advanced International Federation of Gynaecology and Obstetrics (FIGO) stages (Coleman, Forman *et. al.*, 2011) and characterised by a 5-year survival rate of only 43 % (Siegel, DeSantis *et. al.*, 2012). This disease is notoriously known as a ‘silent killer’ due to its asymptomatic prevalence and it is estimated that newly diagnosed cases and death rates are expected to rise on a global level each year (Jemal, Siegel *et. al.*, 2009). In Australia alone, 1470 women are expected to be diagnosed with ovarian cancer in 2014 and the number of cases are predicted to rise to 1640 by 2020 (AIHW, 2012). Despite current treatment options for advanced EOC which involves maximal cytoreductive surgery and platinum-based chemotherapy (Kessler, Fotopoulou *et. al.*, 2013), less than a 10 % improvement has been achieved for 5-year survival rates over the past 35 years (Jemal, Siegel *et. al.*, 2008). This poor prognosis is largely due to several factors: (i) the lack of reliable diagnostic markers and screening tests for the early detection of ovarian cancer (Suh, Park *et. al.*, 2010; Erickson, Conner *et. al.*, 2013), (ii) rapid metastasis of the disease which extends beyond the ovaries at the initial time of diagnosis (Bhoola and Hoskins, 2006), (iii) frequent development of drug resistance which further contributes to the lack of effective treatments for ovarian cancer (Agarwal and Kaye, 2003) and (iv) a poor understanding of the aetiology and origin of the precursor lesion which fails to account for the diverse clinical and pathological behaviours of the tumours (Nik, Vang *et. al.*, 2014).

For decades, EOC was traditionally thought to have originated from the ovarian surface epithelium (OSE) and various studies have primarily been focused on the ovary (Fathalla, 1971; Dubeau, 1999; Li, Fadare *et. al.*, 2012). Interestingly, the most prevalent type of EOC, which is of the serous histotype, represents 60-80 % of EOC and is rarely confined to the ovaries, even at tumour initiation (Selvaggi, 2000; Seidman, Horkayne-Szakaly *et. al.*, 2004; Li, Fadare *et. al.*, 2012). Mounting evidence has implicated that serous ovarian tumours together with non-ovarian serous cancers such as tumours of the fallopian tube and peritoneum, are characterised by P53 mutations and can be regarded as fast-growing, high grade serous carcinomas (HGSC), often with a widespread dissemination within the pelvic region (Seidman, Zhao *et. al.*, 2011; Kessler, Fotopoulou *et. al.*, 2013). From a diagnostic perspective, these serous tumours are often designated broadly as pelvic serous carcinomas

especially when the primary site of origin cannot be precisely determined (Nik, Vang *et al.*, 2014). In most cases, a majority of the tumour mass is located on the ovaries and is thus collectively treated and managed in a similar manner, regardless of tumour origin (Kindelberger, Lee *et al.*, 2007; Landen, Birrer *et al.*, 2008). Although recent findings have suggested the involvement of the serous fallopian tube epithelium as a precursor lesion for a majority of high grade serous ovarian cancers (Piek, van Diest *et al.*, 2001; Piek, Verheijen *et al.*, 2003; Li, Fadare *et al.*, 2012; Erickson, Conner *et al.*, 2013), studies investigating the underlying differences within these serous cancer subtypes which are reflective of the individual cellular phenotypes and molecular origin have been rather limited (Lacy, Hartmann *et al.*, 1995; Pere, Tapper *et al.*, 1998; Chen, Yamada *et al.*, 2003). Specifically, the degree to which these serous tumours differ, despite their similarity in terms of pathogenesis, clinical behaviour and chemotherapy response remains relatively unknown.

It has been widely accepted that protein glycosylation is an important post-translational modification which has relevance in many biological processes such as cell signalling, immune responses, extracellular interaction and cell adhesion (Varki, 1993; Ohtsubo and Marth, 2006). In the tumour microenvironment, aberrant protein glycosylation such as the expression of truncated glycans as well as neo-expression of glycans that are usually restricted to embryonic tissues have been well described in various cancers (Hakomori, 2002; Dube and Bertozzi, 2005; Reis, Osorio *et al.*, 2010). These structures may resemble glycomic ‘fingerprints’ which facilitate the discrimination between healthy and cancerous cells or potentially reflect tumour micro-heterogeneity caused by the variation between cancer subtypes (Abbott, Lim *et al.*, 2010; West, Segu *et al.*, 2010). One of the most common glycosylation changes in cancer is the increase in size and branching of *N*-glycans, in which large tetra-antennary structures are formed by the specific enzyme, *N*-acetylglucosaminyltransferase V (GnT-V) (Dennis, Laferte *et al.*, 1987; Seelentag, Li *et al.*, 1998; Lau and Dennis, 2008). The presence of increased branching antennas creates available sites for the addition of sialic acids (Neu5Ac) by sialyltransferases, which in turn, often lead to increased sialylation in cancer (Kim and Varki, 1997; Wang, Lee *et al.*, 2005; Saldova, Royle *et al.*, 2007; Bull, Boltje *et al.*, 2013). Likewise, terminal modifications on glycan structures such as fucosylation on the cancer cell surface can also give rise to the presence of Lewis and sialyl Lewis antigens [sialyl Le^a; Neu5Ac α 2-3Gal β 1-3(Fuc α 1-4)GlcNAc β and sialyl Le^x; Neu5Ac α 2-3Gal β 1-4(Fuc α 1-3)GlcNAc β] which have been shown to correlate with tumour progression and metastasis (Narita, Funahashi *et al.*, 1993; McEver, 1997; Nakagoe, Fukushima *et al.*, 2000; Miyoshi, Moriwaki *et al.*, 2008; Shiozaki, Yamaguchi *et al.*, 2011). It is evident that aberrant glycosylation is indeed a key event in

malignant transformation and therefore affords an excellent opportunity for the identification of cancer-specific markers (Drake, Cho *et. al.*, 2010).

As the field of glycomics continues to gain recognition in this post-genomics era, mass spectrometry (MS)-based methodologies are now becoming indispensable and routinely used for the reliable profiling of numerous glycans from various samples (Chu, Ninonuevo *et. al.*, 2009; Harvey, 2009; Alley, Vasseur *et. al.*, 2012). In fact, MS identification and measurement of glycans are being pursued as a structurally-informative approach as opposed to the clinically-established immunological assays (Scholler, Crawford *et. al.*, 2006; Shirotani, Futakawa *et. al.*, 2011; Wu, Zhu *et. al.*, 2014) or arrays (Yue, Goldstein *et. al.*, 2009) commonly used in biomarker discovery (Alley, Vasseur *et. al.*, 2012). This strategy, also known as glycomic profiling, has been recently employed in several studies to identify *N*- and *O*-glycan changes that were statistically elevated in ovarian cancer patients' plasma (Saldova, Royle *et. al.*, 2007; Alley, Vasseur *et. al.*, 2012; Biskup, Braicu *et. al.*, 2013; Kim, Park *et. al.*, 2014). One study, for instance, noted a significant increase in branching and sialylation patterns as well as increased expression of $\alpha 2$ -6 sialylation in ovarian cancer plasma as compared to healthy controls (Saldova, Royle *et. al.*, 2007). In addition, a recent study on the glycosylation of serum CA125, a membrane-associated glycoprotein clinically used for the diagnosis of ovarian cancer, also revealed that ovarian cancer patient sera displayed increased core-fucosylated bi-antennary monosialylated *N*-glycans and Core 1 and Core 2 *O*-glycans, as compared to healthy controls (Saldova, Struwe *et. al.*, 2013). While most of these studies yielded clinically relevant information on the differential expression of glycans found in patients' plasma, the major focus of their analysis was on differentiating between healthy and diseased patients. To date, there has been no single MS-based glycan profiling study carried out to compare *N*- and *O*- glycan structures on proteins from pelvic serous carcinomas which potentially have different sites of origin, and most likely represent distinct diseases, despite being classified as HGSC. In addition, since the glycomic changes observed in serum represent only a small fraction of the actual glycosylation directly associated with the tumour, there is also a crucial need to identify the precise glycan structural changes that occur at a cellular level (Anderson and Anderson, 2002; Alley, Vasseur *et. al.*, 2012). These less abundant glycan differences due to the presence of a tumour remain elusive since abundant levels of glycoproteins synthesised and secreted by the liver are present in the serum (Arnold, Saldova *et. al.*, 2008), thereby masking the detection of sensitive and specific biomarkers with clinical potential.

To address this challenge, we have employed the glycomic profiling strategy to identify *N*- and *O*- glycan changes on membrane glycoproteins extracted from serous cancer tissues clinically diagnosed as serous ovarian, peritoneal and tubal cancer, respectively. Specifically, we aim to (i) identify structural glycan features that are characteristic of all serous cancer specimens, (ii) identify a panel of tissue-specific glycan markers to discriminate between the three serous cancer origins, and (iii) perform a rigorous statistical evaluation of the diagnostic potential of these glycan structures. It is envisioned that the identification of serous-subtype specific glycan structures may improve diagnosis and further lead to novel therapeutic strategies to improve survival rates for this malignancy.

3.1 Materials and Methods

Serous cancer tissue specimens

The clinical tissue specimens were obtained surgically from patients diagnosed with high grade, advanced stage serous ovarian, peritoneal or tubal cancer. The bio-bank establishment of tissue specimens was carried out in separate stages through our collaborative initiatives with Dr. Viola Heinzelmann-Schwarz at hospitals and gynaecological centres in Switzerland and Australia. The first patient cohort (n=14) tissue specimens were obtained from various gynaecological cancer centres in Switzerland and established at the University Hospital Zurich from 2006-2010. The second patient cohort (n=18) was established in the Lowy Cancer Research Centre, Prince of Wales Clinical School, University of New South Wales (UNSW) since 2009 and the samples were obtained from the John Hunter Hospital, Newcastle and the Royal Hospital for Women in Sydney. All patient specimens were processed identically in both cohorts. Formalin-fixed and paraffin-embedded tissue-blocks were evaluated by a specially trained gynaecological pathologist. Tissue collection was carried out with patient's consent using standardised clinical and ethical protocols approved through independent, board-approved institutions during the entire collection period (SPUK Canton of Zurich, Switzerland, Hunter Area Research Ethics- Ref: 04/04/07/3.04, South Eastern Sydney Illawarra HREC/AURED-Ref: 08/09/17/3.02 and Macquarie University-Ref: 26/09/11/ 5201100778). Clinico-pathological data for these tissue samples are listed in **Table 1**.

Cohort	No	Patient ID	Age	Blood Type	Tumour stage/Grade	Discriminant		BRCA Carrier
						1-Diagnosis	2-Tissue Source	
Sydney	1	S69	52		III/ 3	Serous ovarian cancer	Left ovary	
	2	S70	58	O	III/ 3	Serous ovarian cancer	Right ovary	
	3	S75	61	A	III/ 3	Serous ovarian cancer	Right ovary	
	4	S102	66		III/ 3	Serous ovarian cancer	Left ovary	
	5	S308	47	O	III/ 3	Serous ovarian cancer	Omentum	
	6	S450	56	A	IV/ 3	Serous ovarian cancer	Right ovary	
	7	S520	77	A	III/ unknown	Serous ovarian cancer	Ovary	
	8	S565	57		II/ 3	Serous ovarian cancer	Right ovarian mass	
	9	S153	67		III/ 3	Serous peritoneal cancer	Omentum	
	10	S155	62		III/ 2	Serous peritoneal cancer	Omentum	
	11	S164	87		III/ 3	Serous peritoneal cancer	Peritoneal mass	
	12	S362	77	A	III/ 3	Serous peritoneal cancer	Omentum	
	13	S366	61	A	III/ 2	Serous peritoneal cancer	Cancer mass	
	14	S418	73	O	IV/ 3	Serous peritoneal cancer	Left ovary	
	15	S521	56	B	unknown/ 3	Serous peritoneal cancer	Omentum	
	16	S524	83	A	III/ 3	Serous peritoneal cancer	Omentum	BRCA1
	17	S467	66	O	III/ 3	Serous tubal cancer	Left ovary	
	18	S448	77		III/ 3	Serous tubal cancer	Ovary	
Switzerland	19	Z6	65	O	II/ 3	Serous ovarian cancer	Ovary	
	20	L6	63	B	III/ 2	Serous ovarian cancer	Ovary	
	21	Z17	63	B	III/ 3	Serous ovarian cancer	Ovary	
	22	Z55	56			Serous ovarian cancer	Right ovary	
	23	Z21	67	A	IV/ 3	Serous ovarian cancer	Right ovary	
	24	Z10	78	A	III/ 3	Serous ovarian cancer	Right ovary	
	25	L11	78	A	III/ 3	Serous peritoneal cancer	Omentum	
	26	L13	71	A	III/ 3	Serous peritoneal cancer	Peritoneum	
	27	L15	67	O	III/ 3	Serous peritoneal cancer	Omentum	
	28	L18	60	O	III/ 3	Serous peritoneal cancer	Omentum	
	29	L8	69	O	III/ 3	Serous peritoneal cancer	Omentum	
	30	Z30	71	O	IV/ 3	Serous peritoneal cancer	Omentum	
	31	Z5	66	A	IV/ 2	Serous tubal cancer	Omentum	
	32	Z22	65	A	II/ 3	Serous tubal cancer	Left tube	

Table 1. Source and clinico-pathological information of serous cancer specimens. The cancer specimens derived from the ovary, peritoneum and fallopian tube obtained from tissue cohorts in Sydney (n=18) and in Switzerland (n=14), were selected based on their serous histotype. All patient specimens were processed identically from both cohorts and evaluated based on tumour stage and grade by a specially trained gynaecological pathologist. Serous cancer specimens have been assigned respective discriminants (diagnosis and source) for the purpose of statistical analyses. Blood group information and hereditary gene mutations (BRCA1/2) are indicated (where available).

Ovarian cancer tissue processing

Fresh tissue specimens obtained during surgery were kept in RNAlater® solution at -80 °C until use. RNAlater® solution (Ambion) was removed as previously described with a few minor modifications (Rader, Malone *et. al.*, 2008). Briefly, intact tissue specimens (~ 40 mg) were removed from RNAlater® solution using sterile forceps, transferred to a Ultracell MC 0.45µ filter unit and placed into a 1.5 ml Eppendorf collection tube. A volume of 500 µl of ice-cold acetonitrile: water (80:20) was added to the tissue sample, resulting in the formation of RNA ice crystals in the tissue. The RNAlater® ice crystals were precipitated by centrifugation at 1500 x g for 20 mins at RT and the biphasic liquid in the collection tube was discarded. Removal of the RNAlater® with acetonitrile:water was repeated several times until the formation of RNAlater® ice crystals stopped and no visible biphasic layer was observed in the collection tube. Tissues were washed twice in 10 ml of phosphate buffered saline and cut into small (1 mm x 1 mm) pieces prior to tissue homogenisation.

Membrane protein extraction from tissue

Membrane protein extraction was carried out as previously described (Lee, Kolarich *et. al.*, 2009). Tissues (~40 mg) were re-suspended in 2 ml of lysis buffer (50 mM Tris-HCl, 100 mM NaCl, 1 mM EDTA and protease inhibitor at pH 7.4) and stored on ice for 20 mins. The tissues were lysed using a Polytron homogeniser (Omni TH, Omni International Inc, VA) for 20 mins. Unlysed cells and cellular debris were removed by centrifugation at 2,000 x g for 20 mins at 4 °C. Tissue homogenates were collected and diluted with 2 ml of Tris buffer (20 mM Tris-HCl, 100 mM NaCl at pH 7.4) and membranes were sedimented by ultracentrifugation at 120 000 x g for 80 mins at 4 °C. After discarding the supernatant, 140 µl of Tris binding buffer was added into each sample to re-suspend the membrane pellet. A volume of 450 µl of Tris binding buffer containing 1 % (v/v) Triton X-114 was then added to the mixture and chilled on ice for 10 mins. Samples were heated at 37 °C for 20 mins and further subjected to centrifugation at 1000 x g for 3 mins. The upper aqueous layer was carefully removed and stored at -20 °C. The detergent-soluble membrane proteins were precipitated from the lower layer with 1 ml of ice-cold acetone and left overnight at -20 °C. Precipitated membrane proteins were pelleted by centrifugation at 1000 x g for 3 mins and solubilised in 10 µl of 8 M urea.

Enzymatic release and purification of *N*-glycans from tissue membrane proteins

N-glycans were prepared as previously described (Kolarich, Jensen *et. al.*, 2012). Briefly, ~30 µg of membrane proteins and a glycoprotein standard (10 µg of fetuin) were spotted (2.5 µl x 4 times) onto a polyvinylidene difluoride (PVDF) membrane and dried overnight at room temperature. The stained membrane-bound protein spots were cut and placed in separate wells of a 96-well microtiter plate, to which 100 µl of blocking buffer was added. The wells were washed with MilliQ water after removing the blocking buffer and PNGase F enzyme (2 µl of 1 U/µl PNGase F and 8 µl of MilliQ water) was added to each well. A volume of 10 µl MilliQ water was added and the microtiter plate was sealed with parafilm prior to an overnight incubation at 37 °C. After sonication of the plate for 10 mins, approximately 20 µl of released *N*-glycans were collected and transferred to a new Eppendorf tube, together with combined washings (50 µl of MilliQ water, twice) from each sample well. To regenerate the reducing terminus of the released *N*-glycans, 20 µl of 100 mM ammonium acetate (pH 5.0) was added to each sample (~120 µl) and kept at room temperature for 1 h. After evaporation of the samples, the released *N*-glycans were reduced to alditols with 10 µl of 2 M NaBH₄ in 50 mM KOH and 10 µl of 50 mM KOH at 50 °C for 2 h and the reduction was quenched using 2 µl of glacial acetic acid. For purification of *N*-glycan alditols, 45 µl of cation exchange resin beads (AG50W-X8) were deposited into reversed phase µ-C18 ZipTips (Perfect Pure, Millipore) placed in individual microfuge tubes. Approximately 20 µl of *N*-glycan alditols were applied to the column, eluted with MilliQ water (50 µl, twice) and dried. Residual borate was removed by drying the samples under vacuum after the addition of methanol (100 µl, thrice). The purified *N*-glycan alditols were re-suspended in 15 µl of MilliQ water prior to mass spectrometry analysis.

Chemical release of *O*-glycans

The remaining PVDF spots in the 96- well microtiter plate were then re-wet with 2.5 µl methanol and further subjected to reductive β-elimination of the *O*-linked oligosaccharides by treating the spots with 2.0 µl of 0.5 M sodium borohydride in 50 mM potassium hydroxide. The plate was then sealed with parafilm and incubated for 16 h at 50 °C. The reaction was quenched using 2 µl of glacial acetic acid and desalted by cation exchange chromatography as previously described for *N*-glycans.

LC-ESI-MS/MS and data interpretation of released *N*- and *O*-glycan alditols

The separation of *N*- and *O*-glycans was performed on a Hypercarb porous graphitised carbon capillary column (5 μm Hypercarb KAPPA, 180 μm x 100 mm, Thermo Hypersil, Runcorn, UK) over a linear gradient of 0–45 % (v/v) acetonitrile/10 mM ammonium bicarbonate for 85 mins for *N*-glycans and 0–90% (v/v) acetonitrile/10 mM ammonium bicarbonate for 45 mins for *O*-glycans. The sample injection volume was 7 μl and 4 μl for *N*- and *O*-glycans respectively, and the flow rate was set at 2 $\mu\text{l}/\text{min}$ using an Agilent HPLC (Agilent 1100). The MS instrument used in this study consisted of an ion-trap mass spectrometer (LC/MSD Trap XCT Plus Series 1100, Agilent Technologies, USA) connected to an ESI source (Agilent 6330, USA). The temperature of the transfer capillary was maintained at 300 °C and the capillary voltage was set at 3 kV. *N*- and *O*-glycans were detected in negative ionisation mode as $[M-H]^{-1}$ and $[M-2H]^{-2}$ ions within the mass range of m/z 600– m/z 2200. MS data was analysed using Compass Data Analysis Version 4.0 software (Bruker Daltonics, USA).

Monoisotopic masses detected in negative mode were assigned to possible monosaccharide compositions using the GlycoMod tool (Cooper, Gasteiger *et. al.*, 2001) available on the ExPASy server (<http://au.expasy.org/tools/glycomod>) using a mass tolerance of ± 0.5 Da. Glycan structures were proposed based on manual annotation of tandem MS fragmentation spectra and were further characterised with the aid of software-generated mass fragments using GlycoWorkBench (Ceroni, Maass *et. al.*, 2008). The *N*-glycan structures of cancer tissues diagnosed as serous ovarian, peritoneal and tubal cancers (**Discriminant 1**) were classified into four major categories [high mannose/oligomannose, hybrid, complex (neutral and sialylated) and core fucosylated] based on the proposed nomenclature (Stanley, Schachter *et. al.*, 2009). The MS ion intensity of each *N*- and *O*-glycan was relatively quantified based on the peak areas of their extracted ion chromatogram (EIC) and expressed as a percentage of summed ion intensities for total glycans within each sample.

Data processing and statistical analyses

Following normalisation to 100 %, the relative ion intensities were used to generate glycomic profiles for individual serous cancers and subsequent statistical analyses were carried out based on a) serous cancers diagnosed as ‘ovarian’, ‘peritoneal’ and ‘tubal’ (**Discriminant 1**) and b) serous cancers derived from the ovary, peritoneum/omentum and fallopian tube (**Discriminant 2**). In **Discriminant 1**, glycomic profiles were analysed based on the diagnosis of these serous cancers, irrespective of their location from which the tumour has been surgically-derived. For instance, a cancer tissue sample may have been derived from the ovary of a patient diagnosed with serous ‘tubal’ cancer. In **Discriminant 2**, glycomic profiles were analysed based on the location from which the tumour has been surgically removed from, ie. ovary (left and right ovary), peritoneum (omentum) or tube. As an initial statistical assessment for **Discriminant 1** and **2**, one-way analysis of variance (ANOVA) using SPSS (version 19.0) was carried out to assess statistical significance ($p < 0.05$) between the overall *N*- and *O*-glycan expressions for each glycan category. An additional *post-hoc* analysis, known as the Bonferroni correction (two-tailed) was applied to compare between the three serous cancer groups. Two analyses, namely the Principal Component Analysis (PCA) and Partial Least Squares Discriminant Analysis (PLSDA) were carried out to assess the discriminatory potential of individual *N*- and *O*-glycans, respectively. Specifically, Principal Component Analysis (PCA) was employed to visualize clustering based on **Discriminant 1** and **2**, while the Partial Least Squares Discriminant Analysis (PLSDA) was used to predict the accuracy of the classification of serous cancers based on **Discriminant 1**. For the Receiver-Operating Characteristics (ROC) analysis, the biomarker potential of diagnostic *N*- and *O*-glycans was assigned to specific rankings based on the resulting area-under-the-curve (AUC) values, ranging between 0-1. Statistical evaluations for ROC (‘ROCR’ package), PLSDA (‘caret’ package) and PCA (‘stats’ package) were performed using the R statistical programming language, version 2.15.1 (<http://www.r-project.org/>).

3.2 Results

In view of the complexity surrounding the early detection of serous ovarian cancers and the potential involvement of non-ovarian tissues (distal fallopian tube and peritoneum), *N*- and *O*-MSglycomic profiling of clinically diagnosed serous ovarian (n=14), peritoneal (n=14) and tubal (n= 4) cancers from two independent cohorts, Australia (n=18) and Switzerland (n=14), were carried out. The membrane proteins were extracted and the released *N*- and *O*-glycan alditols were analysed using negative ion mode LC-MS/MS, which resulted in the detection of well-resolved chromatographic peaks that corresponded to generally recognised glycan masses. The extracted ion chromatograms (EIC) for each of the observed MS signals were analysed and detailed glycan structures were manually assigned *via* the following steps: a) a monosaccharide compositional prediction approach based on residue masses (GlycoMod) (Cooper, Gasteiger *et. al.*, 2001), b) a fragmentation mass spectral-matching approach of fragment ions produced by negative ion tandem MS of each glycan mass and c) use of diagnostic fragment ions in negative ion mode that have been previously reported for the identification of specific glycan structural features (Harvey, 2009; Everest-Dass, Abrahams *et. al.*, 2013; Everest-Dass, Kolarich *et. al.*, 2013) and d) known synthesis of glycan structures based on biological pathway constraints. Upon the identification of characteristic glycan features for each serous cancer type, glycan profiles were subjected to a series of statistical evaluations to potentially distinguish between serous ovarian, tubal and peritoneal cancers. The workflow employed in this study is outlined in **Figure 1**.

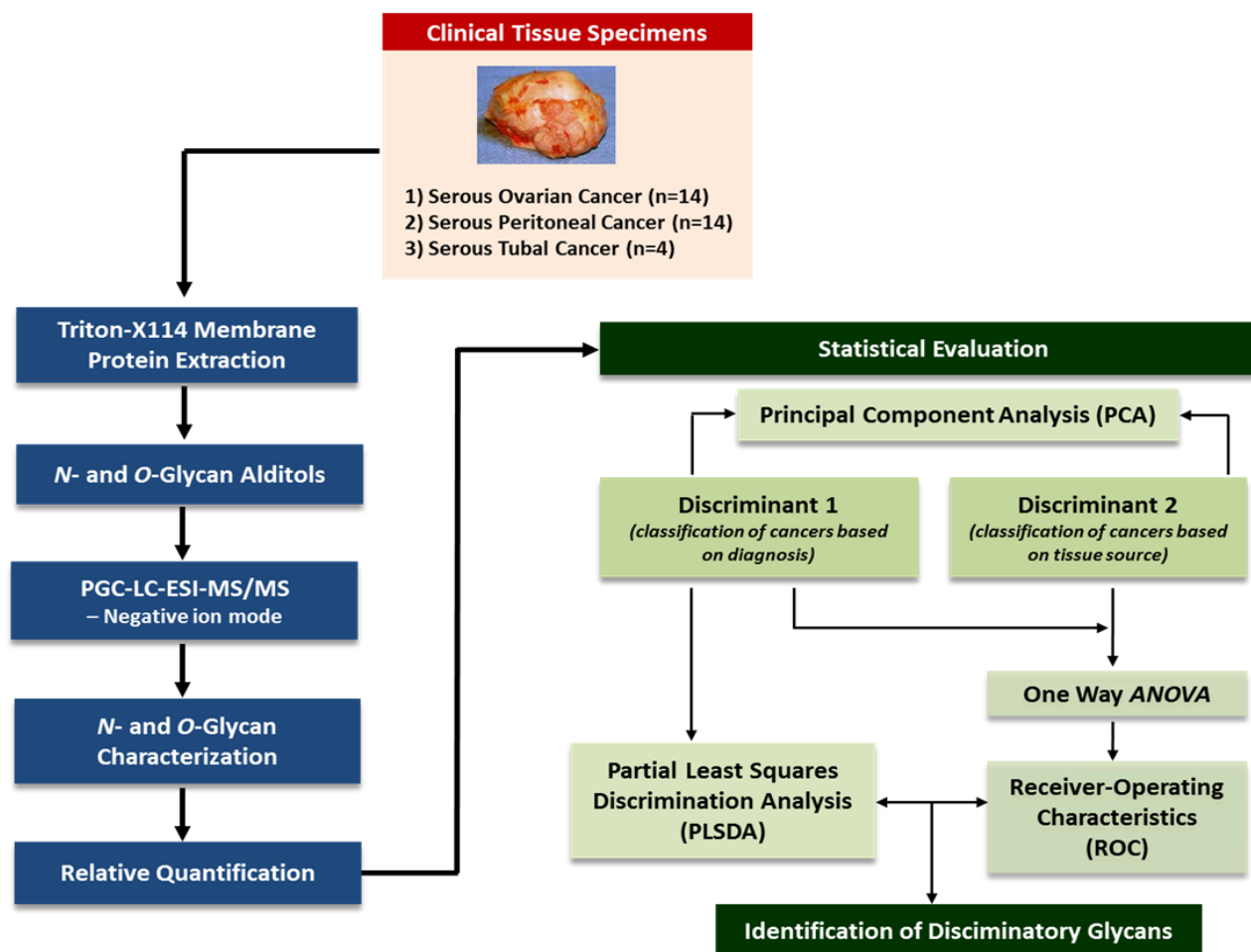


Figure 1. Graphic illustration of workflow employed in the extraction, profiling and analysis of *N*- and *O*-glycans of pelvic serous cancers. Briefly, membrane proteins extracted from serous cancers and released *N*- and *O*-glycan alditols were separated on porous graphitised carbon (PGC) and analysed using electrospray ionisation mass spectrometry (ESI-MS/MS). Glycans were structurally characterised using tandem MS and subjected to a battery of statistical evaluations to identify discriminatory glycans implicated in the distinction of serous ovarian, peritoneal and tubal cancers.

Serous cancers display highly similar membrane *N*- and *O*-glycan profiles

For *N*-glycans, 55 distinct masses were identified across all the serous cancers at varying intensities within a mass range of m/z 600 - m/z 2200. The structures of these glycans, including their isobaric isomers, were then characterized and quantified based on their relative ion intensities (**Table 2A**) and classified into five major categories, namely the high mannose, hybrid, complex neutral, complex sialylated and core fucosylated based on the proposed nomenclatures (Stanley, Schachter *et. al.*, 2009). The representative average MS spectra (**Figure 2**) were overall similar and showed that a majority of the peaks in the global MS profiles of all three serous cancer groups were associated with sialylated *N*-glycans which appeared to be comparable in terms of their relative ion intensities. Several other peaks which comprised of neutral and high-mannose type glycans were also observed, appearing at lower intensities. Due to the potential biological variation which would occur in the individual tissues of each serous cancer type, the total ion intensities of the five *N*-glycan structural categories within all samples were represented individually (box plots) for all tissue samples to gain an insight into their heterogeneity (**Figure 3A**). One-way ANOVA was performed to assess the statistical significance between the average *N*-glycan expression of each structural category in all three serous cancer groups. No significant differences were observed between the three serous cancer groups for all five *N*-glycan categories. *O*-glycans were released from the extracted membrane proteins by alkaline β -elimination and analysed using negative ion mode LC-MS/MS. In total, nine *O*-glycan masses were detected across all the serous cancer tissue samples and the proposed *O*-glycan structures and their relative intensities for each cancer type are listed in **Table 2B**. Based on the representative MS spectra shown in **Figure 4**, the *O*-glycans appeared as singly charged ions in all samples which mainly comprised of Core 1 and Core 2 *O*-glycan structures. The total ion intensities for *O*-glycan structures based on the respective core-type are shown in **Figure 3B**, in which no significant differences were observed for the overall *O*-glycan expression across the individuals comprising the three serous cancer groups.

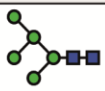
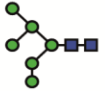
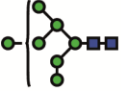
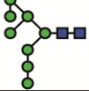

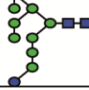
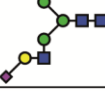
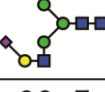

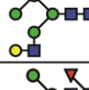
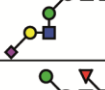
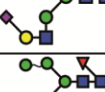
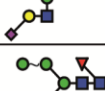
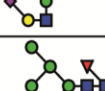
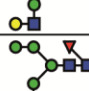
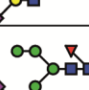

Type	No	Glycan Mass [M-H] ⁻	[M-2H] ²⁻	Glycan Structures	Average Relative Intensity (%)		
					Serous Ovarian Cancer (n=14)	Serous Peritoneal Cancer (n=14)	Serous Tubal Cancer (n=4)
N-glycans-High Mannose	1	1235.4	617.2		2.08 ± 0.70	1.68 ± 1.29	3.08 ± 0.96
	2	1397.6	698.3		2.76 ± 1.27	2.10 ± 1.31	2.48 ± 1.70
	3	1559.6	779.3		3.20 ± 1.80	2.45 ± 1.41	3.42 ± 1.59
	4	1721.6	860.3		4.02 ± 2.02	3.82 ± 2.47	4.71 ± 2.30
	5	1883.8	941.4		5.40 ± 3.33	5.80 ± 4.28	6.88 ± 3.41
	6	2045.6	1022.3		0.39 ± 0.17	0.38 ± 0.23	0.47 ± 0.22
N-glycans-Hybrid	7	1567.6	783.3		0.12 ± 0.29	0.28 ± 0.46	0.22 ± 0.44
	7a	1567.6	783.3		0.76 ± 0.38	0.51 ± 0.32	0.60 ± 0.14
	8	1584.6	791.8		0.04 ± 0.09	0.05 ± 0.13	0.07 ± 0.09
	9	1600.6	799.8		0.72 ± 0.40	0.62 ± 0.22	0.76 ± 0.23
	10	1713.6	856.3		0.40 ± 0.58	0.23 ± 0.59	0.20 ± 0.42
	10a	1713.6	856.3		0.91 ± 0.52	0.49 ± 0.60	0.86 ± 0.54
	11	1729.6	864.3		0.48 ± 0.32	0.42 ± 0.37	0.53 ± 0.85
	11a	1729.6	864.3		0.58 ± 0.23	0.64 ± 0.31	0.75 ± 0.54
	12	1746.6	872.8		0.01 ± 0.03	0.1 ± 0.10	0.07 ± 0.08
	13	1875.6	937.3		0.30 ± 0.40	0.19 ± 0.22	0.32 ± 0.30
	13a	1875.6	937.3		0.45 ± 0.35	0.10 ± 0.15	0.73 ± 0.41

Table 2A

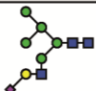

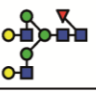


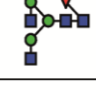



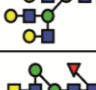
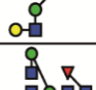
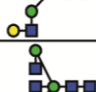





Type	No	Glycan Mass [M-H] ⁺	[M-2H] ²⁻	Glycan Structures	Average Relative Intensity (%)		
					Serous Ovarian Cancer (n=14)	Serous Peritoneal Cancer (n=14)	Serous Tubal Cancer (n=4)
	14	1891.6	945.3		0.63 ± 0.44	0.49 ± 0.40	0.57 ± 0.36
	14a	1891.6	945.3		0.67 ± 0.33	0.57 ± 0.31	0.75 ± 0.37
N-glycans-Complex Neutral	15	1787.6	893.3		2.51 ± 1.59	3.05 ± 1.58	1.94 ± 0.15
	16	1666.4	832.8		1.07 ± 0.94	0.83 ± 0.41	0.62 ± 0.20
	17	1641.6	820.3		0.99 ± 0.75	1.10 ± 0.44	0.86 ± 0.47
	18	1463.6	731.2		1.03 ± 0.77	1.15 ± 0.71	1.02 ± 0.66
	19	2006.8 *	1002.9		0.04 ± 0.10	0.06 ± 0.11	0.01 ± 0.03
	20	1625.6	812.3		1.40 ± 0.82	1.40 ± 0.69	1.10 ± 0.35
	21	2152.8 *	1075.9		0.32 ± 0.42	0.45 ± 0.46	0.34 ± 0.30
	22	2518	1258.5		0.06 ± 0.11	0.06 ± 0.08	0.09 ± 0.15
	23	1828.8	913.9		0.48 ± 0.63	0.14 ± 0.49	0.58 ± 0.42
	23a	1828.8	913.9		1.78 ± 0.88	1.71 ± 0.70	1.41 ± 0.66
	24	1520.8	759.9		0.36 ± 0.52	0.26 ± 0.17	0.18 ± 0.28
	25	1990.8	994.9		1.14 ± 0.33	1.76 ± 0.84	1.26 ± 0.78
	26	1479.6	739.3		0.20 ± 0.33	0.33 ± 0.26	0.34 ± 0.28
	27	1682.6	840.8		0.29 ± 0.25	0.39 ± 0.21	0.16 ± 0.25
	28	1844.8	921.9		0.17 ± 0.10	0.20 ± 0.18	0.07 ± 0.08

Table 2A

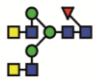


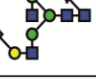
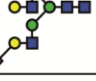
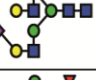




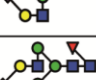

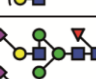


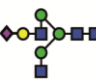

Type	No	Glycan Mass [M-H] ⁻	[M-2H] ²⁻	Glycan Structures	Average Relative Intensity (%)		
					Serous Ovarian Cancer (n=14)	Serous Peritoneal Cancer (n=14)	Serous Tubal Cancer (n=4)
	29	1869.8	934.4		0.32 ± 0.54	0.13 ± 0.27	0.31 ± 0.63
N-glycans-Complex Sialylated	30	2136.0	1067.5		0.19 ± 0.24	0.14 ± 0.15	0.00
	31	1916.6	957.8		0.47 ± 0.35	0.38 ± 0.38	0.65 ± 0.37
	31a	1916.6	957.8		0.42 ± 0.22	0.41 ± 0.37	0.40 ± 0.16
	32	1932.8	965.9		1.53 ± 3.15	1.80 ± 3.80	1.61 ± 3.94
	32a	1932.8	965.9		6.29 ± 3.14	7.88 ± 3.78	8.57 ± 3.53
	33	2078.8	1038.9		4.70 ± 3.90	6.34 ± 4.27	5.00 ± 3.40
	33a	2078.8	1038.9		4.30 ± 2.40	6.08 ± 2.50	3.76 ± 1.20
	34	2223.8	1111.4		0.96 ± 0.28	0.74 ± 0.60	0.48 ± 0.77
	34a	2223.8	1111.4		1.57 ± 3.20	2.00 ± 1.24	1.67 ± 0.50
	34b	2223.8	1111.4		16.41 ± 5.16	18.02 ± 8.80	18.01 ± 10.49
	35	2370.0	1184.5		7.34 ± 5.50	3.80 ± 2.80	4.28 ± 5.26
	35a	2370.0	1184.5		2.59 ± 1.32	3.63 ± 1.85	2.52 ± 1.15
	35b	2370.0	1184.5		4.14 ± 1.94	3.60 ± 1.97	3.00 ± 0.53
	36	2282.0	1140.5		1.47 ± 0.60	1.33 ± 0.67	1.77 ± 0.80
	37	2297.8 *	1148.5		0.25 ± 0.30	0.41 ± 0.52	0.27 ± 0.18
	38	1770.8	884.9		0.65 ± 0.28	0.70 ± 0.27	1.32 ± 0.87

Table 2A

Type	No	Glycan Mass [M-H] ⁻	[M-2H] ²⁻	Glycan Structures	Average Relative Intensity (%)		
					Serous Ovarian Cancer (n=14)	Serous Peritoneal Cancer (n=14)	Serous Tubal Cancer (n=4)
N-glycans-Complex Sialylated	39	2158.8	1078.9		0.18 ± 0.19	0.48 ± 1.42	0.19 ± 0.00
	40	2160.8	1079.9		0.21 ± 0.22	0.01 ± 0.05	0.00
	41	2265.8*	1132.5		1.22 ± 1.70	0.41 ± 0.67	0.43 ± 0.53
	42	2119.8*	1059.4		0.93 ± 1.73	0.19 ± 0.41	0.85 ± 0.62
	42a	2119.8	1059.4		0.41 ± 0.49	0.42 ± 0.35	0.13 ± 0.21
	43	1974.0	986.5		0.24 ± 0.19	0.27 ± 0.31	0.10 ± 0.12
	44	2573.0	1286.0		0.74 ± 0.51	0.44 ± 0.21	0.55 ± 0.43
	45	2411.0	1205.0		0.83 ± 0.48	0.14 ± 0.36	0.34 ± 0.40
	46	2444.0*	1221.5		1.15 ± 0.80	1.61 ± 0.70	1.44 ± 0.75
	47	2589.0*	1294		0.38 ± 0.25	0.52 ± 0.36	0.48 ± 0.33
	48	3026.0*	1512.5		0.65 ± 0.34	0.71 ± 0.55	0.56 ± 0.38
	49	2735.0*	1367		0.84 ± 0.40	1.07 ± 0.42	0.79 ± 0.43
	50	2809.2*	1404.1		0.10 ± 0.11	0.20 ± 0.27	0.25 ± 0.21
	51	2881*	1440		0.78 ± 0.36	0.88 ± 0.64	0.69 ± 0.67
	52	3101.2*	1550.1		0.13 ± 0.16	0.20 ± 0.17	0.23 ± 0.15
Pauci Mannose	53	895.4	—		0.62 ± 0.74	0.39 ± 0.22	0.65 ± 0.62
	54	911.4	—		0.46 ± 0.25	0.37 ± 0.24	0.40 ± 0.22
	55	1057.4	—		0.77 ± 0.59	0.47 ± 0.32	0.85 ± 0.59

Table 2A

Type	No	Glycan Mass [M-H] ⁺	[M-2H] ²⁺	Glycan Structures	Average Relative Intensity (%)		
					Serous Ovarian Cancer (n=14)	Serous Peritoneal Cancer (n=14)	Serous Tubal Cancer (n=4)
O-glycans (Core 1)	1	675.3	–		41.70 ± 23.57	36.50 ± 14.19	28.00 ± 11.43
	2	966.3	–		35.90 ± 20.17	39.19 ± 16.98	43.61 ± 22.14
	3	755.3	–		2.06 ± 1.03	2.30 ± 0.90	0.27 ± 0.00
	4	530.2	–		3.83 ± 0.00	0.00	0.00
O-glycans (Core 2)	5	749.3	–		2.20 ± 1.77	3.45 ± 2.12	4.08 ± 3.81
	6	1040.5	–		6.50 ± 7.26	10.58 ± 7.07	9.50 ± 3.75
	7	1331.5	665.3		4.08 ± 6.14	6.50 ± 5.47	10.09 ± 9.16
	8	1120.3	–		2.32 ± 4.00	1.48 ± 0.92	1.62 ± 1.87
	9	1411.4	705.2		1.41 ± 0.00	0.00	2.83 ± 3.82
<p>Legend:</p> <ul style="list-style-type: none"> Mannose (Man) Fucose (Fuc) Galactose (Gal) Sulphate N-acetylneuraminic acid (Neu5Ac; sialic acid) N-acetylglucosamine (GlcNAc) N-acetylgalactosamine (GalNAc) <p>Monosaccharide Linkage:</p>							

Table 2B

Table 2. Proposed A) *N*- and B) *O*-glycan structures detected on the membrane proteins of serous cancers derived from the ovary, peritoneum and tube. *N*- and *O*-glycan structures released from serous cancer tissue membrane proteins were separated by PGC-LC-ESI and their structures were assigned based on MS/MS fragmentation (where possible), retention time differences and biological pathway constraints. Structures were depicted according to the Consortium of Functional Glycomics (CFG) notation with linkage placement to indicate linkages for sialic acid and fucose residues (where known). Specific linkages corresponding to Type 1 (Galβ1-3GlcNAc) or Type 2 (Galβ1-4GlcNAc) lactosamine linkages and sulphate residues were not distinguished. *N*-glycan masses determined to consist of two or more isomer(s) but were not structurally resolved are indicated with asterisks (*). Values represent mean ± SD of biological replicates [serous ovarian (n=14), serous peritoneal (n=14), serous tubal (n=4)]. Position of sulphate is not determined and represented by parentheses ().

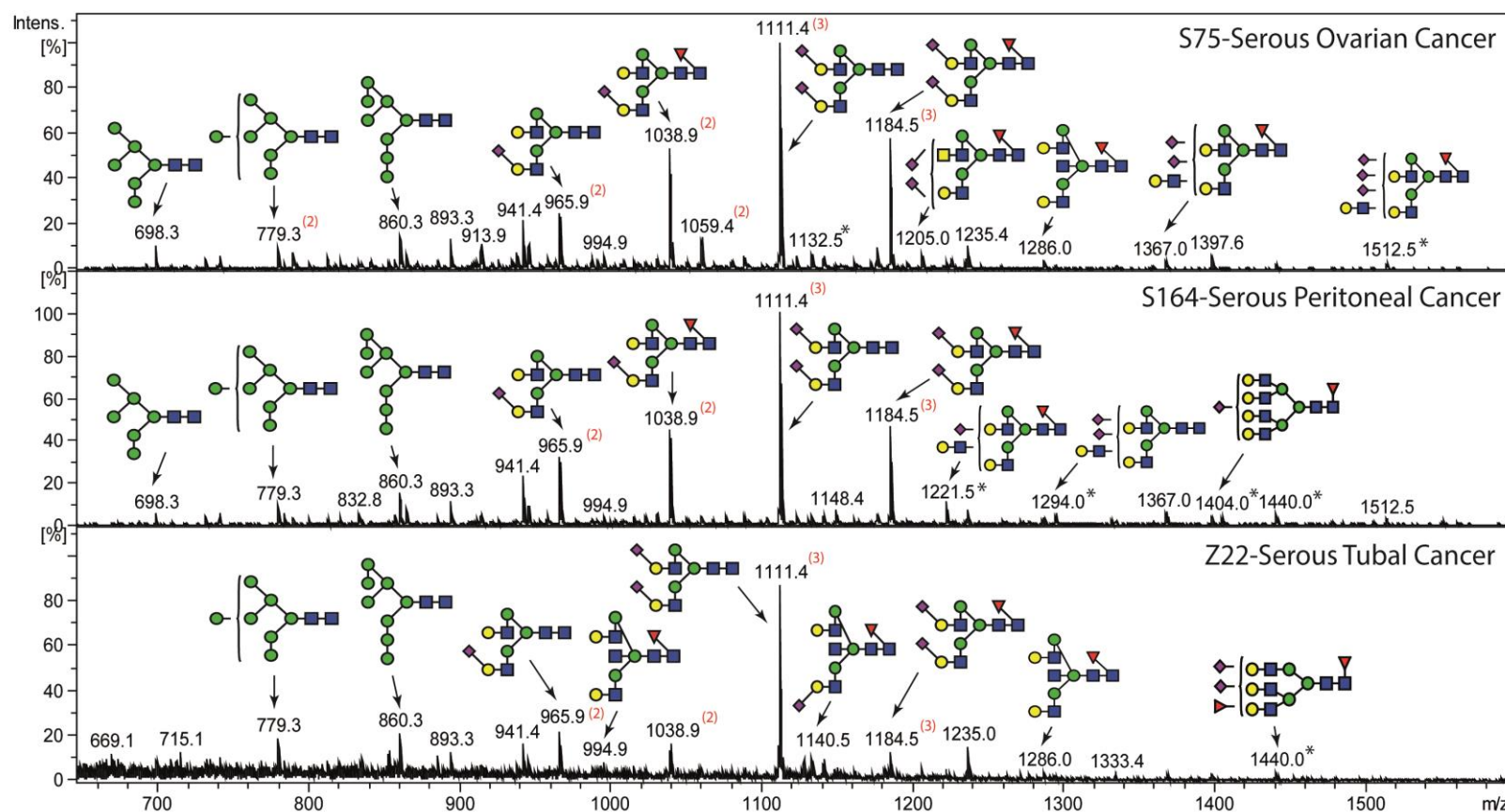


Figure 2. Representative average MS glycomic profiles of *N*-glycans released from membrane proteins of serous cancer tissues. An overview of the representative average MS *N*-glycan profiles in the range of m/z 640– m/z 1540 of serous ovarian (S75), serous peritoneal (S164) and serous tubal (Z22) cancer (LC elution time: 30 to 70 mins). The *N*-glycan structures were identified by tandem MS and are represented mainly by the doubly charged species ion, m/z $[M-2H]^{2-}$. Number of isomers corresponding to structurally resolved mass ions is indicated in parentheses (). *N*-glycan masses that were determined to consist of two or more isomer(s) but not structurally resolved are indicated with asterisks (*).

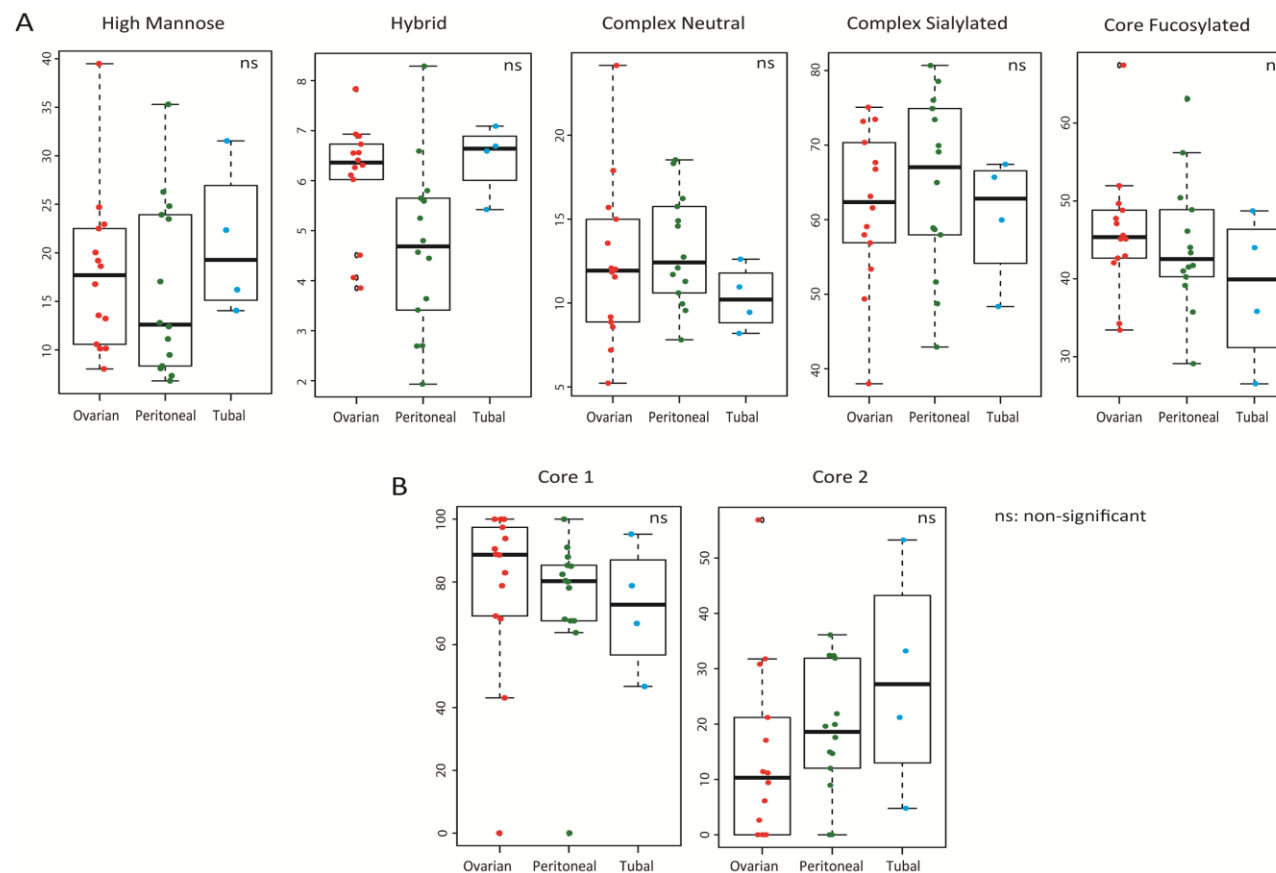


Figure 3. Quantitation of total relative abundances based on structural *N*- and *O*-glycan type as shown in **Table 1**. Box plots indicating changes in the relative ion intensities of A) 55 common *N*-glycans (high mannose, hybrid, complex neutral, complex sialylated and core fucosylated) and B) 9 *O*-glycans expressed in pelvic serous cancers. Data points for each serous cancer [serous ovarian (n=14), serous peritoneal (n=14), serous tubal (n=4)] represent total ion intensities of glycans in each category. Level of significance is indicated by ns (non-significant) for all categories.

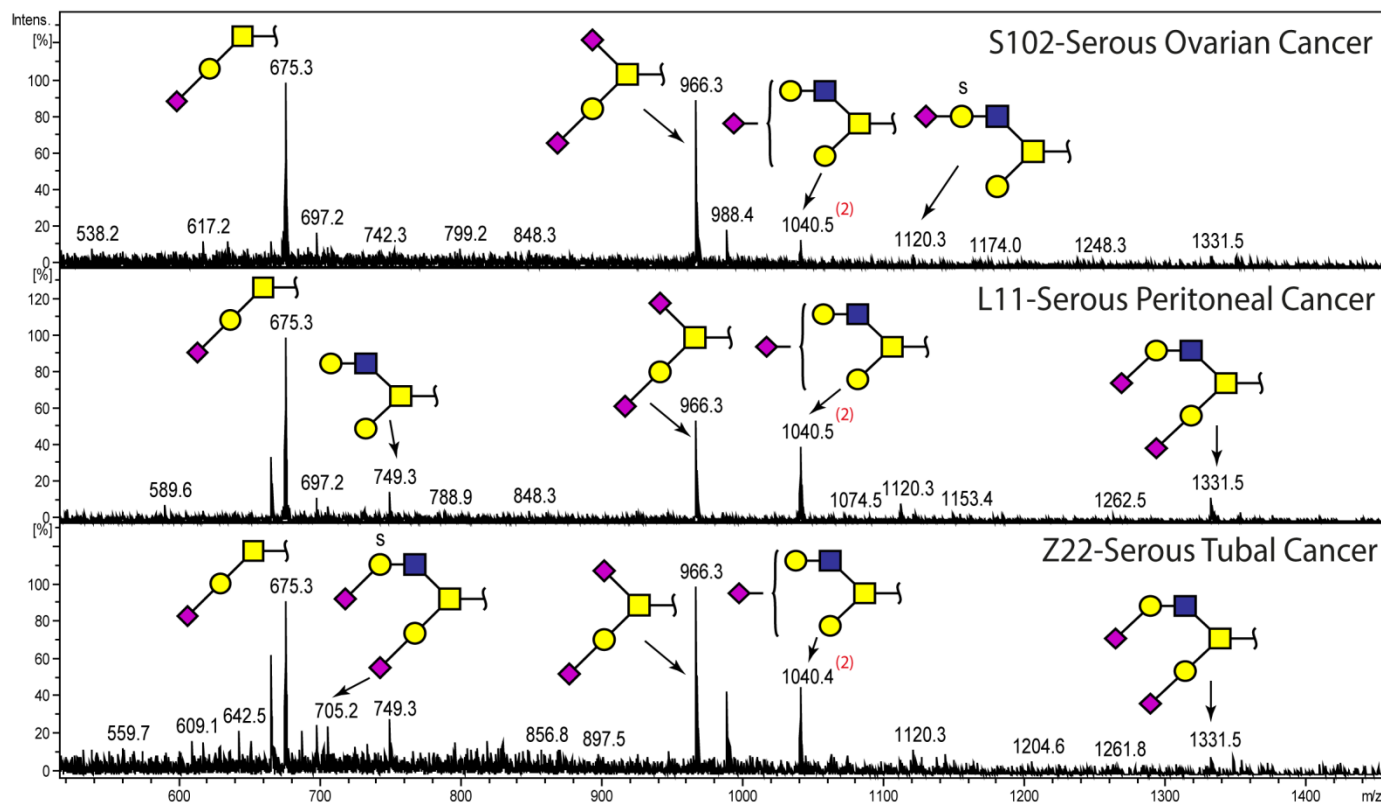


Figure 4. Representative glycomic profiles of *O*-glycans released from membrane proteins of serous cancer tissues. An overview of the representative average MS *O*-glycan profiles in the range of m/z 600- m/z 1400 of serous ovarian (S102), serous peritoneal (L11) and serous tubal (Z22) cancer tissue (LC elution time: 20 to 45 mins). The *O*-glycan structures were identified by tandem MS and are represented mainly by the singly charged species ion, m/z $[M-H]^{-}$. Doubly charged $[M-H]^{2-}$ ion with m/z 705.2 $^{-}$ is also shown in the figure. Number of glycan isomers is represented in parentheses ().

Serous cancers express a common subset of glycan structural features

The initial relative quantitative assessment of the overall expression of *N*- and *O*-glycans failed to reveal any significant changes between the populations of the three serous cancer types, thereby prompting an in-depth investigation of individual *N*- and *O*-glycan structures for possible more specific substructure differences. Many individual mass signals corresponded to a combination of structural and compositional isomers. For instance, some glycan compositions existed as several structural isomers with sialic acids located at various positions on the branched antennae of the *N*-glycan or with differences in sialic acid linkages (**Table 2A**: #32, #32a, #34, #34a and #34b; **Figure 2**). These positional isomers typically do not affect their categorisation into the five *N*-glycan subtypes but they can be classified differently, taking into account different properties. For example, glycan masses with compositional isomers, such as bi-antennary *N*-glycan compositions with an additional HexNAc (GlcNAc or GalNAc) both have an additional residue mass of m/z 203 (**Table 2A**: #23 and #23a; **Figure 2**). This composition can correspond to either a tri-antennary (GlcNAc attached to α 1-3 or α 1-6 Man residue), bisecting-type (GlcNAc attached to branching core Man residue), or LacdiNAc-type antennae (GalNAc attached to GlcNAc). The determination of the detailed glycan structures was performed by the use of specific feature mass ions that are characteristic for negative ion fragmentation, and was used to classify the specific glycan epitopes expressed in each of the serous cancer groups as follows:

a) Sialylation

Sialylation appeared to be a major *N*-glycan feature of serous cancers of the ovary (n=14), peritoneum (n=14) and tube (n=4). In all three serous cancer groups, the total relative ion intensities of sialylated structures ranged between 65.6 to 68.5 % of all the *N*-glycan structures across all samples investigated, and therefore comprise the most abundant membrane glycans. Sialylated *N*-glycans were further classified based on the number of sialic acid residues, in which mono-, di- and tri-sialylated *N*-glycans were all observed to be present. Of the three types, the total ion intensities for mono- and di-sialylated *N*-glycans were similar, with few tri-sialylated *N*-glycans identified ($p < 0.0001$) (**Figure 5A**). Specifically, the four most abundant glycan masses were comprised of mono-sialylated *N*-glycans with m/z 965.9²⁻ and m/z 1038.9²⁻ (**Table 2A**: #32, #32a, #33 and #33a) and di-sialylated *N*-glycans, m/z 1111.4²⁻ and m/z 1184.5²⁻ (**Table 2A**: #34, #34a, #34b, #35, #35a and #35b) which represented approximately 49.83 % \pm 10.84 % and 48.90 % \pm 7.80 % of total ion intensities for the serous ovarian and tubal cancers and 53.89 % \pm 12.0 % for serous peritoneal cancers.

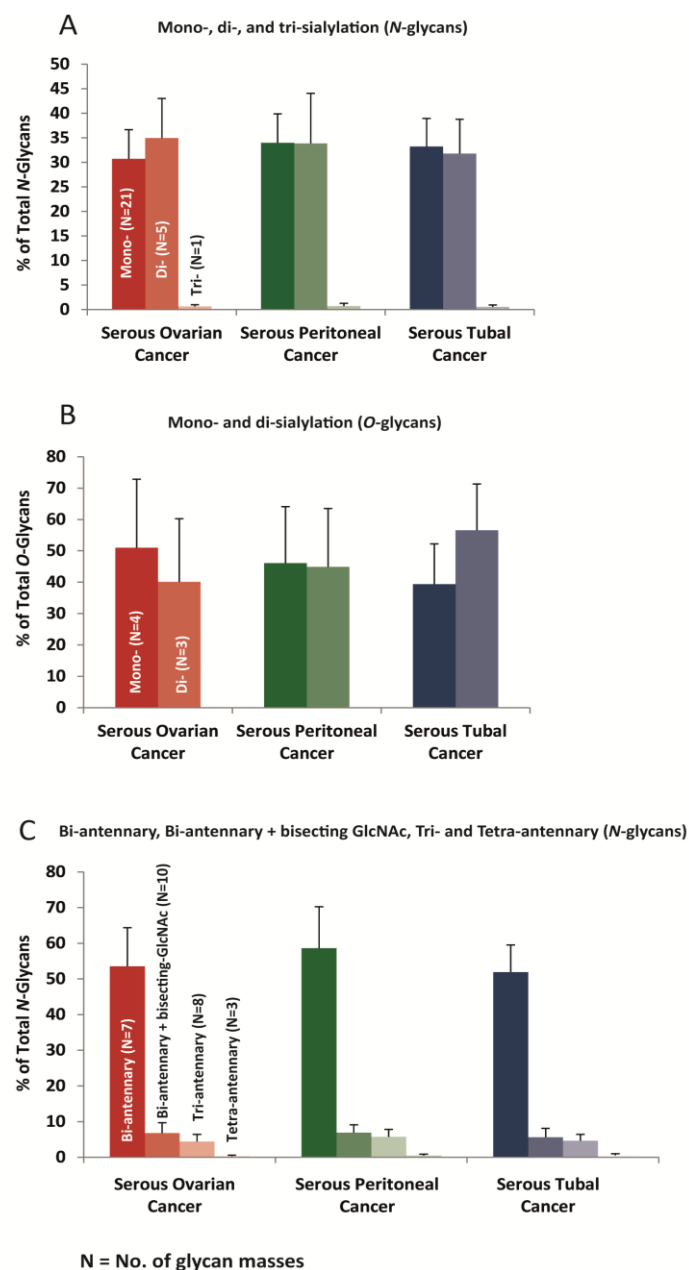


Figure 5. Relative quantitation of abundances of sialylation levels (mono-, di- and tri-) and branching patterns of *N*- and *O*-glycans. Sialylation of *N*- and *O*-glycans can be classified based on the number of sialic acid residues attached to the terminal non-reducing end of the glycan. The relative ion intensities for glycans bearing varying levels of sialylation are illustrated in (A) mono-, di- and tri-sialylated epitopes of *N*-glycans and (B) mono- and di-sialylated epitopes of *O*-glycans for each serous cancer group. Branching patterns of *N*-glycans consisting of bi-antennary, bisecting-biantennary, tri- and tetra-antennary are illustrated in (C). Bar graphs represent total ion intensities for N number of glycan masses in each category for each serous cancer group. Error bars represent SD of biological replicates [serous ovarian (n=14), serous peritoneal (n=14), serous tubal (n=4)].

Likewise, for the *O*-glycans, sialylation was also a prominent feature, in which the two most abundant structures identified in all three serous cancer types were the mono- and di-

sialylated *O*-glycans (**Table 2B**: #1 and #2; **Figure 5B**). Specifically, Core 1 *O*-glycan structures with m/z 675.3¹⁻ [(Neu5Ac)₁(Gal)₁(GalNAc)₁] and m/z 966.3¹⁻ [(Neu5Ac)₂(Gal)₁(GalNAc)₁] comprised 77.60 % ± 22.78 %, 75.69 % ± 23.58 % and 71.61 % ± 20.0 % of the total ion intensities of all the *O*-glycans in serous ovarian, serous peritoneal and serous tubal cancer tissues, respectively.

Several glycans with structural isomers corresponding to differences in sialic acid linkage were also observed for some of the *N*-glycan masses. For example, mono-sialylated hybrid and complex-type *N*-glycans with m/z 945.3²⁻ [(Neu5Ac)₁(Gal)₁(GlcNAc)₁(Man)₂+(Man)₃(GlcNAc)₂] and m/z 965.9²⁻ [(Neu5Ac)₁(Gal)₂(GlcNAc)₂+(Man)₃(GlcNAc)₂], respectively were found to contain isomers with terminal α2-3 or α2-6-linked sialic acids which were able to be differentiated based on their chromatographic retention times as shown in **Figure 6A (i)** and **(ii)**. For both these *N*-glycans, the sialylated α2,6-linked glycan was shown to elute from the porous graphitised carbon column approximately 8 minutes earlier than the sialylated α2,3-linked glycan isomer. The chromatographic behaviour and retention times of these sialylated isomeric structures have been previously identified (Townsend, Hardy *et. al.*, 1989; Nakano, Saldanha *et. al.*, 2011) and were confirmed by exoglycosidase (sialidase) treatments in our recently published cell line study which is also part of this thesis (**Chapter 2** and published as Anugraham *et. al.*) (Anugraham, Jacob *et. al.*, 2014). Similarly, the most abundant di-sialylated *N*-glycan of m/z 1111.4²⁻ [(Neu5Ac)₂(Gal)₂(GlcNAc)₂+(Man)₃(GlcNAc)₂] was also found to comprise of structural isomers bearing α2-3 or/and α2-6 sialic acid linkages. For this *N*-glycan, the most abundant bi-antennary di-sialylated α2,6-linked glycan (α2,6/α2,6-) isomeric structure eluted from the column earlier than the remaining two structural isomers containing α2,6/α2,3- and α2,3/α2,3- linked sialic acids, respectively [**Figure 6A(iii)**]. In total, 10 sialylated *N*-glycan masses (**Table 2A**: #7, #10, #11, #13, #14, #31, #32, #33, #34 and #35) were found to contain these isomeric structures which were distinguished by distinct extracted ion chromatograms. Specifically, 5 of these *N*-glycans were mono-sialylated hybrid structures (**Table 2A**: m/z 783.3²⁻, m/z 856.3²⁻, m/z 864.3²⁻, m/z 937.3²⁻, m/z 945.3²⁻), of which the α2-6 mono-sialylated isomer accounted for 58.4 -66.6 % of the total hybrid-type isomeric structures for all three serous cancers [**Figure 6B(i)**]. Likewise, the remaining 5 isomeric *N*-glycans were mono- (m/z 957.8²⁻, m/z 965.9²⁻ and m/z 1038.9²⁻) and di-sialylated (m/z 1111.4²⁻ and m/z 1184.5²⁻) complex-type glycans, which displayed α2-6 sialylation for approximately 62 % [**Figure 6B(ii)**] and 62-70.0 % of the total complex-type isomeric structures [**Figure 6B(iii)**], respectively for all three serous cancer groups.

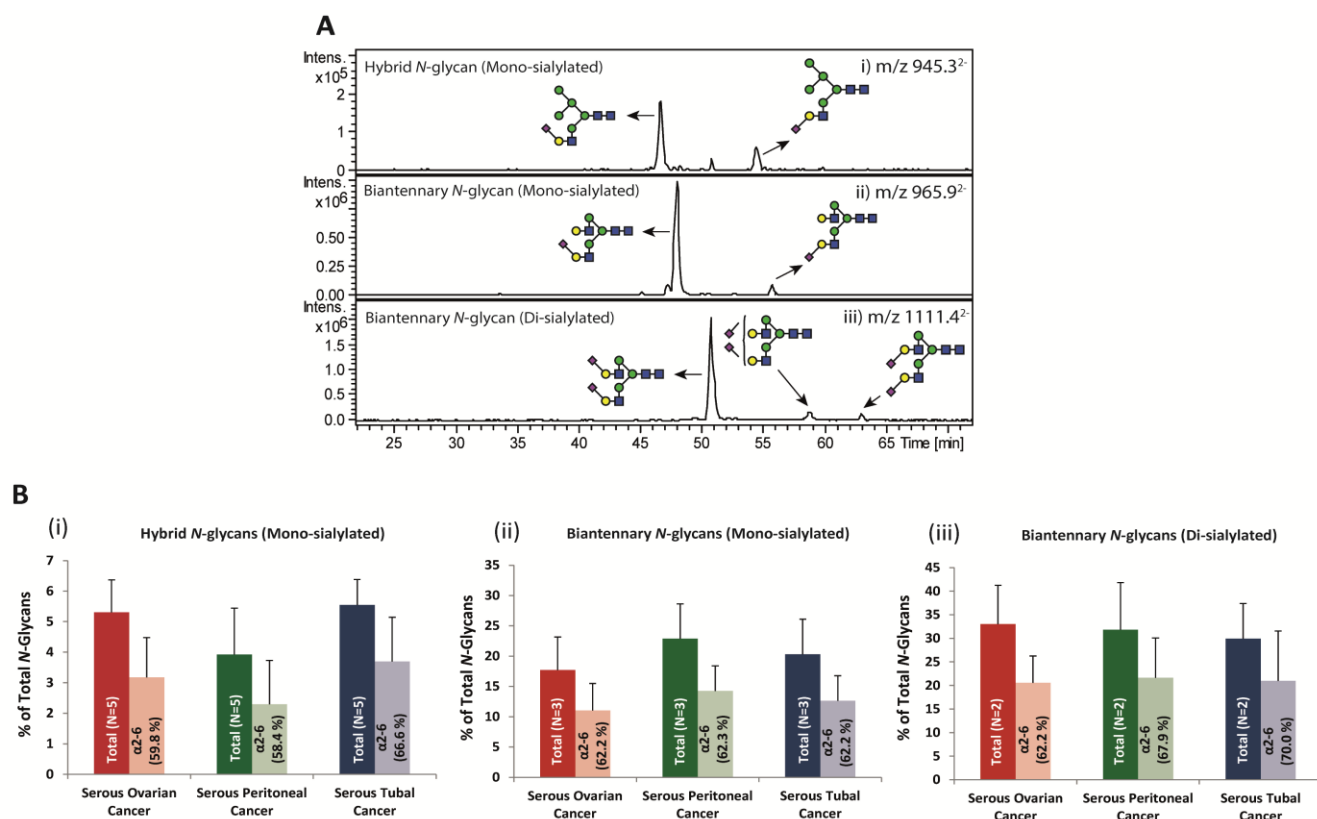


Figure 6. Representative extracted ion chromatograms (EIC) of mono- and di-sialylated *N*-glycans and the corresponding relative abundances for total and α 2-6 sialylation. (A) PGC- LC allows for the separation of α 2-6 and α 2-3 sialylated *N*-glycans based on retention time. The representative EICs depicting the separate retention times for isomers with α 2-6-linked and α 2-3-linked sialic acids are represented for mono-sialylated *N*-glycans, $m/\approx 945.3^{2-}$ [(Neu5Ac)₁(Gal)₁(GlcNAc)₁(Man)₂+(Man)₃(GlcNAc)₂](i) and $m/\approx 965.9^{2-}$ [(Neu5Ac)₁(Gal)₂(GlcNAc)₂+(Man)₃(GlcNAc)₂](ii) and di-sialylated *N*-glycan, $m/\approx 1111.4^{2-}$ [(Neu5Ac)₂(Gal)₂(GlcNAc)₂+(Man)₃(GlcNAc)₂](iii). (B) Relative abundances for N number of *N*-glycans bearing sialylated isomeric structures and the percentage of α 2-6 sialylation of these isomers is displayed for hybrid mono-sialylated [Table 2: 5 *N*-glycans; $m/\approx 783.3^{2-}$, $m/\approx 864.3^{2-}$, $m/\approx 856.3^{2-}$, $m/\approx 937.3^{2-}$ and $m/\approx 945.3^{2-}$] (i), complex mono-sialylated [3 *N*-glycans; $m/\approx 957.8^{2-}$, $m/\approx 965.9^{2-}$ and $m/\approx 1038.9^{2-}$] (ii) and complex di-sialylated [2 *N*-glycans; $m/\approx 1111.4^{2-}$ and $m/\approx 1184.5^{2-}$] (iii) for each serous cancer group. Error bars represent SD of biological replicates [serous ovarian (n=14), serous peritoneal (n=14), serous tubal (n=4)].

b) Bi-antennary N-glycans

Branching patterns in a typical N-glycan structure, formed by the action of specific N-acetylglucosaminyltransferases, can vary in size and are reflective of the number of antennae (Stanley, Schachter *et. al.*, 2009). Bi-antennary N-glycans, for instance, are formed initially through the addition of β 1-2-linked GlcNAc (N-acetylglucosamine) residues by the enzyme GlcNAcT-II on both the α 1-3 and α 1-6-linked Man residues of the N-glycan core [(Man)₃(GlcNAc)₂] which are typically elongated with a Gal residue to form an antenna on each arm. The definitive assignment of an antenna in this study was performed based on the presence of a complete LacNAc (Gal-GlcNAc) antenna, regardless of the presence of other modifications such as sialylation or sulphation. In total, seven N-glycan compositions (including isomers) corresponding to neutral (m/z 820.3²⁻ and m/z 893.3²⁻) (Table 2A: #17 and #15) and sialylated (m/z 965.9²⁻, m/z 1038.9²⁻, m/z 1078.9²⁻, m/z 1111.4²⁻ and m/z 1184.5²⁻) (Table 2A: #32, #33, #39, #34 and #35) bi-antennary N-glycans were observed in serous cancer tissues, accounting for 53.51 % \pm 10.86 %, 58.52 % \pm 11.64 % and 51.89 % \pm 7.62 %, of the total glycans on membrane proteins of serous ovarian, peritoneal and tubal cancers, respectively (Figure 5C). In regards to the more highly branched N-glycan structures which are synthesised by the enzyme, GlcNAcT-IV and GlcNAcT-V to form β 1-4- and β 1-6-linked GlcNAc, respectively, 11 N-glycans comprising of tri- and tetra-antennary structures were identified, despite having very significantly lower relative ion intensities in all three serous cancer groups as compared to the bi-antennary N-glycans ($p < 0.0001$). Specifically, eight tri-antennary N-glycans (m/z 1002.9²⁻, m/z 1075.9²⁻, m/z 1221.5²⁻, m/z 1367.0²⁻, m/z 1148.5²⁻, m/z 1512.5²⁻, m/z 1294.0²⁻, m/z 1440.0²⁻) (Table 2A: #19, #21, #46, #49, #37, #48, #47, and #51), ranged between 4.4 % and 5.7 % while three tetra-antennary N-glycans (m/z 1258.5²⁻, m/z 1404.1²⁻ and m/z 1550.1²⁻) (Table 2A: #22, #50, and #52) accounted for less than 1 %, of the total membrane N-glycans in the serous ovarian, peritoneal and tubal cancers (Figure 5C).

c) Bisecting GlcNAc N-glycans

Interestingly, we also observed the presence of bisecting-type N-glycans which accounted for approximately 6.78 % \pm 2.89 %, 6.89 % \pm 2.22 % and 5.63 % \pm 2.48 % of the total ion intensities of N-glycans in serous ovarian, peritoneal and tubal cancer respectively (Figure 5C). A bisecting-type N-glycan is formed when a GlcNAc residue is attached to the innermost mannose of the N-glycan core by the action of a specific enzyme, β 1-4-N-acetylglucosaminyltransferase III (GlcNAcT-III), encoded by the *MGAT3* gene. In total, there were 10 structures which corresponded to bisecting N-glycan structures, of which several

forms were observed such as the agalactosylated bisecting (m/z 759.9²⁻, m/z 840.8²⁻ and m/z 913.9²⁻) (**Table 2A**: #24, #27, and #23a), bi-antennary bisecting (m/z 921.9²⁻ and m/z 994.9²⁻) (**Table 2A**: #28 and #25), mono-sialylated bi-antennary bisecting (m/z 986.5²⁻, m/z 1059.4²⁻, m/z 1067.5²⁻ and m/z 1140.4²⁻) (**Table 2A**: #43, #42a, #30 and #36) and disialylated bi-antennary bisecting (m/z 1286.0²⁻) (**Table 2A**: #44) *N*-glycans. The presence of the 'bisecting' GlcNAc group is characterised by a diagnostic D-221⁻ [203⁻ (mass of bisecting GlcNAc) + 18⁻(H₂O)] cleavage ion which occurs specifically in the negative ion mode. This ion can be visualized in the MS/MS fragmentation spectra of bi-antennary *N*-glycans as m/z 670.1¹⁻ which corresponds to the loss of the GlcNAc residue from the D ion (mass of 6-arm antennae composition and two remaining branching core Man residues), accompanied by the loss of a water molecule (**Figure 7**). As observed in **Figure 7A-C**, when the parent ion masses were fragmented, the D-221 fragment ion mass at m/z 670.1¹⁻ which corresponds to the composition, Gal-GlcNAc-Man-Man-18⁻ (H₂O) was observed in the MS/MS spectra. In **Figure 7D**, the D-221⁻ ion was observed as m/z 508.1¹⁻, for the agalactosylated *N*-glycan with m/z 759.9²⁻, thereby corresponding to the mass of GlcNAc-Man-Man-18⁻ (H₂O).

d) Terminal fucosylation

Terminal fucosylation of *N*- and *O*-glycans typically gives rise to the presence of Lewis and sialylated Lewis antigens (e.g. Le^x and sLe^x) as well as blood group antigens (e.g. H antigen). The expression of these structures, despite their low intensities and poor MS/MS fragmentation patterns, was observed on some of the proteins of the serous cancer tissues. Specifically, one *N*-glycan composition corresponding to a core fucosylated tri-antennary (m/z 1440.1²⁻) (**Table 2A**: #51) *N*-glycan was found to contain one fucose residue at the terminal end while another tetra-antennary *N*-glycan structure (m/z 1550.1²⁻) (**Table 2A**: #52) contained two fucose residues. These structures only accounted for 0.91 % ± 0.42 %, 1.08 % ± 0.75 %, and 0.92 % ± 0.72 % of the total relative ion intensities in serous ovarian, peritoneal and tubal cancers, respectively. Terminal fucosylation on *O*-glycans was observed in only one of the serous ovarian cancer tissues and identified as Core 1 *O*-glycan m/z 530.2¹⁻ (**Table 2B**: #4), in which the MS/MS fragment spectrum tentatively identified this structure to contain the fucose α1-2-linked to the Gal residue as evidenced by the B and C fragment ions at m/z 307.1¹⁻ and m/z 325.1¹⁻ respectively (**Figure 8A**).

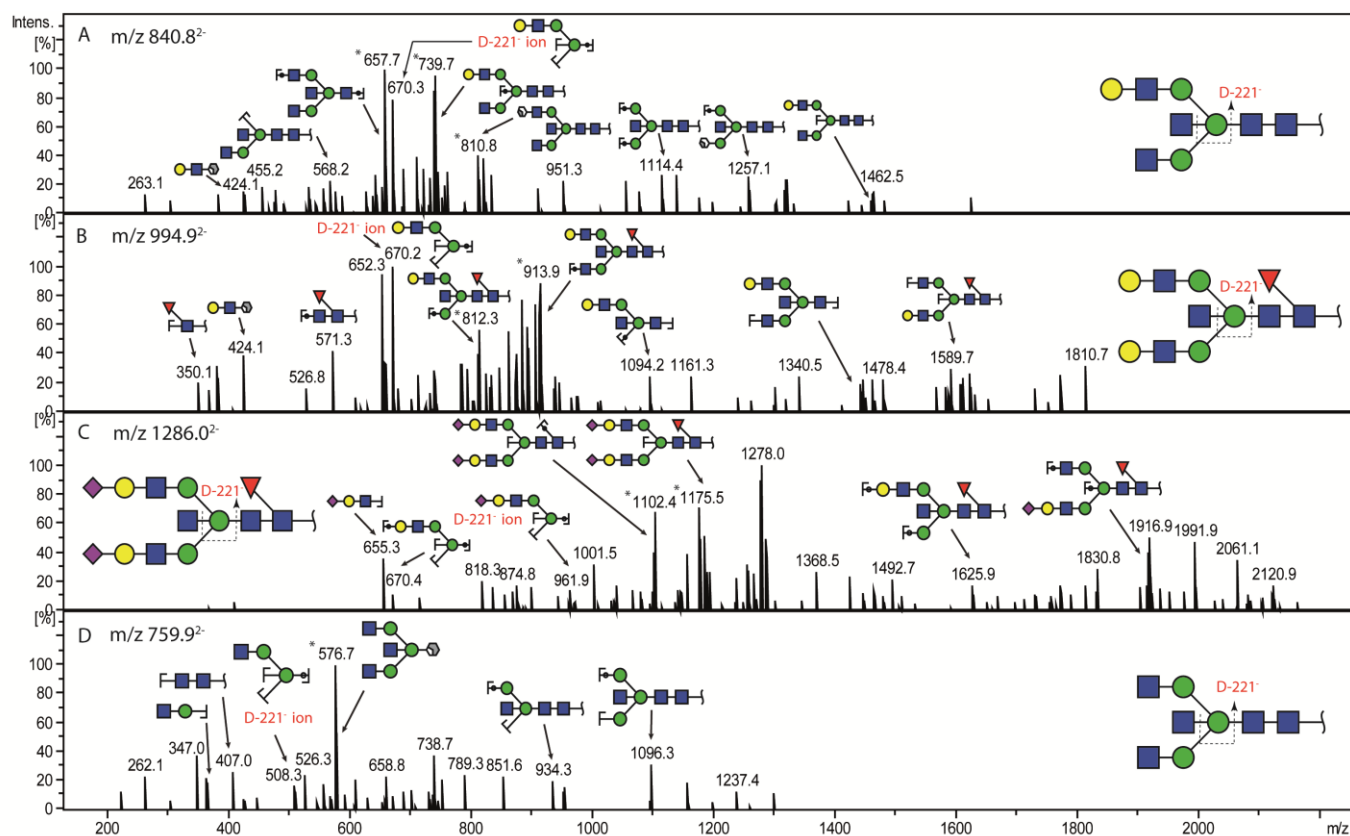


Figure 7. Representative MS² fragment ion spectra depicting the diagnostic ions of bisecting GlcNAc type *N*-glycans in serous cancers. A bisecting-type *N*-glycan is formed when a GlcNAc residue is attached to the innermost mannose of the *N*-glycan core by the action of a specific enzyme, β 1-4-*N*-acetyl-glucosaminyltransferase III (GlcNAcT-III). In *N*-glycans, the diagnostic ion, D-221- ion, is formed through the cleavage of the bisecting GlcNAc attached to the innermost Man residue of the 6-antenna arm comprising of Gal-GlcNAc-bisecting GlcNAc-Man-Man. The fragment ion resulting from this specific cleavage is shown to appear at m/z 670.3¹⁻ in the representative *N*-glycan MS² spectra of m/z 840.8²⁻ (A), m/z 994.9²⁻ (B) and m/z 1286.0²⁻ (C). For the agalactosylated *N*-glycan with m/z 759.9²⁻, this diagnostic fragment ion is observed at m/z 508.3¹⁻.

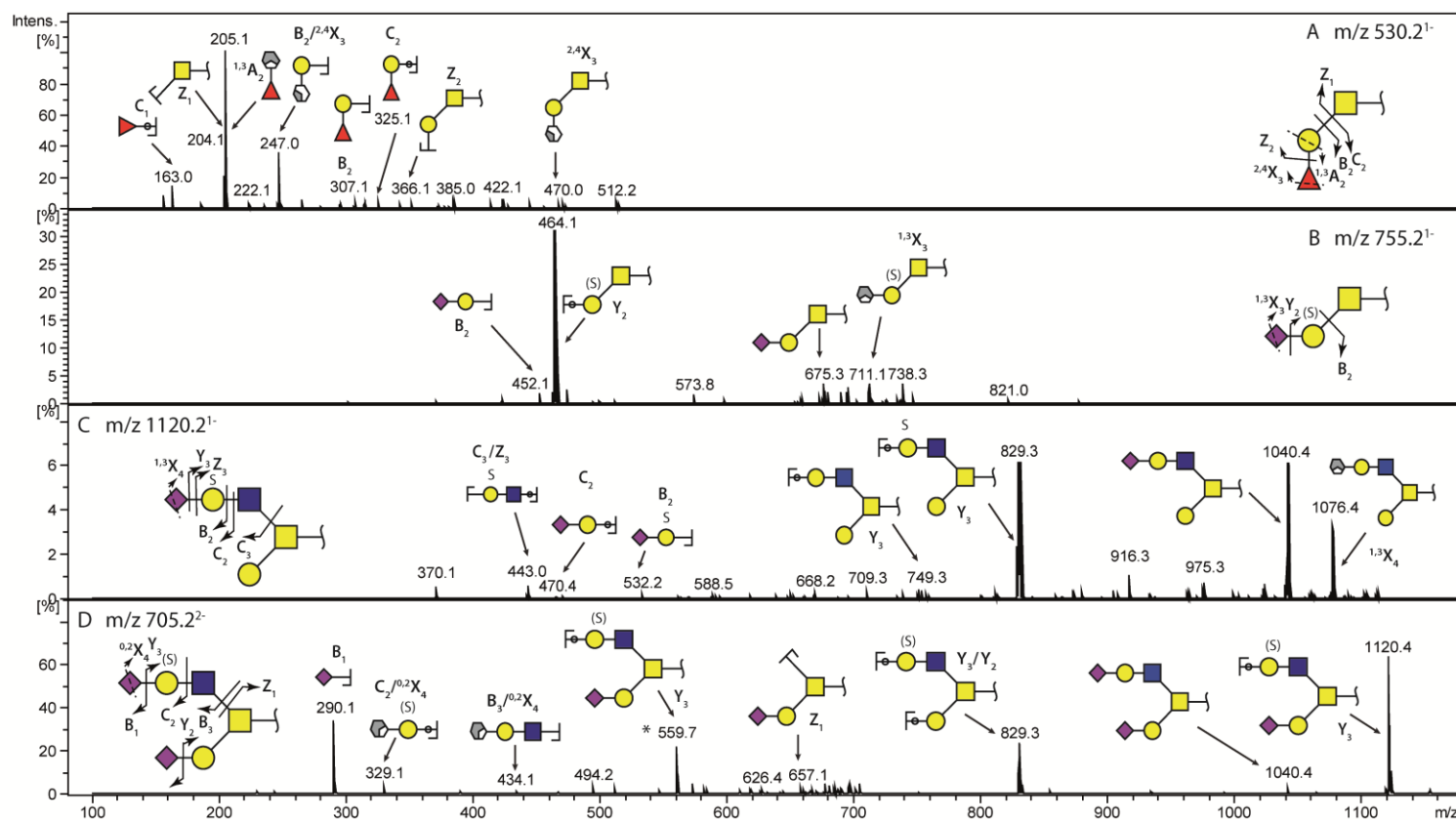


Figure 8. Representative MS² fragment ion spectra depicting terminal modifications of *O*-glycans with fucose, sulphate and sialic acid residues. Diagnostic fragment ions characteristic for the identification of terminal modifications in *O*-glycans are illustrated for fucosylated Core 1 *O*-glycan with m/z 530.2¹⁻(A), sulphated Core 1 *O*-glycan with m/z 755.2¹⁻(B), monosialylated and sulphated Core 2 *O*-glycan with m/z 1120.2¹⁻(C) and di-sialylated and sulphated Core 2 *O*-glycan with m/z 705.2²⁻(D). Position of sulphate is not determined and represented by parentheses ().

e) Terminal sulphation

Apart from sialic acid modifications to the non-reducing end of the *N*-glycan, acidic *N*-glycans in the form of sulphated *O*-glycans have been previously observed in ovarian cancer ascites fluid (Karlsson and McGuckin, 2012). Sulphated structures were also observed in the serous cancer tissues analysed in this study, in which one *N*-glycan with m/z 1078.9²⁻ (**Table 2A**: #39) was found to be present in eight serous ovarian cancer tissues (0.18 % \pm 0.19 %), five serous peritoneal cancer tissues (0.48 % \pm 1.42 %) and one serous tubal tissue (0.19 % \pm 0.00 %). Similarly, terminal sulphation was also observed at varying intensities on a few Core 1 and Core 2 *O*-glycans. The characterisation of these low abundance sulphated *O*-glycans is shown in their MS/MS fragment spectra in **Figure 8B-D**. Core 1 sulphated and mono-sialylated *O*-glycan with m/z 755.3¹⁻ [(Sulph)₁(Neu5Ac)₁(Gal)₁(GalNAc)₁] (**Table 2B**: #3) was observed in three serous ovarian (2.06 % \pm 1.03 %), two serous peritoneal (2.30 % \pm 0.90 %) and one tubal cancer tissue (0.27 % \pm 0.00 %). The position of the sulphate residue on either the Gal or the GalNAc residue for *O*-glycan with m/z 755.2¹⁻ however was not able to be precisely determined due to insufficient fragmentation ions (**Figure 8B**).

For Core 2 *O*-glycans, sulphated mono-sialylated *O*-glycans with m/z 1120.3¹⁻ [(Sulph)₁(Neu5Ac)₁(Gal)₂(GlcNAc)₁(GalNAc)₁] (**Table 2B**: #8) were identified in seven serous ovarian (2.32 % \pm 4.00 %), five serous peritoneal (1.48 % \pm 0.92 %) and two tubal cancer tissues (1.62 % \pm 1.87 %). Based on the MS/MS fragment spectra, the identification of the B₂ glycosidic cleavage ion at m/z 532.2¹⁻ clearly determined the position of the sulphate residue on the Gal residue (**Figure 8C**). In addition, a sulphated di-sialylated *O*-glycan with m/z 705.2¹⁻ [(Sulph)₁(Neu5Ac)₂(Gal)₂(GlcNAc)₁(GalNAc)₁] (**Table 2B**: #9) was also observed in one serous ovarian cancer (1.41 \pm 0.00 %) and two serous tubal cancer tissues (2.83 % \pm 3.82 %) (**Figure 8D**). Once again, the location of the sulphate residue was found to be linked to the Gal, although the precise identification of the Gal residue linked to either the GlcNAc or Core GalNAc was not determined (**Figure 8D**). The linkage of the sulphate residue, however, either as 4- or 6-linked *O*-sulphate, was not determined and beyond the scope of this study.

***N,N'*-diacetyl-lactosamine-type (LacdiNAc) *N*-glycans are present in serous ovarian and tubal cancer tissues**

While the separation of sialylated isomers has been clearly demonstrated in this study, the isomer-resolving capabilities of the porous graphitised carbon were once again utilised for the identification of other compositional isomers which were differentiated based on their separate retention times and MS/MS fragmentation. For instance, the neutral *N*-glycan m/z 913.9²⁻ with a composition of (Hex)₁(HexNAc)₃(dHex)₁ + (Man)₃(GlcNAc)₂, consists of two compositional isomers with separate retention times [Figure 9A(i) -insert and A(ii) -insert]. The first isomer was shown to elute at 40 mins and the tandem MS spectra corresponded to a bisecting-GlcNAc-type core-fucosylated *N*-glycan with a monosaccharide composition of (Gal)₁(GlcNAc)₃(Fuc)₁ + (Man)₃(GlcNAc)₂. This was confirmed by the presence of the diagnostic D-221⁻ cleavage ion at m/z 508.1¹⁻ [Figure 9A(i)]. The second-eluting isomer at 48 mins consisted of a monosaccharide composition of (Gal)₁(GalNAc)₁(GlcNAc)₂(Fuc)₁ + (Man)₃(GlcNAc)₂ which corresponded to a 'LacdiNAc'-type *N*-glycan. The presence of the LacdiNAc antenna (GalNAc β 1-4GlcNAc) was indicated by the B ion at m/z 405.1¹⁻ and the ^{1,3}A cross-ring cleavage ion at m/z 465.1¹⁻. This ion is also termed as 'F ion' (Harvey, 2005) and has a composition of GalNAc-GlcNAc-O-CH=CH-O- (GalNAc + GlcNAc + 59¹⁻) which comprises the LacdiNAc disaccharide and two carbon atoms of the branching Man residue. The location of the LacdiNAc on either the 3-arm or 6-arm antenna of the *N*-glycan core was further distinguished by the D ion at m/z 729.8¹⁻ which corresponds to the mass of the 6-arm antenna, comprising of GalNAc-GlcNAc and two remaining branching core Man residues, thereby confirming the presence of the LacdiNAc on the 6-arm antenna [Figure 9A(ii)].

In total, five *N*-glycan compositions that corresponded to neutral (m/z 913.9²⁻ and m/z 934.4²⁻) (Table 2A: #23 and #29), and sialylated LacdiNAc (m/z 1059.4²⁻, m/z 1079.9²⁻ and m/z 1205.0²⁻) (Table 2A: #42, #40 and #45) motifs were identified, accounting for approximately 2.77 % \pm 2.00 %, and 2.09 % \pm 2.30 %, of the total *N*-glycans in serous ovarian and tubal cancers respectively, while only 0.62 % \pm 1.31 %, was found in the serous peritoneal cancer group (Figure 9B). MS/MS spectra of *N*-glycans bearing neutral (m/z 934.4²⁻) and sialylated LacdiNAc antennae (m/z 1079.9²⁻ and m/z 1205.0²⁻) are represented in Figure 9A (iii-v). The *N*-glycan with m/z 1205.0²⁻ [(Neu5Ac)₁(Gal)₁(GlcNAc)₂(GalNAc)₁(dHex)₁ + (Man)₃(GlcNAc)₂] was found to display antenna containing both the sialylated form of the LacdiNAc (Neu5Ac-GalNAc-GlcNAc) and the sialylated LacNAc (Neu5Ac-Gal-GlcNAc), observed as mass fragments of m/z

696.2¹⁻ and m/z 655.2¹⁻, respectively [Figure 9A (iv)] and was present in thirteen of the fourteen serous ovarian cancer tissues analysed in this study. Likewise, in serous tubal cancers, this structure was detected in three of the four serous tubal cancers analysed. However, in the peritoneal serous cancer tissues, it was only found two of the fourteen serous cancer tissues analysed. A proposed pathway of the synthesis of these unique *N*-glycan structures by the action of specific glycosyltransferases is shown in Figure 10.

Figure 9. Representative MS² fragment ion spectra depicting the differentiation of bisecting-biantennary and LacdiNAc-type *N*-glycans and quantitation of relative abundances of LacdiNAc-type structures in serous cancers. (A) The neutral *N*-glycan m/z 913.9²⁻ with a composition of (Hex)₁(HexNAc)₃(dHex)₁ + (Man)₃(GlcNAc)₂ consists of two compositional isomers with separate retention times [i-(insert)]. The first isomer was shown to elute at 40 mins and the tandem MS spectra corresponded to a bisecting-GlcNAc-type core-fucosylated *N*-glycan with a monosaccharide composition of (Gal)₁(GlcNAc)₃(Fuc)₁ + (Man)₃(GlcNAc)₂. This was confirmed by the presence of the diagnostic D-221⁻ cleavage ion at m/z 508.1¹⁻. The second-eluting isomer at 48 mins consisted of a monosaccharide composition of (Gal)₁(GalNAc)₁(GlcNAc)₂(Fuc)₁ + (Man)₃(GlcNAc)₂ which corresponded to a ‘LacdiNAc’-type *N*-glycan [ii-(insert)]. The presence of the LacdiNAc antenna (GalNAcβ1-4GlcNAc) was indicated by the B ion at m/z 405.1¹⁻ and the ^{1,3}A cross-ring cleavage ion at m/z 465.1¹⁻. This ion is also termed as ‘F ion’ and has a composition of GalNAc-GlcNAc-O-CH=CH-O- (GalNAc + GlcNAc + 59¹⁻) which comprises the LacdiNAc disaccharide and two carbon atoms of the branching Man residue. Several forms of LacdiNAc-type *N*-glycans identified in serous ovarian cancer are illustrated for neutral LacdiNAc *N*-glycan with m/z 934.4²⁻ (iii), sialylated LacdiNAc *N*-glycan with m/z 1079.9²⁻ (iv) and sialylated LacdiNAc/LacNAc *N*-glycan with m/z 1205.0²⁻ (v). (B) Box plot representing relative abundances of LacdiNAc-type *N*-glycans in serous cancers. Data points for each serous cancer group [serous ovarian (n=14), serous peritoneal (n=14), serous tubal (n=4)] represent total ion intensities of glycans in each category. Level of significance is indicated by *p* value.

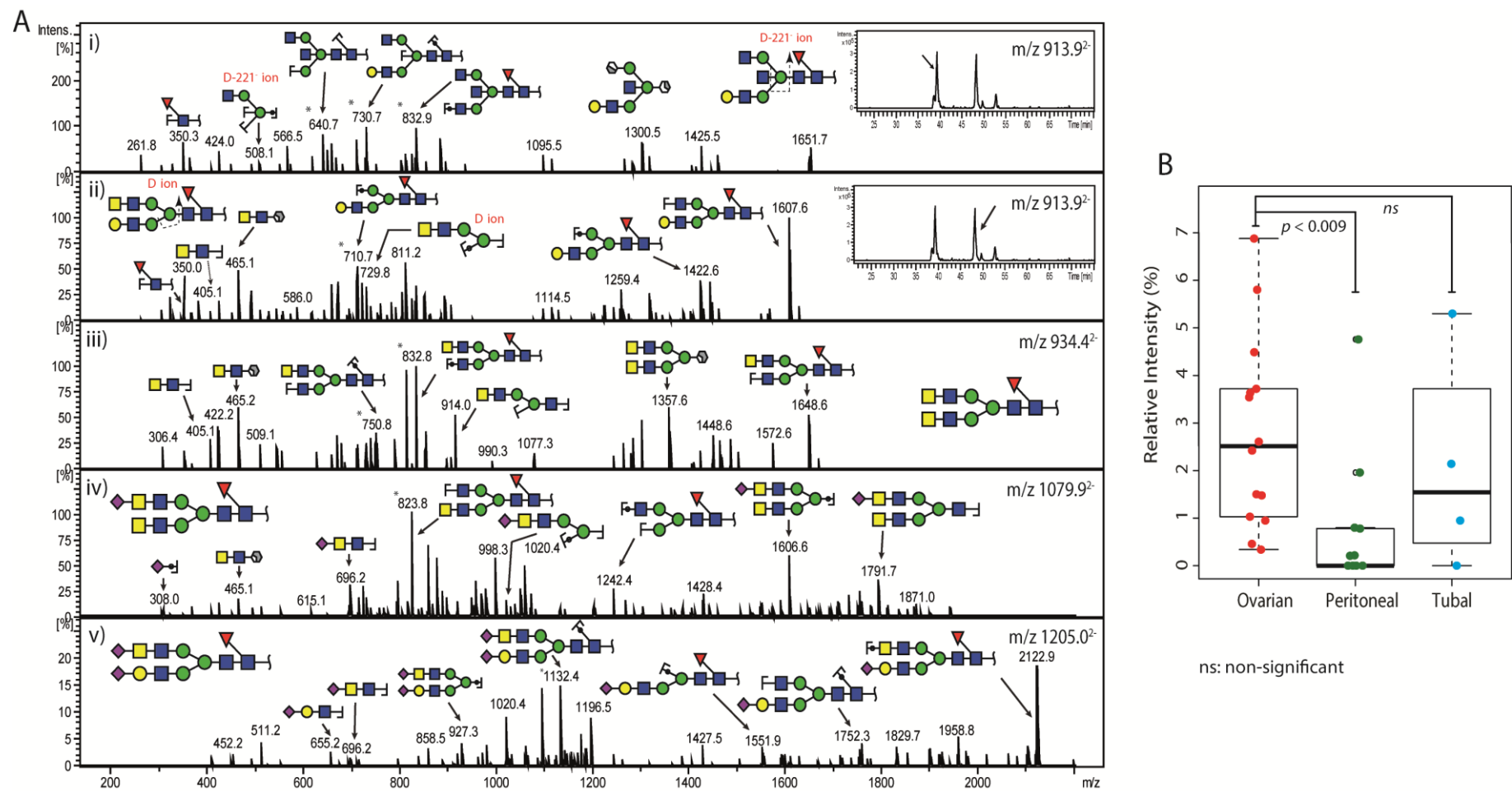


Figure 9

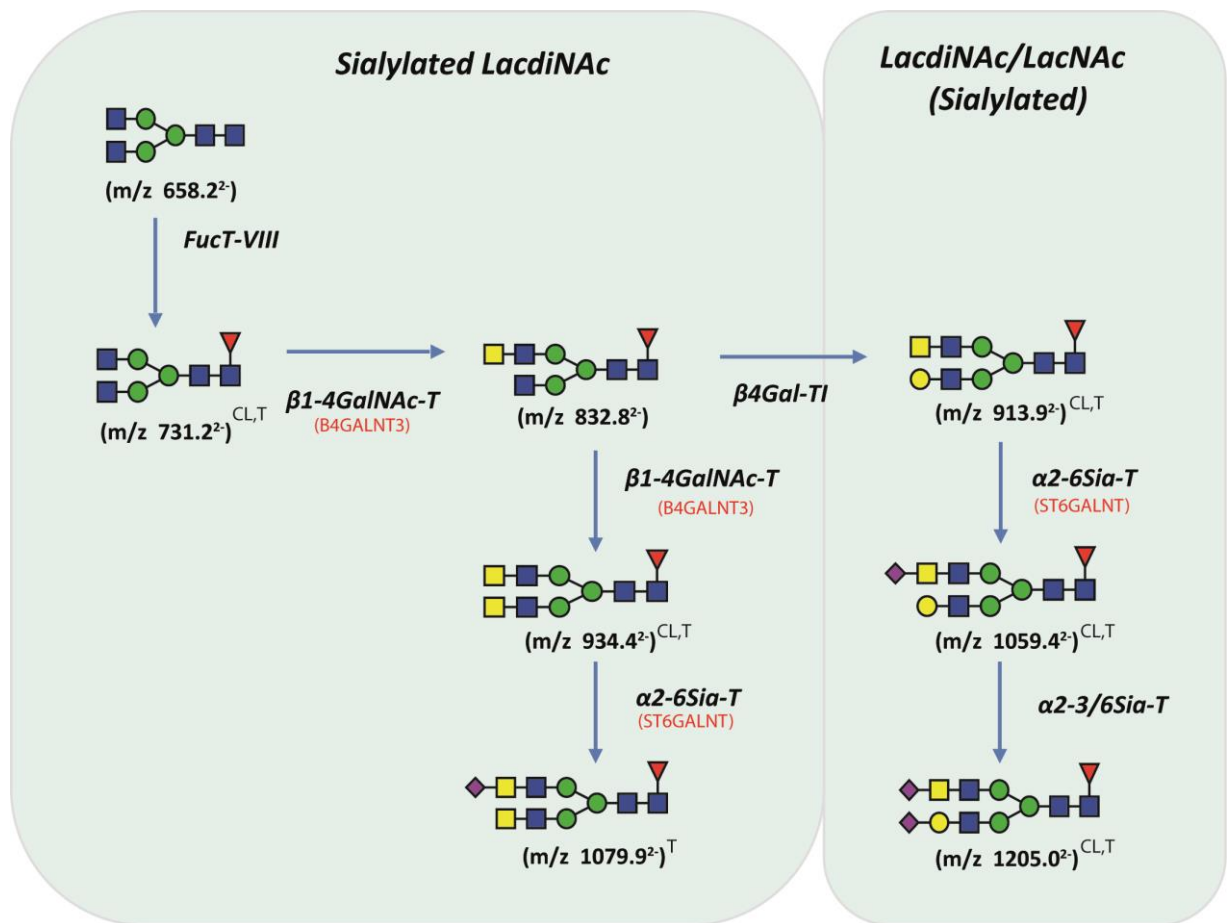


Figure 10. Proposed biosynthetic pathway for synthesis of LacdiNAc-type *N*-glycans. LacdiNAc-type *N*-glycans that were identified in this study and found to be up-regulated in serous ovarian cancer tissues (T) and in previously analysed ovarian cancer cell lines, SKOV3 and IGROV1 (CL) (**Chapter 2**). Glycosyltransferase genes involved in the transfer of β 1-4GalNAc and α 2-6Neu5Ac are represented in parentheses ().

Statistical analysis for potential glycan biomarker discovery and diagnosis of pelvic serous cancers

Several statistical analyses were employed to evaluate the discriminatory potential of *N*- and *O*-glycans identified in this study. An important factor that was taken into consideration was the prior classification of these serous cancers based on their diagnosis at the time of collection. As noted previously, most of the tumours that were classified as serous ovarian, peritoneal or tubal were surgically removed from their respective location (ie. ovary, peritoneal/omentum or fallopian tube) at the time of diagnosis. However, in some cases, the diagnosis of the serous cancers did not correspond to the location from which it was derived. For instance, two of the four serous cancers diagnosed as ‘tubal’ cancers were surgically removed from the ovary and not from their corresponding tubal tissue. To overcome discrepancies which could potentially arise from the assignment of glycans that are specific to a particular serous cancer or tissue origin, the subsequent statistical analyses were carried out for two individual classifiers, namely the diagnosis of these serous cancers (**Discriminant 1**) and the tissue from which the tumour was surgically removed from (**Discriminant 2**) as listed in **Table 1**.

Specific *N*- and *O*-glycan structures are differentially expressed in serous cancers

As an initial statistical assessment, one-way analysis of variance (ANOVA) was performed to identify potential differences between the individual glycans. In this analysis, the mean relative ion intensities of individual *N*- and *O*-glycans were compared to provide an indicative evaluation of their differential expression. Statistical significance using *p* values to signify the confidence level of assigning their differences were obtained for **Discriminant 1** and **2**. Several *N*- and *O*-glycans that were found to be statistically significantly different in terms of their expression in all three serous cancers are listed in **Table 3A** and **B**. For **Discriminant 1** (diagnosis) (**Table 3A**), the distinction between serous ovarian (SOC) and serous peritoneal (SPC) cancer revealed four statistically significantly ($0.001 < p < 0.025$) different *N*-glycans which were found to be up-regulated in serous ovarian cancer. Three of these *N*-glycans with m/z 1205.0²⁻, m/z 1059.4²⁻ and m/z 1079.9²⁻ and contained the LacdiNAc-type motif while the other *N*-glycan corresponded to a hybrid-type of m/z 937.3²⁻. Serous tubal cancers (STC) also appeared to be differentiated by the hybrid structure (m/z 937.3²⁻) from SPC, and from both SOC and SPC based on the significant increase in abundance observed for the sulphated di-sialylated *O*-glycan (m/z 705.2²⁻).

For **Discriminant 2** (tissue origin), serous cancers were re-analysed as majority of the tumours were surgically derived from either the ovary or the peritoneum/omentum (**Table 1**). The single surgically-derived tubal specimen was thus excluded from this analysis due to insufficient number of biological replicates. In total, 10 *N*-glycans and 2 *O*-glycans were identified to be significantly altered ($0.0001 < p < 0.028$) between the serous ovarian and serous peritoneal/omentum tissues in their relative intensities (**Table 3B**). As well as the specific LacdiNAc-type *N*-glycans previously identified in **Discriminant 1** (m/z 1205.0²⁻, m/z 1059.4²⁻ and m/z 1079.9²⁻), we identified four other *N*-glycan structures which comprised of a LacdiNAc-type (m/z 913.9²⁻) and three mono-sialylated hybrid glycans (m/z 856.4²⁻, m/z 937.3²⁻ and m/z 945.3²⁻) which were elevated in ovarian-derived tissues, relative to peritoneum/omentum-derived serous tissues. On the other hand, the latter expressed statistically elevated glycan structures comprising of complex bisecting-type (m/z 994.9²⁻), mono-sialylated (m/z 1038.9²⁻, and m/z 1221.5²⁻) and Core 2 sialylated *O*-glycans (m/z 1040.5¹⁻, and m/z 1331.5²⁻) compared to ovarian-derived tissues (**Table 3B**).

Table 3. Statistical evaluation of *N*- and *O*-glycan structures involved in the distinction of serous cancers of the ovary, peritoneum and tube. The statistically performance of individual *N*- and *O*-glycans implicated in the distinction of serous cancers based on their diagnosis (**Discriminant 1-Table 3A**) and tissue source (**Discriminant 2-Table 3B**) were evaluated using one-way ANOVA analysis ($p < 0.05$) and represented by area-under-the curve (AUC) values obtained through ROC analyses. Average relative intensities for *N*- and *O*-glycan structures are displayed according to respective classifiers (**Discriminant 1 and 2**).



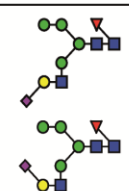



Glycan Mass [M-H] ⁻	[M-2H] ²⁻	Structure(s)	Cancer Discriminant 1 (Diagnosis)								
			% of Total Glycans			Serous Ovarian vs Serous Peritoneal		Serous Ovarian vs Serous Tubal		Serous Peritoneal vs Serous Tubal	
			Serous Ovarian (n=14)	Serous Peritoneal (n=14)	Serous Tubal (n=4)	<i>p value</i>	AUC	<i>p value</i>	AUC	<i>p value</i>	AUC
2411.0	1205.0		0.83	0.14	0.34	0.001	0.929				
2119.8	1059.4		0.93	0.19	0.85	0.009	0.825				
1875.6	937.3		0.75	0.29	1.05	0.003	0.890			0.001	1.0
2160.8	1079.9		0.21	0.01	0	0.006	0.805				
1770.8	884.9		0.65	0.7	1.32			0.014	0.932	0.025	0.818
1411.4	705.2		1.41	0	2.83			0.015	0.268	0.001	0.250

Table 3A




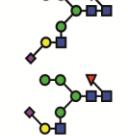



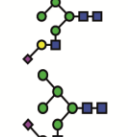
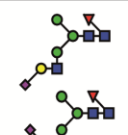
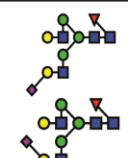

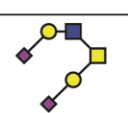
Glycan Mass [M-H]	[M-2H] ²⁻	Structure(s)	Cancer Discriminant 2 (Tissue Source)			
			% of Total Glycans		Serous Ovarian vs Serous Peritoneal	
			Ovarian-derived Cancer Tissues (n=16)	Peritoneum/Omentum- derived Cancer Tissues (n=15)	p value	AUC
2411.0	1205.0		0.79	0.09	0.0001	0.951
2119.8	1059.4		1.02	0.11	0.0001	0.902
1828.8	913.9		0.68	0.01	0.003	0.751
1875.6	937.3		0.74	0.38	0.007	0.835
2160.8	1079.9		0.19	0.01	0.006	0.751
1990.8	994.9		1.08	1.83	0.002	0.182
2444.0	1221.5		1.03	1.81	0.003	0.206
1891.6	945.3		1.34	1.01	0.028	0.737
1713.6	856.3		1.28	0.75	0.021	0.762
2078.8	1038.9		9.01	12.42	0.022	0.266
1040.5	—		6.72	9.50	0.014	0.242
1331.5	665.3		3.88	7.26	0.002	0.177

Table 3B

***N*-glycans derived from serous cancers of the ovary and peritoneum reveal distinct clustering patterns**

The one-way ANOVA analyses thus revealed some statistically significant differences in specific glycan structures which could potentially distinguish between serous cancers, particularly between the *N*-glycans of serous ovarian and serous peritoneal cancers. Therefore, it is important to note that the specific *N*- and *O*-glycan profiles generated for each serous cancer tissue in this study, although mostly similar for the major glycan structures, are nonetheless quite unique. These profiles are truly representative of individual biological differences and contain glycan features that pertain to the different serous tissue types. Hence, with this wealth of glycan expression data acquired using ESI-MS/MS, various clustering techniques, prediction and classification tools were selectively used to interpret the data for their potential utility in clinical application. Typically, relative quantitative glycan profiling experiments are characterised by many variables (different glycan structures) on only a few number of observations (experiments or samples). As demonstrated in our study, the number of samples for each serous cancer group was reasonably small (serous ovarian, $n=14$; serous peritoneal, $n=14$; serous tubal, $n=4$) and the total number of *N*-glycan compositions identified was 57. Hence, the number of variables, \mathbf{p} , easily exceeds the number of observations, \mathbf{N} . It is therefore important to note that while the number of glycans identified is comparatively large, there may be only a few underlying glycan combinations that account for most of the data variation. Dimension reduction methods can help to focus attention on a lower K -dimensional glycan component space. Here in this study, two dimensional reduction methods of PCA and PLS-DA have been employed to achieve this as described below:

a) Principal Component Analysis (PCA)

To visualize the representation of the various *N*- and *O*-glycan profiles of these cancers based on their similarities and differences, a statistical tool known as Principal Component Analysis (PCA), is utilized to help focus on the directions (glycan linear combinations) of highest variability in the data. The main objective of PCA is to find common factors, also known as ‘*principal components*’ which represent linear combinations of the variables under investigation. Briefly, a data set is represented in terms of an $m \times n$ matrix, X where the n columns are the samples (e.g. observations) and the m rows are the variables as shown in the formula below:

$$X = \begin{pmatrix} x_{1,1} & x_{1,2} & \cdots & x_{1,n} \\ x_{2,1} & x_{2,2} & \cdots & x_{2,n} \\ \vdots & \vdots & \ddots & \vdots \\ x_{m,1} & x_{m,2} & \cdots & x_{m,n} \end{pmatrix} = \begin{pmatrix} x_1 \\ x_2 \\ \vdots \\ x_m \end{pmatrix} \in \mathbb{R}^{m \times n}, \quad x_i^T \in \mathbb{R}^n$$

This matrix is represented in terms of m row vectors, each of length, n , and transformed to a covariance matrix which can be used to calculate eigenvectors and eigenvalues which subsequently form the ‘*principal components*’. The eigenvector with the largest eigenvalue has the direction of the largest variance and corresponds to the first principal component (PC1), while the second largest eigenvalue is the (orthogonal) direction with the next highest variation which forms the second principal component (PC2) and so on. The outcome of this analysis is achieved without prior knowledge of the specific diagnosis (unsupervised classification). The N - and O -glycan data set acquired for all the individual serous cancers were subjected to PCA analysis and the scores for each sample were represented in the plot based on **Discriminant 1** (diagnosis) [Figure 11(i) and 12(i)] and **Discriminant 2** (tissue source) [Figure 11(ii) and 12(ii)]. For N -glycan score plots, there appeared to be a reasonable clustering of data based on **Discriminant 1** [Figure 11(i)], in which serous peritoneal cancer could be differentiated from serous ovarian cancer to a certain extent based on Principal Component 2, although a varying degree of heterogeneity was observed for both groups. For the O -glycan score plots, although a majority of serous peritoneal cancers appeared to be reasonably separated from serous ovarian cancers based on the direction of Principal Component 3 for **Discriminant 1** [Figure 12(i)], there seemed to be a small proportion of serous peritoneal cancer samples that appear to be clustered near the serous ovarian cancer group.

Using the identical PCA score plots generated for individual serous cancers in **Discriminant 1** (diagnosis) [n=32; SOC=14; SPC=14; STC=4], we re-assigned each serous cancer sample with the respective tissue identifier based on **Discriminant 2** (tissue source) [n=32; ovarian=16; peritoneum/omentum=15; tube=1] to further investigate if their N - and O -glycomic profiles were reflective of the various tissues from which these samples were surgically derived from (ie. left and right ovary, peritoneum/omentum and tube) [Figure 11(ii) and 12(ii)]. A majority of serous cancer samples appeared to be clustered based on their specific tissue identifier, however, we noted a few ‘non-conformists’ that could pertain to discrepancies in diagnosing these serous cancers. For instance, based on the N - and O -glycan score plot, the serous tubal cancer sample (#TB.448) is clustered together with the

serous ovarian group [**Discriminant 1-Figure 11(i)** and **12(i)**] and was actually surgically-derived from the ovary [**Discriminant 2-Figure 11(ii)** and **12(ii)**]. Likewise, a discrepancy was observed for the diagnosed serous peritoneal cancer sample (#PT.418) which is seen to rather cluster within the serous ovarian group [**Discriminant 1-Figure 11(i)** and **12(i)**], and was surgically-derived from the ovary [**Discriminant 2-Figure 11(ii)** and **12(ii)**]. These discrepancies are interesting in that the glycan profiles may provide a more reliable diagnosis of cancer origin and facilitate the histo-pathological staging of tumours based on their respective tissues.

N-Glycans (Discriminant 1 and Discriminant 2)

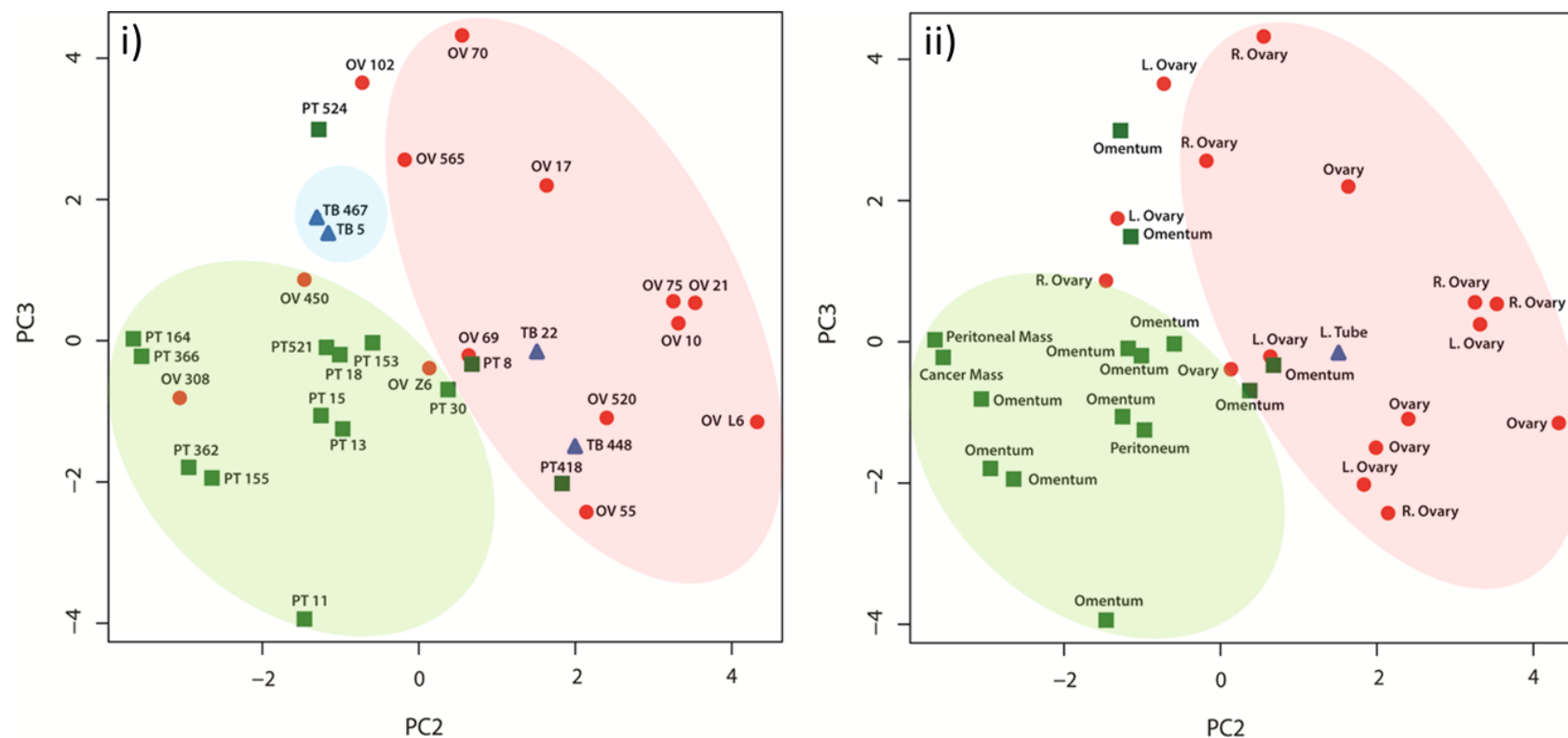


Figure 11. Two-dimensional PCA score plot depicting clustering of serous cancers according to their respective *N*-glycan profiles for **Discriminant 1** and **2**. The *N*-glycan data set ($n=57$ compositions) acquired for all the individual serous cancers were subjected to PCA analysis and the scores for each sample were represented in the plot for Component 2 and Component 3 based on **Discriminant 1** (cancer diagnosis) (ovarian: $n=14$; peritoneal: $n=14$; tubal: $n=4$) (i) and **Discriminant 2** (tissue source) (ovarian: $n=16$; peritoneum/omentum: $n=15$; fallopian tube: $n=1$) (ii). Red circles: OV-serous ovarian cancer; green squares: PT-serous peritoneal cancer; blue triangles: TB-serous tubal cancer.

O-Glycans (Discriminant 1 and Discriminant 2)

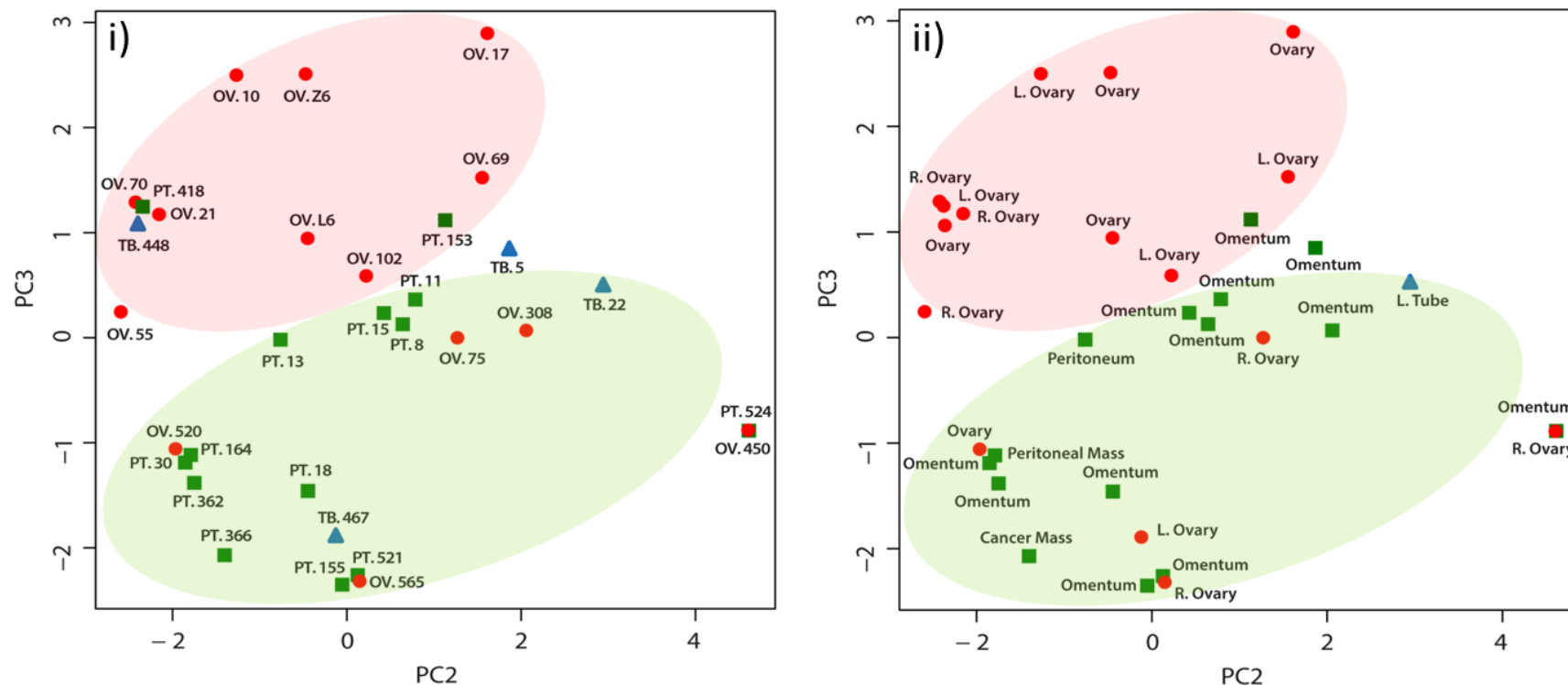


Figure 12. Two-dimensional PCA score plot depicting clustering of serous cancers according to their respective *O*-glycan profiles for **Discriminant 1** and **2**. The *O*-glycan data set ($n=9$ compositions) acquired for all the individual serous cancers were subjected to PCA analysis and the scores for each sample were represented in the plot for Component 2 and Component 3 based on **Discriminant 1** (cancer diagnosis) (ovarian: $n=14$; peritoneal: $n=14$; tubal: $n=4$) (i) and **Discriminant 2** (tissue source) (ovarian: $n=16$; peritoneum/omentum: $n=15$; fallopian tube: $n=1$) (ii). Red circles: OV-serous ovarian cancer; green squares: PT-serous peritoneal cancer; blue triangles: TB-serous tubal cancer.

b) PLSDA analysis

Partial least squares discriminant analysis (PLSDA) represents a form of supervised classification, in which the components of PLS are selected so that the sample co-variance between the response and a linear combination of the p predictors (glycans) are maximized. This specific criterion employed in PLS is thus, directly driven by the knowledge of the response variable, and thus should yield a better classification (eg. cancer diagnosis) (Nguyen and Rocke, 2002). The PLS approach undertaken in this study consists of two main steps; a) generating a classifier using the data and the known response and b) predicting the classification of a new sample, by assigning it to a category that its most like to have come from. This analysis is modelled using the logistic functional form illustrated below, where \mathbf{x} is the column vector of p predictor values and y denotes the binary response value. For instance, $y = 0$ for serous ovarian cancer, $y = 1$ for serous peritoneal cancer and \mathbf{x} is the corresponding expression value of p glycans. In logistic regression, $\pi = P(y=1 | \mathbf{x}) = P(\text{tumor with glycan profile } \mathbf{x})$ and parameter $\boldsymbol{\beta}$ represents the Maximum Likelihood Estimates (MLE).

$$\pi = \frac{\exp(\mathbf{x}'\boldsymbol{\beta})}{1 + \exp(\mathbf{x}'\boldsymbol{\beta})}$$

The predicted class of each cancer tissue (serous ovarian or serous peritoneal) is $\hat{y} = I(\hat{\pi} > 1 - \hat{\pi})$, where $I(\cdot)$ is the indicator function; $I(A) = 1$ if condition A is true and zero otherwise. Hence, a sample is classified as cancer ($\hat{y} = 1$) if the estimated probability of observing a serous peritoneal tumour sample given the glycan profile, \mathbf{x} , is greater than the probability of observing a serous ovarian cancer with the same glycan expression profile (Nguyen and Rocke, 2002). In order to utilize the linear discriminant analysis (LDA), corresponding glycan profiles in the reduced dimensional space must be obtained from PLS or PCA. To quantitatively evaluate the accuracy of this approach, we used leave-one-out cross-validation. In turn, each one of the samples was excluded and a model was fitted based on the remaining samples except for the excluded sample. This new fitted model was then used to predict the classification of the excluded sample and the classification success of all samples was combined and reported as the overall accuracy.

In this study, the PLSDA-derived statistical analysis was applied and the statistical model was validated using the above leave-one-out-cross-validation. Specifically, twenty-eight (serous ovarian=14; serous peritoneal=14) cancer tissue samples of **Discriminant 1** (diagnosis) were analysed. Serous tubal cancers were excluded due to too low sample number. Overall classification results demonstrated 78.57 % accuracy, in which 11/14

samples were correctly classified ($p = 0.00186$) for serous ovarian and peritoneal cancer, respectively. As shown in **Figure 13**, each point in the PLSDA plot contains information which is reflective of the explicit measurement of specific glycan structures which correspond to each serous cancer group. Hence, the clustering of same coloured points indicates the ability of this statistical analysis to define the similarity between the biological replicates of each tissue group. In regard to the discrimination between serous ovarian and serous peritoneal cancer tissues, there is a clear trend in the statistical output which supports the validity of this analysis for the diagnosis and discrimination of serous ovarian from peritoneal cancers. Specifically, as one moves from the left to the right along the x axis (Component 1), it becomes increasingly evident that serous peritoneal cancer cluster quite closely compared to serous ovarian cancers. In total, 11 *N*-glycans (**Table 2A**: #13, #21, #22, #23, #26, #29, #40, #41, #42, #45 and #52) contributed to the separation based on Component 1, of which five *N*-glycans with m/z 913.9²⁻, m/z 1079.9²⁻, m/z 1059.4²⁻ and m/z 1205.0²⁻ as previously mentioned (**Table 3A**), and together with the *N*-glycan with m/z 934.4²⁻ were found to contain LacdiNAc motifs.

Interestingly, some of the mis-diagnoses as observed in the PLSDA were not particularly random, in that there was a definitive correlation to the tissue source from which the tumour was surgically-derived, rather than from the assigned diagnosis, as shown by the PCA analysis. For instance, of the three tissues, #OV 450, #OV 308 and #OV 55, that indicated incorrect diagnosis of SOC by PLSDA (**Figure 13**), #OV 308 clustered within the SPC group (**Discriminant 1**) as indicated by the PCA analysis of the *N*-glycans [**Figure 11(i)**] and this tissue was in fact derived from the omentum [**Discriminant 2-Figure 11(ii)**]. Likewise of the three samples, #PT 418, #PT 524 and #PT 153 that were incorrectly diagnosed as SPC by PLSDA (**Figure 13**), #PT 418, originally derived from the left ovary [**Discriminant 2-Figure 11(ii)**] was seen to cluster within SOC group (**Discriminant 1**) as indicated by the PCA analysis of the *N*-glycans [**Figure 11(i)**]. This tissue was also present as an outlier from both clusters in the PLSDA analysis. The remaining two tissues that were apparently mis-diagnosed as SOC (#OV 450 and #OV 55) and SPC (#PT 524 and #PT 153) samples were found to cluster around the overlap of the ellipses for each serous cancer group in the PLSDA analysis. When compared to their respective PCA clustering, both tissues #OV 450 and #OV 55, were surgically removed from the right ovary, while #PT 524 and #PT 153 were removed from the omentum [**Discriminant 2-Figure 11(ii)**]. The PLSDA analysis was not performed for *O*-glycans due to the few glycan structures identified across both SOC and SPC groups. Overall, the PLSDA analysis thus reveals similar clustering patterns to PCA analysis, with even more significant correlations between the

individual glycan profiles and their corresponding serous cancer diagnosis. More importantly, both analyses indicate that serous cancers of the ovary and peritoneal can be distinguished based on specific structures in their *N*-glycan profiles.

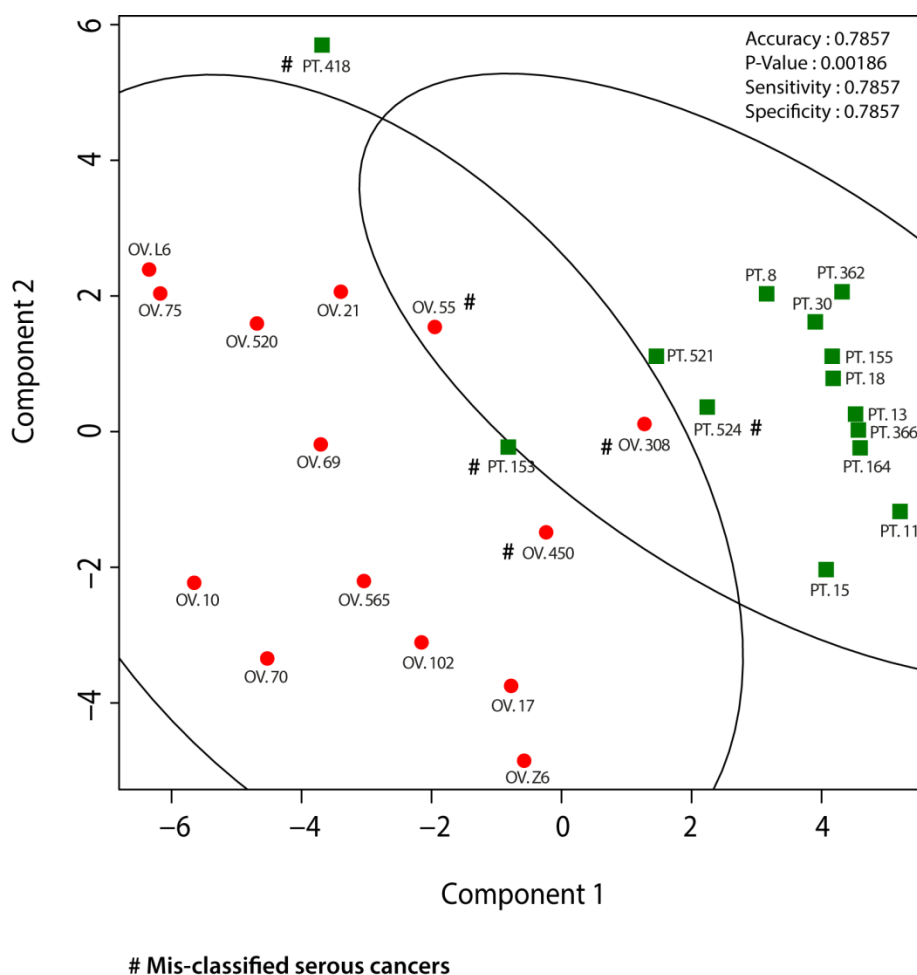


Figure 13. PLSDA classification of serous ovarian and peritoneal cancers using leave-out-one cross validation for **Discriminant 1**. PLSDA-derived statistical analysis was applied and the statistical model was validated using leave-one-out-cross-validation which resulted in the overall classification accuracy of 78.57 % ($p = 0.00186$) for serous cancers (ovarian: $n=14$; peritoneal: $n=14$). In total, 11 out of 14 serous cancers were correctly classified for each serous cancer group based on their individual *N*-glycan profiles. Samples marked with # were incorrectly classified. Red circles: OV-serous ovarian cancer ($n=14$); green squares: PT-serous peritoneal cancer ($n=14$)

Sialylated LacdiNAc-type N-glycans distinguish between serous cancers of the ovary and peritoneum

As with most biomarker-associated studies, the choice of statistical tools employed in this study was a crucial factor in determining the diagnostic potential of glycan biomarkers in differentiating between the three serous cancer types (Hanley and McNeil, 1982; Ringner, 2008). Hence, the Receiver Operating Characteristics (ROC) and corresponding area-under the curve (AUC) values were calculated as a measure of classification potential for each glycan. Other mass spectrometric-based ovarian cancer studies have demonstrated the use of ROC values as an effective diagnostic tool, particularly for evaluating discriminatory glycans in healthy vs. diseased conditions as well as between pre- and post-cancer treatments (Alley, Vasseur *et. al.*, 2012; Hua, Williams *et. al.*, 2013; Mitra, Alley *et. al.*, 2013). In this test, ROC curves were generated for N- and O-glycan relative ion intensities that were significantly altered ($p < 0.05$) and the resulting area-under-the curve (AUC) was used as an indicator of the test's accuracy. Typically, these AUC values can range from 0 to 1, with 0 corresponding to an accurate negative test and 1 representing a perfectly accurate or positive test (Bewick, Cheek *et. al.*, 2004). By using recommendations from previous studies (Alley, Vasseur *et. al.*, 2012), the following rankings were designated as a) 'highly accurate' ($0.9 < \text{AUC} < 1.0$ or $0 < \text{AUC} < 0.1$), b) 'accurate' ($0.8 < \text{AUC} < 0.9$ or $0.1 < \text{AUC} < 0.2$), c) 'moderately accurate' ($0.7 < \text{AUC} < 0.8$ or $0.2 < \text{AUC} < 0.3$) and d) 'uninformative' ($0.5 < \text{AUC} < 0.7$ or $0.3 < \text{AUC} < 0.5$). Examples of ROC curves generated for specific N-glycans with respect to their discriminatory potential are shown in **Supplementary Figure 1**. The statistical comparisons displaying favourable correlations with AUC values for potential N- and O-glycan 'biomarkers' based on the respective Discriminants are listed in **Table 3**. Several N- and O-glycans, specifically those containing the unusual LacdiNAc sequence (GalNAc β 1-4GlcNAc) were found to be implicated in the distinction between the serous tumours. For **Discriminant 1** (diagnosis) (**Table 3A**), the biomarker potential of LacdiNAc N-glycan with m/z 1205.0²⁻ (AUC: 0.929) was considered as 'highly accurate' while the two other N-glycans with m/z 1059.4²⁻ (AUC: 0.825) and 1079.9²⁻ (AUC: 0.805) were 'accurate' biomarkers, thereby distinguishing serous ovarian from serous peritoneal cancers. The hybrid-type N-glycan with m/z 937.3²⁻ was shown to be classified as 'accurate' (AUC: 0.890) and 'highly accurate' (AUC: 1.0) for the discrimination of serous ovarian cancer and serous tubal cancers, respectively, from serous peritoneal cancers. On the other hand, the sulphated Core 2 O-glycan with m/z 705.2²⁻ appeared to discriminate serous tubal cancers from serous ovarian and peritoneal cancers and was classified as 'moderately accurate' (AUC: 0.268; AUC: 0.250). For **Discriminant 2** (tissue source) (**Table 3B**), the same LacdiNAc N-glycans

(m/z 1205.0²⁻ and m/z 1059.4²⁻) which were found to be significantly diagnostic for serous ovarian cancer (**Discriminant 1**) were also associated with ovarian cancer tissue origin and considered as ‘highly accurate’ and ‘accurate’ with AUC values of 0.951 and 0.902, respectively. In peritoneal/omentum-derived serous cancer tissues, structures such as the bisecting-GlcNAc type (m/z 994.9²⁻) and sialylated Core 2 *O*-glycan (m/z 1331.5²⁻) were classified as ‘accurate’ glycan biomarkers as indicated by their AUC values of 0.182 and 0.177, respectively, thereby discriminating peritoneal cancer tissues from ovarian tissues.

3.3 Discussion

High-grade serous cancers derived from the ovary, fallopian tube and peritoneum represent a group of highly aggressive cancers which exhibit remarkable homogeneity, both in their morphology and clinical behaviour (Kurman and Shih Ie, 2008; Kurman and Shih Ie, 2010). From a clinical perspective, these cancers are diagnosed and treated identically (Ozols, 2002a; Ozols, 2002b), despite their distinct anatomic sites and genetic origins. The difficulty in identifying the site of origin at the time of clinical diagnosis remains a challenge, particularly due to their wide-spread dissemination at early stages and lack of reliable diagnostic biomarkers. The discrimination of these cancers at an early stage, therefore, is important, not just to facilitate the development of personalised treatment, but also to offer the possibility of bilateral oophorectomy salpingectomy (removal of ovaries and tubes) as a means of primary prevention for high risk patients. In the pursuit of discovering novel approaches to diagnosing this diverse group of serous cancers, the field of glycomics has become increasingly investigated for its potential to unravel tumour-specific glycans which are associated with the cell surface of ovarian cancer cells (Dennis, 1991; Drake, Cho *et. al.*, 2010). Here, in this study, *N*- and *O*-glycans were analysed from serous cancers using the glycomic profiling strategy which has been successfully employed in recent glycan biomarker studies (Alley, Vasseur *et. al.*, 2012; Biskup, Braicu *et. al.*, 2013; Kim, Ruhaak *et. al.*, 2014). Specifically, the total membrane protein glycans were released and subjected to a rigorous, structural MS-based characterization of glycans, including the identification of specific isomeric structures that present different terminal epitopes. In addition, various statistical methods were applied to assess the diagnostic performance of these glycans which subsequently led to the identification of discriminatory *N*- and *O*-glycan features between the serous cancer groups.

To the best of our knowledge, comparative glycan profiling of high grade pelvic serous carcinomas has not been performed before. The specific cellular glycosylation and phenotypic alterations that occur as a result of molecular genetic mutations are unknown, particularly for these serous cancers. As opposed to ovarian cancers which have been extensively studied and characterized by high levels of genetic instability and frequent mutations of the tumour suppressor gene, TP53 (Folkins, Jarboe *et. al.*, 2008; Kurman and Shih Ie, 2011), serous fallopian tube and primary serous peritoneal cancers have been less frequently investigated (Jordan, Green *et. al.*, 2008; Nik, Vang *et. al.*, 2014). This group of serous cancers, however, are thought to share a common aetiology based on their close histological and clinical similarities (Kessler, Fotopoulou *et. al.*, 2013). It is therefore not

surprising that this close association between the three serous cancers was also reflected in their membrane protein *N*- and *O*-glycomic profiles, as evidenced broadly by the similar abundances when grouped into glycan types (high mannose, hybrid and complex). Interestingly, the most prominent feature of the *N*-glycosylation was the abundant expression of mono- and di-sialylated bi-antennary glycans, with more than 50 % of the total *N*-glycans comprising these sialylated structures in all three serous cancer tissues. Similarly, for *O*-glycans, mono- and di-sialylated Core 1 and Core 2 structures also represented the major glycans for all three serous cancer tissues. A similar observation of the increase in sialylation has also been reflected in a recent sera-based study by Hua *et. al.*(2013), in which mono- and di-sialylated bi-antennary *N*-glycans were found to be significantly increased on ovarian cancer patients' plasma proteins (Hua, Williams *et. al.*, 2013). Interestingly, a majority of the mono and di-sialylated *N*-glycans analyzed in this study which appeared to be implicated in serous cancers, contained mostly α 2-6-linked sialic acids. This observation is consistent with some of the previous observations in ovarian cancer serum glycoproteins (Salдова, Wormald *et. al.*, 2008) as well as in ovarian cancer cell lines (**Chapter 2**, published as Anugraham *et. al.*) (Anugraham, Jacob *et. al.*, 2014). Of all the glycosylation forms, the over-expression of sialylated antigens on cancer cell membranes has been widely investigated, particularly in the event of metastasis which involves a multi-step series of cell adhesion and signalling events (Zhang, Zhang *et. al.*, 2002; Casey, Oegema *et. al.*, 2003; Seales, Jurado *et. al.*, 2005). In fact, it has been shown that hypersialylation of the integral membrane glycoprotein, β 1 Integrin, conferred a more metastatic phenotype to ovarian cancer cells (Christie, Shaikh *et. al.*, 2008), consistent with previous observations from other cancers such as in breast (Lin, Kemmner *et. al.*, 2002) and colon (Seales, Jurado *et. al.*, 2005). These findings, together with the extensive display of cell membrane sialylation identified in this study in all three serous cancers, suggest the potential involvement of these antigens in the early dissemination of tumour cells via metastasis.

Another characteristic feature that was common in all of the three serous cancer groups was the relatively low abundant levels of bisecting *N*-acetylglucosamine on some of the complex neutral and sialylated *N*-glycans. The bisecting GlcNAc is a unique modification which occurs on hybrid and complex *N*-glycans and is catalyzed by β 1-4 *N*-acetylglucosaminyl transferase (GlcNAcT-III), by the expression of the *MGAT3* gene (Narasimhan, 1982). In recent years, however, the conflicting 'yin' and 'yang' roles of bisected *N*-glycans on cell surface glycoproteins have been noted in cancer, with studies indicating varying effects on tumour progression and metastasis in various cancers (Song, Aglipay *et. al.*, 2010; Kang, Wang *et. al.*, 2012; Miwa, Song *et. al.*, 2012). For instance, on mammary tissue membrane

glycoproteins, bisecting GlcNAc serves to protect mammary epithelial cells from tumour progression (Song, Aglipay *et. al.*, 2010), while in other cancers such as in hepatocellular carcinomas, the overexpression of *MGAT3* has been shown to be associated with higher metastatic potential (Kang, Wang *et. al.*, 2012). In ovarian cancer, however, GlcNAcT-III expression is thought to play an important role in the maintenance of cell-cell adhesion via the cell surface glycosylation of E-cadherin (Abbott, Lim *et. al.*, 2010). Another possible role for these *N*-glycans in facilitating early stage peritoneal dissemination of ovarian cancer has also been suggested in a recent study involving the use of serous ovarian cancer cell line (SKOV 3) and its highly metastatic derivative, SKOV 3-ip. Specifically, it was revealed that bisecting GlcNAc *N*-glycans were found to be significantly decreased in the metastatic cell line (Zhang, Wang *et. al.*, 2014). It is also worth noting that the regulation of *MGAT3* gene which lead to the presence of bisecting GlcNAc type *N*-glycans in several serous ovarian cancer cell lines, including SKOV3 has been shown by us to be influenced by DNA hypomethylation (**Chapter 2**, published as Anugraham *et. al.*) (Anugraham, Jacob *et. al.*, 2014). The absence of these structures in non-cancerous ovarian surface epithelial cells together with DNA hypermethylation of *MGAT3* gene and the low level expression of *MGAT3* in normal ovaries (Abbott, Nairn *et. al.*, 2008) may partially explain the presence of these structures as a feature of all serous cancers in general.

The highlight of this study, however, was the identification of a family of structurally related *N*-glycans containing LacdiNAc and sialylated LacdiNAc motifs, primarily present on serous cancers surgically-derived from ovarian tissue (**Discriminant 2**). Most mammalian *N*-glycans contain LacNAc (Gal β 1-3/4GlcNAc) antennae which form bi-antennary or branched tri- and tetra-antennary structures that are usually capped by sialylation or extended to form poly-LacNAc chains. The less common LacdiNAc disaccharide (GalNAc β 1-4GlcNAc), is synthesized by the action of specific β 4-GalNAc transferases, β 4GalNAcT3 and β 4GalNAcT4, and is found to be expressed in various organs of the human body such as stomach, colon, ovaries, testes and brain (Sato, Gotoh *et. al.*, 2003; Gotoh, Sato *et. al.*, 2004). A few cancer studies have shown that tumour-associated glycoproteins such as secreted tissue plasminogen activator from Bowes melanoma cells (Chan, Morris *et. al.*, 1991), secreted ribonuclease I from pancreatic tumour cells (Peracaula, Royle *et. al.*, 2003) and alpha-fetoprotein (AFP) from hepatic cancer cell lines (Ito, Kuno *et. al.*, 2009) were found to contain LacdiNAc type *N*- and *O*-glycans. The identification of this motif in serous ovarian cancer tissues, facilitated through ESI-MS/MS is consistent with our published cell-line based glycosylation model (**Chapter 2**), in which LacdiNAc-type *N*-glycans were found to

be present on membrane proteins of serous ovarian cancer cell lines, SKOV 3 and IGROV 1 and not on non-cancerous HOSE ovarian cell line membrane proteins (Anugraham, Jacob *et al.*, 2014). In this tissue-based study, we identified three sialylated LacdiNAc-type *N*-glycans (m/z 1205.0²⁻, m/z 1059.4²⁻ and m/z 1079.9²⁻) which were all ranked as ‘highly accurate’, and ‘accurate’ biomarkers respectively, thereby distinguishing serous ‘ovarian’ cancer from serous ‘peritoneal’ and ‘tubal’ cancers. Two of the three LacdiNAc structures (m/z 1205.0²⁻ and m/z 1059.4²⁻) were also noted to have improved AUC values upon the re-classification of diagnosed these serous cancers with respect to their ovarian and peritoneal tissue origin (**Discriminant 2**). It is also interesting to note that these unique structures have never been reported in the serum glycans of ovarian cancer (Saldiva, Royle *et al.*, 2007; Alley, Vasseur *et al.*, 2012; Hua, Williams *et al.*, 2013), possibly due to the low abundance (2.77 % ± 2.00 %) of these *N*-glycan epitopes. At this point in time, it is not clear if, as in the cell line models, the LacdiNAc motifs are indeed cancer specific glycan determinants in tissues. Likewise, at this stage, it is also not known whether these structures are displayed on a specific glycoprotein from serous ovarian cancer tissues or are present as an altered glycan structure on many serous ovarian cancer membrane proteins. Nevertheless, it is evident that a closer investigation into the specific regulation of the LacdiNAc-type pathway in serous ovarian cancer is warranted. Of future interest also is the expression of sialylated LacdiNAc structures and of the associated sialyltransferases; *N*-acetyl-galactosaminide alpha-2,6-sialyltransferase known to preferentially sialylate GalNAc residues.

In recent years, much interest towards understanding ovarian carcinogenesis has been developed due to the dismal survival statistics associated with the late-stage detection of ovarian cancer. More specifically, the origin of these serous cancers has been a widely debated topic, with accumulating evidence pointing to the fallopian tube as an occult source of high grade serous cancers which were previously thought to be of peritoneal or ovarian origin (Crum, Drapkin *et al.*, 2007; Seidman, Zhao *et al.*, 2011; Erickson, Conner *et al.*, 2013). Given the early events in molecular alterations which are thought to arise from the tubal epithelium, it is possible to speculate that these cancerous tubal intraepithelial cells could have resulted in serous tumours that have evolved to become quite distinct upon implantation onto the ovary or peritoneum/omentum. This event could explain why some of the serous cancers initially diagnosed as serous tubal cancers (#TB22 and #TB448), were clustered with the ovarian-derived cancer tissues based on the PCA analysis for *N*-glycans in **Discriminant 2** (tissue source). Although compelling, but inconclusive, it is also evident that the discrepancies observed in the PCA cluster analysis for some of the diagnosed

samples could potentially indicate that these tumours could have conformed to the various metastasized sites, and thus developed a morphology that no longer resembles the primary site of tumour origin (e.g. tubal). It would, therefore, have been of interest to more confidently characterize the *N*- and *O*- glycans of serous ‘tubal’ cancers in this study. However, only a small number of clinical samples are ever diagnosed as serous tubal cancers ($n=4$; obtained from both sample cohorts reflect this fact) and only one of these was surgically-derived from the tube while the remaining samples were removed from the ovaries and omentum. Nevertheless, two of the four diagnosed serous tubal cancers displayed the presence of the sulphated and di-sialylated *O*-glycan structure (m/z 705.2²⁻); interestingly, the one sample actually derived from the tube displayed the highest expression of this glycan ($p < 0.01$). Furthermore, this structure has also been previously observed in the ascites’ fluid of serous ovarian cancer patients and was structurally characterized by ESI-LC-MS/MS (Karlsson and McGuckin, 2012). The sulphation of plasma glycoproteins is quite rare (Karlsson and McGuckin, 2012), but the expression of this unique terminal epitope in ascitic fluid, reflected by the characterization of a structurally-related sulphated *O*-glycan on the membrane glycoproteins in this study could represent a novel biological function and serve as a diagnostic marker for general ovarian cancer detection.

The potential discriminatory *N*-glycan features implicated in the classification of serous ovarian and peritoneal cancers were also assessed and validated using the partial least square discriminant analysis (PLSDA) and leave-one-out-cross-validation analysis, respectively. Typically, these analyses involve larger and more diverse sample cohorts and are useful in the classification of healthy and diseased states, thereby allowing for the identification of not just a few, but a panel of specific biomarkers. However, in this study, the utilization of this statistical analysis proved to be quite reliable in the differential diagnosis of serous ovarian and peritoneal cancers. More importantly, the panel of discriminating structures comprising of LacdiNAc *N*-glycans, as well as a few other structures, that were independently identified by ANOVA and AUC, were also found to be implicated in the PLSDA classification of serous cancers. Despite an overall classification accuracy of only 78.57 %, it is remarkable that only a few mis-classifications were observed, given the extensive glycan similarities observed for both these serous cancers. Hence, the identification of these diagnostic membrane glycan biomarkers further attests to the strength of the PLSDA analysis for the distinction and classification of these neoplasms. It is worth mentioning that another factor that has not been taken into consideration in this study is the extent of metastasis. For instance, two of the mis-classified tissues, PT418 and

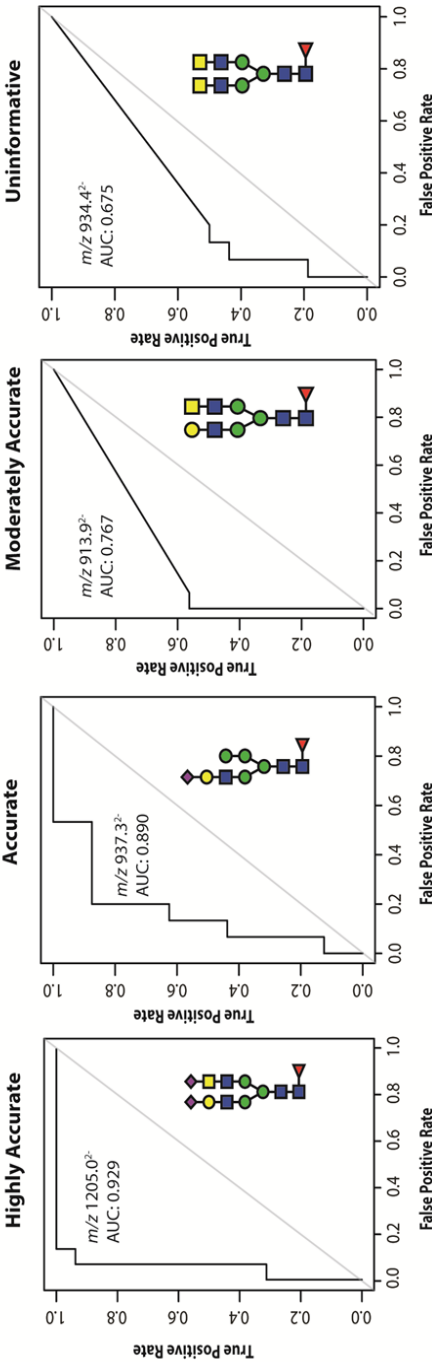
OV308, were classified by PLSDA as serous ‘ovarian’ and ‘peritoneal’ cancers, respectively and these samples were also found to be clustered within the ovarian and peritoneum tissue group, respectively using PCA. In the event that the initial diagnosis was true, these tumours may have metastasised, thereby displaying glycan features that are representative of their respective metastatic sites. Hence, these underlying morphological changes may be complicating the clinical diagnosis of late stage serous cancers, as well as the subsequent treatment and management of serous cancers.

It has been previously shown that the similarities between serous peritoneal and serous ovarian cancers do not enable a clinical preoperative distinction between both the neoplasms (Barda, Menczer *et. al.*, 2004). In fact, in the last decade, up to 18-28 % of serous ovarian carcinomas have been re-classified as primary peritoneal cancers, as compared to just 10 % of previously mis-diagnosed cases (Eltabbakh, Piver *et. al.*, 1998; Chen, Ruiz *et. al.*, 2003; Quirk and Natarajan, 2005). In retrospect, the peritoneal origin of serous cancers by itself remains unclear as the normal peritoneum is composed of a layer of mesothelium which forms the lining of the abdominal cavity and can undergo malignant transformation to form a tumour entirely different from serous peritoneal carcinoma (Seidman, Zhao *et. al.*, 2011). However, the serous-type epithelium from which serous peritoneal cancer is thought to be derived, positioned just underneath the peritoneal surface, is ciliated and considered identical to that of the normal fallopian tube (Halperin, Zehavi *et. al.*, 2001). Surprisingly, a majority of fallopian tubes examined from patients with primary peritoneal cancer have been found with the presence of serous tubal intraepithelial lesions, thereby giving the tumour cells access to the peritoneal cavity (Seidman, Zhao *et. al.*, 2011). If this reasoning is true, the identification of glycans such as the bisecting-type (m/z 994.9²⁻, $p < 0.002$), mono-sialylated *N*-glycans (m/z 1038.9²⁻, $p < 0.022$; m/z 1221.5²⁻, $p < 0.003$) and sialylated Core 2 *O*-glycans (m/z 1040.5¹⁻, $p < 0.014$; m/z 1331.1¹⁻, $p < 0.002$) in serous cancers derived from the peritoneum and omentum could potentially discriminate serous peritoneal cancer from serous ovarian and tubal cancers.

To our knowledge, the findings of this study represent the first in-depth MS-based glycan structural characterization carried out to identify biomarkers that distinguish between serous cancers of various origins, namely the ovary, peritoneum and tube. This study provides the additional level of glycan profiling, in the form of the identification of compositional and structural isomers, which is required for the determination of low abundance discriminatory structures. Despite the prevailing evidence surrounding the elusive and silent nature of this ‘killer’ disease, the structural determination of these membrane protein glycan biomarkers may hold substantial promise in understanding the

complex carcinogenesis process of serous cancers, and potentially aid in the distinction between ovarian cancer and other gastro-intestinal tumours which involve the peritoneal dissemination of tumour cells. The findings reported here point to increasing evidence that specific glycans are indeed tissue specific and can further be exploited for discrimination between various serous cancers of differing cellular origin. Furthermore, this study serves as an initial clinical validation of the presence of specific glycan determinants such as the (sialylated) LacdiNAc-type which have not been reported in membrane proteins of serous ovarian cancer tissues to date. It is envisaged that the understanding of the differences in specific membrane glycosylation determinants between these serous cancers could provide alternative approaches for the disease to be diagnosed and could facilitate the development of targeted ovarian cancer therapies.

3.4 Supplementary Data



Discriminatory Potential	AUC Values
Highly Accurate	0.9 < AUC < 1.0 or 0 < AUC < 0.1
Accurate	0.8 < AUC < 0.9 or 0.1 < AUC < 0.2
Moderately Accurate	0.7 < AUC < 0.8 or 0.2 < AUC < 0.3
Uninformative	0.5 < AUC < 0.7 or 0.3 < AUC < 0.5

Figure 1

3.5 Overview of Chapter III

- Serous cancers derived from the ovary, peritoneum and tube are diagnosed and treated identically, despite their distinct anatomic sites and genetic origins
- The *N*-glycan profiles of all three serous cancer groups (ovarian vs. peritoneum vs. tubal tissues) are overall similar and mainly associated with abundant mono- and di-sialylated bi-antennary *N*-glycans
- α 2-6 sialylation accounts for more than 50 % of the total sialylation of *N*-glycans in all three serous cancer groups
- *O*-glycans for all three serous cancer groups are mainly comprised of sialylated Core 1 structures
- Many individual mass signals corresponded to a combination of structural and compositional isomers which were further elucidated based on their MS/MS fragmentation patterns and LC column retention time
- Some of the unique structural features (as observed in Chapter II for ovarian cancer cell lines) such as the bisecting type *N*-glycans are present in all three serous cancer groups
- The presence of low abundant *N*- and *O*-glycan structures in all three serous cancer groups contained informative structural features that appear to have discriminatory potential. For instance, *N*-glycan structures bearing the unique LacdiNac motif (GalNAc β 1-4GlcNAc) and sialylated LacdiNac (Neu5Ac-GalNAc β 1-4GlcNAc) were expressed in majority of serous ovarian cancers but not on peritoneal serous cancers
- Several statistical tools were used in this study for the evaluation of discriminatory glycan features based on the a) type of serous cancer diagnosis-ovarian, peritoneal or tubal and b) location of the tumour (right/left ovary, peritoneum, omentum and tube)
- Glycan profiles representative of the location from which the specific tumor is derived from, regardless of the cancer diagnosis, potentially affords a better discrimination potential between serous cancers

CHAPTER IV

Rationale

Apart from the structural characterisation of membrane proteins in serous cancer tissues and cell lines, the glycosylation profiles of membrane glycosphingolipids (GSLs) were also investigated to identify specific cancer-associated glycan structures. The first section of this chapter entails the optimisation and development of a new method for the enzymatic release of glycans from PVDF-immobilised GSLs and the elucidation of various isobaric and isomeric glycans by PGC-LC-ESI-MS/MS. The second section of this chapter utilises this method, established for the analysis of glycan-derived GSLs, for the identification of P blood group-related and fucosylated /non-fucosylated Type 1 and Type 2 glycan structures that are implicated in the immune recognition by auto-antibodies present in ovarian cancer patients' plasma.

4.0 Publication III: A platform for the structural characterization of glycans enzymatically released from glycosphingolipids extracted from tissue and cells

Research Article



Received: 5 September 2014

Revised: 7 November 2014

Accepted: 15 December 2014

Published online in Wiley Online Library

Rapid Commun. Mass Spectrom. **2015**, *29*, 545–561
(wileyonlinelibrary.com) DOI: 10.1002/rcm.7130

A platform for the structural characterization of glycans enzymatically released from glycosphingolipids extracted from tissue and cells

Merrina Anugraham¹, Arun Vijay Everest-Dass¹, Francis Jacob² and Nicolle H. Packer^{1*}

¹Department of Chemistry and Biomolecular Sciences, Biomolecular Frontiers Research Centre, Faculty of Science, Macquarie University, Sydney 2109, Australia

²Gynecological Research Group, Department of Biomedicine, University Hospital Basel, University of Basel, Basel 4031, Switzerland

RATIONALE: Glycosphingolipids (GSLs) constitute a highly diverse class of glyco-conjugates which are involved in many aspects of cell membrane function and disease. The isolation, detection and structural characterization of the carbohydrate (glycan) component of GSLs are particularly challenging given their structural heterogeneity and thus rely on the development of sensitive, analytical technologies.

METHODS: Neutral and acidic GSL standards were immobilized onto polyvinylidene difluoride (PVDF) membranes and glycans were enzymatically released using endoglycoceramidase II (EGCase II), separated by porous graphitized carbon (PGC) liquid chromatography and structurally characterized by negative ion mode electrospray ionization tandem mass spectrometry (PGC-LC/ESI-MS/MS). This approach was then employed for GSLs isolated from 100 mg of serous and endometrioid cancer tissue and from cell line (10⁷ cells) samples.

RESULTS: Glycans were released from GSL standards comprising of ganglio-, asialo-ganglio- and the relatively resistant globo-series glycans, using as little as 1 mU of enzyme and 2 µg of GSL. The platform of analysis was then applied to GSLs isolated from tissue and cell line samples and the released isomeric and isobaric glycan structures were chromatographically resolved on PGC and characterized by comparison with the MS² fragment ion spectra of the glycan standards and by application of known structural MS² fragment ions. This approach identified several (neo)-lacto-, globo- and ganglio-series glycans and facilitated the discrimination of isomeric structures containing Lewis A, H type 1 and type 2 blood group antigens and sialyl-tetraosylceramides.

CONCLUSION: We describe a relatively simple, detergent-free, enzymatic release of glycans from PVDF-immobilized GSLs, followed by the detailed structural analysis afforded by PGC-LC-ESI-MS/MS, to offer a versatile method for the analysis of tumour and cell-derived GSL-glycans. The method uses the potential of MS² fragmentation in negative ion ESI mode to characterize, in detail, the biologically relevant glycan structures derived from GSLs. Copyright © 2015 John Wiley & Sons, Ltd.

Glycosphingolipids (GSLs) are ubiquitous membrane constituents that collectively form a large and heterogeneous family of amphipathic lipid molecules, anchored to the outer leaflet of the cell membrane of most vertebrates.^[1,2] These glyco-conjugates comprise of hydrophilic carbohydrate residues that are linked to a hydrophobic ceramide moiety consisting of long-chain fatty acids.^[3,4] They typically constitute about 5% of the total membrane lipids,^[5] where up to 30% of GSLs are found in neuronal membranes of the brain.^[6] To date, GSLs have been shown to be involved in many cellular functions in biological systems, such as cell-cell adhesion,^[7,8] signal transduction^[9] and immune recognition.^[10] The carbohydrate residues, also known as

glycans, are structurally diverse due to variation in monosaccharide composition, monosaccharide sequence, branching as well as linkage positions.^[11] The structural diversity exhibited in the glycan structures of GSLs reported so far, in a variety of vertebrate tissues and organs, accounts for approximately 188 acidic, 172 neutral and 24 sulfated glycans.^[12] Unlike N- and O-glycosylation on proteins, these carbohydrate residues are covalently linked to the ceramide through a β-linkage, to form galactosylceramide (Gal-Cer) or the more abundant glycosylceramide (Glc-Cer). Most members of the GSL family are built on Glc-Cer, which are further extended to generate a series of neutral 'core' structures that have been described in the nomenclature of GSLs.^[11] The isolation and structural characterization of these glycan constituents are highly desirable as alterations in the carbohydrate component of GSLs have been implicated in diseases such as in cancer.^[13,14]

In many cancers, membrane-bound GSLs represent an unexplored source of novel tumour-associated antigens, reflecting alterations such as (a) incomplete synthesis of

* Correspondence to: N. H. Packer, Building E8C, Room 307, Department of Chemistry and Biomolecular Sciences, Macquarie University, Sydney 2109, New South Wales, Australia.
E-mail: nicki.packer@mq.edu.au

glycans, (b) neo-synthesis through the appearance of aberrant glycans, and (c) over-expression of glycans due to increased glycosyltransferase activity or gene activation.^[15] These specific glycosylation patterns on their cell surface membranes have been shown to be intimately linked to specific functions in tumour growth and development. For instance, in colorectal cancer, the overexpression of fucosylated and sialylated structures such as sialyl Lewis X^[16] and sialyl Lewis A^[17] have been observed on GSLs and are found to correlate with tumour metastasis, prognosis and survival outcomes. Likewise, the accumulation of the globo-series GSL Gb3 was shown to be associated with enhanced invasiveness in metastatic colorectal cancer cells.^[18] In cancers such as in breast, prostate and lung, the expression of globo-H epitope on GSLs was found to be over-expressed and, in some cases, the sera of patients were shown to contain high levels of antibodies to this epitope.^[19,20]

As opposed to the use of conventional methods such as thin-layer chromatography (TLC) and monoclonal antibodies for the detection of biologically relevant lipid-linked glycans, mass spectrometry (MS) offers a valuable alternative that is well established for the structural characterization of glycans. A few studies have successfully employed matrix-assisted laser desorption/ionization time-of-flight (MALDI-TOF)MS^[21,22] and porous graphitized carbon liquid chromatography electrospray ionization (PGC-LC/ESI)-MS^[3] for the elucidation of GSL-derived glycan structures. Owing to the structural complexity of these glycans with respect to the sequence, composition and linkage differences, the use of porous graphitized carbon (PGC) chromatography with ESI-MS/MS analysis is particularly attractive for the differentiation of isobaric and isomeric glycans and has facilitated the label-free analysis of *N*- and *O*-glycans released from glycoproteins based on their differences in chromatographic retention times and fragmentation patterns.^[23] One such example is the elegant characterization of native and reduced oligosaccharides released from well-characterized non-acidic reference GSL standards and GSL-derived glycans isolated from complex sample mixtures using PGC-LC/ESI-MS.^[3] It was demonstrated that precise structural information obtained from characteristic cross-ring cleavage ions such as the ^{0,2}A-type fragment ions was useful in the discrimination of isoglobo- and globo-series as well as type 1 (Galβ1-3GlcNAc) and type 2 (Galβ1-4GlcNAc) LacNAc chains. In the majority of these studies, the enzymatic isolation of GSL-derived glycans using a specific ceramide endoglycanase, endoglycoceramidase II, is preferred as this enzyme specifically cleaves the glycans from the ceramide of GSLs, thus enabling the structural analysis of the released intact glycans. The in-solution detergent-based system that is commonly used requires long incubation times and high enzyme concentrations with limitations in specificity and with the subsequent requirement of detergent removal to obtain purified glycans for analysis. This potentially results in the substantial loss of glycans, especially when sample quantity is a limiting factor.

In this study, the enzymatically released glycans from reference GSL standards were analyzed as reduced glycan alditols using porous graphitized carbon (PGC) liquid chromatography/negative ion electrospray ionization mass

spectrometry (PGC-LC/ESI-MS/MS) to determine specific glycan linkages and monosaccharide sequence composition. However, in contrast to the common in-solution enzyme digestion approach, we utilized an enzymatic release of PVDF-immobilized extracted GSLs that has been previously described for the characterization of *N*- and *O*-glycans released from glycoproteins.^[23] This method was then applied to the detailed structural characterization of GSLs extracted from ovarian cancer tissues and cell lines and immobilized on PVDF membrane in a 96-well plate format. The described approach eliminates the use of detergent, minimizes sample loss, decreases contamination and increases detection sensitivity. This method can be used for the rapid profiling of glycans of the GSL-derived ganglio, globo- and (neo-)lacto-series as demonstrated in this study. It is also envisaged that this simple detergent-free approach can be optimized, if required, for further qualitative and quantitative experiments investigating GSL function.

EXPERIMENTAL

Materials

Endoglycoceramidase II (EGCase II, recombinant clone derived from *Rhodococcus* spp. and expressed in *Escherichia coli*) was purchased from Sigma-Aldrich (MO, USA). Glycosphingolipid standards from Matreya LLC (Neutral glycosphingolipid qualmix 1505, globotriosylceramide (Gb3)/ceramide trihexose (CTH), mono-sialoganglioside mixture 1508, non-acidic tetrahexosylganglioside 1064) were obtained from Adela Scientific (SA, Australia). Immobilon-P polyvinylidene difluoride (PVDF, 0.2 μm) was obtained from Millipore (MA, USA). Microtiter plates (Corning, 96-well clear flat bottom, polypropylene) were purchased from In Vitro Technologies (Victoria, Australia). Cation-exchange resin beads (AG50W-X8) were obtained from BioRad (Hercules, CA, USA) and PerfectPure C18 Zip Tips were obtained from Eppendorf (Hamburg, Germany). Potassium hydroxide and sodium borohydride were obtained from Sigma-Aldrich. Other reagents and solvents such as methanol, ethanol, chloroform and acetonitrile were of HPLC or LC/MS grade.

Preparation of glycolipid standards

For PVDF blotting experiments to determine the minimum amount of working ceramide endoglycanase, pure reference standards, non-acidic tetrahexosylganglioside (asialo-GM₁) and globotriosyl-ceramide (Gb3) were diluted to a final concentration of 1 mg/mL and aliquots of 2 μL, 4 μL, 6 μL, 8 μL and 10 μL were used. Neutral and acidic glycolipid mixtures were diluted to final concentrations of 1 and 0.5 mg/mL, respectively, and used as controls for subsequent MS/MS characterization.

Isolation of GSLs from cancer tissues

Glycosphingolipids were extracted from ovarian and peritoneal cancer tissues (S565 and S566) using a modified Bligh and Dyer extraction method as previously described for tissues.^[24] Briefly, approximately 100 mg of tissue was

homogenized in 5 mL of chloroform/methanol (2:1) and stored for 2 h at room temperature, with intermittent mixing every 30 min. Methanol (2.5 mL) was added to the tissue suspension prior to centrifugation at 1800 g for 15 min. The supernatant was collected and the residual tissue was homogenized again in 5 mL of chloroform/methanol/water (1:2:0.8), stored for 2 h at room temperature and pelleted by centrifugation at 1800 g for 15 min. The supernatant was combined with the previous supernatant and evaporated to dryness under vacuum. The dried residue containing the glycosphingolipid mixtures was re-dissolved in 50 μ L of chloroform/methanol (2:1).

Isolation of GSLs from ovarian cancer cell line, IGROV 1

The extraction of GSLs from the ovarian cancer cell line, IGROV 1,^[25] was carried out with some modifications based on a Folch method.^[26] Cells (1×10^7) were harvested, washed thrice in 10 mL of phosphate-buffered saline and pelleted by centrifugation at 1800 g for 20 min. Then 5 mL of chloroform/methanol (2:1) was added to the cell pellet and the tube was left overnight in a 4 °C incubator shaker. The supernatant was collected after centrifugation at 1800 g for 20 min and the pellet was re-extracted again as described above. The combined supernatants were evaporated to dryness under vacuum and the dried glycosphingolipid mixture was re-dissolved in 50 μ L of chloroform/methanol (2:1).

PVDF spotting of GSLs

Polyvinylidene difluoride (PVDF) membrane spots were cut and placed in a chloroform-compatible 96-well microplate (Supplementary Fig. S1, see Supporting Information). For the optimization experiment to determine the minimum amount of working ceramide endoglycanase, aliquots of 2, 4, 6, 8, and 10 μ L of non-acidic tetrahexosylganglioside (asialo-GM₁) and globotriosylceramide (Gb3) reference standards (1 mg/mL) were spotted on the individual PVDF spots and treated with 1 mU (0.5 μ L) and 4 mU (2 μ L) of endoglycoceramidase II in 50 μ L of 0.05 M sodium acetate buffer, pH 5.0, and incubated for 16 h (overnight) at 37 °C, with modifications.^[3,24] For the validation experiment, 10 μ L (2.5 μ L \times 4 times) of neutral and acidic glycosphingolipid standards were spotted on the individual PVDF spots. 50 μ L of re-dissolved glycosphingolipid mixtures from tissue and cell line samples were also spotted (5 μ L \times 10 times) on the same plate and air-dried at room temperature to ensure proper binding of GSLs. To ensure the complete release of the glycans from the membrane-bound glycosphingolipids, 2 μ L (4 mU) of endoglycoceramidase II in 50 μ L of 0.05 M sodium acetate buffer, pH 5.0, was added to each sample well and incubated for 16 h (overnight) at 37 °C. Approximately 50 μ L of released glycans was recovered from the individual sample wells and transferred to Eppendorf tubes containing 1 mL of chloroform/methanol/water (8:4:3).^[3] The sample well was then washed with 50 μ L of water and residual glycans were added to the Eppendorf tube. The upper methanol/water layer containing the released oligosaccharides (~400 μ L) was dried and kept for subsequent analysis. As controls, blank PVDF spots with

(a) 0.5 μ L (1 mU) and 2 μ L (4 mU) of enzyme, respectively, and (b) immobilized glycolipid standards without the addition of the enzyme were treated in the same way.

Reduction and purification of released glycans

The released glycans were reduced to alditols with 20 μ L of 200 mM sodium borohydride in 50 mM potassium hydroxide at 50 °C for 2 h. The reaction mixture was quenched using 2 μ L of 100% glacial acetic acid. Glycan alditols (~20 μ L) were applied to individually prepared cation-exchange columns which consisted of 45 μ L of cation-exchange resin beads (AG50W-X8) deposited onto reversed-phase μ -C18 ZipTips (Perfect Pure, Millipore) and placed in microfuge tubes. The columns were conditioned by a series of pre-washing steps with (a) 50 μ L of 1 M HCl, (b) 50 μ L of methanol and (c) 50 μ L of water. Glycan alditols were eluted with Milli Q water (50 μ L, twice) and dried. Subsequent drying steps with methanol (100 μ L, thrice) were performed to remove residual borate. Purified glycan alditols were re-suspended in 15 μ L of water prior to MS analysis.

LC/ESI-MS/MS of released GSL glycan alditols

Glycans were analyzed by LC/MS/MS using an ion-trap mass spectrometer (LC/MSD Trap XCT Plus Series 1100, Agilent Technologies, USA) which was connected to an ESI source (Agilent 6330, USA). A volume of 4 μ L of sample was injected onto a Hypercarb porous graphitized carbon (PGC) capillary column (5 μ m Hypercarb KAPPA, 180 μ m \times 100 mm, Thermo Hypersil, Runcom, UK) using an Agilent autosampler. The separation of glycans was carried out over a linear HPLC gradient of 0–45% (v/v) acetonitrile/10 mM ammonium bicarbonate for 35 min followed by a 10-min wash-step using 90% (v/v) acetonitrile/10 mM ammonium bicarbonate at a flow rate of 3 μ L/min. The MS spectra were obtained within the mass range of m/z 200–1500. The temperature of the transfer capillary was maintained at 300 °C and the capillary voltage was set at 3 kV. Neutral and acidic glycans were detected in the negative ion reflector mode as [M–H][–] ions and their signal intensities were analyzed using ESI Compass 1.3, Data Analysis software (version 4.0, Bruker Daltonics). Structural feature ions previously identified in negative ion mode for GSLs^[3] and protein-derived glycans,^[27] together with comparisons based on MS/MS fragment ions and retention times obtained from specific glycan masses of released glycans from glycosphingolipid standards, were used to characterize and verify proposed glycan structures.

Peak area calculation for relative quantification of glycans

For the optimization experiment, the peak area-under-the-curve (AUC) was obtained using ESI Compass 1.3, Data Analysis software (version 4.0, Bruker Daltonics) for glycans released from 2, 4, 6, 8, and 10 μ g of pure GSL standards which were digested with 1 mU and 4 mU of endoglycoceramidase II enzyme. Scatter plots depicting the obtained peak area values against the various GSL standard concentrations were generated using Microsoft Excel Version 2010.

RESULTS

Determination of the minimum amount of working ceramide endoglycanase for release of glycans from PVDF-immobilized GSLs

To reliably establish the minimum amount of working enzyme (endoglycoceramidase II) for the release of the glycan from the ceramide component of PVDF-immobilized GSLs, a 5-point standard curve scatter plot for 1 mU and 4 mU enzyme was constructed using a range of PVDF-immobilized GSL standard concentrations (2, 4, 6, 8 and 10 $\mu\text{g}/\mu\text{L}$) which were plotted against the peak area-under-the-curve of glycan elution from the PGC column. For this relative quantitative analysis, two pure reference compounds, globotriosylceramide (Gb3) and asialo-GM1, were used in separate experiments. The scatter plots displaying the linear relationships (R^2) for the selected standards at different enzyme amounts are shown in Fig. 1. With Gb3 as a reference compound, we observed a low corresponding increase (1.01-fold) in the peak area when the higher enzyme (4 mU) was used. Good linearity with R^2 values of 0.9682 and 0.9970 were obtained over the range of Gb3 standard concentrations for both amounts of enzyme. Using asialo-GM1 as substrate, the hydrolytic efficiency of the ceramidase increased proportionately (4.31-fold change) upon increasing enzyme amount from 1 mU to 4 mU with linear relationships (R^2) of 0.9941 and 0.9585 using 4 mU and 1 mU of enzyme, respectively. At both enzyme amounts, sufficient fragment ions were obtained to give detailed linkage information, using as little as 2 μg of Gb3 and asialo-GM1 standard (data not shown). The differences observed in the enzymatic hydrolysis of Gb3 and asialo-GM1 have previously been attributed to the limited hydrolytic capacity of the enzyme towards oligosaccharides of the globo-series.^[3] All peak area measurements were performed in duplicates to determine the intra-assay reproducibility (Supplementary Table 1, see Supporting Information). The values of these measurements were consistent, as represented

by their standard deviation (SD) values, indicating that this method of release of glycans from GSLs is reliable for subsequent quantitation and statistical analyses to be carried out in a reproducible manner for small amounts of GSLs.

PGC-LC/ESI-MS/MS characterization of glycans released from immobilized GSL standards

Glycans were enzymatically released from GSL standards non-covalently immobilized on PVDF membranes using 4 mU endoglycoceramidase II, as illustrated in Fig. 2. The released glycans were separated on a PGC column and analyzed as underivatized, reduced alditols by an ion-trap mass spectrometer connected to a negative-mode ESI source. The chromatographic peaks observed for the standards were well resolved with low signal-to-noise ratio, yielding singly charged $[M-H]^-$ ions. The chromatographic features of the enzymatically released glycans from pure reference glycosphingolipids, singly and mixed together, were investigated in terms of their resolution, retention time and MS/MS fragmentation patterns. The structural characterization of the GSL-derived glycans was carried out based on retention times and by using the diagnostic fragment ions that have been previously reported to occur in glycans fragmented in negative mode ionization.^[3,27] The major glycosidic and cross-ring fragment ions are described for the released glycans from seven standard structures of the two different GSL classes representative of neutral GSLs (globosides and asialo-ganglio) and acidic GSLs (mono-sialylated gangliosides) and form the basis for the subsequent structural characterization of the glycans released from the GSLs extracted from ovarian cancer tissues and cell line as reported in this study.

(a) Neutral glycosphingolipids

The released glycans from immobilized neutral GSL standards consisting of lactosylceramide (LacCer), globotriosylceramide (Gb3), globotetraosylceramide (Gb4)

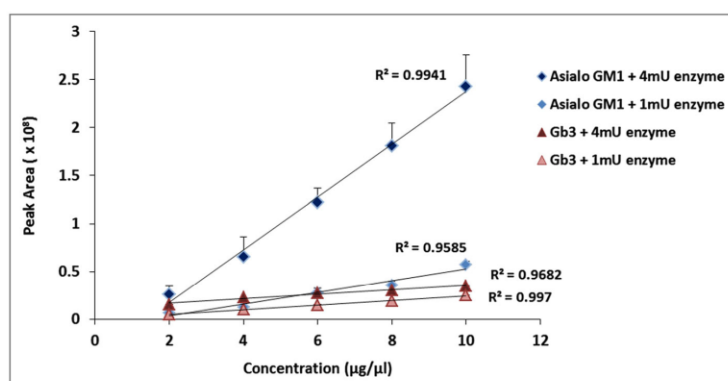


Figure 1. Determination of minimum amount of working ceramide endoglycanase for the release of glycans from PVDF-immobilized GSLs. A five-point standard curve scatter plot for 1 mU and 4 mU enzyme (endoglycoceramidase II) was constructed against the peak area-under-the-curve of elution of glycans from the PGC column released from 2, 4, 6, 8 and 10 $\mu\text{g}/\mu\text{L}$ of asialo-GM1 (ganglio-series) and Gb3 (globo-series) GSL standards.

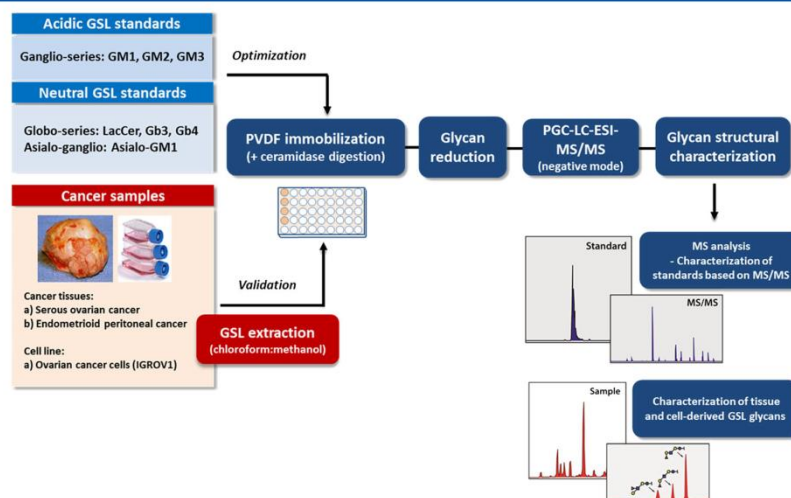


Figure 2. Illustration of the proposed workflow for analysis of glycosphingolipids (GSLs). GSL-glycans were enzymatically released from PVDF-immobilized GSL standards and extracted GSLs of cancer tissue and cell line using endoglycoceramidase II. Released glycan alditols were separated by PGC-LC/ESI and characterized based on MS/MS fragmentation of GSL standards and previously reported fragment ions in negative mode ionization.

and non-acidic tetrahexosylganglioside (asialo-GM1) which were detected as singly charged ions at retention times 5, 7, 9.8 and 18 min, respectively, are shown in Figs. 3(A)(i) and (ii). The disaccharide constituent of the lactosylceramide, Gal β 1-4Glc β 1-, was detected as m/z 343.3 $^{1-}$ (Fig. 3(B)(i)). The MS/MS spectra was characterized by glycosidic cleavages depicting the loss of the terminal Gal residue such as the prominent C $_1$ ion at m/z 179.1 $^{1-}$ and the B $_1$ ion at m/z 161.1 $^{1-}$ which was accompanied by the loss of H $_2$ O at m/z 143.1 $^{1-}$. The disaccharide glycan also contained low-abundance cross-ring cleavages such as the $^{0,2}X_2$ (m/z 223.1 $^{1-}$) and $^{2,4}X_2$ (m/z 283.1 $^{1-}$) ions occurring at the non-reducing end Gal residue. A low-abundance cross-ring cleavage ion, $^{0,2}A_2$ (m/z 281.1 $^{1-}$), of the reducing end Glc residue was also observed and this cleavage ion is most likely derived from the 4-substituted Glc residue at the reducing end of the disaccharide. The $^{0,2}A$ -type cleavage ion has been previously reported in negative ion fragmentation of oligosaccharides, observed to be characteristic of the C-4 substitution of the GlcNAc residue.^[28,29]

The MS/MS spectrum of the glycan released from globotriaosylceramide (Gb3), Gal α 1-4Gal β 1-4Glc β 1-, detected as m/z 505.3 $^{1-}$ at 7.0 min, contained prominent B $_1$ (m/z 161.1 $^{1-}$) and C $_1$ (m/z 179.2 $^{1-}$) fragment ions from the non-reducing end (Fig. 3(B)(ii)). Y ions from the reducing end of the trisaccharide were also evident such as Y $_2$ (m/z 343.1 $^{1-}$) and Y $_1$ (m/z 181.1 $^{1-}$) ions that have been previously observed in the MS 2 spectrum of native globotriaosylceramide oligosaccharides analyzed in negative mode ionization.^[3] The MS 2 spectra also contained an abundant cross-ring cleavage ion, the $^{2,4}A_2$ fragment ion observed as m/z 221.0 $^{1-}$. This ion has also been previously observed,^[3] confirming the 4-linked Gal to the internal Gal β 1-4Glc β 1 of the Gb3 trisaccharide.

The glycan released from globotetraosylceramide (Gb4), GalNAc β 1-3Gal α 1-4Gal β 1-4Glc β 1-, was detected as m/z 708.3 $^{1-}$ at 10 min. The fragmentation of this larger oligosaccharide resulted in B- and C-type fragment ions such as the C $_1$ ion at m/z 220.1 $^{1-}$, the C $_2$ ion at m/z 382.1 $^{1-}$ and the B $_3$ ion at m/z 526.0 $^{1-}$ (Fig. 3(B)(iii)). Fragmentation from the reducing end also resulted in several Y-ion fragments identified as m/z 343.2 $^{1-}$ (Y $_2$ ion) and m/z 505.2 $^{1-}$ (Y $_3$ ion) while the Z $_3$ (m/z 487.2 $^{1-}$) ion resulting from the loss of the terminal GalNAc residue was also present. The sequential loss of monosaccharide residues resulting in the glycosidic cleavage ions B, C, Y and Z corresponded well to the identification and verification of the tetrasaccharide glycan. The cross-ring cleavage ion, $^{0,2}A_3/Z_3$, at m/z 263.1 $^{1-}$ was also observed with a relatively high intensity. The prominent cross-ring cleavage corresponding to $^{2,4}A_3$ at m/z 424.1 $^{1-}$ further confirmed the presence of 4-linked Gal to the internal Gal β 1-4Glc β 1 of the Gb4 tetrasaccharide as described previously.^[3]

The non-sialylated ganglioside, asialo-GM1, was also structurally characterized by negative ion fragmentation. The gangliotetraosylceramide, Gal β 1-3GalNAc β 1-4Gal β 1-4Glc β 1-, was detected by PGC chromatography as m/z 708.3 $^{1-}$ at 18 min (Fig. 3(A)(ii)). This structure, although identical to the mass of the previously described globotetraosylceramide (Fig. 3(A)(i); GalNAc β 1-3Gal α 1-4Gal β 1-4Glc β 1) differs in sequence and linkage of the terminal GalNAc and Gal residues. Negative ion PGC-LC/ESI-MS/MS fragmentation was utilized to differentiate these isomeric structures based on their different retention times and fragmentation patterns (Fig. 3(B)(iv)). The tandem mass spectra of this oligosaccharide showed a prominent Y $_2$ ion at m/z 343.1 $^{1-}$ which corresponded to the Gal-Glc disaccharide sequence at the reducing terminal end while the non-reducing end disaccharide was defined by the B $_2$ ion at m/z 364.1 $^{1-}$. In

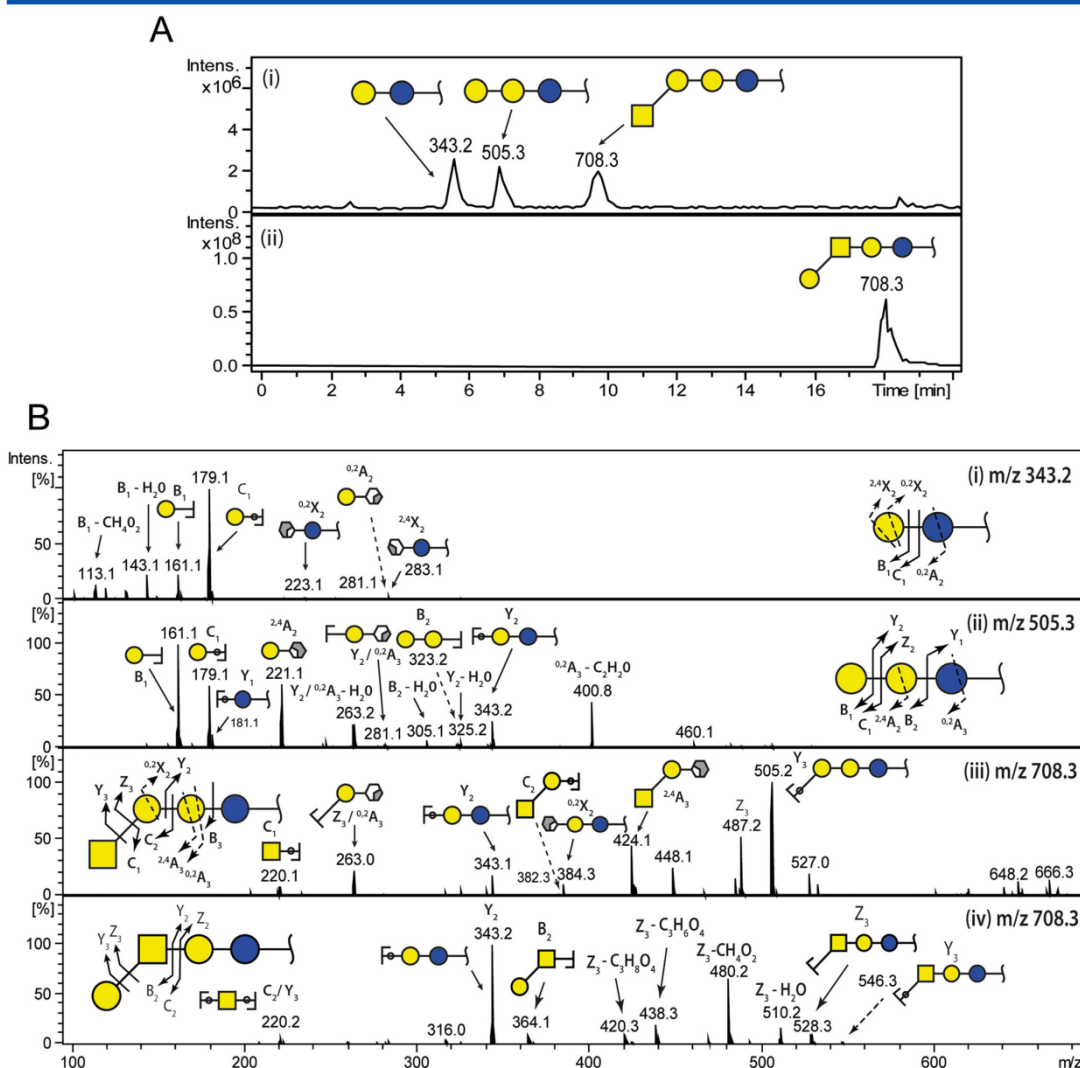


Figure 3. LC/MS of glycans released from PVDF-immobilized neutral GSL standards, lactosylceramide (LacCer; Gal β 1-4Glc β 1), globotriaosylceramide (Gb3; Gal α 1-4Gal β 1-4Glc β 1), globotetraosylceramide (Gb4; GalNAc β 1-3Gal α 1-4Gal β 1-4Glc β 1) and non-acidic tetrahexosylganglioside (asialo-GM1; Gal β 1-3GalNAc β 1-4Gal β 1-4Glc β 1). Base peak chromatograms of these glycans are represented for LacCer (m/z 343.0¹⁻; retention time: 5.0 min), Gb3 (m/z 505.3¹⁻; retention time: 7.0 min), Gb4 (m/z 708.3¹⁻; retention time: 9.8 min) and asialo-GM1 (m/z 708.3¹⁻; retention time: 18.0 min (lower panel-ii)] (A). MS² spectrum of the precursor ion at m/z 343.0¹⁻, 505.3¹⁻ and 708.3¹⁻ derived from LacCer (i), Gb3 (ii), Gb4 (iii), and asialo-GM1 (iv), respectively (B).

addition to these ions, the MS/MS spectrum of this structure also yielded a Z ion cleavage at m/z 528.3¹⁻ that was further accompanied by fragment ions in the MS² spectrum which corresponded to the loss of acetyl ($M = 42$ Da; C₂H₂O) and acetate ($M = 60$ Da; C₂H₄O₂) groups from the precursor ion. For example, there was an abundant Z₃-CH₂O₂ ion at m/z 480.2¹⁻ while several low-abundance ions at m/z 468¹⁻, 438.2¹⁻ and 420.2¹⁻ were also observed which corresponded to Z₃-C₂H₄O₂, Z₃-C₃H₆O₄ and Z₃-C₃H₈O₄, respectively. The diagnostic cross-ring fragment ion, ^{2,4}A₂

(m/z 221.0¹⁻), characteristic for the 4-linked terminal Gal, was not observed, further confirming the C-3 substitution of the GalNAc residue of the Gal β 1-3GalNAc β 1-4Gal β 1-4Glc β tetrasaccharide.

(b) Mono-sialylated glycosphingolipids

The released glycans of the mono-sialylated ganglioside GSL standards were comprised of GM1, GM2, and GM3 oligosaccharides containing a α 2-3-linked sialic acid linked

to the innermost Gal residue attached to the reducing end glucose moiety. As previously noted in negative ion mode fragmentation, abundant cross-ring cleavages which are commonly observed in neutral glycans are found to be low or absent in the fragmentation patterns of sialylated glycans.^[27] The loss of the acidic species requires intense energy for the dissociation of these highly charged residues, and as a result subdues the fragmentation of other ions such as A- and X-type cleavages that can provide greater structural detail.^[30] Nevertheless, the fragmentation spectra of these mono-sialylated structures contained sufficient information to be useful in confirming their composition. Figure 4(A)

shows the extracted ion chromatogram (EIC) of the first eluting compound GM2, GalNAc β 1-4(NeuAc α 2-3)Gal β 1-4Glc β 1-, which was detected as a singly charged ion of m/z 837.4¹⁻ at 5 min. The cleavage of the sialic acid residue was observed as intense B_{1a} and Y_{2a} ions at m/z 290.1¹⁻ and m/z 546.2¹⁻ respectively (Fig. 4(B)(i)). Double cleavages resulting from the loss of both the sialic acid and GalNAc residues were also observed at m/z 343.0¹⁻ (Y_{2a}/Y_{2b}).

GM1, Gal β 1-3GalNAc β 1-4(NeuAc α 2-3)Gal β 1-4Glc β 1-, was detected as m/z 999.4¹⁻ and was observed to elute at 6 min (Fig. 4(A)). Similar to the previous GM2, the abundant ions were the fragments formed due to the loss of the sialic acid

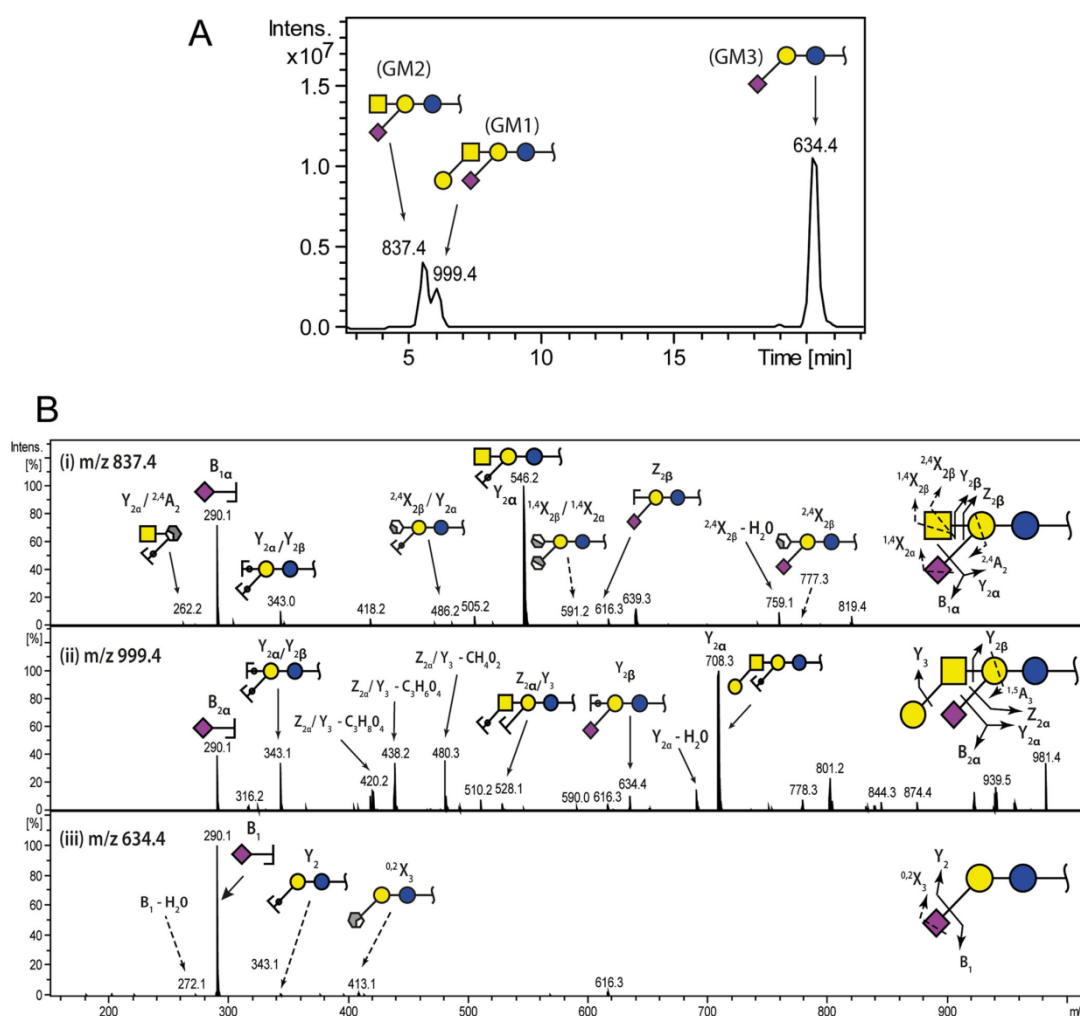


Figure 4. LC/MS of glycans released from PVDF-immobilized acidic (mono-sialylated) glycosphingolipid standards, mono-sialotetrahexosylganglioside (GM1; Gal β 1-3GalNAc β 1-4(NeuAc α 2-3)Gal β 1-4Glc β 1), mono-sialotrihexosylganglioside (GM2; GalNAc β 1-4 (NeuAc α 2-3)Gal β 1-4Glc β 1) and mono-sialodihexosylganglioside (GM3; (NeuAc α 2-3) Gal β 1-4Glc β 1). Base peak chromatograms of these glycans are represented for GM2 (m/z 837.4¹⁻; retention time: 5.0 min), GM1 (m/z 999.4¹⁻; retention time: 6.0 min) and GM3 (m/z 634.4¹⁻; retention time: 21.0 min) (A). MS² spectrum of the precursor ion at m/z 837.4¹⁻, 999.4¹⁻ and 634.4¹⁻ derived from GM2 (i), GM1 (ii), and GM3 (iii), respectively (B).

residue, as exemplified by the B_{2a} and Y_{2a} ions at m/z 290.1¹⁻ and 708.3¹⁻, respectively. Likewise, the double cleavages of both the sialic acid and terminal Gal residues resulting in the Z_{2a}/Y_3 fragment ion were observed at m/z 528.2¹⁻ and the Y_{2a}/Y_{2b} fragment ion at m/z 343.0¹⁻ corresponding to the loss of the sialic acid, Gal and GalNAc residues. Several neutral losses from the glycosidic fragment ion Z_{2a}/Y_3 were also observed, such as m/z 480.2¹⁻, 438.2¹⁻ and 420.2¹⁻ fragment ions which correspond to $Z_{2a}/Y_3-CH_4O_2$, $Z_{2a}/Y_3-C_3H_6O_4$ and $Z_{2a}/Y_3-C_3H_8O_4$, respectively (Fig. 4(B)(ii)).

The late elution of the trisaccharide, GM3 [(NeuAcα2-3Galβ1-4Glcβ1)], illustrates the non-linear retention characteristics of PGC chromatography. This structure was detected as a singly charged ion at m/z 634.2¹⁻ and was shown to elute at 21.0 min. The fragmentation spectra contained mainly the B_1 ion at m/z 290.1¹⁻ with the corresponding Y_2 ion at m/z 343.0¹⁻ from the loss of the sialic acid residue with little further fragmentation (Fig. 4(B)(iii)).

Method validation on GSLs extracted from ovarian and peritoneal cancer samples

1. Structural characterization of GSL-derived glycans from cancer tissues

To validate that this platform of GSL analysis is applicable for complex tissue samples, GSLs were extracted from ovarian and peritoneal cancer tissues using the Bligh and Dyer extraction procedure. This method is commonly employed in many studies involving extraction of lipids from tissue samples with high water content and is comprised of a methanol/chloroform/water extraction.^[31] The extracted lipids were immobilized on PVDF membrane and ceramide endoglycanase-released oligosaccharides were analyzed using negative ion LC/ESI-MS/MS. Nine mass ions corresponding to 16 glycan structures (including isomeric structures) were detected in the base peak chromatograms, as listed in Table 1. The characterization of these isomeric glycans is described in detail in the following sections.

(a) Neutral fucosylated pentaglycosylceramides

The extracted ion chromatogram (EIC) of m/z 854.3¹⁻ of both types of cancer tissues (S565 and S566) revealed three and two isomeric structures, respectively, corresponding to the fucosylated pentasaccharide composition of Gal(Fuc)HexNAc-Gal-Glc (Figs. 5(A)(i) and (ii)). The first isomer eluted at 19.4 min and the MS/MS spectrum consisted of an abundant Y_2 fragment ion at m/z 343.1¹⁻ (Gal-Glc), a double cleavage Y_{3a}/Y_{3b} ion at m/z 546.0¹⁻ (HexNAc-Gal-Glc) and a Y_{3a} ion at m/z 692.4¹⁻ (HexNAc(Fuc)-Gal-Glc) which helped resolve the monosaccharide sequence of this structure (Fig. 5(B)(i)). The B_2 fragment ion at m/z 510.2¹⁻ in the MS/MS spectrum is comprised of Gal-Fuc-HexNAc and is commonly observed for terminal fucosylated trisaccharides in *N*- and *O*-glycans.^[27,32] The fragment ion at m/z 348.1¹⁻ is diagnostic for the internal 3-linked HexNAc substituted with a Fuc residue at C-4, and is a result of the double glycosidic cleavages (B_2/Y_{3a}) of the 3-linked Gal residue (m/z 162.0¹⁻ loss from the m/z 510.2¹⁻ fragment ion). This phenomenon is thought to occur as the C-3 linkage residue is more labile when the GlcNAc is di-substituted at C-3 and C-4 and is

consistent with previous reports of the fragmentation of Lewis-type fucosylated glycans analyzed in negative ion mode.^[27] Cross-ring cleavage of the terminal Gal at m/z 438.2¹⁻ and m/z 420.2¹⁻ resulting from the m/z 510.2¹⁻ ion was also observed. The absence of the characteristic ^{0,2}A₃ cross-ring cleavage of the inner Gal residue further confirms a Lewis A pentasaccharide [Galβ1-3(Fucα1-4)GlcNAcβ1-3Galβ1-4Glc] for this structure.

The second and third eluting isomers were shown to elute at 22.0 and 24.2 min, respectively (Fig. 5(A)(ii)). The tandem spectra for both isomers (Figs. 5(B)(ii) and (iii)) showed a series of prominent B- and C-ions at m/z 510.2¹⁻ (B_3), 325.2¹⁻ (C_2), 528.3¹⁻ (C_3) and 690.2¹⁻ (C_4), which tentatively identified the pentasaccharide sequence of (Fuc)Gal-HexNAc-Gal-Glc. Unlike the first isomer which has a fucose residue linked to the GlcNAc, both these later eluting isomeric structures contain the H epitope where the fucose residue is attached to the terminal Gal residue in a α1-2 linkage. This is substantiated by the fragment ions at m/z 307.0¹⁻ (B_2) and 325.2¹⁻ (C_2) corresponding to a fragment ion comprising of a galactose and fucose residue.

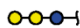
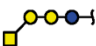
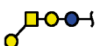

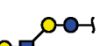
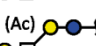

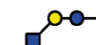


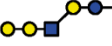
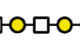


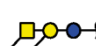
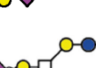
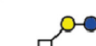
The third eluting isomer was found to contain the H type 2 epitope, that is distinguished from the H type 1 epitope observed in the second eluting isomer by the presence of the diagnostic cross-ring cleavage ion at m/z 409.3¹⁻ (^{0,2}A₃-H₂O) and ^{0,2}A₃ fragment ion at m/z 427.3¹⁻ previously observed in negative ion fragmentation of type 2 chains (Galβ1-4GlcNAc).^[3] Similar to the first eluting isomer, the MS/MS spectra of both these late-eluting isomers (Figs. 5(B)(ii) and (iii)) did not contain the ^{0,2}A₄ fragment ion which is characteristic of C-4 substitution of the inner Gal residue, suggesting that the GalNAc residue is β1-3 linked to the inner Gal residue. These structures were tentatively identified as type 1 H antigen [(Fucα1-2)Galβ1-3GlcNAcβ1-3Galβ1-4Glc] and type 2 H antigen [(Fucα1-2)Galβ1-4GlcNAcβ1-3Galβ1-4Glc], respectively.

(b) Neutral tetraosylceramides

Several isomers of the neutral tetrasaccharide with m/z 708.3¹⁻ were also detected in both tissue samples (Fig. 6(A)). Four isomers of this glycan were characterized based on the informative spectra and specific structural feature ions obtained from the negative ion fragmentation. The first isomer eluted at 16.9 min (Figs. 6(A)(i) and (ii)) and the MS/MS spectra consisted of a prominent Y_3 ion (m/z 505.3¹⁻) and Y_2 (m/z 343.3¹⁻) ion which were characteristic for the Gal-Gal-Glc and Gal-Glc sequences, arising from cleavages to the non-reducing terminal (Fig. 6(B)(i)). The loss of the HexNAc residue at the terminal end as a result of the glycosidic cleavage at m/z 220.0¹⁻ (C_1) further confirmed the tetrasaccharide sequence, HexNAc-Gal-Gal-Glc. The presence of the diagnostic cross-ring cleavage ions at m/z 424.1¹⁻ (^{2,4}A₃) and 263¹⁻ (^{0,2}A₃/Z₃) corresponded to the C-4 substitution of the Gal-Glc lactose residue at the reducing end, thereby identifying this structure as GalNAcβ1-3Galα1-4Galβ1-4Glcβ1 or globotetraosylceramide, Gb4. The fragmentation pattern of this isomer is also consistent with the elution time of the Gb4 standard that was ran concurrently (Fig. 6(A)(iv)).

The tandem mass spectrum for the second isomeric mass which eluted at 18.6 min was observed to be quite different to the first isomer (Fig. 6(B)(ii)). The Y_3 ion at m/z 505.3¹⁻,

Table 1. Proposed GSL-glycan structures detected on the glycolipid membranes of serous ovarian cancer tissue (S565), endometrioid peritoneal cancer tissue (S566) and epithelial ovarian cancer cells (IGROV1). Structures were assigned based on MS/MS fragmentation (where possible) and known biological GSL synthetic pathway constraints. Glycan masses that were either partially assigned or determined to consist of acetyl modifications are indicated with asterisks (*). All structures were depicted according to the CFG (Consortium of Functional Glycomics) notation with linkage placement to indicate linkages for fucose and sialic acid residues. Specific linkages corresponding to Gal-GlcNAc (type 1/type 2) lactosamine linkages are also indicated (where possible)

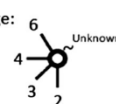
Type	Glycan mass [M-H] ⁻	GSL series/type	Proposed structure	Relative intensity (%)		
				S565	S566	IGROV1
Neutral GSL-glycans	505.3	Globo (Gb3)		4.16	3.59	-
	708.3a	Globo (Gb4)		1.94	4.98	-
	708.3b	Ganglio (Asialo-GM1)		9.85	7.58	-
	708.3c*	-		-	9.86	-
	708.3d	Neo-lacto		52.49	46.91	7.64
	750.3*	-		15.99	-	-
	854.3a	Lacto (Lewis A)		1.56	4.86	-
	854.3b	Lacto (H epitope)		1.92	-	-
	854.3c	Neo-lacto (H epitope)		5.92	4.26	-
	870.3	Neo-lacto		2.08	9.95	2.43
	1032.4*	-		1.86	4.35	-
	634.4	Ganglio (GM3)		1.74	3.67	12.86
Acidic GSL-glycans	837.4	Ganglio (GM2)		0.49	-	73.11
	999.4a	Ganglio (GM1)		-	-	0.68
	999.4b	Neo-lacto		-	-	2.15
	999.4c	Lacto		-	-	1.14
						

Legend:

● Glucose
▲ Fucose
● Galactose

◆ N-acetylneuraminic acid
■ N-acetylglucosamine
■ N-acetylgalactosamine

Monosaccharide Linkage:



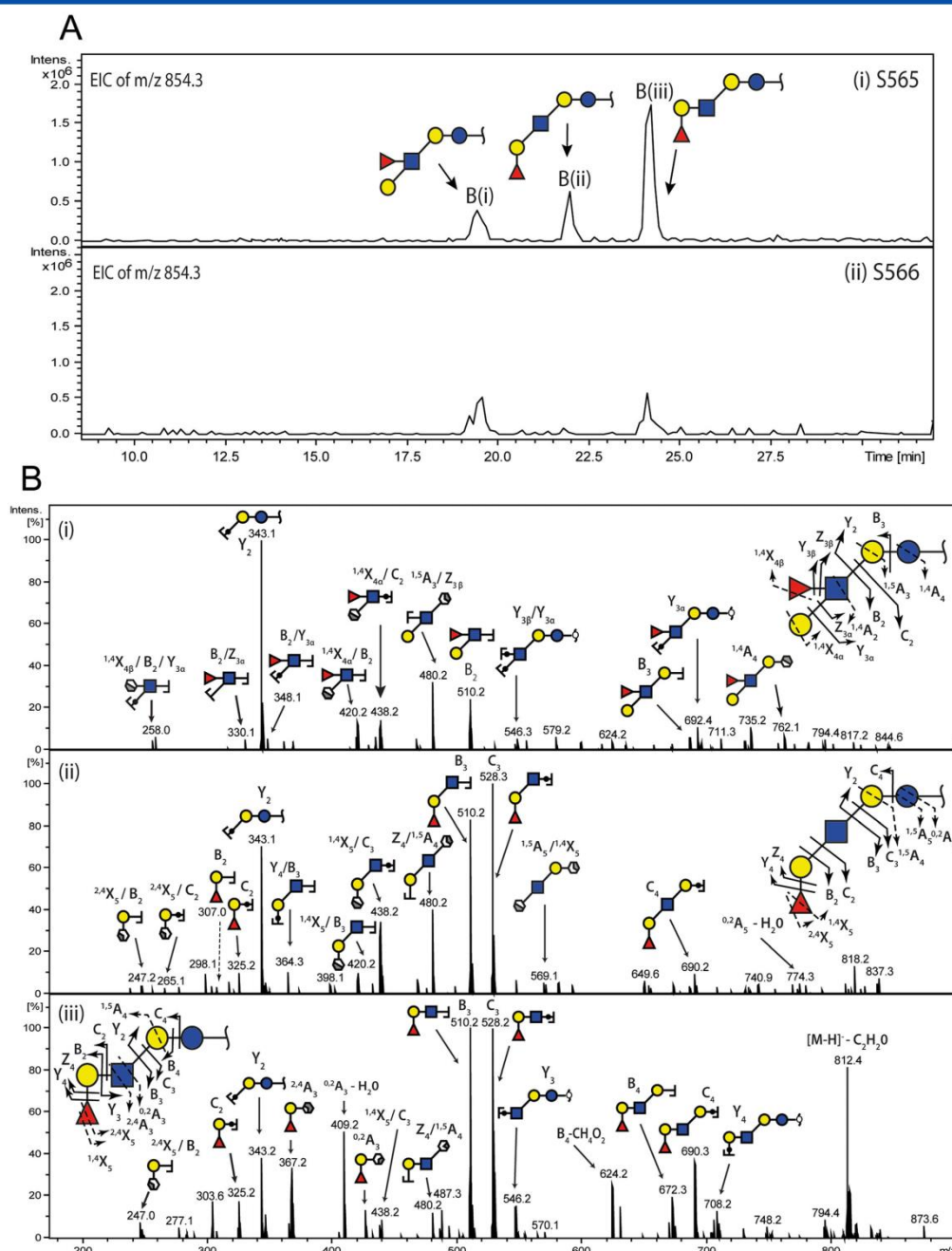


Figure 5. Extracted ion chromatograms (EICs) of pentasaccharide GSL-glycan with m/z 854.3¹⁻ from serous ovarian cancer (S565) and endometrioid peritoneal cancer (S566) tissues. The EICs obtained from serous ovarian cancer (S565) depict three isomeric structures eluting at 19.4 min (i), 22.0 min (ii), and 24.2 min (iii), respectively, while endometrioid peritoneal cancer (S566) tissues displayed only two isomeric structures eluting at 19.4 min (i) and 24.2 min (ii), respectively (A). MS² spectrum of the precursor ion at 854.3¹⁻ tentatively identified these structures as Lewis A pentasaccharide [Gal β 1-3(Fuc α 1-4)GlcNAc β 1-3Gal β 1-4Glc] (i), H type 1 pentasaccharide [(Fuc α 1-2Gal β 1-3GlcNAc β 1-3Gal β 1-4Glc] (ii), and H type 2 pentasaccharide [(Fuc α 1-2Gal β 1-4GlcNAc β 1-3Gal β 1-4Glc] (iii) (B).

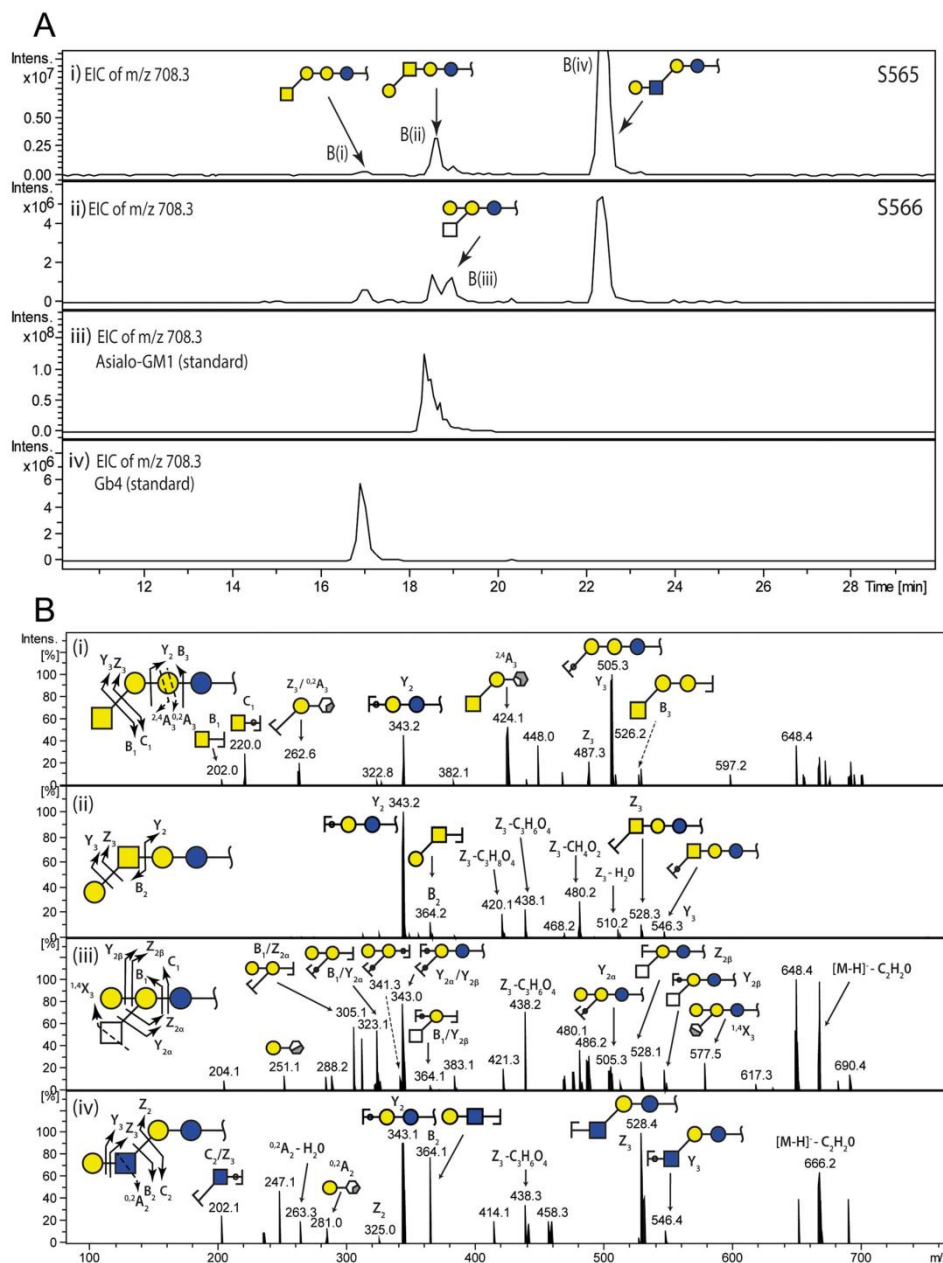


Figure 6. Extracted ion chromatograms (EICs) of tetrasaccharide GSL-glycan with m/z 708.3¹⁻ from serous ovarian cancer (S565) and endometrioid peritoneal cancer (S566) tissues. The EICs obtained from serous ovarian cancer (S565) depict three isomeric structures eluting at 16.9 min (i), 18.6 min (ii), and 22.4 min (iii), respectively, while endometrioid peritoneal cancer (S566) tissues displayed four isomeric structures eluting at 16.9 min (i), 18.6 min (ii), 19.0 min (iii), and 22.4 min (iv), respectively (A). MS² spectrum of the precursor ion at m/z 708.3¹⁻ tentatively identified these structures as Gb4 [GalNAc β 1-3Gal α 1-4Gal β 1] (i), Asialo-GM1 [Gal β 1-3GalNAc β 1-4Gal β 1] (ii), branched-type [Gal α 1-?Gal(HexNAc β 1-?) β 1-?Glc β 1] (iii), and [Gal β 1-4GlcNAc β 1-3Gal β 1-4Glc β 1] (iv) (B).

characteristic for the Gal-Gal-Glc sequence, was found to be absent, while the Z_3 ion at m/z 528.2¹⁻ resulting from the loss of the terminal Gal residue was observed, thereby confirming the Gal-HexNAc-Gal-Glc sequence. In addition, and similar to the fragment ions that were previously observed for the asialo-GM1 (Fig. 3(B)(iv)), neutral losses from the glycosidic fragment ion, Z_3 (528.2¹⁻), were also present, such as the fragment ions at m/z 480.2¹⁻, 438.1¹⁻ and 420.1¹⁻. The tetrasaccharide was identified as Gal β 1-3GalNAc β 1-4Gal β 1-4Glc β -asialo, which is the precursor to the formation of the ganglioside, GM1.

The MS/MS spectrum of the third eluting isomer of m/z 708.3¹⁻ at 19.0 min (Fig. 6(B)(iii)) displayed a mixture of fragment ions that resembled a branched-type glycan structure as opposed to a linear tetrasaccharide. This observation was substantiated by fragment ions at Z_{2a} (m/z 528.3¹⁻) and Y_{2a} (m/z 546.3¹⁻) which confirmed the HexNAc-Gal-Glc sequence, while the fragment ion at Y_{2b} (m/z 505.3¹⁻) corresponded tentatively to the Gal-Gal-Glc sequence. Glycosidic cleavages corresponding to the terminal Gal-Gal sequence were also observed as m/z 341.3¹⁻ (C_1/Y_{2a}), 323.1¹⁻ (B_1/Y_{2a}) and 305.1¹⁻ (B_1/Z_{2a}) fragment ions. The sequence proposed for this structure is Gal-Gal(HexNAc)-Glc β as insufficient fragment ions diagnostic for specific linkages and monosaccharide composition were not observed in the MS² spectrum.

The last eluting and most abundant structure, detected as m/z 708.3¹⁻ in both tissues, eluted at 22.4 min (Figs. 6(A)(i) and (ii)). The MS/MS spectrum was dominated by a prominent Y_2 ion at m/z 343.1¹⁻, Z_3 ion at m/z 528.2¹⁻ and B_2 ion at m/z 364.1¹⁻ indicative of the Gal-HexNAc-Gal-Glc sequence (Fig. 6(B)(iv)). In addition, the spectrum also contained a fragment ion at m/z 325.2¹⁻ (Z_2), resulting from the cleavage of the terminal Gal-HexNAc. The absence of the ^{2,4}A₃ cross-ring cleavage ion (m/z 424.1¹⁻), which was previously described as diagnostic for 4-linked HexNAc, suggests that the HexNAc is possibly linked to the internal Gal via a β 1-3 linkage. Several fragment ions arising from cleavages at the non-reducing terminal end were also present, such as the ^{0,2}A₂ and ^{0,2}A₂-H₂O cross-ring cleavages which confirmed the terminal Gal β 1-4 linkage to the HexNAc. Based on the assignment of these fragment ions and the longer retention time on the column as noted previously for GlcNAc-containing glycans,^[3] the tetrasaccharide was assigned as Gal β 1-4GlcNAc β 1-3Gal β 1-4Glc β 1.

2. Structural characterization of gangliosides from ovarian cancer cell line, IGROV 1

To further investigate the applicability of this method, glycolipids were extracted from approximately 1×10^7 cells of the ovarian cancer cell line, IGROV 1. The modified Folch extraction procedure was used in this case as it has been previously used as a reliable method for the enrichment of the sialylated acidic gangliosides from cells grown in culture.^[26] After ceramide-glycanase treatment of the PVDF-immobilized extracted glycolipids, we were able to identify several acidic released glycans eluting as m/z 837.4¹⁻, 634.4¹⁻ and 999.4¹⁻ as well as neutral structures (Table 1). Three isomeric glycan structures of m/z 999.4¹⁻ were detected (Fig. 7(A)) and were characterized based on their retention times and diagnostic fragments as observed in the analysis of the

mono-sialylated glycan standards previously described in Fig. 4. The tandem mass spectra of the sialylated glycans predominantly consisted of Y and Z ion cleavages corresponding to the loss of the acidic residue (m/z 343.1¹⁻, 708.3¹⁻ and 528.4¹⁻) (Figs. 7(B)(i), (ii) and (iii)). The first eluting glycan, at 20.9 min (Fig. 7(B)(i)), contained fragment ions identical to those of the pentasaccharide structure of GM1 (Gal β 1-3GalNAc β 1-4(NeuAc α 2-3)Gal β 1-4Glc β 1), as described in the standard (Fig. 4(B)(ii)). Glycosidic cleavage depicting the loss of the sialic acid at m/z 290.1¹⁻ (B_1) was present in abundance. The position of the sialic acid at the inner Gal residue was further confirmed by the loss of the Gal-GalNAc disaccharide from the terminal end of the pentasaccharide, thereby resulting in fragment ion masses at m/z 616.3¹⁻ (Z_3) and 634.4¹⁻ (Y_{2b}), respectively.

The second and third glycan structures of m/z 999.4¹⁻ eluted later at 24.5 and 25.5 min, respectively (Figs. 7(B)(ii) and (iii)). The MS² spectra contained a characteristic fragment ion at m/z 655.3¹⁻ which was indicative of the sialic acid being linked to the Hex-HexNAc moiety of the pentasaccharide. Previous studies have observed diagnostic ions which could potentially distinguish between the α 2-3 and α 2-6 Neu5Ac linkage to the Gal in negative ion mode.^[33,34] Specifically, using argon as the collision gas, it was shown that the ^{0,2}A-CO₂ cross-ring cleavage ion at m/z 306¹⁻ corresponded to the α 2-6 Neu5Ac linkage in small, unreduced glycans. This ion was not present in any of the MS² spectra of these pentasaccharide isomeric structures, which is consistent with the fact that this fragment is not formed when the collision gas used is helium,^[27] as was the case in this study. These pentasaccharide structures were further differentiated into type 1 and type 2 chains based on the presence of the diagnostic ^{0,2}A₃-H₂O fragment ion at m/z 554.3¹⁻ which is characteristic of the C-4-substituted HexNAc observed only in MS² fragmentation of the second eluting isomer (Fig. 7(B)(ii)). These two structures were tentatively assigned as NeuAc α 2-7Gal β 1-4HexNAc β 1-3Gal β 1-4Glc and NeuAc α 2-7Gal β 1-3HexNAc β 1-3Gal β 1-4Glc, respectively. As previously noted in the analysis of neutral tetraosylceramides, it is also possible that these structures contain GlcNAc as GlcNAc-containing glycan moieties are retained relatively longer as compared to GalNAc-containing glycans in PGC liquid chromatography.^[3]

DISCUSSION

Glycosphingolipids (GSLs) constitute a unique class of membrane glyco-conjugates which exhibit diverse complexity in both their carbohydrate moiety and lipid backbone structure.^[11] To date, many studies have been performed to elucidate the expression of GSLs, with regard to their organization and function within the membrane.^[35,36] The glycosylated motifs in GSLs, however, are less extensively studied as compared to other glycolipids. In fact, in some cases, glycolipids have been shown to contain specific carbohydrate motifs that are not present on glycoproteins such as the Gal α 1-4Gal sequence of the (neo-)lacto-, globo-series or the GalNAc β 1-4Gal β 1-4Glc β - sequence of the gangliosides.^[3] In this study, we employed the use of the hydrophobic PVDF membrane to efficiently immobilize the extracted GSLs prior to the release

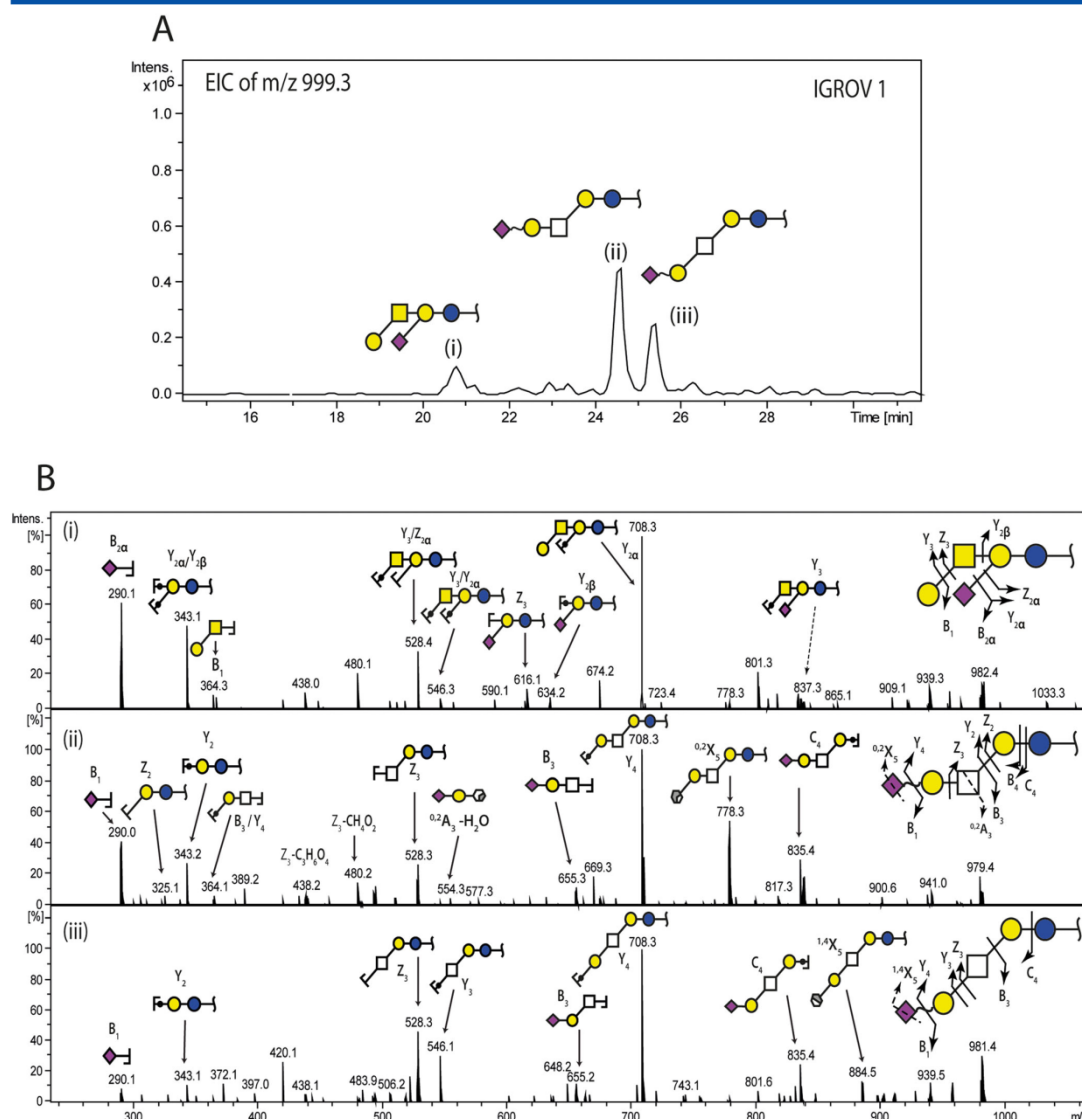


Figure 7. Extracted ion chromatograms (EICs) of pentasaccharide GSL-glycan with m/z 999.4¹⁻ in ovarian epithelial cancer cell line, IGROV1. The EICs obtained depict three glycan structures eluting at 20.9 min (i), 24.5 min (ii), and 25.5 min (iii), respectively (A). MS² spectrum of the precursor ion at m/z 999.4¹⁻ tentatively identified these structures as GM1 [Gal β 1-3GalNAc β 1-4(NeuAc α 2-3)Gal β 1-4Glc β 1] (i), type 2 sialyl-tetraosylceramide [NeuAc α 2-?Gal β 1-4HexNAc β 1-3Gal β 1-4Glc] (ii), and type 1 sialyl-tetraosylceramide [NeuAc α 2-?Gal β 1-3HexNAc β 1-3Gal β 1-4Glc] (iii) (B).

of glycans by the commercially available enzyme, endoglycoceramidase II (EGCase II). This method, as demonstrated in our study, is sensitive and compatible with subsequent PGC-LC/ESI-MS/MS detection of label-free glycans and presents an efficient platform for the detailed analysis of the glycosylation of the GSLs. As proof of concept, we structurally characterized neutral and acidic glycans derived from reference GSL standards. We further applied the workflow to ovarian cancer tissue and cell line

samples, in which the entire protocol, inclusive of GSL extraction, PVDF immobilization, enzymatic release of glycans and the LC/MS detection of glycans, was performed within 5 days. The detailed structural characterization of these glycans, however, was more time-consuming as it still requires manual assignment of structures based on prior knowledge of negative mode fragmentation patterns. We have also recently used this approach to validate the P blood group-related antigens on ovarian cancer cells and tissues.^[37]

As previously demonstrated for glycoproteins,^[23] the efficient immobilization of the glycolipids to the PVDF membrane is thought to occur *via* hydrophobic surface interactions; in this case between the hydrophobic ceramide portion of the extracted GSLs and the hydrophobic PVDF membrane. Hence, the binding of the hydrophobic lipid portion of the GSL to the PVDF membrane allows the hydrophilic glycans on the surface of the PVDF membrane to be more accessible to the enzyme.^[38] In addition, there are also the added advantages of increased sensitivity/activity of solid-phase chemistry where the analyte is concentrated on the surface; increased ease of washing for removal of contaminants and decreased non-specific binding of the endoglycoceramidase which has been previously shown to have binding domains that recognize both the glycan and the lipid portion of the GSL.^[39,40] Recent structural and mechanistic analysis of the EGC enzyme showed that it is amphiphilic, bearing both hydrophilic and hydrophobic domains which allow for the differential recognition of GSL substrates.^[41] Specifically, the active site of this enzyme displays a broad, polar cavity which is lined with polar residues which facilitate the binding to the oligosaccharide moiety as compared to a narrow, hydrophobic channel which preferentially binds to the ceramide head of GSLs. Unlike the EGC I enzyme isolated from *M. decore* sp., which exhibits a hydrolytic specificity towards a broad range of GSL series,^[39] the only commercially available EGC II enzyme, which is presently available and isolated from *Rhodococcus* sp., preferentially binds to the carbohydrate moieties which include the ganglio-, neolacto- and lacto-GSL series.^[40] This limiting factor has been noted in several studies whereby several acidic GSLs of the cerebroside- and ganglio-series such as sulfatides, GD1b and fucosyl-GM1 as well as other GSLs of the galactosylceramide and globo series have been proven to be relatively resistant to the enzyme.^[3,40]

In view of the inherent limitations of the enzyme, several attempts have been made to enhance the enzyme specificity by increasing the glycolipid concentration, enzyme concentration as well as incubation hours of the reaction mixture. In one study, final concentrations of glycolipid standards ranged from 20–50 µg for 1 mU of enzyme with incubation hours ranging from 16 to 48 h.^[42] Similarly, in a more recent study by Karlsson *et al.*, the authors indicated that while 1 mU of endoglycoceramidase II enzyme was sufficient to hydrolyze 50 µg of GSLs of the iso-globo-GSL series, higher enzyme concentrations together with a 48-h incubation period were required for the partial release of globo series GSLs, Gb3 and Gb4.^[3] However, as shown in our experiments using the PVDF membrane to immobilize the glycolipids, we were able to detect glycans derived from 2 to 10 µg of asialo-GM1 and Gb3 standards using as little as 1 mU of enzyme with a 16-h incubation period. This improved sensitivity may be attributed to the immobilization of GSLs on the PVDF membrane providing a larger surface area for the interaction between the enzyme and the glycan portion of the GSLs as compared to an in-solution digestion. Nevertheless, we did observe a 10-fold decreased release of glycans from Gb3 compared to asialo-GM1, even when the enzyme was increased to 4 mU. To validate the approach in biological samples, glycans were

released from lipids extracted from approximately 100 mg of serous ovarian and endometrioid peritoneal cancer tissues and 1×10^7 ovarian cancer cells using 4 mU of EGC II enzyme. Other studies have used varying enzyme concentrations to optimize the recovery of glycans from GSLs for subsequent MS analysis. One study^[24] used 10 mU of enzyme for approximately 20 mg of tissue sample over a 16-h incubation period, while another study^[43] used a lower enzyme concentration of 2 mU for 20 mg of tissue samples (100 mU = 1 g of tissue) with an incubation time of 24 h. These studies utilized the in-solution digestion system, in which enzyme concentrations appear to be significantly higher than those used in this study to ensure sufficient hydrolysis of glycans from GSLs.

In addition, to date, various studies investigating the enzymatic de-glycosylation of GSLs have been usually carried out in detergent-based solutions,^[3,22,43] which include the addition of non-ionic detergents such as Triton X-100^[44] as well as bile salts such as sodium cholate and sodium taurodeoxycholate^[40] to solubilize the GSLs and increase enzyme activity. The use of Triton X-100 has been thought to increase the initial reaction velocity of the enzyme,^[44] and this effect was substantiated in another study where the authors concluded that the addition of this detergent played dual roles in enhancing both the solubility of the enzyme and that of the GSLs by the formation of GSL-detergent micelles in the solution.^[40] Due to the difficulties associated with the removal of Triton X-100 and potential contamination of the detergent in MS analysis, bile salts are more commonly used, for example, for the hydrolysis of GSLs by glycosidases such as endo- β -galactosidase,^[45,46] because of their compatibility with downstream mass spectrometry analysis.^[3,22,43] Alternatively, organic solvents such as dimethyl sulfoxide (DMSO), dimethylformamide (DMF) and tetrahydrofuran (THF) that can be removed *via* evaporation have also been used to facilitate the release of glycans from GSLs.^[47] Utilizing the PVDF-immobilization of GSLs, we have shown that the use of detergents or bile salts is not necessary for the enzymatic hydrolysis, as there is no requirement for solubility of the lipids that have been immobilized. By doing so, we were also able to eliminate the subsequent clean-up steps thereby reducing the workflow, decreasing sample losses and preventing detergent contamination of the subsequent MS analysis. The advantages of the methods were evidenced by the high-quality mass spectra obtained from various neutral and acidic GSL-derived glycans released *via* the PVDF-immobilization of GSLs extracted from cancer tissues and culture cells.

As demonstrated in this study, the PVDF-based glycan release method proposed here is well suited for the chromatographic separation of glycans on porous graphitized carbon (PGC) and characterization of structure-specific glycan isomers and isobars using negative mode fragmentation. Moreover, there is also no requirement for additional labelling steps such as permethylation to be carried out, thereby resulting in less experimental procedures, decrease in loss of material and thus increased sensitivity of glycan detection. The determination of the glycan structures was facilitated using diagnostic MS² fragment ions previously described for the analysis of GSL-derived glycans as well as N- and O-glycans released from glycoproteins using negative mode LC/ESI-MS/MS.^[3,27] Specifically, we

used the fragment masses of the diagnostic $^{0,2}A$ and $^{2,4}A$ cross-ring fragment ions to distinguish between type 1 (Gal β 1-3GlcNAc) and type 2 (Gal β 1-4GlcNAc) disaccharide constituents of the glycan structures. The fragment ion $^{0,2}A$, in particular, has been previously reported in several studies^[27–29] to be characteristic of glycans with GlcNAc or Glc residues substituted at C-4. As shown in our study, this diagnostic ion was observed in the MS/MS spectra of the globo-series GSL standards, Gb3 (Gal α 1-4Gal β 1-4Glc β 1) and Gb4 (GalNAc β 1-3Gal α 1-4Gal β 1-4Glc β 1), and is indicative of the C-4 substitution of the inner Gal residue of the Gal α 1-4Gal sequence. In addition, characteristic MS/MS feature ions were also observed in the fragmentation spectra of the neutral fucosylated pentasaccharide isomeric structures on the GSLs which were found to be expressed in cancer tissues. For instance, in the serous ovarian cancer tissue sample, we detected neutral GSL-glycans bearing terminal fucosylation which corresponded to Lewis A [Gal β 1-3(Fuc α 1-4)GlcNAc β 1-3Gal β 1-4Glc] and H type 1 [(Fuc α 1-2)Gal β 1-3GlcNAc β 1-3Gal β 1-4Glc] and H type 2 [(Fuc α 1-2)Gal β 1-4GlcNAc β 1-3Gal β 1-4Glc] blood group antigens, while the peritoneal cancer tissue sample appeared to contain only Lewis A and H type 2 antigens. It must also be mentioned that isobaric pentasaccharide structures of different composition could also be released from fucosyl-gangliotetraosylceramides (e.g. Fuc α 1-2Gal β 1-3GalNAc β 1-4Gal β 1-4Glc β 1) which were not detected in this. Nevertheless, the LC/MS analysis of this structure has been performed in a previous study,^[3] in which the authors noted a shorter retention time on the PGC column for these GalNAc-containing structures as compared to the later eluting GlcNAc-containing H type 1 and 2 pentasaccharides observed in our study.

In regard to the expression of gangliosides in ovarian cancer, sialylated gangliosides such as GM3, GD3, GM2 and GD1a have been previously observed in epithelial ovarian cancer cell lines by immunohistochemistry.^[48] The significance of these selected gangliosides is far from clear, although the cells are thought to escape ceramide-mediated apoptosis through the glycosylation of ceramides.^[48,49] This conversion leads to the accumulation of gangliosides which are shed into the tumour micro-environment to suppress cell-mediated immune functions. In a separate study involving serous ovarian cancer-derived KF28 cells and KF28-derived paclitaxel- and cisplatin-resistant cells, Gb3 was increased in both KF28-derived paclitaxel- and cisplatin-resistant cells, while GM3 was elevated only in the paclitaxel-resistant cells, thereby suggesting their role in chemotherapy resistance.^[50,51] Here in this study, several mono-sialylated gangliosides such as GM3, GM2 and GM1 were detected in the ovarian cancer cell line, IGROV 1, and characterized using PGC-LC/ESI-MS/MS. Of particular interest were the late-eluting isoforms of a pentasaccharide which displayed slightly different fragmentation patterns to those of the earlier-eluting GM1 (Gal β 1-3GalNAc β 1-4(NeuAc α 2-3)Gal β 1-4Glc β 1-) isomer. These isoforms were characterized as type 1 and 2 sialyl-tetraosylceramide structures which had a characteristic fragment ion at m/z 655¹⁻ which corresponded to the Neu5Ac-Gal-HexNAc fragment. This fragment ion has also been previously observed in *N*- and *O*-glycan fragmentation in the negative ion mode,^[27] irrespective of the sialic acid linkage.

The successful application of this platform of detailed GSL-derived glycan analysis to ovarian cancer samples demonstrates the potential for this approach to discovering new tumour-associated glycan cancer antigens (TACAs). A majority of the initial work carried out to determine TACAs in ovarian cancer has been performed using immunohistochemistry. For instance, in several studies involving ovarian cancer tissues^[52–54] and cell lines,^[55,56] the di-fucosylated Lewis y antigen bearing terminal α 1-2 fucosylation (Fuc α 1-2Gal β 1-4GlcNAc β 1-3(Fuc α 1-3)Gal β 1-4Glc) has been identified on surface glycoproteins and glycolipids using specific monoclonal antibodies, and a majority of this antigen was primarily carried by the two major glycoproteins, CA125 and MUC1, in ovarian cancer.^[57] While we were not able to detect this structure in the tissue samples analyzed in this study, the presence of the mono-fucosylated structure, Fuc α 1-2Gal β 1-4GlcNAc β 1-3Gal β 1-4Glc, also known as the H type 2 antigen, was detected in abundance in both the investigated tissue samples. Interestingly, this latter structural glycan antigen has also been noted previously distinguishing between ovarian cancers of the serous, endometrioid and mucinous sub-types. Specifically, the H type 2 antigen, together with the Lewis Y antigens, were found to be exclusively expressed in the serous and endometrioid subtypes, thereby distinguishing them from the mucinous subtype.^[52] The corresponding accumulation in α 1-2 H epitopes, including the less abundant H type 1 epitope in serous ovarian cancer tissue, as observed in this study could be potentially implicated in the escape of immune surveillance mechanisms *via* cellular resistance to apoptosis, as demonstrated in colon carcinoma cells^[58,59] and may require a closer investigation into their specific expression in ovarian cancer.

It is widely acknowledged that there is a lack of reliable diagnostic markers for early ovarian cancer detection and the importance of the GSL-derived glycan structures in tumour development and progression is relatively unexplored. The herein described, relatively simple, detergent-free, enzymatic release of glycans from PVDF-immobilized GSLs using a 96-well plate assay, followed by the detailed structural analysis afforded by PGC-LC/ESI-MS/MS, offers a versatile method for the analysis of tumour-derived GSL-glycans. The method displays excellent intra-assay reproducibility and can detect glycans derived from pure sample amounts as low as 2 μ g, and, importantly, from 100 mg of cancer tissue or 10⁷ cells. The platform of analysis provides the means for characterizing the repertoire of GSL-derived glycans as a potential new molecular diagnostic, albeit clearly the analysis will need to be done on statistically significant numbers of samples.

Acknowledgements

We thank Dr Viola Heinzlmann-Schwarz for provision of ovarian cancer tissue samples and cell lines, and Cheah Wai Yuen for helpful discussions. This research was supported by a Macquarie University International Research Scholarship and Postgraduate Research Fund award, and a Research Scholar award (Aris Project No: 9201200676) from the Northern Translational Cancer Research Unit, Cancer Institute NSW, Australia.

REFERENCES

- [1] H. F. Maccioni, C. Giraudo, J. Daniotti. Understanding the stepwise synthesis of glycolipids. *Neurochem. Res.* **2002**, *27*, 629.
- [2] B. K. Gillard, L. T. Thurmon, D. M. Marcus. Variable subcellular localization of glycosphingolipids. *Glycobiology* **1993**, *3*, 57.
- [3] H. Karlsson, A. Halim, S. Teneberg. Differentiation of glycosphingolipid-derived glycan structural isomers by liquid chromatography/mass spectrometry. *Glycobiology* **2010**, *20*, 1103.
- [4] M. Malhotra. Membrane glycolipids: Functional heterogeneity: A review. *Biochem. Anal. Biochem.* **2012**, *1*, 108.
- [5] M. Fukasawa, M. Nishijima, H. Itabe, T. Takano, K. Hanada. Reduction of sphingomyelin level without accumulation of ceramide in Chinese hamster ovary cells affects detergent-resistant membrane domains and enhances cellular cholesterol efflux to methyl-beta-cyclodextrin. *J. Biol. Chem.* **2000**, *275*, 34028.
- [6] P. Singh, Y. D. Paila, A. Chattopadhyay. Role of glycosphingolipids in the function of human serotonin1A receptors. *J. Neurochem.* **2012**, *123*, 716.
- [7] S. I. Hakomori. Cell adhesion/recognition and signal transduction through glycosphingolipid microdomain. *Glycoconjugate J.* **2000**, *17*, 143.
- [8] A. Regina Todeschini, S. I. Hakomori. Functional role of glycosphingolipids and gangliosides in control of cell adhesion, motility, and growth, through glycosynaptic microdomains. *Biochim. Biophys. Acta* **2008**, *1780*, 421.
- [9] K. Kasahara, Y. Sanai. Functional roles of glycosphingolipids in signal transduction via lipid rafts. *Glycoconjugate J.* **2000**, *17*, 153.
- [10] S. Hakomori, Y. Zhang. Glycosphingolipid antigens and cancer therapy. *Chem. Biol.* **1997**, *4*, 97.
- [11] R. L. Schnaar, A. Suzuki, P. Stanley, in *Essentials of Glycobiology*, (Eds: A. Varki, R. D. Cummings, J. D. Esko, H. H. Freeze, P. Stanley, C. R. Bertozzi, G. W. Hart, M. E. Etzler). Cold Spring Harbor Laboratory Press, Cold Spring Harbor, New York, **2009**.
- [12] R. K. Yu, M. Yanagisawa, T. Ariga, in *Comprehensive Glycoscience*, (Ed: H. Kamerling). Elsevier, Oxford, **2007**, p. 73.
- [13] J. L. Daniotti, A. A. Vilcas, V. Torres Demichelis, F. M. Ruggiero, M. Rodriguez-Walker. Glycosylation of glycolipids in cancer: basis for development of novel therapeutic approaches. *Front. Oncol.* **2013**, *3*, 306.
- [14] L. G. Durrant, P. Noble, I. Spendlove. Immunology in the clinic review series; focus on cancer: glycolipids as targets for tumour immunotherapy. *Clin. Exp. Immunol.* **2012**, *167*, 206.
- [15] S. Hakomori. Tumor malignancy defined by aberrant glycosylation and sphingo(glyco)lipid metabolism. *Cancer Res.* **1996**, *56*, 5309.
- [16] L. Schiffmann, F. Schwarz, M. Linnebacher, F. Prall, J. Pahnke, H. Krentz, B. Vollmar, E. Klar. A novel sialyl LeX expression score as a potential prognostic tool in colorectal cancer. *World J. Surg. Oncol.* **2012**, *10*, 95.
- [17] T. Nakayama, M. Watanabe, T. Katsumata, T. Teramoto, M. Kitajima. Expression of sialyl Lewis(a) as a new prognostic factor for patients with advanced colorectal carcinoma. *Cancer* **1995**, *75*, 2051.
- [18] O. Kovbasnjuk, R. Mourtaizina, B. Baibakov, T. Wang, C. Elowsky, M. A. Choti, A. Kane, M. Donowitz. The glycosphingolipid globotriaosylceramide in the metastatic transformation of colon cancer. *Proc. Natl. Acad. Sci. USA* **2005**, *102*, 19087.
- [19] R. Kannagi, S. B. Levery, F. Ishigami, S. Hakomori, L. H. Shevinsky, B. B. Knowles, D. Solter. New globoseries glycosphingolipids in human teratocarcinoma reactive with the monoclonal antibody directed to a developmentally regulated antigen, stage-specific embryonic antigen 3. *J. Biol. Chem.* **1983**, *258*, 8934.
- [20] C. C. Wang, Y. L. Huang, C. T. Ren, C. W. Lin, J. T. Hung, J. C. Yu, A. L. Yu, C. Y. Wu, C. H. Wong. Glycan microarray of Globo H and related structures for quantitative analysis of breast cancer. *Proc. Natl. Acad. Sci. USA* **2008**, *105*, 11661.
- [21] S. Parry, V. Ledger, B. Tissot, S. M. Haslam, J. Scott, H. R. Morris, A. Dell. Integrated mass spectrometric strategy for characterizing the glycans from glycosphingolipids and glycoproteins: direct identification of sialyl Lex in mice. *Glycobiology* **2007**, *17*, 646.
- [22] S. Holst, K. Stavenhagen, C. I. Balog, C. A. Koeleman, L. M. McDonnell, O. A. Mayboroda, A. Verhoeven, W. E. Mesker, R. A. Tollenaar, A. M. Deelder, M. Wührer. Investigations on aberrant glycosylation of glycosphingolipids in colorectal cancer tissues using liquid chromatography and matrix-assisted laser desorption time-of-flight mass spectrometry (MALDI-TOF-MS). *Mol. Cell. Proteomics* **2013**, *12*, 3081.
- [23] P. H. Jensen, N. G. Karlsson, D. Kolarich, N. H. Packer. Structural analysis of N- and O-glycans released from glycoproteins. *Nat. Protocols* **2012**, *7*, 1299.
- [24] H. Korekane, S. Tsuji, S. Noura, M. Ohue, Y. Sasaki, S. Imaoka, Y. Miyamoto. Novel fucogangliosides found in human colon adenocarcinoma tissues by means of glycomic analysis. *Anal. Biochem.* **2007**, *364*, 37.
- [25] J. Benard, J. Da Silva, M. C. De Blois, P. Boyer, P. Duvillard, E. Chiric, G. Riou. Characterization of a human ovarian adenocarcinoma line, IGROV1, in tissue culture and in nude mice. *Cancer Res.* **1985**, *45*, 4970.
- [26] L. G. Durrant, S. J. Harding, N. H. Green, L. D. Buckberry, T. Parsons. A new anticancer glycolipid monoclonal antibody, SC104, which directly induces tumor cell apoptosis. *Cancer Res.* **2006**, *66*, 5901.
- [27] A. V. Everest-Dass, J. L. Abrahams, D. Kolarich, N. H. Packer, M. P. Campbell. Structural feature ions for distinguishing N- and O-linked glycan isomers by LC-ESI-IT MS/MS. *J. Am. Soc. Mass Spectrom.* **2013**, *24*, 895.
- [28] W. Chai, V. Piskarev, A. M. Lawson. Negative-ion electrospray mass spectrometry of neutral underivatized oligosaccharides. *Anal. Chem.* **2001**, *73*, 651.
- [29] C. Robbe, C. Capon, B. Coddeville, J. C. Michalski. Diagnostic ions for the rapid analysis by nano-electrospray ionization quadrupole time-of-flight mass spectrometry of O-glycans from human mucins. *Rapid Commun. Mass Spectrom.* **2004**, *18*, 412.
- [30] J. L. Seymour, C. E. Costello, J. Zaia. The influence of sialylation on glycan negative ion dissociation and energetics. *J. Am. Soc. Mass Spectrom.* **2006**, *17*, 844.
- [31] E. G. Bligh, W. J. Dyer. A rapid method of total lipid extraction and purification. *Can. J. Biochem. Physiol.* **1959**, *37*, 911.
- [32] W. Chai, V. E. Piskarev, B. Mulloy, Y. Liu, P. G. Evans, H. M. Osborn, A. M. Lawson. Analysis of chain and blood group type and branching pattern of sialylated oligosaccharides by negative ion electrospray tandem mass spectrometry. *Anal. Chem.* **2006**, *78*, 1581.
- [33] D. J. Harvey, L. Royle, C. M. Radcliffe, P. M. Rudd, R. A. Dwek. Structural and quantitative analysis of N-linked glycans by matrix-assisted laser desorption ionization and negative ion nanospray mass spectrometry. *Anal. Biochem.* **2008**, *376*, 44.
- [34] S. F. Wheeler, D. J. Harvey. Negative ion mass spectrometry of sialylated carbohydrates: Discrimination of N-acetylneuraminic

- acid linkages by MALDI-TOF and ESI-TOF mass spectrometry. *Anal. Chem.* **2000**, *72*, 5027.
- [35] S. Hakomori. Bifunctional role of glycosphingolipids. Modulators for transmembrane signaling and mediators for cellular interactions. *J. Biol. Chem.* **1990**, *265*, 18713.
- [36] C. A. Lingwood. Glycosphingolipid Functions, Cold Spring Harbor Perspectives in Biology, **2011**, vol. 3.
- [37] F. Jacob, M. Anugraham, T. Pochechueva, B. W. Tse, S. Alam, R. Guertler, N. V. Bovin, A. Fedier, N. F. Hacker, M. E. Huflejt, N. Packer, V. A. Heinzelmann-Schwarz. The glycosphingolipid P is an ovarian cancer-associated carbohydrate antigen involved in migration. *Br. J. Cancer* **2014**.
- [38] A. Lee, D. Kolarich, P. A. Haynes, P. H. Jensen, M. S. Baker, N. H. Packer. Rat liver membrane glycoproteome: enrichment by phase partitioning and glycoprotein capture. *J. Proteome Res.* **2009**, *8*, 770.
- [39] B. Zhou, S. C. Li, R. A. Laine, R. T. Huang, Y. T. Li. Isolation and characterization of ceramide glycanase from the leech, *Macrobdella decora*. *J. Biol. Chem.* **1989**, *264*, 12272.
- [40] M. Ito, T. Yamagata. Purification and characterization of glycosphingolipid-specific endoglycosidases (endoglyco-ceramidas) from a mutant strain of *Rhodococcus* sp. Evidence for three molecular species of endoglyco-ceramidase with different specificities. *J. Biol. Chem.* **1989**, *264*, 9510.
- [41] M. E. C. Caines, M. D. Vaughan, C. A. Tarling, S. M. Hancock, R. A. J. Warren, S. G. Withers, N. C. J. Strynadka. Structural and mechanistic analyses of endo-glycoceramidase II, a membrane-associated family 5 glycosidase in the Apo and GM3 ganglioside-bound forms. *J. Biol. Chem.* **2007**, *282*, 14300.
- [42] Y. T. Li, C. W. Chou, S. C. Li, U. Kobayashi, Y. H. Ishibashi, M. Ito. Preparation of homogenous oligosaccharide chains from glycosphingolipids. *Glycoconjugate J.* **2009**, *26*, 929.
- [43] S. Parry, V. Ledger, B. Tissot, S. M. Haslam, J. Scott, H. R. Morris, A. Dell. Integrated mass spectrometric strategy for characterizing the glycans from glycosphingolipids and glycoproteins: direct identification of sialyl Le(x) in mice. *Glycobiology* **2007**, *17*, 646.
- [44] H. Ashida, K. Yamamoto, H. Kumagai, T. Tochikura. Purification and characterization of membrane-bound endoglycoceramidase from *Corynebacterium* sp. *Eur. J. Biochem.* **1992**, *205*, 729.
- [45] M. N. Fukuda, M. Fukuda, S. Hakomori. Cell surface modification by endo-beta-galactosidase. Change of blood group activities and release of oligosaccharides from glycoproteins and glycosphingolipids of human erythrocytes. *J. Biol. Chem.* **1979**, *254*, 5458.
- [46] M. Kitamikado, M. Ito, Y. T. Li. Isolation and characterization of a keratan sulfate-degrading endo-beta-galactosidase from *Flavobacterium keratolyticus*. *J. Biol. Chem.* **1981**, *256*, 3906.
- [47] Y. Ishibashi, U. Kobayashi, A. Hijikata, K. Sakaguchi, H. M. Goda, T. Tamura, N. Okino, M. Ito. Preparation and characterization of EGCase I, applicable to the comprehensive analysis of GSLs, using a rhodococcal expression system. *J. Lipid Res.* **2012**, *53*, 2242.
- [48] M. H. Ravindranath, S. Muthugounder, N. Presser, S. R. Selvan, A. D. Santin, S. Bellone, T. S. Saravanan, D. L. Morton. Immunogenic gangliosides in human ovarian carcinoma. *Biochem. Biophys. Res. Commun.* **2007**, *353*, 251.
- [49] M. C. Cabot, in *Ceramide Signaling*, (Ed: A. H. Futerman). Kluwer Academic, New York, **2002**, p. 133.
- [50] K. Kiguchi, Y. Iwamori, N. Suzuki, Y. Kobayashi, B. Ishizuka, I. Ishiwata, T. Kita, Y. Kikuchi, M. Iwamori. Characteristic expression of globotriaosyl ceramide in human ovarian carcinoma-derived cells with anticancer drug resistance. *Cancer Sci.* **2006**, *97*, 1321.
- [51] K. Tanaka, H. Takada, S. Isonishi, D. Aoki, M. Mikami, K. Kiguchi, M. Iwamori. Possible involvement of glycolipids in anticancer drug resistance of human ovarian serous carcinoma-derived cells. *J. Biochem.* **2012**, *152*, 587.
- [52] M. F. Federici, V. Kudryashov, P. E. Saigo, C. L. Finstad, K. O. Lloyd. Selection of carbohydrate antigens in human epithelial ovarian cancers as targets for immunotherapy: serous and mucinous tumors exhibit distinctive patterns of expression. *Int. J. Cancer* **1999**, *81*, 193.
- [53] J. Gao, Z. Hu, D. Liu, J. Liu, C. Liu, R. Hou, S. Gao, D. Zhang, S. Zhang, B. Lin. Expression of Lewis y antigen and integrin alphav, beta3 in ovarian cancer and their relationship with chemotherapeutic drug resistance. *J. Exp. Clin. Cancer Res.* **2013**, *32*, 36.
- [54] I. Hellstrom, H. J. Garrigues, U. Garrigues, K. E. Hellstrom. Highly tumor-reactive, internalizing, mouse monoclonal antibodies to Le(y)-related cell surface antigens. *Cancer Res.* **1990**, *50*, 2183.
- [55] J. J. Liu, B. Lin, Y. Y. Hao, F. F. Li, D. W. Liu, Y. Qi, L. C. Zhu, S. L. Zhang, M. Iwamori. Lewis(y) antigen stimulates the growth of ovarian cancer cells via regulation of the epidermal growth factor receptor pathway. *Oncol. Rep.* **2010**, *23*, 833.
- [56] J. Liu, B. Lin, Y. Hao, Y. Qi, L. Zhu, F. Li, D. Liu, J. Cong, S. Zhang, M. Iwamori. Lewis y antigen promotes the proliferation of ovarian carcinoma-derived RMG-1 cells through the PI3K/Akt signaling pathway. *J. Exp. Clin. Cancer Res.* **2009**, *28*, 154.
- [57] B. W. Yin, C. L. Finstad, K. Kitamura, M. G. Federici, M. Welshinger, V. Kudryashov, W. J. Hoskins, S. Welt, K. O. Lloyd. Serological and immunochemical analysis of Lewis y (Ley) blood group antigen expression in epithelial ovarian cancer. *Int. J. Cancer* **1996**, *65*, 406.
- [58] C. Goupille, F. Hallouin, K. Meflah, J. Le Pendu. Increase of rat colon carcinoma cells tumorigenicity by alpha(1-2) fucosyltransferase gene transfection. *Glycobiology* **1997**, *7*, 221.
- [59] N. Labarriere, J. P. Piau, C. Otry, M. Denis, P. Lustenberger, K. Meflah, J. Le Pendu. H blood group antigen carried by CD44V modulates tumorigenicity of rat colon carcinoma cells. *Cancer Res.* **1994**, *54*, 6275.

SUPPORTING INFORMATION

Additional supporting information may be found in the online version of this article at the publisher's website.

4.1 Supplementary Data

Supplementary Info

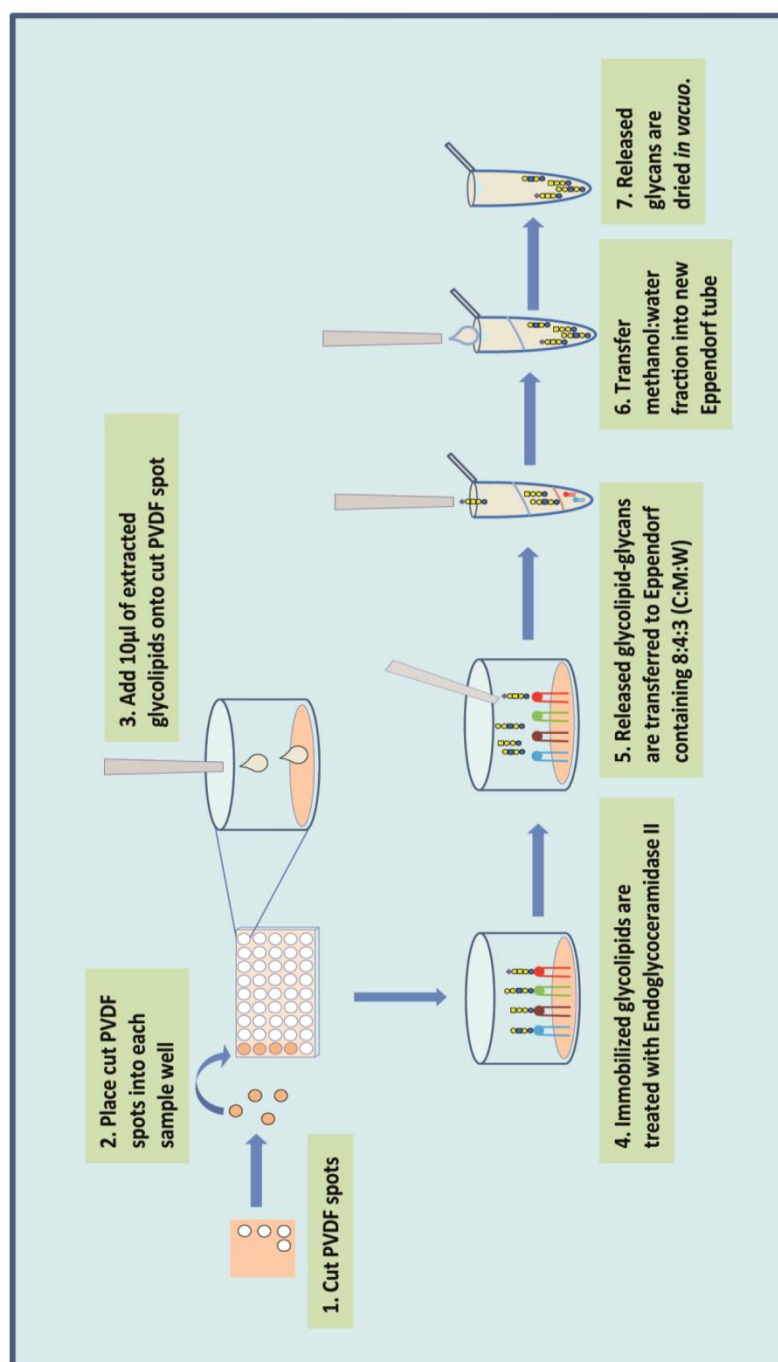


Figure 1: Detailed workflow of enzymatic release of PVDF-immobilized GSLs

Substrate	Enzyme Concentration (mU)	Substrate Concentration ($\mu\text{g}/\mu\text{l}$)				
		2	4	6	8	10
		Peak Area Intensity ($\times 10^8$)				
Asialo- GM1	1	0.068 ± 0.00	0.126 ± 0.00	0.239 ± 0.05	0.391 ± 0.05	0.603 ± 0.04
	4	0.257 ± 0.09	0.653 ± 0.21	1.22 ± 0.15	1.808 ± 0.24	2.325 ± 0.33
Globotriaosylceramide (Gb3)	1	0.054 ± 0.00	0.106 ± 0.00	0.145 ± 0.01	0.194 ± 0.00	0.25 ± 0.01
	4	0.151 ± 0.01	0.229 ± 0.01	0.275 ± 0.01	0.304 ± 0.01	0.349 ± 0.00

Table 1: Peak area intensities for 1 mU and 4 mU of enzyme concentration for GSL standards (Asialo-GM1 and Gb3). Values represent mean \pm SD of two technical replicates.

4.2 Overview of Chapter IV: Publication III

- Apart from membrane protein glycosylation, glycosphingolipids (GSLs) represent an important class of glycoconjugates that are highly diverse due to structural heterogeneity exhibited in both their glycan and lipid moieties
- The isolation of glycans from GSLs extracted from ovarian cancer tissues and cells in this study was accomplished using Endoglycoceramidase II, an enzyme that specifically cleaves the Glc residue from the ceramide portion of the lipid
- This enzyme has a broad-based recognition of specific core GSL glycans (ganglio and isoglobo series) but displays limited specificities for certain GSL glycans (eg. globo series)
- Using a PVDF-based immobilization of GSLs, the limited specificities of the enzyme was overcome, thereby allowing various glycans from core GSLs to be enzymatically released directly from the PVDF surface.
- This technique not only allows for the isolation of various glycans from ganglio, globo, neo-lacto and isoglobo GSL series, but also requires substantially lower amounts of enzyme concentration to be used.
- Several PGC-LC-resolved isomeric GSL-derived glycans were isolated from both serous cancer tissues and IGROV1 cell line and characterized using negative ion mode MS/MS diagnostic fragment ions.
- Typical fragmentation patterns observed in negative ion mode for glycans with terminal fucosylation (H antigen and Lewis-type) and Type1/2 linkages were successfully characterized using a combination of standards and previous diagnostic ions reported in literature

4.3 Publication IV: The glycosphingolipid P₁ is an ovarian cancer-associated carbohydrate antigen involved in migration



The glycosphingolipid P₁ is an ovarian cancer-associated carbohydrate antigen involved in migration

F Jacob^{*,1,2}, M Anugraham³, T Pochechueva¹, B W C Tse^{2,4}, S Alam¹, R Guertler^{1,2}, N V Bovin⁵, A Fedier¹, N F Hacker⁶, M E Huflejt⁷, N Packer³ and V A Heinzelmann-Schwarz^{1,2,6}

¹Gynecological Research Group, Department of Biomedicine, University Hospital Basel, University of Basel, Hebelstrasse 20, Basel 4031, Switzerland; ²Ovarian Cancer Group, Adult Cancer Program, Lowy Cancer Research Centre, University of New South Wales, Prince of Wales Clinical School, Building C25 Kensington Campus, Sydney, NSW 2052, Australia; ³Department of Chemistry and Biomolecular Sciences, Biomolecular Frontiers Research Centre, Faculty of Science, Macquarie University, Balacava Road, North Ryde, Sydney, NSW 2109, Australia; ⁴Australian Prostate Cancer Research Centre Queensland, Institute of Health and Biomedical Innovation, Queensland University of Technology, Translational Research Institute, Brisbane, QLD 4102, Australia; ⁵Shemyakin-Ovchinnikov Institute of Bioorganic Chemistry, Russian Academy of Sciences, Ul. Miklukho-Maklaya, 16/10, Moscow 117997, Russian Federation; ⁶Gynaecological Cancer Centre, Royal Hospital for Women, School of Women's and Children's Health, Barker Street, Randwick, NSW 2031, Australia and ⁷Division of Thoracic Surgery and Thoracic Oncology, Department of Cardiothoracic Surgery, New York University School of Medicine, 550 First Avenue, New York, NY 10016, USA

Background: The level of plasma-derived naturally circulating anti-glycan antibodies (AGA) to P₁ trisaccharide has previously been shown to significantly discriminate between ovarian cancer patients and healthy women. Here we aim to identify the Ig class that causes this discrimination, to identify on cancer cells the corresponding P₁ antigen recognised by circulating anti-P₁ antibodies and to shed light into the possible function of this glycosphingolipid.

Methods: An independent Australian cohort was assessed for the presence of anti-P₁ IgG and IgM class antibodies using suspension array. Monoclonal and human derived anti-glycan antibodies were verified using three independent glycan-based immunoassays and flow cytometry-based inhibition assay. The P₁ antigen was detected by LC-MS/MS and flow cytometry. FACS-sorted cell lines were studied on the cellular migration by colorimetric assay and real-time measurement using xCELLigence system.

Results: Here we show in a second independent cohort ($n = 155$) that the discrimination of cancer patients is mediated by the IgM class of anti-P₁ antibodies ($P = 0.0002$). The presence of corresponding antigen P₁ and structurally related epitopes in fresh tissue specimens and cultured cancer cells is demonstrated. We further link the antibody and antigen (P₁) by showing that human naturally circulating and affinity-purified anti-P₁ IgM isolated from patients ascites can bind to naturally expressed P₁ on the cell surface of ovarian cancer cells. Cell-sorted IGROV1 was used to obtain two study subpopulations (P₁-high, 66.1%; and P₁-low, 33.3%) and observed that cells expressing high P₁-levels migrate significantly faster than those with low P₁-levels.

Conclusions: This is the first report showing that P₁ antigen, known to be expressed on erythrocytes only, is also present on ovarian cancer cells. This suggests that P₁ is a novel tumour-associated carbohydrate antigen recognised by the immune system in patients and may have a role in cell migration. The clinical value of our data may be both diagnostic and prognostic; patients with low anti-P₁ IgM antibodies present with a more aggressive phenotype and earlier relapse.

*Correspondence: Dr F Jacob; E-mail: francis.jacob@unibas.ch

Received 19 March 2014; revised 5 June 2014; accepted 21 July 2014

© 2014 Cancer Research UK. All rights reserved 0007–0920/14



www.bjcancer.com | DOI:10.1038/bjc.2014.455

Advance Online Publication: 28 August 2014

1

Glycosphingolipids (GSLs) have critical roles in embryonic development, signal transduction, cell signalling, apoptosis, receptor modulation, cell adhesion, growth and cell differentiation and carcinogenesis (Jarvis *et al.*, 1996; Hakomori, 1998; Kasahara and Sanai, 1999). The presence of tumour-associated GSLs antigens have been observed in epithelial ovarian cancer (Pochechueva *et al.*, 2012), which is the fifth most common cause of death from all cancers in women and the leading cause of death from gynaecological malignancies (Ozols, 2006).

Printed glycan array technology (a glycan-based discovery approach) previously demonstrated that naturally occurring anti-glycan antibodies (AGA) in plasma of ovarian cancer patients exhibited specificities towards synthetic P₁ trisaccharide. In our previous study, we have demonstrated using a printed glycan array that anti-P₁ antibodies can discriminate healthy controls from ovarian cancer patients (Jacob *et al.*, 2012). This study (on a Swiss Discovery Cohort) showed that anti-P₁ antibodies of IgM, IgG and IgA together were significantly lower in ovarian cancer patients, thereby discriminating them from healthy controls. The predictive value of the printed glycan array was validated by two independent glycan-based immunoassays, ELISA and suspension array (Pochechueva *et al.*, 2011b).

The P^K, P and P₁ carbohydrate antigens, commonly expressed on GSL, are members of the P blood group system that differ in their specificity based on their oligosaccharide sequences. In cancer, the globo (P^K and P) and neolacto (P₁) series are precursor GSL that give rise to well-known tumour-associated carbohydrate antigens, such as Forssman antigen (Hakomori *et al.*, 1977; Taniguchi *et al.*, 1981) and Globo H (Gilewski *et al.*, 2001; Chang *et al.*, 2008; Wang *et al.*, 2008). High levels of P^K (Gal α 1-4Gal β 1-4Glc β 1-1Ceramide; Gb3, CD77), P (GalNAc β 1-3Gal α 1-4Gal β 1-4Glc β 1-1Ceramide; Gb4) and Globo H were described in the past (Wenk *et al.*, 1994).

As shown previously, naturally occurring AGA to P₁ have the potential to be used diagnostically in plasma of ovarian cancer patients. However, it remains unknown whether P₁-bearing GSL are present on ovarian cancer cells and whether naturally occurring anti-P₁ antibodies to chemically synthesised carbohydrates in glycan-based immunoassays bind to these GSL antigens. To our knowledge, no published reports regarding the role of P₁ in malignant transformation, particularly in ovarian cancer, are available, and the molecular mechanisms underlying GSL expression on the cell surface, as well as its function, have yet to be elucidated. Therefore, this study aims (A) to determine the responsible naturally occurring AGA immunoglobulin class discriminating cancer from normal; (B) to determine whether the level of these antibodies are predictive of patient outcome; (C) to investigate whether the related P₁ glycan epitopes are present on cells isolated from ovarian cancer tissues as well as on ovarian cancer cell lines; (D) to compare the AGA profiles in ascites and matched plasma; (E) to compare monoclonal anti-P₁ antibodies produced in humans and affinity purified anti-P₁ antibodies isolated from ascites; and finally (F) to investigate the functional role of the P₁ antigen in ovarian cancer.

MATERIALS AND METHODS

Biospecimens. Two independent patient cohorts from two different continents were used for the experiments: (A) matched plasma and ascites from 11 serous FIGO stage III/IV cancer patients from the previously described Swiss Discovery Cohort (Jacob *et al.*, 2012); (B) plasma from 155 Australian samples (Australian Validation Cohort) comprising healthy controls, borderline tumour and ovarian cancer patients. The Australian Validation Cohort was split into: (1) borderline tumours and

adenocarcinomas of the ovary, tube and peritoneum ('tumour group'), and (2) healthy control women ('control group'). Patients were either admitted with an adnexal mass to the Gynaecological Cancer Centre of the Royal Hospital for Women, Randwick, Australia or were seen as outpatients to the Hereditary Cancer Centre of The Prince of Wales Hospital, Randwick, Australia. All patients were prospectively included after giving informed consent in accordance with ethical regulations (Hunter Area Research Ethics 04/04/07/3.04; South Eastern Sydney Illawarra HREC/AURED Ref:08/09/17/3.02). The processing of blood plasma samples was performed constantly on ice within 3 h after collection as previously described (Jacob *et al.*, 2011a, 2012). All clinicopathological data (Supplementary Table S1) such as FIGO stage and grade were incorporated in a specifically designed in-house database ('PEROV'), which was developed using Microsoft Access (Microsoft Corporation, Redmond, WA, USA). Diagnosis and histopathological features were independently re-evaluated by a pathologist specialised in gynaecological oncology (JS). Blood samples were stored in aliquots at -80°C .

Glycan-based immunoassays (printed glycan array, suspension array and ELISA). The printed glycan array was performed as previously described (Huflejt *et al.*, 2009; Bovin *et al.*, 2012; Jacob *et al.*, 2012). AGA were detected by ImmunoPure goat anti-human IgA + IgG + IgM conjugated to long chain biotin (1:100, 'Combo', Pierce, Rockford, IL, USA). To detect the immunoglobulin class, developed printed glycan array slides were individually incubated with 1:50-diluted biotin-conjugated goat anti-human IgA, IgG or IgM (ZYMED Laboratories, Invitrogen, Carlsbad, CA, USA). The coupling procedures for end-biotinylated glycopolymers and antibody binding were described before (Pochechueva *et al.*, 2011a, b). Experimental protocol was performed as described previously (Pochechueva *et al.*, 2011b). Exceptions were made with respect to the use of goat anti-human IgG-R-PE or IgM-R-PE secondary antibodies (Southern Biotech Ass. Inc., Birmingham, AL, USA). ELISA was performed as described previously (Pochechueva *et al.*, 2011b).

Extraction and identification of GSLs from cancer tissue samples and IGROV1 cell line. Fresh primary tissue samples (~100 mg) from a serous ovarian cancer and an endometrioid peritoneal cancer patient were collected to analyse glycolipids by negative ion electrospray ionisation mass spectrometry (LC-ESI-MS/MS). Detailed analysis of the procedure is described in Supplementary Information.

Affinity purification of anti-P₁ antibodies. Ascites fluid was collected from a late-stage serous ovarian cancer patient during primary surgery. The ascites was processed by centrifugation at 4°C , 3000 g for 15 min. Supernatant was aliquoted and kept frozen at -80°C . Thawed ascites (50 ml) was filtered through a 0.22- μm filter (Millipore, Billerica, MA, USA) and diluted three times in PBS (pH 7.4). Glycan-polyacrylamide-Sepharose stored in 20% (v/v) ethanol was washed with 10 volumes 20% ethanol, 20 volumes milliQ water and equilibrated with 10 volumes of PBS. Preprocessed ascites affinity purified against Gal α 1-4Gal β 1-4GlcNAc β -polyacrylamide-Sepharose (P₁-PAA-Seph; 10 ml). A constant flow rate of 1 ml min^{-1} was controlled by the use of an auxiliary pump (Model EP-1 Econo Pump, Bio-Rad, Hercules, CA, USA). Protein content and buffer composition was recorded by UV at 280 nm and conductivity, respectively (BioLogic DuoFlow Workstation, Bio-Rad). The column was washed with PBS containing 0.05% (v/v) Tween 20, unplugged and stored overnight at 4°C . The next day, the column was inserted back into the chromatography system and washed until no protein was detected anymore. Bound anti-P₁ antibodies were eluted using 0.2 M TrisOH (pH 10.2) and neutralised by 2.0 M Glycine HCl (pH 2.5). Eluted anti-P₁ antibodies were concentrated using the Amicon Ultra-0.5

centrifugal filter (Millipore), and their concentration was determined using spectrophotometrically at 280 nm.

Flow cytometry. GSL expression on the cell surface membranes was analysed by flow cytometry (CyAn ADP Analyzer, Beckman Coulter, Nyon, CH, USA) prior to antibody labelling. Unconjugated antibodies included anti-P₁ human IgM (clone P3NIL100; Immucor Gamma, Rödermark, Germany), anti-P₁ murine monoclonal IgM (clone OSK17; Immucor Gamma) and anti-Gb3 monoclonal IgG2b (CD77, P^k) (clone BGR23; Seikagaku Biobusiness Corporation, Tokyo, Japan). Biotin-conjugated antibodies included anti-human mouse IgM (BD Bioscience, Basel, Switzerland), rat anti-mouse IgM and rat anti-mouse IgG2b (BD Bioscience). Streptavidin conjugated to FITC (BD Bioscience) was used for fluorescence detection. Dead and apoptotic cells were separated from live cells using propidium iodide (BD Bioscience). Matching isotype monoclonal antibodies conjugated to FITC were used as controls (BD Bioscience). All investigated cell lines were gated individually to exclude debris, followed by single cell gating to remove dead cells and doublets. Data acquisition was performed using Summit v4.3 (CyAn ADP Analyzer, Beckman Coulter). Data analysis was performed using FlowJo v9 (Tree Star Inc., Ashland, OR, USA).

FACS sorting. IGROV1 cells were grown to 80% confluence, washed twice in PBS and harvested using non-enzymatic cell dissociation buffer (Sigma Aldrich, Buchs, Switzerland). Cells were then washed in PBS containing 1% FCS and resuspended to 10⁶ cells ml⁻¹. Cell suspension (100 µl) was stained with human anti-P₁ IgM (BD Bioscience) as mentioned above and run on a BD FACS Vantage SE DiVa Cell Sorter (BD Bioscience). IGROV1 cell line was sorted using >90% and <10% fluorescence signal intensity for P₁-positive cells to receive P₁-high and P₁-low fractions, respectively.

Flow cytometry-based inhibition assay. Monoclonal human IgM antibody directed to P₁ (Immucor Gamma, Rödermark) was preincubated either with Sepharose-P₁-PAA or Sepharose-P^k-PAA (Lectinity Holdings, Moscow, Russia) in different amounts ranging from 0.015 µmol to 0.06 µmol for 60 min at RT. The supernatant was further processed as described in the flow cytometry section.

Colorimetric cell migration assay. Sub-confluent tumour cells were 'starved' from serum by incubation in serum-free media for 24 h, before harvesting using a non-enzymatic cell dissociation buffer (Sigma Aldrich, Buchs, Switzerland), washed twice and resuspended in serum-free media containing 5% (w/v) BSA. Tumour cells (7.5 × 10⁵ in 300 µl) were loaded into cell culture inserts containing a polyethylene terephthalate membrane with 8-micron pores (Millipore). The inserts were assembled into 24-well plates with each well containing 700 µl of media with 10% supplemented with fetal calf serum, which was used as chemoattractant. After incubation for 18 h at 37 °C, the media in the interior of the insert was removed, and the entire insert was immersed in 400 µl of 0.2% crystal violet/10% ethanol for 20 min. The insert was washed several times in water, and the non-migrated cells in the interior of the insert were removed using a cotton-tip swab. After air-drying, five random areas of the inserts showing the migrated cells were photographed, and cell counts were performed. Colorimetric cell migration assay was performed three times.

In addition, parental IGROV1 cells were preincubated with 1% (w/v) BSA in PBS, the corresponding isotype control (ChromPure human IgM, Jackson ImmunoResearch Laboratories, Inc., MILAN Analytica AG, Rheinfelden, Switzerland) and human anti-P₁ IgM (clone P3NIL100), both antibodies in a final concentration of 500 µg ml⁻¹. After 1 h incubation, cells were processed according to previously described cell migration protocol.

MTT assay. Cultures were incubated with 500 µg ml⁻¹ (final concentration) MTT dye (Sigma-Aldrich, Buchs, Switzerland) in PBS for 3 h, followed by removal of the medium and dissolution of the violet crystals in 200 µl of DMSO. The optical density (absorbance at 540 nm) was measured with a SynergyH1 Hybrid Reader (Biotek, Luzern, Switzerland). The data are given as absorbance at 540 nm, representing cell viability as a function of araC concentration. Each experiment was performed independently twice from multiple cultures.

Real-time cell migration analysis (xCELLigence). Real-time cell analysis (RTCA; xCELLigence System, Roche Diagnostics GmbH, Mannheim, Germany) was used to investigate cell migration in P₁-low and -high serous ovarian cancer IGROV1 cells in a label-free environment (Solly *et al*, 2004; Ke *et al*, 2011). Migration was examined on 16-transwell plates (Roche Diagnostics GmbH) with microelectrodes attached to the underside bottom of the membrane for impedance-based detection of the migrated cells. Prior to each experiment, cells were deprived of FCS over a period of 24 h. Initially, 160 µl 'chemoattractant' media (RPMI 1640 containing 10% FCS) and 50 µl RPMI 1640 containing 1% FCS was added to the lower and upper chambers, respectively. Sterile PBS was loaded into the evaporation troughs. CIM-16 plates were further prepared according to the manufacturer's protocol. Background signals generated by the cell-free media were recorded. Cells were harvested using trypsin, counted and re-suspended in an appropriate volume of RPMI 1640 containing 1% FCS. Cells (100 000 cells per 100 µl medium) were seeded onto the upper chamber of the CIM-16 plate and allowed to settle onto the membrane. Cell-free media was used as negative control. Each experiment was performed two times in duplicates. The programmed signal detection for quantification of the cell index was measured every 15 min over a period of 30 h. In an independent migration assay, 5 µM of 1-beta-D-arabinofuranosylcytosine (araC; Sigma-Aldrich), a DNA polymerase inhibitor, was added to avoid possible effects on migration caused by cell proliferation.

Statistical analysis. Detailed statistical procedure applied is described in Supplementary Information.

RESULTS

IgM antibodies in plasma against P₁ trisaccharide are reduced in patients with tubal, peritoneal and ovarian cancer. In our previous study, the use of three glycan-based immunoassays (printed glycan array, ELISA and suspension array), detecting IgM, IgG and IgA together, revealed significant AGA interactions with the members of the P blood group system (Pochechueva *et al*, 2011a, b; Jacob *et al*, 2012). Overall, less AGA to P₁ trisaccharide (printed glycan array, ELISA and suspension array) and P^k (printed glycan array) were observed in the plasma of the cancer patient group compared with the control group (Pochechueva *et al*, 2011b; Jacob *et al*, 2012).

In this study, we investigated the levels of IgM and IgG AGA in the plasma of an independent Australian Validation Cohort (*n* = 155). The cohort consisted of a 'benign' control group (healthy controls and benign gynaecological conditions; *n* = 81) and a 'tumour' group (ovarian borderline tumours, ovarian, tubal and peritoneal cancers; *n* = 74) (Supplementary Table S1). Based on suspension array data, AGA to the P₁ trisaccharide belonged mainly to the IgM class (median, IQR; 9.948log(MFI), 9.351–10.090log(MFI)) in all the tested samples. Significantly lower IgM anti-P₁ antibody levels were observed in the blood plasma samples of the tumour as compared with the control group (*P* = 0.0002) (Figure 1A). The tumour group revealed 15/74 (20.3%) samples having lower AGA levels compared with the lowest control group sample. Logistic regression did not reveal any relationship between

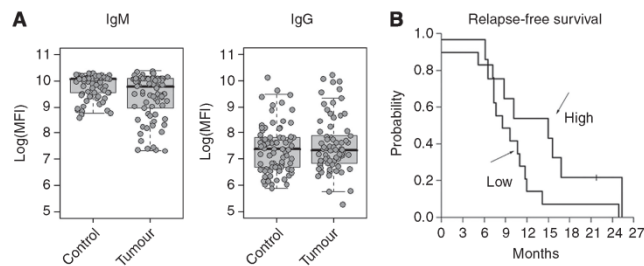


Figure 1. Significantly lower levels of anti-P₁ IgM in cancer patients in the Australian validation cohort ($n=155$). **(A)** Box-and-whisker plots showing distribution of AGA levels of IgM and IgG to covalently attached P₁ trisaccharide using suspension array. Decreased AGA levels in cancer patients were observed for IgM. **(B)** Kaplan–Meier curve on relapse-free survival showing that patients with low antibody levels ($n=33$; lower than median fluorescence signal) have slightly earlier relapse ($P=0.055$) than those with high antibody levels ($n=25$, higher than median fluorescence signal).

clinicopathological parameters and anti-P₁ IgM antibody signatures in the tumour group. In contrast to IgM, generally lower IgG antibody levels (median, IQR; 7.35log(MFI), 6.726–7.858log(MFI)) were observed. Both the control and tumour groups were similar in IgG AGA levels, with no significant difference in between both the groups ($P=0.7248$, Figure 1A). We have compared various clinical parameters recorded along with collection of plasma samples for each patient. Statistical evaluation revealed a significant discrimination in FIGO stage of the non-mucinous cancer of ovary, tube and peritoneum group (FIGO Stage, non-mucinous cancer of the ovary, tube and peritoneum I/II vs III/IV, $P=0.01773$, t -test). The remaining investigated clinical parameters were not significantly different in their anti-P₁ IgM antibody levels mentioning Grade (G1 vs G2/3, $P=0.2883$; t -test) or tumour origin (ovary vs tube vs peritoneum, $P=0.322$; ANOVA). An increasing age has previously been demonstrated to be associated with reduction of AGA in a cohort of 48 control plasma samples using glycopeptide arrays (Oyeleran *et al*, 2009). To investigate the influence of age on anti-P₁ antibodies (IgG and IgM), we have applied Pearson's correlation to suspension array data and found a moderate negative correlation ($\rho=-0.33$, $P<0.01$) in the entire cohort (mean age 56.4 (28–87) years). However, in contrast to the control group that showed a moderate negative correlation ($\rho=-0.37$, $P<0.01$), there was no correlation between age and anti-P₁ IgM levels in the tumour group ($\rho=-0.18$, $P=0.123$). This demonstrates that the reduction of anti-P₁ IgM is independent of age in the tumour group and further indicates an association of these lowered IgM levels with the disease. In contrast, we observed no correlation between age and anti-P₁ IgG levels in the control and tumour groups (Supplementary Figure S1). With regards to the risk of cancer recurrence (relapse-free survival), we observed that women with low IgM AGA levels to P₁ (lower than median fluorescence intensity, $n=33$) were associated with a slightly higher risk ($P=0.055$) of having an earlier recurrence than patients ($n=25$) with higher levels of IgM anti-P₁ antibodies (hazard rate ratio 2.328, 95% CI 0.96–5.64) (Figure 1B). The disease-free survival analysis did not reveal any significant effect ($P=0.605$).

Identification of P blood group-related GSL in cancer tissues. GSLs were extracted from fresh collected cancer tissues, and the glycans released from the glycolipids in the form of alditols (see 'Materials and methods') were analysed in the negative ion mode using LC-ESI-MS/MS to identify P blood group-related GSLs (Figure 2). The MS² spectra contained adequate information to facilitate the structural assignment of the glycans based on the fragment ions arising from various glycosidic and cross-ring cleavages, which were described previously (Domon and Costello, 1988).

The base peak chromatograms of the glycan alditols released from the GSLs extracted from serous ovarian (Figure 2A (a)) and peritoneal (Figure 2B (a)) cancer tissue showed several components. Globotriaosylceramide (Gb3, P₁) was detected as $[M-H]^{-}$ m/z 505.3¹⁻ at low intensities, and the extracted ion chromatogram (EIC) showed it eluting at 15.4 min (Figures 2A b(i) and B b(i)). The MS² spectra of the precursor ion at m/z 505.3¹⁻ (Figure 2C (i)) showed prominent B- and C-type fragment ions (B₁ at m/z 161.1¹⁻, C₁ at m/z 179.2¹⁻ and C₂ at m/z 341.1¹⁻) corresponding to a (Hex)₃ or Gal-Gal-Glc sequence of P₁. Characteristic cross ring fragment ions corresponding to ^{2,4}A₂ at m/z 221.2¹⁻ and ^{0,2}A₂ at m/z 281.0¹⁻ were also present in the spectrum, thereby confirming the presence of the 4-linked terminal Gal to the (Gal-Glc) disaccharide (Karlsson *et al*, 2010). A similar study indicated the absence of ^{0,2}A₂ fragment ion in the MS² spectrum of isoglobotriaosylceramide (Galx1-3Galβ1-4Glcβ1) (Karlsson *et al*, 2010) while previous reports have also noted that this characteristic cross ring cleavage was useful in distinguishing between Type 1 (Galβ1-3GlcNAc) and Type 2 (Galβ1-4GlcNAc) chains commonly found in mucins (Chai *et al*, 2001; Robbe *et al*, 2004; Everest-Dass *et al*, 2012).

Globotetraosylceramide (P antigen, Gb4) was detected at $[M-H]^{-}$ m/z 708.3¹⁻ and the EIC showed it to elute at 17.0 min (Figures 2A c(ii) and B c(ii)). Despite appearing at low intensities, the MS² spectra of the precursor ion at m/z 708.3¹⁻ (Figure 2C (ii)) was indicated by the B- and C-type fragment ions (B₁ at m/z 202.0¹⁻, B₃ at m/z 526.0¹⁻, C₁ at m/z 220.0¹⁻ and C₂ at m/z 382.1¹⁻), which corresponded to the tetrasaccharide sequence, HexNAc₁Hex₃ or GalNAc-Gal-Gal-Glc of the P antigen. Several Y-ion fragments seen from the reducing-end were also identified at m/z 343.2¹⁻ (Y₂) and m/z 505.2¹⁻ (Y₃) while the diagnostic cross ring cleavages corresponding to ^{2,4}A₃ at m/z 424.1¹⁻ and ^{0,2}A₃-H₂O at m/z 467.1¹⁻ further confirmed the presence of 4-linked Gal to the internal Galβ1-4Glcβ1 of the Gb4 tetrasaccharide.

The pentasaccharide P₁, HexNAc₁Hex₄ or Gal-Gal-GlcNAc-Gal-Glc, was detected at $[M-H]^{-}$ m/z 870.3¹⁻ at 18.0 min in both tissue samples (Figures 2A d(iii) and B d(iii)). The glycosidic fragment ions occurring at m/z 305.1¹⁻ (B₂-H₂O ion) and m/z 341.0¹⁻ (C₂ ion) indicated the presence of the terminal Gal-Gal epitope while the Y-type fragment ions at m/z 546.2¹⁻ (Y₃) and a prominent m/z 708.2¹⁻ (Y₄ ion) corresponded to the loss of the Gal-Gal epitope and terminal Gal, respectively, from the precursor ion, $[M-H]^{-}$ m/z 870.3¹⁻ (Figure 2C (iii)). Besides that, the prominent ^{2,4}x₄ fragment ion observed at m/z 648.3¹⁻ in the MS² spectra was also characteristic of the terminal Gal residue linked via a 4-linkage to the Gal-GlcNAc-Gal-Glc tetrasaccharide. The cross ring cleavage at ^{0,2}A₃-H₂O at m/z 425.1¹⁻ and the

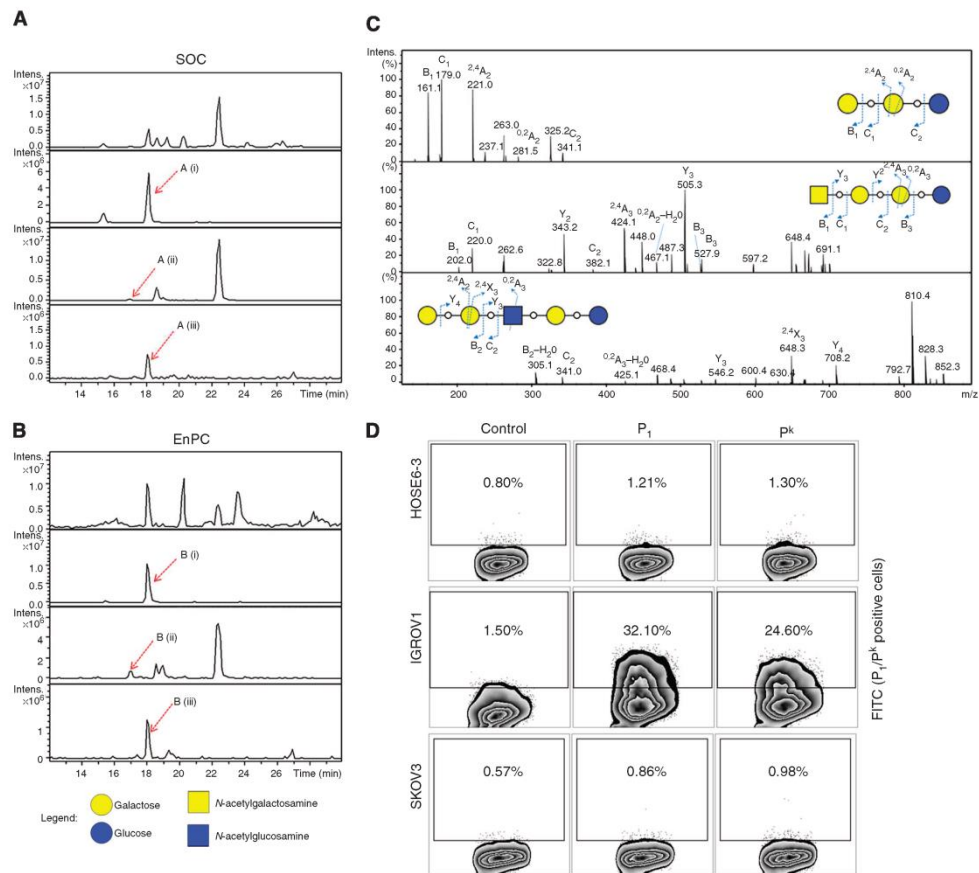


Figure 2. P₁ is expressed on cancer tissue cells. (A, B) Base peak chromatograms shown for serous ovarian cancer (A (a)) and endometrioid peritoneal cancer tissue (B (a)). Selected mass peaks (red arrow) corresponding to the composition of the P^k trisaccharide (Hex₃) (A and B b(i); m/z 505.3¹⁻), P tetrasaccharide (Hex₃HexNAc₁) (A and B c (ii); m/z 708.3¹⁻), and P₁ pentasaccharide (Hex₄HexNAc₁) (A and B d(iii); m/z 870.3¹⁻) are represented as an extracted ion chromatogram (EIC). (C) MS² spectrum of P^k trisaccharide (Galx1-4Galβ1-4Glcβ1) (i), P tetrasaccharide (Galx1-4Galβ1-3Galx1-4Galβ1-4Glcβ1) (ii) and P₁ pentasaccharide (Galx1-4Galβ1-4GlcNAcβ1-3Galβ1-4Glcβ1) (iii). (D) Representative flow cytometry results shown as contour plots with outliers demonstrate P₁ and P^k negative cell lines HOSE6-3 and SKOV3. IGROV1 was detected positive with IgMs for both P₁ and P^k. Representative contour plots showing P₁ and P^k expression (FITC; ordinate) and forward scatter (FSC; abscissa). Given percentage corresponds to P₁/P^k-positive cells.

absence of the ^{0,2}A₄ at m/z 646.1¹⁻ further demonstrates the 4-substitution of the GlcNAc residue and the 3-substitution of the internal Gal and thus tentatively identified this compound as Galx1-4Galβ1-4GlcNAcβ1-3Galβ1-4Glc, the P₁ antigen. The three P blood group antigens were thus shown to be expressed on the GSL of serous ovarian and peritoneal cancer tissues. There was insufficient tubal cancer tissue sample to identify the presence of these antigens.

P₁ is expressed on IGROV1 cell surface. As IgMs were raised against the P₁ antigen in plasma from all types of ovarian cancer patients, and the P₁ (P^k and P) antigens were found to be expressed on the GSL extracted from the cancer tissue of these patients, we established an experimental cell culture model for the investigation into the functional role of P₁. Our panel of immortal cell lines, including human ovarian surface epithelial cells (HOSE6-3 and

HOSE17-1) and various ovarian cancer cell lines ($n=6$), were profiled for P₁ and P^k expression using flow cytometry (Figure 2D). Serous ovarian cancer cell line IGROV1 was heterogenic for P₁ expression (mean 34.1% ranging from 22.8% to 52.8%) based on human anti-P₁ IgM (clone P3NIL100) antibody. The second antibody used in this study, monoclonal murine anti-P₁ IgM (clone OSK17), confirmed P₁ expression on IGROV1 (mean 22.3% ranging from 22.0% to 33.6%). IGROV1 cells were also positive for P^k (mean 33.6% ranging from 12.0% to 54.0%). The normal control cell line HOSE6-3 was negative for both P₁ and P^k as were the remaining ovarian cancer cell lines ($n=5$).

To verify the presence of P₁ on IGROV1 cell line, we isolated GSLs from this cell line and analysed the released glycan alditols using negative ion mode LC-ESI-MS/MS. The P₁ pentasaccharide at m/z 870.3¹⁻ was shown to elute at 20.3 min, and the MS² spectra consisted of B₂ (m/z 323.1¹⁻), Y₃ (m/z 546.3¹⁻) and Y₄

(m/z 708.3¹⁻) fragment ions, which corresponded to the Gal-Gal-GlcNAc-Gal-Glc sequence. The terminal Gal α 1-4Gal linkage was also determined by the cross ring fragment ion at $^{2,4}x_4$ fragment ion observed at m/z 648.3¹⁻ (Supplementary Figure S2).

Monoclonal anti-P₁ IgM bind IGROV1 cells. Both P₁ and P^k share terminal disaccharide structure of composition Gal α 1-4Gal β 1-4Glc(NAc). The monoclonal antibody to P₁ (clone P3NIL100) was used in a flow cytometry-based inhibition assay. Sepharose conjugated PAA-lactose, -N-acetylglucosamine (LacNAc), -P₁ trisaccharide, -P^k was incubated with the monoclonal antibody to P₁ before immunostaining of IGROV1 cells to observe the degree of inhibition of IgM antibody binding to the expressed P₁ on IGROV1 cell surface. In this experiment, repeated three times, flow cytometry of 52.8% P₁-positive IGROV1 cells revealed complete inhibition of monoclonal anti-P₁ antibody by preincubating with 0.015 μ mol P₁ glycoabsorbents (0.04%). In contrast, less reduction (28.3% by 0.06 μ mol P^k) of bound anti-P₁ antibodies to IGROV1 cells was observed in case of P^k glycoabsorbent (Figure 3). Anti-P₁ antibodies were only slightly inhibited by preincubation with glycoabsorbents Lactose (0.06 μ mol; 46.8%) and LacNAc (0.06 μ mol, 44.8%). This clearly demonstrates that IGROV1 cells express P₁ on their cell surface, and monoclonal antibody to P₁ shows clearly higher affinity to P₁ compared with P^k. It also demonstrates specifically that galactose α 1-4 link is required for antibody binding and that lactose and LacNAc are not primarily epitopes of P₁.

Anti-glycan antibodies levels are similar in ascites and blood plasma. To determine whether anti-tumour antibodies were expressed in ascites as well as plasma of patients, we investigated the presence and distribution of AGA in matched ascites and blood plasma samples ($n=11$ patients) for IgA, IgG and IgM together

and separately using the printed glycan array. This was also done for epitope mapping of ascites-derived human anti-P₁ antibodies.

We detected a broad spectrum of AGA in both plasma and ascites (Figure 4). The fluorescence scan of the binding to the immobilised glycans on the array showed high amplitude of AGA in ascites of IgG, IgM and IgA in both 50 μ M and 10 μ M glycan-printed arrays (Supplementary Figure S3). We observed the highest median relative fluorescence signals in ascites (median, 32.75×10^4 RFU) and in plasma (43.33×10^4 RFU) for anti-glycan IgM antibodies. Anti-glycan IgG antibodies showed lower interaction with the glycans (ascites (8.11×10^4 RFU), plasma (9.80×10^4 RFU) as well as anti-glycan IgA (ascites (8.8×10^4 RFU), plasma (10.4×10^4 RFU)). Different levels of AGA to P₁ trisaccharide were detected in all the tested ascites and plasma samples (Figure 4). Highest binding to P₁ was observed for IgM (ascites (18.1×10^4 RFU), plasma (14.3×10^4 RFU)) compared with IgG and IgA.

Matched ascites and plasma AGA signals were not dependent on the volume of patient's ascites. Based on raw data sets of 50 μ M printed glycan arrays, strong correlation between matched ascites and blood plasma samples was observed (Figure 4): IgA + IgG + IgM (CCC = 0.889), IgA (CCC = 0.888), IgG (CCC = 0.961), and IgM (CCC = 0.950). Correlations were similar for 10 μ M printed glycans. This demonstrates that detected AGA levels were independent of the volume of ascites.

Naturally occurring anti-P₁ antibodies in ascites bind to cancer cells expressing P₁ on their cell surface. The results achieved from the above experiments demonstrated that (A) anti-P₁ antibodies detected by glycan-based immunoassays are reduced in plasma of cancer patients, (B) P blood group-related glycans are detectable in tissue samples of cancer patients, (C) IGROV1

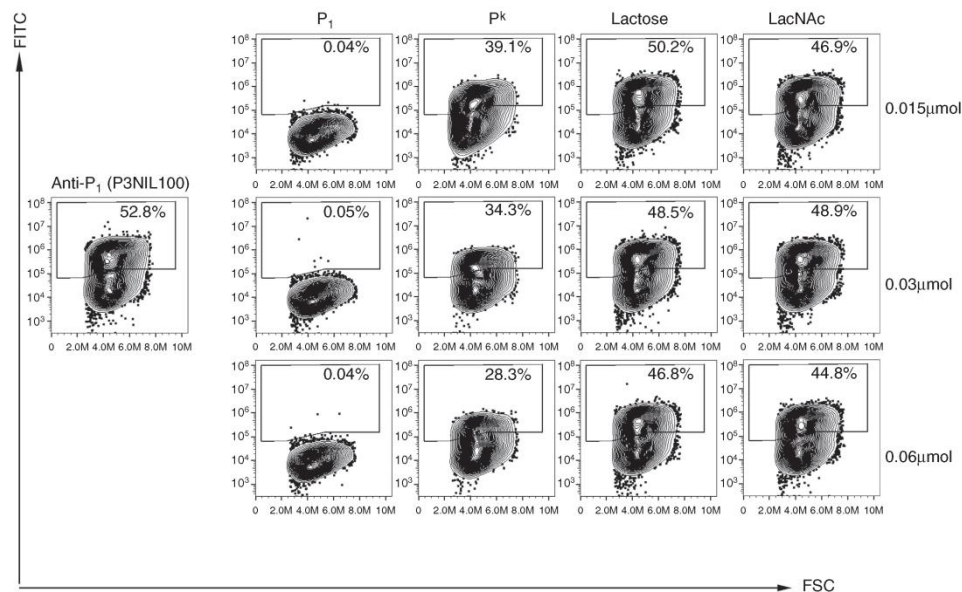


Figure 3. Monoclonal anti-P₁ IgM bind specifically to P₁. Monoclonal anti-P₁ antibody (P3NIL100, positive control) was incubated with different glycan amounts (0.015–0.06 μ mol) prior to flow cytometric measurement of binding to IGROV1 cells. Glycoconjugates Sepharose-PAA (-Lactose, -LacNAc, -P₁, -P^k) were applied to test specificity of antibodies to P₁ by testing the inhibition of binding of the anti-P₁ antibody. Representative contour plots out of three independent experiments showing P₁ expression (FITC; ordinate) and forward scatter (FSC; abscissa). Complete inhibition is shown by increasing Seph-PAA-P₁ amount with only minor inhibition of anti-P₁ antibodies using Seph-PAA-P^k.

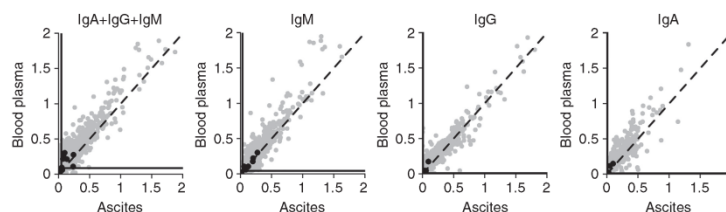


Figure 4. Ascites and blood plasma from cancer patients contain comparable levels of anti-glycan antibodies independent of immunoglobulin class and volume of ascites. Matched ascites and blood plasma samples ($n=11$) were profiled for binding of IgA + IgG + IgM ($n=22$ printed glycan array slides) and independently for IgA ($n=22$), IgG ($n=22$) and IgM ($n=22$) to printed glycan array slides. One scatterplot represents signals for 11 patients each with ascites and blood plasma. AGA to P₁ trisaccharide are highlighted in black. Median signal intensity over all signals calculated for ascites and plasma are shown by horizontal and vertical solid lines, respectively. Antibody signals ($\text{RFU} \times 10^4$) are shown on ascites and blood plasma axis. Cutoff (5%) separating background signals from real AGA binding are indicated by a solid line for ascites and plasma in the same scatterplot.

ovarian cancer cell line was found to express P₁ on its cell surface among all the tested cell lines and (D) profiled ascites contained AGA to P₁ trisaccharide. Therefore the following series of experiments were aimed to investigate whether IgM antibodies derived from ascites bind to IGROV1 and in particular to P₁ presented on its cell surface in the same way as the plasma-derived autoantibodies.

We investigated AGA to P₁ trisaccharide from an ascites sample of a late-stage serous ovarian cancer patient. The ascites fluid was first applied to the IGROV1 cell line in a 1:3 dilution, in which 24.3% of cells were stained positive with ascites-derived IgM antibodies (Figure 5A). Based on this result, we proceeded to affinity purify antibodies bound specifically to P₁ trisaccharide conjugated to sepharose beads. Affinity-purified proteins yielded a maximum amount of IgM of 24 μg after concentration. Detection of purified anti-P₁ antibodies of class IgM revealed binding to P₁-expressing IGROV1 (15.1%) (Figure 5A). In contrast, the ovarian cancer cell line SKOV3, negative for P₁ and P^k expression, had a positive staining of only 0.29% using the purified IgM-P₁ antibodies. This demonstrates for the first time that ascites-derived AGA directed to P₁ trisaccharide also bind to naturally expressed P₁ on cell surface of ovarian cancer cells. In the following ELISA experiment on purified IgM-P₁ antibodies (Figure 5B), higher values for IgM ($\text{OD}_{450\text{ nm}} = \text{mean } 3.23 \pm \text{s.d. } 0.08$) compared with IgG ($\text{OD}_{450\text{ nm}} = 1.08 \pm 0.02$) were observed.

Next, we investigated whether purified IgM-P₁ antibodies bind to glycan structures other than P₁ (potential cross-reactivity). ELISA to a limited number of glycoconjugates revealed in the case of IgM specific binding to P₁ trisaccharide, with cross-reactivity to Galz1-3GalNAc and Galz1-4GlcNAc (Figure 5B). Suspension and printed glycan array were additionally utilised to study the cross-reactivity to broader range of glycan structures, other than P₁. In suspension array, the binding of ascites-derived anti-P₁ antibodies to P₁, P^k, Le^y and α -rhamnose was tested. No preferential binding was observed comparing P₁ and P^k (P₁ 4.11log(MFI); P^k 4.24log(MFI), IgM class). In contrast, Le^y and α -rhamnose coupled beads revealed only minor binding. In the printed glycan array (Figure 5C), we applied a threshold of 5% to the highest median fluorescence signal (19 443 RFU; Galz1-4Gal β 1-4Glc-sp3) to eliminate potentially unspecific binding as described previously (Huflejt *et al.*, 2009). We identified that affinity-purified IgM-P₁ antibodies bound to P blood group-related structures as the top 10 glycans (Supplementary Table S2). Most of the identified low-affinity binding to glycan structures had substructures of the P₁ antigen such as Gal β 1-4Glc(NAc) with 63.0% and Galz1-4Gal β with 22.2% binding reactivity (Supplementary Table S2). This demonstrates that affinity-purified IgM-P₁ antibodies preferentially bound to both P^k and P₁ trisaccharide.

P₁ expression leads to elevated migration rate in ovarian cancer cells. GSLs on the cell surface are described to have several functions in cellular processes, such as pathogen recognition, angiogenesis, cell motility and cell migration (Panjwani *et al.*, 1995; Todeschini *et al.*, 2008; Hakomori, 2010). Migration is a common feature in cancer cells, and therefore we investigated whether or not the presence of P₁ affects cell migration by using a flow cytometry-based cell sorting of IGROV1 cells to separate P₁-high from P₁-low-expressing subpopulations. After further sub-cultivation, P₁ expression in P₁-low IGROV1 cells was determined by murine monoclonal anti-P₁ IgM (OSK17; 18%) or human anti-P₁ IgM (P3NIL100; 33.3%). In contrast, P₁-high-expressing IGROV1 cells were 50.0% and 66.1% positive for P₁, respectively, for these antibodies (Figure 6A).

Utilising these P₁-sorted cell lines, we hypothesised that the presence of P₁ affects cell migration. Significantly higher migration was detected in P₁-high-expressing when compared with P₁-low-expressing IGROV1 cells after an 18 h incubation period ($P=0.0006$) (Figure 6B), as shown by colorimetric cell migration assay. In addition to end-point migration assay, real-time and label-free measurement of P₁-sorted IGROV1 cells was performed using the xCELLigence system. A number of 100 000 cells was seeded into each well of the upper chamber, and migration through the microporous membrane were recorded as cell index. IGROV1 cells with higher P₁ were significantly faster after 20 h ($P=0.035$) than low P₁ cells. Longer incubation periods resulted in no difference between both subpopulations (30 h; $P=0.1337$, 40 h; $P=1$; Figure 6C). To avoid the influence of potentially elevated proliferation effects, 5 μM cytosine arabinoside (araC) was added to the cell culture (Supplementary Figure S4). In concordance with results on the colorimetric cell migration assay and observations on initial xCELLigence experiment, cells with elevated P₁ displayed high basal migratory activity as indicated by the increases in cell index values, reflecting the number of migrating cells. In contrast, P₁-low-expressing cells failed to migrate under experimental conditions. With regard to migratory kinetics, P₁-high-expressing cells migrated rapidly and demonstrated elevated (4.7-fold) cell index of 0.3434 ± 0.054 (mean \pm s.d.) as compared with P₁-low-expressing cells (0.0726 ± 0.029 ; $P=0.004$, CI 0.1–0.45). This difference remained constant throughout the 40 h time course experiment (20 h–3.6-fold ($P<0.001$, CI 0.32–0.66); 30 h–3.6-fold ($P<0.001$, CI 0.40–0.75); 40 h–4.6-fold ($P<0.001$, CI 0.49–0.84); Figure 6C). These findings demonstrate that ovarian cancer cells expressing P₁ on their cell surface migrate faster compared with low-P₁-expressing cells originated from the same parental cell line.

In order to confirm that P₁ is involved in cell migration, we performed the colorimetric cell migration assay with anti-P₁ IgM-pretreated IGROV1 cells. The results (Figure 6D) showed that the

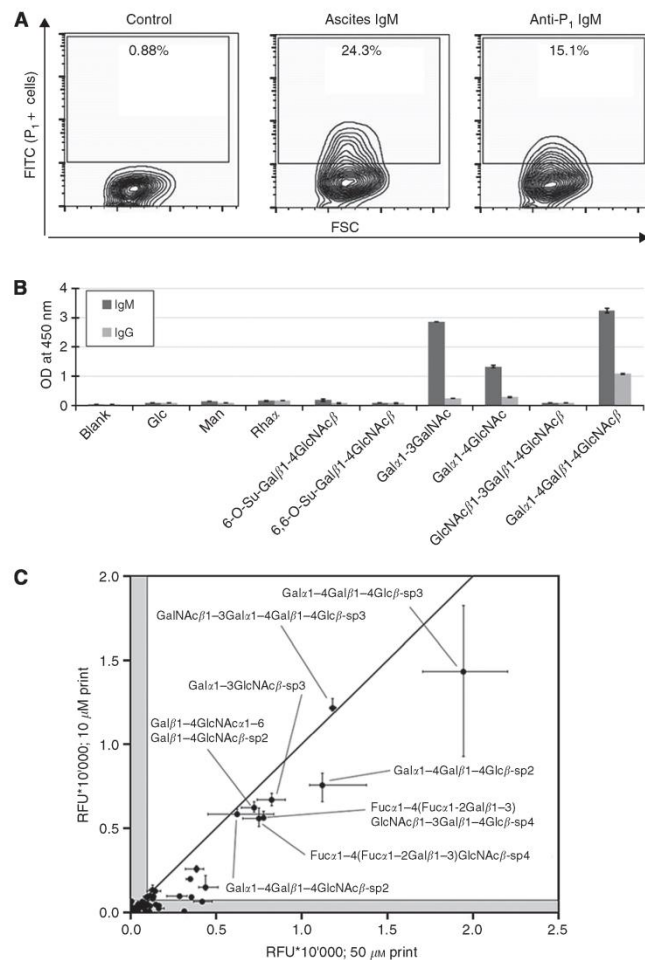


Figure 5. Human ascites-derived affinity-purified anti-P₁ antibodies bind to IGROV1 cells. **(A)** Flow cytometry-based contour plots demonstrate the presence of IgM antibodies in ascites (1:3 diluted in PBS) bound to IGROV1 cells (ascites IgM, 24.3%) compared with unstained sample (control). Affinity-purified anti-P₁ IgM (1:20) bound to IGROV1 cells (15.1% of P₁-positive cells). **(B)** Representative ELISA demonstrating the cross-reactivity of affinity-purified anti-P₁ antibodies of class IgM (dark grey) and IgG (light grey) to investigated glycans linked to PAA. **(C)** Printed glycan array data (scatterplot for 50 μM vs 10 μM saccharide prints) showing cross-reactivity to glycans sharing related carbohydrate structures. Grey area indicates unspecific binding of AGA as determined by 5% threshold. Inter-quartile range is shown for each glycan horizontally and vertically for 50 μM and 10 μM, respectively.

percentage of migrated cells was significantly lower (reduction by 64%; $P < 0.001$) in cultures preincubated with the anti-P₁ IgM antibody. Pretreatment with the respective IgM isotype control did not affect the migration of IGROV1 cells.

DISCUSSION

Unlike P^k, which has been extensively studied in the areas of verotoxin-mediated cytotoxicity, human immunodeficiency virus infection, immunology and epithelial carcinogenesis, there is, to our knowledge, no published study of P₁ and its potential

presence, immunogenicity and its functional role in oncogenesis. Using glycan-based immunoassays, we have previously demonstrated that naturally occurring AGA significantly distinguish healthy controls from ovarian cancer patients (Pochechueva *et al*, 2011b; Jacob *et al*, 2012). The present study demonstrates that: (A) an unknown subpopulation of cancer patients show reduced levels of anti-P₁ IgM antibodies in an extended and independent cohort from another continent (Australian Validation Cohort), (B) P^k, P and P₁ carbohydrate antigens are detectable in cancer tissue as well as on the cell surface of cultured ovarian cancer cells, (C) ascites contains similar anti-glycan IgM-P₁ antibody levels compared with blood plasma independent of its volume at the primary diagnosis, (D) naturally occurring AGA of IgM class derived from ascites of a

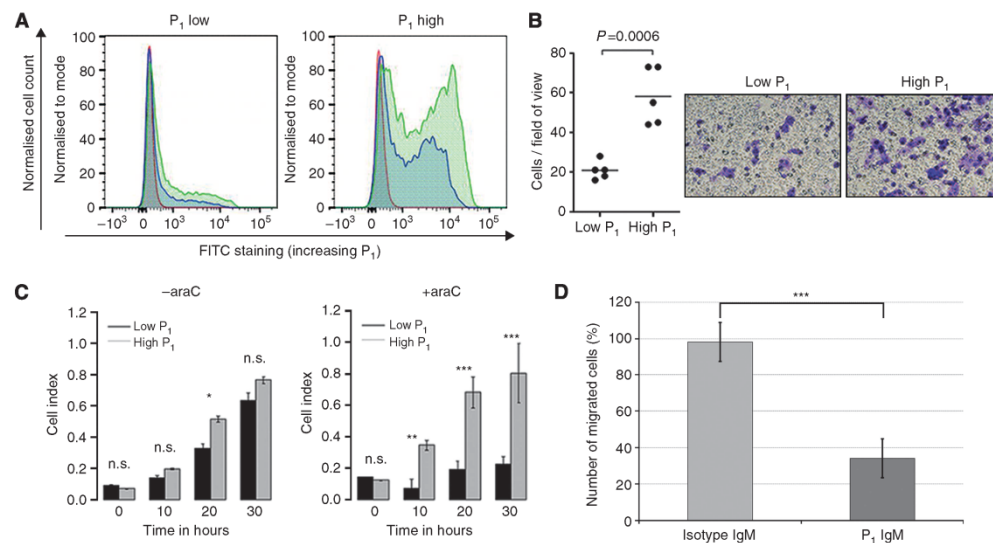


Figure 6. Elevated P₁ expression results in increased migration rate. (A) FACS-sorted subpopulations of P₁-low- and -high-expressing IGROV1 cells. Representative histograms showing P₁ expression (abscissa) on cell-sorted IGROV1 cells to normalised cell count (ordinate). P₁ distribution for unstained controls (red), P₁-positivity P3NIL100 antibody (green) and OSK17 antibody (blue). (B) Colorimetric cell migration assay showing enhanced migratory ability of IGROV1 cells expressing high compared with low levels of P₁. Stained cells counted in five fields and averaged. Representative image of cell sorted subpopulations of migrated cells (stained violet) after 18 h. (C) RTCA assay for P₁-sorted IGROV1 cells showing the migrated cells (cell index) in bar graphs at the time points 0 h, 10 h, 20 h and 30 h. Left bar graph shows RTCA experiment without araC, right bar graph with araC as proliferation inhibitor. Representative figure out of two independent experiments. (D) Bar chart showing the inhibition of cell migration of human IGROV1 cells incubated with anti-P₁ IgM compared with corresponding incubation with IgM isotype control. Number of migrated cells was normalised to control. Not significant (NS); *P < 0.05, **P < 0.01, ***P < 0.001.

ovarian cancer patient bind to naturally expressed and chemically synthesised P₁ on glycan arrays, and (E) the presence of P₁ on ovarian cancer cultured IGROV1 cells leads to enhanced migration.

Our results demonstrate that the significantly lower anti-P₁ antibody levels observed in cancer patients were primarily due to the reduction of IgM but not IgG antibodies. This is in full concordance with the literature on the IgM type anti-Thomsen Friedenreich antibodies (Desai *et al*, 1995) and anti-Lewis C antibodies in breast cancer (Bovin, 2013). A very recently published work demonstrated significantly reduced human IgM antibodies to another GSL (N-glycolylneuraminyl)-lactosylceramide (NeuGcGM3) in non-small cell lung cancer patients (Rodriguez-Zhurbenko *et al*, 2013). Therefore we can assume that IgM class of naturally occurring AGA was able to discriminate between cancer and healthy controls. Natural IgM antibodies belong to the innate immune system and are primarily produced by B1 or CD5+ cells (Boes, 2000; Martin and Kearney, 2001; Viau and Zouali, 2005). As part of the natural immunity, the binding of IgM to conserved carbohydrate structures acts as a first barrier to all invasive particles ('external') and alterations on proteins and lipids within an organism ('internal') (Vollmers and Brandlein, 2007). To date, several human monoclonal antibodies directed to tumour-associated carbohydrate antigens have been isolated. For instance, the monoclonal IgM antibody, SAM-6, specific for cancerous tissue was first derived from a gastric cancer patient (Pohle *et al*, 2004). Later, it was found that the receptor for SAM-6 is a tumour-specific O-linked carbohydrate epitope on GRP78, a central regulator of endoplasmic reticulum in protein folding (Li and Lee, 2006). PAM-1, another monoclonal IgM antibody, binds to a tumour-specific N-linked carbohydrate epitope, a posttranslational modification on cysteine-rich fibroblast growth

factor receptor, CFR-1. This antibody also inhibited tumour growth *in vitro* and in animal model systems by inducing apoptosis (Brandlein *et al*, 2003, 2004a, b). Consistent with the findings of Vollmers and colleagues regarding SAM-6 and PAM-1, our observation based on hierarchical clustering indicates that AGA preferentially bind to substructures of the glycan epitope (Jacob *et al*, 2012). Besides that the decrease of AGA mainly of the IgM class in gynaecological cancer patients (Jacob *et al*, 2012) also points to an involvement of naturally occurring IgM autoantibodies, which recognise GSL structures. We further propose that Galz1-4Galβ1-4Glc(NAc) (present in P, P^h and P₁ antigens) are a result of malignant transformation and could serve as an 'internal' epitope on GSLs that is recognised by naturally circulating anti-glycan IgM antibodies.

The observation of lower levels of anti-P₁ IgM compared with anti-P₁ IgG in cancer patients is very intriguing, and although exploring the underlying mechanisms was beyond the scope of the study, we speculate on a number of possibilities. The elevated presence of corresponding antigens on cancer cells, in our case P₁ GSL, may be bound by circulating anti-P₁ IgM and therefore no longer be freely floating in the plasma and ascites. Another potential mechanism may be tumour-induced immune suppression. It is known that ovarian cancers employ a range of strategies, such as secretion of immunosuppressive cytokines, to facilitate their escape from immune destruction (Lavoue *et al*, 2013). It is possible that this may lead to reduced antibody production against cancer-associated antigens, for example, P₁, conferring a survival advantage to cancer cells. The antibody repertoire in cancer patients would therefore be different. Another possible mechanism is the occupation of anti-P₁ IgMs by cancer cells (including circulating tumour cells) by virtue of their surface expression of

P₁, leading to a reduction in the amount of unbound antibody in plasma and/or ascites. The formation of immune complexes consisting of P₁ antigen shed from cancer cells, and anti-P₁ IgMs, may further contribute to this reduction. A prominent example in the literature for the formation of circulating immune complexes consisting of Lewis x and antibodies has been shown in *Helicobacter pylori*-infected human (Chmiela *et al*, 1998). With regards to no change being observed in the anti-P₁ IgG levels, we expected differences preferentially in the case of IgM rather than of IgG as glycan-based antigens are T-cell-independent antigens and are recognised by the innate immune system.

Our mass spectrometry results demonstrated that these P₁, P^k and P antigens are expressed on ovarian and peritoneal cancer tissues. The functional role of the GSL that carry these structures in carcinogenesis is poorly understood, especially in the case of P₁ and P. It was recently described that a monoclonal anti-P^k antibody (E3E2) inhibited angiogenesis and tumour development (Desselle *et al*, 2012). Enhanced expression of P^k has also been shown to cause doxorubicin resistance in breast cancer cells (Gupta *et al*, 2012). Cisplatin-resistant pleural mesothelioma cells were shown to be sensitised to cisplatin by the addition of sub-toxic concentrations of Verotoxin 1 (Johansson *et al*, 2010). In addition, we also demonstrate that P₁ and P^k antigens are also present on the surface of the IGROV1 serous ovarian cancer cells. IGROV1 is, therefore, to the best of our knowledge, the only immortal cell line from several investigated that expresses P₁. Using monoclonal antibodies against P₁, only minor cross-reactivity to other glycan structures was observed in glycan-based immunoassays (not shown). Furthermore, based on the flow cytometry inhibition assay using IGROV1 cells as an investigative model, the specificity of monoclonal antibodies to P₁ as shown by the full saturation of anti-P₁ antibodies by inhibition with 0.06 µmol glycan on sepharose beads indicates that IGROV1 expresses P₁ on the cell surface.

Serous pelvic masses commonly present with malignant ascites, a plasma-protein-rich intraperitoneal exudate of up to several litres. Several pathophysiological mechanisms are necessary for malignant ascites occur: (a) decreased lymphatic ascites absorption, (b) increased capillary permeability, (c) increased overall capillary membrane-surface area available for filtration, and consequently (d) an increased intraperitoneal oncotic pressure due to intraperitoneal protein concentration (Tamsma *et al*, 2001). Using the printed glycan array, we observed an unexpectedly rich spectrum of AGA with similar amounts in plasma and ascites. These findings suggested that there is an equilibrium between both body fluids. Early lymphatic obstruction is one of the first manifestations of an inflammatory reaction (Feldman, 1975). As IgM has an important role in inflammation with multivalent antigen binding due to its pentameric structure and as the first immunoglobulin class produced in a primary response to an antigen, lymphatic obstruction may result in a rapid increase in IgM secreting plasma cells. Natural circulating AGA have also been described in various inflammatory conditions, including diabetes mellitus type 1 (Gillard *et al*, 1989), chronic inflammatory bowel and Crohn's disease (Malickova *et al*, 2006) and in patients with cancer (Young *et al*, 1979; Springer, 1984; Springer *et al*, 1988; Desai *et al*, 1995).

We also investigated the expression of A4GALT P₁- and P^k-profiled cell lines. As seen in our study, A4GALT is overexpressed in the P₁- and P^k-positive ovarian cancer cell line IGROV1 (Jacob *et al*, 2011b), suggesting that A4GALT is not only involved in P^k but also in P₁ synthesis in ovarian cancer cells. We propose that A4GALT is involved in the progression of various ovarian and peritoneal cancers; however, the molecular link between A4GALT mRNA levels and P₁ expression remains unknown. This is consistent with suspension array results in which no tested clinical parameters were shown to correlate with lower AGA levels to P₁ trisaccharide. A recently identified single nucleotide polymorphism

(CT conversion) encoding an additional exon in the genomic region of A4GALT (Thuresson *et al*, 2011) could probably explain the presence of P₁ in cancer cells. However, it is unclear whether the overexpression of A4GALT is causative for the synthesis of P₁ or P^k in profiled cancer cell lines. The invasive phenotype of colon cells lacking P^k could be induced and inhibited by the transfection of Gb3 synthase (A4GALT) or RNA interference, respectively (Kovbasnjuk *et al*, 2005). Another immunohistochemistry-based study showed that P^k expression was elevated in colorectal cancers and their metastases; however, A4GALT mRNA levels, protein expression or galactosyltransferase activity were not investigated (Falguières *et al*, 2008). The potential role of A4GALT in cancer initiation or progression needs to be elucidated in future studies with respect to all P blood group-related glycans.

For the first time, we also observed migration rate in P₁-high-expressing cells, and this was even more obvious when araC, a proliferation inhibitor, was added to the cultures (Roy *et al*, 2006). The addition of araC confirmed that the observed difference in migration was indeed due to altered cell migration and not cell proliferation. Our results suggest an involvement of P₁ in cell migration, but the underlying molecular mechanisms are unknown.

Finally, this study provides further evidence that P blood group-related antigens have a role in carcinogenesis and those naturally occurring anti-glycan IgM antibodies against them may have the potential to discriminate ovarian cancer patients from healthy individuals. If these surface antigens prove to be indeed tumour-specific, they may become candidate molecular targets for potential imaging tools for confocal fluorescence endoscopy and positron emission tomography and as tools in targeted immunotherapy (Janssen *et al*, 2006; Viel *et al*, 2008).

ACKNOWLEDGEMENTS

This work was supported by Cancer Institute NSW grant (09/CRF/2-02) to VHS, the William Maxwell Trust, the Mary Elisabeth Courier Scholarship (RANZCOG) to VHS, the Swiss National Foundation grants PBZHP3-133289 (to FJ) and 320030-120543 (to VHS), the OncoSuisse grant (OCS-02115-08-2007) to VHS and the Novartis Foundation (13B093) to FJ. We would like to acknowledge the following people for their various contributions to this publication: Jim Scurry, Andreas Schoetzau, Sheri Nixdorf, Monica Nunez Lopez, Renato Mueller and Daniel Fink.

REFERENCES

- Boes M (2000) Role of natural and immune IgM antibodies in immune responses. *Mol Immunol* 37(18): 1141–1149.
- Bovin N, Obukhova P, Shilova N, Rapoport E, Popova I, Navakouski M, Unverzagt C, Vuskovic M, Huflejt M (2012) Repertoire of human natural anti-glycan immunoglobulins. Do we have auto-antibodies? *Biochim Biophys Acta* 1820(9): 1373–1382.
- Bovin NV (2013) Natural antibodies to glycans. *Biochemistry (Moscow)* 78(7): 786–797.
- Brandlein S, Beyer I, Eck M, Bernhardt W, Hensel F, Muller-Hermelink HK, Vollmers HP (2003) Cysteine-rich fibroblast growth factor receptor 1, a new marker for precancerous epithelial lesions defined by the human monoclonal antibody PAM-1. *Cancer Res* 63(9): 2052–2061.
- Brandlein S, Eck M, Strobel P, Wozniak E, Muller-Hermelink HK, Hensel F, Vollmers HP (2004a) PAM-1, a natural human IgM antibody as new tool for detection of breast and prostate precursors. *Hum Antibodies* 13(4): 97–104.
- Brandlein S, Pohle T, Vollmers C, Wozniak E, Ruoff N, Muller-Hermelink HK, Vollmers HP (2004b) CFR-1 receptor as target for tumor-specific apoptosis induced by the natural human monoclonal antibody PAM-1. *Oncol Rep* 11(4): 777–784.

- Chai W, Piskarev V, Lawson AM (2001) Negative-ion electrospray mass spectrometry of neutral underivatized oligosaccharides. *Anal Chem* **73**(3): 651–657.
- Chang WW, Lee CH, Lee P, Lin J, Hsu CW, Hung JT, Lin JJ, Yu JC, Shao LE, Yu J, Wong CH, Yu AL (2008) Expression of Globo H and SSEA3 in breast cancer stem cells and the involvement of fucosyl transferases 1 and 2 in Globo H synthesis. *Proc Natl Acad Sci USA* **105**(33): 11667–11672.
- Chmiela M, Wadstrom T, Folkesson H, Planeta Malecka I, Czkwianiec E, Rechinski T, Rudnicka W (1998) Anti-Lewis X antibody and Lewis X-anti-Lewis X immune complexes in *Helicobacter pylori* infection. *Immunol Lett* **61**(2-3): 119–125.
- Desai PR, Ujjainwala LH, Carlstedt SC, Springer GF (1995) Anti-Thomsen-Friedenreich (T) antibody-based ELISA and its application to human breast carcinoma detection. *J Immunol Methods* **188**(2): 175–185.
- Desselle A, Chaumette T, Gaugler MH, Cochonneau D, Fleurence J, Dubois N, Hulin P, Aubry J, Birkle S, Paris F (2012) Anti-gb3 monoclonal antibody inhibits angiogenesis and tumor development. *PLoS One* **7**(11): e45423.
- Domon B, Costello CE (1988) Structure elucidation of glycosphingolipids and gangliosides using high-performance tandem mass spectrometry. *Biochemistry* **27**(5): 1534–1543.
- Everest-Dass AV, Jin D, Thaysen-Andersen M, Nevalainen H, Kolarich D, Packer NH (2012) Comparative structural analysis of the glycosylation of salivary and buccal cell proteins: innate protection against infection by *Candida albicans*. *Glycobiology* **22**(11): 1465–1479.
- Falguieres T, Maak M, von Weyhern C, Sarr M, Sastre X, Poupon MF, Robine S, Johannes L, Janssen KP (2008) Human colorectal tumors and metastases express Gb3 and can be targeted by an intestinal pathogen-based delivery tool. *Mol Cancer Ther* **7**(8): 2498–2508.
- Feldman GB (1975) Lymphatic obstruction in carcinomatous ascites. *Cancer Res* **35**(2): 325–332.
- Gilewski T, Ragupathi G, Bhuta S, Williams LJ, Musselli C, Zhang XF, Bornmann WG, Spassova M, Bencath KP, Panageas KS, Chin J, Hudis CA, Norton L, Houghton AN, Livingston PO, Danishefsky SJ (2001) Immunization of metastatic breast cancer patients with a fully synthetic globo H conjugate: a phase I trial. *Proc Natl Acad Sci USA* **98**(6): 3270–3275.
- Gillard BK, Thomas JW, Nell LJ, Marcus DM (1989) Antibodies against ganglioside GT3 in the sera of patients with type I diabetes mellitus. *J Immunol* **142**(11): 3826–3832.
- Gupta V, Bhinge KN, Hosain SB, Xiong K, Gu X, Shi R, Ho MY, Khoo KH, Li SC, Li YT, Ambudkar SV, Jazwinski SM, Liu YY (2012) Ceramide glycosylation by glucosylceramide synthase selectively maintains the properties of breast cancer stem cells. *J Biol Chem* **287**(44): 37195–37205.
- Hakomori S (1998) Cancer-associated glycosphingolipid antigens: their structure, organization, and function. *Acta Anat* **161**(1-4): 79–90.
- Hakomori S, Wang SM, Young Jr. WW (1977) Isoantigenic expression of Forssman glycolipid in human gastric and colonic mucosa: its possible identity with "A-like antigen" in human cancer. *Proc Natl Acad Sci USA* **74**(7): 3023–3027.
- Hakomori SI (2010) Glycosynaptic microdomains controlling tumor cell phenotype through alteration of cell growth, adhesion, and motility. *FEBS Lett* **584**(9): 1901–1906.
- Huflejt ME, Vuskovic M, Vasiliu D, Xu H, Obukhova P, Shilova N, Tuzikov A, Galanina O, Arun B, Lu K, Bovin N (2009) Anti-carbohydrate antibodies of normal sera: findings, surprises and challenges. *Mol Immunol* **46**(15): 3037–3049.
- Jacob F, Goldstein DR, Bovin NV, Pochechueva T, Spengler M, Caduff R, Fink D, Vuskovic MI, Huflejt ME, Heinzelmann-Schwarz V (2012) Serum antiglycan antibody detection of nonmucinous ovarian cancers by using a printed glycan array. *Int J Cancer* **130**(1): 138–146.
- Jacob F, Meier M, Caduff R, Goldstein D, Pochechueva T, Hacker N, Fink D, Heinzelmann-Schwarz V (2011a) No benefit from combining HE4 and CA125 as ovarian tumor markers in a clinical setting. *Gynecol Oncol* **121**(3): 487–491.
- Jacob F, Tse BWC, Guertler R, Nixdorf S, Bovin NV, Hacker N, Heinzelmann-Schwarz V (2011b) P1 antigen is present on the serous ovarian cancer cell line, IGROV1, correlating with A4GALT overexpression and altered cell behaviour. *Glycobiology* **21**(11): 1454–1531.
- Janssen KP, Vignjevic D, Boisgard R, Falguieres T, Bousquet G, Decaudin D, Dolle F, Louvard D, Tavittian B, Robine S, Johannes L (2006) In vivo tumor targeting using a novel intestinal pathogen-based delivery approach. *Cancer Res* **66**(14): 7230–7236.
- Jarvis WD, Grant S, Kolesnick RN (1996) Ceramide and the induction of apoptosis. *Clin Cancer Res* **2**(1): 1–6.
- Johansson D, Andersson C, Moharer J, Johansson A, Behnam-Motlagh P (2010) Cisplatin-induced expression of Gb3 enables verotoxin-1 treatment of cisplatin resistance in malignant pleural mesothelioma cells. *Br J Cancer* **102**(2): 383–391.
- Karlsson H, Halim A, Teneberg S (2010) Differentiation of glycosphingolipid-derived glycan structural isomers by liquid chromatography/mass spectrometry. *Glycobiology* **20**(9): 1103–1116.
- Kasahara K, Sanai Y (1999) Possible roles of glycosphingolipids in lipid rafts. *Biophys Chem* **82**(2-3): 121–127.
- Ke N, Wang X, Xu X, Abassi YA (2011) The xCELLigence system for real-time and label-free monitoring of cell viability. *Methods Mol Biol* **740**: 33–43.
- Kovbasnjuk O, Mourtazina R, Baibakov B, Wang T, Elowsky C, Choti MA, Kane A, Donowitz M (2005) The glycosphingolipid globotriaosylceramide in the metastatic transformation of colon cancer. *Proc Natl Acad Sci USA* **102**(52): 19087–19092.
- Lavoue V, Thedrez A, Leveque J, Foucher F, Henno S, Jauffret V, Belaud-Rotureau MA, Catros V, Cabillic F (2013) Immunity of human epithelial ovarian carcinoma: the paradigm of immune suppression in cancer. *J Transl Med* **11**: 147.
- Li J, Lee AS (2006) Stress induction of GRP78/BiP and its role in cancer. *Curr Mol Med* **6**(1): 45–54.
- Malickova K, Lukas M, Donoval R, Sandova P, Janatkova I (2006) Novel anti-carbohydrate autoantibodies in patients with inflammatory bowel disease: are they useful for clinical practice? *Clin Lab* **52**(11-12): 631–638.
- Martin F, Kearney JF (2001) B1 cells: similarities and differences with other B cell subsets. *Curr Opin Immunol* **13**(2): 195–201.
- Oyleran O, McShane LM, Dodd L, Gildersleeve JC (2009) Profiling human serum antibodies with a carbohydrate antigen microarray. *J Proteome Res* **8**(9): 4301–4310.
- Ozols RF (2006) Challenges for chemotherapy in ovarian cancer. *Ann Oncol* **17**(Suppl 5): v181–v187.
- Panjwani N, Zhao Z, Ahmad S, Yang Z, Jungwalwa F, Baum J (1995) Neolactoglycosphingolipids, potential mediators of corneal epithelial cell migration. *J Biol Chem* **270**(23): 14015–14023.
- Pochechueva T, Chinarev A, Spengler M, Korchagina E, Heinzelmann-Schwarz V, Bovin N, Rieben R (2011a) Multiplex suspension array for human anti-carbohydrate antibody profiling. *Analyst* **136**(3): 560–569.
- Pochechueva T, Jacob F, Fedier A, Heinzelmann-Schwarz V (2012) Tumor-associated glycans and their role in gynecological cancers: accelerating translational research by novel-high throughput approaches. *Metabolites* **2**(4): 913–939.
- Pochechueva T, Jacob F, Goldstein DR, Huflejt ME, Chinarev A, Caduff R, Fink D, Hacker N, Bovin NV, Heinzelmann-Schwarz V (2011b) Comparison of printed glycan array, suspension array and ELISA in the detection of human anti-glycan antibodies. *Glycoconj J* **28**(8-9): 507–517.
- Pohle T, Brandlein S, Ruoff N, Muller-Hermelink HK, Vollmers HP (2004) Lipoptosis: tumor-specific cell death by antibody-induced intracellular lipid accumulation. *Cancer Res* **64**(11): 3900–3906.
- Robbe C, Capon C, Coddeville B, Michalski JC (2004) Diagnostic ions for the rapid analysis by nano-electrospray ionization quadrupole time-of-flight mass spectrometry of O-glycans from human mucins. *Rapid Commun Mass Spectrom* **18**(4): 412–420.
- Rodriguez-Zhurbenko N, Martinez D, Blanco R, Rondon T, Grinan T, Hernandez AM (2013) Human antibodies reactive to NeuGcGM3 ganglioside have cytotoxic antitumor properties. *Eur J Immunol* **43**(3): 826–837.
- Roy AM, Tiwari KN, Parker WB, Secrist 3rd JA, Li R, Qu Z (2006) Antiangiogenic activity of 4'-thio-beta-D-arabinofuranosylcytosine. *Mol Cancer Ther* **5**(9): 2218–2224.
- Solly K, Wang X, Xu X, Strulovici B, Zheng W (2004) Application of real-time cell electronic sensing (RT-CES) technology to cell-based assays. *Assay Drug Dev Technol* **2**(4): 363–372.
- Springer GF (1984) T and Tn, general carcinoma autoantigens. *Science* **224**(4654): 1198–1206.
- Springer GF, Chandrasekaran EV, Desai PR, Tegtmeyer H (1988) Blood group Tn-active macromolecules from human carcinomas and erythrocytes: characterization of and specific reactivity with mono- and poly-clonal

- anti-Tn antibodies induced by various immunogens. *Carbohydr Res* **178**: 271.
- Tamsma JT, Keizer HJ, Meinders AE (2001) Pathogenesis of malignant ascites: Starling's law of capillary hemodynamics revisited. *Ann Oncol* **12**(10): 1353–1357.
- Taniguchi N, Yokosawa N, Narita M, Mitsuyama T, Makita A (1981) Expression of Forssman antigen synthesis and degradation in human lung cancer. *J Natl Cancer Inst* **67**(3): 577–583.
- Thureson B, Westman JS, Olsson ML (2011) Identification of a novel A4GALT exon reveals the genetic basis of the P1/P2 histo-blood groups. *Blood* **117**(2): 678–687.
- Todeschini AR, Dos Santos JN, Handa K, Hakomori SI (2008) Ganglioside GM2/GM3 complex affixed on silica nanospheres strongly inhibits cell motility through CD82/cMet-mediated pathway. *Proc Natl Acad Sci USA* **105**(6): 1925–1930.
- Viau M, Zouali M (2005) B-lymphocytes, innate immunity, and autoimmunity. *Clin Immunol* **114**(1): 17–26.
- Viel T, Dransart E, Nemat F, Henry E, Theze B, Decaudin D, Lewandowski D, Boissard R, Johannes L, Tavitian B (2008) In vivo tumor targeting by the B-subunit of shiga toxin. *Mol Imaging* **7**(6): 239–247.
- Vollmers HP, Brandlein S (2007) Natural antibodies and cancer. *J Autoimmun* **29**(4): 295–302.
- Wang CC, Huang YL, Ren CT, Lin CW, Hung JT, Yu JC, Yu AL, Wu CY, Wong CH (2008) Glycan microarray of Globo H and related structures for quantitative analysis of breast cancer. *Proc Natl Acad Sci USA* **105**(33): 11661–11666.
- Wenk J, Andrews PW, Casper J, Hata J, Pera MF, von Keitz A, Damjanov I, Fenderson BA (1994) Glycolipids of germ cell tumors: extended globo-series glycolipids are a hallmark of human embryonal carcinoma cells. *Int J Cancer* **58**(1): 108–115.
- Young Jr. WW, Hakomori SI, Levine P (1979) Characterization of anti-Forssman (anti-Fs) antibodies in human sera: their specificity and possible changes in patients with cancer. *J Immunol* **123**(1): 92–96.



This work is licensed under the Creative Commons Attribution-NonCommercial-Share Alike 3.0 Unported License. To view a copy of this license, visit <http://creativecommons.org/licenses/by-nc-sa/3.0/>

Supplementary Information accompanies this paper on British Journal of Cancer website (<http://www.nature.com/bjc>)

4.4 Supplementary Information

SUPPLEMENTARY INFORMATION

Material and Methods

Cell cultures

Normal human ovarian surface epithelial cell line originated from the ovary (HOSE6-3) and ovarian cancer cell lines OVCAR3, SKOV3, A2780, IGROV1 were cultured in RPMI 1640 medium containing penicillin/streptomycin and 10% fetal calf serum (FCS). Ovarian cancer cells TOV112D and TOV21G (clear cell) were cultivated in DMEM containing 10% FCS and penicillin/streptomycin. Cell cultures were maintained at 37°C in 5% CO₂ and tested routinely for mycoplasma infection (VenorGeM® Mycoplasma Detection Kit (Biocene Pty Ltd, Rozelle, Australia) and (Uphoff & Drexler, 2005)).

Extraction of GSLs from cancer tissue samples

Fresh primary tumor samples from patients with serous ovarian cancer and endometrioid peritoneal cancer were washed twice with PBS. GSLs were extracted as previously described (Korekane *et al*, 2007). Briefly, tissues (~100mg) were homogenized in 5ml of chloroform:methanol (2:1) and stored for 2h at room temperature (RT), with intermittent sonication for 30sec every 30min. Prior to centrifugation at 1800xg for 15min, 2.5 ml of methanol was added to the homogenate. Supernatant was collected and residual tissue was homogenized again in 5ml of chloroform:methanol:water (1:2:0.8). The tissue homogenate was stored for 2h at RT and subjected to centrifugation at 1800xg for 15min. Supernatant was collected and combined with the previous supernatant and evaporated under vacuum. The dried residue containing the glycosphingolipid mixture was then re-dissolved in 100µl of chloroform:methanol (2:1).

Extraction of GSLs from IGROV1 cells

Ovarian cancer cell line IGROV1 was grown in large quantities (1×10^8), harvested and stored in -80°C until use. GSLs were extracted as previously described with some modifications (Durrant *et al*, 2006). Cells were harvested and washed thrice in 10ml of PBS and centrifuged at 1800xg for 15min. A volume of 5ml of chloroform: methanol (2:1) was added to the cell pellet and the tube was kept overnight in a 4°C incubator shaker prior to centrifugation at 1800xg for 15min. Supernatant was collected and pellet was re-extracted again as described above. The combined supernatants were subjected to centrifugation at 1800xg for 15min to remove residual protein pellet. The supernatant was evaporated to dryness under vacuum and the dried residue containing the glycosphingolipid mixtures was re-dissolved in 50 μl of chloroform: methanol (2:1).

PVDF blotting of extracted GSLs, enzymatic release of glycans and purification of glycan alditols

GSLs were blotted onto a polyvinylidene difluoride (PVDF) membrane, an adaptation from a previous method developed for the release of *N*- and *O*-glycans (Jensen *et al*, 2012). Re-dissolved glycosphingolipid mixtures (50 μl) were blotted (10 μl x 5 times) onto cut pre-activated PVDF spots which were placed in a chloroform-compatible 96-well microtitre plate. Neutral and acidic glycosphingolipid standards (10 μl) were blotted (2.5 μl x 4 times) on individual PVDF spots. The spots were air-dried at RT to ensure proper binding of GSLs to the membrane. Once the spots were dried, the glycosphingolipid mixture (acidic and neutral) was digested with 5mU of *Endoglycoceramidase* II (EGCase II, recombinant clone derived from *Rhodococcus* sp. and expressed in *Escherichia coli*, Sigma-Aldrich, St. Louis, USA) in 50 μl of 0.05M Sodium acetate buffer pH 5.0 for 16h at 37°C . The 96-well microtiter plate was sealed with parafilm to avoid sample evaporation. After incubation, approximately 50 μl was recovered from the individual PVDF spots and transferred to 1.5ml Eppendorf tubes. The sample wells were washed with 50 μl of water and combined with the enzyme mixture of

released glycans for each sample. The reaction was stopped by adding 1ml of chloroform:methanol:water (8:4:3) (Karlsson *et al*, 2010). The upper layer (methanol:water) containing the released oligosaccharides (~400µl) was dried and used for subsequent reduction and desalting steps.

Released glycans were reduced to alditols with 20µl of 200mM sodium borohydride in 50mM potassium hydroxide at 50°C for 2h. The reduction mixture was quenched using 3µl of 100% glacial acetic acid.

Glycan alditols were desalted using cation exchange columns that were prepared individually. Approximately 45µl of cation exchange resin beads (BioRad, Hercules, USA; AG50W-X8) were deposited onto reversed phase µ-C18 ZipTips (Perfect Pure, Millipore, Billerica, USA) that were placed in individual microfuge tubes. The tubes were then subjected to a brief spin and followed by a series of individual pre-washing steps with a) 50µl of 1M HCl, b) 50µl of methanol and c) 50µl of water. Each washing step was repeated three times, in which the columns were subjected to a brief spin after the addition of each solution. Approximately 20µl of glycan alditols were applied to the previously prepared cation exchange columns and they were eluted with water (50µl, twice) and dried. Residual borate was removed by drying the samples under vacuum after the addition of methanol (100µl, thrice). The purified glycan alditols were re-suspended in 15µl of water prior to mass spectrometry analysis.

Negative-mode LC-ESI-MS of released glycan alditols mixtures

Samples (4µl) were injected onto a Hypercarb porous graphitized carbon (PGC) capillary column (5 µm Hypercarb KAPPA, 180µm x 100mm, Thermo Hypersil, Runcorn, UK) using a Surveyor auto-sampler. The separation of glycans was carried out over a linear HPLC gradient of 0-45 % (v/v) acetonitrile/ 10mM ammonium bicarbonate for 35min followed by a 10min wash-step using 90 % (v/v) acetonitrile/ 10mM ammonium bicarbonate at a flow rate

of 3 μ l/ min. Glycans were analyzed by nanoLC-MS/MS using a LTQ linear ion-trap mass spectrometer (LC/MSD Trap XCT Plus Series 1100, Agilent Technologies, USA) which was connected to an ESI source (Agilent 6330, Agilent Technologies, USA). The MS spectra were obtained within the mass range of m/z 200 - m/z 1500. The temperature of the transfer capillary was maintained at 300°C and the capillary voltage was set at 3kV. Neutral and acidic glycans were detected in the negative ion reflector mode as $[M-H]^-$ ions and their signal intensities analyzed using Compass Data Analysis Version 1.1 software (Bruker Daltonics, Billerica, USA). The proposed oligosaccharide structures of experimental samples were verified through annotation using a fragmentation mass matching approach based on the MS/MS data and further validated based on the retention times of specific glycan masses of released glycans from glycosphingolipid standards.

Statistical analysis

All evaluations were performed using the R statistical programming language, version 2.15.1 (<http://www.r-project.org/>). Suspension array data are presented as logarithmized median fluorescence intensity ($\log(\text{MFI})$) which is defined as relative fluorescence unit (RFU). Two-group comparison was performed by Welch Two Sample *t*-test. Logistic regression was performed to predict low anti-P₁ trisaccharide antibody levels in the tumor group, with linear predictors being “cancer histotype”, “FIGO stage”, “grade”, “CA125”, “tumor origin”, “ABO blood group”, “past history of infections”, “BRCA1/2 status” and “smoking”. Cox regression was performed on relapse- and disease-free survival to investigate the prediction of anti-P₁ trisaccharide antibodies. Results are presented as differences of mean values with corresponding 95% confidence intervals (CI) and *p*-values. A *p*-value <0.05 was considered significant. Pearson’s correlation was applied to investigate the relationship between age and AGA levels.

In regards to printed glycan array experiments, the concordance correlation coefficient (CCC) was applied on total signal intensities as a median out of eight replicates (relative fluorescence unit, RFU) in order to calculate the correlation of AGA comparing ascites and blood plasma. The CCC was calculated on both printed glycan concentrations (10 and 50 μ M) for IgA+IgG+IgM together, as well as individually for IgA, IgG and IgM. The results were summarized in scatter plots.

In regards to xCELLigence experiment, to compare the effects of "P₁-high *versus* P₁-low" expressing IGROV1 cells with and without inhibitor araC, a linear mixed effects-model was applied across time points. Factors "high-low", "with/without inhibitor" and "time" were modified parameters. Measured cell indices were treated as a random effect. "P₁high-low" was nested in "Inhibitor", "Inhibitor" was nested in "time".

References

- Durrant LG, Harding SJ, Green NH, Buckberry LD, Parsons T (2006) A new anticancer glycolipid monoclonal antibody, SC104, which directly induces tumor cell apoptosis. *Cancer research* **66**(11): 5901-9
- Jensen PH, Karlsson NG, Kolarich D, Packer NH (2012) Structural analysis of N- and O-glycans released from glycoproteins. *Nature protocols* **7**(7): 1299-310
- Karlsson H, Halim A, Teneberg S (2010) Differentiation of glycosphingolipid-derived glycan structural isomers by liquid chromatography/mass spectrometry. *Glycobiology* **20**(9): 1103-16
- Korekane H, Tsuji S, Noura S, Ohue M, Sasaki Y, Imaoka S, Miyamoto Y (2007) Novel fucogangliosides found in human colon adenocarcinoma tissues by means of glycomic analysis. *Analytical biochemistry* **364**(1): 37-50
- Uphoff CC, Drexler HG (2005) Detection of mycoplasma contaminations. *Methods in molecular biology* **290**: 13-23

4.5 Supplementary Data

Table 1S Clinicopathological characteristics of ovarian cancer cohort (n=155)

Disease status		n	%	Total in %
Control group (81)	Healthy and benign	81	100	52.3
Tumors (74)	Borderline tumor	8	10.8	47.7
	Ovarian cancer	38	51.3	
	Peritoneal Cancer	19	25.7	
	Tubal Cancer	9	12.2	
FIGO Stage (74)	I	17	23.0	
	II	3	4.0	
	III	40	54.0	
	IV	9	12.2	
	unknown	5	6.8	
Grade (74)	Borderline	8	10.8	
	1	7	9.5	
	2	4	5.4	
	3	55	74.3	
Histotype (74)	Serous	53	71.6	
	Mucinous	10	13.6	
	Endometrioid	3	4.0	
	Mixed	3	4.0	
	Clear cell	2	2.7	
	Transitional cell	2	2.7	
	Undifferentiated	1	1.4	

Figure 1S Identification of P₁ in ovarian cancer cell line (IGROV 1) using negative ion mode LC-ESI-MS/MS Base peak chromatogram is shown for glycans extracted from GSLs of ovarian cancer cell line, IGROV 1 **(A)**. Representative extracted ion chromatogram (EIC) of the P₁ pentasaccharide (Hex₄HexNAC₁) at m/z 870.3¹⁻ as indicated by the selected mass peak (red arrow) **(B)**. MS² spectrum of the m/z 870.3¹⁻ ion which corresponds to P₁ pentasaccharide (Gal α 1-4Gal β 1-4GlcNAc β 1-3Gal β 1-4Glc β 1)(C).

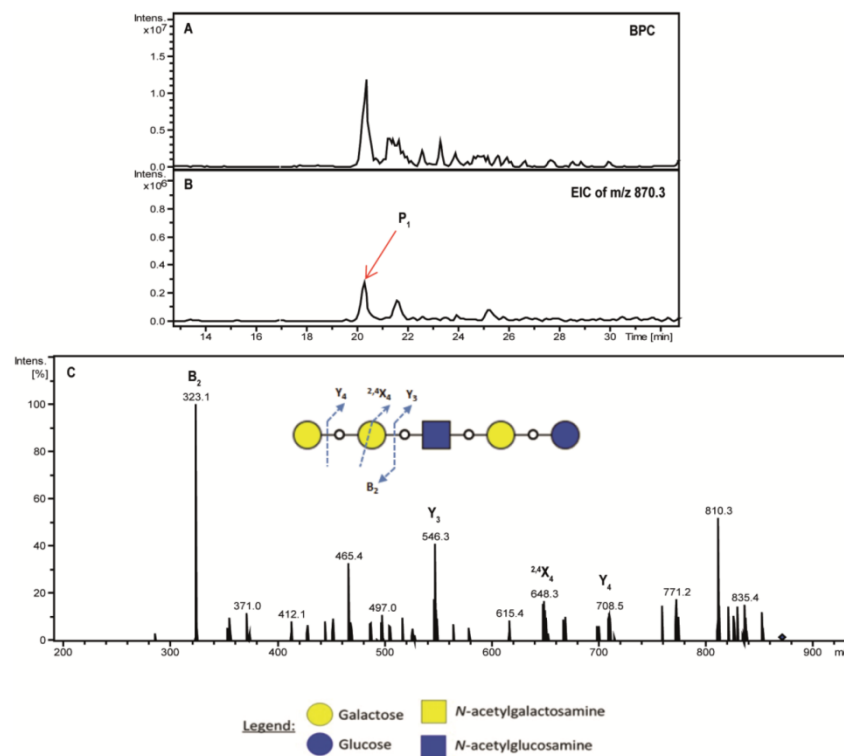


Figure 2S Representative fluorescence scan of randomly selected patient profiled for AGA in ascites (right panel) and blood plasma (left panel) on 50 μ M and 10 μ M prints

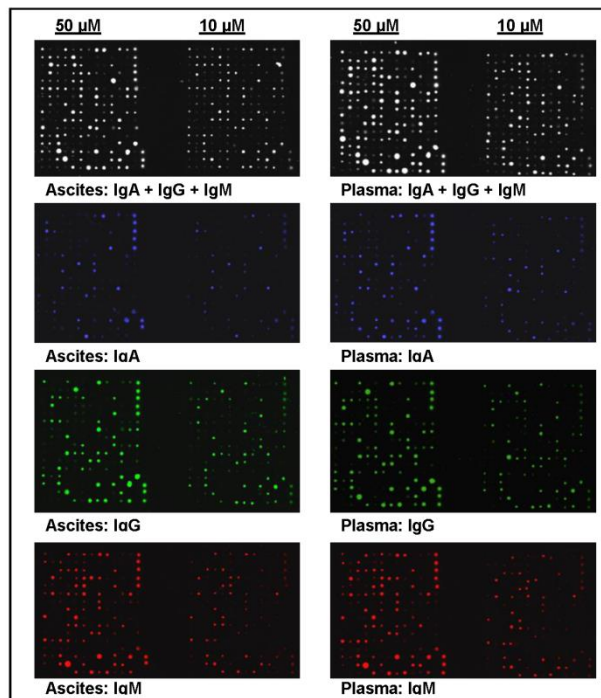


Table 2S Summary of profiled printed glycans showed binding with ascites-derived anti-P₁ antibodies

Glycans are ranked from highest to lowest median RFU referring to AGA levels. The presence of particular disaccharide motifs is indicated by “X”. P₁ trisaccharide is highlighted in bold. Abbreviations: Lewis x (Le^x); Lewis y (Le^y); Lewis b (Le^b); H antigen (H); Tn antigen (TnSer); Lacto-N-fucopentaose I (LNFP-1).

	Median RFU	Spacered form of saccharide	Common name	Galβ1-4GlcNAc	Galα1-4Galβ
1.	19443	Galα1-4Galβ1-4Glcβ-sp3	P ^k , Gb3	X	X
2.	11807.5	GalNAcβ1-3Galα1-4Galβ1-4Glcβ-sp3	Gb4, P	X	X
3.	11209.5	Galα1-4Galβ1-4Glcβ-sp2	P ^k , Gb3	X	X
4.	8251	Galα1-3GlcNAcβ-sp3			
5.	7772	Fucα1-4(Fucα1-2Galβ1-3)GlcNAcβ1-3Galβ1-4Glcβ-sp4	Le ^b -Lac	X	
6.	7501	Fucα1-4(Fucα1-2Galβ1-3)GlcNAcβ-sp3	Le ^b		
7.	7218	Galβ1-4GlcNAcα1-6Galβ1-4GlcNAcβ-sp2		X	
8.	6224	Galα1-4Galβ1-4GlcNAcβ-sp2	P₁	X	X
9.	4380	Galα1-4(Galα1-3)Galβ1-4GlcNAcβ-sp3		X	X
10.	3855.5	Fucα1-2Galβ1-4(Fucα1-3)GlcNAcβ-sp3	Le ^y	X	
11.	3557	GalNAcβ-sp3	β-GalNAc		
12.	3492	Galα1-4(Fucα1-2)Galβ1-4GlcNAc		X	X
13.	3142.5	4-O-Su-Galβ1-4GlcNAcβ-sp3	4'-O-Su-LacNAc	X	
14.	2863.5	Manα1-6(Manα1-3)Manα1-6(Manα1-3)Manβ-sp4	Man5		
15.	1655	ManNAcβ-sp4	β-ManNAc		
16.	1647	Fucα1-2Galβ1-4(Fucα1-3)GlcNAcβ1-3Galβ1-4Glcβ-sp4	Le ^y -Lac	X	
17.	1471	GalNAcα-sp0	TnSer		
18.	1435	Galα1-4GlcNAcβ-sp3	α-LacNAc		
19.	1335.5	(Glcα1-6) ₆ β-sp4	maltohexaose		

20.	1302	Fuc α 1-2Gal β 1-3GlcNAc β 1-3Gal β 1-4GlcNAc β -sp2	H(type 1) penta	X
21.	1289	Gal β 1-3GlcNAc α 1-3Gal β 1-4GlcNAc β -sp3		X
22.	1250.5	Fuc α 1-2Gal β 1-4GlcNAc β -sp3	H (type 2)	X
23.	1132	Gal α 1-3Gal β 1-4GlcNAc β -sp3	α GalLe ^x	X
24.	1095.5	6-O-Su-GalNAc β 1-4GlcNAc β -sp3	6'-O-Su- LacdiNAc	
25.	1057.5	GlcNAc β 1-4Mur-L-Ala-D-i-Gln-Lys	GMDP-Lys	
26.	1020.5	Gal α 1-4GlcNAc β 1-3Gal β 1-4GlcNAc β -sp3		X
27.	985.5	Fuc α 1-2Gal β 1-3GlcNAc β 1-3Gal β 1-4Glc β -sp4	LNFP-I	X

4.6 Overview of Chapter IV: Publication IV

- Naturally circulating, plasma-derived anti-glycan antibodies (AGA) to glycans have been previously shown to significantly discriminate between ovarian cancer patients and healthy women using printed glycan array (PGA)
- In this study, a second independent patient cohort validated using suspension array revealed that the discrimination of cancer patients is mediated by the IgM class of anti-glycan antibodies
- Specifically, these IgM class of anti-glycan antibodies recognized the P1 antigen, a GSL-derived glycan which comprises of the globo series GSLs
- The presence of GSL-derived glycan structures bearing the P1 glycan motif and its structurally related counterparts (P and Pk) on ovarian cancer tissues and cell line was also detected using mass spectrometry (using method established in Publication III) and flow cytometry-based inhibition assay
- It is also shown that human naturally circulating and affinity-purified anti-P1 IgM isolated from patients ascites can bind to naturally expressed P1 on the cell surface of ovarian cancer cells
- Using IGROV1 as a cell line model, two study subpopulations (P1-high and P1-low) were investigated for their role in cell migration, in which cells expressing high P1-levels were found to migrate significantly faster than those with low P1-levels

CHAPTER V: CONCLUSIONS AND FUTURE DIRECTIONS

5.0 Thesis Overview

Serous epithelial cancers of ovarian, peritoneal and tubal origin are collectively regarded as a single disease, given their close histological and clinical similarities and are treated identically with maximal cytoreductive surgery and platinum-based chemotherapy. From a genetic perspective, these serous tumours display high levels of chromosomal instability and are mostly characterised by TP53 gene mutations. Despite significant efforts that have been made in recent years to improve early detection and to understand the complex association between these cancers, five-year survival rates for this heterogeneous disease has remained at only ~20 % for the last 50 years, the lowest among all gynaecological cancers. Perhaps, the most promising evidence-based hypothesis that has recently gained momentum and will likely have important implications for the future detection, prevention and therapy in serous cancers is the significant role of the fallopian tube in the early development of pelvic serous cancers. This important discovery is synonymous to the missing ‘piece’ of the jigsaw puzzle that surrounds the elusive nature of this asymptomatic disease, which has, for years, traditionally been thought to arise from the ovaries. Nevertheless, with respect to this discovery, many other questions pertaining to the development and degree to which these tumours differ, is far from clear, pointing to the need for detailed characterisation of these malignant tumours to accurately diagnose their distinct entities and predict the progression of these cancers, with respect to their clinical management and survival outcomes.

In the pursuit of identifying truly informative ‘molecular’ markers that have diagnostic or therapeutic implications for the early detection and treatment of this deadly disease, omics-based technologies such as glycomics have the potential to explore beyond the morphological and genetic constituents defining serous cancers of the ovary, peritoneum and fallopian tube. Glycans are structurally diverse hydrophilic molecules which have been implicated in many diseases including cancer and can act as promising candidates for the development of biomarkers and the design of novel therapeutics. The primary focus of this study, therefore, has been the detailed structural investigation of *N*- and *O*- glycans of membrane proteins of a number of serous ovarian cancer and non-cancerous cell lines and serous cancer tissues of the ovary, peritoneum and fallopian tube. Specifically, this study is centred upon the establishment of a preliminary cell line-based glycosylation model that identified the differential expression of membrane glycans that are characteristic of serous ovarian cancers, and relates to the expression and the regulation of specific glycosyltransferase genes implicated in the membrane glycosylation. Specific glycosylation features identified using this model were then subsequently verified using biological serous

cancer tissues, yielding both the same ovarian cancer-associated structures, as well as other *N*- and *O*-glycan structural features which could distinguish between serous ovarian, peritoneal and tubal cancers. Apart from the structural elucidation of ovarian cancer membrane protein glycosylation, this thesis also explores the less investigated glycosylated structural motifs of glycosphingolipids derived from selected serous cancer samples which had been implicated by the immune recognition of these motifs by specific auto-antibodies in ovarian cancer patients serum. The detection and characterisation of these biologically relevant glycans, both from membrane glycoproteins and glycosphingolipids, therefore, build upon the existing knowledge and understanding of serous cancers, in the context of their specific glycosylation status.

5.1 Methodology and Analytical Considerations

Mass spectrometry provides an alternative approach for the discovery and discrimination of biologically and clinically relevant glycans

As opposed to the application of conventional detection methods such as lectins or immunohistochemistry to identify specific glycan features on cell membrane proteins, the elucidation of glycan structures by the use of tandem mass spectrometry unravels the possibility of discovering novel branching patterns or linkages of glycan structures on specific glycoconjugates which are representative of various forms of diseases. For instance, as evidenced in this study, the heterogeneity of glycan structures arising from the differential biosynthetic pathway of glycans in cancer cells and tissues was described for both glycoproteins and glycolipids. Besides that, the presentation of different glycan epitopes on both *N*-, *O*-glycans of glycoproteins and glycolipids were also distinguished. To date, there are limitations of other methods to discriminate between specific glycan determinants. For example, monoclonal antibodies directed towards Lewis X or sialyl Lewis A structures are not able to distinguish which specific glycoconjugates carry these epitopes (Cummings and Etzler, 2009). Likewise, the identification of sulphate modifications on both *N*- and *O*-glycans observed in this study could not have possibly been characterised by the use of commercial lectins or monoclonal antibodies since they are not readily available for the identification of these specific glycan determinants. More importantly, PGC-LC-ESI-MS/MS afforded the rapid detection and characterisation of structures in the serous cancer tissue samples based on the prior characterisation of *N*- and *O*-glycans on the membrane proteins of ovarian cancer cell lines, in regard to their specific glycan masses, retention time differences on PGC and MS² fragmentation patterns. This workflow, together with the accumulated knowledge of chromatographic retention order and negative ion fragmentation

of glycans established in our laboratory (Everest-Dass, Abrahams *et. al.*, 2013; Everest-Dass, Kolarich *et. al.*, 2013) and made available in UniCarb-KB (Campbell, Peterson *et. al.*, 2013), eliminated the need for orthogonal-based confirmatory approaches such as sequential enzymatic digestion. The structural elucidation of glycosphingolipid-derived glycans, however, was more challenging, mainly due to the lack of structural-based studies performed in the negative ion mode and curated, structural databases containing biologically-possible lipid-derived glycans. Nevertheless, the use of informative tandem mass spectra at MS² level, using the similar fragmentation pathways occurring to protein-derived glycans, sufficiently characterised various fucosylated and sialylated glycan motifs and residue linkages of the glycolipids.

Differential procedures of membrane extraction of glycoproteins may result in selective detection of specific glycan epitopes

The *N*- and *O*-glycans investigated in this study were isolated from total membrane fractions or microsomes of the ovarian cancer cells and tissues. The membrane protein extraction process employed in this study involved the use of ultracentrifugation and Triton-X114 phase partitioning which has been previously optimised for the isolation of membrane proteins (Lee, Kolarich *et. al.*, 2009). The *N*- and *O*-glycan microheterogeneity described in this study, therefore, although partly a result of aberrant expression of enzymes in ovarian cancer, is also representative of various subcellular membrane fractions contained in this membrane preparation which include plasma membranes as well as membranes of the Golgi, ER and endosomes. A recent study has shown that extracted microsomes of various breast cancer cell lines contain a high proportion of ER-residing proteins that were found to display high mannose-type *N*-glycans (Lee, Lin *et. al.*, 2014). This observation is consistent with the significant increase of immature, unprocessed high mannose type *N*-glycans observed across all four ovarian cancer cell lines analysed in this study. Specifically, 34 to 48 % of *N*-glycans from ovarian cancer cell lines were composed of Man₈₋₉GlcNAc₂ *N*-glycans, thereby comprising the majority glycans identified in these cell lines as compared to 9.42 - 11.59 % of *N*-glycans observed in the serous cancer tissues. This is perhaps, not surprising as various glycosylation studies have noted the elevated expression of these high mannose glycans in cultured cells. Interestingly, a previous study on the use of media such as RPMI was found to influence the glycosylation of CHO cells producing IFN- γ by altering the intracellular nucleotide and nucleotide sugar contents (Kochanowski, Blanchard *et. al.*, 2008). Specifically, the increase in intracellular GDP-man corresponded with changes in IFN- γ glycosylation patterns. It is therefore unclear, if the presence of high mannose structures represents a common feature of cell lines in general.

5.2 Biological Insights Derived From Membrane Glycosylation of Serous Cancers

An overview of the major findings based on the biological significance and relevant clinical implications of this in-depth, glyco-explorative study is described below, highlighting specific relevance to previously published findings.

a) Ovarian cancer cell lines retain some, but not all serous cancer glycan features observed in serous cancer tissues

The preliminary investigation of *N*-glycans, as demonstrated using the cell line model, revealed the unique presence of bisecting-type *N*-glycans in all four of the serous ovarian cancer cell lines analysed (**Chapter 2**). These structures were not found to be present in the non-cancerous ovarian epithelium cells. Likewise, increase in $\alpha 2$ -6 sialylation was also observed for the cancer cell lines as compared to the non-cancerous cells. These characteristic glycan features were reflected consistently throughout the entire glycosylation analysis of all serous ovarian, peritoneal and tubal cancer tissues (**Chapter 3**). In fact, several forms of bisecting-type structures were present in the tissue samples, while the overall sialylation, displaying increased $\alpha 2$ -6 sialylation, was the most prominent feature in all three serous cancers.

For decades, experimental ovarian cancer *in-vitro* models have provided researchers with an avenue for investigating numerous molecular processes governing the development of ovarian tumours. Despite underlying limitations of using continuously laboratory grown cell cultures, the specific glycan features mentioned above that were observed in cell lines and validated in clinically derived tissue samples indicate that these glycomic changes are cancer-relevant. More importantly, the cell-based system established in this study also permitted the correlation with the corresponding glycosyltransferase gene expression, *MGAT3* and *ST6GAL1*, that code for the enzymes responsible for the addition of bisecting-type *N*-glycans and $\alpha 2$ -6 sialylation (**Chapter 2**). This subsequently led to the observation that *MGAT3* gene expression, was epigenetically regulated with its absence in non-cancerous ovarian cell lines being due to DNA hypermethylation. The expression of bisecting structures in cancer cell lines, and the gene regulation of the synthetic enzyme by DNA hypomethylation, warrants a closer investigation as to why this gene remains expressed, thus leading to the synthesis of these bisecting type *N*-glycan structures in serous cancers. This is the first evidence of characterization of bisecting GlcNAc on the membrane proteins of serous cancer tissues of ovary, peritoneum and tubal origin, apart from the previous lectin-based identification of bisecting GlcNAc glycosylation on proteins

of mucinous ovarian cancer tissues (Abbott, Lim *et. al.*, 2010), indicating that their specific presence could also be a common feature of serous cancers, regardless of their origin. Nevertheless, as expected, there were also instances in which the expression of certain glycan structures in the serous cancer tissues were not represented in the serous cancer cell lines. For example, the sulphated *N*- and *O*-glycans identified in some of the tissue samples (**Chapter 3**), at varying intensities, were not identified in any of the cell lines investigated.

b) N-glycans bearing LacdiNAc motifs differentiate serous ovarian cancers from serous peritoneal cancer

The non-reducing terminal GalNAc β 1-4GlcNAc (LacdiNAc or LDN) disaccharide which occurs in *N*- and *O*-glycans has been widely considered as a rare motif and has been found only on selected mammalian glycoproteins such as the bovine pituitary hormones. In regard to their expression in cancer, a few studies have shown that the regulation of this disaccharide expression is tumour-dependent and has been previously isolated from prostate (LNCaP) (Peracaula, Tabarés *et. al.*, 2003), pancreatic (Capan-1) (Peracaula, Royle *et. al.*, 2003) and ovarian cancer cell lines (RMG-1 and SKOV 3) (Machado, Kandzia *et. al.*, 2011; Yu, Chang *et. al.*, 2013). In this study, this unique glycan structural feature was found to be expressed on membrane *N*-glycoproteins of two of the four serous ovarian cancer cell lines analysed and not on the non-cancerous ovarian cell lines. The corresponding increase in gene expression for the enzyme responsible for the addition of the *N*-acetylgalactosamine residue was also investigated, in which *B4GALNT3* was found to be significantly increased in the ovarian cancer cell lines as compared to the non-cancerous cells. Interestingly, the expression of LacdiNAc on β 1 integrin has been implicated in the suppression of tumour growth for neuroblastoma (Hsu, Che *et. al.*, 2011), while the expression of *B4GALNT3* and *B4GALNT4* were found to be implicated in tumour progression of colon (Huang, Liang *et. al.*, 2007) and prostate cancers, respectively (Fukushima, Satoh *et. al.*, 2010).

The ability of cell lines to retain glycans features that may potentially be cancer-specific was once again demonstrated through the validation of these LacdiNAc *N*-glycan structures on the membrane glycoproteins of serous cancer tissue samples which have not been previously reported. More specifically, their expression was limited to the serous cancer tissues that were diagnosed as serous ovarian cancer. This finding was also verified to be significant by independent statistical ANOVA and ROC analyses. It is also interesting to note that specifically, the sialylated biantennary *N*-glycan bearing LacdiNAc and LacNAc motifs

(m/z 1205.0²⁻) was consistently present in most of the ovarian cancer tissue samples and was classified as a highly accurate biomarker of cancer of ovarian origin. This structure, together with other related LacdiNAc-type *N*-glycans were also able to accurately differentiate between serous ovarian and peritoneal cancers based on the PLSDA analysis. The sialylated LacdiNAc structure was also observed in both the serous ovarian cancer cell lines, SKOV 3 and IGROV 1 while fucosylated LacdiNAc motifs were found only in IGROV1 cell lines. A previous study by Dell, A. *et. al.*, (1995) showed that glycodelin, a human glycoprotein, also known as placental protein 14 (PP14) or progesterone-associated endometrial protein (PAEP), was extensively glycosylated with complex *N*-glycans which displayed sialylated and fucosylated LacdiNAc motifs. The increased expression of glycodelin has also been found in several carcinomas such as serous ovarian (Mandelin, Lassus *et. al.*, 2003), endometrioid ovarian (Lenhard, Heublein *et. al.*, 2013) and breast (Shabani, Mylonas *et. al.*, 2005) cancers in which its role in these cancers remains unknown. Although the membrane proteins carrying these LacdiNAc *N*-glycans were not identified in our study, the work presents the first comparative analysis of glycan structures on membrane proteins of pelvic serous cancers and depicts the presence of these LacdiNAc structures exclusively on serous ovarian cancers.

c) Glycoproteins and glycosphingolipid-derived glycosylation of ovarian tumours exhibit unique glycan motifs that are potentially antigenic

Apart from the characterization of *N*- and *O*-glycans from serous cancer tissues and cell lines, glycosphingolipid (GSL)-derived glycans were also isolated and characterized from selected tissue samples as an initiative to validate some of the research work established by our collaborator in the gynaecological cancer group in Basel, Switzerland. The researchers from this group have previously observed significantly lower levels of auto-antibodies, specifically anti-IgMs, in plasma from non-mucinous ovarian cancer patients, as compared to healthy controls using printed glycan arrays (Jacob, Goldstein *et. al.*, 2012). One of the reasons speculated to account for this observation was that circulating auto-antibodies against the cancer may potentially be bound to the corresponding glycan antigen on the tumour surface, thus resulting in lesser, free-floating anti-glycan IgM antibodies in the blood plasma. Some of the glycan sub-structures recognised by the plasma IgMs were found to consist of the chitobiose core (GlcNAc β 1-4GlcNAc β -Asn) present on *N*-glycoproteins and globo-series P_k (Gal α 1-4Gal β 1-4Glc β 1) and P₁ (Gal α 1-4Gal β 1-4GlcNAc β 1) terminal motifs which are primarily found on glycolipids. In addition, several other terminal sub-structures recognised by the plasma IgM auto-antibodies were found to consist of sulphated

(Neu5Ac α 2-3Gal β 1-4-(6-Su)GlcNAc β , Neu5Ac α 2-3Gal β 1-3-(6-Su)GalNAc α) and Type 2 chains (Gal β 1-4 GlcNAc β 1-6Gal β 1-4GlcNAc β) which were also identified in this thesis to be present on the membrane protein *N*- and *O*-glycans (**Chapter 2**) and glycolipids (**Chapter 4**), respectively, of serous cancer tissues.

The P-blood group-related antigens (P_k, P₁ and P) were not found to be present on the membrane *N*- and *O*-glycoproteins of all the serous cancer samples investigated in our study. The presence of these structures, however, was validated and structurally characterised in two cancer tissue samples, while only the P₁ antigen was detected in the IGROV1 cells (**Chapter 4**). It is important to note that the structural motifs on the printed glycan array, although developed primarily based on diverse glycans such as blood group antigens, pathogen-related glycans and well-known tumour associated antigens, may not truly reflect the spectrum of glycans implicated in ovarian cancer specifically and the auto-antibodies may have wide specificities (Oyelaran and Gildersleeve, 2009). This was substantiated in our study where the ascites-derived anti-P₁ antibodies were shown to recognise other structures such as the H Type 1 and Type 2 structures which were also detected in GSL-derived glycans analysed in this study. Nevertheless, as demonstrated in this study, we have shown that the identification of specific glycan structures on proteins and lipids derived from ovarian tumour cell lines and tissue samples can be useful for the development of functional, curated arrays that are cancer-relevant with respect to specific isomeric and linkage specifications. Potentially, these arrays subsequently can be used for the diagnosis of these cancer specific auto-antibodies in patient plasma.

d) Glycoproteins and glycosphingolipid-derived glycosylation of ovarian tumours are differentially expressed

The heterogeneity of glycans displayed on various forms of glycoconjugates, although fascinating, reflects on the broader significance of their specific roles in regard to tumour development and progression. Glycolipids, for instance, differ significantly from glycoproteins, based on the different glycan core structures that are synthesised such as the ganglio-, globo-, neolacto-series. Whilst cancer-specific expression in regards to their specific cores were detected and characterised in this study, the differential expression of unique terminal glycan motifs observed between the membrane glycoproteins and glycolipids of a single serous ovarian cancer tissue (e.g. S565) and cell line (e.g. IGROV 1) was quite intriguing. For example, the glycoproteins of S565 comprised of mostly sialylated LacNAc structures, while the membrane glycolipid from the same tissue was dominated by the neo-lacto Type 2 tetrasaccharides and H Type 2 mono-fucosylated tetrasaccharides.

Interestingly, the H Type 2 antigen (Fuc α 1-2Gal β 1-4GlcNAc β 1-3Gal β 1-4Glc), is also a precursor of the Lewis Y antigen bearing (Fuc α 1-2Gal β 1-4(Fuc α 1-3)GlcNAc β 1-3Gal β 1-4Glc). Both of these antigens (H Type 2 and Lewis Y) have been previously identified using immunohistochemistry to be exclusively expressed in the serous and endometrioid cancer subtypes and not on the mucinous subtype (Federici, Kudryashov *et. al.*, 1999).

Similarly, the H Type 1 epitope which was also observed on glycolipids of S565 ovarian cancer tissue, together with H Type 2 epitopes, are precursors of blood group A and B and the progressive loss of these blood group antigens in tumours of advanced stages has been observed in ovarian cancer (Metoki, Kakudo *et. al.*, 1989; Welshinger, Finstad *et. al.*, 1996). The loss of blood group antigens has also been associated with bad prognosis in cancers such as lung (Lee, Ro *et. al.*, 1991; Matsumoto, Muramatsu *et. al.*, 1993), head and neck (Wolf, Carey *et. al.*, 1990) and bladder (Malmstrom, Busch *et. al.*, 1988). It is therefore evident that the differential expression of specific glycoforms on serous cancer membrane glycoconjugates, as demonstrated in this study can be exploited not just for diagnosis, but also to monitor disease progression. While the profiling of glycan-GSL of all the ovarian cancer cell lines and tissues was beyond the primary scope of this study, the investigation of these structures is warranted to fully understand why some motifs are more closely associated glycolipids as opposed to glycoproteins. This apparent discrepancy has also been recently observed in colon cancer, in which sulphated glycans were found to be decreased in the GSL-derived glycans, while an increase in sulphation was observed on the *N*-glycans, thereby adding to the complexity of tumorigenesis and the potential role of these glycans in adaptive strategies such as host immune evasion (Holst, Stavenhagen *et. al.*, 2013).

5.3 Translational ('bench-to bedside') Implications for Ovarian Cancer Research

One of the most prevailing questions pertaining to the discovery of specific glycans associated with cancer, perhaps, is their potential utility in the clinic, not just for early detection and diagnosis, but also to provide appropriate treatments for the disease. The post-genomic era has undoubtedly opened the door to a wide range of omics-based technologies which have the capacity to be incorporated into current clinical research to deliver more effective screening and targeted treatments. The past two decades have brought about the identification of over 200 potential biomarkers for ovarian cancer, of which only a few have been successfully validated using clinical samples. Likewise, more than half of the 137 gene mutations reported for ovarian cancer have been derived from one single cell line or tumour sample (Suh, Park *et. al.*, 2010). The strength of this study is therefore centred on the identification and characterisation of unique glycan structures that have also been validated at a membrane tissue level using serous cancer samples that are linked with clinically accurate data.

Some of the discriminatory glycan structures (eg. LacdiNAc) reported in this study, however, have not yet been identified in bodily fluids such as plasma, urine or saliva and could potentially be translated into diagnostic biomarkers which could be detected using minimally-invasive methods. In fact, recent studies have shown that *O*-glycans bearing various sulphated and fucosylated forms have been detected in ovarian cancer ascites fluid (Karlsson and McGuckin, 2012) while *N*-glycans have been reported to be differentially expressed in ovarian cancer patients' sera (Alley, Vasseur *et. al.*, 2012). The identification of these glycans in bodily fluids of patients indicates that their presence is not only reflective of an individual's state of health, but also useful as diagnostic and prognostic biological indicators of ovarian cancer (Saldiva, Royle *et. al.*, 2007). One notable example is the clinical utility of glycans in liver cancer, whereby the changes in the glycosylation profile of alpha-fetoprotein (AFP-L3), a serum glycoprotein, have been used to distinguish hepatocellular carcinoma (HCC) from chronic liver disease (Kim, Kim *et. al.*, 2014). Besides that, the detection of these structures on tissues also offers the ability to use imaging techniques such as mass spectrometry-based tools that are currently being developed (Gustafsson, Oehler *et. al.*, 2011). In addition, the identification of these glycans, combined with the knowledge of interacting anti-glycan auto-antibodies could lead to the development of molecular diagnostic assays which could effectively distinguish between serous cancer origins. Owing to the heterogeneity displayed in the membrane lipid and protein glycan profiles of serous ovarian cancers, it is envisioned that a panel of candidate glycan biomarkers together with

the corresponding genes identified in this study, could be further developed and validated on a larger number of bio-specimens and result in personalised targets that are directly associated with the molecular profiles of individual ovarian cancers.

5.4 Future Directions/ Suggestions

In line with the objective of discovering a combination of serous cancer-specific biomarkers (proteins, glycans and genes) for early detection, diagnosis and disease progression monitoring, the following future work is proposed as a continuation from this thesis.

- Comparison of membrane glycoconjugates from non-cancerous surface epithelial tissues derived from the fallopian tube and ovaries, with the observed ovarian cancer changes
- Further investigation of the gene regulatory mechanisms associated with the expression of the corresponding glycosyltransferase genes in serous cancers
- Identification of membrane proteins from serous ovarian cancer tissues that specifically carry the unique LacdiNAc N- glycans observed
- Characterisation of intact glycolipids in serous cancer tissues to determine any structural changes in the lipid component
- Purification of anti-glycan auto-antibodies from serum and validation of binding to specific glycans implicated in ovarian cancer by this study
- Development of a plasma-based test to quantify the auto-antibody levels using the ovarian cancer-specific glycan structures
- Site-specific glycoproteomics analysis to define the glycosylation sites of membrane proteins and their microheterogeneity
- Investigation of membrane protein and lipid glycosylation from a larger cohort of cancer tissue samples derived from various anatomic sites as well as benign tumour samples

CHAPTER VI: REFERENCES

References

- Abbott, K. L., J. M. Lim, L. Wells, B. B. Benigno, J. F. McDonald and M. Pierce (2010). "Identification of candidate biomarkers with cancer-specific glycosylation in the tissue and serum of endometrioid ovarian cancer patients by glycoproteomic analysis." *Proteomics* **10**(3): 470-481.
- Abbott, K. L., A. V. Nairn, E. M. Hall, M. B. Horton, J. F. McDonald, K. W. Moremen, D. M. Dinulescu and M. Pierce (2008). "Focused glycomic analysis of the N-linked glycan biosynthetic pathway in ovarian cancer." *Proteomics* **8**(16): 3210-3220.
- Adams, A. T. and N. Auersperg (1981). "Transformation of cultured rat ovarian surface epithelial cells by Kirsten murine sarcoma virus." *Cancer Res* **41**(6): 2063-2072.
- Agarwal, Roshan and Stan B. Kaye (2003). "Ovarian cancer: strategies for overcoming resistance to chemotherapy." *Nat Rev Cancer* **3**(7): 502-516.
- Ahmed, F. Y., E. Wiltshaw, R. P. A'Hern, B. Nicol, J. Shepherd, P. Blake, C. Fisher and M. E. Gore (1996). "Natural history and prognosis of untreated stage I epithelial ovarian carcinoma." *J Clin Oncol* **14**(11): 2968-2975.
- AIHW (2012). Breast cancer in Australia: an overview. Canberra, Australian Institute of Health and Welfare & Cancer Australia. Cancer series no. 71. Cat. no. CAN 67.
- AIHW (2012). Cancer incidence projections: Australia, 2011 to 2020, Canberra: AIHW. Cancer Series no. 66. Cat. No. CAN 62.
- AIHW (2014). Australian Cancer Incidence and Mortality (ACIM) Books. Canberra, Australian Institute of Health and Welfare.
- Allen, H. J., C. Porter, M. Gamarra, M. S. Piver and E. A. Johnson (1987). "Isolation and morphologic characterization of human ovarian carcinoma cell clusters present in effusions." *Exp Cell Biol* **55**(4): 194-208.
- Alley, W. R., Jr. and M. V. Novotny (2010). "Glycomic analysis of sialic acid linkages in glycans derived from blood serum glycoproteins." *J Proteome Res* **9**(6): 3062-3072.
- Alley, W. R., Jr., J. A. Vasseur, J. A. Goetz, M. Svoboda, B. F. Mann, D. E. Matei, N. Menning, A. Hussein, Y. Mechref and M. V. Novotny (2012). "N-linked glycan structures and their expressions change in the blood sera of ovarian cancer patients." *J Proteome Res* **11**(4): 2282-2300.
- Alvarado-Cabrero, Isabel, Robert H. Young, Eleftherios C. Vamvakas and Robert E. Scully (1999). "Carcinoma of the Fallopian Tube: A Clinicopathological Study of 105 Cases with Observations on Staging and Prognostic Factors." *Gynecologic Oncology* **72**(3): 367-379.
- Anderson, N. L. and N. G. Anderson (2002). "The human plasma proteome: history, character, and diagnostic prospects." *Mol Cell Proteomics* **1**(11): 845-867.
- Ando, H., M. Kobayashi, S. Toda, F. Kikkawa, T. Masahashi and S. Mizutani (2000). "Establishment of a ciliated epithelial cell line from human Fallopian tube." *Hum Reprod* **15**(7): 1597-1603.
- Anugraham, M., F. Jacob, S. Nixdorf, A. V. Everest-Dass, V. Heinzelmann-Schwarz and N. H. Packer (2014). "Specific glycosylation of membrane proteins in epithelial ovarian cancer cell lines: glycan structures reflect gene expression and DNA methylation status." *Mol Cell Proteomics*.
- Apweiler, R., H. Hermjakob and N. Sharon (1999). "On the frequency of protein glycosylation, as deduced from analysis of the SWISS-PROT database." *Biochim Biophys Acta* **1473**(1): 4-8.
- Ariga, T., T. Kohriyama, L. Freddo, N. Latov, M. Saito, K. Kon, S. Ando, M. Suzuki, M. E. Hemling, K. L. Rinehart, Jr. and et al. (1987). "Characterization of sulfated

- glucuronic acid containing glycolipids reacting with IgM M-proteins in patients with neuropathy." *J Biol Chem* **262**(2): 848-853.
- Arnold, J. N., R. Saldiva, U. M. Hamid and P. M. Rudd (2008). "Evaluation of the serum N-linked glycome for the diagnosis of cancer and chronic inflammation." *Proteomics* **8**(16): 3284-3293.
- Ashline, D., S. Singh, A. Hanneman and V. Reinhold (2005). "Congruent strategies for carbohydrate sequencing. 1. Mining structural details by MSn." *Anal Chem* **77**(19): 6250-6262.
- Auersperg, N., A. S. Wong, K. C. Choi, S. K. Kang and P. C. Leung (2001). "Ovarian surface epithelium: biology, endocrinology, and pathology." *Endocr Rev* **22**(2): 255-288.
- Azad, N. S., E. M. Posadas, V. E. Kwitkowski, S. M. Steinberg, L. Jain, C. M. Annunziata, L. Minasian, G. Sarosy, H. L. Kotz, A. Premkumar, L. Cao, D. McNally, C. Chow, H. X. Chen, J. J. Wright, W. D. Figg and E. C. Kohn (2008). "Combination targeted therapy with sorafenib and bevacizumab results in enhanced toxicity and antitumor activity." *J Clin Oncol* **26**(22): 3709-3714.
- Backstrom, M., K. A. Thomsson, H. Karlsson and G. C. Hansson (2009). "Sensitive liquid chromatography-electrospray mass spectrometry allows for the analysis of the O-glycosylation of immunoprecipitated proteins from cells or tissues: application to MUC1 glycosylation in cancer." *J Proteome Res* **8**(2): 538-545.
- Badiglian Filho, L., C. T. Oshima, F. De Oliveira Lima, H. De Oliveira Costa, R. De Sousa Damiao, T. S. Gomes and W. J. Goncalves (2009). "Canonical and noncanonical Wnt pathway: a comparison among normal ovary, benign ovarian tumor and ovarian cancer." *Oncol Rep* **21**(2): 313-320.
- Baldwin, R. L., E. Nemeth, H. Tran, H. Shvartsman, I. Cass, S. Narod and B. Y. Karlan (2000). "BRCA1 promoter region hypermethylation in ovarian carcinoma: a population-based study." *Cancer Res* **60**(19): 5329-5333.
- Bannatyne, P. and P. Russell (1981). "Early adenocarcinoma of the fallopian tubes. A case for multifocal tumorigenesis." *Diagn Gynecol Obstet* **3**(1): 49-60.
- Barber, M., R. Bordoli, G. Elliott, R. Sedgwick and A. Tyler (1982). "Fast atom bombardment mass spectrometry." *Analytical Chemistry* **54**: 645-657.
- Barber, M., Bordoli, R., Sedgwick, R and Tyler, A. (1981). "Fast atom bombardment of solids (FAB): a new ion source for mass spectrometry." *Journal of the Chemical Society, Chemical Communications* **81**: 325-327.
- Barbolina, M. V., B. P. Adley, E. V. Ariztia, Y. Liu and M. S. Stack (2007). "Microenvironmental regulation of membrane type 1 matrix metalloproteinase activity in ovarian carcinoma cells via collagen-induced EGR1 expression." *J Biol Chem* **282**(7): 4924-4931.
- Barda, G., J. Menczer, A. Chetrit, F. Lubin, D. Beck, B. Piura, M. Glezerman, B. Modan, S. Sadetzki and Group National Israel Ovarian Cancer (2004). "Comparison between primary peritoneal and epithelial ovarian carcinoma: a population-based study." *Am J Obstet Gynecol* **190**(4): 1039-1045.
- Bast, R. C., Jr., M. Feeney, H. Lazarus, L. M. Nadler, R. B. Colvin and R. C. Knapp (1981). "Reactivity of a monoclonal antibody with human ovarian carcinoma." *J Clin Invest* **68**(5): 1331-1337.
- Bast, R. C., Jr., B. Hennessy and G. B. Mills (2009). "The biology of ovarian cancer: new opportunities for translation." *Nat Rev Cancer* **9**(6): 415-428.
- Bereman, M. S., T. I. Williams and D. C. Muddiman (2009). "Development of a nanoLC LTQ orbitrap mass spectrometric method for profiling glycans derived from plasma from healthy, benign tumor control, and epithelial ovarian cancer patients." *Anal Chem* **81**(3): 1130-1136.
- Bewick, V., L. Cheek and J. Ball (2004). "Statistics review 13: receiver operating characteristic curves." *Crit Care* **8**(6): 508-512.

- Bhoola, S. and W. J. Hoskins (2006). "Diagnosis and management of epithelial ovarian cancer." *Obstet Gynecol* **107**(6): 1399-1410.
- Biskup, Karina, Elena I. Braicu, Jalid Sehoul, Christina Fotopoulou, Rudolf Tauber, Markus Berger and Véronique Blanchard (2013). "Serum Glycome Profiling: A Biomarker for Diagnosis of Ovarian Cancer." *Journal of Proteome Research* **12**(9): 4056-4063.
- Blagden, S. and H. Gabra (2008). "Future directions in the management of epithelial ovarian cancer." *Future Oncol* **4**(3): 403-411.
- Blaustein, A. (1984). "Peritoneal mesothelium and ovarian surface cells—shared characteristics." *Int J Gynecol Pathol* **3**(4): 361-375.
- Blixt, Ola and Nahid Razi (2008). Enzymatic Glycosylation by Transferases. Glycoscience. B. Fraser-Reid, K. Tatsuta and J. Thiem, Springer Berlin Heidelberg: 1361-1385.
- Bloss, J. D., S. Y. Liao, R. E. Buller, A. Manetta, M. L. Berman, S. McMeekin, L. P. Bloss and P. J. DiSaia (1993). "Extraovarian peritoneal serous papillary carcinoma: a case-control retrospective comparison to papillary adenocarcinoma of the ovary." *Gynecol Oncol* **50**(3): 347-351.
- Bol, G. M., K. P. Suijkerbuijk, J. Bart, M. Vooijs, E. van der Wall and P. J. van Diest (2010). "Methylation profiles of hereditary and sporadic ovarian cancer." *Histopathology* **57**(3): 363-370.
- Bon, G. G., P. Kenemans, J. J. Dekker, P. G. Hompes, R. A. Verstraeten, G. J. van Kamp and J. Schoemaker (1999). "Fluctuations in CA 125 and CA 15-3 serum concentrations during spontaneous ovulatory cycles." *Hum Reprod* **14**(2): 566-570.
- Bookman, M. A., K. M. Darcy, D. Clarke-Pearson, R. A. Boothby and I. R. Horowitz (2003). "Evaluation of monoclonal humanized anti-HER2 antibody, trastuzumab, in patients with recurrent or refractory ovarian or primary peritoneal carcinoma with overexpression of HER2: a phase II trial of the Gynecologic Oncology Group." *J Clin Oncol* **21**(2): 283-290.
- Boyd, W. C. and E. Shapleigh (1954). "Specific precipitating activity of plant agglutinins (lectins)." *Science* **119**(3091): 419-419.
- Bray, F., J. S. Ren, E. Masuyer and J. Ferlay (2013). "Global estimates of cancer prevalence for 27 sites in the adult population in 2008." *Int J Cancer* **132**(5): 1133-1145.
- Brockhausen, I. (2006). "Mucin-type O-glycans in human colon and breast cancer: glycodynamics and functions." *EMBO Rep* **7**(6): 599-604.
- Brockhausen, I., H. Schachter and P. Stanley (2009). O-GalNAc Glycans. Essentials of Glycobiology. A. Varki, R. D. Cummings, J. D. Esko et al. Cold Spring Harbor (NY).
- Brose, M. S., T. R. Rebbeck, K. A. Calzone, J. E. Stopfer, K. L. Nathanson and B. L. Weber (2002). "Cancer risk estimates for BRCA1 mutation carriers identified in a risk evaluation program." *J Natl Cancer Inst* **94**(18): 1365-1372.
- Brown, D. A. and E. London (2000). "Structure and function of sphingolipid- and cholesterol-rich membrane rafts." *J Biol Chem* **275**(23): 17221-17224.
- Bruggink, C., M. Wuhler, C. A. Koeleman, V. Barreto, Y. Liu, C. Pohl, A. Ingendoh, C. H. Hokke and A. M. Deelder (2005). "Oligosaccharide analysis by capillary-scale high-pH anion-exchange chromatography with on-line ion-trap mass spectrometry." *J Chromatogr B Analyt Technol Biomed Life Sci* **829**(1-2): 136-143.
- Bull, C., T. J. Boltje, M. Wassink, A. M. de Graaf, F. L. van Delft, M. H. den Brok and G. J. Adema (2013). "Targeting aberrant sialylation in cancer cells using a fluorinated sialic acid analog impairs adhesion, migration, and in vivo tumor growth." *Mol Cancer Ther* **12**(10): 1935-1946.
- Burger, R. A., M. W. Sill, B. J. Monk, B. E. Greer and J. I. Sorosky (2007). "Phase II trial of bevacizumab in persistent or recurrent epithelial ovarian cancer or primary peritoneal cancer: a Gynecologic Oncology Group Study." *J Clin Oncol* **25**(33): 5165-5171.

- Burges, A., P. Wimberger, C. Kumper, V. Gorbounova, H. Sommer, B. Schmalfeldt, J. Pfisterer, M. Lichinitser, A. Makhson, V. Moiseyenko, A. Lahr, E. Schulze, M. Jager, M. A. Strohlein, M. M. Heiss, T. Gottwald, H. Lindhofer and R. Kimmig (2007). "Effective relief of malignant ascites in patients with advanced ovarian cancer by a trifunctional anti-EpCAM x anti-CD3 antibody: a phase I/II study." *Clin Cancer Res* **13**(13): 3899-3905.
- Buys, S. S., E. Partridge, A. Black, C. C. Johnson, L. Lamerato, C. Isaacs, D. J. Reding, R. T. Greenlee, L. A. Yokochi, B. Kessel, E. D. Crawford, T. R. Church, G. L. Andriole, J. L. Weissfeld, M. N. Fouad, D. Chia, B. O'Brien, L. R. Ragard, J. D. Clapp, J. M. Rathmell, T. L. Riley, P. Hartge, P. F. Pinsky, C. S. Zhu, G. Izmirlian, B. S. Kramer, A. B. Miller, J. L. Xu, P. C. Prorok, J. K. Gohagan, C. D. Berg and Plco Project Team (2011). "Effect of screening on ovarian cancer mortality: the Prostate, Lung, Colorectal and Ovarian (PLCO) Cancer Screening Randomized Controlled Trial." *JAMA* **305**(22): 2295-2303.
- Cabezas, J.A. (1994). "The origins of glycobiology." *Biochemical Education* **22**: 3-7.
- Campbell, Matthew P., Robyn Peterson, Julien Mariethoz, Elisabeth Gasteiger, Yukie Akune, Kiyoko F. Aoki-Kinoshita, Frederique Lisacek and Nicolle H. Packer (2013). "UniCarbKB: building a knowledge platform for glycoproteomics." *Nucleic Acids Research*.
- Campbell, S., V. Bhan, P. Royston, M. I. Whitehead and W. P. Collins (1989). "Transabdominal ultrasound screening for early ovarian cancer." *BMJ* **299**(6712): 1363-1367.
- Campone, M., V. Levy, E. Bourbouloux, D. Berton Rigaud, D. Bootle, C. Dutreix, U. Zoellner, N. Shand, F. Calvo and E. Raymond (2009). "Safety and pharmacokinetics of paclitaxel and the oral mTOR inhibitor everolimus in advanced solid tumours." *Br J Cancer* **100**(2): 315-321.
- Cannistra, S. A. (2004). "Cancer of the ovary." *N Engl J Med* **351**(24): 2519-2529.
- Cao, Y., P. Stosiek, G. F. Springer and U. Karsten (1996). "Thomsen-Friedenreich-related carbohydrate antigens in normal adult human tissues: a systematic and comparative study." *Histochem Cell Biol* **106**(2): 197-207.
- Casagrande, J. T., E. W. Louie, M. C. Pike, S. Roy, R. K. Ross and B. E. Henderson (1979). "'Incessant ovulation' and ovarian cancer." *Lancet* **2**(8135): 170-173.
- Casey, M. J., C. Bewtra, L. L. Hoehne, A. D. Tatpati, H. T. Lynch and P. Watson (2000). "Histology of prophylactically removed ovaries from BRCA1 and BRCA2 mutation carriers compared with noncarriers in hereditary breast ovarian cancer syndrome kindreds." *Gynecol Oncol* **78**(3 Pt 1): 278-287.
- Casey, R. C., T. R. Oegema, Jr., K. M. Skubitz, S. E. Pambuccian, S. M. Grindle and A. P. Skubitz (2003). "Cell membrane glycosylation mediates the adhesion, migration, and invasion of ovarian carcinoma cells." *Clin Exp Metastasis* **20**(2): 143-152.
- Cass, I., C. Holschneider, N. Datta, D. Barbuto, A. E. Walts and B. Y. Karlan (2005). "BRCA-mutation-associated fallopian tube carcinoma: a distinct clinical phenotype?" *Obstet Gynecol* **106**(6): 1327-1334.
- Ceroni, A., K. Maass, H. Geyer, R. Geyer, A. Dell and S. M. Haslam (2008). "GlycoWorkbench: a tool for the computer-assisted annotation of mass spectra of glycans." *J Proteome Res* **7**(4): 1650-1659.
- Ceroni, Alessio, Kai Maass, Hildegard Geyer, Rudolf Geyer, Anne Dell and Stuart M. Haslam (2008). "GlycoWorkbench: A Tool for the Computer-Assisted Annotation of Mass Spectra of Glycans†." *Journal of Proteome Research* **7**(4): 1650-1659.
- Chai, W., V. Piskarev and A. M. Lawson (2001). "Negative-ion electrospray mass spectrometry of neutral underivatized oligosaccharides." *Anal Chem* **73**(3): 651-657.
- Chai, W., V. Piskarev and A. M. Lawson (2002). "Branching pattern and sequence analysis of underivatized oligosaccharides by combined MS/MS of singly and doubly charged

- molecular ions in negative-ion electrospray mass spectrometry." *J Am Soc Mass Spectrom* **13**(6): 670-679.
- Chait, E.M. (1972). "Ionization Sources in Mass Spectrometry " *Analytical Chemistry* **44**(3): 77A-91a.
- Chan, A. L., H. R. Morris, M. Panico, A. T. Etienne, M. E. Rogers, P. Gaffney, L. Creighton-Kempsford and A. Dell (1991). "A novel sialylated N-acetylgalactosamine-containing oligosaccharide is the major complex-type structure present in Bowes melanoma tissue plasminogen activator." *Glycobiology* **1**(2): 173-185.
- Chang, S. H., J. L. Han, S. Y. Tseng, H. Y. Lee, C. W. Lin, Y. C. Lin, W. Y. Jeng, A. H. Wang, C. Y. Wu and C. H. Wong (2010). "Glycan array on aluminum oxide-coated glass slides through phosphonate chemistry." *J Am Chem Soc* **132**(38): 13371-13380.
- Chen, L. M., S. D. Yamada, Y. S. Fu, R. L. Baldwin and B. Y. Karlan (2003). "Molecular similarities between primary peritoneal and primary ovarian carcinomas." *Int J Gynecol Cancer* **13**(6): 749-755.
- Chen, V. W., B. Ruiz, J. L. Killeen, T. R. Cote, X. C. Wu and C. N. Correa (2003). "Pathology and classification of ovarian tumors." *Cancer* **97**(10 Suppl): 2631-2642.
- Chen, X. and G. C. Flynn (2007). "Analysis of N-glycans from recombinant immunoglobulin G by on-line reversed-phase high-performance liquid chromatography/mass spectrometry." *Anal Biochem* **370**(2): 147-161.
- Cheng, W., J. Liu, H. Yoshida, D. Rosen and H. Naora (2005). "Lineage infidelity of epithelial ovarian cancers is controlled by HOX genes that specify regional identity in the reproductive tract." *Nat Med* **11**(5): 531-537.
- Cheng, Y. M., S. T. Wang and C. Y. Chou (2002). "Serum CA-125 in preoperative patients at high risk for endometriosis." *Obstet Gynecol* **99**(3): 375-380.
- Chester, M. A. (1998). "IUPAC-IUB Joint Commission on Biochemical Nomenclature (IUBCN). Nomenclature of glycolipids—recommendations 1997." *Eur J Biochem* **257**(2): 293-298.
- Chianese-Bullock, K. A., W. P. Irvin, Jr., G. R. Petroni, C. Murphy, M. Smolkin, W. C. Olson, E. Coleman, S. A. Boerner, C. J. Nail, P. Y. Neese, A. Yuan, K. T. Hogan and C. L. Slingluff, Jr. (2008). "A multi-peptide vaccine is safe and elicits T-cell responses in participants with advanced stage ovarian cancer." *J Immunother* **31**(4): 420-430.
- Cho, K. R. and M. Shih Ie (2009). "Ovarian cancer." *Annu Rev Pathol* **4**: 287-313.
- Chodankar, R., S. Kwang, F. Sangiorgi, H. Hong, H. Y. Yen, C. Deng, M. C. Pike, C. F. Shuler, R. Maxson and L. Dubeau (2005). "Cell-nonautonomous induction of ovarian and uterine serous cystadenomas in mice lacking a functional Brca1 in ovarian granulosa cells." *Curr Biol* **15**(6): 561-565.
- Choi, J. H., A. S. Wong, H. F. Huang and P. C. Leung (2007). "Gonadotropins and ovarian cancer." *Endocr Rev* **28**(4): 440-461.
- Christie, D. R., F. M. Shaikh, J. A. th Lucas, J. A. Lucas, 3rd and S. L. Bellis (2008). "ST6Gal-I expression in ovarian cancer cells promotes an invasive phenotype by altering integrin glycosylation and function." *J Ovarian Res* **1**(1): 3.
- Chu, C. S., M. R. Ninonuevo, B. H. Clowers, P. D. Perkins, H. J. An, H. Yin, K. Killeen, S. Miyamoto, R. Grimm and C. B. Lebrilla (2009). "Profile of native N-linked glycan structures from human serum using high performance liquid chromatography on a microfluidic chip and time-of-flight mass spectrometry." *Proteomics* **9**(7): 1939-1951.
- Ciucanu, I. and C. E. Costello (2003). "Elimination of oxidative degradation during the per-O-methylation of carbohydrates." *J Am Chem Soc* **125**(52): 16213-16219.
- Cohen, C.J., G.M. Thoas, G.S. Hagopian, D.W. Kufe, R.E. Pollock and J.F. Holland (2000). Neoplasms of the fallopian tube cancer medicine. British Columbia, Canada, Decker Inc.: 1683.
- Coleman, M. P., D. Forman, H. Bryant, J. Butler, B. Rachet, C. Maringe, U. Nur, E. Tracey, M. Coory, J. Hatcher, C. E. McGahan, D. Turner, L. Marrett, M. L. Gjerstorff, T. B.

- Johannesen, J. Adolfsson, M. Lambe, G. Lawrence, D. Meechan, E. J. Morris, R. Middleton, J. Steward, M. A. Richards and Icbp Module 1 Working Group (2011). "Cancer survival in Australia, Canada, Denmark, Norway, Sweden, and the UK, 1995-2007 (the International Cancer Benchmarking Partnership): an analysis of population-based cancer registry data." *Lancet* **377**(9760): 127-138.
- Colombo, N., M. Peiretti, G. Parma, M. Lapresa, R. Mancari, S. Carinelli, C. Sessa and M. Castiglione (2010). "Newly diagnosed and relapsed epithelial ovarian carcinoma: ESMO Clinical Practice Guidelines for diagnosis, treatment and follow-up." *Annals of Oncology* **21**(suppl 5): v23-v30.
- Cooper, C. A., E. Gasteiger and N. H. Packer (2001). "GlycoMod—a software tool for determining glycosylation compositions from mass spectrometric data." *Proteomics* **1**(2): 340-349.
- Cooper, C. A., H. J. Joshi, M. J. Harrison, M. R. Wilkins and N. H. Packer (2003). "GlycoSuiteDB: a curated relational database of glycoprotein glycan structures and their biological sources. 2003 update." *Nucleic Acids Res* **31**(1): 511-513.
- Costello, C. E., J. M. Contado-Miller and J. F. Cipollo (2007). "A glycomics platform for the analysis of permethylated oligosaccharide alditols." *J Am Soc Mass Spectrom* **18**(10): 1799-1812.
- Cramer, D. W., G. B. Hutchison, W. R. Welch, R. E. Scully and K. J. Ryan (1983). "Determinants of ovarian cancer risk. I. Reproductive experiences and family history." *J Natl Cancer Inst* **71**(4): 711-716.
- Cramer, D. W. and W. R. Welch (1983). "Determinants of ovarian cancer risk. II. Inferences regarding pathogenesis." *J Natl Cancer Inst* **71**(4): 717-721.
- Crocker, P. R. and T. Feizi (1996). "Carbohydrate recognition systems: functional triads in cell-cell interactions." *Curr Opin Struct Biol* **6**(5): 679-691.
- Crum, C. P., R. Drapkin, A. Miron, T. A. Ince, M. Muto, D. W. Kindelberger and Y. Lee (2007). "The distal fallopian tube: a new model for pelvic serous carcinogenesis." *Curr Opin Obstet Gynecol* **19**(1): 3-9.
- Culf, A. S., M. Cuperlovic-Culf and R. J. Ouellette (2006). "Carbohydrate microarrays: survey of fabrication techniques." *OMICS* **10**(3): 289-310.
- Cummings, R. D. and J. D. Esko (2009). Principles of Glycan Recognition. Essentials of Glycobiology. A. Varki, R. D. Cummings, J. D. Esko et al. Cold Spring Harbor (NY).
- Cummings, R. D. and M. E. Etzler (2009). Antibodies and Lectins in Glycan Analysis. Essentials of Glycobiology. A. Varki, R. D. Cummings, J. D. Esko et al. Cold Spring Harbor (NY).
- Cummings, R. D. and S. Kornfeld (1982). "Fractionation of asparagine-linked oligosaccharides by serial lectin-agarose affinity chromatography. A rapid, sensitive, and specific technique." *Journal of Biological Chemistry* **257**(19): 11235-11240.
- Czekierdowski, A., S. Czekierdowska, M. Wielgos, A. Smolen, P. Kaminski and J. Kotarski (2006). "The role of CpG islands hypomethylation and abnormal expression of neuronal protein synuclein-gamma (SNCG) in ovarian cancer." *Neuro Endocrinol Lett* **27**(3): 381-386.
- Davies, M. J. and E. F. Hounsell (1996). "Carbohydrate chromatography: towards yoctomole sensitivity." *Biomed Chromatogr* **10**(6): 285-289.
- Davies, M. J. and E. F. Hounsell (1998). "HPLC and HPAEC of oligosaccharides and glycopeptides." *Methods Mol Biol* **76**: 79-100.
- Dell, A. (1990). "Preparation and desorption mass spectrometry of permethyl and peracetyl derivatives of oligosaccharides." *Methods Enzymol* **193**: 647-660.
- Dell, A. and C. E. Ballou (1983). "Fast-atom-bombardment, negative-ion mass spectrometry of the mycobacterial O-methyl-D-glucose polysaccharide and lipopolysaccharides." *Carbohydr Res* **120**: 95-111.

- Dell, A., A. J. Reason, K. H. Khoo, M. Panico, R. A. McDowell and H. R. Morris (1994). "Mass spectrometry of carbohydrate-containing biopolymers." *Methods Enzymol* **230**: 108-132.
- Dennis, J. W. (1991). "N-linked oligosaccharide processing and tumor cell biology." *Semin Cancer Biol* **2**(6): 411-420.
- Dennis, J. W., S. Laferte, C. Waghorne, M. L. Breitman and R. S. Kerbel (1987). "Beta 1-6 branching of Asn-linked oligosaccharides is directly associated with metastasis." *Science* **236**(4801): 582-585.
- Dietel, M. (1983). "Discrimination between benign, borderline, and malignant epithelial ovarian tumors using tumor markers: an immunohistochemical study." *Cancer Detect Prev* **6**(1-2): 255-262.
- Domon, B. and C.E. Costello (1988). "A systematic nomenclature for carbohydrate fragmentations in FAB-MS/MS spectra of glycoconjugates." *Glycoconjugate Journal* **5**(4): 397-409.
- Drake, P. M., W. Cho, B. Li, A. Prakobphol, E. Johansen, N. L. Anderson, F. E. Regnier, B. W. Gibson and S. J. Fisher (2010). "Sweetening the pot: adding glycosylation to the biomarker discovery equation." *Clin Chem* **56**(2): 223-236.
- Drapkin, R. and J.L. Hecht (2002). "The origins of ovarian cancer: Hurdles and progress." *Women's Oncology Reviews* **2**: 261-268.
- Dube, D. H. and C. R. Bertozzi (2005). "Glycans in cancer and inflammation—potential for therapeutics and diagnostics." *Nat Rev Drug Discov* **4**(6): 477-488.
- Dubeau, L. (1999). "The cell of origin of ovarian epithelial tumors and the ovarian surface epithelium dogma: does the emperor have no clothes?" *Gynecol Oncol* **72**(3): 437-442.
- Dwek, R. A. (1996). "Glycobiology: Toward Understanding the Function of Sugars." *Chem Rev* **96**(2): 683-720.
- Eddy, G. L. (1984). "Fallopian tube carcinoma." *Obstetrics and gynecology (New York. 1953)* **64**(4): 546-552.
- Eden, A., F. Gaudet, A. Waghmare and R. Jaenisch (2003). "Chromosomal instability and tumors promoted by DNA hypomethylation." *Science* **300**(5618): 455.
- Egge, H., A. Dell and H. Von Nicolai (1983). "Fucose containing oligosaccharides from human milk. I. Separation and identification of new constituents." *Arch Biochem Biophys* **224**(1): 235-253.
- Ehrlich, M. (2002). "DNA hypomethylation, cancer, the immunodeficiency, centromeric region instability, facial anomalies syndrome and chromosomal rearrangements." *J Nutr* **132**(8 Suppl): 2424S-2429S.
- Ehrlich, M. (2002). "DNA methylation in cancer: too much, but also too little." *Oncogene* **21**(35): 5400-5413.
- El-Aneel, A., A. Cohen and J. Banoub (2009). "Mass Spectrometry, Review of the Basics: Electrospray, MALDI, and Commonly Used Mass Analyzers." *Applied Spectroscopy Reviews* **44**(3): 210-230.
- Eltabbakh, G. H. and M. S. Piver (1998). "Extraovarian primary peritoneal carcinoma." *Oncology (Williston Park)* **12**(6): 813-819; discussion 820, 825-816.
- Eltabbakh, G. H., M. S. Piver, N. Natarajan and C. J. Mettlin (1998). "Epidemiologic differences between women with extraovarian primary peritoneal carcinoma and women with epithelial ovarian cancer." *Obstet Gynecol* **91**(2): 254-259.
- Emery, M. F. (1989). "Separation of cationic technetium-99m amine complexes on porous graphitic carbon." *Journal of chromatography* **479**: 212-215.
- Erickson, B. K., M. G. Conner and C. N. Landen, Jr. (2013). "The role of the fallopian tube in the origin of ovarian cancer." *Am J Obstet Gynecol* **209**(5): 409-414.
- Escrevente, C., E. Machado, C. Brito, C. A. Reis, A. Stoeck, S. Runz, A. Marme, P. Altevogt and J. Costa (2006). "Different expression levels of alpha3/4 fucosyltransferases and

- Lewis determinants in ovarian carcinoma tissues and cell lines." *Int J Oncol* **29**(3): 557-566.
- Esteller, M. (2008). "Epigenetics in cancer." *N Engl J Med* **358**(11): 1148-1159.
- Esteller, M., P. G. Corn, S. B. Baylin and J. G. Herman (2001). "A gene hypermethylation profile of human cancer." *Cancer Res* **61**(8): 3225-3229.
- Everest-Dass, A. V., J. L. Abrahams, D. Kolarich, N. H. Packer and M. P. Campbell (2013). "Structural feature ions for distinguishing N- and O-linked glycan isomers by LC-ESI-IT MS/MS." *J Am Soc Mass Spectrom* **24**(6): 895-906.
- Everest-Dass, A. V., D. Jin, M. Thaysen-Andersen, H. Nevalainen, D. Kolarich and N. H. Packer (2012). "Comparative structural analysis of the glycosylation of salivary and buccal cell proteins: innate protection against infection by *Candida albicans*." *Glycobiology* **22**(11): 1465-1479.
- Everest-Dass, A. V., D. Kolarich, M. P. Campbell and N. H. Packer (2013). "Tandem mass spectra of glycan substructures enable the multistage mass spectrometric identification of determinants on oligosaccharides." *Rapid Commun Mass Spectrom* **27**(9): 931-939.
- Fan, J. Q., A. Kondo, I. Kato and Y. C. Lee (1994). "High-performance liquid chromatography of glycopeptides and oligosaccharides on graphitized carbon columns." *Anal Biochem* **219**(2): 224-229.
- Farwanah, H. and T. Kolter (2012). "Lipidomics of Glycosphingolipids." *Metabolites* **2**(1): 134-164.
- Fathalla, M. F. (1971). "Incessant ovulation—a factor in ovarian neoplasia?" *Lancet* **2**(7716): 163.
- Federici, M. F., V. Kudryashov, P. E. Saigo, C. L. Finstad and K. O. Lloyd (1999). "Selection of carbohydrate antigens in human epithelial ovarian cancers as targets for immunotherapy: serous and mucinous tumors exhibit distinctive patterns of expression." *Int J Cancer* **81**(2): 193-198.
- Ferlay, J., I. Soerjomataram, M. Ervik, R. Dikshit, S. Eser, C. Mathers, M. Rebelo, D. M. Parkin, D. Forman and F. Bray (2013). GLOBOCAN 2012 Version 1.0, Cancer Incidence and Mortality Worldwide: IARC CancerBase No. 11. Lyon, France, IARC Press.
- Finch, Amy, Patricia Shaw, Barry Rosen, Joan Murphy, Steven A. Narod and Terence J. Colgan (2006). "Clinical and pathologic findings of prophylactic salpingo-oophorectomies in 159 BRCA1 and BRCA2 carriers." *Gynecologic Oncology* **100**(1): 58-64.
- Folkins, A. K., E. A. Jarboe, A. Saleemuddin, Y. Lee, M. J. Callahan, R. Drapkin, J. E. Garber, M. G. Muto, S. Tworoger and C. P. Crum (2008). "A candidate precursor to pelvic serous cancer (p53 signature) and its prevalence in ovaries and fallopian tubes from women with BRCA mutations." *Gynecol Oncol* **109**(2): 168-173.
- Ford, D., D. F. Easton, D. T. Bishop, S. A. Narod and D. E. Goldgar (1994). "Risks of cancer in BRCA1-mutation carriers. Breast Cancer Linkage Consortium." *Lancet* **343**(8899): 692-695.
- Frank, M. and S. Schloissnig (2010). "Bioinformatics and molecular modeling in glycobiology." *Cell Mol Life Sci* **67**(16): 2749-2772.
- Freire-de-Lima, Leonardo (2014). "Sweet and Sour: The Impact of Differential Glycosylation in Cancer Cells Undergoing Epithelial-Mesenchymal Transition." *Frontiers in Oncology* **4**.
- Fromm, G. L., D. M. Gershenson and E. G. Silva (1990). "Papillary serous carcinoma of the peritoneum." *Obstet Gynecol* **75**(1): 89-95.
- Frost, C. and M. P. Coleman (1997). "Obesity and ovarian cancer." *Eur J Cancer* **33**(10): 1529-1531.

- Fujii, Yuko, Shin-ichiro Numata, Yoko Nakamura, Takashi Honda, Keiko Furukawa, Takeshi Urano, Joelle Wiels, Makoto Uchikawa, Noriyuki Ozaki, Sei-ichi Matsuo, Yasuo Sugiura and Koichi Furukawa (2005). "Murine glycosyltransferases responsible for the expression of globo-series glycolipids: cDNA structures, mRNA expression, and distribution of their products." *Glycobiology* **15**(12): 1257-1267.
- Fukushima, Keiko, Takefumi Satoh, Shiro Baba and Katsuko Yamashita (2010). " α 1,2-Fucosylated and β -N-acetylgalactosaminylated prostate-specific antigen as an efficient marker of prostatic cancer." *Glycobiology* **20**(4): 452-460.
- Fuster, M. M. and J. D. Esko (2005). "The sweet and sour of cancer: glycans as novel therapeutic targets." *Nat Rev Cancer* **5**(7): 526-542.
- Ghazarian, H., B. Idoni and S. B. Oppenheimer (2011). "A glycobiology review: carbohydrates, lectins and implications in cancer therapeutics." *Acta Histochem* **113**(3): 236-247.
- Ghazizadeh, M., T. Oguro, Y. Sasaki, K. Aihara, T. Araki and G. F. Springer (1990). "Immunohistochemical and ultrastructural localization of T antigen in ovarian tumors." *Am J Clin Pathol* **93**(3): 315-321.
- Gilbert, M.T., J.H. Knox and B. Kaur (1982). "Porous glassy carbon, a new columns packing material for gas chromatography and high-performance liquid chromatography." *Chromatographia* **16**(1): 138-146.
- Gilead, A. and M. Neeman (1999). "Dynamic remodeling of the vascular bed precedes tumor growth: MLS ovarian carcinoma spheroids implanted in nude mice." *Neoplasia* **1**(3): 226-230.
- Godwin, A. K., J. R. Testa, L. M. Handel, Z. Liu, L. A. Vanderveer, P. A. Tracey and T. C. Hamilton (1992). "Spontaneous transformation of rat ovarian surface epithelial cells: association with cytogenetic changes and implications of repeated ovulation in the etiology of ovarian cancer." *J Natl Cancer Inst* **84**(8): 592-601.
- Goff, B. A., L. Mandel, H. G. Muntz and C. H. Melancon (2000). "Ovarian carcinoma diagnosis." *Cancer* **89**(10): 2068-2075.
- Gohlke, M. and V. Blanchard (2008). Separation of N-glycans by HPLC. Post-translational Modifications of Proteins: Tools for Functional Proteomics. C. Kannicht. Totowa, New Jersey, Human Press. **446**: 239-254.
- Goldstein, I.J., R.C. Hughes, M. Monsigny, T. Osawa and N. Sharon (1980). "What should be called a lectin?" *Nature* **285**: 66.
- Gordon, A. N., N. Finkler, R. P. Edwards, A. A. Garcia, M. Crozier, D. H. Irwin and E. Barrett (2005). "Efficacy and safety of erlotinib HCl, an epidermal growth factor receptor (HER1/EGFR) tyrosine kinase inhibitor, in patients with advanced ovarian carcinoma: results from a phase II multicenter study." *Int J Gynecol Cancer* **15**(5): 785-792.
- Gotoh, M., T. Sato, K. Kiyohara, A. Kameyama, N. Kikuchi, Y. D. Kwon, Y. Ishizuka, T. Iwai, H. Nakanishi and H. Narimatsu (2004). "Molecular cloning and characterization of beta1,4-N-acetylgalactosaminyltransferases IV synthesizing N,N'-diacetylglucosamine." *FEBS Lett* **562**(1-3): 134-140.
- Grant, O. C., H. M. Smith, D. Firsova, E. Fadda and R. J. Woods (2014). "Presentation, presentation, presentation! Molecular-level insight into linker effects on glycan array screening data." *Glycobiology* **24**(1): 17-25.
- Gras, E., J. Cortes, O. Diez, C. Alonso, X. Matias-Guiu, M. Baiget and J. Prat (2001). "Loss of heterozygosity on chromosome 13q12-q14, BRCA-2 mutations and lack of BRCA-2 promoter hypermethylation in sporadic epithelial ovarian tumors." *Cancer* **92**(4): 787-795.
- Greenlee, R. T., T. Murray, S. Bolden and P. A. Wingo (2000). "Cancer statistics, 2000." *CA Cancer J Clin* **50**(1): 7-33.

- Gross, Amy L., Robert J. Kurman, Russell Vang, Ie-Ming Shih and Kala Visvanathan (2010). "Precursor Lesions of High-Grade Serous Ovarian Carcinoma: Morphological and Molecular Characteristics." *Journal of Oncology* **2010**.
- Guignard, C., L. Jouve, M. B. Bogeat-Triboulot, E. Dreyer, J. F. Hausman and L. Hoffmann (2005). "Analysis of carbohydrates in plants by high-performance anion-exchange chromatography coupled with electrospray mass spectrometry." *J Chromatogr A* **1085**(1): 137-142.
- Gustafsson, Johan O. R., Martin K. Oehler, Andrew Ruszkiewicz, Shaun R. McColl and Peter Hoffmann (2011). "MALDI Imaging Mass Spectrometry (MALDI-IMS)—Application of Spatial Proteomics for Ovarian Cancer Classification and Diagnosis." *International Journal of Molecular Sciences* **12**(1): 773-794.
- Hakomori, S. (1984). "Tumor-associated carbohydrate antigens." *Annu Rev Immunol* **2**: 103-126.
- Hakomori, S. (1989). "Aberrant glycosylation in tumors and tumor-associated carbohydrate antigens." *Adv Cancer Res* **52**: 257-331.
- Hakomori, S. (1991). "Possible functions of tumor-associated carbohydrate antigens." *Curr Opin Immunol* **3**(5): 646-653.
- Hakomori, S. (2002). "Glycosylation defining cancer malignancy: new wine in an old bottle." *Proc Natl Acad Sci U S A* **99**(16): 10231-10233.
- Hakomori, S. (2003). "Structure, organization, and function of glycosphingolipids in membrane." *Curr Opin Hematol* **10**(1): 16-24.
- Halperin, R., S. Zehavi, E. Hadas, L. Habler, I. Bukovsky and D. Schneider (2001). "Immunohistochemical comparison of primary peritoneal and primary ovarian serous papillary carcinoma." *Int J Gynecol Pathol* **20**(4): 341-345.
- Halperin, R., S. Zehavi, R. Langer, E. Hadas, I. Bukovsky and D. Schneider (2001). "Primary peritoneal serous papillary carcinoma: a new epidemiologic trend? A matched-case comparison with ovarian serous papillary cancer." *Int J Gynecol Cancer* **11**(5): 403-408.
- Hanisch, F. G. (2001). "O-glycosylation of the mucin type." *Biol Chem* **382**(2): 143-149.
- Hanisch, F. G., C. Hanski and A. Hasegawa (1992). "Sialyl Lewis(x) antigen as defined by monoclonal antibody AM-3 is a marker of dysplasia in the colonic adenoma-carcinoma sequence." *Cancer Res* **52**(11): 3138-3144.
- Hanley, J. A. and B. J. McNeil (1982). "The meaning and use of the area under a receiver operating characteristic (ROC) curve." *Radiology* **143**(1): 29-36.
- Hansen, J. E., O. Lund, J. O. Nielsen, J. E. Hansen and S. Brunak (1996). "O-GLYCBASE: a revised database of O-glycosylated proteins." *Nucleic Acids Res* **24**(1): 248-252.
- Hardy, M. R. and R. R. Townsend (1988). "Separation of positional isomers of oligosaccharides and glycopeptides by high-performance anion-exchange chromatography with pulsed amperometric detection." *Proc Natl Acad Sci U S A* **85**(10): 3289-3293.
- Harvey, D. J. (1993). "Quantitative aspects of the matrix-assisted laser desorption mass spectrometry of complex oligosaccharides." *Rapid Commun Mass Spectrom* **7**(7): 614-619.
- Harvey, D. J. (2005). "Fragmentation of negative ions from carbohydrates: part 3. Fragmentation of hybrid and complex N-linked glycans." *J Am Soc Mass Spectrom* **16**(5): 647-659.
- Harvey, D. J. (2005a). "Fragmentation of negative ions from carbohydrates: part 1. Use of nitrate and other anionic adducts for the production of negative ion electrospray spectra from N-linked carbohydrates." *J Am Soc Mass Spectrom* **16**(5): 622-630.
- Harvey, D. J. (2005b). "Fragmentation of negative ions from carbohydrates: part 2. Fragmentation of high-mannose N-linked glycans." *J Am Soc Mass Spectrom* **16**(5): 631-646.

- Harvey, D. J. (2005c). "Fragmentation of negative ions from carbohydrates: part 3. Fragmentation of hybrid and complex N-linked glycans." *J Am Soc Mass Spectrom* **16**(5): 647-659.
- Harvey, D. J. (2009). "Analysis of carbohydrates and glycoconjugates by matrix-assisted laser desorption/ionization mass spectrometry: An update for 2003-2004." *Mass Spectrom Rev* **28**(2): 273-361.
- Harvey, D. J., L. Royle, C. M. Radcliffe, P. M. Rudd and R. A. Dwek (2008). "Structural and quantitative analysis of N-linked glycans by matrix-assisted laser desorption ionization and negative ion nanospray mass spectrometry." *Anal Biochem* **376**(1): 44-60.
- Hase, S. (1996). "Precolumn derivatization for chromatographic and electrophoretic analyses of carbohydrates." *Journal Of Chromatography A* **720**: 137-182.
- Hase, S., T. Ikenaka and Y. Matsushima (1978). "Structure analyses of oligosaccharides by tagging of the reducing end sugars with a fluorescent compound." *Biochem Biophys Res Commun* **85**(1): 257-263.
- Haslam, S. M., H. R. Morris and A. Dell (2001). "Mass spectrometric strategies: providing structural clues for helminth glycoproteins." *Trends Parasitol* **17**(5): 231-235.
- Henderson, Simon R., Randall C. Harper, Omar M. Salazar and Jerome H. Rudolph (1977). "Primary carcinoma of the fallopian tube: Difficulties of diagnosis and treatment." *Gynecologic Oncology* **5**(2): 168-179.
- Hiraishi, K., K. Suzuki, S. Hakomori and M. Adachi (1993). "Le(y) antigen expression is correlated with apoptosis (programmed cell death)." *Glycobiology* **3**(4): 381-390.
- Hitchcock, A. M., K. E. Yates, C. E. Costello and J. Zaia (2008). "Comparative glycomics of connective tissue glycosaminoglycans." *Proteomics* **8**(7): 1384-1397.
- Ho, C. S., C. W. Lam, M. H. Chan, R. C. Cheung, L. K. Law, L. C. Lit, K. F. Ng, M. W. Suen and H. L. Tai (2003). "Electrospray ionisation mass spectrometry: principles and clinical applications." *Clin Biochem Rev* **24**(1): 3-12.
- Hoffmann, E.D. and V. Stroobant (2013). *Mass Spectrometry: Principles and Applications*. Chichester, England, John Wiley & Sons.
- Hofmiester, G.E., Z. Zhou and J. A. Leary (1991). "Linkage position determination in lithium-cationized disaccharides: tandem mass spectrometry and semiempirical calculations." *Journal Of The American Chemical Society* **113**(16): 5964-5970.
- Hollingsworth, M. A. and B. J. Swanson (2004). "Mucins in cancer: protection and control of the cell surface." *Nat Rev Cancer* **4**(1): 45-60.
- Holst, S., K. Stavenhagen, C. I. Balog, C. A. Koeleman, L. M. McDonnell, O. A. Mayboroda, A. Verhoeven, W. E. Mesker, R. A. Tollenaar, A. M. Deelder and M. Wuhler (2013). "Investigations on aberrant glycosylation of glycosphingolipids in colorectal cancer tissues using liquid chromatography and matrix-assisted laser desorption time-of-flight mass spectrometry (MALDI-TOF-MS)." *Mol Cell Proteomics* **12**(11): 3081-3093.
- Horvat, T., V. Zoldos and G. Lauc (2011). "Evolutional and clinical implications of the epigenetic regulation of protein glycosylation." *Clin Epigenetics* **2**(2): 425-432.
- Hou, T., D. Liang, J. He, X. Chen and Y. Zhang (2012). "Primary peritoneal serous carcinoma: a clinicopathological and immunohistochemical study of six cases." *Int J Clin Exp Pathol* **5**(8): 762-769.
- Hsu, Wen-Ming, Mei-Ieng Che, Yung-Feng Liao, Hsiu-Hao Chang, Chia-Hua Chen, Yu-Ming Huang, Yung-Ming Jeng, John Huang, Michael J. Quon, Hsinyu Lee, Hsiu-Chin Huang and Min-Chuan Huang (2011). "B4GALNT3 Expression Predicts a Favorable Prognosis and Suppresses Cell Migration and Invasion via β 1 Integrin Signaling in Neuroblastoma." *The American Journal of Pathology* **179**(3): 1394-1404.
- Hu, C. Y., M. L. Taymor and A. T. Hertig (1950). "Primary carcinoma of the fallopian tube." *Am J Obstet Gynecol* **59**(1): 58-67, illust.

- Hu, L., J. Hofmann, J. Holash, G. D. Yancopoulos, A. K. Sood and R. B. Jaffe (2005). "Vascular endothelial growth factor trap combined with paclitaxel strikingly inhibits tumor and ascites, prolonging survival in a human ovarian cancer model." *Clin Cancer Res* **11**(19 Pt 1): 6966-6971.
- Hua, S., C. C. Williams, L. M. Dimapasoc, G. S. Ro, S. Ozcan, S. Miyamoto, C. B. Lebrilla, H. J. An and G. S. Leiserowitz (2013). "Isomer-specific chromatographic profiling yields highly sensitive and specific potential N-glycan biomarkers for epithelial ovarian cancer." *J Chromatogr A* **1279**: 58-67.
- Hua, W., T. Christianson, C. Rougeot, H. Rochefort and G. M. Clinton (1995). "SKOV3 ovarian carcinoma cells have functional estrogen receptor but are growth-resistant to estrogen and antiestrogens." *J Steroid Biochem Mol Biol* **55**(3-4): 279-289.
- Huang, John, Jin-Tung Liang, Hsiu-Chin Huang, Tang-Long Shen, Hsiao-Yu Chen, Neng-Yu Lin, Mei-Ieng Che, Wei-Chou Lin and Min-Chuan Huang (2007). " β 1,4-N-Acetylgalactosaminyltransferase III Enhances Malignant Phenotypes of Colon Cancer Cells." *Molecular Cancer Research* **5**(6): 543-552.
- Ibanez de Caceres, I., C. Battagli, M. Esteller, J. G. Herman, E. Dulaimi, M. I. Edelson, C. Bergman, H. Ehya, B. L. Eisenberg and P. Cairns (2004). "Tumor cell-specific BRCA1 and RASSF1A hypermethylation in serum, plasma, and peritoneal fluid from ovarian cancer patients." *Cancer Res* **64**(18): 6476-6481.
- Inoue, M., H. Ogawa, K. Nakanishi, O. Tanizawa, K. Karino and J. Endo (1990). "Clinical value of sialyl Tn antigen in patients with gynecologic tumors." *Obstet Gynecol* **75**(6): 1032-1036.
- Inoue, M., S. M. Ton, H. Ogawa and O. Tanizawa (1991). "Expression of Tn and sialyl-Tn antigens in tumor tissues of the ovary." *Am J Clin Pathol* **96**(6): 711-716.
- Iribarne, J. V. and B. A. Thomson (1976). "On the evaporation of small ions from charged droplets." *Journal of Chemical Physics* **64**: 2287-2294.
- Isaji, T., Y. Sato, Y. Zhao, E. Miyoshi, Y. Wada, N. Taniguchi and J. Gu (2006). "N-glycosylation of the β -propeller domain of the integrin $\alpha 5$ subunit is essential for $\alpha 5\beta 1$ heterodimerization, expression on the cell surface, and its biological function." *Journal of Biological Chemistry* **281**(44): 33258-33267.
- Ismail, M. A., J. Rotmensch, L. J. Mercer, B. S. Block, G. I. Salti and J. A. Holt (1994). "CA-125 in peritoneal fluid from patients with nonmalignant gynecologic disorders." *J Reprod Med* **39**(7): 510-512.
- Ito, H., A. Kuno, H. Sawaki, M. Sogabe, H. Ozaki, Y. Tanaka, M. Mizokami, J. Shoda, T. Angata, T. Sato, J. Hirabayashi, Y. Ikehara and H. Narimatsu (2009). "Strategy for glycoproteomics: identification of glyco-alteration using multiple glycan profiling tools." *J Proteome Res* **8**(3): 1358-1367.
- Ito, H., K. Yamada, K. Deguchi, H. Nakagawa and S. Nishimura (2007). "Structural assignment of disialylated biantennary N-glycan isomers derivatized with 2-aminopyridine using negative-ion multistage tandem mass spectral matching." *Rapid Commun Mass Spectrom* **21**(2): 212-218.
- Iwai, T., N. Inaba, A. Naundorf, Y. Zhang, M. Gotoh, H. Iwasaki, T. Kudo, A. Togayachi, Y. Ishizuka, H. Nakanishi and H. Narimatsu (2002). "Molecular cloning and characterization of a novel UDP-GlcNAc:GalNAc-peptide beta1,3-N-acetylglucosaminyltransferase (beta 3Gn-T6), an enzyme synthesizing the core 3 structure of O-glycans." *J Biol Chem* **277**(15): 12802-12809.
- Jackson, K. S., K. Inoue, D. A. Davis, T. S. Hilliard and J. E. Burdette (2009). "Three-dimensional ovarian organ culture as a tool to study normal ovarian surface epithelial wound repair." *Endocrinology* **150**(8): 3921-3926.
- Jacob, Francis, Darlene R. Goldstein, Nicolai V. Bovin, Tatiana Pochechueva, Marianne Spengler, Rosemarie Caduff, Daniel Fink, Marko I. Vuskovic, Margaret E. Huflejt and Viola Heinzelmann-Schwarz (2012). "Serum antiglycan antibody detection of

- nonmucinous ovarian cancers by using a printed glycan array." *International Journal of Cancer* **130**(1): 138-146.
- Jacob, Francis, Sheri Nixdorf, Neville Hacker and Viola Heinzelmann-Schwarz (2014). "Reliable in vitro studies require appropriate ovarian cancer cell lines." *Journal of Ovarian Research* **7**(1): 60.
- Jemal, A., T. Murray, E. Ward, A. Samuels, R. C. Tiwari, A. Ghafoor, E. J. Feuer and M. J. Thun (2005). "Cancer statistics, 2005." *CA Cancer J Clin* **55**(1): 10-30.
- Jemal, A., R. Siegel, E. Ward, Y. Hao, J. Xu, T. Murray and M. J. Thun (2008). "Cancer statistics, 2008." *CA Cancer J Clin* **58**(2): 71-96.
- Jemal, A., R. Siegel, E. Ward, Y. Hao, J. Xu and M. J. Thun (2009). "Cancer statistics, 2009." *CA Cancer J Clin* **59**(4): 225-249.
- Jensen, P. H., N. G. Karlsson, D. Kolarich and N. H. Packer (2012). "Structural analysis of N- and O-glycans released from glycoproteins." *Nat Protoc* **7**(7): 1299-1310.
- Jeung, I. C., Y. S. Lee, H. N. Lee and E. K. Park (2009). "Primary carcinoma of the fallopian tube: report of two cases with literature review." *Cancer Res Treat* **41**(2): 113-116.
- Ji, Q., P. I. Liu, P. K. Chen and C. Aoyama (2004). "Follicle stimulating hormone-induced growth promotion and gene expression profiles on ovarian surface epithelial cells." *Int J Cancer* **112**(5): 803-814.
- Jordan, S. J., A. C. Green, D. C. Whiteman, S. P. Moore, C. J. Bain, D. M. Gertig, P. M. Webb, Group Australian Cancer Study and Group Australian Ovarian Cancer Study (2008). "Serous ovarian, fallopian tube and primary peritoneal cancers: a comparative epidemiological analysis." *Int J Cancer* **122**(7): 1598-1603.
- Kakugawa, Y., T. Wada, K. Yamaguchi, H. Yamanami, K. Ouchi, I. Sato and T. Miyagi (2002). "Up-regulation of plasma membrane-associated ganglioside sialidase (Neu3) in human colon cancer and its involvement in apoptosis suppression." *Proc Natl Acad Sci U S A* **99**(16): 10718-10723.
- Kamerling, J.P., W. Heerma, J.F.G. Vliegthart, Green B.N., I.A.S. Lewis, G. Strecker and G. Spik (1983). "Fast atom bombardment mass spectrometry of carbohydrate chains derived from glycoproteins." *Biological Mass Spectrometry* **10**: 420-425.
- Kang, X., N. Wang, C. Pei, L. Sun, R. Sun, J. Chen and Y. Liu (2012). "Glycan-related gene expression signatures in human metastatic hepatocellular carcinoma cells." *Exp Ther Med* **3**(3): 415-422.
- Kanitakis, J, I al-Rifai, M Faure and A Claudy (1998). "Differential expression of the cancer associated antigens T (Thomsen-Friedenreich) and Tn to the skin in primary and metastatic carcinomas." *Journal of Clinical Pathology* **51**(8): 588-592.
- Karlsson, N. G. and M. A. McGuckin (2012). "O-Linked glycome and proteome of high-molecular-mass proteins in human ovarian cancer ascites: Identification of sulfation, disialic acid and O-linked fucose." *Glycobiology* **22**(7): 918-929.
- Karlsson, N. G., B. L. Schulz and N. H. Packer (2004). "Structural determination of neutral O-linked oligosaccharide alditols by negative ion LC-electrospray-MSn." *J Am Soc Mass Spectrom* **15**(5): 659-672.
- Karst, A. M., K. Levanon and R. Drapkin (2011). "Modeling high-grade serous ovarian carcinogenesis from the fallopian tube." *Proc Natl Acad Sci U S A* **108**(18): 7547-7552.
- Karst, Alison M. and Ronny Drapkin (2010). "Ovarian Cancer Pathogenesis: A Model in Evolution." *Journal of Oncology* **2010**: 13.
- Kawasaki, N., M. Ohta, S. Hyuga, O. Hashimoto and T. Hayakawa (1999). "Analysis of carbohydrate heterogeneity in a glycoprotein using liquid chromatography/mass spectrometry and liquid chromatography with tandem mass spectrometry." *Anal Biochem* **269**(2): 297-303.
- Kebarle, P. (2000). "A brief overview of the present status of the mechanisms involved in electrospray mass spectrometry." *J Mass Spectrom* **35**(7): 804-817.

- Kenny, H. A., S. Kaur, L. M. Coussens and E. Lengyel (2008). "The initial steps of ovarian cancer cell metastasis are mediated by MMP-2 cleavage of vitronectin and fibronectin." *J Clin Invest* **118**(4): 1367-1379.
- Kessler, M., C. Fotopoulou and T. Meyer (2013). "The molecular fingerprint of high grade serous ovarian cancer reflects its fallopian tube origin." *Int J Mol Sci* **14**(4): 6571-6596.
- Kim, E. H. and David E. Misek (2011). "Glycoproteomics-Based Identification of Cancer Biomarkers." *International Journal of Proteomics* **2011**: 10.
- Kim, H., K. Kim, J. Jin, J. Park, S. J. Yu, J. H. Yoon and Y. Kim (2014). "Measurement of glycosylated alpha-fetoprotein improves diagnostic power over the native form in hepatocellular carcinoma." *PLoS One* **9**(10): e110366.
- Kim, Jae-Han, Chang Won Park, Dalho Um, Ki Hwang Baek, Yohahn Jo, Hyunjoo An, Yangsun Kim and Tae Jin Kim (2014). "Mass Spectrometric Screening of Ovarian Cancer with Serum Glycans." *Disease Markers* **2014**: 9.
- Kim, K., L. R. Ruhaak, U. T. Nguyen, S. L. Taylor, L. Dimapasoc, C. Williams, C. Stroble, S. Ozcan, S. Miyamoto, C. B. Lebrilla and G. S. Leiserowitz (2014). "Evaluation of glycomic profiling as a diagnostic biomarker for epithelial ovarian cancer." *Cancer Epidemiol Biomarkers Prev* **23**(4): 611-621.
- Kim, Y. J. and A. Varki (1997). "Perspectives on the significance of altered glycosylation of glycoproteins in cancer." *Glycoconj J* **14**(5): 569-576.
- Kindelberger, D. W., Y. Lee, A. Miron, M. S. Hirsch, C. Feltmate, F. Medeiros, M. J. Callahan, E. O. Garner, R. W. Gordon, C. Birch, R. S. Berkowitz, M. G. Muto and C. P. Crum (2007). "Intraepithelial carcinoma of the fimbria and pelvic serous carcinoma: Evidence for a causal relationship." *Am J Surg Pathol* **31**(2): 161-169.
- King, S. M., S. Quartuccio, T. S. Hilliard, K. Inoue and J. E. Burdette (2011). "Alginate hydrogels for three-dimensional organ culture of ovaries and oviducts." *J Vis Exp*(52).
- Kjeldsen, T., H. Clausen, S. Hirohashi, T. Ogawa, H. Iijima and S. Hakomori (1988). "Preparation and characterization of monoclonal antibodies directed to the tumor-associated O-linked sialosyl-2----6 alpha-N-acetylgalactosaminyl (sialosyl-Tn) epitope." *Cancer Res* **48**(8): 2214-2220.
- Knox, J. H. and P. Ross (1997). Carbon-based packing materials for liquid chromatography—Structure, performance, and retention mechanisms. *Advances in Chromatography*. New York, Marcel Dekker Inc.: 73-119.
- Knox, J.H. and M.T. Gilbert (1981). Depositing polymerizable material onto porous substrate, pyrolysis, graphitization, Google Patents.
- Knox, J.H. and B. Kaur (1986). "Structure and performance of porous graphitic carbon in liquid chromatography." *Journal Of Chromatography A* **352**: 3-25.
- Kochanowski, N., F. Blanchard, R. Cacan, F. Chirat, E. Guedon, A. Marc and J. L. Goergen (2008). "Influence of intracellular nucleotide and nucleotide sugar contents on recombinant interferon-gamma glycosylation during batch and fed-batch cultures of CHO cells." *Biotechnol Bioeng* **100**(4): 721-733.
- Kolarich, D., P. H. Jensen, F. Altmann and N. H. Packer (2012). "Determination of site-specific glycan heterogeneity on glycoproteins." *Nat Protoc* **7**(7): 1285-1298.
- Konner, J., R. J. Schilder, F. A. DeRosa, S. R. Gerst, W. P. Tew, P. J. Sabbatini, M. L. Hensley, D. R. Spriggs and C. A. Aghajanian (2008). "A phase II study of cetuximab/paclitaxel/carboplatin for the initial treatment of advanced-stage ovarian, primary peritoneal, or fallopian tube cancer." *Gynecol Oncol* **110**(2): 140-145.
- Kornfeld, R. and S. Kornfeld (1985). "Assembly of asparagine-linked oligosaccharides." *Annu Rev Biochem* **54**: 631-664.
- Kosary, C. and E. L. Trimble (2002). "Treatment and survival for women with Fallopian tube carcinoma: a population-based study." *Gynecol Oncol* **86**(2): 190-191.

- Kuberan, B., M. Lech, L. Zhang, Z. L. Wu, D. L. Beeler and R. D. Rosenberg (2002). "Analysis of heparan sulfate oligosaccharides with ion pair-reverse phase capillary high performance liquid chromatography-microelectrospray ionization time-of-flight mass spectrometry." *J Am Chem Soc* **124**(29): 8707-8718.
- Kuhn, E., R. J. Kurman, R. Vang, A. S. Sehdev, G. Han, R. Soslow, T. L. Wang and M. Shih Ie (2012). "TP53 mutations in serous tubal intraepithelial carcinoma and concurrent pelvic high-grade serous carcinoma—evidence supporting the clonal relationship of the two lesions." *J Pathol* **226**(3): 421-426.
- Kui Wong, N., R. L. Easton, M. Panico, M. Sutton-Smith, J. C. Morrison, F. A. Lattanzio, H. R. Morris, G. F. Clark, A. Dell and M. S. Patankar (2003). "Characterization of the oligosaccharides associated with the human ovarian tumor marker CA125." *J Biol Chem* **278**(31): 28619-28634.
- Kuo, K. T., B. Guan, Y. Feng, T. L. Mao, X. Chen, N. Jinawath, Y. Wang, R. J. Kurman, M. Shih Ie and T. L. Wang (2009). "Analysis of DNA copy number alterations in ovarian serous tumors identifies new molecular genetic changes in low-grade and high-grade carcinomas." *Cancer Res* **69**(9): 4036-4042.
- Kurman, R. J. and M. Shih Ie (2008). "Pathogenesis of ovarian cancer: lessons from morphology and molecular biology and their clinical implications." *Int J Gynecol Pathol* **27**(2): 151-160.
- Kurman, R. J. and M. Shih Ie (2010). "The origin and pathogenesis of epithelial ovarian cancer: a proposed unifying theory." *Am J Surg Pathol* **34**(3): 433-443.
- Kurman, R. J. and M. Shih Ie (2011). "Molecular pathogenesis and extraovarian origin of epithelial ovarian cancer—shifting the paradigm." *Hum Pathol* **42**(7): 918-931.
- Kusakari, T., M. Kariya, M. Mandai, Y. Tsuruta, A. A. Hamid, K. Fukuhara, K. Nanbu, K. Takakura and S. Fujii (2003). "C-erbB-2 or mutant Ha-ras induced malignant transformation of immortalized human ovarian surface epithelial cells in vitro." *Br J Cancer* **89**(12): 2293-2298.
- Kwon, M. J. and Y. K. Shin (2011). "Epigenetic regulation of cancer-associated genes in ovarian cancer." *Int J Mol Sci* **12**(2): 983-1008.
- Lacy, M. Q., L. C. Hartmann, G. L. Keeney, S. C. Cha, H. S. Wieand, K. C. Podratz and P. C. Roche (1995). "c-erbB-2 and p53 expression in fallopian tube carcinoma." *Cancer* **75**(12): 2891-2896.
- Lamari, F.N., R. Kuhn and N.K. Karamanos (2003). "Derivatization of carbohydrates for chromatographic, electrophoretic, and mass spectrometric structure analysis." *Journal Of Chromatography B* **793**: 15-36.
- Lambe, M., J. Wu, M. A. Rossing and C. C. Hsieh (1999). "Twinning and maternal risk of ovarian cancer." *Lancet* **353**(9168): 1941.
- Lanctot, P. M., F. H. Gage and A. P. Varki (2007). "The glycans of stem cells." *Curr Opin Chem Biol* **11**(4): 373-380.
- Landen, C. N., Jr., M. J. Birrer and A. K. Sood (2008). "Early events in the pathogenesis of epithelial ovarian cancer." *J Clin Oncol* **26**(6): 995-1005.
- Lapadula, A. J., P. J. Hatcher, A. J. Hanneman, D. J. Ashline, H. Zhang and V. N. Reinhold (2005). "Congruent strategies for carbohydrate sequencing. 3. OSCAR: an algorithm for assigning oligosaccharide topology from MSn data." *Anal Chem* **77**(19): 6271-6279.
- Lau, K. S., E. A. Partridge, A. Grigorian, C. I. Silvescu, V. N. Reinhold, M. Demetriou and J. W. Dennis (2007). "Complex N-glycan number and degree of branching cooperate to regulate cell proliferation and differentiation." *Cell* **129**(1): 123-134.
- Lau, Ken S and James W Dennis (2008). "N-Glycans in cancer progression." *Glycobiology* **18**(10): 750-760.

- Lee, A., D. Kolarich, P. A. Haynes, P. H. Jensen, M. S. Baker and N. H. Packer (2009). "Rat liver membrane glycoproteome: enrichment by phase partitioning and glycoprotein capture." *J Proteome Res* **8**(2): 770-781.
- Lee, J. S., J. Y. Ro, A. A. Sahin, W. K. Hong, B. W. Brown, C. F. Mountain and W. N. Hittelman (1991). "Expression of blood-group antigen A—a favorable prognostic factor in non-small-cell lung cancer." *N Engl J Med* **324**(16): 1084-1090.
- Lee, Ling Yen, Chi-Hung Lin, Susan Fanayan, Nicolle H. Packer and Morten Thaysen-Andersen (2014). "Differential site accessibility mechanistically explains subcellular-specific N-glycosylation determinants." *Frontiers in Immunology* **5**.
- Lee, Y., A. Miron, R. Drapkin, M. R. Nucci, F. Medeiros, A. Saleemuddin, J. Garber, C. Birch, H. Mou, R. W. Gordon, D. W. Cramer, F. D. McKeon and C. P. Crum (2007). "A candidate precursor to serous carcinoma that originates in the distal fallopian tube." *J Pathol* **211**(1): 26-35.
- Lengyel, E., J. E. Burdette, H. A. Kenny, D. Matei, J. Pilrose, P. Haluska, K. P. Nephew, D. B. Hales and M. S. Stack (2014). "Epithelial ovarian cancer experimental models." *Oncogene* **33**(28): 3619-3633.
- Lenhard, M., S. Heublein, C. Kunert-Keil, T. Vrekoussis, I. Lomba, N. Ditsch, D. Mayr, K. Friese and U. Jeschke (2013). "Immunosuppressive Glycodelin A is an independent marker for poor prognosis in endometrial cancer." *BMC Cancer* **13**: 616.
- Levanon, K., C. Crum and R. Drapkin (2008). "New insights into the pathogenesis of serous ovarian cancer and its clinical impact." *J Clin Oncol* **26**(32): 5284-5293.
- Levanon, K., V. Ng, H. Y. Piao, Y. Zhang, M. C. Chang, M. H. Roh, D. W. Kindelberger, M. S. Hirsch, C. P. Crum, J. A. Marto and R. Drapkin (2010). "Primary ex vivo cultures of human fallopian tube epithelium as a model for serous ovarian carcinogenesis." *Oncogene* **29**(8): 1103-1113.
- Lewallen, D. M., D. Siler and S. S. Iyer (2009). "Factors affecting protein-glycan specificity: effect of spacers and incubation time." *Chembiochem* **10**(9): 1486-1489.
- Li, J., O. Fadare, L. Xiang, B. Kong and W. Zheng (2012). "Ovarian serous carcinoma: recent concepts on its origin and carcinogenesis." *J Hematol Oncol* **5**: 8.
- Lin, R. Z. and H. Y. Chang (2008). "Recent advances in three-dimensional multicellular spheroid culture for biomedical research." *Biotechnol J* **3**(9-10): 1172-1184.
- Lin, S., W. Kemmner, S. Grigull and P. M. Schlag (2002). "Cell surface alpha 2,6 sialylation affects adhesion of breast carcinoma cells." *Exp Cell Res* **276**(1): 101-110.
- Litkouhi, B., J. Kwong, C. M. Lo, J. G. Smedley, 3rd, B. A. McClane, M. Aponte, Z. Gao, J. L. Sarno, J. Hanners, W. R. Welch, R. S. Berkowitz, S. C. Mok and E. I. Garner (2007). "Claudin-4 overexpression in epithelial ovarian cancer is associated with hypomethylation and is a potential target for modulation of tight junction barrier function using a C-terminal fragment of Clostridium perfringens enterotoxin." *Neoplasia* **9**(4): 304-314.
- Liu, Q., J. X. Lin, Q. L. Shi, B. Wu, H. H. Ma and G. Q. Sun (2011). "Primary peritoneal serous papillary carcinoma: a clinical and pathological study." *Pathol Oncol Res* **17**(3): 713-719.
- Lloyd, K. O. and L. J. Old (1989). "Human monoclonal antibodies to glycolipids and other carbohydrate antigens: dissection of the humoral immune response in cancer patients." *Cancer Res* **49**(13): 3445-3451.
- Lynch, H. T., M. J. Casey, C. L. Snyder, C. Bewtra, J. F. Lynch, M. Butts and A. K. Godwin (2009). "Hereditary ovarian carcinoma: heterogeneity, molecular genetics, pathology, and management." *Mol Oncol* **3**(2): 97-137.
- Maass, K., R. Ranzinger, H. Geyer, C. W. von der Lieth and R. Geyer (2007). "'Glyco-peakfinder'—de novo composition analysis of glycoconjugates." *Proteomics* **7**(24): 4435-4444.

- Mabuchi, S., D. A. Altomare, D. C. Connolly, A. Klein-Szanto, S. Litwin, M. K. Hoelzle, H. H. Hensley, T. C. Hamilton and J. R. Testa (2007). "RAD001 (Everolimus) delays tumor onset and progression in a transgenic mouse model of ovarian cancer." *Cancer Res* **67**(6): 2408-2413.
- Maccioni, Hugo J F., Claudio G Giraudo and José Luis Daniotti (2002). "Understanding the Stepwise Synthesis of Glycolipids." *Neurochemical Research* **27**(7-8): 629-636.
- Machado, E., S. Kandzia, R. Carilho, P. Altevogt, H. S. Conradt and J. Costa (2011). "N-Glycosylation of total cellular glycoproteins from the human ovarian carcinoma SKOV3 cell line and of recombinantly expressed human erythropoietin." *Glycobiology* **21**(3): 376-386.
- Madera, M., Y. Mechref, I. Klouckova and M. V. Novotny (2007). "High-sensitivity profiling of glycoproteins from human blood serum through multiple-lectin affinity chromatography and liquid chromatography/tandem mass spectrometry." *Journal of Chromatography B: Analytical Technologies in the Biomedical and Life Sciences* **845**(1): 121-137.
- Madore, J., F. Ren, A. Filali-Mouhim, L. Sanchez, M. Kobel, P. N. Tonin, D. Huntsman, D. M. Provencher and A. M. Mes-Masson (2010). "Characterization of the molecular differences between ovarian endometrioid carcinoma and ovarian serous carcinoma." *J Pathol* **220**(3): 392-400.
- Maemura, K. and M. Fukuda (1992). "Poly-N-acetyllactosaminyl O-glycans attached to leukosialin. The presence of sialyl Le(x) structures in O-glycans." *J Biol Chem* **267**(34): 24379-24386.
- Maines-Bandiera, S. L. and N. Auersperg (1997). "Increased E-cadherin expression in ovarian surface epithelium: an early step in metaplasia and dysplasia?" *Int J Gynecol Pathol* **16**(3): 250-255.
- Maines-Bandiera, S. L., P. A. Kruk and N. Auersperg (1992). "Simian virus 40-transformed human ovarian surface epithelial cells escape normal growth controls but retain morphogenetic responses to extracellular matrix." *Am J Obstet Gynecol* **167**(3): 729-735.
- Makhija, S., L. C. Amler, D. Glenn, F. R. Ueland, M. A. Gold, D. S. Dizon, V. Paton, C. Y. Lin, T. Januario, K. Ng, A. Strauss, S. Kelsey, M. X. Sliwowski and U. Matulonis (2010). "Clinical activity of gemcitabine plus pertuzumab in platinum-resistant ovarian cancer, fallopian tube cancer, or primary peritoneal cancer." *J Clin Oncol* **28**(7): 1215-1223.
- Malmstrom, P. U., C. Busch, B. J. Norlen and B. Andersson (1988). "Expression of ABH blood group isoantigen as a prognostic factor in transitional cell bladder carcinoma." *Scand J Urol Nephrol* **22**(4): 265-270.
- Mandelin, E., H. Lassus, M. Seppala, A. Leminen, J. A. Gustafsson, G. Cheng, R. Butzow and R. Koistinen (2003). "Glycodelin in ovarian serous carcinoma: association with differentiation and survival." *Cancer Res* **63**(19): 6258-6264.
- Marchal, I., G. Golfier, O. Dugas and M. Majed (2003). "Bioinformatics in glycobiology." *Biochimie* **85**(1-2): 75-81.
- Marino, K., J. J. Bones, J. J. Kattla and P. M. Rudd (2010). "A systematic approach to protein glycosylation analysis: a path through the maze." *Nat Chem Biol* **6**(10): 713-723.
- Matsumoto, H., H. Muramatsu, T. Shimotakahara, M. Yanagi, H. Nishijima, N. Mitani, K. Baba, T. Muramatsu and H. Shimazu (1993). "Correlation of expression of ABH blood group carbohydrate antigens with metastatic potential in human lung carcinomas." *Cancer* **72**(1): 75-81.
- McCluggage, W. G. and N. Wilkinson (2005). "Metastatic neoplasms involving the ovary: a review with an emphasis on morphological and immunohistochemical features." *Histopathology* **47**(3): 231-247.

- McEver, R. P. (1997). "Selectin-carbohydrate interactions during inflammation and metastasis." *Glycoconj J* **14**(5): 585-591.
- McKeage, M. J., J. Von Pawel, M. Reck, M. B. Jameson, M. A. Rosenthal, R. Sullivan, D. Gibbs, P. N. Mainwaring, M. Serke, J. J. Lafitte, C. Chouaid, L. Freitag and E. Quoix (2008). "Randomised phase II study of ASA404 combined with carboplatin and paclitaxel in previously untreated advanced non-small cell lung cancer." *Br J Cancer* **99**(12): 2006-2012.
- Melmer, M., T. Stangler, A. Premstaller and W. Lindner (2011). "Comparison of hydrophilic-interaction, reversed-phase and porous graphitic carbon chromatography for glycan analysis." *J Chromatogr A* **1218**(1): 118-123.
- Merritt, M. A., S. Bentink, M. Schwede, M. P. Iwanicki, J. Quackenbush, T. Woo, E. S. Agoston, F. Reinhardt, C. P. Crum, R. S. Berkowitz, S. C. Mok, A. E. Witt, M. A. Jones, B. Wang and T. A. Ince (2013). "Gene expression signature of normal cell-of-origin predicts ovarian tumor outcomes." *PLoS One* **8**(11): e80314.
- Metoki, R., K. Kakudo, Y. Tsuji, N. Teng, H. Clausen and S. Hakomori (1989). "Deletion of histo-blood group A and B antigens and expression of incompatible A antigen in ovarian cancer." *J Natl Cancer Inst* **81**(15): 1151-1157.
- Miller, K. A., J. L. Deaton and D. E. Pittaway (1996). "Evaluation of serum CA 125 concentrations as predictors of pregnancy with human in vitro fertilization." *Fertil Steril* **65**(6): 1184-1189.
- Mink, P. J., A. R. Folsom, T. A. Sellers and L. H. Kushi (1996). "Physical activity, waist-to-hip ratio, and other risk factors for ovarian cancer: a follow-up study of older women." *Epidemiology* **7**(1): 38-45.
- Mitra, I., W. R. Alley, Jr., J. A. Goetz, J. A. Vasseur, M. V. Novotny and S. C. Jacobson (2013). "Comparative profiling of N-glycans isolated from serum samples of ovarian cancer patients and analyzed by microchip electrophoresis." *J Proteome Res* **12**(10): 4490-4496.
- Miwa, H. E., Y. Song, R. Alvarez, R. D. Cummings and P. Stanley (2012). "The bisecting GlcNAc in cell growth control and tumor progression." *Glycoconj J* **29**(8-9): 609-618.
- Miyajima, Y., R. Nakano and M. Morimatsu (1995). "Analysis of expression of matrix metalloproteinases-2 and -9 in hypopharyngeal squamous cell carcinoma by in situ hybridization." *Ann Otol Rhinol Laryngol* **104**(9 Pt 1): 678-684.
- Miyoshi, E., K. Moriwaki and T. Nakagawa (2008). "Biological function of fucosylation in cancer biology." *J Biochem* **143**(6): 725-729.
- Mock, K. K., M. Davey and J. S. Cottrell (1991). "The analysis of underivatized oligosaccharides by matrix-assisted laser desorption mass spectrometry." *Biochem Biophys Res Commun* **177**(2): 644-651.
- Monk, B. J., E. Han, C. A. Josephs-Cowan, G. Pugmire and R. A. Burger (2006). "Salvage bevacizumab (rhuMAB VEGF)-based therapy after multiple prior cytotoxic regimens in advanced refractory epithelial ovarian cancer." *Gynecol Oncol* **102**(2): 140-144.
- Moorman, Patricia G., Joellen M Schildkraut, Brian Calingaert, Susan Halabi, Marilyn F Vine and Andrew Berchuck (2002). "Ovulation and ovarian cancer: a comparison of two methods for calculating lifetime ovulatory cycles (United States)." *Cancer Causes & Control* **13**(9): 807-811.
- Mueller, D. R., B. M. Domon, W. Blum, F. Raschdorf and W. J. Richter (1988). "Direct stereochemical assignment of sugar subunits in naturally occurring glycosides by low energy collision induced dissociation. Application to papulacandin antibiotics." *Biomed Environ Mass Spectrom* **15**(8): 441-446.
- Mullen, P., A. Ritchie, S. P. Langdon and W. R. Miller (1996). "Effect of Matrigel on the tumorigenicity of human breast and ovarian carcinoma cell lines." *Int J Cancer* **67**(6): 816-820.

- Munson, M. S. B. and F. H. Field (1966). "Chemical Ionization Mass Spectrometry. I. General Introduction." *Journal of the American Chemical Society* **88**(12): 2621-2630.
- Murphy, S. K., Z. Huang, Y. Wen, M. A. Spillman, R. S. Whitaker, L. R. Simel, T. D. Nichols, J. R. Marks and A. Berchuck (2006). "Frequent IGF2/H19 domain epigenetic alterations and elevated IGF2 expression in epithelial ovarian cancer." *Mol Cancer Res* **4**(4): 283-292.
- Nakagoe, T., K. Fukushima, A. Nanashima, T. Sawai, T. Tsuji, M. Jibiki, H. Yamaguchi, T. Yasutake, H. Ayabe, T. Matuo, Y. Tagawa and K. Arisawa (2000). "Expression of Lewis(a), sialyl Lewis(a), Lewis(x) and sialyl Lewis(x) antigens as prognostic factors in patients with colorectal cancer." *Can J Gastroenterol* **14**(9): 753-760.
- Nakano, M., R. Saldanha, A. Gobel, M. Kavallaris and N. H. Packer (2011). "Identification of glycan structure alterations on cell membrane proteins in desoxyepothilone B resistant leukemia cells." *Mol Cell Proteomics* **10**(11): M111 009001.
- Naora, H. (2005). "Developmental patterning in the wrong context: the paradox of epithelial ovarian cancers." *Cell Cycle* **4**(8): 1033-1035.
- Narasimhan, S. (1982). "Control of glycoprotein synthesis. UDP-GlcNAc:glycopeptide beta 4-N-acetylglucosaminyltransferase III, an enzyme in hen oviduct which adds GlcNAc in beta 1-4 linkage to the beta-linked mannose of the trimannosyl core of N-glycosyl oligosaccharides." *J Biol Chem* **257**(17): 10235-10242.
- Narimatsu, H., H. Sawaki, A. Kuno, H. Kaji, H. Ito and Y. Ikehara (2010). "A strategy for discovery of cancer glyco-biomarkers in serum using newly developed technologies for glycoproteomics." *FEBS J* **277**(1): 95-105.
- Narita, T., H. Funahashi, Y. Satoh, T. Watanabe, J. Sakamoto and H. Takagi (1993). "Association of expression of blood group-related carbohydrate antigens with prognosis in breast cancer." *Cancer* **71**(10): 3044-3053.
- Newsom-Davis, T. E., D. Wang, L. Steinman, P. F. Chen, L. X. Wang, A. K. Simon and G. R. Screaton (2009). "Enhanced immune recognition of cryptic glycan markers in human tumors." *Cancer Res* **69**(5): 2018-2025.
- Nguyen, D. V. and D. M. Roche (2002). "Tumor classification by partial least squares using microarray gene expression data." *Bioinformatics* **18**(1): 39-50.
- Ni, W., J. Bones and B. L. Karger (2013). "In-depth characterization of N-linked oligosaccharides using fluoride-mediated negative ion microfluidic chip LC-MS." *Anal Chem* **85**(6): 3127-3135.
- Nik, N. N., R. Vang, M. Shih Ie and R. J. Kurman (2014). "Origin and pathogenesis of pelvic (ovarian, tubal, and primary peritoneal) serous carcinoma." *Annu Rev Pathol* **9**: 27-45.
- Nimeiri, H. S., A. M. Oza, R. J. Morgan, G. Friberg, K. Kasza, L. Faoro, R. Salgia, W. M. Stadler, E. E. Vokes, G. F. Fleming, I. I. Consortium Chicago Phase, P. M. H. Phase II Consortium and I. I. Consortium California Phase (2008). "Efficacy and safety of bevacizumab plus erlotinib for patients with recurrent ovarian, primary peritoneal, and fallopian tube cancer: a trial of the Chicago, PMH, and California Phase II Consortia." *Gynecol Oncol* **110**(1): 49-55.
- Ninonuevo, M. R., P. D. Perkins, J. Francis, L. M. Lamotte, R. G. LoCascio, S. L. Freeman, D. A. Mills, J. B. German, R. Grimm and C. B. Lebrilla (2008). "Daily variations in oligosaccharides of human milk determined by microfluidic chips and mass spectrometry." *J Agric Food Chem* **56**(2): 618-626.
- Nordin, A. J. (1994). "Primary carcinoma of the fallopian tube: A 20-year literature review." *Obstetrical & gynecological survey* **49**(5): 349-361.
- Noske, A., M. Schwabe, W. Weichert, S. Darb-Esfahani, A. C. Buckendahl, J. Sehouli, E. I. Braicu, J. Budczies, M. Dietel and C. Denkert (2011). "An intracellular targeted antibody detects EGFR as an independent prognostic factor in ovarian carcinomas." *BMC Cancer* **11**: 294.
- Nucci, M.R. and E. Oliva (2009). *Gynecologic Pathology*, Churchill Livingstone/Elsevier.

- Oei, A. L., F. C. Sweep, A. Geurts-Moespot, D. van Tienoven, S. Von Mensdorff-Pouilly, C. M. Thomas and L. F. Massuger (2008). "Human anti-mouse IgM and IgG responses in ovarian cancer patients after radioimmunotherapy with 90Y-muHMF1." *Anticancer Res* **28**(5A): 2721-2725.
- Ogawa, H., M. Ghazizadeh and T. Araki (1996). "Tn and sialyl-Tn antigens as potential prognostic markers in human ovarian carcinoma." *Gynecol Obstet Invest* **41**(4): 278-283.
- Ohtsubo, K. and J. D. Marth (2006). "Glycosylation in cellular mechanisms of health and disease." *Cell* **126**(5): 855-867.
- Okamura, H. and H. Katabuchi (2001). "Detailed morphology of human ovarian surface epithelium focusing on its metaplastic and neoplastic capability." *Ital J Anat Embryol* **106**(2 Suppl 2): 263-276.
- Orlando, Ron, C. Allen Bush and Catherine Fenselau (1990). "Structural analysis of oligosaccharides by tandem mass spectrometry: Collisional activation of sodium adduct ions." *Biological Mass Spectrometry* **19**(12): 747-754.
- Orsulic, S., Y. Li, R. A. Soslow, L. A. Vitale-Cross, J. S. Gutkind and H. E. Varmus (2002). "Induction of ovarian cancer by defined multiple genetic changes in a mouse model system." *Cancer Cell* **1**(1): 53-62.
- Oyelaran, O. and J. C. Gildersleeve (2009). "Glycan arrays: recent advances and future challenges." *Curr Opin Chem Biol* **13**(4): 406-413.
- Oyelaran, O., Q. Li, D. Farnsworth and J. C. Gildersleeve (2009). "Microarrays with varying carbohydrate density reveal distinct subpopulations of serum antibodies." *J Proteome Res* **8**(7): 3529-3538.
- Ozcan, S., H. J. An, A. C. Vieira, G. W. Park, J. H. Kim, M. J. Mannis and C. B. Lebrilla (2013). "Characterization of novel O-glycans isolated from tear and saliva of ocular rosacea patients." *J Proteome Res* **12**(3): 1090-1100.
- Ozols, R. F. (2002a). "Update on the management of ovarian cancer." *Cancer J* **8 Suppl 1**: S22-30.
- Ozols, R. F. (2002b). "Future directions in the treatment of ovarian cancer." *Semin Oncol* **29**(1 Suppl 1): 32-42.
- Pabst, M. and F. Altmann (2008). "Influence of electrosorption, solvent, temperature, and ion polarity on the performance of LC-ESI-MS using graphitic carbon for acidic oligosaccharides." *Anal Chem* **80**(19): 7534-7542.
- Pabst, M., J. S. Bondili, J. Stadlmann, L. Mach and F. Altmann (2007). "Mass + retention time = structure: a strategy for the analysis of N-glycans by carbon LC-ESI-MS and its application to fibrin N-glycans." *Anal Chem* **79**(13): 5051-5057.
- Pabst, M., S. Q. Wu, J. Grass, A. Kolb, C. Chiari, H. Viernstein, F. M. Unger, F. Altmann and S. Toegel (2010). "IL-1beta and TNF-alpha alter the glycophenotype of primary human chondrocytes in vitro." *Carbohydr Res* **345**(10): 1389-1393.
- Packer, N. H., M. A. Lawson, D. R. Jardine and J. W. Redmond (1998). "A general approach to desalting oligosaccharides released from glycoproteins." *Glycoconj J* **15**(8): 737-747.
- Packer, N. H., M. A. Lawson, D. R. Jardine, J. C. Sanchez and A. A. Gooley (1998). "Analyzing glycoproteins separated by two-dimensional gel electrophoresis." *Electrophoresis* **19**(6): 981-988.
- Padler-Karavani, V., X. Song, H. Yu, N. Hurtado-Ziola, S. Huang, S. Muthana, H. A. Chokhawala, J. Cheng, A. Verhagen, M. A. Langereis, R. Kleene, M. Schachner, R. J. de Groot, Y. Lasanajak, H. Matsuda, R. Schwab, X. Chen, D. F. Smith, R. D. Cummings and A. Varki (2012). "Cross-comparison of protein recognition of sialic acid diversity on two novel sialoglycan microarrays." *J Biol Chem* **287**(27): 22593-22608.

- Palmisano, G., M.R. Larsen, N.H. Packer and M. Thaysen-Andersen (2013). "Structural analysis of glycoprotein sialylation – part II: LC-MS based detection." *RSC Advances* **3**: 22706.
- Parrott, J. A., V. Doraiswamy, G. Kim, R. Mosher and M. K. Skinner (2001). "Expression and actions of both the follicle stimulating hormone receptor and the luteinizing hormone receptor in normal ovarian surface epithelium and ovarian cancer." *Mol Cell Endocrinol* **172**(1-2): 213-222.
- Peracaula, R., L. Royle, G. Tabares, G. Mallorqui-Fernandez, S. Barrabes, D. J. Harvey, R. A. Dwek, P. M. Rudd and R. de Llorens (2003). "Glycosylation of human pancreatic ribonuclease: differences between normal and tumor states." *Glycobiology* **13**(4): 227-244.
- Peracaula, R., G. Tabarés, L. Royle, D. J. Harvey, R. A. Dwek, P. M. Rudd and R. de Llorens (2003). "Altered glycosylation pattern allows the distinction between prostate-specific antigen (PSA) from normal and tumor origins." *Glycobiology* **13**(6): 457-470.
- Pere, H., J. Tapper, M. Seppala, S. Knuutila and R. Butzow (1998). "Genomic alterations in fallopian tube carcinoma: comparison to serous uterine and ovarian carcinomas reveals similarity suggesting likeness in molecular pathogenesis." *Cancer Res* **58**(19): 4274-4276.
- Pereira, Luisa (2008). "Porous Graphitic Carbon as a Stationary Phase in HPLC: Theory and Applications." *Journal of Liquid Chromatography & Related Technologies* **31**(11-12): 1687-1731.
- Permuth-Wey, J. and T.A. Sellers (2009). *Epidemiology of Ovarian Cancer. Methods of Molecular Biology, Cancer Epidemiology*. M. Verma. Totowa, New Jersey, Humana Press., **472**: 413-437.
- Petrescu, Andrei-J., Adina-L. Milac, Stefana M. Petrescu, Raymond A. Dwek and Mark R. Wormald (2004). "Statistical analysis of the protein environment of N-glycosylation sites: implications for occupancy, structure, and folding." *Glycobiology* **14**(2): 103-114.
- Pfenninger, A., M. Karas, B. Finke and B. Stahl (2002). "Structural analysis of underivatized neutral human milk oligosaccharides in the negative ion mode by nano-electrospray MS(n) (part 2: application to isomeric mixtures)." *J Am Soc Mass Spectrom* **13**(11): 1341-1348.
- Piek, J. M., J. C. Dorsman, A. Shvarts, A. C. Ansink, L. F. Massuger, P. Scholten, P. J. van Diest, J. C. Dijkstra, J. Weegenaar, P. Kenemans and R. H. Verheijen (2004). "Cultures of ovarian surface epithelium from women with and without a hereditary predisposition to develop female adnexal carcinoma." *Gynecol Oncol* **92**(3): 819-826.
- Piek, J. M., P. J. van Diest, R. P. Zweemer, J. W. Jansen, R. J. Poort-Keesom, F. H. Menko, J. J. Gille, A. P. Jongsma, G. Pals, P. Kenemans and R. H. Verheijen (2001). "Dysplastic changes in prophylactically removed Fallopian tubes of women predisposed to developing ovarian cancer." *J Pathol* **195**(4): 451-456.
- Piek, J. M., R. H. Verheijen, P. Kenemans, L. F. Massuger, H. Bulten and P. J. van Diest (2003). "BRCA1/2-related ovarian cancers are of tubal origin: a hypothesis." *Gynecol Oncol* **90**(2): 491.
- Piek, J. M., R. H. Verheijen, F. H. Menko, A. P. Jongsma, J. Weegenaar, J. J. Gille, G. Pals, P. Kenemans and P. J. van Diest (2003). "Expression of differentiation and proliferation related proteins in epithelium of prophylactically removed ovaries from women with a hereditary female adnexal cancer predisposition." *Histopathology* **43**(1): 26-32.
- Piura, Benjamin and Alex Rabinovich (2000). "Primary carcinoma of the fallopian tube: study of 11 cases." *European Journal of Obstetrics & Gynecology and Reproductive Biology* **91**(2): 169-175.

- Plavina, T., E. Wakshull, W. S. Hancock and M. Hincapie (2007). "Combination of abundant protein depletion and Multi-Lectin Affinity Chromatography (M-LAC) for plasma protein biomarker discovery." *Journal of Proteome Research* **6**(2): 662-671.
- Pochechueva, T., F. Jacob, D. R. Goldstein, M. E. Huflejt, A. Chinarev, R. Caduff, D. Fink, N. Hacker, N. V. Bovin and V. Heinzelmann-Schwarz (2011). "Comparison of printed glycan array, suspension array and ELISA in the detection of human anti-glycan antibodies." *Glycoconj J* **28**(8-9): 507-517.
- Pochechueva, Tatiana, Francis Jacob, Andre Fedier and Viola Heinzelmann-Schwarz (2012). "Tumor-Associated Glycans and Their Role in Gynecological Cancers: Accelerating Translational Research by Novel High-Throughput Approaches." *Metabolites* **2**(4): 913-939.
- Posadas, E. M., M. S. Liel, V. Kwitkowski, L. Minasian, A. K. Godwin, M. M. Hussain, V. Espina, B. J. Wood, S. M. Steinberg and E. C. Kohn (2007). "A phase II and pharmacodynamic study of gefitinib in patients with refractory or recurrent epithelial ovarian cancer." *Cancer* **109**(7): 1323-1330.
- Prat, J. (2012). "New insights into ovarian cancer pathology." *Annals of Oncology* **23**(suppl 10): x111-x117.
- Provencher, D. M., H. Lounis, L. Champoux, M. Tetrault, E. N. Manderson, J. C. Wang, P. Eydoux, R. Savoie, P. N. Tonin and A. M. Mes-Masson (2000). "Characterization of four novel epithelial ovarian cancer cell lines." *In Vitro Cell Dev Biol Anim* **36**(6): 357-361.
- Przybycin, C. G., R. J. Kurman, B. M. Ronnett, M. Shih Ie and R. Vang (2010). "Are all pelvic (nonuterine) serous carcinomas of tubal origin?" *Am J Surg Pathol* **34**(10): 1407-1416.
- Purdie, D. M., C. J. Bain, P. M. Webb, D. C. Whiteman, S. Pirozzo and A. C. Green (2001). "Body size and ovarian cancer: case-control study and systematic review (Australia)." *Cancer Causes Control* **12**(9): 855-863.
- Purdie, David M., Christopher J. Bain, Victor Siskind, Penelope M. Webb and Adèle C. Green (2003). "Ovulation and risk of epithelial ovarian cancer." *International Journal of Cancer* **104**(2): 228-232.
- Quemener, B., C. Desire, M. Lahaye, L. Debrauwer and L. Negroni (2003). "Structural characterisation by both positive- and negative-ion electrospray mass spectrometry of partially methyl-esterified oligogalacturonides purified by semi-preparative high-performance anion-exchange chromatography." *Eur J Mass Spectrom (Chichester, Eng)* **9**(1): 45-60.
- Quirk, J. T. and N. Natarajan (2005). "Ovarian cancer incidence in the United States, 1992-1999." *Gynecol Oncol* **97**(2): 519-523.
- Rademacher, T. W., R. B. Parekh and R. A. Dwek (1988). "Glycobiology." *Annu Rev Biochem* **57**: 785-838.
- Rader, J. S., J. P. Malone, J. Gross, P. Gilmore, R. A. Brooks, L. Nguyen, D. L. Crimmins, S. Feng, J. D. Wright, N. Taylor, I. Zighelboim, M. C. Funk, P. C. Huettner, J. H. Ladenson, D. Gius and R. R. Townsend (2008). "A unified sample preparation protocol for proteomic and genomic profiling of cervical swabs to identify biomarkers for cervical cancer screening." *Proteomics Clin Appl* **2**(12): 1658-1669.
- Raja, F. A., N. Chopra and J. A. Ledermann (2012). "Optimal first-line treatment in ovarian cancer." *Ann Oncol* **23 Suppl 10**: x118-127.
- Raju, U., G. Fine, K. A. Greenawald and J. M. Ohorodnik (1989). "Primary papillary serous neoplasia of the peritoneum: a clinicopathologic and ultrastructural study of eight cases." *Hum Pathol* **20**(5): 426-436.
- Ramos-Vara, J. A. (2005). "Technical Aspects of Immunohistochemistry." *Veterinary Pathology Online* **42**(4): 405-426.

- Rauthe, G. (1998). "Primary cancer of the fallopian tube. Treatment and results of 37 cases." *European journal of gynaecological oncology* **19**(4): 356-362.
- Reis, C. A., H. Osorio, L. Silva, C. Gomes and L. David (2010). "Alterations in glycosylation as biomarkers for cancer detection." *J Clin Pathol* **63**(4): 322-329.
- Remmers, N., J. M. Anderson, E. M. Linde, D. J. DiMaio, A. J. Lazenby, H. H. Wandall, U. Mandel, H. Clausen, F. Yu and M. A. Hollingsworth (2013). "Aberrant expression of mucin core proteins and o-linked glycans associated with progression of pancreatic cancer." *Clin Cancer Res* **19**(8): 1981-1993.
- Resta, L., S. Russo, G. A. Colucci and J. Prat (1993). "Morphologic precursors of ovarian epithelial tumors." *Obstet Gynecol* **82**(2): 181-186.
- Richardson, D. L., F. J. Backes, L. G. Seamon, V. Zanagnolo, D. M. O'Malley, D. E. Cohn, J. M. Fowler and L. J. Copeland (2008). "Combination gemcitabine, platinum, and bevacizumab for the treatment of recurrent ovarian cancer." *Gynecol Oncol* **111**(3): 461-466.
- Ringner, M. (2008). "What is principal component analysis?" *Nat Biotechnol* **26**(3): 303-304.
- Riska, A., A. Leminen and E. Pukkala (2003). "Sociodemographic determinants of incidence of primary fallopian tube carcinoma, Finland 1953-97." *Int J Cancer* **104**(5): 643-645.
- Roberts, W. L., S. Santikarn, V. N. Reinhold and T. L. Rosenberry (1988). "Structural characterization of the glycoinositol phospholipid membrane anchor of human erythrocyte acetylcholinesterase by fast atom bombardment mass spectrometry." *J Biol Chem* **263**(35): 18776-18784.
- Roboz, J. (2002). *Mass Spectrometry in Cancer Research*. Florida, CRC Press: 567.
- Roby, K. F., C. C. Taylor, J. P. Sweetwood, Y. Cheng, J. L. Pace, O. Tawfik, D. L. Persons, P. G. Smith and P. F. Terranova (2000). "Development of a syngeneic mouse model for events related to ovarian cancer." *Carcinogenesis* **21**(4): 585-591.
- Rosen, A. (1993). "Primary carcinoma of the Fallopian tube - A retrospective analysis of 115 patients." *British journal of cancer* **68**(3): 605-609.
- Rosen, A. C., C. Ausch, M. Klein, A. H. Graf, M. Metzenbauer, K. Philipp and A. Reiner (2000). "p53 expression in fallopian tube carcinomas." *Cancer Letters* **156**(1): 1-7.
- Rosen, D. G., L. Wang, J. N. Atkinson, Y. Yu, K. H. Lu, E. P. Diamandis, I. Hellstrom, S. C. Mok, J. Liu and R. C. Bast, Jr. (2005). "Potential markers that complement expression of CA125 in epithelial ovarian cancer." *Gynecol Oncol* **99**(2): 267-277.
- Roth, J. (2002). "Protein N-glycosylation along the secretory pathway: relationship to organelle topography and function, protein quality control, and cell interactions." *Chem Rev* **102**(2): 285-303.
- Ruhaak, L. R., A. M. Deelder and M. Wührer (2009). "Oligosaccharide analysis by graphitized carbon liquid chromatography-mass spectrometry." *Anal Bioanal Chem* **394**(1): 163-174.
- Ryuko, K., O. Iwanari, M. Kitao and S. Moriwaki (1993). "Immunohistochemical evaluation of sialosyl-Tn antigens in various ovarian carcinomas." *Gynecol Oncol* **49**(2): 215-224.
- Sagi, D., J. Peter-Katalinic, H. S. Conradt and M. Nimtz (2002). "Sequencing of tri- and tetraantennary N-glycans containing sialic acid by negative mode ESI QTOF tandem MS." *J Am Soc Mass Spectrom* **13**(9): 1138-1148.
- Saito, T., E. Miyoshi, K. Sasai, N. Nakano, H. Eguchi, K. Honke and N. Taniguchi (2002). "A secreted type of beta 1,6-N-acetylglucosaminyltransferase V (GnT-V) induces tumor angiogenesis without mediation of glycosylation: a novel function of GnT-V distinct from the original glycosyltransferase activity." *J Biol Chem* **277**(19): 17002-17008.
- Salani, R., F.J. Backes and L.J. Copeland (2009). "Overview of Epithelial Ovarian Cancer and Updates in Management Strategies: Role of Chemotherapy." *Expert Review of Obstetrics & Gynecology* **4**(4): 1-17.
- Salazar, H., A. K. Godwin, M. B. Daly, P. B. Laub, W. M. Hogan, N. Rosenblum, M. P. Boente, H. T. Lynch and T. C. Hamilton (1996). "Microscopic benign and invasive

- malignant neoplasms and a cancer-prone phenotype in prophylactic oophorectomies." *J Natl Cancer Inst* **88**(24): 1810-1820.
- Saldova, R., E. Dempsey, M. Perez-Garay, K. Marino, J. A. Watson, A. Blanco-Fernandez, W. B. Struwe, D. J. Harvey, S. F. Madden, R. Peracaula, A. McCann and P. M. Rudd (2011). "5-AZA-2'-deoxycytidine induced demethylation influences N-glycosylation of secreted glycoproteins in ovarian cancer." *Epigenetics* **6**(11): 1362-1372.
- Saldova, R., L. Royle, C. M. Radcliffe, U. M. Abd Hamid, R. Evans, J. N. Arnold, R. E. Banks, R. Hutson, D. J. Harvey, R. Antrobus, S. M. Petrescu, R. A. Dwek and P. M. Rudd (2007). "Ovarian cancer is associated with changes in glycosylation in both acute-phase proteins and IgG." *Glycobiology* **17**(12): 1344-1356.
- Saldova, R., W. B. Struwe, K. Wynne, G. Elia, M. J. Duffy and P. M. Rudd (2013). "Exploring the glycosylation of serum CA125." *Int J Mol Sci* **14**(8): 15636-15654.
- Saldova, R., M. R. Wormald, R. A. Dwek and P. M. Rudd (2008). "Glycosylation changes on serum glycoproteins in ovarian cancer may contribute to disease pathogenesis." *Dis Markers* **25**(4-5): 219-232.
- Sankaranarayanan, R. and J. Ferlay (2006). "Worldwide burden of gynaecological cancer: the size of the problem." *Best Pract Res Clin Obstet Gynaecol* **20**(2): 207-225.
- Sato, T., M. Gotoh, K. Kiyohara, A. Kameyama, T. Kubota, N. Kikuchi, Y. Ishizuka, H. Iwasaki, A. Togayachi, T. Kudo, T. Ohkura, H. Nakanishi and H. Narimatsu (2003). "Molecular cloning and characterization of a novel human beta 1,4-N-acetylgalactosaminyltransferase, beta 4GalNAc-T3, responsible for the synthesis of N,N'-diacetyllactosediamine, galNAc beta 1-4GlcNAc." *J Biol Chem* **278**(48): 47534-47544.
- Schachter, H. (2000). "The joys of HexNAc. The synthesis and function of N- and O-glycan branches." *Glycoconj J* **17**(7-9): 465-483.
- Schiffenbauer, Y. S., R. Abramovitch, G. Meir, N. Nevo, M. Holzinger, A. Itin, E. Keshet and M. Neeman (1997). "Loss of ovarian function promotes angiogenesis in human ovarian carcinoma." *Proc Natl Acad Sci U S A* **94**(24): 13203-13208.
- Schilder, R. J., M. W. Sill, X. Chen, K. M. Darcy, S. L. Decesare, G. Lewandowski, R. B. Lee, C. A. Arciero, H. Wu and A. K. Godwin (2005). "Phase II study of gefitinib in patients with relapsed or persistent ovarian or primary peritoneal carcinoma and evaluation of epidermal growth factor receptor mutations and immunohistochemical expression: a Gynecologic Oncology Group Study." *Clin Cancer Res* **11**(15): 5539-5548.
- Schildkraut, J. M., P. J. Schwingl, E. Bastos, A. Evanoff and C. Hughes (1996). "Epithelial ovarian cancer risk among women with polycystic ovary syndrome." *Obstet Gynecol* **88**(4 Pt 1): 554-559.
- Schnaar, R. L., A. Suzuki and P. Stanley (2009). Glycosphingolipids. Essentials of Glycobiology. A. Varki, R. D. Cummings, J. D. Esko et al. Cold Spring Harbor (NY).
- Scholler, N., M. Crawford, A. Sato, C. W. Drescher, K. C. O'Briant, N. Kiviat, G. L. Anderson and N. Urban (2006). "Bead-based ELISA for validation of ovarian cancer early detection markers." *Clin Cancer Res* **12**(7 Pt 1): 2117-2124.
- Schorge, J. O., M. G. Muto, W. R. Welch, C. A. Bandera, S. C. Rubin, D. A. Bell, R. S. Berkowitz and S. C. Mok (1998). "Molecular evidence for multifocal papillary serous carcinoma of the peritoneum in patients with germline BRCA1 mutations." *J Natl Cancer Inst* **90**(11): 841-845.
- Schwarz, F. and M. Aeibi (2011). "Mechanisms and principles of N-linked protein glycosylation." *Curr Opin Struct Biol* **21**(5): 576-582.
- Scully, R., R. Young and P. Clement (1998). Tumors of the ovary, maldeveloped gonads, fallopian tube, and broad ligament. Washington, Armed Forces Institute of Pathology.

- Scully, R.E., Young, R.H., Clement, P.B. (1998). Tumors of the ovary, maldeveloped gonads, fallopian tube, and broad ligament. Atlas of tumor pathology. Washington, DC, Armed Forces Institute of Pathology. **series 3, fascicle 23**.
- Seales, E. C., G. A. Jurado, B. A. Brunson, J. K. Wakefield, A. R. Frost and S. L. Bellis (2005). "Hypersialylation of beta1 integrins, observed in colon adenocarcinoma, may contribute to cancer progression by up-regulating cell motility." *Cancer Res* **65**(11): 4645-4652.
- Secord, A. A., J. A. Blessing, D. K. Armstrong, W. H. Rodgers, Z. Miner, M. N. Barnes, G. Lewandowski, R. S. Mannel and Group Gynecologic Oncology (2008). "Phase II trial of cetuximab and carboplatin in relapsed platinum-sensitive ovarian cancer and evaluation of epidermal growth factor receptor expression: a Gynecologic Oncology Group study." *Gynecol Oncol* **108**(3): 493-499.
- Seelentag, W. K., W. P. Li, S. F. Schmitz, U. Metzger, P. Aeberhard, P. U. Heitz and J. Roth (1998). "Prognostic value of beta1,6-branched oligosaccharides in human colorectal carcinoma." *Cancer Res* **58**(23): 5559-5564.
- Seidman, J. D., I. Horkayne-Szakaly, M. Haiba, C. R. Boice, R. J. Kurman and B. M. Ronnett (2004). "The histologic type and stage distribution of ovarian carcinomas of surface epithelial origin." *Int J Gynecol Pathol* **23**(1): 41-44.
- Seidman, J. D., P. Zhao and A. Yemelyanova (2011). "'Primary peritoneal' high-grade serous carcinoma is very likely metastatic from serous tubal intraepithelial carcinoma: assessing the new paradigm of ovarian and pelvic serous carcinogenesis and its implications for screening for ovarian cancer." *Gynecol Oncol* **120**(3): 470-473.
- Selvaggi, S. M. (2000). "Tumors of the ovary, maldeveloped gonads, fallopian tube, and broad ligament." *Arch Pathol Lab Med* **124**(3): 477.
- Shabani, N., I. Mylonas, C. Kunert-Keil, V. Briesse, W. Janni, B. Gerber, K. Friese and U. Jeschke (2005). "Expression of glycodefin in human breast cancer: immunohistochemical analysis in mammary carcinoma in situ, invasive carcinomas and their lymph node metastases." *Anticancer Res* **25**(3A): 1761-1764.
- Sharon, N. (1980). "Carbohydrates." *Sci Am* **243**(5): 90-116.
- Sharon, N. and H. Lis (1993). "Carbohydrates in cell recognition." *Sci Am* **268**(1): 82-89.
- Shaw, P. A., J. R. McLaughlin, R. P. Zweemer, S. A. Narod, H. Risch, R. H. Verheijen, A. Ryan, F. H. Menko, P. Kenemans and I. J. Jacobs (2002). "Histopathologic features of genetically determined ovarian cancer." *Int J Gynecol Pathol* **21**(4): 407-411.
- Sheeley, D. M. and V. N. Reinhold (1998). "Structural characterization of carbohydrate sequence, linkage, and branching in a quadrupole Ion trap mass spectrometer: neutral oligosaccharides and N-linked glycans." *Anal Chem* **70**(14): 3053-3059.
- Sherman-Baust, Cheryl A., Elisabetta Kuhn, Blanca L. Valle, Ie-Ming Shih, Robert J. Kurman, Tian-Li Wang, Tomokazu Amano, Minoru S. H. Ko, Ichiro Miyoshi, Yoshihiko Araki, Elin Lehrmann, Yongqing Zhang, Kevin G. Becker and Patrice J. Morin (2014). "A genetically engineered ovarian cancer mouse model based on fallopian tube transformation mimics human high-grade serous carcinoma development." *The Journal of Pathology* **233**(3): 228-237.
- Shih Ie, M., L. Chen, C. C. Wang, J. Gu, B. Davidson, L. Cope, R. J. Kurman, J. Xuan and T. L. Wang (2010). "Distinct DNA methylation profiles in ovarian serous neoplasms and their implications in ovarian carcinogenesis." *Am J Obstet Gynecol* **203**(6): 584 e581-522.
- Shih Ie, M. and R. J. Kurman (2004). "Ovarian tumorigenesis: a proposed model based on morphological and molecular genetic analysis." *Am J Pathol* **164**(5): 1511-1518.
- Shiozaki, K., K. Yamaguchi, K. Takahashi, S. Moriya and T. Miyagi (2011). "Regulation of sialyl Lewis antigen expression in colon cancer cells by sialidase NEU4." *J Biol Chem* **286**(24): 21052-21061.

- Shirotani, Keiro, Satoshi Futakawa, Kiyomitsu Nara, Kyoka Hoshi, Toshie Saito, Yuriko Tohyama, Shinobu Kitazume, Tatsuhiko Yuasa, Masakazu Miyajima, Hajime Arai, Atsushi Kuno, Hisashi Narimatsu and Yasuhiro Hashimoto (2011). "High Throughput ELISAs to Measure a Unique Glycan on Transferrin in Cerebrospinal Fluid: A Possible Extension toward Alzheimer's Disease Biomarker Development." *International Journal of Alzheimer's Disease* **2011**: 5.
- Siegel, R., C. DeSantis, K. Virgo, K. Stein, A. Mariotto, T. Smith, D. Cooper, T. Gansler, C. Lerro, S. Fedewa, C. Lin, C. Leach, R. S. Cannady, H. Cho, S. Scoppa, M. Hachey, R. Kirch, A. Jemal and E. Ward (2012). "Cancer treatment and survivorship statistics, 2012." *CA Cancer J Clin* **62**(4): 220-241.
- Singer, G., R. Oldt, 3rd, Y. Cohen, B. G. Wang, D. Sidransky, R. J. Kurman and M. Shih Ie (2003). "Mutations in BRAF and KRAS characterize the development of low-grade ovarian serous carcinoma." *J Natl Cancer Inst* **95**(6): 484-486.
- Solis, D., J. Jimenez-Barbero, H. Kaltner, A. Romero, H. C. Siebert, C. W. von der Lieth and H. J. Gabius (2001). "Towards defining the role of glycans as hardware in information storage and transfer: basic principles, experimental approaches and recent progress." *Cells Tissues Organs* **168**(1-2): 5-23.
- Song, Y., J. A. Aglipay, J. D. Bernstein, S. Goswami and P. Stanley (2010). "The bisecting GlcNAc on N-glycans inhibits growth factor signaling and retards mammary tumor progression." *Cancer Res* **70**(8): 3361-3371.
- Spengler, B., J. W. Dolce and R. J. Cotter (1990). "Infrared Laser Desorption Mass Spectrometry of Oligosaccharides: Fragmentation Mechanisms and Isomer Analysis." *Analytical Chemistry* **62**(17): 1731-1737.
- Spiro, R. G. (2002). "Protein glycosylation: nature, distribution, enzymatic formation, and disease implications of glycopeptide bonds." *Glycobiology* **12**(4): 43R-56R.
- Stanley, P., H. Schachter and N. Taniguchi (2009). N-Glycans. *Essentials of Glycobiology*. A. Varki, R. D. Cummings, J. D. Esko et al. Cold Spring Harbor (NY).
- Strathdee, G., K. Appleton, M. Illand, D. W. Millan, J. Sargent, J. Paul and R. Brown (2001). "Primary ovarian carcinomas display multiple methylator phenotypes involving known tumor suppressor genes." *Am J Pathol* **158**(3): 1121-1127.
- Strathdee, G., J. K. Vass, K. A. Oien, N. Siddiqui, J. Curto-Garcia and R. Brown (2005). "Demethylation of the MCJ gene in stage III/IV epithelial ovarian cancer and response to chemotherapy." *Gynecol Oncol* **97**(3): 898-903.
- Strupat, K., M. Karas and F. Hillenkamp (1991). "2,5-Dihydroxybenzoic acid: a new matrix for laser desorption—ionization mass spectrometry." *International Journal of Mass Spectrometry and Ion Processes* **111**: 89-102.
- Suh, K. S., S. W. Park, A. Castro, H. Patel, P. Blake, M. Liang and A. Goy (2010). "Ovarian cancer biomarkers for molecular biosensors and translational medicine." *Expert Rev Mol Diagn* **10**(8): 1069-1083.
- Svennerholm, L. (1964). "The Gangliosides." *J Lipid Res* **5**: 145-155.
- Swerdlow, M. (1959). "Mesothelioma of the pelvic peritoneum resembling papillary cystadenocarcinoma of the ovary; case report." *Am J Obstet Gynecol* **77**(1): 197-200.
- Tabak, L. A. (1995). "In defense of the oral cavity: structure, biosynthesis, and function of salivary mucins." *Annu Rev Physiol* **57**: 547-564.
- Takai, D. and P. A. Jones (2002). "Comprehensive analysis of CpG islands in human chromosomes 21 and 22." *Proc Natl Acad Sci U S A* **99**(6): 3740-3745.
- Takeuchi, Toyohide, Takahiro Kojima and Tomoo Miwa (2000). "Ion Chromatography of Inorganic Anions on Graphitic Carbon as the Stationary Phase." *Journal of High Resolution Chromatography* **23**(10): 590-594.
- Tanaka, Nobou, Tetsuya Tanigawa, Kazuhiro Kimata, Ken Hosoya and Takeo Arai (1991). "Selectivity of carbon packing materials in comparison with octadecylsilyl- and

- pyrenylethylsilylsilica gels in reversed- phase liquid chromatography." *Journal of Chromatography A* **549**(0): 29-41.
- Tarp, M. A. and H. Clausen (2008). "Mucin-type O-glycosylation and its potential use in drug and vaccine development." *Biochim Biophys Acta* **1780**(3): 546-563.
- Tashiro, H., H. Katabuchi, M. Begum, X. Li, M. Nitta, H. Ohtake and H. Okamura (2003). "Roles of luteinizing hormone/chorionic gonadotropin receptor in anchorage-dependent and -independent growth in human ovarian surface epithelial cell lines." *Cancer Sci* **94**(11): 953-959.
- Tashiro, Y., S. Yonezawa, Y. S. Kim and E. Sato (1994). "Immunohistochemical study of mucin carbohydrates and core proteins in human ovarian tumors." *Hum Pathol* **25**(4): 364-372.
- Taylor, M.E. and M. Drickamer (2006). Introduction to glycobiology New York, Oxford University Press: 255.
- Testa, J. R., L. A. Getts, H. Salazar, Z. Liu, L. M. Handel, A. K. Godwin and T. C. Hamilton (1994). "Spontaneous transformation of rat ovarian surface epithelial cells results in well to poorly differentiated tumors with a parallel range of cytogenetic complexity." *Cancer Res* **54**(10): 2778-2784.
- Thanawiroon, C., K. G. Rice, T. Toida and R. J. Linhardt (2004). "Liquid chromatography/mass spectrometry sequencing approach for highly sulfated heparin-derived oligosaccharides." *J Biol Chem* **279**(4): 2608-2615.
- Thomsson, K. A., N. G. Karlsson and G. C. Hansson (1999). "Liquid chromatography-electrospray mass spectrometry as a tool for the analysis of sulfated oligosaccharides from mucin glycoproteins." *J Chromatogr A* **854**(1-2): 131-139.
- Townsend, R. R., M. R. Hardy, D. A. Cumming, J. P. Carver and B. Bendiak (1989). "Separation of branched sialylated oligosaccharides using high-pH anion-exchange chromatography with pulsed amperometric detection." *Anal Biochem* **182**(1): 1-8.
- Truong, L. D., M. L. Maccato, H. Awalt, P. T. Cagle, M. R. Schwartz and A. L. Kaplan (1990). "Serous surface carcinoma of the peritoneum: a clinicopathologic study of 22 cases." *Hum Pathol* **21**(1): 99-110.
- Tsao, S. W., S. C. Mok, E. G. Fey, J. A. Fletcher, T. S. Wan, E. C. Chew, M. G. Muto, R. C. Knapp and R. S. Berkowitz (1995). "Characterization of human ovarian surface epithelial cells immortalized by human papilloma viral oncogenes (HPV-E6E7 ORFs)." *Exp Cell Res* **218**(2): 499-507.
- Tung, Ko-Hui, Lynne R. Wilkens, Anna H. Wu, Katharine McDuffie, Abraham M. Y. Nomura, Laurence N. Kolonel, Keith Y. Terada and Marc T. Goodman (2005). "Effect of Anovulation Factors on Pre- and Postmenopausal Ovarian Cancer Risk: Revisiting the Incessant Ovulation Hypothesis." *American Journal of Epidemiology* **161**(4): 321-329.
- Van Damme, ElsJ M. (2011). Lectins as Tools to Select for Glycosylated Proteins. Gel-Free Proteomics. K. Gevaert and J. Vandekerckhove, Humana Press. **753**: 289-297.
- van Haaften-Day, C., Y. Shen, F. Xu, Y. Yu, A. Berchuck, L. J. Havrilesky, H. W. de Bruijn, A. G. van der Zee, R. C. Bast, Jr. and N. F. Hacker (2001). "OVX1, macrophage-colony stimulating factor, and CA-125-II as tumor markers for epithelial ovarian carcinoma: a critical appraisal." *Cancer* **92**(11): 2837-2844.
- van Nagell, J. R., Jr., R. V. Higgins, E. S. Donaldson, H. H. Gallion, D. E. Powell, E. J. Pavlik, C. H. Woods and E. A. Thompson (1990). "Transvaginal sonography as a screening method for ovarian cancer. A report of the first 1000 cases screened." *Cancer* **65**(3): 573-577.
- Vanderschaeghe, D., N. Festjens, J. Delanghe and N. Callewaert (2010). "Glycome profiling using modern glycomics technology: technical aspects and applications." *Biol Chem* **391**(2-3): 149-161.

- Vang, R., M. Shih Ie and R. J. Kurman (2009). "Ovarian low-grade and high-grade serous carcinoma: pathogenesis, clinicopathologic and molecular biologic features, and diagnostic problems." *Adv Anat Pathol* **16**(5): 267-282.
- Varki, A. (1993). "Biological roles of oligosaccharides: all of the theories are correct." *Glycobiology* **3**(2): 97-130.
- Varki, A. (2009). *Essentials of Glycobiology*. A. Varki, R. D. Cummings, J. D. Esko et al. Cold Spring Harbor (NY).
- Vavasseur, F., J. M. Yang, K. Dole, H. Paulsen and I. Brockhausen (1995). "Synthesis of O-glycan core 3: characterization of UDP-GlcNAc: GalNAc-R beta 3-N-acetylglucosaminyltransferase activity from colonic mucosal tissues and lack of the activity in human cancer cell lines." *Glycobiology* **5**(3): 351-357.
- Venkitaraman, A. R. (2002). "Cancer susceptibility and the functions of BRCA1 and BRCA2." *Cell* **108**(2): 171-182.
- Verheijen, R. H., L. F. Massuger, B. B. Benigno, A. A. Epenetos, A. Lopes, J. T. Soper, J. Markowska, R. Vyzula, T. Jobling, G. Stamp, G. Spiegel, D. Thurston, T. Falke, J. Lambert and M. V. Seiden (2006). "Phase III trial of intraperitoneal therapy with yttrium-90-labeled HMFG1 murine monoclonal antibody in patients with epithelial ovarian cancer after a surgically defined complete remission." *J Clin Oncol* **24**(4): 571-578.
- Viseux, N., E. de Hoffmann and B. Domon (1997). "Structural analysis of permethylated oligosaccharides by electrospray tandem mass spectrometry." *Anal Chem* **69**(16): 3193-3198.
- Vollmers, H. P. and S. Brandlein (2006). "Natural IgM antibodies: the orphaned molecules in immune surveillance." *Adv Drug Deliv Rev* **58**(5-6): 755-765.
- von Riedenauer, Wesley, Sumbul Janjua, David Kwon, Ziyang Zhang and Vic Velanovich (2007). "Immunohistochemical identification of primary peritoneal serous cystadenocarcinoma mimicking advanced colorectal carcinoma: a case report." *Journal of Medical Case Reports* **1**(1): 150.
- Wan, Qian H., P. Nicholas Shaw, Martyn C. Davies and David A. Barrett (1995). "Chromatographic behaviour of positional isomers on porous graphitic carbon." *Journal of Chromatography A* **697**(1-2): 219-227.
- Wang, J., F. Luo, J. J. Lu, P. K. Chen, P. Liu and W. Zheng (2002). "VEGF expression and enhanced production by gonadotropins in ovarian epithelial tumors." *Int J Cancer* **97**(2): 163-167.
- Wang, P. H., W. L. Lee, C. M. Juang, Y. H. Yang, W. H. Lo, C. R. Lai, S. L. Hsieh and C. C. Yuan (2005). "Altered mRNA expressions of sialyltransferases in ovarian cancers." *Gynecol Oncol* **99**(3): 631-639.
- Welshinger, M., C. L. Finstad, E. Venkatraman, M. G. Federici, S. C. Rubin, J. L. Lewis, Jr. and K. O. Lloyd (1996). "Expression of A, B, and H blood group antigens in epithelial ovarian cancer: relationship to tumor grade and patient survival." *Gynecol Oncol* **62**(1): 106-112.
- Werness, B. A., A. M. Afify, K. L. Bielat, G. H. Eltabbakh, M. S. Piver and J. M. Paterson (1999). "Altered surface and cyst epithelium of ovaries removed prophylactically from women with a family history of ovarian cancer." *Hum Pathol* **30**(2): 151-157.
- West, C., C. Elfakir and M. Lafosse (2010). "Porous graphitic carbon: A versatile stationary phase for liquid chromatography." *Journal of Chromatography A* **1217**(19): 3201-3216.
- West, M. B., Z. M. Segu, C. L. Feasley, P. Kang, I. Klouckova, C. Li, M. V. Novotny, C. M. West, Y. Mechref and M. H. Hanigan (2010). "Analysis of site-specific glycosylation of renal and hepatic gamma-glutamyl transpeptidase from normal human tissue." *J Biol Chem* **285**(38): 29511-29524.
- Wheeler, S. F., P. Domann and D. J. Harvey (2009). "Derivatization of sialic acids for stabilization in matrix-assisted laser desorption/ionization mass spectrometry and

- concomitant differentiation of alpha(2 --> 3)- and alpha(2 --> 6)-isomers." *Rapid Commun Mass Spectrom* **23**(2): 303-312.
- Wheeler, S. F. and D. J. Harvey (2000). "Negative ion mass spectrometry of sialylated carbohydrates: discrimination of N-acetylneuraminic acid linkages by MALDI-TOF and ESI-TOF mass spectrometry." *Anal Chem* **72**(20): 5027-5039.
- Widschwendter, M., G. Jiang, C. Woods, H. M. Muller, H. Fiegl, G. Goebel, C. Marth, E. Muller-Holzner, A. G. Zeimet, P. W. Laird and M. Ehrlich (2004). "DNA hypomethylation and ovarian cancer biology." *Cancer Res* **64**(13): 4472-4480.
- Wolf, G. T., T. E. Carey, S. P. Schmaltz, K. D. McClatchey, J. Poore, L. Glaser, D. J. Hayashida and S. Hsu (1990). "Altered antigen expression predicts outcome in squamous cell carcinoma of the head and neck." *J Natl Cancer Inst* **82**(19): 1566-1572.
- Wright, J. D., A. A. Secord, T. M. Numnum, R. P. Rocconi, M. A. Powell, A. Berchuck, R. D. Alvarez, R. K. Gibb, K. Trinkaus, J. S. Rader and D. G. Mutch (2008). "A multi-institutional evaluation of factors predictive of toxicity and efficacy of bevacizumab for recurrent ovarian cancer." *Int J Gynecol Cancer* **18**(3): 400-406.
- Wu, H., Y. Cao, D. Weng, H. Xing, X. Song, J. Zhou, G. Xu, Y. Lu, S. Wang and D. Ma (2008). "Effect of tumor suppressor gene PTEN on the resistance to cisplatin in human ovarian cancer cell lines and related mechanisms." *Cancer Lett* **271**(2): 260-271.
- Wu, J., J. Zhu, H. Yin, R. J. Buckanovich and D. M. Lubman (2014). "Analysis of glycan variation on glycoproteins from serum by the reverse lectin-based ELISA assay." *J Proteome Res* **13**(4): 2197-2204.
- Wuhrer, M., C. A. Koeleman, A. M. Deelder and C. H. Hokke (2004). "Normal-phase nanoscale liquid chromatography-mass spectrometry of underivatized oligosaccharides at low-femtomole sensitivity." *Anal Chem* **76**(3): 833-838.
- Yao, X., J. F. Hu, T. Li, Y. Yang, Z. Sun, G. A. Ulaner, T. H. Vu and A. R. Hoffman (2004). "Epigenetic regulation of the taxol resistance-associated gene TRAG-3 in human tumors." *Cancer Genet Cytogenet* **151**(1): 1-13.
- Yin, B. W., C. L. Finstad, K. Kitamura, M. G. Federici, M. Welshinger, V. Kudryashov, W. J. Hoskins, S. Welt and K. O. Lloyd (1996). "Serological and immunochemical analysis of Lewis y (Ley) blood group antigen expression in epithelial ovarian cancer." *Int J Cancer* **65**(4): 406-412.
- Yu, S. Y., L. Y. Chang, C. W. Cheng, C. C. Chou, M. N. Fukuda and K. H. Khoo (2013). "Priming mass spectrometry-based sulfoglycomic mapping for identification of terminal sulfated lacdiNAc glycotope." *Glycoconj J* **30**(2): 183-194.
- Yuan, M., S. H. Itzkowitz, C. R. Boland, Y. D. Kim, J. T. Tomita, A. Palekar, J. L. Bennington, B. F. Trump and Y. S. Kim (1986). "Comparison of T-antigen expression in normal, premalignant, and malignant human colonic tissue using lectin and antibody immunohistochemistry." *Cancer Res* **46**(9): 4841-4847.
- Yue, T., I. J. Goldstein, M. A. Hollingsworth, K. Kaul, R. E. Brand and B. B. Haab (2009). "The prevalence and nature of glycan alterations on specific proteins in pancreatic cancer patients revealed using antibody-lectin sandwich arrays." *Mol Cell Proteomics* **8**(7): 1697-1707.
- Zaia, J. (2004). "Mass spectrometry of oligosaccharides." *Mass Spectrom Rev* **23**(3): 161-227.
- Zaia, J. (2008). "Mass spectrometry and the emerging field of glycomics." *Chem Biol* **15**(9): 881-892.
- Zaia, J. (2010). "Mass spectrometry and glycomics." *OMICS* **14**(4): 401-418.
- Zaia, J. (2013). "Glycosaminoglycan glycomics using mass spectrometry." *Mol Cell Proteomics* **12**(4): 885-892.
- Zeng, G., L. Gao, S. Birkle and R. K. Yu (2000). "Suppression of ganglioside GD3 expression in a rat F-11 tumor cell line reduces tumor growth, angiogenesis, and vascular endothelial growth factor production." *Cancer Res* **60**(23): 6670-6676.

- Zhang, H., S. Singh and V. N. Reinhold (2005). "Congruent strategies for carbohydrate sequencing. 2. FragLib: an MSn spectral library." *Anal Chem* **77**(19): 6263-6270.
- Zhang, X., Y. Wang, Y. Qian, X. Wu, Z. Zhang, X. Liu, R. Zhao, L. Zhou, Y. Ruan, J. Xu, H. Liu, S. Ren, C. Xu and J. Gu (2014). "Discovery of specific metastasis-related N-glycan alterations in epithelial ovarian cancer based on quantitative glycomics." *PLoS One* **9**(2): e87978.
- Zhang, Y., X. Y. Zhang, F. Liu, H. L. Qi and H. L. Chen (2002). "The roles of terminal sugar residues of surface glycans in the metastatic potential of human hepatocarcinoma." *J Cancer Res Clin Oncol* **128**(11): 617-620.
- Zheng, M., H. Fang and S. Hakomori (1994). "Functional role of N-glycosylation in alpha 5 beta 1 integrin receptor. De-N-glycosylation induces dissociation or altered association of alpha 5 and beta 1 subunits and concomitant loss of fibronectin binding activity." *J Biol Chem* **269**(16): 12325-12331.
- Zheng, W., J. J. Lu, F. Luo, Y. Zheng, Yj Feng, J. C. Felix, S. C. Lauchlan and M. C. Pike (2000). "Ovarian epithelial tumor growth promotion by follicle-stimulating hormone and inhibition of the effect by luteinizing hormone." *Gynecol Oncol* **76**(1): 80-88.
- Zhi, Z. L., N. Laurent, A. K. Powell, R. Karamanska, M. Fais, J. Voglmeir, A. Wright, J. M. Blackburn, P. R. Crocker, D. A. Russell, S. Flitsch, R. A. Field and J. E. Turnbull (2008). "A versatile gold surface approach for fabrication and interrogation of glycoarrays." *Chembiochem* **9**(10): 1568-1575.
- Zoldos, V., S. Grgurevic and G. Lauc (2010). "Epigenetic regulation of protein glycosylation." *Biomolecular Concepts* **1**(3): 253-261.
- Zoldos, V., T. Horvat and G. Lauc (2013). "Glycomics meets genomics, epigenomics and other high throughput omics for system biology studies." *Curr Opin Chem Biol* **17**(1): 34-40.
- Zoldos, V., T. Horvat, M. Novokmet, C. Cuenin, A. Muzinic, M. Pucic, J. E. Huffman, O. Gornik, O. Polasek, H. Campbell, C. Hayward, A. F. Wright, I. Rudan, K. Owen, M. I. McCarthy, Z. Herceg and G. Lauc (2012). "Epigenetic silencing of HNF1A associates with changes in the composition of the human plasma N-glycome." *Epigenetics* **7**(2): 164-172.

APPENDICES

Appendix A: FIGO staging

Stage	Characteristics
0	Carcinoma in situ (limited to tubal epithelium [mucosa])
STAGE I: Tumor confined to fallopian tube	
IA	Growth limited to one fallopian tube without extension through or onto serosa, ascites containing malignant cells, or positive peritoneal washings
IA-0	Growth limited to one fallopian tube, tumor mass is intraluminal with no invasion of lamina propria (submucosa) or muscularis
IA-1	Growth limited to one tube with invasion of lamina propria but no extension into muscularis
IA-2	Growth limited to one fallopian tube with invasion of the muscularis
IB	Growth limited to both tubes without extension through or onto serosa, ascites containing malignant cells, or positive peritoneal washings
IB-0	Growth limited to both fallopian tubes, tumor mass is intraluminal with no invasion of lamina propria (submucosa) or muscularis
IB-1	Growth limited to both tubes with invasion of lamina propria but no extension into muscularis
IB-2	Growth limited to both tubes with extension into muscularis
IC	Tumor either stage IA or IB with extension through or onto tubal serosa; or with ascites present containing malignant cells or with positive peritoneal washings
I(F)	Tumor limited to fimbriated end of fallopian tube(s) without invasion of tubal wall
Stage II: Tumor involving one or both fallopian tubes with pelvic extension	
IIA	Extension and/or metastases to uterus and/or ovaries.
IIB	Extension to other pelvic tissues.
IIC	Tumor either stage IIA or IIB and with ascites containing malignant cells or with positive peritoneal washings
Stage III: Tumor involving one or both fallopian tubes with peritoneal implants outside pelvis and/or positive retroperitoneal or inguinal nodes. Superficial liver metastases equal stage III. Tumor appears limited to true pelvis but with histologically proven malignant extension to small bowel or omentum	
IIIA	Tumor grossly limited to true pelvis with negative nodes but with histologically confirmed microscopic seeding of abdominal peritoneal surfaces
IIIB	Tumor involving one or both tubes with histologically confirmed implants of abdominal peritoneal surfaces, none exceeding 2 cm in diameter. Lymph nodes are negative
IIIC	Abdominal implants >2 cm in diameter and/or positive retroperitoneal or inguinal nodes
Stage IV: Growth involving one or both tubes with distant metastases including parenchymal liver metastases. If pleural effusion is present, fluid must be positive for malignant cells.	

Table 1: FIGO staging in PFTSC

STAGE I: Tumor confined to ovaries	
Stage	Characteristics
IA	Tumor limited to one ovary, capsule intact, no tumor on surface, negative washings.
IB	Tumor involves both ovaries otherwise like IA.
IC	Tumor limited to one or both ovaries
IC1	Surgical spill (Intraoperative spill)
IC2	Capsule rupture before surgery or tumor on ovarian surface.
IC3	Malignant cells in the ascites or peritoneal washings.
STAGE II: Tumor involves 1 or both ovaries with pelvic extension (below the pelvic brim) or primary peritoneal cancer	
IIA	Extension and/or implant on uterus and/or Fallopian tubes
IIB	Extension to other pelvic intraperitoneal tissues
STAGE III: Tumor involves 1 or both ovaries with cytologically or histologically confirmed spread to the peritoneum outside the pelvis and/or metastasis to the retroperitoneal lymph nodes	
IIIA	Positive retroperitoneal lymph nodes and /or microscopic metastasis beyond the pelvis
IIIA1	Positive retroperitoneal lymph nodes only
IIIA 1(i)	Metastasis ≤ 10 mm
IIIA 1(ii)	Metastasis > 10 mm
IIIA2	Microscopic, extrapelvic (above the brim) peritoneal involvement ± positive retroperitoneal lymph nodes.
IIIB	Macroscopic, extrapelvic, peritoneal metastasis ≤ 2 cm ± positive retroperitoneal lymph nodes. Includes extension to capsule of liver/spleen.
IIIC	Macroscopic, extrapelvic, peritoneal metastasis > 2 cm ± positive retroperitoneal lymph nodes. Includes extension to capsule of liver/spleen.
STAGE IV: Distant metastasis excluding peritoneal metastasis	
IVA	Pleural effusion with positive cytology
IVB	Hepatic and/or splenic parenchymal metastasis, metastasis to extra-abdominal organs (including inguinal lymph nodes and lymph nodes outside of the abdominal cavity)
<p>Other major recommendations are as follows:</p> <p>a) Histologic type including grading should be designated at staging</p> <p>b) Primary site (ovary, fallopian tube or peritoneum) should be designated where possible</p> <p>c) Tumors that may otherwise qualify for stage I but involved with dense adhesions justify upgrading to stage II if tumor cells are histologically proven to be present in the adhesions</p>	

Table 2: FIGO staging in EOC

SECTION A		 		Biohazard Risk Assessment Form – NON GMO		Notification Number: MEA020712BHA	
Investigator completing assessment :		MERRINA ANUGRAHAM		Date of assessment:		2 nd July 2012	
Department:		CBMS, FACULTY OF SCIENCE		Name of Supervisor submitting this assessment:		PROF NICOLLE H. PACKER	
Contact number/email:		029850 8200/merrina.anugraham@mq.edu.au					
Reason for this assessment							
<input checked="" type="checkbox"/> New research <input type="checkbox"/> New information relating to existing research <input type="checkbox"/> other _____							
Exact location(s) of research: E8C 323							
Control measures: Eliminate risk <input type="checkbox"/> Substitute the hazard <input type="checkbox"/> Isolate the hazard <input checked="" type="checkbox"/> Implement engineering controls <input type="checkbox"/> Administration <input checked="" type="checkbox"/> (e.g. Training) PPE <input type="checkbox"/>							
E.g. eliminated by irradiation prior to use, isolation by class II biological safety cabinets, administration by following SWP as below, PPE as listed below.							
Supporting documents which must be read in conjunction with this assessment. (e.g. Safe Working Procedures, Safety Data Sheets, Guidelines/Protocols)							
-NIL-							
What is the type of the biological material?							
Bacteria <input type="checkbox"/> Fungi <input type="checkbox"/> Virus <input type="checkbox"/> Cell Line <input checked="" type="checkbox"/> Tissue <input checked="" type="checkbox"/> Parasite <input type="checkbox"/> Animal <input type="checkbox"/> Plant <input type="checkbox"/> Soil <input type="checkbox"/> Toxin <input type="checkbox"/> Prions <input type="checkbox"/> Nucleic Acid <input type="checkbox"/> other <input type="checkbox"/> _____							
What is the name of the biological agent?							
Human ovarian cancer cell lines and tissue samples from patients							
List the Personal Protective Equipment required:							
Gloves <input checked="" type="checkbox"/> (e.g. chemical resistant) Eye protection <input checked="" type="checkbox"/> (e.g. safety glasses/goggles) Clothing <input checked="" type="checkbox"/> (e.g. button up lab coat/coveralls/apron)							
Footwear <input checked="" type="checkbox"/> (e.g. Enclosed/Gumboots/overshoe covers) Respiratory Protection <input type="checkbox"/> (e.g. PF2 face mask) Other <input type="checkbox"/> _____							

What are the risks associated with this Biological Agent. (Can be more than one risk group depending on method)			
Risk Group	Details of Biohazards	Biosafety level	Risk Reduction Measures (must be followed by the researcher)
Group 1- Low individual and community risk (Microorganism that is unlikely to cause human, plant or animal disease)	Human cell lines Ovarian Cancer Cell Lines and Ascites: SKOV3, IGROV, TOVII, S458, S129	Normal Laboratory PC2 biosafety cabinet	<ol style="list-style-type: none"> Standard laboratory procedures will be followed in accordance with Laboratory Microbiological Standards AS/NZ 2243:3:2010 and university guidelines (see supporting documents - Section A above) and include spillage and emergency response. Investigator has attended university Biosafety training course (see 3) Supervisor identified in Section A confirms that the investigator has received appropriate training and instruction or has adequate supervision and understands safe laboratory practice according to AS/NZ2243:3:2010 and university guidelines (see supporting documents - Section A above)
Group 2- Moderate individual risk, limited community risk (Microorganism that is unlikely to be a significant risk to laboratory workers, the community/livestock/environment. Laboratory exposures may cause infection but effective treatment and preventative measures are available and the risk of spread is limited).	Ovarian Cancer Tissue: Derived from ovarian cancer patients (ovary, fallopian tube and peritoneum)	PC2 APAF(323)	<ol style="list-style-type: none"> Standard laboratory procedures will be followed in accordance with Laboratory Microbiological Standards AS/NZ 2243:3:2010 and university guidelines which are appropriate for Risk Group 2 (see supporting documents - Section A above) and include spillage and emergency response. Investigator has attended university Biosafety training course (see 3) Supervisor identified in Section A confirms that the investigator has received appropriate training and instruction or has adequate supervision and understands safe laboratory practice according to AS/NZ 2243:3:2010 and university guidelines (see supporting documents - Section A above)
Group 3 -High individual risk, limited community risk (Microorganisms that usually causes serious human or animal disease and may present a significant risk to laboratory workers. It could present a limited to moderate risk if spread in the community or the environment, but there are usually effective preventative measures or treatment available).			<ol style="list-style-type: none"> Standard laboratory procedures will be followed in accordance with Laboratory Microbiological Standards AS/NZ 2243:3:2010 and university guidelines which are appropriate for Risk Group 3 (see supporting documents - Section A above) and include spillage and emergency response. Investigator has attended university Biosafety training course (see 3) Supervisor identified in Section A confirms that the investigator has received appropriate training and instruction or has adequate supervision and understands safe laboratory practice according to AS/NZ 243:3:2010 and university guidelines (see supporting documents - Section A above)

Hardcopies of this document are considered uncontrolled.
Please refer to the Health & Safety internet site for latest version.

Source: Manager, Health & Safety
Created: March 2012
Document No: 68
Revised: N/A
Version No: 1

<p>Process and equipment to be used</p>	<p>You must include: -</p> <ol style="list-style-type: none"> 1 Description and quantity of any chemicals, gasses, substances and radiation used. 2 Any aerosols produced and any controls necessary to ensure the health and safety of investigators and others 3 Any alternative and/or additional control measures to those identified above and explain why these are necessary. 4 Safe Work Procedure if there is no existing SWP* 5 Explain why risks cannot be eliminated. 6 Waste disposal method.
<p>1) Ovarian Cancer Cell Lines and Ascites: Cells (1×10^7) are obtained from the University of New South Wales and have undergone Mycoplasma testing. Cell types include ATCC cell lines (HOSE6.3, SKOV 3, IGROV) and cells from patients' ascites (S458, S129, S521).</p> <p>Ovarian Cancer Tissue: Tissue samples (approx. 100mg) are obtained from the ovaries, fallopian tubes and peritoneum of cancer patients and are restricted only to patients that have been tested negative for HIV, Hepatitis A as well as other potential infective viruses and bacteria. Tissue processing is carried out at the Royal Hospital for Women and samples are kept in RNA later buffer.</p> <p>2) The main biosafety hazard of all experimental procedures occurs during the lysis of frozen cells and tissues. Lysis is necessary to disrupt the cells and separate the cell membrane pellets from other cytosolic and nucleic material. This will be performed mechanically using a homogenizer. This procedure may generate aerosols so it has to be carried out in a Class II safety cabinet in a designated cell culture room (APAF BMD Laboratory E8C 323).</p> <p>3) Upon lysis, the cell membrane pellets will be subjected to a detergent- based extraction protocol which includes Triton X-114, and further inactivates live cells. Membrane protein pellets that are obtained from this procedure are now safe to work with and can be transferred to the designated lab bench for further glycan analysis.</p> <p>4) Handling of all cancer cell cultures will be conducted in a Class II safety cabinet in the designated cell culture room (E8C 323) and all centrifugation of live cells will occur inside cell culture room in sealed containers in a sealed centrifuge. Centrifuge will be left for 10 minutes before opening to allow aerosols to settle. If the centrifuge tube breaks, spillage will occur and aerosol contamination will be minimized by allocating 30 minutes for aerosol's to settle. All standard laboratory protection will be worn including disposable gloves and lab coat whilst handling samples. Used lab coats from the PC2 lab will also be autoclaved after use prior to laundering. Hands will be thoroughly washed with soap and water before leaving the laboratory. To clean up following cell culture or cell lysis procedure, all work/bench areas will be wiped routinely following experimental work using 0.5-1% chlorine for 10 minutes.</p> <p>5) All identified risks will be managed efficiently by practising good aseptic techniques and adhering to the safety working procedures that ensure their proper management and disposal.</p> <p>6) Waste Disposal Method: Cell debris from tissues and cell lines as well as contaminated pipette tips from the PC2 lab will be collected in a plain autoclave bag and then transported to the E8C202 Autoclave room in a sealed unbreakable container. Upon autoclaving, the waste is then transported to the locked yellow bin in the E5A compound for its disposal. Glassware will be decontaminated with 0.5-1% chlorine for 10 minutes prior to rinsing with water. Any spillage on the working lab bench will be cleaned using 0.5-1% chlorine.</p>	<p>1) Ovarian Cancer Cell Lines and Ascites: Cells (1×10^7) are obtained from the University of New South Wales and have undergone Mycoplasma testing. Cell types include ATCC cell lines (HOSE6.3, SKOV 3, IGROV) and cells from patients' ascites (S458, S129, S521).</p> <p>Ovarian Cancer Tissue: Tissue samples (approx. 100mg) are obtained from the ovaries, fallopian tubes and peritoneum of cancer patients and are restricted only to patients that have been tested negative for HIV, Hepatitis A as well as other potential infective viruses and bacteria. Tissue processing is carried out at the Royal Hospital for Women and samples are kept in RNA later buffer.</p> <p>2) The main biosafety hazard of all experimental procedures occurs during the lysis of frozen cells and tissues. Lysis is necessary to disrupt the cells and separate the cell membrane pellets from other cytosolic and nucleic material. This will be performed mechanically using a homogenizer. This procedure may generate aerosols so it has to be carried out in a Class II safety cabinet in a designated cell culture room (APAF BMD Laboratory E8C 323).</p> <p>3) Upon lysis, the cell membrane pellets will be subjected to a detergent- based extraction protocol which includes Triton X-114, and further inactivates live cells. Membrane protein pellets that are obtained from this procedure are now safe to work with and can be transferred to the designated lab bench for further glycan analysis.</p> <p>4) Handling of all cancer cell cultures will be conducted in a Class II safety cabinet in the designated cell culture room (E8C 323) and all centrifugation of live cells will occur inside cell culture room in sealed containers in a sealed centrifuge. Centrifuge will be left for 10 minutes before opening to allow aerosols to settle. If the centrifuge tube breaks, spillage will occur and aerosol contamination will be minimized by allocating 30 minutes for aerosol's to settle. All standard laboratory protection will be worn including disposable gloves and lab coat whilst handling samples. Used lab coats from the PC2 lab will also be autoclaved after use prior to laundering. Hands will be thoroughly washed with soap and water before leaving the laboratory. To clean up following cell culture or cell lysis procedure, all work/bench areas will be wiped routinely following experimental work using 0.5-1% chlorine for 10 minutes.</p> <p>5) All identified risks will be managed efficiently by practising good aseptic techniques and adhering to the safety working procedures that ensure their proper management and disposal.</p> <p>6) Waste Disposal Method: Cell debris from tissues and cell lines as well as contaminated pipette tips from the PC2 lab will be collected in a plain autoclave bag and then transported to the E8C202 Autoclave room in a sealed unbreakable container. Upon autoclaving, the waste is then transported to the locked yellow bin in the E5A compound for its disposal. Glassware will be decontaminated with 0.5-1% chlorine for 10 minutes prior to rinsing with water. Any spillage on the working lab bench will be cleaned using 0.5-1% chlorine.</p>

Hardcopies of this document are considered uncontrolled.
Please refer to the Health & Safety internet site for latest version.

Source: Manager, Health & Safety
Created: March 2012
Document No: 68
Revised: N/A
Version No: 1

SECTION B	
 MACQUARIE UNIVERSITY	Biohazard Safety Committee – Risk Assessment Decision
Notification Number:	MEA020712BHA

Important Information

For non GMO investigations email this assessment to biohazard@mq.edu.au for approval by the Biohazard Safety Committee.

Individual Responsibilities

By submitting this assessment the Supervisor identified in Section A, confirms that any supporting documents, training, guidance, instruction or protocols issued by the University will be followed so far as reasonably practicable to ensure the work is carried out without risk to health, safety or the environment. The named Supervisor confirms that the investigator has received appropriate training and instruction or will have adequate supervision and understands safe laboratory practice according to AS/NZ 2243:3:2010 and university guidelines.

Decision to be completed by the Biohazard Safety Committee:

The Committee has agreed that this risk assessment is sufficient for investigations to commence? Yes ☒ No ☐ Further action required ☐

Further Action/Comments:

Name of Approver (Committee Rep):	Michael Gillings (Chairperson, Biohazard Committee)
Extension and email address:	Michael.gillings@mq.edu.au ext: 8199
Date Approved and submitted to Health and Safety Unit:	4 th September, 2012

Hardcopies of this document are considered uncontrolled.
Please refer to the Health & Safety internet site for latest version.

Source: Manager, Health & Safety
Created: March 2012
Document No: 68
Revised: N/A
Version No: 1



MACQUARIE
UNIVERSITY

Biosafety Workshop

This is to certify that

Merrina Anugraham

*has successfully completed the above workshop which was conducted
by the
Macquarie University Biosafety Committee on 26 July 2011*

*Dr Sinan Ali
Chair, Biosafety Committee
July 2011*

*Expiry Date:
July 2014*

Appendices C - D of this thesis has been removed as they may contain sensitive/confidential content